

MycoKeys issue 100: progress and innovation to enhance rapid publication in fungal systematics

H. Thorsten Lumbsch¹, Pier Luigi Nimis², Dominik Begerow³, Pavel Stoev⁴, Lyubomir Penev⁴

¹ *The Field Museum, Chicago, USA*

² *University of Trieste, Trieste, Italy*

³ *University of Hamburg, Hamburg, Germany*

⁴ *Pensoft Publishers, Sofia, Bulgaria*

Corresponding author: H. Thorsten Lumbsch (tlumbsch@fieldmuseum.org)

Since its inception in 2011 (Lumbsch et al. 2011), MycoKeys has published over 550 articles that have been cited more than 6000 times according to the Web of Science. Twelve years since its launch, and eight years since receiving its first Journal Impact Factor, we are now publishing the journal's 100th issue. This was only made possible by the high quality of submissions from authors who chose the journal as a vehicle to publish their results, the team of subject editors, numerous reviewers, and the efficient editing and publishing of the journal. This issue is a great occasion to look back and evaluate the performance of MycoKeys.

MycoKeys started with only 13 submissions in 2011, whereas the number of submitted manuscripts has been above 130 annually for the past six years (Fig. 1). Similarly, the number of published articles has grown, from 8 in the first year to above 50 annually in the last 6 years. To date, the journal has received a total of 1033 submissions and published 561 articles with an average acceptance rate of 55%. In recent times, the average time from submission to acceptance has been 70 days, and from acceptance to publication: 90 days. The number of article views has also increased to more than 450,000 annually for the last few years (Fig. 2). The articles address issues of systematics and taxonomy of all clades of the kingdom Fungi, however, the majority of papers deal with Ascomycota or Basidiomycota, including lichenized fungi.

MycoKeys has attracted researchers from various parts of the world to publish their results (Fig. 3). Altogether, scientists from 80 countries have published in the journal to date. The greatest number of researchers come from China, Thailand, Germany, the United States of America, Sweden, and Italy.

The top 10 most cited MycoKeys papers up until 31 October 2023 include papers addressing a wide array of issues, including: potential bias in the use of high throughput molecular identification methods (Tedersoo et al. 2015); quality control of generated sequences (Nilsson et al. 2012); orphan taxa in environmental sampling databases (Nilsson et al. 2016); nomenclatural issues (Hawksworth 2011); an exhaustive checklist (Nimis et al. 2018); large scale phylogenies at family and generic levels (Miettinen et al. 2016; Plata et al. 2013); diversity of plant-associated fungi (Tibpromma et al. 2018; Yang et al. 2018); and a fungus isolated from Bison dung (Callaghan et al. 2015).



Academic editor: Yassen Mutafchiev
Published: 13 November 2023

Citation: Lumbsch HT, Nimis PL, Begerow D, Stoev P, Penev L (2023) MycoKeys issue 100: progress and innovation to enhance rapid publication in fungal systematics. MycoKeys 100: 1–4. <https://doi.org/10.3897/mycokeys.100.115344>

Copyright: © H. Thorsten Lumbsch et al.
This is an open access article distributed under terms of the Creative Commons Attribution License (Attribution 4.0 International – CC BY 4.0).

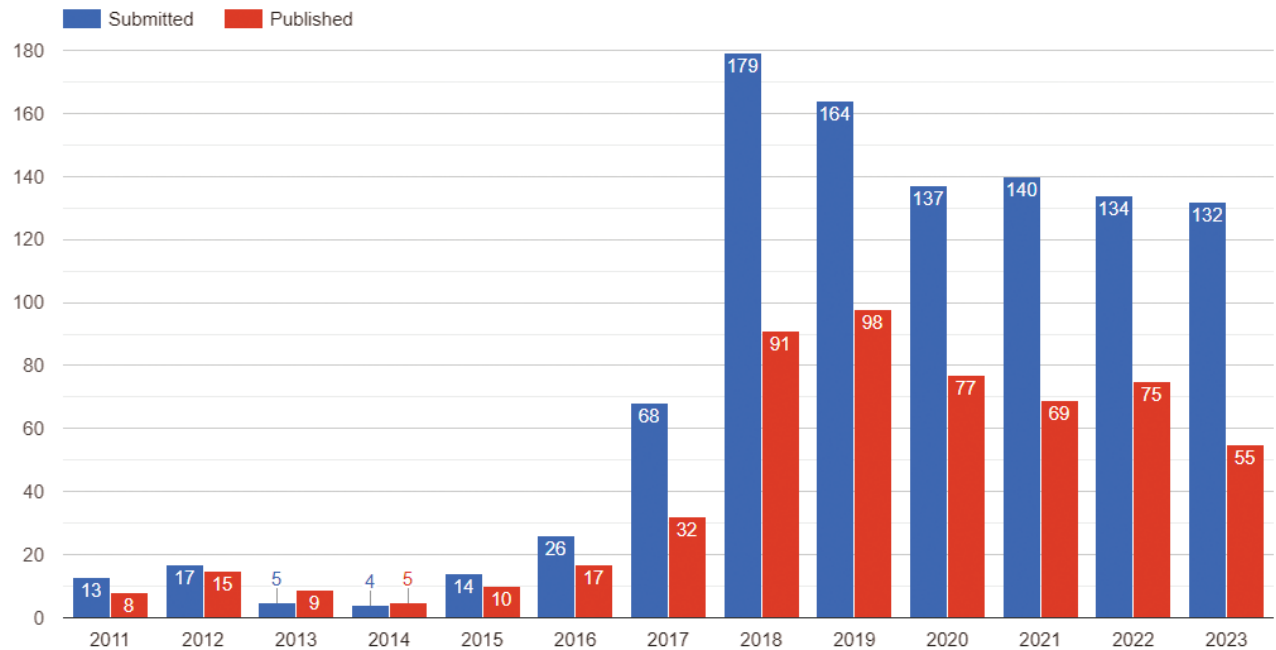


Figure 1. Submitted and published manuscripts in MycoKeys on a yearly basis since the launch of the journal in 2011. Data retrieved on 30 October 2023.

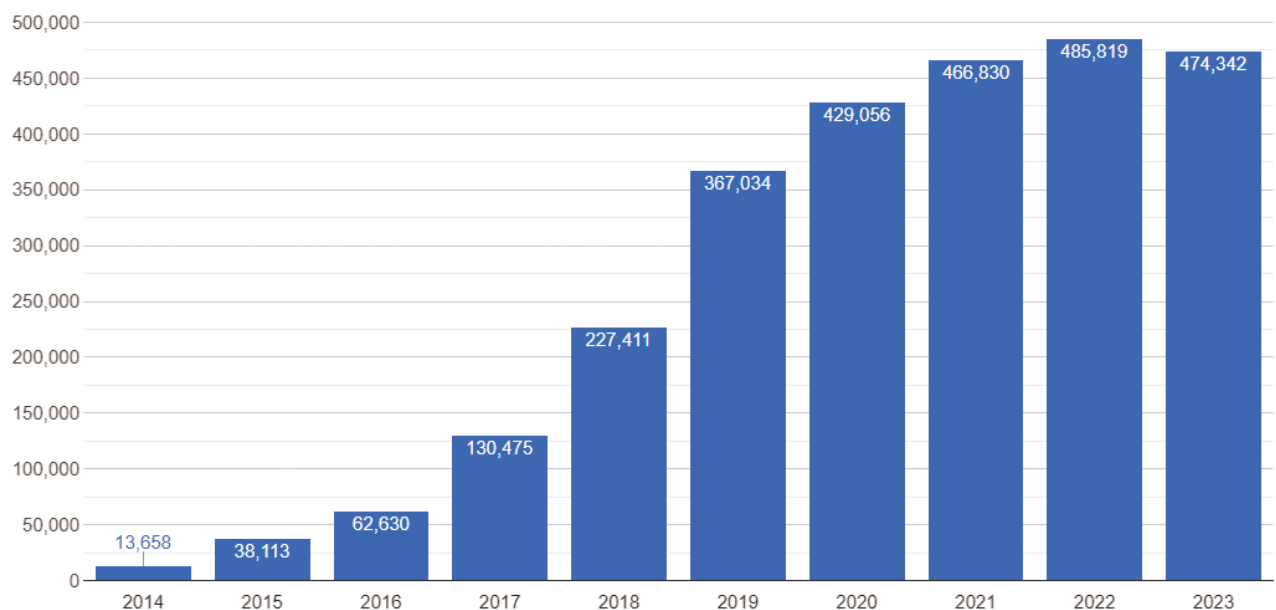


Figure 2. Article views for MycoKeys on a yearly basis since 2014. Data retrieved on 30 October 2023.

All nomenclatural changes in the journal are indexed in MycoBank. Since its launch, 1108 new species, 71 new genera and four new families have been described in MycoKeys. In addition, 248 new combinations of taxa have been proposed in the journal.

When the journal received its first Journal Impact Factor in 2015, it was at 1.846 and has subsequently increased to the current 3.3, demonstrating the quality of the peer review of submitted manuscripts, stringent quality control and management of manuscripts. The current CiteScore – a journal-level citation metric by Scopus – of MycoKeys is 5.8. Although the journal is currently

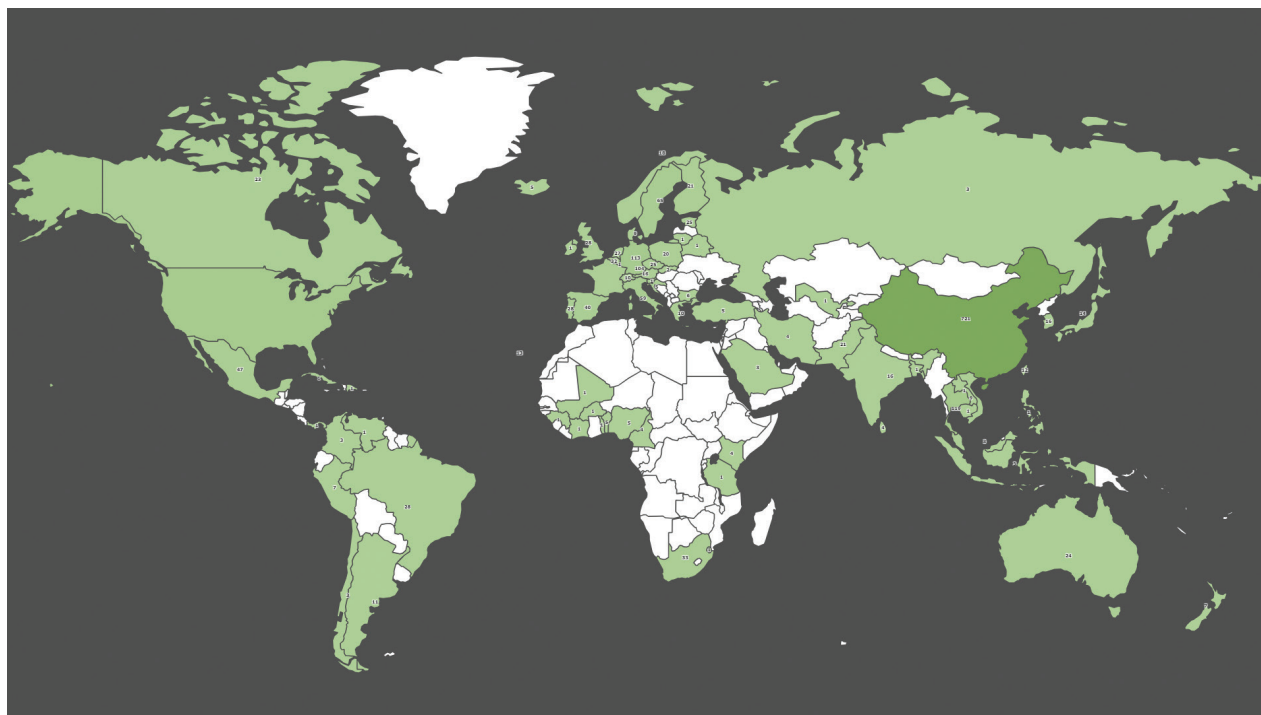


Figure 3. Authors in MycoKeys by country (all-time data). Data retrieved on 30 October 2023.

in the Q2 Mycology quartile of the Web of Science, it is in the Q1 quartile in all three Scopus categories: Agricultural and Biological Sciences; Ecology, Evolution, Behavior and Systematics; and Plant Science.

MycoKeys is also active in popularizing research on social media via its own channels on X and Facebook, where updates about the most recent publications and news from the journal are currently shared to approximately 1,500 and 2,200 followers, respectively. As a result of regular press campaigns, over the years, studies published in MycoKeys have been publicized in major news media outlets, such as The Washington Post, CNN, Newsweek and Spiegel.

In its short history, MycoKeys has already played a vital role in contributing to the understanding of the evolution, diversity and taxonomy of fungi. Exciting new methods provide further insights and allow us to address questions we could not dream of a few decades ago.

Additional information

Conflict of interest

The authors have declared that no competing interests exist.

Ethical statement

No ethical statement was reported.

Funding

No funding was reported.

Author contributions

All authors have contributed equally.

Author ORCIDs

H. Thorsten Lumbsch  <https://orcid.org/0000-0003-1512-835X>

Pavel Stoev  <https://orcid.org/0000-0002-5702-5677>

Lyubomir Penev  <https://orcid.org/0000-0002-2186-5033>

Data availability

All of the data that support the findings of this study are available in the main text.

References

- Callaghan TM, Podmirseg SM, Hohlweck D, Edwards JE, Puniya AK, Dagar SS, Griffith GW (2015) *Buwchfawromyces eastonii* gen. nov., sp. nov.: a new anaerobic fungus (Neocallimastigomycota) isolated from buffalo faeces. *MycoKeys* 9: 11–28. <https://doi.org/10.3897/mycokeys.9.9032>
- Hawksworth DL (2011) A new dawn for the naming of fungi: impacts of decisions made in Melbourne in July 2011 on the future publication and regulation of fungal names. *MycoKeys* 1: 7–20. <https://doi.org/10.3897/mycokeys.1.2062>
- Lumbsch T, Miller A, Begerow D, Penev L (2011) MycoKeys, or why we need a new journal in mycology? *MycoKeys* 1: 1–6. <https://doi.org/10.3897/mycokeys.1.2058>
- Miettinen O, Spirin V, Vlasák J, Rivoire B, Stenroos S, Hibbett DS (2016) Polypores and genus concepts in Phanerochaetaceae (Polyporales, Basidiomycota). *MycoKeys* 17: 1–46. <https://doi.org/10.3897/mycokeys.17.10153>
- Nilsson RH, Tedersoo L, Abarenkov K, Ryberg M, Kristiansson E, Hartmann M, Schoch CL, Nylander JAA, Bergsten J, Porter TM, Jumpponen A, Vaishampayan P, Ovaskainen O, Hallenberg N, Bengtsson-Palme J, Eriksson KM, Larsson KH, Larsson E, Koljalg U (2012) Five simple guidelines for establishing basic authenticity and reliability of newly generated fungal ITS sequences. *MycoKeys* 4: 37–63. <https://doi.org/10.3897/mycokeys.4.3606>
- Nilsson RH, Wurzbacher C, Bahram M, Coimbra VRM, Larsson E, Tedersoo L, Eriksson J, Ritter CD, Svantesson S, Sánchez-García M, Ryberg M, Kristiansson E, Abarenkov K (2016) Top 50 most wanted fungi. *MycoKeys* 12: 29–40. <https://doi.org/10.3897/mycokeys.12.7553>
- Nimis PL, Hafellner J, Roux C, Clerc P, Mayrhofer H, Martellos S, Bilovitz PO (2018) The lichens of the Alps - an annotated checklist. *MycoKeys* 31: 1–634. <https://doi.org/10.3897/mycokeys.31.23568>
- Plata ER, Parnmen S, Staiger B, Mangold A, Frisch A, Weerakoon G, Hernández JE, Cáceres MES, Kalb K, Sipman HJM, Common RS, Nelsen MP, Lücking R, Lumbsch HT (2013) A molecular phylogeny of Graphidaceae (Ascomycota, Lecanoromycetes, Ostropales) including 428 species. *MycoKeys* 6: 55–94. <https://doi.org/10.3897/mycokeys.6.3482>
- Tedersoo L, Anslan S, Bahram M, Polme S, Riit T, Liiv I, Koljalg U, Kisand V, Nilsson RH, Hildebrand F, Bork P, Abarenkov K (2015) Shotgun metagenomes and multiple primer pair-barcode combinations of amplicons reveal biases in metabarcoding analyses of fungi. *MycoKeys* 10: 1–43. <https://doi.org/10.3897/mycokeys.10.4852>
- Tibpromma S, Hyde KD, Bhat JD, Mortimer PE, Xu JC, Promputtha I, Doilom M, Yang JB, Tang AMC, Karunarathna SC (2018) Identification of endophytic fungi from leaves of Pandanaceae based on their morphotypes and DNA sequence data from southern Thailand. *MycoKeys* 33: 25–67. <https://doi.org/10.3897/mycokeys.33.23670>
- Yang Q, Fan XL, Guarnaccia V, Tian CM (2018) High diversity of *Diaporthe* species associated with dieback diseases in China, with twelve new species described. *MycoKeys* 39: 97–149. <https://doi.org/10.3897/mycokeys.39.26914>

Taxonomy and phylogeny of the genus *Ganoderma* (Polyporales, Basidiomycota) in Costa Rica

Melissa Mardones^{1,2}, Julieta Carranza-Velázquez^{1,2}, Milagro Mata-Hidalgo²,
Xavier Amador-Fernández¹, Hector Urbina³

¹ Escuela de Biología, Universidad de Costa Rica, San Pedro de Montes de Oca, 11501-2060, San José, Costa Rica

² Herbario Luis Fournier Origgí (USJ), Centro de Investigación en Biodiversidad y Ecología Tropical (CIBET), Universidad de Costa Rica, San Pedro de Montes de Oca, 11501-2060, San José, Costa Rica

³ Florida Department of Agriculture and Consumer Services, Division of Plant Industry, Section of Plant Pathology, 1911 SW 34th St, Gainesville, Florida, 32608, USA
Corresponding author: Melissa Mardones (melissa.mardones@ucr.ac.cr)

Abstract

Ganoderma species are well recognised by their significant role in the recycling of nutrients in ecosystems and by their production of secondary metabolites of medical and biotechnological importance. *Ganoderma* spp. are characterised by laccate and non-laccate, woody basidiocarps, polypore hymenophores and double-walled basidiospores generally with truncate apex. Despite the importance of this genus, its taxonomy is unclear and it includes several species' complexes with few circumscribed species and incorrect geographic distributions. The aim of this work was to provide detailed morphological descriptions together with phylogenetic analyses using ITS sequences to confirm the presence of seven species of *Ganoderma* in Costa Rica: *G. amazonense*, *G. applanatum* s.l., *G. australe*, *G. curtisii*, *G. ecuadorensis*, *G. oerstedii* and *G. parvulum*. This is the first study that integrates morphological and phylogenetic data of *Ganoderma* from Central America and a key of the neotropical species. Besides, the distribution range of *G. curtisii*, previously reported from North America and *G. ecuadorensis* from South America, is expanded to Central America.

Key words: Central America, fungal diversity, ITS, key neotropical species



Academic editor: Bao-Kai Cui

Received: 23 May 2023

Accepted: 21 August 2023

Published: 13 November 2023

Citation: Mardones M, Carranza-Velázquez J, Mata-Hidalgo M, Amador-Fernández X, Urbina H (2023) Taxonomy and phylogeny of the genus *Ganoderma* (Polyporales, Basidiomycota) in Costa Rica. MycoKeys 100: 5–47. <https://doi.org/10.3897/mycokeys.100.106810>

Copyright: © Melissa Mardones et al.
This is an open access article distributed under the terms of the CC0 Public Domain Dedication.

Introduction

The genus *Ganoderma* P. Karst. (Ganodermataceae, Agaricomycetes) was erected by Karsten (1881), based on *Polyporus lucidus* (Curtis) Fr., to include species with a laccate and stipitate basidiocarp. The *Ganoderma* species are characterised by laccate and non-laccate, coriaceous to wood polypore basidiomes and double-walled basidiospores generally with a truncate apex and column-like endosporic projections (Moncalvo and Ryvarden 1997; Costa-Rezende et al. 2017). *Ganoderma* is a widely distributed genus, mostly represented by tropical species and some temperate ones; approximately 278 species have been described (Sun et al. 2022), most of them laccate (Cabarroí-Hernández et al. 2019; Index Fungorum <http://www.indexfungorum.org/names/names.asp>). The genus includes both ecologically and economically important species (wood decomposers, pathogens and metabolites producers of medical importance).

Due to the high phenotypic plasticity present in the *Ganoderma* species, the taxonomy of this genus is ambiguous and confusing. Several species complexes have led to few circumscribed species and incorrect geographic distributions (Moncalvo and Ryvarden 1997; Ryvarden 2000; Loyd et al. 2018; Fryssouli et al. 2020; Sun et al. 2022). Traditionally, the species delimitation within *Ganoderma* is based on basidiomata morphology and host preference. However, phylogenetic analyses using ribosomal RNA (rRNA) of global collections showed that morphological features and cultural characteristics appeared highly polyphyletic and most of the species are geographically restricted (Gottlieb et al. 2000; Loyd et al. 2018).

In the past few decades, molecular analyses have brought some clarifications for species delimitation in *Ganoderma*. Currently, only 50% of accepted *Ganoderma* species have molecular data (Sun et al. 2022). However, several studies have shown that numerous available sequences in public repositories are incorrectly annotated (Moncalvo et al. 1995; Hong and Jung 2004; Fryssouli et al. 2020). Moncalvo's et al. paper (1995), one of the first molecular studies on *Ganoderma* using ITS sequence data, showed the delimitation of six clades in this genus, but vouchers labelled as *G. lucidum* (Curtis) P. Karst. were found scattered in five of the six clades. Fryssouli et al. (2020) found that only 40% of the ITS sequences deposited in GenBank (www.ncbi.nlm.nih.gov/Genbank) were correctly annotated.

In the Neotropics, approximately 39 species of *Ganoderma* have been reported in literature. Most of these studies were based on morphology and host associations (Ryvarden 2000, 2004; Costa-Rezende et al. 2020) and were focused on the species of a country or region, i.e. Brazil (Gomes-Silva et al. 2011; Torres-Torres et al. 2012; de Lima et al. 2014), Colombia (Bolaños et al. 2016), Ecuador (Crous et al. 2016, 2017, 2018), French West Indies (Welti and Courtecuisse 2010) and Mexico (Torres-Torres and Guzmán-Dávalos 2005; Torres-Torres et al. 2015; Cabarroi-Hernández et al. 2019). However, the circumscription of several species and their geographic distribution ranges remains largely unknown.

Recently, several studies have included molecular characterisation on some neotropical species of *Ganoderma*. Loyd et al. (2018) studied the laccate species of *Ganoderma* in the USA, using morphology, host preference data and a multilocus phylogeny employing the Internal Transcribed Spacer of the rRNA gene (ITS), elongation factor (*TEF*) and RNA polymerase II subunit 1 (*rpb1*) and subunit 2 (*rpb2*) and delimited four species with neotropical distribution [*G. curtisii* (Berk.) Murrill, *G. martinicense* Welti & Courtec., *G. tuberosum* Murrill, *G. cf. weberianum*]. De Lima et al. (2014) and Bolaños et al. (2016), using ITS and the large subunit (LSU) of the rRNA gene, phylogenetically delimited *G. chalconeum* (Cooke) Steyaert, *G. multiplicatum* (Mont.) Pat., *G. orbiforme* (Fr.) Ryvarden and *G. parvulum* Murrill from Brazil and Colombia. Cabarroi-Hernández et al. (2019), using morphology and multilocus phylogeny using ITS, *rpb2* and *TEF*, found at least two phylogenetic species (*G. mexicanum* Pat. and *G. parvulum*) within the neotropical species in the *G. weberianum-resinaceum* complex. Fryssouli et al. (2020) identified and curated the ITS sequences of *Ganoderma* in GenBank, including 14 neotropical species [*G. australe* (Fr.) Pat., *G. chocoense* J.A. Flores, C.W. Barnes & Ordoñez, *G. concinnum* Ryvarden, *G. curtisii*, *G. martinicense*, *G. mexicanum*, *G. multiplicatum*, *G. orbiforme*, *G. parvulum*, *G. podocarpense* J.A. Flores, C.W. Barnes & Ordoñez, *G. subfornicatum* Murrill, *G. tuberosum* and two undescribed species of non-laccate *Ganoderma*].

There are two studies on *Ganoderma* in Costa Rica (Ruiz-Boyer 1998; Carranza & Ruiz-Boyer 2005); however, none includes molecular data or phylogenetic anal-

yses. Nowadays, nine species have been reported in Costa Rica: *G. amazonense* Weir, *G. applanatum*, *G. australe*, *G. colossus* (Fr.) C.F. Baker, *G. lucidum sensu lato* (s.l.), *G. oerstedii* (Fr.) Torrend, *G. orbiforme*, *G. parvulum*, *G. stipitatum* (Murrill) Murrill and *G. tuberculosum* (Ruiz-Boyer 1998; Ryvarden 2004; Carranza and Ruiz-Boyer 2005; Cabarroi-Hernández et al. 2019). However, only *G. parvulum* and *G. tuberculosum* have been confirmed by molecular sequence data (Cabarroi-Hernández et al. 2019; Sun et al. 2022), while *G. stipitatum* was recently synonymised with *G. parvulum* (Cabarroi-Hernández et al. 2019). Besides, current data indicate that *G. lucidum* is restricted to Europe and only to some parts of China (Cao et al. 2012; Wang et al. 2012); hence, there is a need for confirming the diversity of *Ganoderma* of Costa Rica using both morphological and molecular analyses.

The geographical location of Costa Rica in the Central American isthmus has allowed the flow of species from North and South America, turning this country into a unique biogeographic region. Therefore, it is expected that *Ganoderma* species can be shared throughout the regions. Nevertheless, the geographic distribution of several neotropical species of *Ganoderma* is uncertain and molecular data of *Ganoderma* species from Central America is almost non-existent. The aims of this work are: I) to re-examine the species of *Ganoderma* present in Costa Rica using morphology and ITS sequences of fresh collections, herbarium specimens and pure cultures; II) to describe, illustrate and expand the knowledge on distribution and biogeography of neotropical *Ganoderma* species and III) to propose a key of the neotropical species of *Ganoderma*. This study represents the first attempt to include *Ganoderma* species from Central America under morphological and phylogenetic frameworks worldwide.

Methods

Fungal material and morphological studies

Selected voucher collections from the Herbarium of the University of Costa Rica (**USJ**), the National Herbarium of Costa Rica (**CR**) and the Plant Industry Herbarium Gainesville (**PIHG**) of the Florida Department of Agriculture and Consumer Services (**FDACS**) were used for this study. Additionally, several specimens were collected during field trips throughout Costa Rica. In total, 370 specimens were macroscopically examined. Afterwards, 117 specimens were selected to be examined in detail, including microscopical characteristics. Representative basidiomata collected from this study have been deposited into the USJ collection. Collection sites with ecological details are mentioned together with the records below. In addition, type specimens from the United States National Herbarium (**BPI**) and The New York Botanical Garden Herbarium (**NY**) were re-examined. Overall, more than 120 specimens of nine morphotypes, including nine types, were examined.

Specimens were photographed in situ. Descriptions of macromorphological features (colour and texture of the basidiocarp and tissue context, presence/absence of stipe, melanoid deposits or concentric zones) were observed from fresh material. Microscopical preparations of the hyphal system, cuticular cells, basidiospores and chlamydospores were made in 3% potassium hydroxide (KOH), cotton blue (1 mg/ml), and Melzer's reagent (to test dextrinoid and/or amyloid reactions). Slides were examined with a Nikon Eclipse 80i microscope with bright field and phase contrast optics. Imaging and measurements were

done using a camera Nikon DS-Fi2 adapted to the microscope and operated by the Imaging Software NIS-Elements D 2.2. At least 30 individual basidiospores and chlamydospores were measured for at least three representative collections for each species. Outlying measurements observed in less than 5% of the measurements of a given structure are placed in parentheses. The number is indicated in brackets if less than 30 values were measured.

DNA extraction, PCR and sequencing

We extracted DNA from 19 fresh specimens. Basidiome samples were ground by a Fastprep24 machine (MP Biomedicals, CA, USA). The isolation of total genomic DNA was performed using the FastDNA SPIN Kit (MP Biomedicals), following the protocol provided by the manufacturer. DNA was quantified using a Nanodrop ND-1000 spectrometer (Nanodrop Technologies, DE, USA), after which it was adjusted to a final concentration of 50 ng μl^{-1} before PCR. DNA extracts were stored in aliquots at $-20\text{ }^{\circ}\text{C}$.

The complete ITS (ITS1-5.8S-ITS2) region with primers ITS5 and ITS4 (White et al. 1990) was amplified and sequenced. Each PCR tube contained 1 μl of DNA template, 1 μl of each primer (10 μM), 25 μl of iProof HF 2 \times Master Mix (BioRad, Hercules, CA, USA) and 22 μl of sterile distilled water. PCR reactions were performed on a PEQSTAR 2 \times GRADIENT Thermal Cycler (PEQLAB, Erlangen, Germany). Conditions of the PCR were as follows: DNA denaturation 98 $^{\circ}\text{C}$ for 3 min; 35 cycles of DNA denaturation 98 $^{\circ}\text{C}$ for 10 s, primer annealing 55 $^{\circ}\text{C}$ for 30 s and *Taq* extension 72 $^{\circ}\text{C}$ for 30 s and a final *Taq* extension 72 $^{\circ}\text{C}$ for 10 min, followed by storage at 8 $^{\circ}\text{C}$. PCR-products were checked on 1.5% agarose electrophoresis gels stained with ethidium bromide. Amplified PCR products were purified with Cycle Pure Kit (VWR-Omega, GA, USA). The Sanger sequencing in both directions was performed with the same PCR primers in MACROGEN (South Korea) for the specimens collected in Costa Rica, while samples collected in Florida were sequenced in-house at the headquarters of FDACS-Division of Plant Industry in Gainesville. Additionally, one fragment of the LSU with primers NL1 and NL2 (O'Donnell 1993) and one fragment of *TEF* with primers EF1-983f and EF1-2218r (Rehner and Buckley 2005) were also amplified and sequenced, but not used in the phylogenetic analyses. The LSU and *TEF* sequences generated from Costa Rican specimens are provided and the accession numbers of these sequences are mentioned together with the records of each specimen below.

Phylogenetic analyses

We assembled an ITS dataset comprising sequences from 159 specimens worldwide, 82 originating from the Neotropics and 15 from type specimens. This analysis aimed to infer the position of the *Ganoderma* specimens from Costa Rica in a global context. Sequences were downloaded from GenBank, mostly from studies published by Costa-Rezende et al. (2017), Loyd et al. (2018), Cabarroi-Hernández et al. (2019) and Sun et al. (2022). *Tomophagus colossus* (Fr.) Murrill vouchers URM80450 and TC-02 were selected as out-group taxa, based on Loyd et al. (2018). The newly-generated ITS sequences and the sequences retrieved from GenBank are given in Table 1, together with their voucher/strain numbers, location and accession numbers.

Table 1. Specimen data and accession numbers of the taxa used in the phylogenetic analyses. The (T) indicated type material.

Species	Voucher	ITS	Country	Reference
<i>Ganoderma adpersum</i>	GAD3	JN222418	Poland	Retrieve from GenBank
<i>Ganoderma adpersum</i>	GAT000	AM906057	Italy	Costa-Rezende et al. (2017)
<i>Ganoderma amazonense</i>	GA-54	OQ845454	Costa Rica	This study
<i>Ganoderma applanatum</i>	Cui 14062	MZ354913	China	Sun et al. (2022)
<i>Ganoderma applanatum</i>	Cui 14070	MZ354914	China	Sun et al. (2022)
<i>Ganoderma applanatum</i>	GA-64	OQ845455	Costa Rica	This study
<i>Ganoderma applanatum</i>	KM120830	AY884178	UK	Retrieve from GenBank
<i>Ganoderma applanatum</i>	Wei5787a	KF495001	China	Retrieve from GenBank
<i>Ganoderma applanatum</i>	SFC20141001-24	KY364255	Korea	Jargalmaa et al. (2017)
<i>Ganoderma applanatum</i>	SFC20150930-02	KY364258	Korea	Jargalmaa et al. (2017)
<i>Ganoderma aridicola</i>	DAI 12588 (T)	KU572491	South Africa	Xing et al. (2016)
<i>Ganoderma australe</i>	DHCR411 (HUEFS)	MF436675	Australia	Costa-Rezende et al. (2017)
<i>Ganoderma australe</i>	DHCR417 (HUEFS)	MF436676	Australia	Costa-Rezende et al. (2017)
<i>Ganoderma australe</i>	GA-19	OQ845456	Costa Rica	This study
<i>Ganoderma austroafricanum</i>	CBS 1387.24	KM507324	South Africa	Coetzee et al. (2015)
<i>Ganoderma boninense</i>	WD2028 (FFPRI)	KJ143905	Japan	Zhou et al. 2015
<i>Ganoderma boninense</i>	WD2085 (FFPRI)	KJ143906	Japan	Zhou et al. 2015
<i>Ganoderma</i> cf. <i>chocoense</i>	GA-03	OQ845457	Costa Rica	This study
<i>Ganoderma chocoense</i>	QCAM3123 (T)	MH890527	Ecuador	Crous et al. (2018)
<i>Ganoderma concinnum</i>	Robledo 3192	MN077522	Brazil	Costa-Rezende et al. (2020)
<i>Ganoderma concinnum</i>	Robledo 3235	MN077523	Brazil	Costa-Rezende et al. (2020)
<i>Ganoderma cupreum</i>	GANOTK4	JN105701	Camerun	Retrieve from GenBank
<i>Ganoderma cupreum</i>	GANOTK7	JN105702	Camerun	Retrieve from GenBank
<i>Ganoderma curtisii</i>	102NC	MG654074	NC, USA	Loyd et al. (2018)
<i>Ganoderma curtisii</i>	223FL	MG654167	FL, USA	Loyd et al. (2018)
<i>Ganoderma curtisii</i>	CBS 100132	JQ781849	NC, USA	Cao et al. (2012)
<i>Ganoderma curtisii</i>	CBS100131	JQ781848	NC, USA	Cao et al. (2012)
<i>Ganoderma curtisii</i>	GA-00	OQ845458	Costa Rica	This study
<i>Ganoderma curtisii</i>	GA-22	OQ845459	Costa Rica	This study
<i>Ganoderma curtisii</i>	GA-63	OQ845460	Costa Rica	This study
<i>Ganoderma curtisii</i>	GA-65	OQ845461	Costa Rica	This study
<i>Ganoderma curtisii</i>	P559-03202022-2284	OQ845462	FL, USA	This study
<i>Ganoderma curtisii</i>	UMNFL28	MG654097	FI, USA	Loyd et al. (2018)
<i>Ganoderma curtisii</i> f.sp. <i>meredithiae</i>	124FL	MG654188	FI, USA	Loyd et al. (2018)
<i>Ganoderma ecuadorensense</i>	Dai 17397	MZ354950	Brazil	Sun et al. (2022)
<i>Ganoderma ecuadorensense</i>	Dai 17418	MZ354951	Brazil	Sun et al. (2022)
<i>Ganoderma ecuadorensense</i>	GA-52	OQ845463	Costa Rica	This study
<i>Ganoderma ecuadorensense</i>	GA-57	OQ845464	Costa Rica	This study
<i>Ganoderma ecuadorensense</i>	JV 1808/85	MZ354952	French Guiana	Sun et al. (2022)
<i>Ganoderma ecuadorensense</i>	MMG-181A	OQ845465	Costa Rica	This study
<i>Ganoderma ecuadorensense</i>	MMG-209	OQ845466	Costa Rica	This study
<i>Ganoderma ecuadorensense</i>	PMC-126	KU128525	Ecuador	Crous et al. (2016)

Species	Voucher	ITS	Country	Reference
<i>Ganoderma ecuadorensis</i>	Poly-2.4	KU128526	Ecuador	Crous et al. (2016)
<i>Ganoderma ecuadorensis</i>	QCAM3430/ASL799 (T)	KU128524	Ecuador	Crous et al. (2016)
<i>Ganoderma ellipsoideum</i>	GACP14080966 (T)	MH106867	China	Hapuarachchi et al. (2018)
<i>Ganoderma ellipsoideum</i>	GACP14080968	MH106868	China	Hapuarachchi et al. (2018)
<i>Ganoderma enigmaticum</i>	DAI 15970	KU572486	South Africa	Xing and Cui (2016)
<i>Ganoderma enigmaticum</i>	DAI 15971	KU572487	South Africa	Xing and Cui (2016)
<i>Ganoderma enigmaticum</i>	CBS 139792 (T)	NR_132918	South Africa	Coetzee et al. (2015)
<i>Ganoderma flexipes</i>	Wei5200	JN383978	China	Cao and Yuan (2013)
<i>Ganoderma flexipes</i>	Wei5491	JQ781850	China	Cao and Yuan (2013)
<i>Ganoderma flexipes</i>	Wei5494	JN383979	China	Cao and Yuan (2013)
<i>Ganoderma gibbosum</i>	JFL14070442	MH106880	China	Hapuarachchi et al. (2018)
<i>Ganoderma gibbosum</i>	KUT0805	AB733121	Japan	Costa-Rezende et al. (2017)
<i>Ganoderma gibbosum</i>	XSD34	EU273513	China	Retrieve from GenBank
<i>Ganoderma hoehnelianum</i>	Dai12096	KU219989	China	Song et al. (2016)
<i>Ganoderma hoehnelianum</i>	Yuan 6337	MG279160	China	Xing et al. (2018)
<i>Ganoderma leucocontextum</i>	GDGM44303	KJ027607	China	Li et al. (2015)
<i>Ganoderma lingzhi</i>	Cui9166	KJ143907	China	Cao et al. (2012)
<i>Ganoderma lingzhi</i>	Dai12574	KJ143908	China	Cao et al. (2012)
<i>Ganoderma lingzhi</i>	HKAS-76642 (T)	KC222318	China	Yang and Feng (2013)
<i>Ganoderma lingzhi</i>	SFC20150624.06	KY364245	Korea	Jargalmaa et al. (2017)
<i>Ganoderma lingzhi</i>	SFC20150630.14	KY364246	Korea	Jargalmaa et al. (2017)
<i>Ganoderma lobatum</i>	GVL-36	MT232631	Mexico	Espinoza et al. (2021)
<i>Ganoderma lucidum</i>	MUCL 35119	MK554779	France	Cabarroi-Hernández et al. (2019)
<i>Ganoderma lucidum</i>	RYV 33217 (T)	Z37096	Norway	Smith and Sivasithamparam (2000)
<i>Ganoderma martinicense</i>	231NC	MG654182	NC, USA	Loyd et al. (2018)
<i>Ganoderma martinicense</i>	246TX	MG654185	TX, USA	Loyd et al. (2018)
<i>Ganoderma martinicense</i>	LIP SW-Mart08-55 (T)	KF963256	Martinique	Retrieve from GenBank
<i>Ganoderma mastoporum</i>	PM21	JQ409361	Malasia	Retrieve from GenBank
<i>Ganoderma mastoporum</i>	TNM-F0018835	JX840351	China	Wang et al. (2012)
<i>Ganoderma meredithae</i>	CBS 271.88 (T)	NR_164435	USA	Vu et al. (2019)
<i>Ganoderma mexicanum</i>	MUCL 49453	MK531811	Martinique	Cabarroi-Hernández et al. (2019)
<i>Ganoderma mexicanum</i>	XAL D.Jarvio 143	MK531823	México	Cabarroi-Hernández et al. (2019)
<i>Ganoderma mizoramense</i>	UMN-MZ4 (T)	KY643750	India	Crous et al. (2017)
<i>Ganoderma mizoramense</i>	UMN-MZ5	KY643751	India	Crous et al. (2017)
<i>Ganoderma multipileum</i>	CWN04670	KJ143913	China	Retrieve from GenBank
<i>Ganoderma multipileum</i>	Dai9447	KJ143914	China	Zhou et al. 2015
<i>Ganoderma multiplicatum</i>	CC8	KU569515	Colombia	Bolaños et al. (2016)
<i>Ganoderma multiplicatum</i>	URM 83346	JX310823	Brazil	de Lima et al. (2014)
<i>Ganoderma oerstedii</i>	GA-24	OQ845469	Costa Rica	This study
<i>Ganoderma oerstedii</i>	5191	OQ845467	FL, USA	This study
<i>Ganoderma oerstedii</i>	FDACS-DPI 2019-100390	OQ845468	FL, USA	This study
<i>Ganoderma orbiforme</i>	Cui 13880	MG279187	China	Sun et al. (2022)
<i>Ganoderma orbiforme</i>	Cui 13891	MZ354953	China	Sun et al. (2022)
<i>Ganoderma orbiforme</i>	Cui 18301	MZ354954	China	Sun et al. (2022)

Species	Voucher	ITS	Country	Reference
<i>Ganoderma orbiforme</i>	Cui 18302	MZ354955	China	Sun et al. (2022)
<i>Ganoderma orbiforme</i>	Cui 18317	MZ354956	China	Sun et al. (2022)
<i>Ganoderma orbiforme</i>	Cui 18326	MZ354957	China	Sun et al. (2022)
<i>Ganoderma orbiforme</i>	URM 83332	JX310813	Brazil	de Lima et al. (2014)
<i>Ganoderma orbiforme</i>	URM 83334	JX310814	Brazil	de Lima et al. (2014)
<i>Ganoderma orbiforme</i>	URM 83335	JX310815	Brazil	de Lima et al. (2014)
<i>Ganoderma orbiforme</i>	URM 83336	JX310816	Brazil	de Lima et al. (2014)
<i>Ganoderma oregonense</i>	CBS 265.88	JQ781875	OR, USA	Cao et al. (2012)
<i>Ganoderma oregonense</i>	CBS 266.88	JQ781876	WA, USA	Cao et al. (2012)
<i>Ganoderma parvulum</i>	GA-04	OQ845470	Costa Rica	This study
<i>Ganoderma parvulum</i>	GA-08	OQ845471	Costa Rica	This study
<i>Ganoderma parvulum</i>	GA-09	OQ845472	Costa Rica	This study
<i>Ganoderma parvulum</i>	GA-10	OQ845473	Costa Rica	This study
<i>Ganoderma parvulum</i>	GA-46	OQ845474	Costa Rica	This study
<i>Ganoderma parvulum</i>	GA-56	OQ845475	Costa Rica	This study
<i>Ganoderma parvulum</i>	INB E.Fletes-7619	MK531821	Costa Rica	Cabarroi-Hernández et al. (2019)
<i>Ganoderma parvulum</i>	MUCL 43863	MK554769	Cuba	Cabarroi-Hernández et al. (2019)
<i>Ganoderma parvulum</i>	MUCL 44148	MK531132	Cuba	Cabarroi-Hernández et al. (2019)
<i>Ganoderma parvulum</i>	MUCL 52655	MK554770	French Guiana	Cabarroi-Hernández et al. (2019)
<i>Ganoderma parvulum</i>	MUCL53123	MK531814	French Guiana	Cabarroi-Hernández et al. (2019)
<i>Ganoderma philippii</i>	E7092	AJ608710	Indonesia	Retrieve from GenBank
<i>Ganoderma philippii</i>	E7098	AJ536662.2	Indonesia	Retrieve from GenBank
<i>Ganoderma podocarpense</i>	JV 1504/126	MZ354942	Costa Rica	Sun et al. (2022)
<i>Ganoderma podocarpense</i>	QCAM6422 (T)	MF796661	Ecuador	Crous et al. (2017)
<i>Ganoderma polychromum</i>	3300R	MG654196	OR, USA	Loyd et al. (2018)
<i>Ganoderma polychromum</i>	BJ280CA	MG910492	CA, USA	Loyd et al. (2018)
<i>Ganoderma resinaceum</i>	URM 83400	JX310824	Brazil	de Lima et al. (2014)
<i>Ganoderma resinaceum</i>	BR 4150	KJ143915	France	Zhou et al. 2015
<i>Ganoderma resinaceum</i>	MUCL 38956	MK554772	Netherlands	Cabarroi-Hernández et al. (2019)
<i>Ganoderma resinaceum</i>	MUCL 52253	MK554786	France	Cabarroi-Hernández et al. (2019)
<i>Ganoderma rywardenii</i>	HKAS58053 (T)	HM138671	Cameroon	Kinge and Mih (2011)
<i>Ganoderma sessile</i>	MUCL 38061	MK554778	USA	Cabarroi-Hernández et al. (2019)
<i>Ganoderma sessile</i>	UMNFL10	MG654227	FL, USA	Loyd et al. (2018)
<i>Ganoderma sessile</i>	UMNMI24	MG654271	MI, USA	Loyd et al. (2018)
<i>Ganoderma sichuanense</i>	HMAS 42798 (T)	JQ781877	China	Zhou et al. 2015
<i>Ganoderma sinense</i>	Wei5327	KF494998	China	Costa-Rezende et al. (2017)
<i>Ganoderma</i> sp.	JMCR128	AF255148	Costa Rica	Moncalvo and Buchanan (2008)
<i>Ganoderma</i> sp.	JMCR132	AF255137	Costa Rica	Moncalvo and Buchanan (2008)
<i>Ganoderma</i> sp.	JMCR142	AF255138	Costa Rica	Moncalvo and Buchanan (2008)
<i>Ganoderma</i> sp.	JMCR25	AF255134	Costa Rica	Moncalvo and Buchanan (2008)
<i>Ganoderma</i> sp.	JMCR41	AF255135	Costa Rica	Moncalvo and Buchanan (2008)
<i>Ganoderma</i> sp.	JMCR55	AF255136	Costa Rica	Moncalvo and Buchanan (2008)
<i>Ganoderma</i> sp.	VPB202	KJ832060	Brazil	Martin et al. (2015)
<i>Ganoderma</i> sp.	GA-27	OQ845476	Costa Rica	This study

Species	Voucher	ITS	Country	Reference
<i>Ganoderma steyaertanum</i>	MEL2382783	KP012964	Australia	Retrieve from GenBank
<i>Ganoderma stipitatum</i>	CM-UDEA110	MT945605	Colombia	Jaramillo et al. (2020)
<i>Ganoderma subamboinense</i>	Ule.2748/F 15183 (T)	MK531824	Brazil	Cabarroi-Hernández et al. (2019)
<i>Ganoderma subamboinense</i> var. <i>laevisporum</i>	UMNFL100	MG654373	FL, USA	Loyd et al. (2018)
<i>Ganoderma subamboinense</i> var. <i>laevisporum</i>	UMNFL32	MG654372	FL, USA	Loyd et al. (2018)
<i>Ganoderma subfornicatum</i>	BRFM 1024	JX082352	French Guiana	Berrin et al. (2012)
<i>Ganoderma tornatum</i>	GVL-05	MT232633	Mexico	Espinoza et al. (2021)
<i>Ganoderma tornatum</i>	URM82776	JQ514110	Brazil	de Lima et al. (2014)
<i>Ganoderma tropicum</i>	KUMCC 18–0046	MH823539	Thailand	Luangharn et al. (2019)
<i>Ganoderma tropicum</i>	Yuan3490	JQ781880	China	Cao et al. (2012)
<i>Ganoderma tsugae</i>	Dai 12760 (IFP)	KJ143920	USA	Zhou et al. 2015
<i>Ganoderma tsugae</i>	UMNMI20	MG654324	MI, USA	Loyd et al. (2018)
<i>Ganoderma tuberculosum</i>	GVL-40	MT232634	Mexico	Espinoza et al. (2021)
<i>Ganoderma tuberculosum</i>	PLM684	MG654369	FL, USA	Loyd et al. (2018)
<i>Ganoderma tuberculosum</i>	Dai 17412	MZ354943	Brazil	Sun et al. (2022)
<i>Ganoderma tuberculosum</i>	JV 1607/62	MZ354944	Costa Rica	Sun et al. (2022)
<i>Ganoderma weberianum</i>	B18	JN637827	Cuba	Torres-Farradá et al. (2016)
<i>Ganoderma weberianum</i>	CBS 1285.81	MK603805	Taiwan	Cabarroi-Hernández et al. (2019)
<i>Ganoderma weberianum</i>	CBS 219.36	MK603804	Philippines	Cabarroi-Hernández et al. (2019)
<i>Ganoderma weberianum</i>	Guzmán-Dávalos 9569	MK554771	México	Cabarroi-Hernández et al. (2019)
<i>Ganoderma wiioense</i>	UMN20GHA (T)	KT952363	Ghana	Crous et al. (2015)
<i>Ganoderma wiioense</i>	UMN21GHA (T)	KT952361	Ghana	Crous et al. (2015)
<i>Ganoderma zonatum</i>	FDACS-DPI 2019-102200	OQ845478	FL, USA	This study
<i>Ganoderma zonatum</i>	UMNFL105	MG654408	FL, USA	Loyd et al. (2018)
<i>Ganoderma zonatum</i>	UMNFL85	MG654402	FL, USA	Loyd et al. (2018)
<i>Ganoderma zonatum</i>	FDACS-DPI 2021-107113	OQ845477	FL, USA	This study
<i>Tomophagus colossus</i> (outgroup)	TC02	KJ143923	Vietnam	Zhou et al. 2015
<i>Tomophagus colossus</i> (outgroup)	URM80450	JX310825	Brazil	de Lima et al. (2014)

Sequence assembly and editing were performed in GENEIOUS v. 11.1.5 (Kearse et al. 2012). Alignments for each gene and both datasets were generated using MAFFT v.7.490 (Katoh and Standley 2013) with the L-INS-i algorithm. The software GBLOCKS v.0.91b (Talavera and Castresana 2007) was used to remove poorly-aligned positions and divergent regions from the DNA alignments with parameters for a less stringent selection.

PARTITION FINDER v.2.1 (Lanfear et al. 2016), implemented in the CIPRES Science Gateway web portal (http://www.phylo.org/sub_sections/portal/), following the Akaike Information Criterion (AIC), was used to select the best-fit model of evolution and the GTR+G model was applied.

Bayesian Inference (BI) and Maximum Likelihood (ML) phylogenetic analyses were applied to the dataset. The ML analysis was carried out in RAxML v.8.2.12 (Stamatakis 2014) implemented in the CIPRES Science Gateway web portal (http://www.phylo.org/sub_sections/portal/), with 1,000 non-parametric bootstrap iterations using the GTRGAMMA model and discrete gamma distribution.

Bayesian analysis was performed with the programme MrBayes v.3.2.7a (Ronquist et al. 2012) on XSEDE (Miller et al. 2010) on the CIPRES Science Gateway web portal. Two parallel runs with eight chains of Metropolis-coupled Markov Chain Monte Carlo (MC)³ iterations were performed. Analysis was run for 100 million generations, with trees sampled every 1000th generation. Burn-ins were determined by checking the likelihood trace plots in Tracer v.1.7 (Rambaut et al. 2018) and subsequently discarded. To confirm the convergence of trees, the average standard deviation of split frequencies was monitored to ensure that it fell below 0.01 and log files from the Bayesian analyses were analysed with Tracer. No indication of a lack of convergence was detected. Bayesian posterior probabilities (BPP) ≥ 0.95 and Bootstrap values (BS) ≥ 70 were considered significant. The final alignment and the phylogenetic trees are given as Suppl. materials.

Results

Molecular phylogeny

A total of 25 ITS sequences were generated from eight neotropical species of *Ganoderma* that were aligned with other 62 congenetic species. The dataset contained 159 sequences and 465 base pairs in length. The BI and ML phylogeny showed similar tree topologies with *Ganoderma* as a robust monophyletic clade (1/100) comprising eight core clades (I to VIII) including 42 terminal clades that varied in terms of support (Fig. 1, only the BI tree is shown).

The sister-group relationships amongst these eight clades remained with low to moderate support (average BPP: 0.58). On the other hand, the support of several terminal clades, which may represent the circumscription of species, was moderate to strong in most terminal branches (average BPP: 0.96). The sequences obtained from Costa Rican specimens clustered in six of the eight clades (except V and VII).

Clade I is a weakly-supported clade (0.89/34) and included sequences labelled as *G. wiioense* E.C. Otto, Blanchette, C.W. Barnes & Held from Ghana, *G. flexipes* Pat. from China, *G. philippii* (Bres. & Henn. ex Sacc.) Bres. from Indonesia and China and *G. tuberculosum* - *G. oerstedii* from Brazil, Mexico and the USA. The sequences from specimens collected in Costa Rica GA-24 and JV-1607/62 clustered with sequences of *G. tuberculosum* and *G. oerstedii*, forming a well-supported monophyletic group (1/99). Within this clade, where species were represented by more than two sequences, the terminal clades were strongly supported, i.e., *G. flexipes* (1/94), *G. philippi* (1/99) and *G. wiioense* (1/100).

Clade II is divided into two major subclades (0.61/40): clade II.A contains sequences of non-laccate species labelled as *G. multiplicatum* from Brazil and Colombia, *G. tropicum* from China and Thailand, *G. steyaertanum* from Australia, *G. mizoramense* Zothanz., Blanchette, Held & C.W. Barnes from India, *G. multipileum* from China and *G. martinicense* from Martinique and southern USA. The support for this subclade and the internal relationships amongst the species were weak (0.81/54). Clade II.B, resolved with strong support (1/92) and is divided into two subclades: one with sequences labelled as *G. lingzhi* from China and Korea (1/98) and another one with sequences named as *G. curtisii* and *G. meredithae* Adask. & Gilb. (including the type) from North America and the sequences of the Costa Rican specimens GA-00, GA-22, GA-63 and GA-65 (0.58/74).

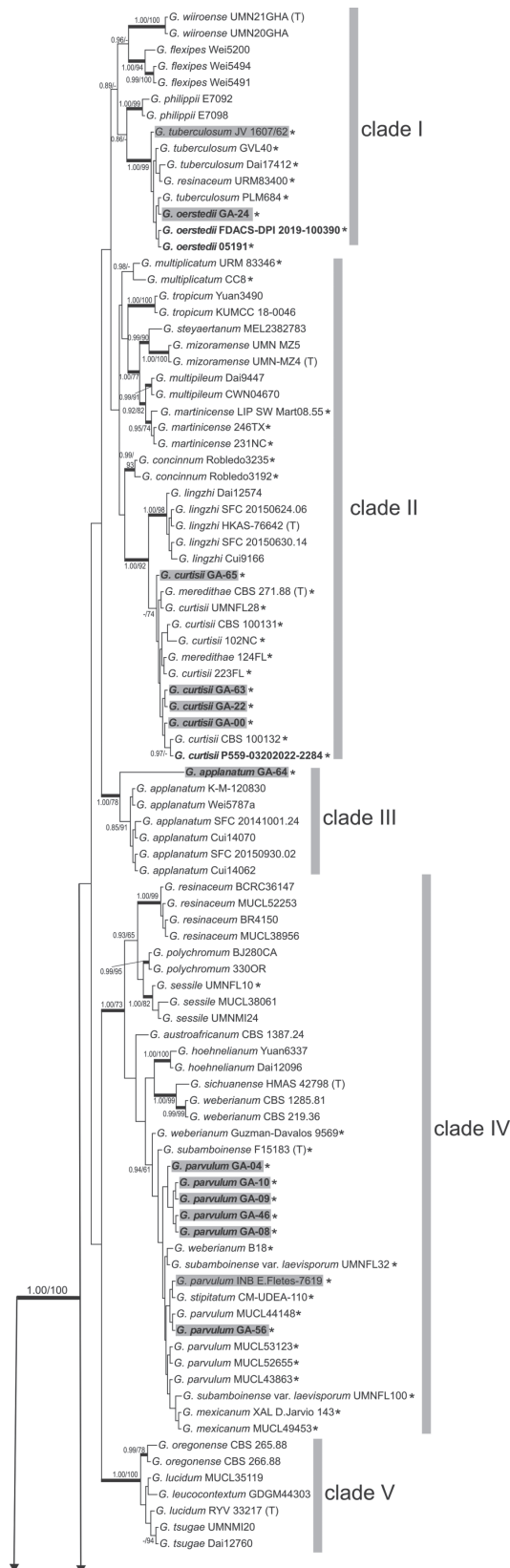


Figure 1. Phylogenetic tree of *Ganoderma* inferred from a Bayesian analysis, based on ITS sequence data. Bayesian posterior probabilities (BPP) > 0.84 and Maximum Likelihood Bootstrap scores (BS) > 70% are shown at the nodes at the first and second positions. BPP \geq 0.95 and BS \geq 70 were significant and are indicated by thickened branches. The phylogenetic position of the species occurring in Costa Rica is highlighted in grey. Sequences generated in this study are shown in bold. The (T) indicates type material and the asterisk (*) indicates specimens from sub-neotropical and neotropical regions.

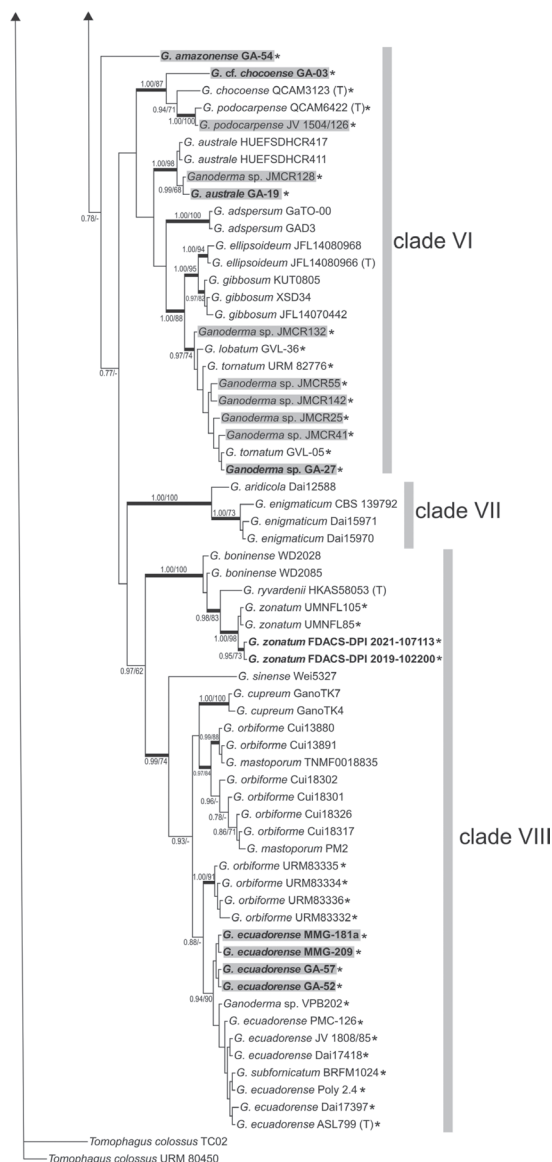


Figure 1. Continued.

Clade III grouped sequences tagged as *G. applanatum* (1/78). The vouchers of several collections in China and UK were grouped together and the sequence obtained from the Costa Rican specimen GA-64 formed an independent lineage.

Clade IV was divided into two subclades (1/73). Clade IV.A contained sequences labelled as *G. resinaceum* from Europe and *G. sessile* Murrill and *G. polychromum* (Copel.) Murrill from the USA (0.93/65). Clade IV.B was divided into two subclades (0.94/61): Clade IV.B.1 grouped sequences of *G. hoehnelianum* Bres., *G. sichuanense* and *G. weberianum* from East Asia and Clade IV.B.2 with sequences of *G. mexicanum*, *G. parvulum*, *G. stipitatum* and *G. subamboinense* (Henn.) Bazzalo & J.E. Wright from the Neotropics. Sequences of seven specimens of *G. parvulum* from Costa Rica (Fletes 7619, GA-04, GA-08, GA-09, GA-10, GA-46 and GA-56) were placed within this subclade.

Clade VI was a weakly supported clade (0.66/16) that contained several non-laccate species. This clade was divided into three subclades. Clade VI.A (1/87) with sequences of *G. chocoense* and *G. podocarpense* from Ecuador (including type specimens) and the Costa Rican specimen GA-03. Clade

VI.B (1/98) with sequences of *G. australe* from Australia and the Costa Rican specimens JMCR-128 and GA-19. Clade VI.C was subdivided into three terminal clades with strong support. Clade VI.C.1 with sequences from *G. adpersum* (Schulzer) Donk from Europe (1/100), Clade VI.C.2 that groups sequences of *G. gibbosum* (Blume & T. Nees) Pat. and *G. ellipsoideum* Hapuar., T.C. Wen & K.D. Hyde from East Asia (0.97/82) and Clade VI.C.3 with several sequences from the Neotropics (0.97/74), including vouchers labelled as *G. lobatum* (Cooke) G.F. Atk. and *G. tornatum* (Pers.) Bres. from Brazil and Mexico and several unidentified specimens from Costa Rica (JMCR25, JMCR55, JMCR142, JMCR41, JMCR132 and GA-27). A single sequence from the Costa Rican specimen GA-54, identified as *G. amazonense*, was grouped within this clade with low support as an independent lineage in both phylogenies (0.73/23).

Clade VIII was divided into two strongly-supported subclades (0.97/62). Clade VIII.A that grouped sequences of *G. boninense* Pat. from Japan, *G. rywardenii* Tonjock & Mih from Cameroon and *G. zonatum* Murrill from Florida (USA) (1/100). Clade VIII.B (0.99/74) was divided into two poorly-supported subclades: Clade VIII.B.1 that included sequences labelled as *G. sinense* J.D. Zhao, L.W. Hsu & X.Q. Zhang from China, *G. cupreum* from Cameroon, *G. mastoporium* from China and Malaysia and *G. orbiforme* from China; and Clade VIII.B.2 that grouped sequences labelled as *G. orbiforme* from Brazil and *G. ecuadorensis* A. Salazar, C.W. Barnes & Ordoñez from several neotropical countries. Four sequences from Costa Rican specimens (MMG-181a, MMG-209, GA-57, GA-52) were placed within a well-supported terminal clade (0.94/90) with sequences of *G. ecuadorensis* from Brazil, Ecuador and French Guyana, including the type specimen.

Identification of *Ganoderma* collections

In this study, 117 specimens of *Ganoderma* were studied in detail. Collections originated from all over the country. Seven taxa were identified: *G. amazonense* (n = 9), *G. applanatum* (n = 5), *G. australe* (n = 31), *G. curtisii* (n = 15), *G. ecuadorensis* (n = 9), *G. oerstedii* (n = 10) and *G. parvulum* (n = 24). The following type specimens were examined: *Fomes stipitatus* Murr., *Ganoderma amazonense* Weir, *G. dorsale* (Lloyd) Torrend, *G. oerstedii* (Fr.) Torrend, *G. perzonatum* Murrill, *G. pulverulentum* Murrill, *G. sessile* Murrill, *G. sessiliforme* Murrill and *G. tuberculosum* Murrill. We also include a map showing the distribution of *Ganoderma* in Costa Rica, based on the altitudinal gradient in Costa Rica and the location of the studied vouchers (Fig. 2).

Taxonomy

Based on the phylogenetic relationships, morphological characteristics and geographic distribution, the *Ganoderma* specimens collected from Costa Rica were identified as: *G. amazonense*, *G. applanatum* s.l., *G. australe* s.l., *G. curtisii*, *G. ecuadorensis*, *G. oerstedii* and *G. parvulum* (Fig. 3). The detail morphological descriptions of seven species, as well as important information about two doubtful species: *G. applanatum* var. *laevisporum* C.J. Humphrey & Leus-Palo and *G. chocoense*, are provided.

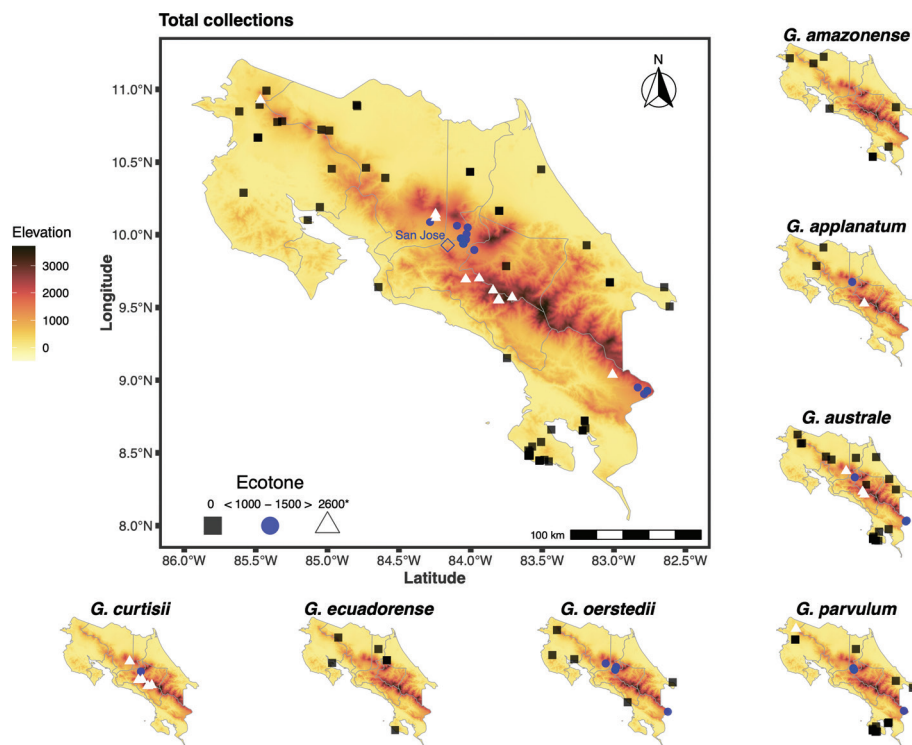


Figure 2. Distribution map of the seven *Ganoderma* species from Costa Rica.

1. *Ganoderma amazonense* Weir, A pathological survey of the para rubber tree (*Hevea brasiliensis* Müll. Arg.) in the Amazon Valley: 12 (1926).

Figs 3A, 4

Type. BRAZIL. Amazonas: Cocal Grande, Para, on *Hevea brasiliensis* (Willd. ex A.Juss.) Müll.Arg., 20 Aug 1923, James R. Weir. Pathological & Mycol. s.n. (lectotype: BPI62043!).

Description. *Basidiocarps* perennial, pileate, stipitate, sessile or with a contracted lateral base, corky to woody, solitary, applanate, irregular to tuberculate, 8.5 × 11 × 1 cm; *pileus* surface sulcate, glabrous, dull, brownish-grey to reddish-brown azonate or with zones close to the margin, margin obtuse, yellowish-brown; *context* yellowish-white, without resinous deposits or with fine discontinuous light brown horizontal bands; *pore surface* pinkish-brown to yellowish-brown, pores circular 4–6 per mm; *tube layer* pinkish-brown to yellowish-brown, simple, up to 20 mm thick. *Stipe* concolour with the pileus surface, up to 5 cm long. *Hyphal system* dimitic; contextual generative hyphae hyaline, thin-walled, with clamps, 2–5 µm in diam., difficult to observe; skeletal hyphae thick-walled, yellowish-brown, aseptate, 3–5 µm in diam., occasionally branched. *Cuticular cells* from the pileus absent. *Basidia* not observed. *Basidiospores* ovoid to ellipsoid, truncate at the distal end; with two walls, connected by inter-wall pillars, hyaline to yellowish-brown, negative in Melzer's Reagent, 8–10 × 6–7 µm. *Chlamydospores* not observed.

Descriptions and illustrations. Weir (1926), Furtado (1967), Steyaert (1980), Gottlieb and Wright (1999a), Ryvardeen (2004), Torres-Torres et al. (2012).

Substrata. On hardwood logs.

Altitudinal distribution. Lowlands.

Geographic distribution. *G. amazonense* is reported in the Caribbean (Jamaica and Puerto Rico) and Central and South America (Costa Rica,

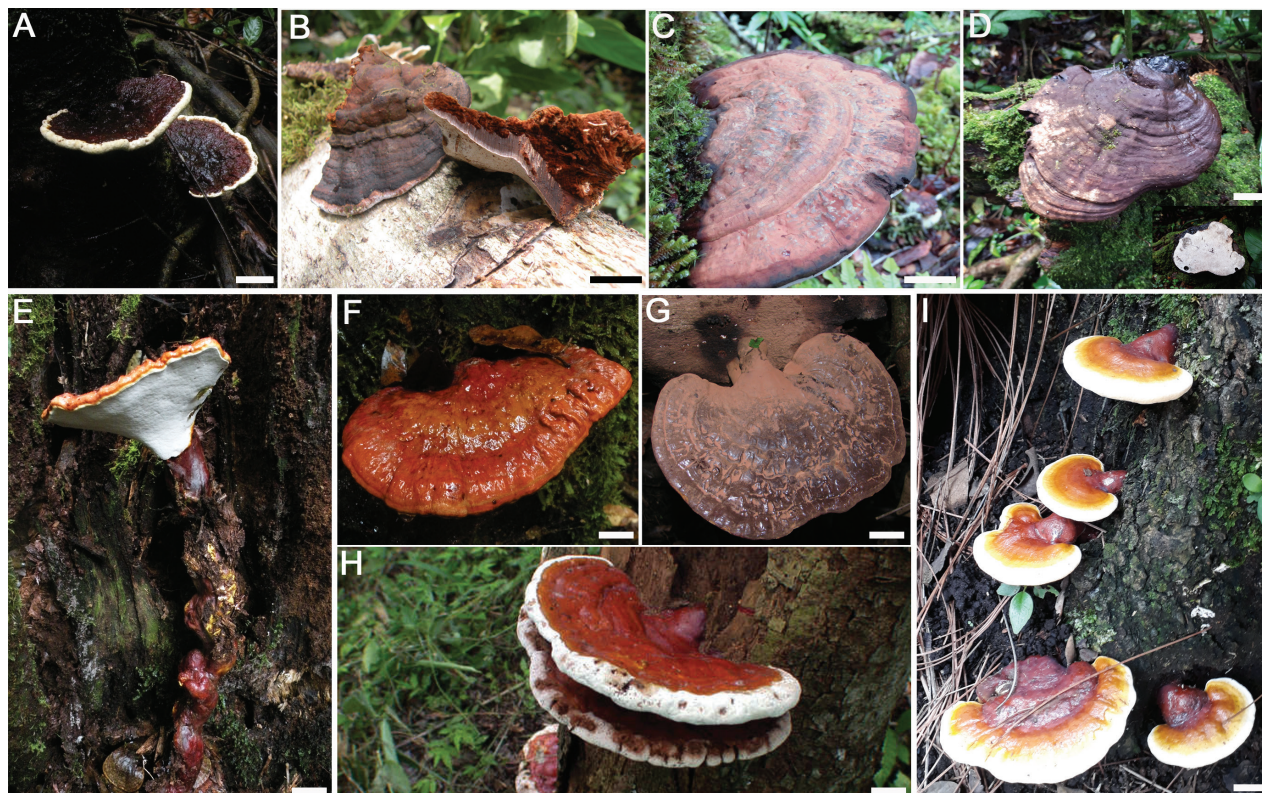


Figure 3. In-situ photos of basidiocarps of *Ganoderma* spp. in Costa Rica **A** *G. amazonense* (GA-30) **B** *G. applanatum* (GA-54) **C** *G. australe* (GA-58) **D** *G. cf. chocoense* (GA-03) **E**, **F** *G. curtisii* (JCV 128-10) **G** *G. ecuadorensis* (MMG-181) **H** *G. oerstedii* (Saenz 2049) **I** *G. parvulum* (GA-09). Scale bars: 20 cm (**A**, **H**); 3 cm (**B**, **C**); 1 cm (**D**, **E**, **I**).

Honduras and Brazil). Reports in West and Central Africa (Steyaert 1980) need further confirmation.

Specimens examined. Costa Rica. Alajuela: Los Chiles, Reserva Nacional de Vida Silvestre Caño Negro, 10°53'6.71"N, 84°47'28.27"W, 30 m elev., 03 Aug 1991, A. Ruiz-Boyer 7-91 (USJ36351). Upala, Bijagua, Albergue Heliconias, 10°43'21.05"N, 85°2'30.47"W, 500 m elev., on log, 12 Jul 2001, L. Ryvar-den 43716 (CR3802379). Guanacaste: Liberia, Parque Nacional Santa Rosa, sector Bosque Húmedo, 10°50'57.49"N, 85°36'57.89"W, 300 m elev., on log, 24 Oct 1996, I. Lindblad 2144.2 (CR3131819). Limón: Cantón Central, Reserva Biológica Hitoy Cerere, Sendero Tepezcuintle, 9°40'19.97"N, 83°01'42.96"W, 100 m elev., on log, 23 Jul 2003, E. Navarro 6843 (CR3727415). Puntarenas: Garabito, Jacó, Sector Garabú, Finca Quebrada Bonita, 9°38'22.81"N, 84°38'40.81"W, 100 m elev., on log, 24 Nov 2008, E. Navarro 10912 (CR4188987); Osa, Parque Nacional Piedras Blancas, Estación Río Bonito, Sendero Tacho, 9°38'22.81"N, 84°38'40.81"W, 100 m elev., on log, 14 Mar 2003, E. Fletes 4933 (CR3700169); Osa, Parque Nacional Corcovado, Estación Sirena, Sendero Espaveles, 8°28'57.75"N, 83°35'28.87"W, 0–10 m elev., on log, 14 Sep 2001, E. Fletes 2847 (CR3756152); 8°28'59.54"N, 83°35'29.69"W, 0–10 m elev., 14 Jul 2021, J. Carranza, M. Mardones, E. Fletes GA-30 (USJ109778); Sendero Sirena, 8°28'56.01"N, 83°35'49.16"W, 0–30 m elev., on log, 06 Jul 2022, J. Carranza, M. Mardones, E. Fletes GA-54 (USJ109779, sequence ITS OQ845454).

Discussion. *Ganoderma amazonense* was described by Weir (1926) as a new species from the Amazonas (Brazil) decaying the roots of *Hevea* spp. It

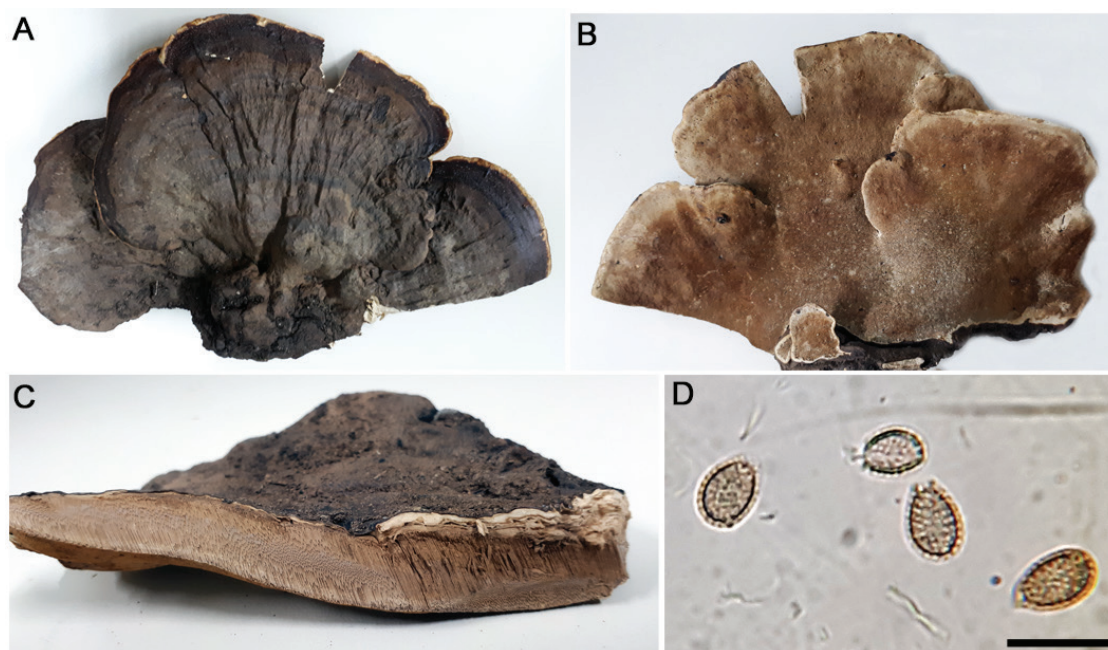


Figure 4. *Ganoderma amazonense* **A** basidiocarp pileus (Fletes 2847) **B** pore surface (Fletes 2847) **C** context tissue (Navarro 6843) **D** basidiospores (Fletes 4933). Scale bar: 10 μ m (**D**).

is characterised by the dull-brown, non-laccate pileus surface, the pale context and the small, light yellow basidiospores. The basidiospores of the specimens from Costa Rica examined in this study are ellipsoid, echinulate and truncate and measure $8-10 \times 6-7 \mu\text{m}$ that agree with measurements reported by Welti and Courtecuisse (2010) and Torres-Torres et al. (2012). However, slightly smaller basidiospores have been observed in the type specimen ($6-9.35 \times 4-6 \mu\text{m}$) and in descriptions by Gottlieb and Wright (1999a), Ryvarden (2004) and Gomes-Silva et al. (2011). All the specimens of *G. amazonense* examined in this study were collected in lowlands.

The *G. amazonense* sequence (GA-54) was placed in our phylogeny as a sister lineage of clade VI with moderate support in the BI analysis (0.78). Our sequence constitutes the first molecular record for this species deposited in GenBank. More sequences from additional molecular markers are needed to confirm the species' evolutionary relationships with other *Ganoderma* species, but its position as a separate lineage within the genus is confirmed.

2. *Ganoderma australe* (Fr.) Pat., Bull. Soc. mycol. Fr. 5(2,3): 65 (1889).

Figs 3C, 5

\equiv *Polyporus australis* Fr., Elench. fung. 1: 108 (1828).

Type. An island in Pacific Ocean, on log, *s.d.*, *s.n.* (type lost).

Description. *Basidiocarps* perennial, sessile or with a contracted lateral base, dimidiate, woody, solitary, applanate to unguulate, irregular to tuberculate, $1.6-21.2 \times 1.5-32 \times 0.3-5.1 \text{ cm}$; *pileus* surface crustose, rugulose, sulcate, glabrous, dull, greyish-brown, yellowish-brown, reddish-brown to brownish-black, margin obtuse, yellowish-brown to pinkish-brown, azonate or with

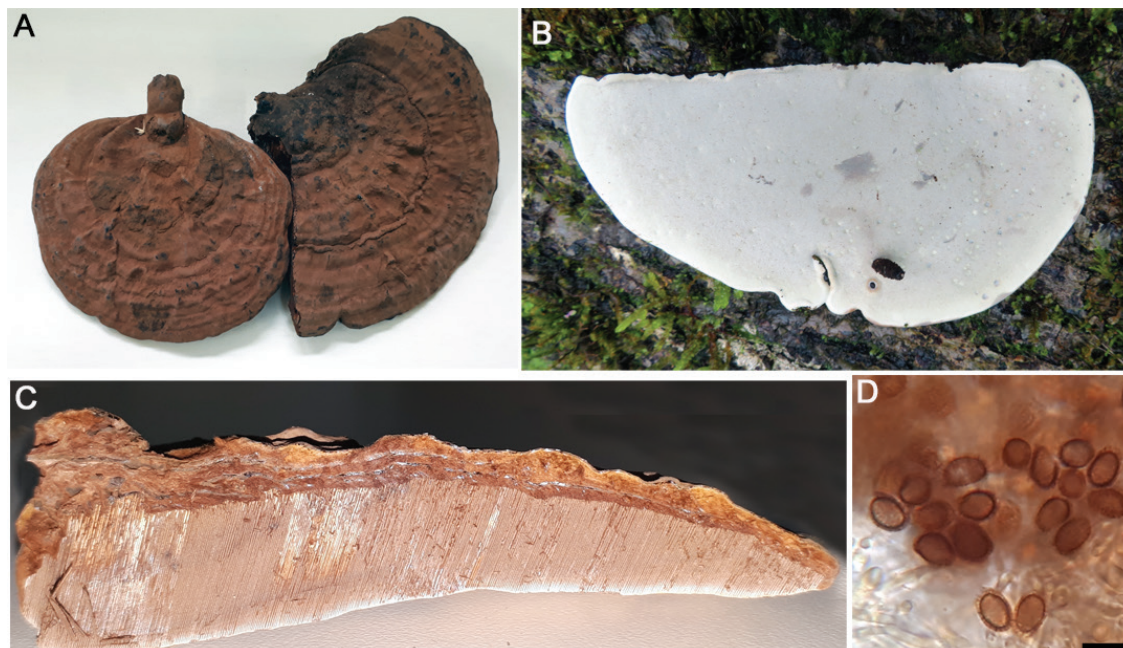


Figure 5. *Ganoderma australe* **A** basidiocarp pileus (Fletes 341) **B** pore surface (GA-64) **C** context tissue (Fletes 1403) **D** basidiospores (Fletes 1403). Scale bar: 10 μ m (**D**).

brownish-black, reddish-brown or yellowish-brown zones; **context** corky, vinaceous, purple-brown or yellowish-brown, with horizontal bands of melanoid substances, 1–30 mm thick, becoming dark with KOH; **pore surface** pinkish-brown to yellowish-brown, pores circular, 3–5 per mm; **tube layers** concolorous with context or yellowish-brown, sometimes whitish within, tubes simple to stratified, up to 0.5–25 mm thick. **Hyphal system** dimitic or trimitic; contextual generative hyphae inconspicuous, thin-walled, with clamps, hyaline, 1.5–3 μ m diam.; skeletal hyphae thick-walled, yellowish-brown, aseptate, up to 6 μ m in diam., occasionally branched; binding hyphae thin-walled, 1–2 μ m in diam. **Cuticular cells** from the pileus: absent. **Basidia** difficult to find. **Basidiospores** ovoid, truncate at the distal end; with two walls, connected by inter-wall pillars, yellowish-brown, negative in Melzer's Reagent, 7–12 \times 5–8 μ m. **Chlamydospores** not observed.

Descriptions and illustrations. Furtado (1967), Ruiz-Boyer (1998), Ryvarden (2004), Welti and Courtecuisse (2010).

Substrata. Dead-standing hardwood trees, stumps or logs.

Altitudinal distribution. Lowlands to highlands.

Geographic distribution. Pantropical, common in tropical America.

Specimens examined. Costa Rica. Alajuela: Arenal, Parque Nacional Arenal, sendero Pilón, 10°27'39.29"N, 84°43'51.83"W, 600–700 m elev., 15 Jul 2001, A. Ruiz 521 (CR3802311); Poás, Parque Nacional Volcán Poás, Sendero hacia el Bosque del Niño, 10°7'3.27"N, 84°14'36.88"W, 2500–2600 m elev., 27 Jun 2007, E. Navarro 10184 (CR4089856); San Carlos, Pocosol, Finca Latite, 10°23'26.51"N, 84°35'49.69"W, 110 m elev., 29 May 2002, J. Carranza JCV 13-02 (USJ72910). Cartago: Jimenez, Pejibaye, Refugio de Vida Silvestre El Copal, 9°47'6.90"N, 83°45'7.77"W, 650 m elev., 26 Apr 2006, E. Navarro 9620 (CR4014312). Guanacaste: La Cruz, Parque Nacional Guanacaste, Estación Biológica Pitilla, camino a la Esperanza, 10°59'28.61"N, 85°25'33.17"W, 700–

800 m elev., 23 Mar 1997, C. Cano 1012 (CR1544454); Liberia, Parque Nacional Rincón de la Vieja, Estación San Cristóbal, Sendero La Danta, 10°46'31.27"N, 85°21'0.51"W, 600–700 m elev., 28 Sep 1996, C. Cano 615 (CR144376); Sector Santa María, Los Naranjales, 10°46'53.11"N, 85°19'1.38"W, 800–900 m elev., 05 Dec 1997, C. Cano 1237 (CR3495780). Heredia: Sarapiquí, La Virgen, Estación Biológica La Selva, 10°25'56.52"N, 84°0'13.96"W, 40 m elev., on log, 06 Nov 2016, J. Carranza JCV 2-16 (USJ109687). Limón, Cantón Central, Reserva Veragua, Sendero Los Valientes, 9°55'40.63"N, 83°11'28.53"W, 200–300 m elev., 26 Jun 2009, E. Navarro 11165 (CR4222697); Reserva Biológica Hitoy Cerere, Sendero Tepezcuintle, 9°40'19.97"N, 83°01'42.96"W, 0–100 m elev., 19 Sep 2001, R. Valladares 536 (CR3464661). Pocosí, Colorado, Tortuguero, Reserva Biológica del Bosque Lluvioso, 10°26'58.96"N, 83°30'25.19"W, 300–400 m elev., 29 Jan 2004, E. Alvarado 111 (CR3802764). Puntarenas: Cantón Central, Parque Nacional Isla del Coco, orillas del Río Genio, 5°30'15.64"N, 87°4'32.05"W, 0–100 m elev., 04 Jun 2005, E. Fletes 7607 (CR3976554). Coto Brus, San Vito, Parque Nacional La Amistad, Zona Protegida Las Tablas, Fila Chiquizá, 8°55'34.40"N, 82°46'00.950"W, 1500–1600 m elev., 18 Feb 2003, E. Fletes 4870 (CR3575822); Finca Cafrosa, Pizote, 8°54'15.82"N, 82°47'21.22"W, 1400–1500 m elev., 28 Nov 1998, E. Navarro 520 (CR4109271). Osa, Puerto Escondido, Playa Colibrí, 8°39'36.96"N, 83°26'12.46"W, 0–100 m elev., 5 Nov 2006, E. Alvarado 367 (CR4044781); Parque Nacional Piedras Blancas, Estación Río Bonito, sendero a San Josecito, 8°43'16.18"N, 83°12'14.64"W, 400 m elev., 18 Apr 1999, E. Fletes 341 (CR1546010); Karate, Finca Exótica, 8°26'29.64"N, 83°27'15.39"W, 0–10 m elev., 11 Aug 2019, M. Mata JCV 4-19 (USJ109489); Parque Nacional Corcovado, Estación San Pedrillo, Sendero Llorona, 8°29'1.96"N, 83°35'30.31"W, 10–100 m elev., 16 Feb 2000, E. Fletes 1219 (CR3097854); Sector Sirena, Sendero Espaveles, 8°29'3.30"N, 83°35'30.64"W, 0–100 m elev., 08 Feb 2003, E. Fletes 4860 (CR3575815); 8°28'46.91"N, 83°35'22.30"W, 0–100 m elev., 01 Jun 2012, J. Carranza JCV 310-12 (USJ109694); Sendero Ollas-Sirena, 8°29'5.14"N, 83°35'24.33"W, 0–100 m elev., 01 Jun 2012, J. Carranza JCV 42-12 (USJ109489); Sector Sirena, sendero a Río Pavo, 8°30' 23.51"N, 83°35'19.34"W, 0–100 m elev., 25 Mar 2003, E. Fletes 1403 (CR1547383); Sendero Espaveles a sendero la Olla, 8°29'4.60"N, 83°35'22.49"W, 0–30 m elev., on log, 07 Jul 2022, J. Carranza, M. Mardones, E. Fletes GA-58 (USJ109795); Sector Aguas Azules, 8°32'35.08"N, 83°34'13.43"W, 0–100 m elev., 12 Mar 2005, E. Fletes 7302 (CR3994940); Estación La Leona, Sendero Paraíso, 8°26'50.34"N, 83°31'6.19"W, 0–100 m elev., 10 Sep 2009, J. Carranza JCV 25-09 (USJ109489); 8°26'49.55"N, 83°31'8.89"W, 0–100 m elev., 9 Dec 2016, J. Carranza JCV 8-16 (USJ109686); 8°26' 50.79"N, 83°31'14.79"W, 0–100 m elev., 08 Jan 2009, J. Carranza JCV 104-09 (USJ109489). San José, Dota, Reserva Forestal Los Santos, Albergue de Montaña Savegre, Sendero Los Robles, 9°33'00.00"N, 83°48'00.0"W, 2400–2500 m elev., 20 Jun 2005, R. Rodríguez 505 (CR3968596); Finca La Neblina, sendero de las Torres a Savegre, 9°37'3.65"N, 83°50'33.3"W, 2500–2600 m elev., 14 Oct 2006, E. Navarro 99712 (CR4043836); Cerro de la Muerte, Km 92.5, Estación Los Nimbos, sendero en el robledal, 10°25'18.9"N, 84°01'30.6"W, 3100 m elev., 09 Jun 2019, M. Mardones GA-19 (USJ109713, sequences ITS OQ845456, LSU OQ835180). Moravia, Jardines, 9°58'1.31"N, 84°1'58.2"W, 1300 m elev., 12 Sep 2021, J. Carranza JCV 2-21 (USJ109781).

Discussion. *Ganoderma australe* is a common species in the Tropics that traditionally is considered a cosmopolitan species; but recent studies suggest that *G. australe* is only present in America and Oceania (Fryssouli et al. 2020). Macroscopically, the main characteristics of *G. australe* are tough and sessile basidiocarp with distinct black cuticle, greyish to brown pileus and context with resinous deposits or melanoid bands. Microscopically can be recognised by its cylindrical and hyaline basidiospores.

The Costa Rican specimens have a wide range of colour variations of the pileus and spore sizes. Steyaert, cited by Ryvarden and Johansen (1980), reported spore sizes that range from $6\text{--}13 \times 4.5\text{--}8 \mu\text{m}$, while Ruiz Boyer (1998) found $6\text{--}8 \times 4\text{--}6 \mu\text{m}$ and Ryvarden (2004) mentioned spore sizes of $7\text{--}12 \times 5\text{--}8 \mu\text{m}$. The spore sizes of the specimens observed in our study were in the range of the ones mentioned by these authors. Morphologically, amongst the neotropical species of *Ganoderma* with non-laccate basidiocarps, *G. australe* and *G. applanatum* are difficult to differentiate. However, both species can be distinguished by the resinous deposits or melanoid bands present only in the context of *G. australe*. From the morphological examination of ca. 40 herbarium specimens within the *G. applanatum-australe* complex in Costa Rica, we determined that most specimens belong to *G. australe*, with a few occurrences of *G. applanatum* (see below). There are some specimens of *G. australe* that do not show resinous deposits or melanoid bands or are very inconspicuous. In these cases, the size of the spores (larger in *G. australe* than in *G. applanatum*) is a criterion to distinguish both species. In other cases, the morphological distinction is complex and molecular characterisation should be used.

Identifying *G. australe* using the ITS region is challenging since, according to Fryssouli et al. (2020), about 5% of the *Ganoderma* sequences deposited in GenBank are labelled as *G. australe*. Still, only 22% of them are correctly tagged. We selected two reference sequences of *G. australe* from Australia (DHCR411 and DHCR417) to be included in the phylogeny. The sequences JMCR128 and GA-19 grouped with them in a strongly supported subclade (1/98) within clade VI.

3. *Ganoderma applanatum* (Pers.) Pat., Hyménomyc. Eur. (Paris): 143 (1887)

Fig. 3B

≡ *Boletus applanatus* Pers., Obs. Mycol. 2:2. 1799.

Description. **Basidiocarps** perennial, sessile or with a contracted lateral base, dimidiate, woody, solitary, applanate to unguulate, irregular to tuberculate, $2\text{--}13 \times 2\text{--}22 \times 0.5\text{--}10 \text{ cm}$; **pileus** surface rugulose, glabrous, dull, greyish-brown to black, margin obtuse, zonate, whitish; **context** firm, reddish-brown, 10–50 mm thick, becoming dark with KOH; **pore surface** light brown to yellowish-brown, pores circular, 4–6 per mm; **tube layers** concolorous with context or yellowish-brown, up to 40 mm thick. **Hyphal system** dimitic or trimitic; contextual generative hyphae thin-walled, with clamps, hyaline, 2–4 μm diam.; skeletal hyphae thick-walled, yellowish-brown, aseptate, 2–4 μm diam., branched; binding hyphae thick-walled, branched, hyaline, 1–2 μm diam. **Cuticular cells** from the pileus: absent. **Basidia** not observed. **Basidiospores** ovoid, truncate; with two walls, yellow, negative in Melzer's Reagent, $7\text{--}10 \times 5\text{--}6 \mu\text{m}$. **Chlamydospores** not observed.

Descriptions and illustrations. Gilbertson and Ryvardeen (1986), Ruiz-Boyer (1998).

Substrata. Dead-standing hardwood trees or logs.

Altitudinal distribution. Lowlands to highlands.

Geographic distribution. Pantropical, common in tropical America.

Specimens examined. Costa Rica. Alajuela: Los Chiles, Refugio Nacional de Vida Silvestre Caño Negro, 10°53'36.73"N, 84°47'45.49"W, 10 m elev., 07 Sep 1991, A. Ruiz-Boyer 13-91 (USJ36357). Guanacaste: Tilarán, 10°27'13.66"N, 84°58'13.61"W, 534 m elev., 10 Oct 1980, J. A. Saénz & J. Carranza 314-80 (USJ21274). Heredia: BosquedeLaHoja, 10°3'44.38"N, 84°5'43.09"W, 1496 m elev., 05 Mar 1986, J. Carranza JCV 67-86 (USJ22291). San José: Dota, San Gerardo, 9°33'1.63"N, 83°48'9.66"W, 2000–2300 m elev., 18 Sep 2022, M. Mardones GA-64 (USJ109782, sequences ITS OQ845455, LSU OQ835179); El Empalme, Ojo de agua, 2250 m elev., 28 Oct 1979, J. Carranza JCV 131-79 (USJ21297).

Discussion. As mentioned above, the species *G. applanatum* is morphologically similar to *G. australe*, but the shorter basidiospores and the absence of resinous deposits or melanoid substances in the context of *G. applanatum* can distinguish them. According to Ryvardeen (2004), *G. applanatum* is a species restricted to temperate zones and, according to Fryssouli et al. (2020), it has a Holarctic distribution. However, our results show the presence of this species or a species closely related to *G. applanatum*, in Costa Rica. The sequence from the GA-64 specimen clusters, as an independent lineage, with several sequences identified as *G. applanatum* from Europe and Asia in a strongly-supported terminal clade (1/78) within clade III. This result would be the first record of this species in the Tropics confirmed by molecular data. Therefore, considering the morphological examination and the phylogenetic position of the sequence, we have decided to identify this specimen as *G. applanatum*. Increasing the number of collections and molecular data is essential to determine if the species observed in Costa Rica is *G. applanatum* or a closely-related species.

While examining the *G. applanatum* specimens from Costa Rica, we found four specimens with smooth basidiospores, which agree with the description of *G. applanatum* var. *laevisporum* C.J. Humphrey & Leus-Palo. For details on these specimens, see the Excluded Species section below.

4. *Ganoderma curtisii* (Berk.) Murrill, N. Amer. Fl. (New York) 9(2): 120 (1908).
Figs 3E, F, 6

≡ *Polyporus curtisii* Berk. 1849.

Type. USA, South Carolina, s.d., s.n. (type: PH00042681).

Descriptions. *Basidiocarps* solitary, laterally and long stipitate, reniform, dimidiate or circular, 10.5–11.1 × 6.3–9.9 × 0.7–2.5 cm; *pileus* single or several arising from a branching stipe, cespitose, glabrous, shiny both when fresh and dry, laccate, upper surface yellow, yellowish-brown to reddish-brown with purple hues; *context* firm, buff to light brown, duplex, without concentric growth zones, 7–13 mm thick, with continuous melanoid bands embedded in context tissue, originating from the stipe and running parallel to the upper surface; *pore surface* pinkish-brown to yellowish, darkening when handled, pores

circular to irregular, 4–6 per mm; **tube layers** ochraceous-tawny, 10–12 mm thick. **Stipe** lateral, 30–250 mm long, round, or slightly compressed, 12–18 mm diam. and with a purple to black, shiny cuticle. **Hyphal system** trimitic; contextual generative hyphae thick-walled, with clamps, hyaline, 3.5 µm in diam.; skeletal hyphae thick-walled, 1.5–6 µm in diam., light yellow; binding hyphae thin and thick-walled, 3–5 µm in diam. **Cuticular cells** from the pileus clavate, some nodulose, sometimes with 1 to 2 protuberances, rarely branched, with granulations in the apex, yellowish, with strong amyloid reaction with Melzer's Reagent, 45–55 × 9–14 µm. **Basidia** not observed. **Basidiospores** ellipsoid to oblong, truncate at the distal end; with two walls, yellowish-brown to brown, moderately coarsely echinulate, (9–)11–17 × (7–)8–10 µm. **Chlamydospores** not observed.

Descriptions and illustrations. Torres-Torres and Guzmán-Dávalos (2005, 2012), Lopez-Peña et al. (2016).

Substrata. On *Quercus* spp. or *Pinus* spp., on decaying wood.

Altitudinal distribution. In Costa Rica, this species is found only in the highlands.

Geographic distribution. Mexico and the USA. This is the first report in Costa Rica and Central America.

Specimens examined. Costa Rica. Alajuela: Grecia, Reserva Forestal Grecia, Bosque del Niño, sendero al acueducto, 10°8'30.90"N, 84°14'49.39"W, 1800–1900 m elev., 26 Jun 2006, E. Navarro 10132 (CR4089789); on soil, 10 Jul 2016, M. Mata 2647 (USJ109166). Cartago: Paraíso, Reserva Forestal Río Macho, Villa Mills, finca Los Abarca, 31 Aug 2008, 9°34'11.15"N, 83°42'37.40"W, 2600–2700 m elev., E. Alvarado 417 (CR4164678); Sector La Chonta, km. 55 de la carretera Interamericana Sur, 9°42'00.0"N, 83°56'30.0"W, 2400–2500 m elev., 20 Jul 2007, E. Navarro 10257 (CR4101818); La Unión, Tres Ríos, Zona Protectora de La Carpintera, 9°53'44.38"N, 83°58'31.79"W, 1400 m elev., 2014, Alvarenga and Canessa GA-00 (USJ109783, sequences ITS OQ845458, LSU OQ835182). San José, Desamparados, San Miguel, Jericó, Cerro Tablazo, ladera SO, *Quercus* sp. forest, 9°49'24.34"N, 84°2'26.56"W, 1880 m elev., on log, 30 Mar 2010, Carlos O. Morales s.n. (USJ83642). Dota, San Gerardo, 9°33'0.86"N, 83°48'16.20"W, 2000–2300 m elev., 10 Jul 2000, R. Halling s.n. (USJ 71604); 9°32'59.91"N, 83°48'18.26"W, 2300 m elev., 26 Nov 2010, J. Carranza JCV 128-10 (USJ104499); 9°33'1.13"N, 83°48'22.39"W, 2300 m elev., 10 Feb 2011, J. Carranza JCV 146-11 (USJ109500); 9°33'2.08"N, 83°48'26.31"W, 2200 m elev., 18 Sep 2022, M. Mardones GA-65 (USJ109784, sequences ITS OQ845461, LSU OQ835184); 9°33'3.85"N, 83°48'25.63"W, 2200 m elev., 18 Sep 2022, M. Mardones GA-63 (USJ109785, sequences ITS OQ845460, LSU OQ835183); Santa María, Jardín, 9°43'20.15"N, 83°58'28.91"W, 2200 m elev., 28 Oct 1979, J. Carranza JCV 90-79 (USJ21299). León Cortés, San Pablo, Sector el casquillo, forest of *Quercus* spp., 9°41'37.98"N, 84°2'6.03"W, 2100 m elev., 22 Sep 2019, Beatriz Picado BPH16/GA-22 (USJ109794, sequences ITS OQ845459). Perez Zeledón, Siberia, 9°32'49.12"N, 83°42'48.29"W, 2900 m elev., on log, José Murillo 10 (USJ109055). San Marcos, Tarrazú, Canet, 9°41'38.92"N, 84°2'5.08"W, 2200 m elev., 22 Jan 2018, Beatriz Picado BPH21 (USJ109716).

Discussion. *Ganoderma curtisii* mainly differs from other *Ganoderma* species from Costa Rica by its lateral and long stipe, the colour of the stipe and pileus, the melanoid bands that originate from the stipe and run parallel to the upper

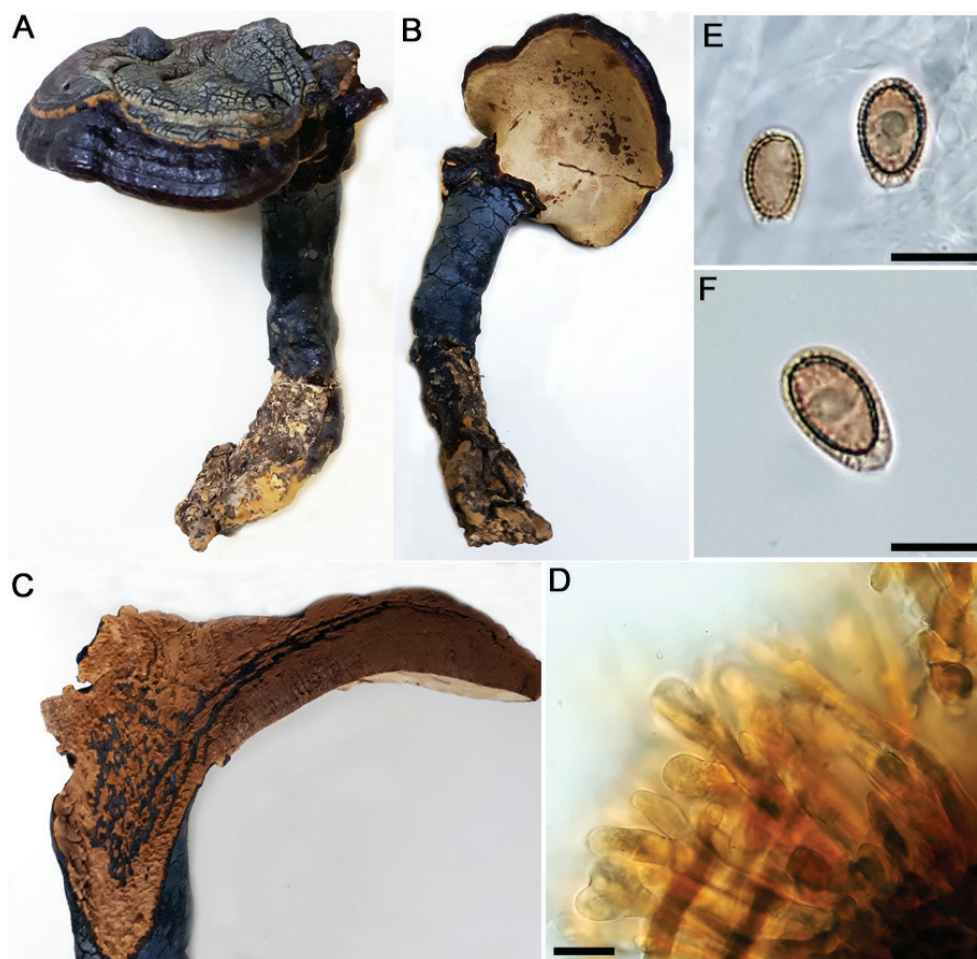


Figure 6. *Ganoderma curtisii* **A, B** basidiocarp (Navarro 10257) **C** context tissue (Navarro 10257) **D** cuticular cells (Navarro 10257) **E, F** basidiospores (Navarro 10132). Scale bars: 10 μm (**D–F**).

surface of the context and the large basidiospores (11–17 \times 8–10 μm). The Costa Rican specimens examined by us showed larger basidiospores than those reported by Murrill (1915, 9–11 \times 5–8 μm), Torres-Torres and Guzmán-Dávalos (2005, 10.4–12.8 \times 5.6–8 μm) and Loyd et al. (2018, 8.3–12.1 \times 5.4–7.5 μm). Additionally, the cuticular cells in our specimens have a very strong amyloid reaction not mentioned by Torres-Torres and Guzmán-Dávalos (2005).

In Costa Rica, this species has been found in highlands and always associated with decaying wood in *Quercus* or *Pinus* forests. Torres-Torres and Guzmán-Dávalos (2012) reported it in Mexico occurring in the same type of forests. *Ganoderma curtisii* f.sp. *meredithiae* was recently erected to include those forms characterised by occurring exclusively on pines and showed slow cultural growth rate (Loyd et al. 2018). Amongst the examined Costa Rican specimens, only one (GA-00) occurred in a pine forest; the other specimens were found in *Quercus* forests. Sequences from four specimens of *G. curtisii* from Costa Rica (GA-00, GA-22, GA-63 and GA-65) clustered in the same clade with *G. lingzhi* (clade II) with strong support (1/92), forming a terminal subclade with sequences labelled as *G. curtisii* and *G. meredithiae* from the USA. This is the first report of the species in Central America and its distribution is probably strongly linked to the distribution of its host plants.

5. *Ganoderma ecuadorensis* A. Salazar, C.W. Barnes & Ordoñez [as 'ecuadoriense'], in Salazar, Ordoñez, Toapanta, Barnes & Gamboa, *Persoonia* 36: 441 (2016)

Figs 3G, 7

Type. ECUADOR. Orellana: Yasuní Research Station, on decaying wood, Mar 2013, A. Salazar s.n. (holotype: QCAM3430).

Description. *Basidiocarps* solitary or gregarious, laterally stipitate, dimidiate, spatulate to circular, woody, 15–21 × 8–11 cm; *pileus* surface laccate, tuberculate, glabrous, zonate reddish-brown to vinaceous-brown, upper surface covered by cinnamon-coloured powder of deposited basidiospore, margin obtuse, yellow when young changing to reddish-brown with age; *context* firm, yellowish-brown, duplex, with melanoid bands or deposits embedded in context tissue; *pore surface* white when young, blackish-brown to vinaceous-black when old, pores circular to irregular, 4–6 per mm; *tube layers* ochraceous-tawny to brownish-black, 10–12 mm thick. *Stipe* lateral, 25–35 cm long, round or slightly compressed, tuberculate or smooth, 12–18 mm diam. and with a reddish-brown, shiny cuticle. *Hyphal system* trimitic; contextual generative hyphae thick-walled, with clamps, hyaline, 3.5 µm in diam.; skeletal hyphae thick-walled, 1.5–6 µm in diam., light yellow; binding hyphae thin and thick-walled, 1–3.5 µm in diam. *Cuticular cells* club-like, yellowish, upper part with small outgrowths, with amyloid reaction with Melzer's Reagent, 40–55 × 7–14 µm. *Basidia* not observed. *Basidiospores* ellipsoid to oblong, truncate at the distal end; with two walls, pale yellow, moderately coarsely echinulate, 8–10 × 5–7 µm. *Chlamydospores* not observed.

Descriptions and illustrations. Crous et al. (2016).

Substrata. On decaying hardwood.

Altitudinal distribution. Lowlands.

Geographic distribution. Brazil, Ecuador, and French Guyana. This is the first report for Costa Rica and Central America.

Specimens examined. Costa Rica. Alajuela: Arenal, Parque Nacional Volcán Tenorio, sector El Pilón, 10°42'58.23"N, 84°59'15.91"W, 700 m elev., 27 Jun 1999, M. Mata Mata-765 (CR3484383). Heredia: Sarapiquí, Puerto Viejo, Estación Biológica La Selva (OET), Sendero Experimental Sur, 10°25'59.6"N, 84°0'16.2"W, 30–100 m elev., 23 Jun 2022, J. Carranza JCV 3-22/GA-52 (USJ109796, sequences ITS OQ845463); 10°25'59.5"N, 84°0'16.3"W, 100 m elev., on log, 06 Nov 2016, J. Carranza JCV 3-16 (USJ109702). Limón: Pococí, Guápiles, Zona Protectora acuíferos de Guácimo y Pococí, bosque sobre colina La Roca, 10°09'57"N, 83°47'59"W, 472 m elev., 06 Jun 2022, M. Montero MMG-181A (USJ109798, sequences ITS OQ845465); en arboleda rodeada de potreros, 10°09'55"N, 83°48'05"W, 410 m elev., 08 Sep 2022 M. Montero MMG-209 (USJ109799, sequences ITS OQ845466). Puntarenas: Cantón Central, Isla Chira, 10°6'5.01"N, 85°8'14.15"W, 0–100 m elev., 29 Jul 2005, I. López Lopez-7241 (CR3970559). Osa, Parque Nacional Corcovado, Estación Sirena, Sendero Espaveles a sendero La Olla, 8°29'12.04"N, 83°35'42.8"W, 0–30 m elev., on log, 07 Jul 2022, J. Carranza, M. Mardones, E. Fletes GA-57 (USJ109797, sequences ITS OQ845464, LSU OQ835185); Estación La Leona, 8°26'49.74"N, 83°31'10.04"W, 10 m elev., on log, 30 Aug 2014, J. Carranza JCV 2-14 (USJ109682); 8°26'49.74"N, 83°31'10.04"W, 10 m elev., on log, 16 Sep 2016, J. Carranza JCV 7-16 (USJ109691).

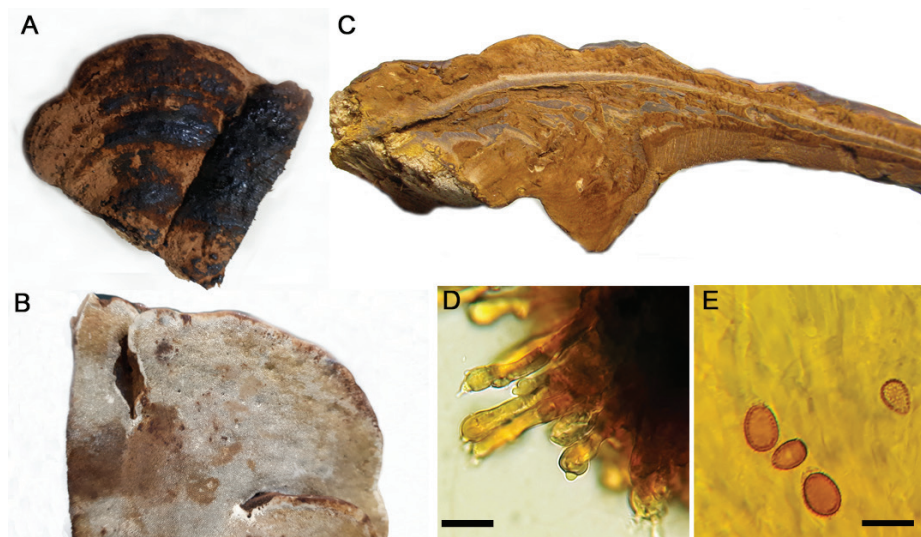


Figure 7. *Ganoderma ecuadorensis* **A** basidiocarp (Mata 765) **B** pore surface (Mata 765) **C** context tissue (MMG-181) **D** cuticular cells (Mata 765) **E** basidiospores (Lopez 7241). Scale bars: 20 μm (**D**); 10 μm (**E**).

Specimens of other species examined for comparison. *Ganoderma perzonatum*. Cuba. Santiago de las Vega, 08 Nov 1904, F.S. Earle 309 (type, NYBG 985702).

Discussion. *Ganoderma ecuadorensis* (as *ecuadoriense*) was recently described from the Amazon Basin in Ecuador (Crous et al. 2016). It is characterised by the laterally stipitate basidiocarp, with dimidiate, laccate, reddish-brown pileus, usually covered by a cinnamon-coloured powder of deposited basidiospores. Microscopically, the main characteristics are their club-shape cuticular cells and the small ($8\text{--}10 \times 5\text{--}7 \mu\text{m}$) and yellow basidiospores. We could not examine the type specimen of *G. ecuadorensis*, but the morphological characteristics observed in our specimens agree well with the description in the protologue.

According to Crous et al. (2016), morphologically, *G. ecuadorensis* is similar to *G. perzonatum* Murrill. The type specimen of *G. perzonatum* has a very short stipe, darker than the pileus, measuring $0.5\text{--}1 \times 0.5\text{--}1.5 \text{ cm}$. Additionally, it has discontinuous melanoid bands; the spores are $8\text{--}10 \times 6\text{--}8.5 \mu\text{m}$ and the cuticular cells do not have projections and are shorter than in *G. ecuadorensis*. Steyaert (1980) considered *G. perzonatum* as a synonym of *G. parvulum*.

Sequences of four specimens from Costa Rica (GA-57, GA-52, MMG-181a, MMG-209) clustered in a subclade with *G. orbiforme* from Brazil (clade II) forming a well-supported terminal subclade (0.94/90) with sequences labelled as *G. ecuadorensis* (including the type) from Brazil, Ecuador and French Guyana and *G. subfornicatum* from French Guyana. Fryssouli et al. (2020) considered *G. ecuadorensis* as a synonym of *G. subfornicatum*, based on the phylogenetic analyses of the ITS region. However, *G. ecuadorensis* still appears as a valid species at Index Fungorum. In the BLASTN search of our sequences, the results gave the highest score to sequences identified as *G. ecuadorensis* (including the holotype).

Therefore, until more data are available, we identify our specimens as *G. ecuadorensis* based on: (i) the similar morphological characteristics of our specimens with the description in the protologue of *G. ecuadorensis*, (ii) the position of our ITS sequences in the phylogenetic analysis within a terminal subclade

with other sequences of *G. ecuadorensis* (including the holotype) and (iii) the lack of more sequences of *G. subfornicatum* (including type material) in GenBank (see Fryssouli et al. (2020) for a complete discussion on the topic).

6. *Ganoderma oerstedii* (Fr.) Murrill, Bull. Torrey bot. Club 29: 606 (1902)

Figs. 3H, 8

= *Ganoderma tuberculosum* Murrill, N. Amer. Fl. (New York) 9(2): 123 (1908).

Type: BELIZE (as British Honduras), 1906, M.E. Peck s.n. (holotype: BPI236681!).

Type. COSTA RICA: s. l., 1846, Oersted. s.n. (neotype: BPI236610!).

Descriptions. **Basidiocarps** gregarious, solitary or imbricate, mostly sessile, sometimes laterally stipitate, dimidiate, unguulate or spatulate woody, rugulose, 2.8–19.1 × 2.1–24.5 × 0.7–3.9 cm; **pileus** surface with laccate zones, glabrous, zonate, brownish-red, vinaceous-brown, vinaceous-red, yellowish-red, gradually changing to yellowish-brown to deep yellow in the margin, margin obtuse; **context** firm, yellowish-brown, up to 6 cm thick, concentrically zonate, with inconspicuous horizontal bands of melanoid substances; **pore surface** yellowish-brown to pinkish-brown, darkening when handled, pores circular to irregular, 3–6 per mm; **tube layers** light brown to yellowish-brown, up to 0.9 cm thick, becoming darker with 5% KOH. **Stipe** glabrous, vinaceous-red or concolorous with pileus surface, with some laccate zones, 1.5–13.1 × 1.2–7.5 cm. **Hyphal system** dimitic or trimitic; contextual generative hyphae thick-walled, with clamps, hyaline, 5 µm in diam.; skeletal hyphae thick walled 3–9 µm in diam.; binding hyphae thin and thick-walled, 2–4 µm in diam. **Cuticular cells** from the pileus cylindrical, clavate, some nodulose, vesiculate and branched, thick-walled, with granulations in the apex, yellowish, with strong amyloid reaction with Melzer's Reagent, 22–52(–100) × 6–20 µm. **Basidia** not observed. **Basidiospores** ovoid, truncate at the distal end; with two walls, connected by inter-wall pillars, subhyaline or yellowish-brown, negative in Melzer's Reagent, (8–)11–14(–15) × (5–)8–11 µm. **Chlamydospores** thick-walled, reddish-brown, 23–30 × 16–21 µm.

Descriptions and illustrations. Murrill (1902, 1908 as *G. tuberculosum*), Steyaert (1980), Gottlieb and Wright (1999b as *G. tuberculosum*), Ryvarden (2000, 2004), Mendoza et al. (2011), Torres-Torres et al. (2015), Lopez-Peña et al. (2016).

Substrata. On living trees and logs.

Altitudinal distribution. Lowlands to highlands.

Geographic distribution. Widespread in the Neotropics.

Specimens examined. Costa Rica. Alajuela: Grecia, Santa Gertrudis, 10°5'13.94"N, 84°17'3.96"W, 1050 m elev., 14 Jul 1991, J. Carranza JCV 16-91 (USJ33286). Guanacaste: Abangares, Higerillas, Finca El Arboreto, 10°11'28.28"N, 85°3'10.8"W, 0–100 m elev., 20 Jun 2007, J.A.Sáenz 2049 (CR4095735); La Cruz, Parque Nacional Guanacaste, Estación Biológica Cacao, sendero Los Naranjos, 10°53'43.2"N, 85°28'24.6"W, 700–1000 m elev., 23 May 1997, E. Fletes and C. Cano 1112 (CR4130985); Santa Cruz, Reserva Ramón Álvarez, 10°17'20.4"N, 85°35'13.2"W, 0–100 m elev., 24 Sep 2011, J. Carranza JCV 7-11 (USJ83002). Heredia: Santo Domingo, San Luis, 10°0'16.4"N, 84°1'44.7"W,

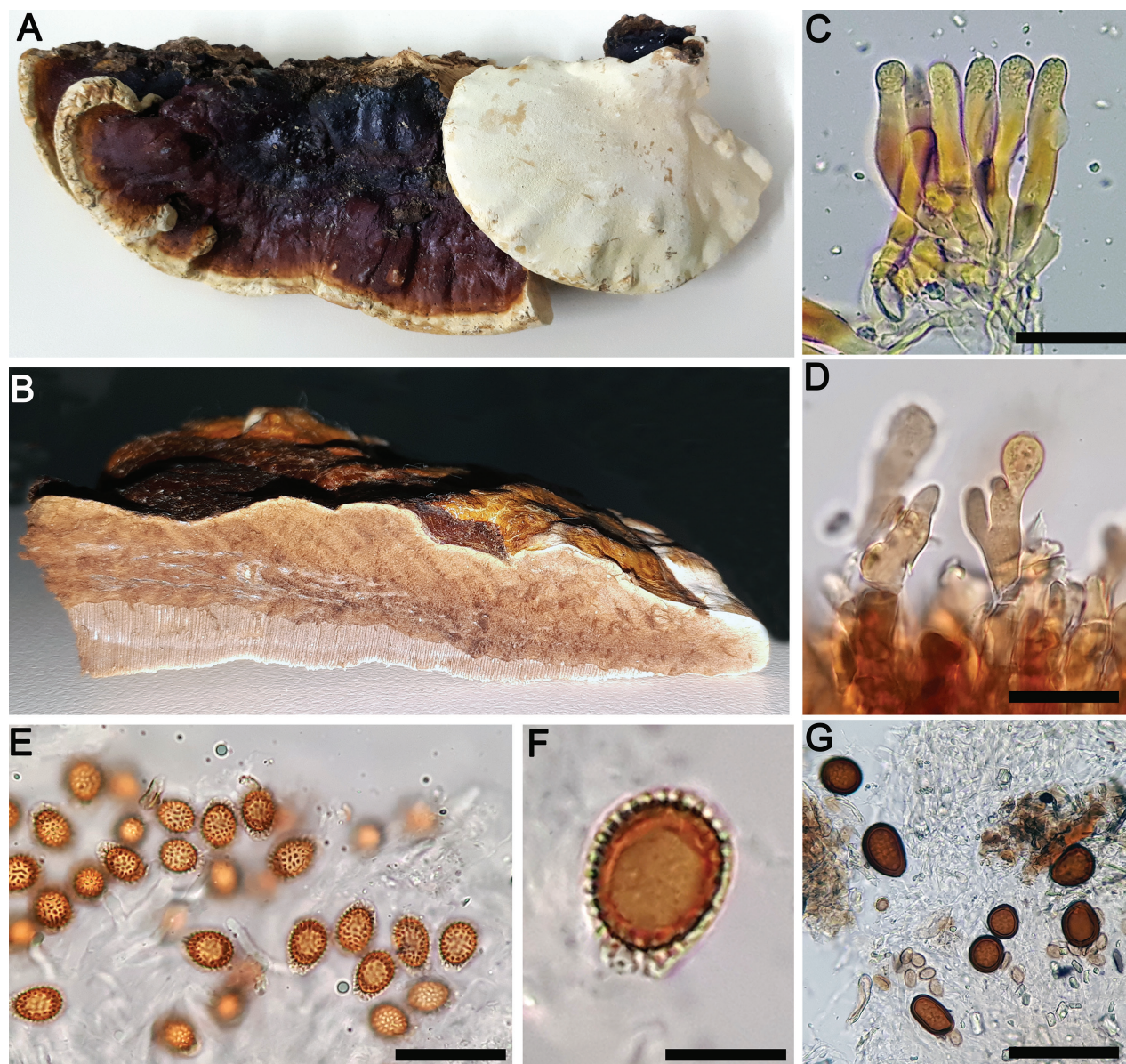


Figure 8. *Ganoderma oerstedii* **A** basidiocarp (Cano 946) **B** context tissue (Fletes 5876) **C, D** nodulose and branched cuticular cells (Navarro 10502, Lopez 4308) **E, F** basidiospores (Fletes 5876) **G** chlamydospores (Navarro 5006). Scale bars: 20 µm (**C, D, E, G**); 10 µm (**F**).

1200 m elev., 06 Nov 2016, J. Carranza JCV 1-16 (USJ109683). Limón: Talamanca, Refugio de Vida Silvestre Gandoca- Manzanillo, sector Manzanillo, alrededores del Centro Operativo, 9°38'19.6"N, 82°38'56.6"W, 0–100 m elev., 26 Sep 2001, R. Valladares RValladares 555 (CR3468098). Puntarenas: Coto Brus, San Vito, Área de Conservación La Amistad Pacífico, Zona Protectora Las Tablas, Fila Chiquizá, 8°55'34.4"N, 82°46'00.95"W, 1500–1600 m elev., 19 Jul 2002, E. Navarro 5006 (CR3516656); Osa, Parque Nacional Marino Ballena, Finca Roca, a orillas de la playa, 9°9'9.02"N, 83°44'46.9"W, 0–100 m elev., 21 Jan 2004, E. Fletes 5876 (CR3813349). San José: Montes de Oca, San Pedro, Universidad de Costa Rica, Finca 1, estacionamiento del CIICLA, 9°56'19.5"N, 84°3'9.4"W, 1100 m elev., 11 Sep 2019, J. Carranza GA-21 (USJ109786); 9°56'19.5"N, 84°3'9.34"W, 1100 m elev., 18 Dec 2019, J. Carranza GA-24 (USJ109787, sequences ITS OQ845469).

Discussion. This species was originally described from Costa Rica. It is characterised by its woody basidiocarp, reddish-brown in the base, to deep yellow in the margin. The species has a yellowish-brown context, with continuous resinous bands and clavate, branched and vesiculate cuticular cells with strong amyloid reaction with Melzer's Reagent. The two walls in the basidiospores are connected by inter-wall pillars.

The piece of the neotype specimen examined under *Polyporus oerstedii* Fr. - *G. oerstedii* (Fr) Murr., collected in Costa Rica, only contained a small portion of the tubes with abundant ovoid, truncate, echinulate spores, $9.3\text{--}13.6 \times 7.65\text{--}9.3 \mu\text{m}$. Annotations done by O. Juel, Xin-Cun Wang, Donjmei Wang and Ryvar-den mentioned spores $9\text{--}10 \times 6.5\text{--}8 \mu\text{m}$ (with wall $11\text{--}12 \mu\text{m}$), $11.5\text{--}13 \times 8.5\text{--}10.5 \mu\text{m}$, $11.5\text{--}15 \times 8\text{--}11.5 \mu\text{m}$ (with wall), $10\text{--}13.5 \times 6.5\text{--}10.5 \mu\text{m}$ (without wall) and $11\text{--}14 \times 7\text{--}10 \mu\text{m}$, respectively. The spores in the specimens studied from Costa Rica are in the range of the ones found on the neotype and the ones mentioned by the above researchers.

In taxonomic studies by Ryvar-den (2000) and Torres-Torres et al. (2015) and in Mycobank (<https://www.mycobank.org/>), *G. oerstedii* is considered a synonym of *G. tuberculosum*, although newer studies by Loyd et al. (2018) and Fryssouli et al. (2020), as well as Index Fungorum contradicted them. We examined the type specimens of both taxa and significant morphological differences were not observed; hence, we concluded that these taxa are co-specific.

According to Loyd et al. (2018), *G. tuberculosum* generally produced sessile basidiomata. However, amongst Costa Rican specimens, we found two forms: sessile and laterally stipitate basidiomes. Additionally, Loyd et al. (2018) mentioned that chlamydospores were lacking in the species, although they are presented in our collections.

The sequences from Costa Rican specimens GA-24 and JV1607/62 (retrieved from GenBank, MZ354944) strongly supported a terminal subclade (1/99), together with other sequences labelled as *G. tuberculosum* or *G. oerstedii* collected from Brazil, Florida (USA) and Mexico, within clade I that also includes the species *G. philippii*, *G. flexipes* and *G. wiioense*.

7. *Ganoderma parvulum* Murrill, Bull. Torrey bot. Club 29: 605 (1902).

Figs 3I, 9

≡ *Fomes parvulus* (Murrill) Sacc. & D. Sacc, Syll. Fung. (Abellini). 17: 123 (1905).

Type: NICARAGUA, s.d., C. L. Smith s.n. (type: NYBG 985699!).

= *Fomes stipitatus* Murrill, Bull. Torrey Bot. Club. 30(4): 229 (1903).

≡ *Ganoderma stipitatum* (Murrill) Murrill, N. Amer. Fl. (New York) 9(2): 122 (1908).

Type: NICARAGUA, 1891, Smith C. L. and Shimek B.s.n. (isotype: NY 985679!).

= *Fomes subamboinensis* Henn., Hedwigia 43(3): 175 (1904) [MB148868].

≡ *Ganoderma subamboinense* (Henn.) Bazzalo & J.E. Wright ex Moncalvo & Ryvar-den, Synopsis Fungorum 11: 82 (1997).

≡ *Ganoderma subamboinense* var. *subamboinense* Bazzalo & J.E. Wright (invalid name).

Description. *Basidiocarps* annual, stipitate or with a contracted base, woody, solitary or gregarious, applanate to sulcate, irregular to tuberculate, dimidiate

to semicircular, 1.5–8 × 0.7–12.3 × 0.5–2 cm; **pileus** surface laccate or dull, sulcate, crustose, rugulose to glabrous, vinaceous-brown, vinaceous-black, reddish-brown, brownish-black to yellowish-brown, yellowish-red, margin obtuse, vinaceous-brown, reddish-brown, yellowish-red or yellowish-brown, azonate or with yellowish-brown, brownish-black or reddish-brown zones; **context** duplex, corky, yellowish-brown to beige, becoming darker, vinaceous-brown to reddish-brown, just above the tubes, with two horizontal bands of melanoid substances, sometimes more like deposits than bands, that originate from the base of the stipe, 2–17 mm thick, becoming dark with KOH; **pore surface** reddish-brown, vinaceous-brown to yellowish-brown, pores circular, 4–7 per mm; tube layers reddish-brown, brownish-black to yellowish-brown, sometimes whitish within; **tubes layers** simple to stratified, 1–8 mm thick. **Stipe** glabrous, sulcate or smooth, laccate or dull, lateral, vinaceous brown, vinaceous-black, vinaceous-red, yellowish-brown or brownish-black, 2.3–8.5 × 0.5–3 × 0.4–3 cm. **Hyphal system** dimitic; contextual generative hyphae inconspicuous, thin or thick-walled, with clamps, 4 µm; skeletal hyphae thick-walled, brown, aseptate, occasionally branched, 3–7 µm in diam. **Cuticular cells** from the pileus cylindrical to clavate, yellowish, with granulations and amyloid reaction on Melzer's Reagent in the apical part, thick-walled, nodulose, 31–66 × 5–10 µm (20–40 × 6–10 µm, Ryvarden (2004)). **Basidia** not observed. **Basidiospores** ovoid, truncate at the distal end; with two walls, connected by inter-wall pillars, brown or subhyaline, negative in Melzer's Reagent, 7–10 × 5–7 µm. **Chlamydo-spores** few, in the context, thick-walled, yellowish-brown, slightly ornamented, 6–8 × 5.5–6 µm; in pure culture, abundant, thick-walled, brown, ornamented, with longitudinal ridges, 8–10 × 6–9 µm.

Descriptions and illustrations. Ryvarden (2000, 2004, as *G. stipitatum*), Cabarroi-Hernández et al. (2019).

Substrata. On hardwood logs.

Altitudinal distribution. Lowlands to highlands. In Costa Rica, this species is more common in the lowlands.

Geographic distribution. Widespread in the Neotropics, reported from south-eastern USA (Florida) to Brazil.

Specimens examined. Costa Rica. Alajuela; Poás, Carrillos, 10°1'41.6"N, 84°16'55.1"W, 800 m elev., M. Mata GA-10 (USJ109860, sequences ITS OQ845473, LSU OQ835189). Cartago; Turrialba, La Amistad Caribe, Parque Nacional Barbilla, sendero El Felino, 9°58'19.7"N, 83°27'50.8"W, 700–800 m elev., 07 Aug 2002, R. Valladares 1372 (CR3537817). Guanacaste: Liberia, Parque Nacional Guanacaste, Estación Biológica Cacao, 10°55'35.4"N, 85°28'2.4"W, 1700 m elev., 4 Jul 1994, J. Carranza JCV 28-94 (USJ53210); Sector Colorado, camino a pozas del Río Colorado, 10°40'3.10"N, 85°29'12.6"W, 150 m elev., 3 Sep 2021, M. Mardones, M. Mata, J. Carranza GA-37 (USJ109790); 10°40'6.9"N, 85°29'9.01"W, 150 m elev., GA-35 (USJ109791); 10°40'5.21"N, 85°28'56.4"W, 150 m elev., GA-38 (USJ109792); GA-46 (USJ109861, sequences ITS OQ845474, LSU OQ835190). Heredia: Santo Domingo, San Luis, carretera Braulio Carrillo, 9°58'28.2"N, 84°4' 4.3"W, 1200 m elev., on *Casuarina* sp., 04 Jul 2018, M. Mardones GA-04 (USJ109789, sequences ITS OQ845470, LSU OQ835187, *TEF* OR022012); 9°58'28.2"N, 84°4'4.3"W, 1200 m elev., 04 Aug 2018, M. Mardones GA-08 (USJ109714, sequence ITS OQ845471). Sarapiquí, Puerto Viejo, Estación Biológica La Selva (OET), 10°26'0.30"N, 84°0'16.8"W,

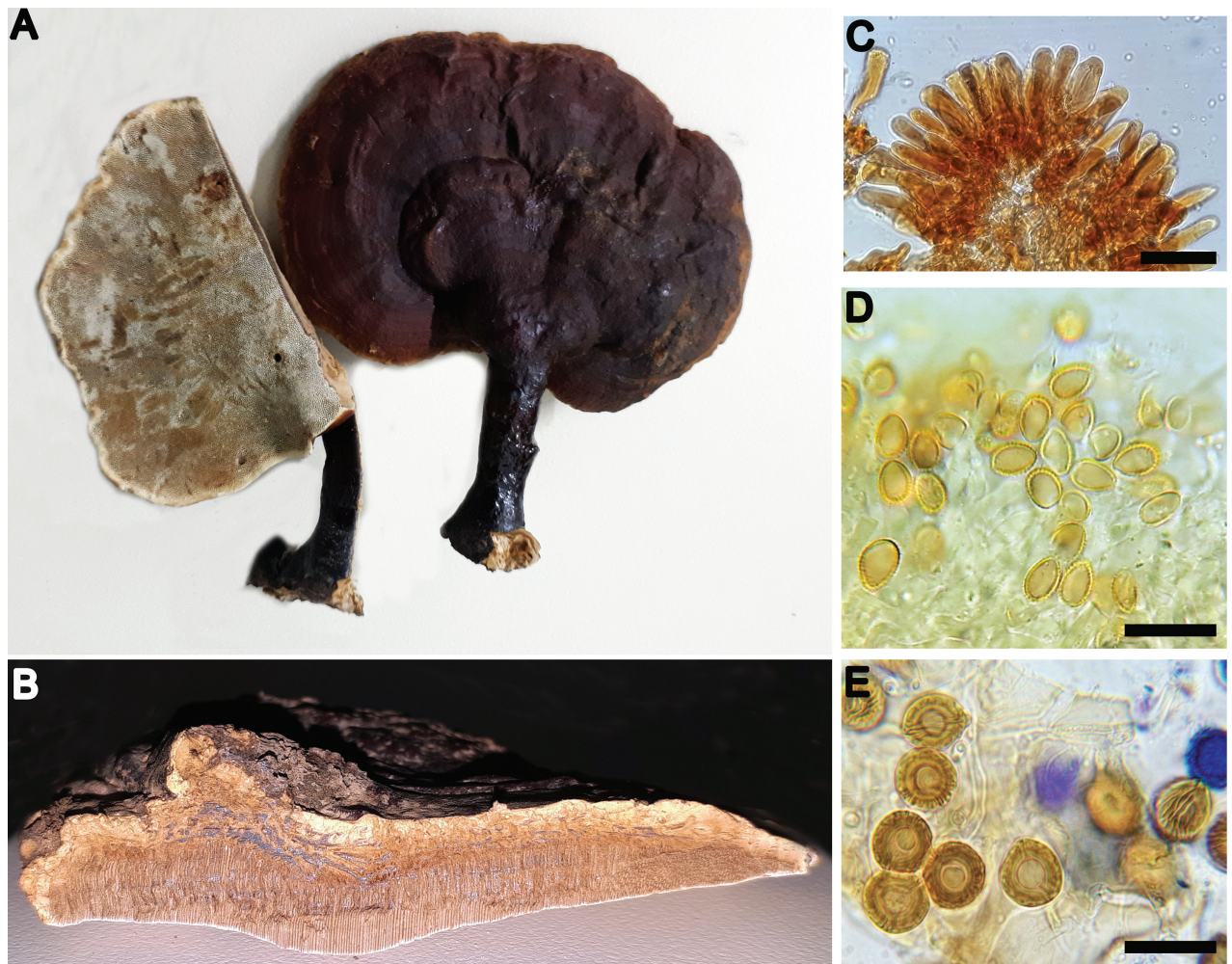


Figure 9. *Ganoderma parvulum* **A** basidiocarp (Fletes 266) **B** context tissue (Fletes 6566) **C** cuticular cells (Fletes 266) **D** basidiospores (Fletes 6566) **E** chlamydospores (GA-09). Scale bars: 10 μ m (**C**); 20 μ m (**D**, **E**).

100 m elev., 23 Jun 2022, J. Carranza JCV 3-16 (USJ109702). Limón: Cantón Central, Reserva Biológica Hitoy Cerere, Sendero Tepezcuintle, 9°40'19.9"N, 83°01'42.9"W, 0–100 m elev., 9 Nov 2002, R. Valladares 1636 (CR3557538); Sixaola, 9°30'25.4"N, 82°36'43.59"W, 10 m elev., 24 Jun 1988, A. Conejo 32-88 (USJ28075). Puntarenas: Coto Brus, San Vito, Área de Conservación La Amistad Pacífico, Zona Protectora Las Tablas, Estación Biológica Las Alturas, sendero a Cerro Echandi, 8°56'56.9"N, 82°49'59.0"W, 1500–1600 m elev., 12 Nov 1999, E. Navarro 1439 (CR1546847). Golfito, Reserva de Vida Silvestre Golfito, sendero La Lechería, 8°39'17.3"N, 83°13'4.8"W, 100–200 m elev., 13 Jun 2003, E. Fletes 5248 (CR3727447); 8°39'18.1"N, 83°13'8.8"W, 100–200 m elev., 09 Feb 1991, J. Carranza JCV 4-91 (USJ33128); Sector el Tajo, 8°40'11.2"N, 83°11'55.4"W, 0–100 m elev., 05 Sep 2004, E. Fletes 6566 (CR3881862). Osa, Parque Nacional Corcovado, Rio Madrigal, quebrada Ceniza, 8°26'53.9"N, 83°30'54.6"W, 200–300 m elev., 19 Mar 2003, E. Fletes 4943 (CR3700175); Parque Nacional Corcovado, Estación Los Patos, márgenes del Rio Rincón, 8°34'27.7"N, 83°30'27.6"W, 80 m elev., 21 Aug 1999, E. Fletes 631 (CR1546789); Parque Nacional Corcovado, orillas del río Pavón, 8°31'1.03"N, 83°35'52.8"W, 100–200 m elev., 27 Feb 2005, E. Fletes 7239 (CR3932787); Parque Nacional Corcovado, Estación Sirena, márgenes del río Sirena, 8°28'51.12"N, 83°35'51.2"W, 0–100 m elev.,

09 Apr 2003, E. Fletes 4999 (CR3717017); sendero Guanacaste, 8°28'56.0"N, 83°35'21.72"W, 10 m elev., 25 Mar 1999, E. Fletes 266 (CR1546586); Sendero Sirena, 8°28'47.8"N, 83°35'46.9"W, 0–30 m elev., on log, 07 Jul 2022, J. Carranza, M. Mardones, E. Fletes GA-56 (USJ109780, sequences ITS OQ845475, LSU OQ835191); Parque Nacional Corcovado, Estación La Leona, Sendero Paraíso, 8°26'49.1"N, 83°31'21.6"W, 0–30 m elev., on log, 10 Sep 2009, J. Carranza JCV 114-09 (USJ83245); Reserva Biológica Isla del Caño, sendero al mirador, 8°42'21.1"N, 83°53'27.0"W, 0–100 m elev., 20 Aug 2003, E. Navarro 7005 (CR3752717). San José: Montes de Oca, San Pedro, Campus UCR, frente a facultad de Medicina, 9°56'19.2"N, 84°3'0.2"W, 1100 m elev., on log of *Casuarina* sp., 04 Oct 1999, J. Carranza JCV 2-99 (USJ71256); 9°56'19.2"N, 84°3'0.2"W, 1100 m elev., 02 Oct 2018, M. Mardones GA-09 (USJ109788, sequences ITS OQ845472, LSU OQ835188); frente a la Facultad de Educación, on log, Nov 1999, A. Ruiz s.n (USJ71255); on log, 09 Aug 2011, J. De León, O. Morales, R. Doss JDL 15-2011 (USJ109685).

Specimens of other species examined for comparison. *Ganoderma pulverulentum*. Grenada. Sep 1905, W.E. Broadway s.n. (lectotype, NYBG 985708). *Ganoderma sessile*. USA. New York: Westchester Co., White Plains, May 1897, L. M. Underwood s.n. (type, NYBG 985711). *Ganoderma sessiliforme*. Mexico. Morelos: Cuernavaca, Gardens, and Barrancas within 3 miles of Cuernavaca, 24 Dec 1909, W. A. Murrill 392 (type, NYBG 985713).

Discussion. *Ganoderma parvulum* is characterised by a laterally stipitate basidiocarp and light-coloured context on the upper part and darker close to the tubes, with melanoid encrustations or bands running from the base of the stipe (like the ones found on *G. curtisii*). According to Cabarroi-Hernández et al. (2019), ornamented chlamydospores in the context and pure culture is the only morphological characteristic distinguishing *G. parvulum* from *G. mexicanum* s.l. Few chlamydospores were observed in *G. parvulum* vouchers collected in Costa Rica and, in some specimens, were totally absent. However, in pure cultures of specimens GA-08 and GA-09, ornamented chlamydospores were numerous (Fig. 9E). In Carranza and Ruiz-Boyer (2001), chlamydospores of the culture JCV 2-99 (as *G. lucidum*) were reported as round to ovoid or elongate and 14–21 × 11–19 µm.

Cabarroi-Hernández et al. (2019) reported much larger basidiospores (11–16 × 9–14.5 µm) than those observed in the Costa Rican specimens (7–10 × 5–7 µm). The size of the basidiospores reported by Ryvar den (2000), as *G. stipitatum*, (7–9.5 × 5–6.5 µm) and Torres-Torres et al. (2012, 8–9 × 6–6.8 µm) agree with our observations. The type specimen under the name *Fomes stipitatus* Murr. collected on dead wood in Nicaragua was examined. It had very much deteriorated, with only a small portion of the pileus and context. No spores were observed, but it had cuticular cells amyloid at the apex, 19.5–24 × 6.8 µm and two melanoid bands are observed in the context. Murrill (1915) reported for *G. parvulum* spores 5 × 4 µm and for *G. stipitatum* 3.5 × 5 µm, both measurements were very small compared with those described by the above authors. The spores observed in the specimen of *G. perzonatum* considered by Steyaert (1980) as *G. parvulum* are larger, 7.7–9.4(–10) × 6–7.7(–8.5) µm, but closer to the ones found on the Costa Rican specimens and the ones reported by other researchers.

Several sequences of specimens of *G. parvulum* are represented in our dataset (GA-04, GA-08, GA-09, GA-10, GA-46, GA-56). The sequences are grouped

in clade IV with good support (1/73) within a subclade containing sequences from several neotropical specimens labelled as *G. parvulum*, *G. mexicanum*, *G. stipitatum*, *G. weberianum* and *G. subamboinense*. *Ganoderma subamboinense* var. *subamboinense* and *G. stipitatum*, neotropical species within the *Ganoderma weberianum-resinaceum* complex, were recently synonymised under *Ganoderma parvulum* (Cabarroí-Hernández et al. 2019).

Excluded and doubtful species of *Ganoderma* in Costa Rica

In addition to the species previously described, there are two additional species of *Ganoderma* that may occur in Costa Rica. However, as there is not enough material or DNA sequences to confirm the identification, they are considered in this study as doubtful taxa.

***Ganoderma chocoense* J.A. Flores, C.W. Barnes & Ordoñez, in Crous et al., *Persoonia* 41: 365 (2018)**

Fig. 3D

Discussion. this species was recently described from Ecuador (Crous et al. 2018). We collected a single specimen (GA-03) in the Braulio Carrillo National Park in north-eastern Costa Rica. Macroscopical characteristics agree with the description in the protologue of *G. chocoense* (Crous et al. 2016).

The BLASTN search and the phylogenetic analyses grouped the ITS sequences of the specimen GA-03 with the sequences of the holotypes of *G. chocoense* (QCAM 3123) and *G. podocarpense* (QCAM-6422) with the highest score in similarity and strong support at the nodes (1/87), respectively. The morphological characteristics of *G. podocarpense* (Crous et al. 2017), a recently described species from Ecuador, are similar to *G. chocoense*. The distinction between both species is unclear and they are probably synonyms. Additional collections and molecular markers of both species are necessary to clarify the circumscription of these species. Considering that we only have a single specimen and the lack of basidiospores in the examined specimen, we believe it is necessary to collect more material before confirming the presence of the species in the country.

Specimens examined. Costa Rica. Heredia: Santo Domingo, San Luis, Parque Nacional Braulio Carrillo, entrada San Josecito, 10°02'57.2"N, 84°01'16.6"W, 1200 m elev., 04 Jul 2018, M. Mardones, J. Carranza, M. Mata GA-03 (USJ109707, sequences ITS OQ845457, LSU OQ835181, *TEF* OR022013).

***Ganoderma applanatum* var. *laevisporum* C.J. Humphrey & Leus-Palo, *Philipp. J. Sci.* 45(4): 533 (1931)**

Discussion. During the examination of *G. applanatum* specimens from Costa Rica, we found four relatively old specimens (JCV16-95, Navarro 8458, Navarro 3699, USJ109859) that agreed with the description of *G. applanatum* var. *laevisporum* (Humphrey and Leus 1931; Wang et al. 2009). This species has been reported for Java, Philippines and mainland China. It is characterised

by its sessile basidioma with a dull upper surface and the basidiospores with smooth wall. According to Wang et al. (2009), the species is distributed at higher elevations in the Tropics, matching with our records, since our specimens were collected above 1800 m a.s.l. The basidiospore size of our specimens ($9\text{--}11 \times 6\text{--}7 \mu\text{m}$) agree with those reported by Humphrey and Leus (1931, $9.3\text{--}10.3\text{--}10.8 \times 5.4\text{--}5.9\text{--}6.4 \mu\text{m}$) and Wang et al. (2009, $9.2\text{--}10.5 \times 5.5\text{--}6.5 \mu\text{m}$). According to Steyaert (1972), *G. applanatum* var. *laevisporum* is a synonym of *G. tornatum* (for a complete discussion on this topic, see Wang et al. (2009)). As we only examined four relatively old specimens, have been unable to examine the holotype and it was not possible to obtain DNA or pure cultures from them, this species is excluded from our taxonomic analysis until more specimens and molecular data are available to confirm its presence in Costa Rica.

Specimens examined. Costa Rica. Alajuela: Grecia, Reserva Forestal Grecia, Bosque del Niño, sendero al acueducto, 26 June 2006, $10^{\circ}8'34.62''\text{N}$, $84^{\circ}14'45.3''\text{W}$, 1800–1900 m elev., J. Carranza JCV16-95 (USJ64962). Puntarenas: Buenos Aires, Parque Nacional La Amistad, Estación Altamira, sendero al Cerro Biolley, $9^{\circ}02'21.6''\text{N}$, $83^{\circ}00'35.9''\text{W}$, 1700–1800 m elev., 20 Jul 2004, E. Navarro 8458 (CR3866211); Estación Pittier, Sendero a Cerro Gemelo, $9^{\circ}02'24.5''\text{N}$, $82^{\circ}57'39.9''\text{W}$, 1800–1900 m elev., 18 Aug 2001, E. Navarro 3699 (CR3459327). San José: Dota, San Gerardo, Albergue de montaña Saavegre, $9^{\circ}33'2.08''\text{N}$, $83^{\circ}48'26.31''\text{W}$, 2000–2300 m elev., 09 Nov 2001, s.n. (USJ109859).

Discussion

Morphological and ITS-phylogenetic-species concept in *Ganoderma* species of Costa Rica

This work represents the first effort to compile the *Ganoderma* species present in Costa Rica. More than 100 specimens were examined, including previously reported taxa for the entire country. Each specimen was characterised morphologically, identified and compared with the type specimen, when available. Afterwards, the sequence data were generated to confirm the morphological identification by using phylogenetic analyses, to improve the molecular identification of the neotropical *Ganoderma* spp., based on the broadly used marker ITS (Schoch et al. 2012), in conjunction with re-description, photographs and a key for the neotropical species of *Ganoderma*.

Based on the morphological analyses, we conclude that five morphological characteristics are diagnostic within neotropical *Ganoderma* collections: (i) the distinction between stipitate and sessile basidiome; (ii) the colour of the context tissue; (iii) the presence and shape of melanised deposits in the context; (iv) the presence or absence of chlamydospores; and (v) the shape and size of the basidiospores. These findings agree with previous morphological analyses of neotropical species of *Ganoderma* (Torres-Torres and Guzmán-Dávalos 2012; Loyd et al. 2018). Some variations in the resinous deposits or melanoid bands in the context were related to the state of basidiocarp development, but it seems that they are present in all the laccate species. For example, in *G. curtisii* and *G. parvulum*, the melanoid bands are more prominent in mature specimens. Amongst non-laccate species, only in *G. australe* have these been observed. Regarding the presence/absence of chlamydospores in some species,

it is important to mention that, for some species, it was necessary to confirm their presence in pure cultures because they were not always present in the basidiocarp, i.e. *G. parvulum*. In general, the chlamydospores' characteristics have been used to distinguish species in culture and not based on the basidiocarp, where they are not always present (Adaskaveg and Gilbertson 1986).

A total of 40 consensus sequences of the ITS, LSU and *TEF* regions from Costa Rican specimens of *Ganoderma* were generated in this study. Before this study, sequences of *G. amazonense* were missing in GenBank and several other species were represented by a few sequences from North or South America. These newly-generated sequences provide data from Central American specimens that will be available for further phylogenetic studies of the genus.

On a global scale, the phylogenetic tree topology obtained in this study is mainly congruent with previously-published clade-specific phylogenies of *Ganoderma*, based on the ITS region (Moncalvo and Buchanan 2008; Loyd et al. 2018; Cabarroi-Hernández et al. 2019; Fryssouli et al. 2020; Sun et al. 2022). The ITS has demonstrated high efficacy in resolving relationships amongst terminal clades within the genus (Fryssouli et al. 2020). It has the advantage of being *Ganoderma*'s best-represented gene region in public repositories. This study resolved eight clades and 34 species or terminal clades (BPP \geq 0.95 and BS \geq 70). However, as several authors pointed out, the use of the ITS region is not enough to clarify the relationships at a higher level or identify complex groups (Cabarroi-Hernández et al. 2019; Sun et al. 2022). In this work, we also identified clades and species that require more molecular markers and additional taxon sampling to be resolved: (i) the phylogenetic position of *G. amazonense* and its relationship with other clades within the genus; (ii) the resolution of the terminal clade of the species *G. curtisii*; (iii) the clade comprising the neotropical species within the *Ganoderma weberianum-resinaceum* complex, specifically the circumscription of the species *G. parvulum*, *G. mexicanum*, *G. subamboinense* var. *subamboinense* and *G. subamboinense* var. *laevisporum*.

The species of *Ganoderma* previously reported for Costa Rica in studies based only on morphological data (Ruiz-Boyer 1998; Carranza and Ruiz-Boyer 2005) were consistent with the results obtained by combining morphology and ITS data. Five taxa previously reported in the country (*G. amazonense*, *G. applanatum*, *G. australe*, *G. oerstedii* and *G. parvulum*) are confirmed in this work, two more taxa are recognised in Costa Rica for the first time: *G. curtisii* and *G. ecuadorensis* and the presence of the species *G. lucidum*, commonly recorded in publications on the fungi of Costa Rica, is rejected.

Before this work, there were nine ITS sequences of *Ganoderma* spp. from Costa Rica deposited in GenBank (Fig. 1). According to the position in the terminal clades of our phylogeny, they belong to *G. australe* (JMCR128), *G. parvulum* (INBFletes 7616), *G. podocarpense* (JV1504/126), *G. oerstedii* (as *G. tuberculosum*, JV1607/62) and several unidentified sequences (JMCR132, JMCR55, JMCR142, JMCR25, JMCR41), forming a terminal clade within clade VI. The only one of these species whose presence in Costa Rica was not confirmed by our morphological analyses is *G. podocarpense*. However, the validity of this species must be confirmed (see discussion of *G. chocoense*). The voucher was not deposited in an indexed collection, nor were duplicates deposited in a local collection, so examining it was not possible. On the other hand, the terminal clade that grouped the unidentified sequences correspond to 'clade 7'

in the study of Moncalvo and Buchanan (2008) of the *G. applanatum-australe* species complex and to clade named as *Ganoderma* sp. E1 in Fryssouli et al. (2020). These sequences were grouped within a well-supported clade with the sequence of our specimen GA-27 and two sequences labelled as *G. tornatum* and *G. lobatum*. According to Fryssouli et al. (2020), the identification of the sequences as *G. tornatum* and *G. lobatum* is incorrect and the specimens should be re-examined along with the corresponding type material. Therefore, although this terminal clade could represent a new species, we assume a cautious position here until the type material is examined and more molecular markers and specimens are available.

In this study, we report seven *Ganoderma* species in Costa Rica and, with additional information obtained in further studies, the presence of at least three more species could be confirmed. Costa Rica has high species richness when compared to the number of species registered for other countries in the region with a much larger area. For example, recent studies of the genus by de Lima et al. (2014) in Brazil, Torres-Torres et al. (2015) in Mexico and Loyd et al. (2018) in the USA report 18, 12 and 13 species, respectively.

Species of *Ganoderma* with neotropical distribution

A dichotomous key is presented for the 14 species of *Ganoderma* confirmed for the Neotropics by morphological and molecular analyses (*G. amazonense*, *G. australe*, *G. applanatum*, *G. chocoense*, *G. concinnum*, *G. curtisii*, *G. ecuadorense*, *G. martinicense*, *G. mexicanum*, *G. multiplicatum*, *G. oerstedii*, *G. orbiforme*, *G. parvulum*, *G. zonatum*).

Although we found 38 *Ganoderma* species reported in literature for the Neotropical Region, some species were not considered in the dichotomous key since: (i) lack of molecular data (*G. chalceum* (Cooke) Steyaert, *G. citriporum* Ryvarden & Iturr., *G. elegantum* Ryvarden, *G. guianense* Decock & Ryvarden, *G. longistipitatum* Ryvarden, *G. multicornum* Ryvarden, *G. nitidum* Murrill, *G. platense* Speg., *G. perzonatum*, *G. vivianimercedianum* M. Torres); (ii) recent studies confirm their distribution outside the Neotropics (*G. gibbosum*, *G. resinaceum*); (iii) doubts about the species circumscription or uncertain DNA annotation (*G. podocarpense*, *G. lobatum*, *G. tornatum*, *G. subfornicatum*); or (iv) synonymised names (*G. annulare* (Lloyd) Boedijn, *G. tuberculosum*, *G. meredithae*, *G. sessiliforme*) or transferred to other genera (*Haddowia neurospora* (J.S. Furtado) Teixeira, *Humphreya coffeata* (Berk.) Steyaert, *Tomophagus colossus*).

Key to *Ganoderma* species with neotropical distribution

- 1 Basidiocarp non-laccate, dull, stipitate, sessile or with a contracted base, yellowish-white, yellowish-brown, brownish-grey, reddish-black to brownish-black.....**2**
- Basidiocarp laccate, shiny, stipitate, sessile or with a contracted base, reddish-brown, reddish-orange or yellowish-brown.....**5**
- 2 Basidiocarp stipitate, with contracted base or sessile, context yellowish-white, spores 8–10 × 6–7 μm..... ***G. amazonense***
- Basidiocarp sessile or with contracted base, context yellowish-brown, dark brown, reddish-brown, to vinaceous-brown, spores 7–12 × 4.7–8 μm**3**

- 3 Context yellowish-brown, purple-brown to vinaceous-brown, with resinous deposits or melanoid bands, spores $7-12 \times 5-8 \mu\text{m}$ ***G. australe***
 – Context reddish-brown to vinaceous-brown, without resinous deposits or melanoid bands, spores $7-11 \times 4.7-8 \mu\text{m}$ **4**
- 4 Spores $7-10 \times 5-6 \mu\text{m}$ ***G. applanatum***
 – Spores $8.9-11 \times 4.7-6.4 \mu\text{m}$ ***G. chocoense***
- 5 Context yellowish-brown, light brown, with or without resinous deposits or with discontinuous melanoid bands **6**
 – Context yellowish-brown, dark-brown, reddish-brown, vinaceous-brown, with resinous deposits, continuous or discontinuous melanoid bands..... **10**
- 6 Resinous deposits or several melanoid bands present, chlamydospores absent in the context, spores $12-14 \times 7-8 \mu\text{m}$ ***G. concinnum***
 – Resinous deposits or inconspicuous melanoid bands present or absent, chlamydospores present or absent in context, spores $9-15 \times 5-8.4 \mu\text{m}$ **7**
- 7 Chlamydospores present, melanoid bands present, spores $6.5-15 \times 4.2-11 \mu\text{m}$ **8**
 – Chlamydospores absent, melanoid bands absent, spores $11.2-15 \times 5.6-8.4 \mu\text{m}$ ***G. zonatum***
- 8 Spores $(7.5-)8-10.6 \times (4.2-)6-8 \mu\text{m}$, chlamydospores in context $8-9 \times 6-7 \mu\text{m}$ ***G. mexicanum***
 – Spores $8-15 \times 5-11 \mu\text{m}$, chlamydospores in context $13.5-30 \times 12.2-21 \mu\text{m}$ **9**
- 9 Spores $9-13.6 \times 5-8.3 \mu\text{m}$, chlamydospores $13.5-21.1 \times 12.2-17.3 \mu\text{m}$.
 ***G. martinicense***
 – Spores $(8-)11-14(-15) \times (5-)8-11 \mu\text{m}$, chlamydospores in context, $23-30 \times 16-21 \mu\text{m}$ ***G. oerstedii***
- 10 Context with two conspicuous melanoid bands or resinous deposits that originate from the base of the stipe, without chlamydospores, spores $(9-)11-17 \times (7-)8-10 \mu\text{m}$ ***G. curtisii***
 – Context with discontinuous melanoid bands or resinous deposits, spores $7-11 \times 5-7 \mu\text{m}$ **11**
- 11 Context yellowish-brown, vinaceous-brown, reddish-brown, with two discontinuous melanoid bands that originate from the base of the stipe, with few chlamydospores, $6-8 \times 5.5-6 \mu\text{m}$, spores $7-10 \times 5-7 \mu\text{m}$
 ***G. parvulum***
 – Context yellowish-brown to reddish-brown, with resinous deposits or discontinuous melanoid bands not originate from the base of the stipe, without chlamydospores, spores $7-13 \times 5-8 \mu\text{m}$ **12**
- 12 Context yellowish-brown to reddish-brown, cuticular cells with many irregular protuberances and outgrowths, strongly amyloid, spores $9-11.2(-13) \times (-6)6.9-8.6 \mu\text{m}$ ***G. orbiforme***
 – Context yellowish-brown, cuticular cells amyloid or strongly amyloid with protuberances or apical outgrowths, spores $7-10 \times 5-7 \mu\text{m}$ **13**
- 13 Cuticular cells amyloid or strongly amyloid with few or many protuberances, spores $7-8.4(-10) \times 5-6(-6.8) \mu\text{m}$ ***G. multiplicatum***
 – Cuticular cells amyloid with few apical protuberances, spores $8-10 \times 5-7 \mu\text{m}$ ***G. ecuadoreense***

Geographic and altitudinal distribution of *Ganoderma* species in Costa Rica

Only two of the seven Costa Rican species reported here have wide ranges and pantropical distribution: *G. applanatum* and *G. australe*. *Ganoderma applanatum* is reported by some authors as a cosmopolitan species. However, according to Ryvarden (2004), the species is not present in the Tropics, contrary to our results. Nevertheless, as mentioned above, more collections and molecular data are needed to confirm whether *G. applanatum* is present in the Neotropics or it is a closely-related species. The remaining five species seem to have geographic distribution limitations. For example, *G. amazonense* and *G. parvulum* have a restricted neotropical distribution. *Ganoderma oerstedii* is found in sub-neotropical (south Florida) and neotropical regions. *Ganoderma curtisii* has been only collected in the eastern USA and Mexico and its presence in Costa Rica is the southernmost record of this species. Similarly, *G. ecuadoreense* has been reported only in tropical South America, with the report in this study being the northernmost record for the species.

On the other hand, amongst our collections, there were some different altitudinal distributions for some species (Fig. 2). For example, species such as *G. australe*, *G. oerstedii* and *G. parvulum* have been found occurring indistinctly in both lowlands and highlands. On the other hand, species such as *G. amazonense* and *G. ecuadoreense* have been collected only in lowlands, between 0 to 700 m, mainly under 300 m. On the contrary, *G. curtisii* has been collected primarily in highlands above 2000 m.

Conclusion

In conclusion, based on morphological criteria, ecological data and ITS phylogenetic analyses, we have confirmed the presence of seven species of *Ganoderma* in Costa Rica. This study clearly established the circumscription of several species which were historically combined in *G. lucidum* s.l. and broadened the distribution range of two laccate *Ganoderma* species to Central America. It also provides molecular data for three non-laccate *Ganoderma* species, i.e. *G. australe*, *G. applanatum* and *G. cf. chocoense*. Additionally, it lays the foundation for future studies of *Ganoderma*, focused on collecting more material and using additional molecular markers to confirm the presence of species, such as *G. chocoense* and *G. applanatum* var. *laevisporum* in the country and to elucidate the relationships between neotropical species within the complex *G. weberianum-resinaceum*.

Acknowledgements

The authors thank Eida Fletes for her help during the fieldwork. We thank MINAE (SINAC) in Costa Rica for collecting permits and Comisión Institucional de Biodiversidad of the UCR for genetic access permits. The assistance of the Herbaria CR, BPI, NYBG and PIGH curators is gratefully acknowledged for loaning specimens and type material. We thank Beatriz Picado, Catalina

Rosales and Mario Montero for collecting material studied here and Cristofer Coto and Verónica Nuñez for their help with pure cultures. The authors would like to acknowledge the FDACS-DPI personnel Cheryl Roberts, Callie Jones, Lynn Combee, Matthew Moore, for their assistance in obtaining the Sanger sequences from *Ganoderma* samples collected in Florida. Proofreading of this article was performed by Timothy Hippert Kirkby.

Additional information

Conflict of interest

The authors have declared that no competing interests exist.

Ethical statement

No ethical statement was reported.

Funding

This work was funded by Vicerrectoría de Investigación (UCR), projects number 111-B6-A31, 111-C0-143 and 111-B6-771, and FEES-CONARE, project number 111-B8-661.

Author contributions

MM and JCV contributed to the study conception and design and organised the infrastructure and permits. All the authors contributed with specimens and fieldwork. JCV and MMH contributed detailed morphological analyses and photos. XAF and MM isolated and kept the pure cultures. MM and HU generated the DNA sequences from Costa Rica and Florida, respectively. MM conducted molecular and phylogenetic analyses, compiled figures and tables and submitted sequences to GenBank. HU produced the distribution map. MM and JCV wrote the first draft of the manuscript and all authors commented on previous versions. All authors read and approved the final manuscript.

Author ORCIDs

Melissa Mardones  <https://orcid.org/0000-0002-4402-7817>

Hector Urbina  <https://orcid.org/0000-0002-5570-4537>

Data availability

All of the data that support the findings of this study are available in the main text or Supplementary Information.

References

- Adaskaveg JE, Gilbertson RL (1986) Cultural studies and genetics of sexuality of *Ganoderma lucidum* and *G. tsugae* in relation to the taxonomy of the *G. lucidum* complex. *Mycologia* 78(5): 694–705. <https://doi.org/10.1080/00275514.1986.12025312>
- Berrin G, Navarro D, Couturier M, Olivé C, Grisel S, Haon M, Taussac S, Lechat C, Courteuisse R, Favel A, Coutinho PM, Lesage-Meessen L (2012) Exploring the natural fungal biodiversity of tropical and temperate forests toward improvement of biomass conversion. *Applied and Environmental Microbiology* 78(18): 6483–6490. <https://doi.org/10.1128/AEM.01651-12>
- Bolaños AC, Bononi VLR, Gugliotta AM, Muñoz JE (2016) New records of *Ganoderma multiplicatum* (Mont.) Pat. (Polyporales, Basidiomycota) from Colombia and

- its geographic distribution in South America. *Check List* 12(4): 1948. <https://doi.org/10.15560/12.4.1948>
- Cabarro-Hernández M, Villalobos-Arámbula AR, Torres-Torres MG, Decock C, Guzmán-Dávalos L (2019) The *Ganoderma weberianum-resinaceum* lineage: Multilocus phylogenetic analysis and morphology confirm *G. mexicanum* and *G. parvulum* in the Neotropics. *MycKeys* 59: 95–131. <https://doi.org/10.3897/mycokeys.59.33182>
- Cao Y, Wu S-H, Dai Y-C (2012) Species clarification of the prize medicinal *Ganoderma* mushroom “Lingzhi”. *Fungal Diversity* 56(1): 49–62. <https://doi.org/10.1007/s13225-012-0178-5>
- Cao Y, Yuan HS (2013) *Ganoderma mutabile* sp. nov. from southwestern China based on morphological and molecular data. *Mycological Progress* 12: 121–126. <https://doi.org/10.1007/s11557-012-0819-9>
- Carranza J, Ruiz-Boyer A (2001) Cultural studies on some genera of Basidiomycetes (Basidiomycota) from Costa Rica. *Harvard Papers in Botany* 6: 57–84.
- Carranza J, Ruiz-Boyer A (2005) Checklist of polypores of Costa Rica. *Revista Mexicana de Micología* 20: 45–52.
- Coetzee MP, Marincowitz S, Muthelo VG, Wingfield MJ (2015) *Ganoderma* species, including new taxa associated with root rot of the iconic Jacaranda mimosifolia in Pretoria, South Africa. *IMA Fungus* 6(1): 249–56. <https://doi:10.5598/ima fungus.2015.06.01.16>
- Costa-Rezende DH, Robledo GL, Góes-Neto A, Reck MA, Crespo E, Drechsler-Santos ER (2017) Morphological reassessment and molecular phylogenetic analyses of *Amauroderma* s.lat. raised new perspectives in the generic classification of the Ganodermataceae family. *Persoonia* 39(1): 254–269. <https://doi.org/10.3767/persoonia.2017.39.10>
- Costa-Rezende DH, Robledo GL, Drechsler-Santos ER, Morag Glen M, Genevieve Gates G, Madrignac Bonzi BR, Popoff OF, Crespo E, Góes-Neto A (2020) Taxonomy and phylogeny of polypores with ganodermatoid basidiospores (Ganodermataceae). *Mycological Progress* 19(8): 725–741. <https://doi.org/10.1007/s11557-020-01589-1>
- Crous PW, Wingfield MJ, Le Roux JJ, Richardson DM, Strasberg D, Shivas RG, Alvarado P, Edwards J, Moreno G, Sharma R, Sonawane MS, Tan YP, Altés A, Barasubiye T, Barnes CW, Blanchette RA, Boertmann D, Bogo A, Carlavilla JR, Cheewangkoon R, Daniel R, de Beer ZW, de Jesús Yáñez-Morales M, Duong TA, Fernández-Vicente J, Geering AD, Guest DI, Held BW, Heykoop M, Hubka V, Ismail AM, Kajale SC, Khemmuk W, Kolařík M, Kurlí R, Lebeuf R, Lévesque CA, Lombard L, Magista D, Manjón JL, Marincowitz S, Mohedano JM, Nováková A, Oberlies NH, Otto EC, Paguigan ND, Pascoe IG, Pérez-Butrón JL, Perrone G, Rahi P, Raja HA, Rintoul T, Sanhueza RM, Scarlett K, Shouche YS, Shuttleworth LA, Taylor PW, Thorn RG, Vawdrey LL, Solano-Vidal R, Voitk A, Wong PT, Wood AR, Zamora JC, Groenewald JZ (2015) Fungal Planet description sheets: 371–399. *Persoonia* 35(1): 264–327. <https://doi.org/10.3767/003158515X690269>
- Crous PW, Wingfield MJ, Richardson DM, Le Roux JJ, Strasberg D, Edwards J, Roets F, Hubka V, Taylor PW, Heykoop M, Martín MP, Moreno G, Sutton DA, Wiederhold NP, Barnes CW, Carlavilla JR, Gené J, Giraldo A, Guarnaccia V, Guarro J, Hernández-Restrepo M, Kolařík M, Manjón JL, Pascoe IG, Popov ES, Sandoval-Denis M, Woudenberg JH, Acharya K, Alexandrova AV, Alvarado P, Barbosa RN, Baseia IG, Blanchette RA, Boekhout T, Burgess TI, Cano-Lira JF, Čmoková A, Dimitrov RA, Dyakov MY, Dueñas M, Dutta AK, Esteve-Raventós F, Fedosova AG, Fournier J, Gamboa P, Gouliamova DE, Grebenc T, Groenewald M, Hanse B, Hardy GE, Held BW, Jurjević Ž, Kaewgrajang T, Latha KP, Lombard L, Luangsa-Ard JJ, Lysková P, Mallátová N, Manimohan P, Miller AN, Mirabolfathy M, Morozova OV, Obodai M, Oliveira NT, Ordóñez ME, Otto EC, Paloi

- S, Peterson SW, Phosri C, Roux J, Salazar WA, Sánchez A, Sarria GA, Shin HD, Silva BD, Silva GA, Smith MT, Souza-Motta CM, Stchigel AM, Stoilova-Disheva MM, Sulzbacher MA, Telleria MT, Toapanta C, Traba JM, Valenzuela-Lopez N, Watling R, Groenewald JZ (2016) Fungal Planet description sheets: 400–468. *Persoonia* 36(1): 316–458. <https://doi.org/10.3767/003158516X692185>
- Crous PW, Wingfield MJ, Burgess TI, Carnegie AJ, Hardy GESJ, Smith D, Summerell BA, Cano-Lira JF, Guarro J, Houbraken J, Lombard L, Martín MP, Sandoval-Denis M, Alexandrova AV, Barnes CW, Baseia IG, Bezerra JDP, Guarnaccia V, May TW, Hernández-Restrepo M, Stchigel AM, Miller AN, Ordoñez ME, Abreu VP, Accioly T, Agnello C, Agustin Colmán A, Albuquerque CC, Alfredo DS, Alvarado P, Araújo-Magalhães GR, Arauzo S, Atkinson T, Barili A, Barreto RW, Bezerra JL, Cabral TS, Camello Rodríguez F, Cruz RSHF, Daniëls PP, da Silva BDB, de Almeida DAC, de Carvalho Júnior AA, Decock CA, Delgat L, Denman S, Dimitrov RA, Edwards J, Fedosova AG, Ferreira RJ, Firmino AL, Flores JA, García D, Gené J, Giraldo A, Góis JS, Gomes AAM, Gonçalves CM, Gouliamova DE, Groenewald M, Guéorguiev BV, Guevara-Suarez M, Gusmão LFP, Hosaka K, Hubka V, Huhndorf SM, Jadan M, Jurjević Ž, Kraak B, Kučera V, Kumar TKA, Kušan I, Lacerda SR, Lamlerthton S, Lisboa WS, Loizides M, Luangsa-Ard JJ, Lysková P, Mac Cormack WP, Macedo DM, Machado AR, Malysheva EF, Marinho P, Matočec N, Meijer M, Mešić A, Mongkolsamrit S, Moreira KA, Morozova OV, Nair KU, Nakamura N, Noisripoom W, Olariaga I, Oliveira RJV, Paiva LM, Pawar P, Pereira OL, Peterson SW, Prieto M, Rodríguez-Andrade E, Rojo De Blas C, Roy M, Santos ES, Sharma R, Silva GA, Souza-Motta CM, Takeuchi-Kaneko Y, Tanaka C, Thakur A, Smith MT, Tkalčec Z, Valenzuela-Lopez N, van der Kleij P, Verbeken A, Viana MG, Wang XW, Groenewald JZ (2017) Fungal Planet description sheets: 625–715. *Persoonia* 39: 270–467. <https://doi.org/10.3767/persoonia.2017.39.11>
- Crous PW, Luangsa-Ard JJ, Wingfield MJ, Carnegie AJ, Hernández-Restrepo M, Lombard L, Roux J, Barreto RW, Baseia IG, Cano-Lira JF, Martín MP, Morozova OV, Stchigel AM, Summerell BA, Brandrud TE, Dima B, García D, Giraldo A, Guarro J, Gusmão LFP, Khamsuntorn P, Noordeloos ME, Nuankaew S, Pinruan U, Rodríguez-Andrade E, Souza-Motta CM, Thangavel R, van Iperen AL, Abreu VP, Accioly T, Alves JL, Andrade JP, Bahram M, Baral HO, Barbier E, Barnes CW, Bendiksen E, Bernard E, Bezerra JDP, Bezerra JL, Bizio E, Blair JE, Bulyonkova TM, Cabral TS, Caiafa MV, Cantillo T, Colmán AA, Conceição LB, Cruz S, Cunha AOB, Darveaux BA, da Silva AL, da Silva GA, da Silva GM, da Silva RMF, de Oliveira RJV, Oliveira RL, De Souza JT, Dueñas M, Evans HC, Epifani F, Felipe MTC, Fernández-López J, Ferreira BW, Figueiredo CN, Filippova NV, Flores JA, Gené J, Ghorbani G, Gibertoni TB, Glushakova AM, Healy R, Huhndorf SM, Iturrieta-González I, Javan-Nikkhah M, Juciano RF, Jurjević Ž, Kachalkin AV, Keochanpheng K, Krisai-Greilhuber I, Li YC, Lima AA, Machado AR, Madrid H, Magalhães OMC, Marbach PAS, Melanda GCS, Miller AN, Mongkolsamrit S, Nascimento RP, Oliveira TGL, Ordoñez ME, Orzes R, Palma MA, Pearce CJ, Pereira OL, Perrone G, Peterson SW, Pham THG, Piontelli E, Pordel A, Quijada L, Raja HA, Rosas de Paz E, Ryvarden L, Saitta A, Salcedo SS, Sandoval-Denis M, Santos TAB, Seifert KA, Silva BDB, Smith ME, Soares AM, Sommai S, Sousa JO, Suetrong S, Susca A, Tedersoo L, Telleria MT, Thanakitpipattana D, Valenzuela-Lopez N, Visagie CM, Zapata M, Groenewald JZ (2018) Fungal Planet description sheets: 785–867. *Persoonia* 41(1): 238–417. <https://doi.org/10.3767/persoonia.2018.41.12>
- de Lima N, Baptista G, Malosso E (2014) Delimitation of some Neotropical laccate *Ganoderma* (Ganodermataceae): Molecular phylogeny and morphology. *Revista de Biología Tropical* 62: 1197–1208. <https://doi.org/10.15517/rbt.v62i3.12380>

- Espinosa-García V, Mendoza G, Shnyreva AV, Padrón JM, Trigos Á (2021) Biological activities of different strains of the genus *Ganoderma* spp. (Agaricomycetes) from Mexico. *International Journal of Medicinal Mushrooms* 23: 67–77. <https://doi.org/10.1615/IntJMedMushrooms.2021037451>
- Fryssouli V, Zervakis GI, Polemis E, Typas MA (2020) A global meta-analysis of ITS rDNA sequences from material belonging to the genus *Ganoderma* (Basidiomycota, Polyporales) including new data from selected taxa. *MycKeys* 75: 71–143. <https://doi.org/10.3897/mycokeys.75.59872>
- Furtado JS (1967) Some Tropical species of *Ganoderma* (Polyporaceae) with pale context. *Persoonia* 4: 379–389.
- Gilbertson RL, Ryvarden L (1986) North American polypores. Vol. I. *Fungiflora*, Oslo, Norway, 433 pp.
- Gomes-Silva AC, Ryvarden L, Gibertoni TB (2011) New records of Ganodermataceae (Basidiomycota) from Brazil. *Nova Hedwigia* 92(1–2): 83–94. <https://doi.org/10.1127/0029-5035/2011/0092-0083>
- Gottlieb AM, Wright JE (1999a) Taxonomy of *Ganoderma* from southern South America: Subgenus *Elfvingia*. *Mycological Research* 103(10): 1289–1298. <https://doi.org/10.1017/S095375629800848X>
- Gottlieb AM, Wright JE (1999b) Taxonomy of *Ganoderma* from South America: Subgenus *Ganoderma*. *Mycological Research* 103(6): 661–673. <https://doi.org/10.1017/S0953756298007941>
- Gottlieb AM, Ferrer E, Wright JE (2000) rDNA analyses as an aid to the taxonomy of species of *Ganoderma*. *Mycological Research* 104(9): 1033–1045. <https://doi.org/10.1017/S095375620000304X>
- Hapuarachchi KK, Karunarathna SC, Raspé O, De Silva KHWL, Thawthong A, Wu XL, Kakumyan P, Hyde KD, Wen TC (2018) High diversity of *Ganoderma* and *Amauroderma* (Ganodermataceae, Polyporales) in Hainan Island, China. *Mycosphere* 9: 931–982. <https://doi.org/10.5943/mycosphere/9/5/1>
- Hong SG, Jung HS (2004) Phylogenetic analysis of *Ganoderma* based on nearly complete mitochondrial small-subunit ribosomal DNA sequences. *Mycologia* 96(4): 742–755. <https://doi.org/10.1080/15572536.2005.11832922>
- Humphrey CJ, Leus S (1931) A partial revision of the *Ganoderma applanatum* group, with particular reference to its oriental variants. *Philippine Journal of Science* 45: 483–589.
- Jaramillo DA, Méndez MJ, Vargas G, Stashenko EE, Vasco-Palacios AM, Ceballos A, Caicedo NH (2020) Biocatalytic potential of native basidiomycetes from Colombia for flavour/ aroma production. *Molecules* 25(18): 4344. <https://doi.org/10.3390/molecules25184344>
- Jargalmaa S, Eimes JA, Park MS, Park JY, Oh S-Y, Lim YW (2017) Taxonomic evaluation of selected *Ganoderma* species and database sequence validation. *PeerJ* 5: e3596. <https://doi.org/10.7717/peerj.3596>
- Karsten PA (1881) Enumeratio Boletinearum et Polyporearum Fennicarum, systemate novo dispositarum. *Revue Mycologique Toulouse* 3: 16–19.
- Katoh K, Standley DM (2013) MAFFT multiple sequence alignment software version 7: Improvements in performance and usability. *Molecular Biology and Evolution* 30(4): 772–780. <https://doi.org/10.1093/molbev/mst010>
- Kearse M, Moir R, Wilson A, Stones-Havas S, Cheung M, Sturrock S, Buxton S, Cooper A, Markowitz S, Duran C, Thierer T, Ashton B, Meintjes P, Drummond A (2012) Geneious Basic: An integrated and extendable desktop software platform for the organization and analysis of sequence data. *Bioinformatics* 28(12): 1647–1649. <https://doi.org/10.1093/bioinformatics/bts199>

- Kinge TR, Mih AM (2011) *Ganoderma ryvardense* sp. nov. associated with basal stem rot (BSR) disease of oil palm in Cameroon. *Mycosphere* 2: 179–188.
- Lanfear R, Hua X, Warren DL (2016) Estimating the effective sample size of tree topologies from bayesian phylogenetic analyses. *Genome Biology and Evolution* 8(8): 2319–2332. <https://doi.org/10.1093/gbe/evw171>
- Li TH, Hu HP, Deng WQ, Wu S-H, Wang D-M, Tsering T (2015) *Ganoderma leucocontextum*, a new member of the *G. lucidum* complex from southwestern China. *Mycoscience* 56: 81–85. <https://doi.org/10.1016/j.myc.2014.03.005>
- Lopez-Peña D, Gutierrez A, Hernández-Navarro E, Valenzuela R, Esqueda M (2016) Diversidad y distribución de *Ganoderma* (Polyporales: Ganodermataceae) en Sonora, Mexico. *Botanical Sciences* 94(2): 431–439. <https://doi.org/10.17129/botsci.463>
- Lloyd AL, Held BW, Barnes CW, Schink MJ, Smith ME, Smith JA, Blanchette RA (2018) Elucidating '*lucidum*': Distinguishing the diverse laccate *Ganoderma* species of the United States. *PLoS ONE* 13(7): e0199738. <https://doi.org/10.1371/journal.pone.0199738>
- Luangharn T, Karunaratna SC, Mortimer PE, Hyde KD, Thongklang N, Xu J (2019) A new record of *Ganoderma tropicum* (Basidiomycota, Polyporales) for Thailand and first assessment of optimum conditions for mycelia production. *Mycology* 51: 65–83. <https://doi.org/10.3897/mycokeys.51.33513>
- Martin R, Gazis R, Skaltsas D, Chaverri P, Hibbett D (2015) Unexpected diversity of basidiomycetous endophytes in sapwood and leaves of *Hevea*. *Mycologia* 107(2): 284–297. [Epub2015Jan8] <https://doi.org/10.3852/14-206>
- Mendoza G, Gúzman G, Ramírez-Guillen F, Luna M, Trigos A (2011) *Ganoderma oerstedii* (Fr.) Murrill (Higher Basidiomycetes), a tree parasite species in Mexico: Taxonomic description, rDNA study, and review of its medical applications. *International Journal of Medicinal Mushrooms* 13(6): 545–552. <https://doi.org/10.1615/IntJMedMushr.v13.i6.60>
- Miller MA, Pfeiffer W, Schwartz T (2010) Creating the CIPRES Science Gateway for inference of large phylogenetic trees. 2010 Gateway Computing Environments Workshop (GCE), 8 pp. <https://doi.org/10.1109/GCE.2010.5676129>
- Moncalvo JM, Buchanan PK (2008) Molecular evidence for long distance dispersal across the Southern Hemisphere in the *Ganoderma appplanatum-australe* species complex (Basidiomycota). *Mycological Research* 112(4): 425–436. <https://doi.org/10.1016/j.mycres.2007.12.001>
- Moncalvo JM, Ryvarden L (1997) A nomenclatural study of the Ganodermataceae Donk. *Synopsis Fungorum* 11: 1–114.
- Moncalvo JM, Wang HH, Hseu RS (1995) Phylogenetic relationships in *Ganoderma* inferred from the internal transcribed spacers and 25S ribosomal DNA sequences. *Mycologia* 87(2): 223–238. <https://doi.org/10.1080/00275514.1995.12026524>
- Murrill WA (1902) The Polyporaceae of North America. I. The genus *Ganoderma*. *Bulletin of the Torrey Botanical Club* 29(10): 599–608. <https://doi.org/10.2307/2478682>
- Murrill WA (1908) Polyporaceae, Part 2. *North American Flora* 9(2): 73–131.
- Murrill WA (1915) *Tropical Polypores*. The New Era Printing Co., Pennsylvania, 113 pp.
- O'Donnell K (1993) *Fusarium* and its near relatives. *The Fungal Holomorph: Mitotic, Meiotic and Pleomorphic Speciation in Fungal Systematics*, 225–233.
- Rambaut A, Drummond AJ, Xie D, Baele G, Suchard MA (2018) Posterior summarization in Bayesian phylogenetics using Tracer 1.7. *Systematic Biology* 67(5): 901–904. <https://doi.org/10.1093/sysbio/syy032>
- Rehner SA, Buckley E (2005) A *Beauveria* phylogeny inferred from nuclear ITS and EF1-sequences: Evidence for cryptic diversification and links to *Cordyceps*. *Mycologia* 97(1): 84–98. <https://doi.org/10.3852/mycologia.97.1.84>

- Ronquist F, Teslenko M, van der Mark P, Ayres DL, Darling A, Höhna S, Larget B, Liu L, Suchard MA, Huelsenbeck JP (2012) MrBayes 3.2: Efficient Bayesian phylogenetic inference and model choice across a large model space. *Systematic Biology* 61(3): 539–542. <https://doi.org/10.1093/sysbio/sys029>
- Ruiz-Boyer A (1998) La familia Ganodermataceae (Aphyllophorales) en Costa Rica. *Brevesia* 49–50: 21–37.
- Ryvarden L (2000) Studies in neotropical polypores 2: A preliminary key to neotropical species of *Ganoderma* with laccate pileus. *Mycologia* 92(1): 180–191. <https://doi.org/10.1080/00275514.2000.12061142>
- Ryvarden L (2004) Neotropical polypores, part 1. *Synopsis Fungorum* 19: 69–102.
- Ryvarden L, Johansen I (1980) A preliminary polypores flora of East Africa. *Fungiflora*, Oslo, Norway, 636 pp.
- Schoch CL, Seifert KA, Huhndorf S, Robert V, Spouge JL, Levesque CA, Chen W, Fungal Barcoding Consortium (2012) Nuclear ribosomal internal transcribed spacer (ITS) region as a universal DNA barcode marker for Fungi. *Proceedings of the National Academy of Sciences (PNAS)* 109: 6241–6246. <https://doi.org/10.1073/pnas.1117018109> [Epub 2012 Mar 27. PMID: 22454494; PMCID: PMC3341068]
- Smith BJ, Sivasithamparam K (2000) Internal transcribed spacer ribosomal DNA sequence of five species of *Ganoderma* from Australia. *Mycological Research* 104(8): 943–951. <https://doi.org/10.1017/S0953756200002458>
- Stamatakis A (2014) RAxML version 8: A tool for phylogenetic analysis and post-analysis of large phylogenies. *Bioinformatics* 30(9): 1312–1313. <https://doi.org/10.1093/bioinformatics/btu033>
- Steyaert RL (1972) Species of *Ganoderma* and related genera mainly of the Bogor and Leiden Herbaria. *Persoonia* 7: 55–118.
- Steyaert RL (1980) Study of some *Ganoderma* species. *Bulletin du Jardin botanique national de Belgique* 50: 135–186. <https://doi.org/10.2307/3667780>
- Sun YF, Xing JH, He XL, Wu DM, Song CG, Liu S, Vlasák J, Gates G, Gibertoni TB, Cui BK (2022) Species diversity, systematic revision and molecular phylogeny of Ganodermataceae (Polyporales, Basidiomycota) with an emphasis on Chinese collections. *Studies in Mycology* 101(1): 287–415. <https://doi.org/10.3114/sim.2022.101.05>
- Talavera G, Castresana J (2007) Improvement of phylogenies after removing divergent and ambiguously aligned blocks from protein sequence alignments. *Systematic Biology* 56(4): 564–577. <https://doi.org/10.1080/10635150701472164>
- Torres-Farradá G, Manzano León AM, Rineau F, Ledo Alonso LL, Sánchez-López MI, Thijs S, Colpaert J, Ramos-Leal M, Guerra G, Vangronsveld J (2016) Diversity of ligninolytic enzymes and their genes in strains of the genus *Ganoderma*: Applicable for biodegradation of xenobiotic compounds? *Frontiers in Microbiology* 8: 898. <https://doi.org/10.3389/fmicb.2017.00898>
- Torres-Torres MG, Guzmán-Dávalos L (2005) Notas sobre la variación morfológica de *Ganoderma curtisii* (Ganodermatales, Ganodermataceae) en México. *Revista Mexicana de Micología* 21: 39–47.
- Torres-Torres MG, Guzmán-Dávalos L (2012) The morphology of *Ganoderma* species with a laccate surface. *Mycotaxon* 119(1): 201–216. <https://doi.org/10.5248/119.201>
- Torres-Torres MG, Guzmán-Dávalos L, de Mello Gugliotta A (2012) *Ganoderma* in Brazil: Known species and new records. *Mycotaxon* 121(1): 93–132. <https://doi.org/10.5248/121.93>
- Torres-Torres MG, Ryvarden L, Guzmán-Dávalos L (2015) *Ganoderma* subgenus *Ganoderma* in Mexico. *Revista Mexicana de Micología* 41: 27–45.

- Vu D, Groenewald M, de Vries M, Gehrman T, Stielow B, Eberhardt U, Al-Hatmi A, Groenewald JZ, Cardinali G, Houbraken J, Boekhout T, Crous PW, Robert V, Verkley GJM (2019) Large-scale generation and analysis of filamentous fungal DNA barcodes boosts coverage for kingdom fungi and reveals thresholds for fungal species and higher taxon delimitation. *Studies in Mycology* 92: 135–154. <https://doi.org/10.1016/j.simyco.2018.05.001>
- Wang D-M, Wu S-H, Li T-H (2009) Two records of *Ganoderma* new to mainland China. *Mycotaxon* 108(1): 35–40. <https://doi.org/10.5248/108.35>
- Wang X-C, Xi R-J, Li Y, Wang D-M, Yao Y-J (2012) The species identity of the widely cultivated *Ganoderma*, '*G. lucidum*' (Ling-zhi), in China. *PLoS ONE* 7(7): e40857. <https://doi.org/10.1371/journal.pone.0040857>
- Weir JR (1926) A pathological survey of the para rubber tree (*Hevea brasiliensis*) in the Amazon Valley: 1–130. <https://doi.org/10.5962/bhl.title.108128>
- Welti S, Courtecuisse R (2010) The Ganodermataceae in the French West Indies (Guadeloupe and Martinique). *Fungal Diversity* 43(1): 103–126. <https://doi.org/10.1007/s13225-010-0036-2>
- White TJ, Bruns T, Lee S, Taylor J (1990) Amplification and direct sequencing of fungal ribosomal RNA genes for phylogenetics. In: Innis MA, Gelfand DH, Sninsky JJ, White TJ (Eds) *PCR protocols: A Guide to Methods and Applications*. Academic Press, Cambridge, 315–322. <https://doi.org/10.1016/B978-0-12-372180-8.50042-1>
- Xing J-H, Song J, Decock C, Cui B-K (2016) Morphological characters and phylogenetic analysis reveal a new species within the *Ganoderma lucidum* complex from South Africa. *Phytotaxa* 266(2): 22. <https://doi.org/10.11646/phytotaxa.266.2.5>
- Xing JH, Sun YF, Han YL, Cui BK, Dai YC (2018) Morphological and molecular identification of two new *Ganoderma* species on *Casuarina equisetifolia* from China. *MycKeys* 7: 93–108. <https://doi.org/10.3897/mycokeys.34.22593>
- Yang ZL, Feng B (2013) What is the Chinese “Lingzhi”?—a taxonomic mini-review. *Mycology* 4: 1–4. <https://doi.org/10.1080/21501203.2013.774299>
- Zhou L-W, Cao Y, Wu S-H, Vlasák J, Li D-W, Li M-J, Dai Y-C (2015) Global diversity of the *Ganoderma lucidum* complex (Ganodermataceae, Polyporales) inferred from morphology and multilocus phylogeny. *Phytochemistry* 114: 7–15. <https://doi.org/10.1016/j.phytochem.2014.09.023>

Supplementary material 1

***Ganoderma* of Costa Rica_Linked Data Table Template for Primary Biodiversity Data**

Author: Melissa Mardones

Data type: xlsx

Explanation note: Excel file with linked data table template for primary biodiversity data of the Costa Rican specimens examined in this work.

Copyright notice: This dataset is made available under the Open Database License (<http://opendatacommons.org/licenses/odbl/1.0/>). The Open Database License (ODbL) is a license agreement intended to allow users to freely share, modify, and use this Dataset while maintaining this same freedom for others, provided that the original source and author(s) are credited.

Link: <https://doi.org/10.3897/mycokeys.100.106810.suppl1>

Supplementary material 2

ITS alignment for global *Ganoderma*

Author: Melissa Mardones

Data type: fasta

Explanation note: ITS alignment for global *Ganoderma*, including sequences from Costa Rican specimens included in this work.

Copyright notice: This dataset is made available under the Open Database License (<http://opendatacommons.org/licenses/odbl/1.0/>). The Open Database License (ODbL) is a license agreement intended to allow users to freely share, modify, and use this Dataset while maintaining this same freedom for others, provided that the original source and author(s) are credited.

Link: <https://doi.org/10.3897/mycokeys.100.106810.suppl2>

Supplementary material 3

Bayesian Inference raw phylogenetic tree for ITS sequences of global *Ganoderma*

Author: Melissa Mardones

Data type: tre

Explanation note: Bayesian Inference raw phylogenetic tree for ITS sequences of global *Ganoderma*, performed with the program MrBayes v. 3.2.7a, and including sequences of the Costa Rican specimens generated in this work.

Copyright notice: This dataset is made available under the Open Database License (<http://opendatacommons.org/licenses/odbl/1.0/>). The Open Database License (ODbL) is a license agreement intended to allow users to freely share, modify, and use this Dataset while maintaining this same freedom for others, provided that the original source and author(s) are credited.

Link: <https://doi.org/10.3897/mycokeys.100.106810.suppl3>

Supplementary material 4

Maximum Likelihood raw phylogenetic tree for ITS sequences of global *Ganoderma*

Author: Melissa Mardones

Data type: result

Explanation note: Maximum Likelihood raw phylogenetic tree for ITS sequences of global *Ganoderma*, carried out in RAxML v.8.2.12, and including sequences of the Costa Rican specimens generated in this work.

Copyright notice: This dataset is made available under the Open Database License (<http://opendatacommons.org/licenses/odbl/1.0/>). The Open Database License (ODbL) is a license agreement intended to allow users to freely share, modify, and use this Dataset while maintaining this same freedom for others, provided that the original source and author(s) are credited.

Link: <https://doi.org/10.3897/mycokeys.100.106810.suppl4>

New species of *Hydnotrya* (Ascomycota, Pezizomycetes) from southwestern China with notes on morphological characteristics of 17 species of *Hydnotrya*

Lin Li^{1,2,3}, Shan-Ping Wan⁴, Yun Wang⁵, Naritsada Thongklang^{2,3}, Song-Ming Tang^{2,3}, Zong-Long Luo¹, Shu-Hong Li⁶

1 College of Agriculture and Biological Science, Dali University, Dali 671003, Yunnan, China

2 School of Science, Mae Fah Luang University, Chiang Rai 57100, Thailand

3 Center of Excellence in Fungal Research, Mae Fah Luang University, Chiang Rai, 57100, Thailand

4 College of Resources and Environment, Yunnan Agricultural University, Kunming 650201, Yunnan, China

5 New Zealand Institute for Crop and Food Research Limited, Invermay Agricultural Centre, Private Bag 50034, Mosgiel, New Zealand

6 Biotechnology and Germplasm Resources Institute, Yunnan Academy of Agricultural Sciences, Kunming 650223, Yunnan, China

Corresponding author: Shu-Hong Li (shuhongfungi@126.com)

Abstract

More specimens of *Hydnotrya* have been collected from southwestern China in recent years. Morphological and molecular analyses showed that they belonged to three species of *Hydnotrya*, of which two are new to science, *H. oblongispora* and *H. zayuensis*. The third one was *H. laojunshanensis*, previously reported in 2013. The new species are described, and their relationship to other species of *Hydnotrya* is discussed. *H. laojunshanensis* is re-described in more detail. The main morphological characters of 17 species of *Hydnotrya* are compared and a key to them is provided as well.

Key words: Discinaceae, hypogeous fungi, ITS, morphological diversity, taxonomy



Academic editor: Alfredo Vizzini

Received: 24 May 2023

Accepted: 4 October 2023

Published: 13 November 2023

Citation: Li L, Wan S-P, Wang Y, Thongklang N, Tang S-M, Luo Z-L, Li S-H (2023) New species of *Hydnotrya* (Ascomycota, Pezizomycetes) from southwestern China with notes on morphological characteristics of 17 species of *Hydnotrya*. MycoKeys 100: 49–67. <https://doi.org/10.3897/mycokeys.100.106709>

Copyright: © Lin Li et al.

This is an open access article distributed under terms of the Creative Commons Attribution License (Attribution 4.0 International – CC BY 4.0).

Introduction

Hydnotrya Berk. & Broome is a genus of hypogeous fungi belonging to Pezizomycetes, Ascomycota. It was placed in the family Helvellaceae by Spooner (1992) and Abbott and Currah (1997) but based on the recent molecular analyses it has been shifted into the family Discinaceae (O'Donnell et al. 1997; Hansen and Pfister 2006; Tedersoo et al. 2006; Læssøe and Hansen 2007; Wang et al. 2023). Their ascomata are hollow to convoluted with simple or folded chambers, even nearly solid, lined with recognizable hymenium. *Hydnotrya* species usually forms a symbiotic relationship with both conifer and broadleaf trees and are distributed throughout the northern hemisphere (Trappe 1975; Spooner 1992; Trappe and Castellano 2000; Stielow et al. 2010; Xu et al. 2018; Slavova et al. 2021). There are 22 names listed in the Index Fungorum online database (<http://www.indexfungorum.org/Names/Names.asp>). However, among them, the species *H. jurana* Qué. and *H. carnea* (Corda) Zobel was synonymized with *H. tulasnei* (Berk.) Berk. & Broome (Gilkey 1954; Trappe 1969), *H. ploettneriana*

(Henn.) Hawker, *H. yukonensis* Gilkey and *H. dysodes* Kirschstein with *H. michaelis* (E. Fisch.) Trappe (Soehner 1942; Trappe 1975), and *H. convoluta* (McAlpine) McLennan was renamed as *Peziza jactata* Burds. & Korf (Burdsall-Jr 1968), *H. ellipsospora* Gilkey combined as *P. ellipsospora* (Gilkey) Trappe (Trappe 1979). To date, there are 15 accepted species remaining in the genus *Hydnотrya*.

To date, nine *Hydnотrya* species have been reported in China: *H. cerebri-formis* in Shanxi and Xinjiang, *H. cubispora* in Tibet, *H. michaelis*, *H. tulasnei* and *H. brunneospora* in Jilin (Tao and Liu 1989; Zhang 1991; Xu 2000; Xu et al. 2018), *H. laojunshanensis* and *H. badia* in Yunnan (Li et al. 2013), *H. nigricans* in Sichuan, *H. puberula* in Yunnan and Jilin (Xu et al. 2018).

Over the past two years, more *Hydnотrya* specimens have been collected in southwest China. Based on the morphological and molecular analyses, two new species were detected and described: *H. oblongispora* and *H. zayuensis*. Their relationships with other known *Hydnотrya* species are discussed and a more detailed supplementary description is given to another species *H. laojunshanensis*, previously found in Yunnan. Additionally, the main morphological characteristics of 15 species of *Hydnотrya* are listed and a key to the species of the genus is provided.

Materials and methods

The specimens were collected from Yunnan and Tibet, China. The type and other studied specimens were deposited at the Biological Science Museum of Dali University (BMDLU) and HKAS (Herbarium of Kunming Institute of Botany, Academy Sinica), China.

Descriptions of microscopic and macroscopic characters were based on specimens (BMDLU L20069, L20067, L21197, L21211, L21212, L21215, L21217, L22024, L22027, and HKAS95802) following the methods of Kumar et al. (2017) and Truong et al. (2017). The sections were made with a razorblade by hand, mounted in a 5% KOH solution or water, and then stained with a cotton blue or lactophenol solution. The sections were observed under an Olympus BH-2 microscope. Key colors were obtained from Kornerup and Wanscher (1978).

Total genomic DNA was extracted from the specimen using the OMEGA Plant Genomic DNA Kit. The internal transcribed spacer (ITS) rDNA region was amplified with PCR primers ITS1F and ITS4 (White et al. 1990; Gardes and Bruns 1993; Truong et al. 2017). The large subunit nuclear ribosomal DNA (LSU) region was amplified with the PCR primers LROR and LR5 (Vilgalys and Hester 1990). PCR reactions were performed on a BIO-RAD C1000TM instrument. Thermal cycles with the following settings: initial denaturation for 5 min at 94 °C, followed by 32 cycles of 40 s denaturation at 94 °C, annealing at 56 °C for 40 s for ITS, and 52 °C for 30 s for LSU, extension for 1 min at 72 °C, and final extension at 72 °C for 10 min. The PCR products were verified on 1% agarose electrophoresis gels stained with ethidium bromide. The purification and sequencing of the PCR products was conducted by Sangon Biotech Limited Company (Shanghai, China).

ITS was used for the analysis of *Hydnотrya* species diversity in this study because ITS appears as a useful locus for the delimitation of *Hydnотrya* species. 46 ITS sequences from NCBI and this study representing 14 species of *Hydnотrya* (Table 1), including *Gyromitra infula* (Schaeff.) Qué. and *Gyromitra esculenta*

Table 1. Taxa information and GenBank accession numbers of the sequences used in this study. The newly generated sequences are in bold.

Species name	Voucher	Origin	GenBank No.	Reference
<i>Gyromitra esculenta</i>	Gyr3	France	AJ544208	Kellner et al. (2007)
<i>Gyromitra esculenta</i>	m954	UK	AJ544209	Kellner et al. (2007)
<i>Gyromitra infula</i>	UBC F15196	Canada	DQ384573	GenBank
<i>Gyromitra infula</i>	Vellinga GLM	USA	AJ698480	Kellner et al. (2007)
<i>Hydnотrya badia</i>	BJTC:FAN270	China	NR_161070	Yu et al. (2018)
<i>Hydnотrya badia</i>	BJTC:FAN270	China	MH445399	Yu et al. (2018)
<i>Hydnотrya baillii</i>	PRM 902032	Czech	AM261522	Stielow (2010)
<i>Hydnотrya baillii</i>	P.Reil_2	Germany	GQ140239	Stielow (2010)
<i>Hydnотrya baillii</i>	P.Reil	Germany	GQ140238	Stielow (2010)
<i>Hydnотrya baillii</i>	997	Germany	GQ149465	Stielow (2010)
<i>Hydnотrya baillii</i>	979	Germany	GQ149464	Stielow (2010)
<i>Hydnотrya brunneospora</i>	HMAS 97138	China	NR_161073	Yu et al. (2018)
<i>Hydnотrya brunneospora</i>	HMAS 97138	China	MH445404	Yu et al. (2018)
<i>Hydnотrya cerebriformis</i>	89_A12_Stielow	Germany	GQ140236	Stielow (2010)
<i>Hydnотrya cerebriformis</i>	87_G11_Stielow	Germany	GQ140235	Stielow (2010)
<i>Hydnотrya cerebriformis</i>	BJTC:FAN647	China	MH430537	Yu et al. (2018)
<i>Hydnотrya cerebriformis</i>	GO-2010-097	Mexico	KC152120	Piña-Páez et al. (2017)
<i>Hydnотrya cerebriformis</i>	GO-2009-455	Mexico	KC152118	Piña-Páez et al. (2017)
<i>Hydnотrya cerebriformis</i>	GO-2009-242	Mexico	KC152119	Piña-Páez et al. (2017)
<i>Hydnотrya cubispora</i>	SAT-13-273-01	USA	MZ054357	GenBank
<i>Hydnотrya cubispora</i>	K(M)104976	UK	EU784273	Brock et al. (2009)
<i>Hydnотrya laojunshanensis</i>	YAAS L2425	China	NR_132886	Li et al. (2013)
<i>Hydnотrya laojunshanensis</i>	BMDLU L21211	China	ON982580	This study
<i>Hydnотrya laojunshanensis</i>	BMDLU L21212	China	ON982593	This study
<i>Hydnотrya laojunshanensis</i>	BMDLU L21215	China	ON982594	This study
<i>Hydnотrya laojunshanensis</i>	BMDLU L21197	China	ON982592	This study
<i>Hydnотrya laojunshanensis</i>	HKAS95802	China	OP908303	This study
<i>Hydnотrya michaelis</i>	K(M)61643	UK	EU784275	Brock et al. 2009
<i>Hydnотrya michaelis</i>	K(M)38647	UK	EU784274	Brock et al. 2009
<i>Hydnотrya michaelis</i>	6463-307EMC	Germany	HM146816	Cox et al. 2010
<i>Hydnотrya nigricans</i>	BJTC:FAN349	China	NR_161071	Yu et al. 2018
<i>Hydnотrya nigricans</i>	BJTC:FAN349	China	MH445400	Yu et al. 2018
<i>Hydnотrya oblongispora</i>	BMDLU L20067	China	OM232075	This study
<i>Hydnотrya oblongispora</i>	BMDLU L20069(Holotype)	China	OM232079	This study
<i>Hydnотrya oblongispora</i>	BMDLU L21217	China	OM232084	This study
<i>Hydnотrya puberula</i>	BJTC:FAN721	China	NR_161072	Yu et al. 2018
<i>Hydnотrya puberula</i>	BJTC:FAN721	China	MH445401	Yu et al. 2018
<i>Hydnотrya puberula</i>	HMAS96758	China	MH445402	Yu et al. 2018
<i>Hydnотrya tulasnei</i>	K(M)99871	UK	EU784276	Brock et al. 2009
<i>Hydnотrya tulasnei</i>	Berk. & Broome C34659	Denmark	AJ969621	Tedersoo et al. 2006
<i>Hydnотrya tulasnei</i>	IT8	Germany	GQ140240	Stielow 2010
<i>Hydnотrya tulasnei</i>	605040	Russia	KY401249	GenBank
<i>Hydnотrya variiformis</i>	TK1615	USA	AY558770	Izzo et al. 2005
<i>Hydnотrya zayuensis</i>	BMDLU L22024	China	OP908304	This study
<i>Hydnотrya zayuensis</i>	BMDLU L22027 (Holotype)	China	OP908305	This study
<i>Hydnотrya</i> sp1.	SNF160	USA	AY558768	Izzo et al. 2005
<i>Hydnотrya</i> sp2.	SNF82	USA	AY558769	Izzo et al. 2005
<i>Hydnотrya</i> sp3.	JT19176	USA	MN653030	GenBank
<i>Hydnотrya</i> sp4.	JT19085	USA	MN653044	GenBank
<i>Hydnотrya</i> sp5.	JLF2015	USA	MH220061	GenBank

Pers. ex Fr. as outgroups (Fig. 1). All *Hydnотrya* ITS sequences were extracted with an ascoma. Sequences of *Hydnотrya* species generated in this study were submitted to the GenBank database. We first used the Basic Local Alignment Search Tool for the GenBank database to recheck whether the newly generated sequences were amplified DNA from contaminant or not and examine clusters with closely related sequences. DNA sequences were retrieved and assembled using SeqMan. Sequence alignments were aligned using MAFFT version 7 (Kato and Standley 2013), ITS gene was analyzed using BioEdit v. 7 (Hall 2007) Maximum Likelihood (ML) analysis was performed using RAXML-HPC2 v. 8.2.12 (Stamatakis 2014) as implemented on the Cipres portal (Miller et al. 2011), with the GTR+G+I model and 1,000 rapid bootstrap (BS) replicates for all genes. A reciprocal 70% bootstrap support approach was used to check for conflicts between the tree topologies from individual genes. As the topology of the ML tree and the Bayesian tree are similar, the ITS1, ITS2, and 5.8s sequences were combined using SequenceMatrix (Vaidya et al. 2011), partitioned phylogenetic analyses. For Bayesian Inference (BI), the best substitution model for each partition was determined by MrModeltest 2.2 (Nylander et al. 2004). The result suggested that ITS1: JC+I, 5.8S: GTR+G+I, ITS2: K80+I+G. Bayesian analysis was performed using MrBayes ver. 3.2.7a (Ronquist et al. 2011) on the Cipres (Miller et al. 2011), four parallel runs, were performed for 10 million generations sampling every 100th generation for the single gene trees. Parameter convergence > 200 was verified in Tracer v. 1.7 (Rambaut et al. 2018). The phylogenetic clade was strongly supported if the bootstrap support value (BS) was $\geq 70\%$ and/or a posterior probability (PP) < 0.01.

Results

Phylogenetic analysis

The ML and Bayesian analyses of the 50 ITS sequences, are shown in Fig. 1 with associated bootstrap supports for branches.

In the phylogenetic tree, the 46 ITS sequences from *Hydnотrya* ascomata revealed the phylogenetic relationship of 14 species: Clade 1 includes 5 sequences of *H. bailii* from Europe. Clade 2 includes 2 sequences of *H. brunneospora* from China. Clade 3 includes 4 sequences of *H. tulasnei* from Europe. Clade 4 includes 3 sequences of *H. puberula* from China. Clade 5 includes 2 sequences of *H. badia* from China. Clade 6 includes 2 sequences of *H. nigricans* from China. Clade 7 includes 6 sequences of *H. cerebriformis* from Germany, China, and Mexico; two other distinct clades were revealed, one comprising Eurasian specimens, and the other comprising specimens from Mexico, which is probably because these specimens, respectively, are from Holarctic and Neotropical regions. Clade 8 includes 3 sequences of *H. variiformis* from the USA. Clade 9 includes 2 sequences of *H. cubispora* from the UK and USA. Clade 10 includes 3 sequences of *H. michaelis* from Europe. Clade 11 includes 3 sequences of new species, *H. oblongispora* from China. Clade 12 includes 3 sequences of *Hydnотrya* sp. from the USA. They may be new species from North America that have not yet been reported. Clade 13 includes 6 sequences of *H. laojunshanensis* from China. When the latter was reported, only one specimen was found, and many more were collected over the past few years, so new DNA sequences of

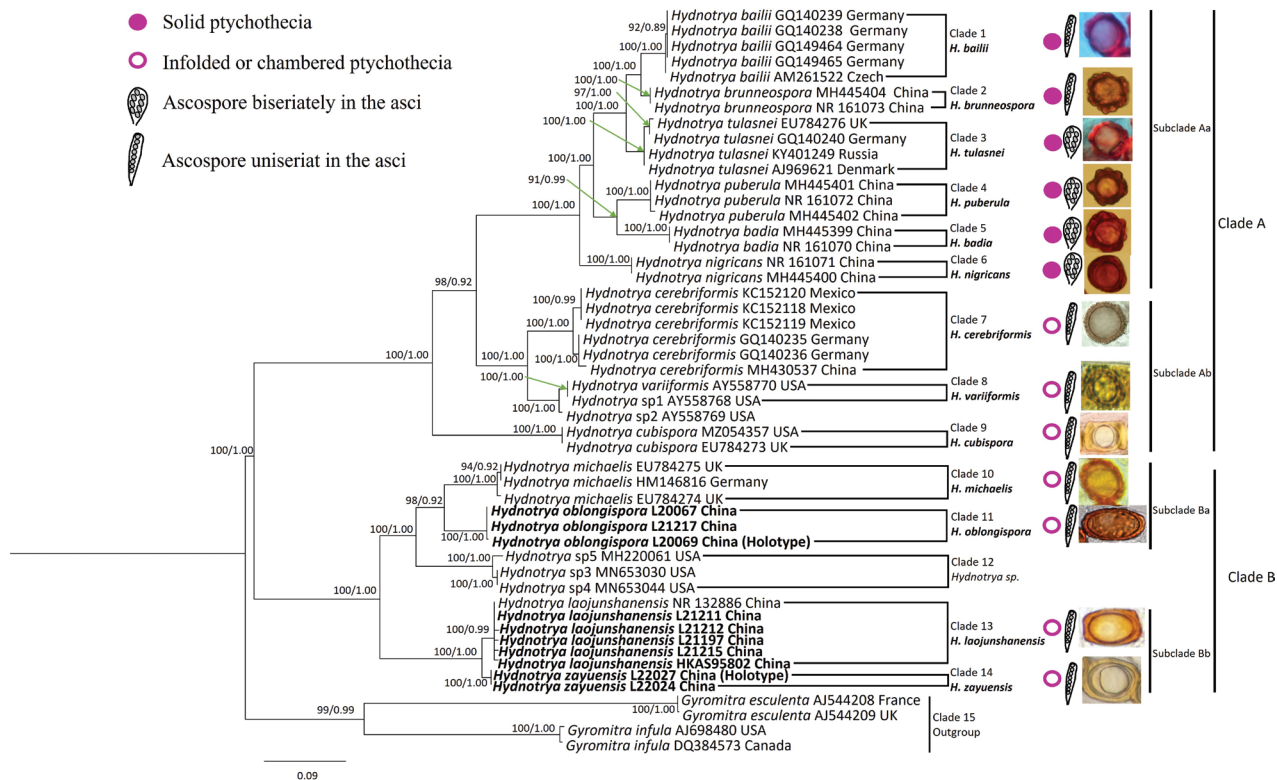


Figure 1. Phylogeny derived from a maximum likelihood (ML) analysis of the nrDNA-ITS sequences from *Hydnотrya* species, using *Gyromitra esculenta* and *G. infula* as outgroup. Values next to nodes reflect, maximum likelihood bootstrap support values (BS), left, and Bayesian posterior probabilities (PP), right. Names of novel species and samples with newly generated sequences in bold. Symbols by taxon names indicate specific fruiting body types, the arrangement of the ascospores in the ascus and ascospore appearance.

H. laojunshanensis were added. Clade 14 includes 2 sequences of a new species, *H. zayuensis* from China. The phylogenetic analysis shows that the new species are distinct from other *Hydnотrya* species. In addition to the ITS sequences used in this phylogenetic analysis, the LSU sequences were amplified from the newly supplemented specimens in this study and uploaded to NCBI for future study.

Based on the ITS locus, two major monophyletic lineages are presented, showing a strong sister relationship (BS=100%; PP = 1.0). They are Clade A (including Clade 1–9) and Clade B (include Clade 10–14) respectively. The species included in these two phylogenetic morphologically share commonalities and uniqueness.

Taxonomy

Hydnотrya oblongispora L. Li & S.H. Li, sp. nov.

Mycobank No: 846735

Plate 1

Diagnosis. Differs from other species in the genus *Hydnотrya* by its nearly single-chambered ascomata and long ellipsoidal ascospores.

Etymology. oblongispora, refers to the long ellipsoidal ascospores.

Holotype. CHINA, Yunnan, Lijiang (26°37.00'N, 99°42.00'E), alt. 3737 m, in the forest of *Abies forrestii* Coltm.-Rog, 12 August 2020, Lin Li, BMDLU L20069.



Plate 1. *Hydnotrya oblongispora* **A** young sarcomata **B** mature ascomata with different openings **C** a piece of section of the ascomata in lactophenol cotton blue **D** a peridium section in lactophenol cotton blue **E** a section of paraphyses in 5% KOH **F** a base of asci in lactophenol cotton blue **G** ascospores released from the ascus **H** asci in lactophenol cotton blue **I** an ascus with 8 ascospores **J–L** ascospores under SEM. Scale bars: 1 cm (**A, B**); 100 μm (**C**); 50 μm (**D**); 10 μm (**E–I**); 5 μm (**J, L**); 2 μm (**K**).

Description. Ascomata irregularly globose, 1.0–2.5 cm in diameter when fresh, smooth, sometimes gently folded inward, surface light khaki (4C5) to reddish brown (8D8); nearly single-chambered with a primary apical opening up to 0.2–0.8 cm in diameter, sometimes the opening is just an almost closed seam, white fluffy inside cavity. Elastic and crisp. No special smell was noticed.

Peridium two-layered, 280–340 μm thick, outer layer 80–100 μm thick, composed of light brown (6D8) ellipsoidal or irregular cells, with a red brown (6E8) pigment deposited on the outermost cells; inner layer, 200–240 μm thick, consists of hyaline interwoven hyphae. Gleba chamber hollow, lined with a milky white (4B2) hymenium, hymenial surface fluffy. *Asci* cylindrical, 102.5–138.5 \times 13.0–25.5 μm , 8-spored, thin-walled, narrowed into a long stalk (20–35 μm) at the base, without croziers, arranged in a palisade. *Ascospore* strictly uniseriate, long ellipsoidal, (20.0–) 26.5–39.0 \times (9.5–) 11.0–21.5 μm , $Q = 2.0 \pm 0.03$, hyaline when immature, golden yellow (5B7) when mature, with a thickened exosporium, surface pitted. *Paraphyses* hyaline, straight stick shape, 2.5–5 μm in diam, septate, exceeding the asci by 60–70 μm .

Ecology and distribution. Hypogeous, solitary, or in groups in soil, under *A. forrestii* mixed with shrubs of *Rhododendron* spp., fruiting from late summer to early autumn. Known only from Yunnan Province, China.

Additional specimens examined. CHINA, Yunnan Province, Lijiang, Jiuhe, (26°38.00'N, 99°42.00'E), alt. 3946 m, in the forest of *A. forrestii*, 12.Aug.2020, Lin Li (BMDLU L20067. GenBank: ITS = OM232075, LSU = ON982626); same locality, 19.Sept.2021, Lin Li (BMDLU L21217. GenBank: ITS = OM232084, LSU = ON982625).

Notes. *H. oblongispora* is characterized by its mostly simple-chambered ascomata and golden yellow long-ellipsoid ascospores, especially with pitted surfaces, which differ from all other species of *Hydnотrya*. Molecular analysis also shows that *H. oblongispora* is distinct from other *Hydnотrya* species, although it is closely related to *H. michaelis*. However, *H. michaelis* has convoluted, lobed ascomata and broadly ellipsoid spores with warty ascospores, which differ from this new species.

***Hydnотrya zayuensis* L. Li & S.H. Li, sp. nov.**

MycoBank No: 846736

Plate 2

Diagnosis. Differs from all other species in *Hydnотrya* by its almost single-chambered ascomata, light golden yellow ellipsoidal ascospores.

Etymology. *zayuensis* from Latin, referring to the type locality.

Holotype. CHINA, Tibet, Zayu (28°35.00'N, 98°06.00'E), alt. 3770 m, in a forest of *Abies* sp., 11 August 2022, Lin Li BMDLU L22027.

Description. Ascomata irregularly globose, 1.5–2.5cm in diameter when fresh, smooth, convoluted, almost single-chambered with a primary apical opening, sometimes the opening nearly closed like a seam, white fluffy inside, surface cinnamon (5E8); shrunken, becoming fuzzy when dried, although there are no protruding hyphae cells from the outermost layer of the peridium. Elastic to crisp. No special smell was noticed.



Plate 2. *Hydnotrya zayuensis* **A** ascomata **B** section of ascomata, with hymenium-lined chambers **C** habitat **D** inner surface of ascomata **E** peridium in 5% KOH **F** hymenium **G** asci in 5% KOH **H** paraphyses **I** ascospores in 5% KOH **J–L** ascospores under SEM (L. SEM of a single ascospore cut in half). Scale bars: 1 cm (**A**); 1 mm (**B**); 0.5cm (**D**); 100 μ m (**E**); 50 μ m (**F**); 20 μ m (**G**); 10 μ m (**H**); 10 μ m (**I**); 5 μ m (**J–L**).

Peridium two-layered, 180–250 µm thick, outer layer 40–80 µm thick, composed of ellipsoid or irregular cells, which grow larger toward the surface, with a yellow brown (4C5) pigment deposited on the outermost cells; inner layer, 110–160 µm thick, consisting of hyaline parallel interwoven hyphae. Gleba chamber hollow, lined with off-white (1A2) hymenium when immature; two-layered when mature, the outer layer golden brown (5C7), the inner layer yellowish to whitish (4A2), hymenial surface fluffy. *Asci* cylindrical, 118.5–130.5 × 15.0–22.5 µm, 8-spored, thin-walled, narrowed into a long stalk (20–40 µm) at the base, without croziers, arranged in a palisade. *Ascospore* strictly uniseriate, ellipsoid (shape including the thickened exosporium), (17–)20–30.5 × 15.5–18.0 µm, $Q = 1.5 \pm 0.16$, hyaline, exosporium thin when immature, surface roughness, and looks crumbly, golden yellow (4B8) when mature. *Paraphyses* hyaline, straight stick shape, 1.5–2.5 µm in diam, septate, apical slightly inflated, exceeding the asci by 120–160 µm.

Ecology and distribution. Hypogeous, solitary in the humus under *Abies* sp. mixed with shrubs of *Rhododendron* spp. Fruiting in summer, from July to September. Known only from Zayu, Tibet, China.

Additional specimen examined. CHINA, Tibet, Zayu, 28°47.00'N, 98°21.00'E, alt. 3840 m, in a forest of *Abies* sp., 15.July.2022, Shucheng He (BMDLU L22024. GenBank: ITS = OP908304, LSU = OP908301).

Notes. Morphologically, *H. zayuensis* is similar to *H. laojunshanensis*. However, *H. zayuensis* has much smaller ascospores, and a thinner peridium, as well as lighter colored ascomata. Molecular analysis showed that *H. zayuensis* is distinct from *H. laojunshanensis* and other species of *Hydnotrya*.

***Hydnotrya laojunshanensis* L. Li, D.Q. Zhou & Y.C. Zhao 2013**

MycoBank No: 803968

Plate 3

Description. *Ascomata* irregularly globose, 1.0–3.0 cm in diameter when fresh, brownish orange (6C8), smooth, mostly single-chambered with a primary apical opening to 0.1–0.5 cm in diameter, the opening rarely narrowing into a slit, sometimes folded forming few channels, lined with white fluffy hymenium. Elastic to crisp. No special smell was noticed.

Peridium two-layered, 350–570 µm thick, outer layer 160–200 µm thick, composed of light brown (6E8) angular or irregular cells, inner layer, 220–350 µm thick, consisting of hyaline interwoven hyphae. Gleba chamber hollow, lined with off-white (1A2) hymenium when immature; two-layered when mature, the outer layer orange (6B8), the inner layer yellowish to whitish (4A2), hymenial surface fluffy. *Asci* cylindrical, 331.5–390.5 × 25.5–35.5 µm, 8-spored, thin-walled, narrowed at the base into a long stalk (30–50 µm), without croziers, arranged in a palisade. *Ascospore* strictly uniseriate, ellipsoid (excluding the thickened exosporium), rectangular (with the exosporium), (26.5–)33.0–50.5 × (15.5–)20.5–35.5(–38.0) µm $Q = 1.35 \pm 0.02$, surface rough, reddish orange to golden (6B8) when mature. *Paraphyses* hyaline, straight stick shape, 2.0–6 µm in diam, apical slightly inflated, septate, exceeding the asci by 180–300 µm.

Ecology and distribution. Hypogeous, solitary, or in groups in soil, under *Abies* spp., fruiting from late summer to early autumn. Known only from Yunnan Province, China.



Plate 3. *Hydnotrya laojunshanensis* **A** young sarcomata cut in half **B** mature ascomata with one cut in half **C** infolded and chambered ascoma **D** section of hymenium in 5% KOH **E** a peridium section in 5% KOH **F** ascospores released from asci in 5% KOH **G–I** ascospores under SEM (I. SEM of a single ascospore cut in half). Scale bars: 1 cm (**A**, **B**); 50 μm (**D**, **E**); 20 μm (**F**); 5 μm (**G–I**).

Additional specimens examined. CHINA, Yunnan Province, Laojun mountains, 26°42.00'N, 99°42.00'E, alt. 3786 m, in a forest of *A. forrestii* var. *smithii*, 30.Aug.2012, Lin Li (Holotype, YAAS L2425; GenBank KC878618); Shangri-La,

28°16.00'N, 99°11.00'E, alt. 3978 m, in a forest of *Abies* sp., 19 Aug. 2014, Shanping Wan (HKAS95802 GenBank: ITS = OP908303), Lijiang, 26°42.00'N, 99°58.00'E, alt. 3540 m, in a forest of *A. forrestii*, 12 Sept. 2019, Lin Li (BMDLU L21197 GenBank: ITS = ON982592, LSU = ON982620); Lijiang, 26°56.00'N, 99°32.00'E, alt. 3805 m, in a forest of *A. forrestii*, 21 Sept. 2021, Lin Li (BMDLU L21211 GenBank: ITS = ON982580, LSU = ON982621, BMDLU L21212 GenBank: ITS = ON982593, LSU = ON982622, BMDLU L21215 GenBank: ITS = ON982594, LSU = ON982623).

Notes. When the species was described in 2013 by Li et al., only one collection from Mt. Laojun in Yunnan Province, China, was reported. More specimens of *H. laojunshanensis* have been found at other places in Yunnan since then. We discovered that this species had not only simple chambered ascomata but also folded, chambered ascomata. This species has large, rectangular ascospores (including thickened exosporium) with a rough surface differentiating from other species in *Hydnотrya*.

Discussion

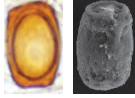
To date, 17 species of *Hydnотrya* (including these two new species) are accepted worldwide (Kirk et al. 2008; Stielow et al. 2010; Li et al. 2013; Xu et al. 2018). The main macroscopic and microscopic characters of these species are provided and discussed based on available literature (Table 2).

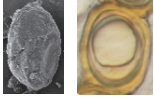
The ascospore morphology is highly variable among different species in *Hydnотrya*, which is useful for distinguishing species. Abbott and Currah (1997) once divided the genus *Hydnотrya* into two subgenera: subg. *Hydnотrya* and *Cerebriformae*, according to the characters of their ornamentation. The subg. *Hydnотrya* had four species of *H. tulasnei*, *H. michaelis*, *H. cubispora*, and *H. variiformis* showing ascospores with rounded or irregular warts. The subg. *Cerebriformae* has only one species of *H. cerebriformi* differs from Subg. *Hydnотrya* in ascospores with short, rounded aculei. However, the current phylogenetic analysis showed that ascospore characteristics were not reliable for differentiating species of *Hydnотrya* into these subgenera (Fig. 1).

Based on ITS analyses, 14 species of *Hydnотrya* are divided into two lineages, A and B. The species in the clade A mostly have nearly solid gleba (6 out of 9) and globose, warty ascospores, either uniseriately or biseriately arranged in asci. The clade A is divided into two subclades: the subclade Aa (clade 1–6) and Ab (clade 7–9). The species in the subclade Aa have solid ascomata. Two groups can be distinguished: the group 1 (clade 1 and 2) and group 2 (clade 3–6), both found in China and Europe. The group 1 contains two species with ascospores uniseriately arranged in asci; the group 2 contains four species with ascospores biseriately arranged in asci. Species in the subclade Ab are distributed in China, Europe, and America, and have hollow ascomata and ascospores uniseriately arranged in asci. The species in the clade B has hollow to chambered gleba and ellipsoidal ascospores (without thickened exosporium), biseriately arranged in asci. The clade B is divided into two groups: Ba and Bb. The group Ba (clade 10 and 11) contains 2 species distributed in China and Europe, with ellipsoidal ascospores, with a pitted surface. The group Bb (clade 13 and 14) contains two species, only found in China, with rectangular and ellipsoidal ascospores (with thickened exosporium), with a rough surface. (Fig. 1).

Table 2. List of main characteristics of *Hydnotrya*.

Species	Ascomata	Gleba	Ascospore	Asci	Host Plants	Distribution	References
<i>Hydnotrya badia</i> L. Fan, Y.W. Wang & Y.Y. Xu 2018	Irregularly subglobose, 7–15 × 14–19 mm diam., surface even, brown to earth brown.	Gleba solid, with numerous variably compacted canals and chambers (usually without empty space).	 Roughly globose, 25–40 µm in diam. including ornamentation, 17.5–27.5 µm in diam. excluding ornamentation, red-brown to reddish, thickened exoperidium with regular large protuberances	Asci broadly clavate to somewhat saccate, sessile, or narrowed at the base into a short stalk, 125–172.5 × 65–75 µm, randomly immersed in paraphyses, 8-spored, spores mostly biseriolate.	<i>Pinus</i> sp.	Huize, China Asia 2000–2900m	Yu et al. 2018
<i>Hydnotrya baijii</i> Soehner 1959	Irregularly subglobose, 10–20(–25) mm diam., dark brown, with deep furrows often with multiple lobes, with one or many openings at the apex, with pleasant aromatic smell.	Gleba solid, dark brown, strongly convoluted cavities.	 Globose, (27.5) 30–34 (–37.5) µm in diam, brown reddish, exoperidium thickening with blistered warts	Asci cylindrical, 250–300×30–40 µm, 8-spored, spores mostly uniseriate.	<i>Picea abies</i>	Europe	Stielow et al. 2010
<i>Hydnotrya brunneospora</i> L. Fan, Y.W. Wang & Y.Y. Xu 2018	Irregularly globose, 20–23 mm diam., dark brown when dry, surface smooth.	Gleba solid, scattered with some small, isolated, and irregularly shaped chambers.	 Roughly globose, 26.25–46.25 µm diam., brown to golden brown at maturity (never reddish), exoperidium thickening with small protuberances.	Asci cylindrical to clavate, narrowed at the base into a short stalk, 162.5–237.5 × 30–47.5 µm, randomly immersed in paraphyses, 8-spored, spores mostly uniseriate.	<i>Betula platyphyllo</i>	Jilin, China Asia	Yu et al. 2018
<i>Hydnotrya cerebriformis</i> Harkn. 1899	Irregular spherical, lobulated, 10–35 × 10–20 mm diam., reddish-brown, cerebriform, with cavities that communicate with the gleba.	Gleba with labyrinthine chambers composed of invagination and fusion from the walls of the ascoma.	 Globose ascospores 20–25µm diam. (x = 22.85 µm), excluding ornamentation, amber-brown, walls 1µm wide. Finely warty ornamentation, warts up to 4µm long.	Asci cylindrical, 175–200 × 25–35 µm, 8-spored, spores mostly uniseriate.	<i>Pinus</i> sp. <i>Abies</i> sp.	Europe North America 3100–4000m	Harkness 1899 Abbott and Currah 1997 Piña-Páez et al. 2017
<i>Hydnotrya confusa</i> Spooner 1992	Ovoid or irregular, size from ca. 20 × 20 × 15 cm up to 40 × 40 × 20 mm, greyish-brown or red-brown, with a primary apical opening and sometimes some smaller secondary openings.	Gleba hollow, with single chambered but mostly cerebriform folded.	 Ovoid or very broad ellipsoid, 38–50 × 28–32 µm, golden brown, exoperidium much thickened, vertically grooved, forming irregular warts.	Asci cylindrical, 290–320 × 38–43 µm, 8-spored, spores mostly uniseriate, clavate at immaturity, with irregular or biseriolate, cylindrical at maturity, strictly uniseriate.	<i>Picea</i> sp.	Europe 361m	Spooner 1992 Bermann and Bandini 2011
<i>Hydnotrya cubispora</i> (E.A. Bessey & B.E. Thoms.) Gilkey 1939	Irregularly globose, 5–10 mm diam., isabella color, with somewhat cerebriform folds radiating distinctly from central opening	Gleba with cavity simple, but somewhat irregular due to surface lobbing.	 Cubical, 47–50 × 23–32µm, including thickening exoperidium, brownish, with maturity.	Asci cylindrical, 100–120 µm long, 8-spored, spores mostly uniseriate.	Coniferous forest	Europe North America	Gilkey 1939 Bryan 2003 K(M)189248
<i>Hydnotrya inordinata</i> Trappe & Castellano, 2000	Irregular globose, 8–30mm diam., dark red-brown, convolute and infolded pythochea with one or a few openings from the interior	Gleba complex, of infolded tramal plates forming canals and chambers 0.5–3mm broad.	 Globose to ellipsoid, 20–30×20–28µm excluding ornamentation, brown-yellow, with aggregated, irregular flexuous spines	Asci cylindrical, ±300 × 25–33 µm, (6–) 8-spored, spores mostly uniseriate.	<i>Abies amabilis</i> <i>Tsuga mertensiana</i>	North America ca 1800m	Trappe and Castellano 2000

Species	Ascomata	Gleba	Ascospore	Asci	Host Plants	Distribution	References
<i>Hydnotrya laojunshanensis</i> Lin Li, D.Q. Zhou & Y.C. Zhao 2013	Irregularly globose, 10–30 mm diam., brownish orange, smooth, mostly single-chambered with a primary apical opening, rare the opening narrowing into a slit, sometimes folded forming a few channels, lined with white fluffy hymenium. No special smell.	Gleba hollow, single-chambered, lined with hyaline, sometimes infolded and whitish to yellowish paraphyses.	 Ellipsoid without thickened exosporium, rectangle (including exosporium), (42.5–) 50.0–57.2(–60.3) × (27.5–)30.4–36.9(–38.2) µm, reddish orange, thickening exosporium with rough surface.	Asci cylindrical, 331.5–390.5 × 25.5–35.5 µm, 8-spored, spores strictly uniseriate	<i>Abies</i> spp.	Yunnan, China Asia 3500–3800m	Li et al. 2013 This study
<i>Hydnotrya michaelsis</i> (E. Fisch.) Trappe 1975	Irregular or subspherical, up to 60 mm across, with rounded opening, wrinkled, lobulate, with numerous invaginations, odor very strong, somewhat pungent, rather persistent.	Gleba labyrinthoid, with large, sinuous cavities, separated by folded inwards portions of ascoma wall.	 Broadly ellipsoid, (21.2–)24.9–29.6(–32.2) × (18.8–)19.8–22.4(–24.9) µm; ornamentation excluded, honey-yellow, exosporium thickened, with conspicuous, irregular, often interconnected warts	Asci cylindrical, 200–220 × 30–35 µm, 8-spored, spores strictly uniseriate	Pinaceae	Europe North America	Trappe 1975 Slavova et al. 2021
<i>Hydnotrya nigricans</i> L. Fan, Y.W. Wang & Y.Y. Xu 2018	Irregular globose, 13 × 9mm, black brown to blackish	Gleba solid, brown, red to dark reddish, with some irregularly shaped and isolated small chambers lined with pale whitish hymenium.	 Irregularly globose, 25.0–37.5 µm in diam., red brown, exosporium unevenly thickened, and usually of trigonal outline in cross section	Asci broadly clavate to saccate, sessile or narrowed at the base into a short stalk, 87.5–190 × 25–62.5 µm, scattered between paraphyses in a hymenium, 8-spored, with spores mostly biseriata.	<i>Pinus</i> sp.	Sichuan, China Asia	Yu et al. 2018
<i>Hydnotrya oblongispora</i> sp. nov.	Irregularly globose, 10–25mm in diam. when fresh, light khaki to reddish brown, smooth, mostly single-chambered with a primary apical opening up to 02–08 mm in diam., sometimes infolded.	Gleba hollow, single-chambered lined with milky white hymenium, hymenium surface fluffy.	 Long-ellipsoid (20.0–) 26.5–39.0 × (9.5–) 11.0–21.5 µm, golden brown, thickened exosporium with pitted surface.	Asci cylindrical, 102.5–138.5 × 13.0–25.5 µm, narrowed at the base into a long stalk (20–30 µm), 8-spored, spores strictly uniseriate	<i>Abies forrestii</i>	Yunnan, China Asia 3500–4000m	This study
<i>Hydnotrya puberula</i> L. Fan, Y.W. Wang & Y.Y. Xu 2018	Irregularly subglobose, 11–20 × 8–19 mm, brown to dark brown, sometimes with purple tints when fresh, much convoluted with deep furrows, ascoma surface tomentulose	Gleba solid, compact, dark brown to purple reddish at maturity, with numerous small chambers.	 Roughly globose, 22.5–42.5 µm in diam., red brown to reddish, exosporium unevenly thickened by irregularly large protuberances.	Asci clavate to saccate, 125–190 × 55–80 µm, sessile or with a short stalk, borne among palisade-like paraphyses in the hymenium, 8-spored, with spores mostly biseriata.	<i>Pinus</i> sp.	Yunnan, China Asia	Yu et al. 2018
<i>Hydnotrya soehneri</i> Svrček, 1955	Irregularly subglobose, tuberous, 10–40 mm wide, reddish and reddish-gray to reddish brown, odor light fragrance	Gleba solid, whitish to yellowish gray, at maturity is colored reddish-brown corridors (from mature spores).	 Spherical, 25–36 (–42), red brown, exosporium thickened, coarsely warty.	Asci mostly cylindrical to saccate, 150–300 × 35–70 µm, 8-spored, mostly incompletely arranged biseriata.	Mixed woods	Europe	Svrček 1955
<i>Hydnotrya subnix</i> Trappe & Castellano, 2000	Irregular subglobose, 50–65mm in diam, dark red-brown, glabrous to minutely roughened. Odor and taste strongly of spicy garlic.	Gleba variable, deeply convoluted and infolded lacking openings from the interior, forming canals and locules 1–10mm broad.	 Globose to rarely ellipsoid, 23–30µm in diam. excluding ornamentation, brown, coarsely warty.	Asci mostly cylindrical, 300–340 × 25–40 µm, 8-spored, mostly incompletely arranged uniseriate	<i>Abies amabilis</i>	North America ca 950m	Trappe and Castellano 2000

Species	Ascomata	Gleba	Ascospore	Asci	Host Plants	Distribution	References
<i>Hydnотrya tulasnei</i> (Berk.) Berk. & Broome, 1846	Irregularly spherical or lobed, sometimes with inward folds, 20–70 mm diam., ochre-reddish to brick red	Gleba solid, later yellow brown, with labyrinthic chambers.	 <p>Globose, 20–30 (–33) µm diam. (including ornamentation), ochre-reddish, with conspicuous, irregular warts.</p>	Asci broadly clavate or cylindrical, 175–210 × 30–62.5 µm, (4–) 8-spored, spores biseriolate.	Coniferous forest	Europe North America ca 1600m	Dimitrova and Gyosheva 2008 Stielow et al. 2010
<i>Hydnотrya variiformis</i> Gilkey, 1947	Globose to subglobose to flattened, somewhat depressed, 7–40 mm broad, cinnamon-buff to cream-buff	Gleba variable, from a simple cavity to extremely lobed with numerous small chambers the interior, usually opening to the exterior at one or more points.	 <p>Ellipsoid, 24–28×36–36 µm, yellow-brown, thickened exosporium wall, surface appearing punctate and with small irregular nodules</p>	Asci 240–280 × 24 µm, 8-spored, clavate at immaturity, spores incompletely biseriolate; cylindrical at maturity, spores strictly uniseriate.	Coniferous forest	North America 1200–2400m	Gilkey 1947 Abbott and Currah 1997 Baug et al. 2014
<i>Hydnотrya zayuensis</i> sp. nov.	Irregularly globose, 15–20 mm in diameter when fresh, smooth, gentle inward folds, surface cinnamon. Mostly single-chambered with a primary apical opening, the opening is just an almost closed seam, white fluffy inside cavity. Elastic and crisp. No special smell.	Gleba hollow, single-chambered with a primary apical opening, sometimes the opening is just an almost closed seam.	 <p>Ellipsoid, (17–)20–30.5 × 15.5–18.0 µm, (including thickened exosporium), golden yellow, surface rough, looking like crumbly.</p>	Asci cylindrical, 118.5–130.5×15.0–22.5 µm, 8-spored, spores strictly uniseriate	Abies sp.	Zayu, China Asia 3770m	This study

Based on the morphological and molecular phylogenetic analyses there seems to be a trend in morphological traits among the species within the genus *Hydnotrya*, that is, the gleba evolved from being hollow or chambered to nearly solid; the ascus becoming shorter and wider, with ascospores arranged from uniseriate to biseriate; ascospores from ellipsoidal to globose, with an ornamentation from smooth to rough as well. This evolutionary trend in the genus *Hydnotrya* is probably related to their hypogeous habits, that is, if the gleba has more chambers, the ascoma will hold more ascospores, and so there are more chances of ascospores to be dispersed by animals that eat them (Hawker 1955; Ławrynowicz 1990; Læssøe and Hansen 2007; Bonito et al. 2013). All of this improves their survival and reproduction. Of course, more collections would be needed for comprehensive morphological and molecular analyses to provide more evidence to support this hypothesis.

In China, 9 species were recorded before this study (Xu et al. 2018). In this paper, two new species are described. 11 species are now known in China, among which 7 species are distributed in southwest China.

Key to species of *Hydnotrya*

- 1 Ascomata hollow, gleba chamber simple or infolded.....2
- Ascomata solid, gleba labyrinthine chambered 11
- 2 Ascospores rectangular or cubical3
- Ascospores ellipsoidal or globose..... 4
- 3 Ascospores cubical.....*H. cubispora*
- Ascospores rectangular..... *H. laojunshanensis*
- 4 Odor distinct, with a special smell5
- Odor not distinct..... 6
- 5 Odor and taste strongly garlic *H. subnix*
- Odor strong pungent and persistent *H. michaelis*
- 6 Ascospores mostly globose 7
- Ascospores ellipsoidal or long ellipsoidal8
- 7 Ascospores globose, with prominent echinate ornamentation
.....*H. cerebriformis*
- Ascospore mostly globose, with aggregated, irregular flexuous spines
..... *H. inordinata*
- 8 Ascospores long ellipsoidal, surface pitted, ascomata mostly single chambered..... *H. oblongispora*
- Ascospores ellipsoidal, Q ratio less than 2..... 9
- 9 Ascospores incompletely biseriate at immaturity, strictly uniseriate at maturity in asci..... 10
- Ascospores strictly uniseriate from immature to mature asci*H. zayuensis*
- 10 Ascospores broadly ellipsoidal, vertically grooved, forming irregular warts *H. confusa*
- Ascospores ellipsoidal, surface appearing punctate and with small irregular nodules *H. variiformis*
- 11 Ascospores mostly uniseriate..... 12
- Ascospores mostly biseriate 13

- 12 Ascospores less than 35 μm^* in length, reddish brown *H. bailii*
- Ascospores up to 46 μm^* in length, brown to golden brown...*H. brunneospora*
- 13 Odor with a light fragrance *H. soehneri*
- Odor not distinct..... **14**
- 14 Ascoma surface tomentose, with purple tints when fresh.....*H. puberula*
- Ascoma not tomentose **15**
- 15 Ascospores without prominent protuberances, trigonal outline in cross section, ascomata blackish*H. nigricans*
- Ascospores with recognizable protuberances **16**
- 16 Ascospores, 20–30 μm diam.* , ochre-reddish, with conspicuous, irregular warts *H. tulasnei*
- Ascospores, 25–40 μm in diam.* , red brown to reddish, with regular large protuberances..... *H. badia*

Acknowledgments

Thanks to Mr. Shucheng He for his help in specimen collection. Thanks to the Fungal Diversity Conservation and Utilization Team in Northwest Yunnan for providing the research platform and team members for their help.

Additional information

Conflict of interest

The authors have declared that no competing interests exist.

Ethical statement

No ethical statement was reported.

Funding

This study was financially supported by the National Natural Science Foundation of China (No. 31800009, 32060008) and the Yunnan Fundamental Research Project (2017FD135).

Author contributions

Data curation: SPW. Methodology: SMT. Writing - original draft: LL. Writing - review and editing: YW, NT, SHL, ZLL.

Author ORCIDs

Lin Li  <https://orcid.org/0009-0000-8167-2965>

Shan-Ping Wan  <https://orcid.org/0000-0002-0794-3701>

Naritsada Thongklang  <https://orcid.org/0000-0001-9337-5001>

Song-Ming Tang  <https://orcid.org/0000-0002-6174-7314>

Zong-Long Luo  <https://orcid.org/0000-0001-7307-4885>

Shu-Hong Li  <https://orcid.org/0000-0001-5806-9148>

Data availability

All of the data that support the findings of this study are available in the main text.

* Including ornamentation.

References

- Abbott SP, Currah RS (1997) The Helvellaceae systematic revision and occurrence in northern and northwestern North America. *Mycotaxon* 62: 1–125.
- Bemmann M, Bandini D (2011) A collection of *Hydnotrya confusa* Spooner 1992 from Southwest Germany. *Ascomycete.Org* 3(3): 55–60.
- Beug M, Bessette AE, Bessette AR (2014) *Ascomycete fungi of North America: a mushroom reference guide*. University of Texas Press. New York, USA, 16–18. <https://doi.org/10.7560/754522>
- Bonito G, Smith ME, Nowak M, Healy RA, Guevara G, Cázares E, Kinoshita A, Nouhra ER, Domínguez LS, Tedersoo L, Murat C, Wang Y, Moreno BA, Pfister DH, Nara K, Zambonelli A, Trappe JM, Vilgalys R (2013) Historical biogeography and diversification of truffles in the Tuberaceae and their newly identified southern hemisphere sister lineage. *PLoS ONE* 8(1): e52765. <https://doi.org/10.1371/journal.pone.0052765>
- Brock PM, Döring H, Bidartondo MI (2009) How to know unknown fungi: The role of a herbarium. *The New Phytologist* 181(3): 719–724. <https://doi.org/10.1111/j.1469-8137.2008.02703.x>
- Bryan L (2003) *Hydnotrya cubispora* in Wales. *Field Mycology* 4(4): 122. [https://doi.org/10.1016/S1468-1641\(10\)60218-6](https://doi.org/10.1016/S1468-1641(10)60218-6)
- Burdsall-Jr HH (1968) A revision of the genus *Hydnocystis* (Tuberales) and of the hypogeous species of *Geopora* (Pezizales). *Mycologia* 60(3): 496–525. <https://doi.org/10.1080/00275514.1968.12018600>
- Cox F, Barsoum N, Lilleskov EA, Bidartondo MI (2010) Nitrogen availability is a primary determinant of conifer mycorrhizas across complex environmental gradients. *Ecology Letters* 13(9): 1103–1113. <https://doi.org/10.1111/j.1461-0248.2010.01494.x>
- Dimitrova E, Gyosheva M (2008) Hypogeous ascomycetes in Bulgaria. *Phytologia Balcanica* 14(3): 309–314.
- Gardes M, Bruns TD (1993) ITS primers with enhanced specificity for basidiomycetes application to the identification of mycorrhizae and rusts. *Molecular Ecology* 2(2): 113–118. <https://doi.org/10.1111/j.1365-294X.1993.tb00005.x>
- Gilkey HM (1939) Tuberales of North America. *Oregon State Monographs. Studies in Botany* 1: 1–63.
- Gilkey HM (1947) New or otherwise noteworthy species of Tuberales. *Mycologia* 39(4): 441–452. <https://doi.org/10.1080/00275514.1947.12017626>
- Gilkey HM (1954) Taxonomic notes on Tuberales. *Mycologia* 46(6): 783–793. <https://doi.org/10.1080/00275514.1954.12024414>
- Hall T (2007) BioEdit 7.0. 5.3 Department of Microbiology, North Carolina State University. <http://www.mbio.ncsu.edu/BioEdit/Bioedit.html>
- Hansen K, Pfister DH (2006) Systematics of the Pezizomycetes—The operculate discomycetes. *Mycologia* 98(6): 1029–1040. <https://doi.org/10.3852/mycologia.98.6.1029>
- Harkness HW (1899) Californian hypogeous fungi. *Proceedings of the California Academy of Sciences* 3: 266.
- Hawker LE (1955) Hypogeous fungi. *Biological Reviews of the Cambridge Philosophical Society* 30(2): 127–158. <https://doi.org/10.1111/j.1469-185X.1955.tb01578.x>
- Izzo AD, Meyer M, Trappe JM, North M, Bruns TD (2005) Hypogeous ectomycorrhizal fungal species on roots and in small mammal diet in a mixed-conifer forest. *Forest Science* 51(3): 243–254.

- Katoh K, Standley DM (2013) MAFFT multiple sequence alignment software version 7: Improvements in performance and usability. *Molecular Biology and Evolution* 30(4): 772–780. <https://doi.org/10.1093/molbev/mst010>
- Kellner H, Luis P, Buscot F (2007) Diversity of laccase-like multicopper oxidase genes in Morchellaceae: Identification of genes potentially involved in extracellular activities related to plant litter decay. *FEMS Microbiology Ecology* 61(1): 153–163. <https://doi.org/10.1111/j.1574-6941.2007.00322.x>
- Kirk PM, Cannon PF, Minter DW, Stalpers JA (2008) *Ainsworth & Bisby's dictionary of the fungi*, 10th edn. CAB International, Wallingford, 325 pp. <https://doi.org/10.1079/9780851998268.0000>
- Kornerup A, Wanscher JH (1978) *Methuen Handbook of Colour* (3rd edn.). Methuen, London, 252 pp.
- Kumar LM, Smith ME, Nouhra ER, Orihara T, Leiva PS, Pfister DH, McLaughlin DJ, Trappe JM, Healy RA (2017) A molecular and morphological re-examination of the generic limits of truffles in the *Tarzetta-Geopyxis* lineage—*Densocarpa*, *Hydnocystis*, and *Paurocotylis*. *Fungal Biology* 121(3): 264–284. <https://doi.org/10.1016/j.funbio.2016.12.004>
- Læssøe T, Hansen K (2007) Truffle trouble: What happened to the Tuberales? *Mycological Research* 111(9): 1075–1099. <https://doi.org/10.1016/j.mycres.2007.08.004>
- Ławrynowicz M (1990) Chorology of the European hypogeous Ascomycetes. II. *Acta Mycologica* 26(1): 7–75. <https://doi.org/10.5586/am.1990.001>
- Li L, Zhao YC, Zhang XL, Su HY, Li SH, Zhou DQ (2013) *Hydnotrya laojunshanensis* sp. nov. from China. *Mycotaxon* 125(1): 277–282. <https://doi.org/10.5248/125.277>
- Miller MA, Pfeiffer W, Schwartz T (2011) The CIPRES science gateway: a community resource for phylogenetic analyses. *Proceedings of the 2011 TeraGrid Conference: extreme digital discovery*. New York, NY, United States, 18 July 2011. Association for Computing Machinery, 1–8. <https://doi.org/10.1145/2016741.2016785>
- Nylander JA, Ronquist F, Huelsenbeck JP, Nieves-Aldrey J (2004) Bayesian phylogenetic analysis of combined data. *Systematic Biology* 53(1): 47–67. <https://doi.org/10.1080/10635150490264699>
- O'Donnell K, Cigelnik E, Weber NS, Trappe JM (1997) Phylogenetic relationships among ascomycetous truffles and the true and false morels inferred from 18S and 28S ribosomal DNA sequence analysis. *Mycologia* 89(1): 48–65. <https://doi.org/10.1080/00275514.1997.12026754>
- Piña-Páez C, Garibay-Orijel R, Guevara-Guerrero G, Castellano MA (2017) Descripción y distribución de *Hydnotrya cerebriformis* (Discinaceae: Pezizales) en México. *Revista Mexicana de Biodiversidad* 88(2): 269–274. <https://doi.org/10.1016/j.rmb.2017.03.017>
- Rambaut A, Drummond AJ, Xie D, Baele G, Suchard MA (2018) Posterior summarization in Bayesian phylogenetics using Tracer 1.7. *Systematic Biology* 67(5): 901–904. <https://doi.org/10.1093/sysbio/syy032>
- Ronquist F, Huelsenbeck J, Teslenko M (2011) Draft MrBayes version 3.2 manual: tutorials and model summaries. [Distributed with the software] <http://brahms.biology.rochester.edu/software.html>
- Slavova M, Assyov B, Denchev TT, Denchev CM (2021) *Hydnotrya michaelis*—an Uncommon Fungus from Unexpected Habitat. *Ecologia Balkanica* 13(1): 167–171.
- Soehner E (1942) *Tuberaceen-Studien*. *Notizblatt des Botanischen Gartens und Museums zu Berlin-Dahlem* 15(5): 762–782. <https://doi.org/10.2307/3995172>

- Spooner BM (1992) A new species of *Hydnотrya* (Helvellaceae) from the British Isles. *Kew Bulletin* 47(3): 502. <https://doi.org/10.2307/4110576>
- Stamatakis A (2014) RAxML version 8: A tool for phylogenetic analysis and post-analysis of large phylogenies. *Bioinformatics* 30(9): 1312–1313. <https://doi.org/10.1093/bioinformatics/btu033>
- Stielow B, Bubner B, Hensel G, Münzenberger B, Hoffmann P, Klenk HP, Göker M (2010) The neglected hypogeous fungus *Hydnотrya bailii* Soehner (1959) is a widespread sister taxon of *Hydnотrya tulasnei* (Berk.) Berk. & Broome (1846). *Mycological Progress* 9(2): 195–203. <https://doi.org/10.1007/s11557-009-0625-1>
- Svrček M (1955) Co jest *Hydnотrya carnea* (Corda) Zobel? *Česká Mykologie* 9(4): 185–189.
- Tao K, Liu B (1989) Preliminary study on *Hydnотrya* from China. *Journal of Shanxi University (Nat. Sci. Ed.)* 12(1): 81–85.
- Tedersoo L, Hansen K, Perry BA, Kjøller R (2006) Molecular and morphological diversity of pezizalean ectomycorrhiza. *The New Phytologist* 170(3): 581–596. <https://doi.org/10.1111/j.1469-8137.2006.01678.x>
- Trappe JM (1969) Comments on Szemere’s “Die Unterirdischen Pilze Des Karpatenbeckens”. *Mycologia* 61(1): 170–174. <https://doi.org/10.1080/00275514.1969.12018711>
- Trappe JM (1975) Generic synonyms in the Tuberales. *Mycotaxon* 2(1): 109–122.
- Trappe JM (1979) The orders, families, and genera of hypogeous Ascomycotina (truffles and their relatives). *Mycotaxon* 9(1): 297–340.
- Trappe JM, Castellano MA (2000) New sequestrate Ascomycota and Basidiomycota covered by the Northwest Forest Plan. *Mycotaxon* 75: 153–179.
- Truong C, Mujic AB, Healy R, Kuhar F, Furci G, Torres D, Niskanen T, Sandoval-Leiva PA, Fernández N, Escobar JM, Moretto A, Palfner G, Pfister D, Nouhra E, Swenie R, Sánchez-García M, Matheny PB, Smith ME (2017) How to know the fungi: Combining field inventories and DNA-barcoding to document fungal diversity. *The New Phytologist* 214(3): 913–919. <https://doi.org/10.1111/nph.14509>
- Vaidya G, Lohman DJ, Meier R (2011) SequenceMatrix: Concatenation software for the fast assembly of multi-gene datasets with character set and codon information. *Cladistics* 27(2): 171–180. <https://doi.org/10.1111/j.1096-0031.2010.00329.x>
- Vilgalys R, Hester M (1990) Rapid genetic identification and mapping of enzymatically amplified DNA from several *Cryptococcus* species. *Journal of Bacteriology* 172(8): 4238–4246. <https://doi.org/10.1128/jb.172.8.4238-4246.1990>
- Wang XC, Yang ZL, Chen SL, Bau T, Li TH, Li L, Fan L, Zhuang WY (2023) Phylogeny and taxonomic revision of the family Discinaceae (Pezizales, Ascomycota). *Microbiology Spectrum* 11(3): e00207–e00223. <https://doi.org/10.1128/spectrum.00207-23>
- White TJ, Bruns T, Lee S, Taylor J (1990) Amplification and direct sequencing of fungal ribosomal RNA genes for phylogenetics. In: Innis MA, et al. (Eds) *PCR Protocols: A Guide to Methods and Applications*. Academic Press, New York, 315–322. <https://doi.org/10.1016/B978-0-12-372180-8.50042-1>
- Xu AS (2000) Two species of *Hydnотrya* in Xizang. *Mycosystema* 19(4): 568–569. [https://doi.org/10.1016/S0167-4048\(00\)07001-2](https://doi.org/10.1016/S0167-4048(00)07001-2)
- Xu YY, Wang YW, Li T, Yan XY, Fan L (2018) DNA analysis reveals rich diversity of *Hydnотrya* with emphasis on the species found in China. *Mycological Progress* 17(10): 1123–1137. <https://doi.org/10.1007/s11557-018-1425-2>
- Zhang BC (1991) Morphology, cytology and taxonomy of *Hydnотrya cerebriformis* (Pezizales). *Mycotaxon* 42: 155–162.

New species and new combinations in the genus *Paraisaria* (Hypocreales, Ophiocordycipitaceae) from the U.S.A., supported by polyphasic analysis

Richard M. Tehan^{1,2}, Connor B. Dooley^{1,3}, Edward G. Barge⁴, Kerry L. McPhail¹, Joseph W. Spatafora³

¹ Department of Pharmaceutical Sciences, College of Pharmacy, Oregon State University, Corvallis, Oregon 97331, USA

² Department of Chemistry and Biochemistry, Utica University, Utica, New York 13502, USA

³ Department of Botany and Plant Pathology, College of Agricultural and Life Sciences, Oregon State University, Corvallis, Oregon 97331, USA

⁴ Seed Testing Laboratory, Idaho State Department of Agriculture, Boise, ID 83712, USA

Corresponding author: Richard M. Tehan (rmtehan@utica.edu)

Abstract

Molecular phylogenetic and chemical analyses, and morphological characterization of collections of North American *Paraisaria* specimens support the description of two new species and two new combinations for known species. *P. cascadenis* **sp. nov.** is a pathogen of *Cyphoderris* (Orthoptera) from the Pacific Northwest USA and *P. pseudoheteropoda* **sp. nov.** is a pathogen of cicadae (Hemiptera) from the Southeast USA. New combinations are made for *Ophiocordyceps insignis* and *O. monticola* based on morphological, ecological, and chemical study. A new cyclopeptide family proved indispensable in providing chemotaxonomic markers for resolving species in degraded herbarium specimens for which DNA sequencing is intractable. This approach enabled the critical linkage of a 142-year-old type specimen to a phylogenetic clade. The diversity of *Paraisaria* in North America and the utility of chemotaxonomy for the genus are discussed.

Key words: Ascomycota, chemotaxonomy, Cicada, Cordyceps, Cyphoderris, entomopathogen, Ophiocordyceps, Prionus



Academic editor: Huzefa Raja

Received: 19 August 2023

Accepted: 12 October 2023

Published: 13 November 2023

Citation: Tehan RM, Dooley CB, Barge EG, McPhail KL, Spatafora JW (2023) New species and new combinations in the genus *Paraisaria* (Hypocreales, Ophiocordycipitaceae) from the U.S.A., supported by polyphasic analysis. MycoKeys 100: 69–94. <https://doi.org/10.3897/mycokeys.100.110959>

Copyright: © Richard M. Tehan et al.

This is an open access article distributed under terms of the Creative Commons Attribution License (Attribution 4.0 International – CC BY 4.0).

Introduction

Paraisaria is an asexual morph-typified genus of entomopathogenic fungi, originally described by Samson and Brady in 1983, characterized by synnemata with verticillately-branched conidiophores and flask-shaped sympodially proliferating phialides (Samson and Brady 1983). These asexual morphs were derived from larvae (Delacroix 1893) and from cultured isolates of the sexual morphs of species in the genus *Cordyceps* (Samson and Brady 1983; Li et al. 2004), which were later transferred to *Ophiocordyceps* (Sung et al. 2007). *Paraisaria* was later proposed for suppression, along with four other genera then in use, in favor of recognizing a broad concept of *Ophiocordyceps* (Quandt et al. 2014). This limited the number of new combinations required to accommodate 1F1N rules following the abolition of the dual system of nomenclature in which sexual states and asexual states of fungi were classified separately. In molecular analyses, *Paraisaria* has been recovered as a distinct monophyletic clade,

being referred to as the “*gracilis* subclade” within the “*ravenelii* subclade” of *Ophiocordyceps* by Sanjuan et al. (2015). *Paraisaria* was ultimately resurrected in 2019, segregated from *Ophiocordyceps*, and amended to include sexual morphology (Mongkolsamrit et al. 2019). *Paraisaria* species possess distinctive sexual morphs characterized by a globose fertile terminal portion of the stroma with immersed perithecia. Thus, *Paraisaria* constitutes a distinct, and robustly monophyletic clade deserving a unique genus classification, though its segregation from *Ophiocordyceps* rendered *Ophiocordyceps* into several paraphyletic clades. Ultimately, a comprehensive analysis of *Ophiocordyceps* sensu Sung et al. (2007), is needed to establish robust generic concepts and restore global monophyly. A major sticking point for this action is the uncertain placement of the type of *Ophiocordyceps*, *O. blattae*, among the paraphyletic subclades of *Ophiocordyceps*.

In North America, *Paraisaria* species are unique among most *Cordyceps* sensu lato in that they form fruiting bodies in the spring, whereas most other insect pathogens fruit in the summer, fall, or winter months, which is evident in herbarium records on MycoPortal (MycoPortal 2023) and observations on the community science platform iNaturalist (<https://www.inaturalist.org/projects/north-american-cordyceps-sensu-lato>). Most *Paraisaria* species, and thus far, all known *Paraisaria* species occurring in North America, form fruiting bodies on subterranean insect hosts.

Some of the insect hosts of *Paraisaria* species are sought as food and their contamination by *Paraisaria* species could pose a human health concern. Doan et al. (2017) reported a series of poisonings and one fatality in Southern Vietnam, among people who had consumed cicadae infected with a fungus identified as *Paraisaria heteropoda* (= *Cordyceps heteropoda*, *Ophiocordyceps heteropoda*), between 2008 and 2015. The toxicity was attributed to the presence of mycotoxins in the otherwise edible cicadae, and the toxic agent was putatively identified as ibotenic acid. The potential role of entomopathogenic fungi in causing food-borne mycotoxin poisonings underscores the need to describe the biological and chemical diversity present in this group of fungi.

In addition to their impact on human and animal health, fungal natural products can be highly useful phenotypic characters for taxonomic purposes. Chemical fingerprints can be used to identify chemical families that constitute a generic chemotype for a taxonomic group, and also unique suites of compounds within a chemical family can be used to resolve species. For example, Cedeño-Sánchez et al. (2023) profiled chemical extracts from stromata to characterize and distinguish species and genera in the family Hypoxylaceae.

Only two studies (Krasnoff et al. 2005; Umeyama et al. 2011) have reported a total of five natural products from *Paraisaria* species, both of which investigated fungi identified as the cicada pathogen, *Paraisaria heteropoda*. A third study reports leucinostatin analogs from an organism reported as *Ophiocordyceps heteropoda* (= *Paraisaria heteropoda*) (Kil et al. 2020), but which is evidently a *Purpureocillium* species based on ITS phylogeny and chemotaxonomy. Doan et al. (2017) also report the amino acid, ibotenic acid from this species, but no analytical chemistry data are presented to confirm this. There are currently no published genome sequences available to mine the specialized metabolic potential of *Paraisaria* species, although the sequenced genomes

of other Ophiocordycipitaceae species display a familial trend of high biosynthetic capacity for specialized metabolites. The first chemical study of a member of this genus resulted in the discovery of the new 8-residue antimicrobial peptaibiotics, cicadapeptins I and II, which possessed a unique two consecutive 4-hydroxyproline residues at the N-terminus (Krasnoff et al. 2005). The known antifungal and immunosuppressant sphingosine analog, myriocin was also isolated in this study. Heteropodamides A and B are N-methylated cyclic heptapeptides reported as cytotoxins from *P. heteropoda* (Umeyama et al. 2011). Their absolute structures are yet to be determined. The further discovery of *Paraisaria* species and their natural products presents fertile grounds for investigation.

In the course of ongoing investigations for the discovery of biologically active natural products from *Paraisaria* species (Tehan 2022), it became critical to perform a taxonomic analysis of North American *Paraisaria* to better understand the biological diversity present in this group. In this study, we examined 29 recent collections of *Paraisaria* to investigate the diversity of North American *Paraisaria*. We also analyzed the type collections of *Ophiocordyceps insignis* and *O. monticola*, both of which were anticipated to belong in *Paraisaria* based on morphological description, ecology, and phenology. One phylogenetically informative DNA sequence was afforded from the 87-year old *O. monticola* specimen. The 142-year old *O. insignis* type did not permit successful DNA sequencing, however, chemical analysis of the newly characterized parasariamide family of compounds by LC-HRMS provided robust support for the combination of both species into *Paraisaria*, as well as the correct identification of a species of importance to human health, as *P. insignis*. This study provides a novel framework for the use of minimally destructive chemical analysis in taxonomic assessment of type specimens where DNA sequencing is not possible. The combined analysis of molecular data, morphology, ecology, phenology, and chemical data support the circumscription of two new species and two new combinations, and provides an initial overview of the diversity of American *Paraisaria* species.

Materials and methods

Specimens and isolates

Twenty nine new collections of *Paraisaria* specimens and their insect hosts were examined. Macroscopic characters were examined from fresh stromata, and microscopic characters were examined from fresh and dried stromata, including ascospores discharged from fresh stromata when possible and sections of dried specimens. Colors are in general terms of the senior author. Specimens are deposited in the Oregon State University Herbarium mycological collection. Culture isolates of fungi were made from tissue dissected from the context of stromata, placed on PDA with 50 µg/ml ampicillin and 100 µg/ml streptomycin, or from ascospores germinated on PDA. Agar plugs were taken from outgrowth of stromatic tissue and subcultured onto PDA and CMA at 20 °C. Cultures are deposited at the USDA ARS Collection of Entomopathogenic Fungal Cultures (ARSEF).

Morphological observations

Fruiting bodies were examined for morphological measurements using a Vernier caliper (Fowler). Sections of ascogenous tissue were mounted in lactophenol cotton blue, 5% KOH, or distilled water, and microanatomical characters were examined with light microscopy using a Leica DM2500. Twenty each, perithecia, asci, and part-spores were measured at magnifications of 10×, 20×, 40×, 63×, or 100×.

DNA extraction and sequencing

DNA was extracted from the ascogenous portion of dried stromata, ground with mortar and pestle in CTAB buffer (1.4 M NaCl, 100 mM Tris-HCl pH 8.0, 20 mM EDTA pH 8.0, 2% CTAB w/v) and processed following the method of Kepler et al. (2012). Samples were extracted with 25:24:1 phenol:chloroform:isoamyl alcohol, (affymetrix), and DNA was precipitated with 3 M sodium acetate (pH 5.2) and 95% ethanol. PCR amplification was performed on the Internal Transcribed Spacer (ITS), amplified using ITS4 and ITS5 primers (White et al. 1990). Alternatively, ITS1F (Gardes and Bruns 1993) was used as a forward primer for samples where ITS4 did not work. For samples in which amplification of the ITS region did not succeed, individual amplification of the ITS1 and ITS2 loci was attempted using primer sets ITS5 and ITS2 (White et al. 1990) for the ITS1 locus, and ITS3 (White et al. 1990) and ITS4 for the ITS2 locus. Nuclear small subunit (nucSSU) was amplified using nucSSU131 and NS24 (Kauff and Lutzoni 2002), nuclear large subunit (nucLSU) using LROR (Rehner and Samuels 1994) and LR7 (Vilgalys and Hester 1990), subunit 1 of RNA polymerase II (RPB1) using RPB1-A_f and RPB1-6R1asc (Hofstetter et al. 2007). Alternatively, CRPB-1 (Castlebury et al. 2004) was used as a forward primer for samples where RPB1-A_f did not work. Elongation factor 1 α (EF-1 α) was amplified using 983F and 2218R (Castlebury et al. 2004). PCR was performed with an iCycler (Bio-Rad, USA), with a total of 20 μ l reaction mixture containing 1 \times PCR Buffer (Promega), 1 \times TBTpar prepared as in Samarakoon et al. (2013), 2.5 mM MgCl₂, 0.5 μ M each forward and reverse primers, 200 μ M of each of the four dNTPs, and 0.5 U Taq polymerase. For ITS, SSU, LSU, and TEF, the PCR thermal cycle consisted of an initial 1 min denaturation at 95 °C; 34 cycles of 30 s at 94 °C, 1 min at 52 °C, 1.5 min at 72 °C, and a termination with an elongation 7 min at 72 °C. For RPB1 and RPB2, the PCR thermal cycle consisted of an initial 1.5 min denaturation at 95 °C; 39 cycles of 30 s at 94 °C, 1 min at 47 °C, 2 min at 72 °C, and a termination with an elongation 4 min at 72 °C. Sequencing was performed by the Sanger method at the Center for Quantitative Life Sciences at Oregon State University. The sequences obtained in this study were deposited to GenBank (Table 1).

Data analysis

Sequences derived from the SSU, LSU, TEF, RPB1, RPB2, and ITS were aligned with MUSCLE 5.1 (Edgar 2004). Ambiguous and phylogenetically uninformative regions were manually removed and the trimmed alignments were concatenated for analysis using Geneious Prime® 2023.0.4. A Maximum Likelihood Tree was made using the GTR+I+A algorithm and 1000 bootstrap replicates.

Table 1. Sequences used in phylogenetic tree construction.

Species	Code	Host	ITS	SSU	LSU	EF1a	RPB1	RPB2	Reference
<i>Cordyceps kyushuensis</i>	EFCC 5886	Lepidoptera	–	EF468960	EF468813	EF468754	EF468863	EF468917	Sung et al. 2007
<i>Cordyceps militaris</i>	OSC.93623	Lepidoptera	JN049825	AY184977	AY184966	DQ522332	DQ522377	–	Kepler et al. 2017
<i>Drechmeria balanoides</i>	CBS 250.82	Nematoda	MH861495	AF339588	AF339539	DQ522342	DQ522388	DQ522442	Vu et al. 2019
<i>Drechmeria sinensis</i>	CBS 567.95	Nematoda	MH862540	AF339594	AF339545	DQ522343	DQ522389	DQ522443	Spatafora et al. 2007
<i>Harposporium anguillulae</i>	ARSEF 5407	Nematoda	–	–	AY636080	–	–	–	Chaverri et al. 2005
<i>Harposporium helicoides</i>	ARSEF 5354	Nematoda	–	AF339577	AF339527	–	–	–	Sung et al. 2001
<i>Ophiocordyceps australis</i>	HUA186147	Hymenoptera	–	KC610784	KC610764	KC610734	KF658678	–	Sanjuan et al. 2015
<i>Ophiocordyceps australis</i>	HUA186097	Hymenoptera	–	KC610786	KC610765	KC610735	KF658662	–	Sanjuan et al. 2015
<i>Ophiocordyceps curculionum</i>	OSC 151910	Coleoptera	–	KJ878918	KJ878885	–	KJ878999	–	Quandt et al. 2014
<i>Ophiocordyceps irangiensis</i>	NBRC101400	Hymenoptera	JN943335	JN941714	JN941426	–	JN992449	–	Schoch et al. 2012
<i>Ophiocordyceps kimflemingiae</i>	SC30	Hymenoptera	–	KX713629	KX713622	KX713699	KX713727	–	Araújo et al. 2018
<i>Ophiocordyceps konnoana</i>	EFCC 7315	Coleoptera	–	EF468959	–	EF468753	EF468861	EF468916	Mongkolsamrit et al. 2019
<i>Ophiocordyceps longissima</i>	TNS F18448	Hemiptera	–	KJ878925	KJ878892	KJ878971	KJ879005	–	Quandt et al. 2014
<i>Ophiocordyceps melolonthae</i>	OSC.110993	Coleoptera	–	DQ522548	DQ518762	DQ522331	DQ522376	–	Mongkolsamrit et al. 2019
<i>Ophiocordyceps monticola</i>	BPI 634610	Orthoptera	OQ709246	–	–	–	–	–	This Study
<i>Ophiocordyceps nigrella</i>	EFCC 9247	Coleoptera	JN049853	EF468963	EF468818	EF468758	EF468866	EF468920	Mongkolsamrit et al. 2019
<i>Ophiocordyceps nutans</i>	OSC 110994	Hemiptera	–	DQ522549	DQ518763	DQ522333	DQ522378	–	Quandt et al. 2014
<i>Ophiocordyceps pulvinata</i>	TNS-F 30044	Hymenoptera	–	GU904208	–	GU904209	GU904210	–	Kepler et al. 2011
<i>Ophiocordyceps ravenelii</i>	OSC 151914	Coleoptera	–	KJ878932	–	KJ878978	KJ879012	KJ878950	Quandt et al. 2014
<i>Ophiocordyceps sinensis</i>	EFCC 7287	Lepidoptera	JN049854	EF468971	EF468827	EF468767	EF468874	EF468924	Quandt et al. 2014
<i>Ophiocordyceps stylophora</i>	OSC_111000	Coleoptera	JN049828	DQ522552	DQ518766	DQ522337	DQ522382	DQ522433	Quandt et al. 2014
<i>Ophiocordyceps variabilis</i>	OSC 111003	Diptera	–	EF468985	EF468839	EF468779	EF468885	EF468933	Mongkolsamrit et al. 2019
<i>Ophiocordyceps variabilis</i>	ARSEF 5365	Diptera	–	DQ522555	DQ518769	DQ522340	DQ522386	DQ522437	Mongkolsamrit et al. 2019
<i>Paraisaria alba</i>	HKAS_102484	Orthoptera	MN947219	MN943843	MN943839	MN929085	MN929078	MN929082	Wei et al. 2021
<i>Paraisaria amazonica</i>	HUA 186143	Orthoptera	–	KJ917562	KJ917571	KM411989	KP212902	KM411982	Sanjuan et al. 2015
<i>Paraisaria amazonica</i>	HUA 186113	Orthoptera	–	KJ917566	KJ917572	–	KP212903	KM411980	Sanjuan et al. 2015
<i>Paraisaria arcta</i>	HKAS_102553	Lepidoptera	MN947221	MN943845	MN943841	MN929087	MN929080	–	Wei et al. 2021
<i>Paraisaria arcta</i>	HKAS 102552	Lepidoptera	MN947220	MN943844	MN943840	MN929086	MN929079	MN929083	Wei et al. 2021
<i>Paraisaria blattarioides</i>	HUA186093	Blattodea	–	KJ917559	KJ917570	KM411992	KP212910	–	Sanjuan et al. 2015
<i>Paraisaria blattarioides</i>	HUA 186108	Blattodea	–	KJ917558	KJ917569	–	KP212912	KM411984	Sanjuan et al. 2015

Species	Code	Host	ITS	SSU	LSU	EF1a	RPB1	RPB2	Reference
<i>Paraisaria cascadenis</i>	OSC-M-052010	Orthoptera	OQ709237	OQ800918	OQ708931	OR199814	OR199828	OR199838	This Study
<i>Paraisaria cascadenis</i>	OSC-M-052012	Orthoptera	OQ709239	OQ800920	OQ708933	OR199816	OR199830	—	This Study
<i>Paraisaria cascadenis</i>	OSC-M-052017	Orthoptera	OQ709240	OQ800921	OQ708934	OR199817	OR199831	—	This Study
<i>Paraisaria coenomyia</i>	NBRC 106964	Diptera	AB968397	AB968385	AB968413	AB968571	—	AB968533	Ban et al. 2015
<i>Paraisaria coenomyia</i>	NBRC 108993	Diptera	AB968396	AB968384	AB968412	AB968570	—	AB968532	Ban et al. 2015
<i>Paraisaria gracilioides</i>	HUA186095	Coleoptera	—	KJ917556	—	KM411994	KP212914	—	Sanjuan et al. 2015
<i>Paraisaria gracilioides</i>	HUA 186092	Coleoptera	—	KJ917555	KJ130992	—	KP212915	—	Sanjuan et al. 2015
<i>Paraisaria gracilis</i>	EFCC 3101	Lepidoptera	—	EF468955	EF468810	EF468750	EF468858	EF468913	Sung et al. 2007
<i>Paraisaria gracilis</i>	EFCC 8572	Lepidoptera	JN049851	EF468956	EF468811	EF468751	EF468859	EF468912	Ban et al. 2015
<i>Paraisaria heteropoda</i>	OSC 106404	Hemiptera	—	AY489690	AY489722	AY489617	AY489651	—	Quandt et al. 2014
<i>Paraisaria heteropoda</i>	EFCC 10125	Hemiptera	JN049852	EF468957	EF468812	EF468752	EF468860	EF468914	Quandt et al. 2014
<i>Paraisaria heteropoda</i>	NBRC 100643	Hemiptera	—	JN941719	JN941422	AB968595	JN992453	AB968556	Ban et al. 2015
<i>Paraisaria heteropoda</i>	BCC 18235	Hemiptera	—	JN941720	JN941421	AB968594	JN992454	AB968555	Ban et al. 2015
	(NBRC 100642)								
<i>Paraisaria heteropoda</i>	BCC 18246	Hemiptera	AB968411	AB113352	—	MK214083	MK214087	—	Ban et al. 2015
	(NBRC 33060)								
<i>Paraisaria insignis</i>	OSC.164134	Coleoptera	OQ709231	OQ800911	OQ708924	OR199807	OR199822	—	This Study
<i>Paraisaria insignis</i>	OSC.164135	Coleoptera	OQ709232	OQ800912	OQ708925	OR199808	OR199823	—	This Study
<i>Paraisaria insignis</i>	OSC.164137	Coleoptera	OQ709233	OQ800913	OQ708926	OR199809	OR199824	—	This Study
<i>Paraisaria insignis</i>	OSC-M-052004	Coleoptera	OQ709234	OQ800914	OQ708927	OR199810	—	—	This Study
<i>Paraisaria insignis</i>	OSC-M-052008	Coleoptera	OQ709236	OQ800917	OQ708930	OR199813	OR199827	—	This Study
<i>Paraisaria insignis</i>	OSC-M-052013	Coleoptera	OQ709244	OQ800924	OQ708938	OR199820	OR199834	—	This Study
<i>Paraisaria orthopterorum</i>	BBC 88305	Orthoptera	MH754742	—	MK332583	MK214080	MK214084	—	Mongkolsamrit et al. 2019
<i>Paraisaria orthopterorum</i>	TBRC 9710	Orthoptera	MH754743	—	MK332582	MK214081	MK214085	—	Mongkolsamrit et al. 2019
<i>Paraisaria phuwiangensis</i>	TBRC 9709	Coleoptera	MK192015	—	MK192057	MK214082	MK214086	—	Mongkolsamrit et al. 2019
<i>Paraisaria phuwiangensis</i>	BBH 43492	Coleoptera	MH188541	—	MH201169	MH211355	MH211352	—	Mongkolsamrit et al. 2019
<i>Paraisaria pseudoheteropoda</i>	OSC-M-052005	Hemiptera	—	OQ800915	OQ708928	OR199811	OR199825	OR199836	This Study
<i>Paraisaria pseudoheteropoda</i>	OSC-M-052007	Hemiptera	OQ709235	OQ800916	OQ708929	OR199812	OR199826	OR199837	This Study
<i>Paraisaria pseudoheteropoda</i>	OSC-M-052022	Hemiptera	OQ709245	OQ800925	OQ708939	OR199821	OR199835	OR199841	This Study
<i>Paraisaria pseudoheteropoda</i>	OSC-M-052020	Hemiptera	OQ709243	OQ800923	OQ708937	OR199819	OR199833	—	This Study
<i>Paraisaria pseudoheteropoda</i>	OSC-M-052009	Hemiptera	OQ709241	OQ800922	OQ708935	OR199818	OR199832	OR199840	This Study
<i>Paraisaria rosea</i>	HKAS_102546	Coleoptera	MN947222	MN943846	MN943842	MN929088	MN929081	MN929084	Wei et al. 2021
<i>Paraisaria</i> sp.	OSC-M-052011	Insecta	OQ709238	OQ800919	OQ708932	OR199815	OR199829	OR199839	This Study
<i>Paraisaria</i> sp.	OSC-M-052026	Insecta	OQ709242	—	OQ708936	—	—	—	This Study
<i>Paraisaria tettigonia</i>	GZUH CS14062709	Orthoptera	KT345954	KT345955	—	KT375440	KT375441	—	Wen et al. 2016
<i>Paraisaria yodhathaii</i>	BBH 43163	Coleoptera	MH188539	—	MK332584	MH211353	MH211349	—	Mongkolsamrit et al. 2019

Species	Code	Host	ITS	SSU	LSU	EF1a	RPB1	RPB2	Reference
<i>Paraisaria yodhathaii</i>	TBRC 8502	Coleoptera	MH188540	–	MH201168	MH211354	MH211350	–	Mongkolsamrit et al. 2019
<i>Perennicordyceps cuboideus</i>	CEM 1514	Coleoptera	–	KF049609	KF049628	KF049683	–	–	Kepler et al. 2013
<i>Perennicordyceps prolifica</i>	TNS-F-18547	Hemiptera	KF049660	KF049613	KF049632	KF049687	KF049649	KF049670	Kepler et al. 2013
<i>Pleurocordyceps nipponicus</i>	BCC_2325	Neuroptera	KF049665	KF049622	KF049640	KF049696	KF049655	KF049677	Kepler et al. 2013
<i>Pleurocordyceps sinensis</i>	ARSEF_1424	Coleoptera	KF049661	KF049615	AY259544	DQ118754	DQ127245	KF049671	Kepler et al. 2013
<i>Pleurocordyceps yunnanensis</i>	NBRC 101760	Hemiptera	MN586827	MN586818	MN586836	MN598051	MN598042	MN598060	Wang et al. 2021
<i>Polycephalomyces formosus</i>	CGMCC_5.2204	Coleoptera	MN586831	MN586821	MN586839	MN598054	MN598045	MN598061	Wang et al. 2021
<i>Polycephalomyces formosus</i>	CGMCC_5.2208	Coleoptera	MN586835	MN586825	MN586843	MN598058	MN598049	MN598065	Wang et al. 2021
<i>Purpureocillium atypicola</i>	CEM 1185	Araneae	–	KJ878907	KJ878872	KJ878955	–	–	Quandt et al. 2014
<i>Purpureocillium atypicola</i>	OSC 151901	Araneae	–	KJ878914	KJ878880	KJ878961	KJ878994	–	Quandt et al. 2014
<i>Purpureocillium takamizusanensis</i>	NHJ_3497	Hemiptera	–	EU369096	EU369033	EU369014	EU369053	EU369074	Johnson et al. 2009
<i>Tolypocladium capitatum</i>	OSC 71233	Fungi (Eurotiales)	–	AY489689	AY489721	AY489615	AY489649	DQ522421	Spatafora et al. 2007
<i>Tolypocladium inflatum</i>	OSC 71235	Coleoptera	JN049844	EF469124	EF469077	EF469061	EF469090	EF469108	Kepler et al. 2012
<i>Tolypocladium ophioglossoides</i>	OSC 106405	Fungi (Eurotiales)	–	AY489691	AY489723	AY489618	AY489652	DQ522429	Castlebury et al. 2004
<i>Tolypocladium japonicum</i>	OSC 110991	Fungi (Eurotiales)	JN049824	DQ522547	DQ518761	DQ522330	DQ522375	DQ522428	Quandt et al. 2014
<i>Torrubiellomyces zombiae</i>	NY04434801	Fungi (Hypocreales)	–	ON493543	ON493602	ON513396	ON513398	ON513402	Araújo et al. 2022

Chemical extraction and LCMS analysis

Excisions (0.4–6.7 mg) were made from the endosclerotia of nineteen dried *Paraisaria* collections, individually placed in MeOH (1 ml, HPLC-grade), sonicated for 5 min, and extracted for 1 hr at 35 °C, then 24 h at ambient temperature. The twenty separate extracts were filtered through syringe filters (0.2 µm PTFE) and dried *in vacuo* before dissolution in MeOH (0.1 mg/ml, LC-MS-grade) for analysis by LC-MS, injecting 3 µl on a Phenomenex Kinetex column (2.6 µm C18 100 Å, 50 × 2.1 mm), with H₂O + 0.1% Formic Acid (A) MeCN + 0.1% Formic Acid (B) as mobile phase solvents at 0.4 ml/min. The LC method was as thus: 0.5 mins at 20% B, a linear gradient from 20–90% B over 14 mins, 4 min at 90% B, a linear gradient from 90–100% B over 0.5 mins, 4.5 mins at 100% B, followed by a linear return to 20% B over 3 mins, and re-equilibration at 20% B for 5 mins, before the next injection. High resolution (Agilent 6545 QToF) mass data were acquired for 26 mins from *m/z* 100–3200, with MS/MS spectra obtained using data-dependent ion selection for up to five precursor ions per duty cycle, excluding precursor ions with *m/z* less than 210, and fragmenting with collision energies of 20, 40, and 60 eV. LCMS data files were converted to mzML format and deposited on the public repository MassIVE (MSV000092591). Extracted ion chromatograms were produced for *m/z* 690–875, corresponding to the mass range for the paraisariamide peptide family (Tehan 2022).

Molecular networking

Unprocessed LC-MS files were converted to mzML format and uploaded to the GNPS online molecular networking platform (version 30) (Wang et al. 2016) using the default network settings but with minimum peak intensity set to 3000. The resulting network was downloaded as a graphML file, analyzed, and visualized using (Cytoscape ver. 3.9.1). The GNPS job is accessible at <https://gnps.ucsd.edu/ProteoSAFe/status.jsp?task=6bd4f858a8704e3fa98cb0c66de02248>.

Principal component analysis

LC-MS data were processed in MZmine v2.53 (Pluskal et al. 2010). Feature detection was performed with noise level set to 1×10^4 . Chromatograms were built using a minimum group size of 5, group intensity threshold set to 1×10^2 , minimum highest intensity set to 2×10^4 , and m/z tolerance was set to m/z 0.001 or 10 ppm. Chromatogram deconvolution was performed with minimum peak height set to 1×10^4 , peak duration was set to 0.1–10 mins, and the baseline was set to 5×10^2 . Isotope peaks were grouped with mass tolerance m/z 0.001 or 15 ppm, RT tolerance was set to 1, with the most intense ion taken as the representative, and max charge was set to 2. Peaks were aligned with mass tolerance m/z 0.001 or 12 ppm, RT tolerance set to 0.8 mins, with m/z weighted 75% and RT weighted 25%. Feature list rows were filtered for features falling within the range m/z 690–875, and RT 5–14 mins, with a minimum of 2 peaks per row, and a minimum of 2 peaks in an isotopic pattern. Gap filling was performed with an intensity tolerance of 10%, mass tolerance m/z 0.001 or 15 ppm, and RT tolerance 0.6 mins. The resulting feature list was subjected to Principal Component Analysis (PCA).

Results

Molecular phylogeny

We generated 82 new sequences (16 SSU, 16 LSU, 15 TEF, 14 RPB1, 6 RPB2, and 16 ITS). The combined dataset of 79 taxa afforded a concatenated multi-locus alignment comprising 5,317 bp (1,030 SSU, 955 LSU, 977 TEF, 702 RPB1, 1,037 RPB2, 616 ITS) which was deposited on TreeBASE (accession URL: <http://purl.org/phylo/treebase/phyloids/study/TB2:S30820>). In the resulting phylogenetic tree (Fig. 1), ten genera in the family Ophiocordycipitaceae are represented. *Cordyceps kyushuensis* and *C. militaris* (Cordycipitaceae) were designated as outgroup taxa. All genera, with the exception of *Ophiocordyceps*, are supported as monophyletic clades. A clade comprising several species morphologically similar to the well-known cicada pathogen, *P. heteropoda*, referred to here as the “*P. heteropoda* complex”, is resolved into five well-defined species as well as additional samples revealing cryptic diversity. Two new species within the *P. heteropoda* complex, *Paraisaria cascadiensis* and *Paraisaria pseudoheteropoda*, are supported as monophyletic clades, and are described below. *Ophiocordyceps insignis* samples produced a monophyletic clade within the *P. heteropoda* complex supporting its combination into *Paraisaria*, and is redescribed based

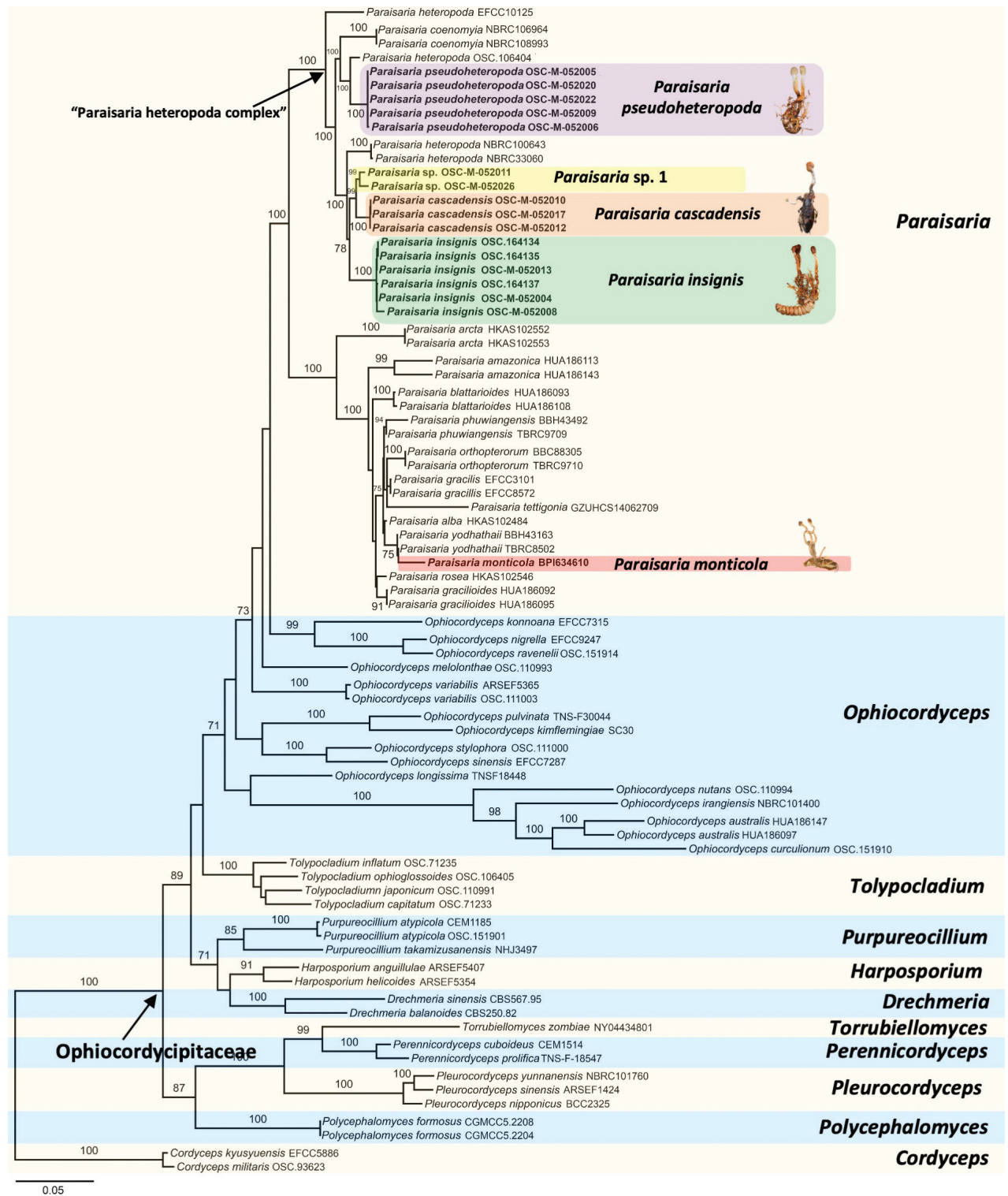


Figure 1. Maximum likelihood tree based on the combined dataset of SSU, LSU, TEF, RPB1, RPB2, and ITS sequences displaying the relationship of *Paraisaria* species within family Ophiocordycipitaceae.

on a fresh collection, which is designated here as an epitype. The type collection of *Ophiocordyceps monticola* also occurred within the genus *Paraisaria*, grouping closely with *P. yodhathaii* and *P. alba*. It was the only North American *Paraisaria* species analyzed in this study which did not fall within the *P. heteropoda* complex.

LC-MS analysis

Molecular Network Analysis of nineteen *Paraisaria* endosclerotium extracts revealed a prominent subnetwork identified as the paraisariamide family of cyclopeptides, with constituent molecular ion masses ($[M+H]^+$) ranging from m/z 694.49–860.56 (Fig. 2A.). All endosclerotium extract samples were observed to possess a subset of paraisariamide congeners with partial overlap between species. Production of paraisariamide cyclopeptides in host/endosclerotium

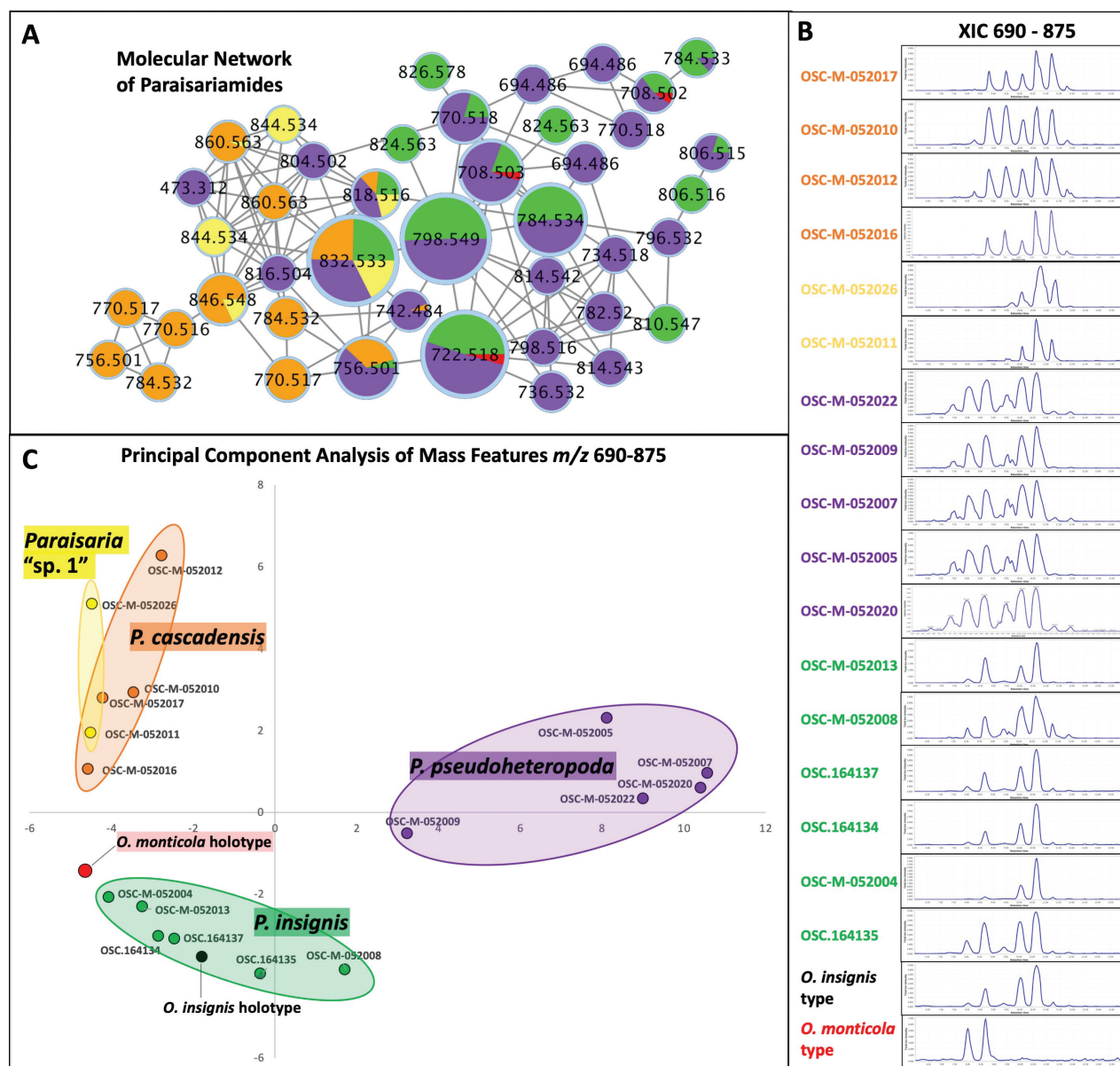


Figure 2. Chemical comparison of paraisariamide content in the endosclerotia of *Paraisaria* species collected in the USA **A** molecular network of the paraisariamide molecular family of cyclic peptides detected in methanol extracts of endosclerotia of *Paraisaria* specimens. Nodes are displayed as pie charts conveying the relative abundance of paraisariamide mass ion features in each *Paraisaria* species (Orange = *P. cascadenis*, Purple = *P. pseudoheteropoda*, Green = *P. insignis*, Yellow = "*Paraisaria* sp. 1", Red = *P. monticola*) **B** extracted ion chromatograms of m/z 690–875 for methanol extracts of endosclerotia of *Paraisaria* specimens **C** principal component analysis of mass features m/z 690–875 from methanol extracts of endosclerotia of *Paraisaria* specimens, color-coded by phylogenetic clade.

is thus supported as a conserved chemotype for *Paraisaria*. Paraisariamides can thus potentially be used as a generic diagnostic character. Chromatograms generated from the extracted ion range m/z 690–875, corresponding to the mass range for the peptide family of paraisariamides, were unique to and consistent within each species (Fig. 2B). From the processed mass data, a feature list was produced comprising 59 LC-MS ion features (Suppl. material 1). A PCA plot generated from this feature list afforded three major clusters (Fig. 2C). Samples derived from *P. insignis* and *P. pseudoheteropoda* were resolved in distinct clusters. Samples derived from *P. cascadiensis* together with samples from its sister clade, "*Paraisaria* sp. 1", grouped apart from other samples. *Ophiocordyceps monticola* afforded two prominent ion peaks with quasimolecular ions, m/z 708.502 and 722.518 eluting at 8.0 and 8.7 min respectively, and grouped most closely with *P. insignis* in the PCA plot. Qualitatively, the general shape of ion chromatograms was highly conserved within each species and distinct between species. The resolution of species by LC-MS analysis overall accorded very well with the phylogenetic analysis.

Taxonomy

Paraisaria cascadiensis Tehan, Dooley & Spatafora, sp. nov.

MycoBank No: 849757

Fig. 3

Type material. Holotype. U.S.A., WASHINGTON. Skamania County, Gifford Pinchot National Forest, Mt. St. Helens, at approximately 46.1771, -121.9224. 1,042 m alt., 9 June 2021, on adult *Cyphoderris monstrosa* buried in the ground, in mixed coniferous forest comprising *Pinus contorta*, *Pseudotsuga menziesii*, and *Abies* sp., collected by R. Tehan, C. Dooley (RMT-2021-072, OSC-M-052017, ex-holotype living culture: ARSEF 14609).

Etymology. *cascadiensis* occurring in the Cascade Mountain range in the Pacific Northwest, USA.

Description. Stroma capitate, solitary, rhizoids solitary arising from heads of adult *Cyphoderris monstrosa* buried in soil. Ascogenous portion globose or subglobose, 8–9 × 6–9 mm, chestnut brown. Stipe white to light brown, inside hollow, fibrous, white, 15–17 mm long, 3–4 mm wide, papillate with ostioles of perithecia. Perithecia obclavate, immersed, ordinaly arranged, 800–970 × 105–150 µm. Asci hyaline, cylindrical, eight-spored, observed up to 350 µm long × 4.5–7 µm wide, possessing abruptly thickened apex. Ascospores hyaline, filiform, multiseptate, breaking into 64 cylindrical part-spores, (6.3–)7.5–9.5(–10.3) × 1.6–2.2(–2.4) µm.

Culture characteristics. Colonies on PDA 61 days at 20 °C, 28 mm, white to yellow, reverse reddish brown to orange. Mycelium septate, smooth-walled hyaline. No conidial state was observed.

Host. *Cyphoderris monstrosa* (Prophalangopsidae, Orthoptera).

Habitat. Specimens occur on hypogeous adult hump-winged grigs, *Cyphoderris monstrosa*, in coniferous forest.

Additional materials examined. U.S.A., WASHINGTON: Skamania County, at approximately 46.177, -121.9167, elevation: 974 m, 29 May 2018, on cf. *Cyphoderris monstrosa* buried in soil, collected by Josh Grefe (OSC-M-052003). U.S.A.,

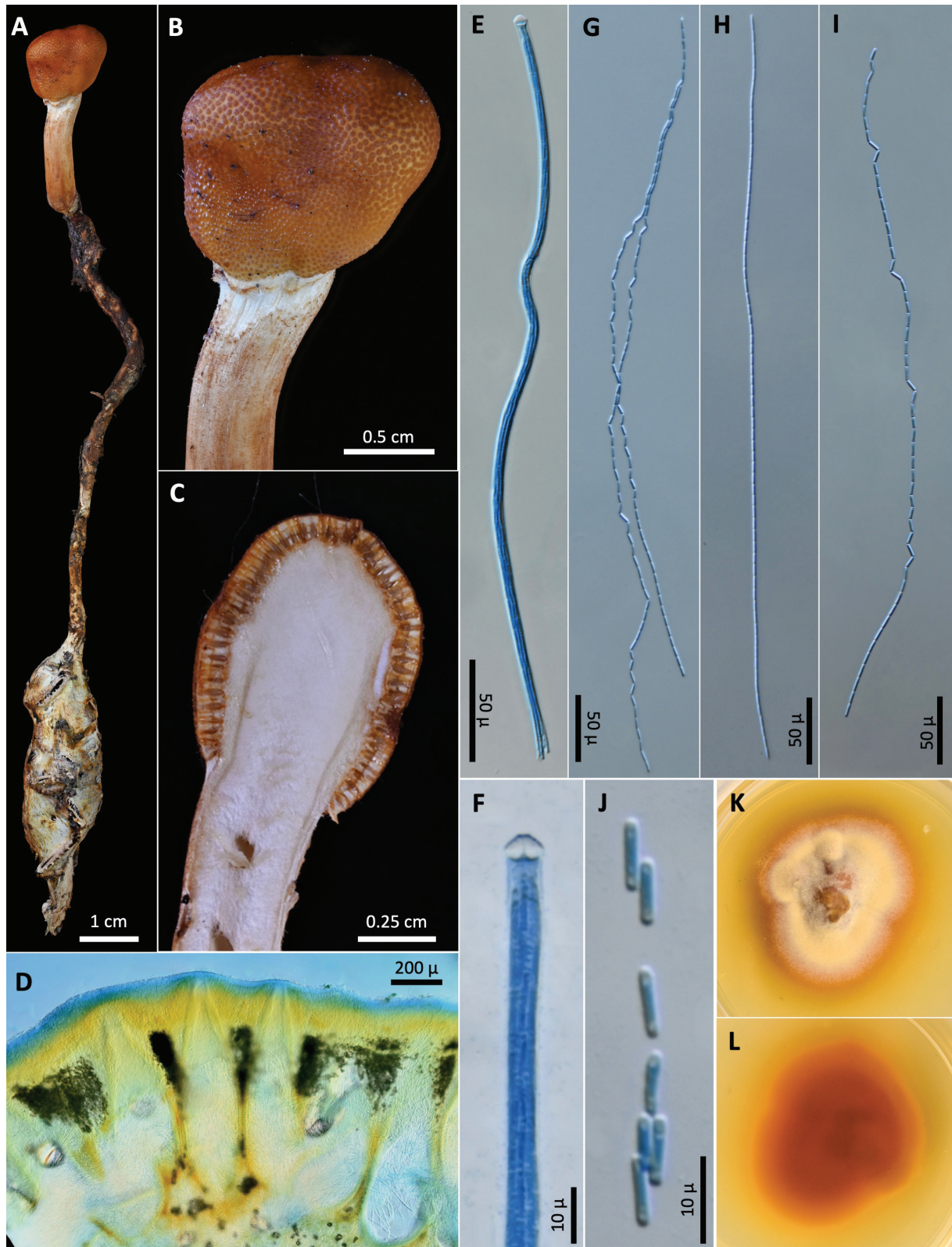


Figure 3. *Paraisaria cascadensis* **A** OSC-M-052017 **B** fertile head **C** cross section of fertile head showing arrangement of perithecia **D** perithecia **E** ascus **F** Ascus apex **G–I** ascospores **J** part-spores **K, L** colonies on PDA 61 d (**K** obverse, **L** reverse).

WASHINGTON: Chelan County, 47.9761, -120.7811, elevation: 865 m, 15 June 2020, on adult *Cyphoderris monstrosa*, buried in soil, collected by Daniel Winkler, Hans Drabicki (OSC-M-052010). U.S.A., WASHINGTON: Skamania County,

at approximately 46.1848, -122.1139, elevation: 12332 m, 12 June 2020, on cf. *Cyphoderris monstrosa*, collected by Ben McCormick (OSC-M-052012). U.S.A., WASHINGTON: Skamania County, Gifford Pinchot National Forest, Mt. St. Helens, at approximately 46.1771, -121,9224. 1,042 m alt., 9 June 2021, on adult *Cyphoderris monstrosa* buried in soil, in mixed coniferous forest comprising *Pinus contorta*, *Pseudotsuga menziesii*, and *Abies* sp., collected by Richard Tehan, Connor Dooley (RMT-2021-071, OSC-M-052016).

Notes. This species is uncommon and has thus far only been collected in the Cascade Mountains of Washington State in the vicinity of Mount St. Helens at elevations above 850 m. It might be expected to have a broader range on the basis of the range of its host, *Cyphoderris monstrosa*, which is known to occur in coniferous forest in several Western U.S. states and Canada (The Orthopterists' Society 2023).

***Paraisaria pseudoheteropoda* Tehan & Spatafora, sp. nov.**

MycoBank No: 849758

Fig. 4

Type material. Holotype. U.S.A. ARKANSAS: Searcy County, Grinder's Ferry, 35.985, -92.732, elevation: 252 m, 15 May 2022, on nymphs of cicadidae (Hemiptera) buried in soil, in near *Quercus* sp., *Carya* sp., and *Juniperus virginiana*, collected by Kerri McCabe (OSC-M-052022, ex-type culture: ARSEF 14616).

Etymology. *pseudoheteropoda* resembling another cicada-pathogenic species, *Paraisaria heteropoda*.

Description. Stromata capitate or subclavate, unbranched, growing singly or up to two stromata attached by rhizoids to hypogeous nymphs of Cicadidae (Hemiptera). Ascogenous portion globose or subglobose, 9–11 × 7–8 mm, cream to chestnut brown. Stipe white to light brown, inside fibrous, white, 20–53 mm long, 4–5 mm wide, papillate with ostioles of perithecia. Perithecia obclavate, immersed, ordinarily arranged 680–745(–760) × (310–)330–420 µm. Asci hyaline, cylindrical, eight-spored, observed up to 420 µm long × 5.5–6.5 µm wide, possessing abruptly thickened apex. Ascospores hyaline, filiform, multiseptate, breaking into 64 cylindrical part-spores, (5.6–)6.2–7.9(–8.7) × 1.6–2.1(–2.4) µm.

Culture characteristics. Colonies on PDA 61 days at 20 °C, 29 mm, white, reverse yellow to orange. Mycelium septate, smooth-walled hyaline. No conidial state was observed.

Host. Nymphs of Cicadidae (Hemiptera).

Habitat. Specimens occur on hypogeous nymphs of cicadae at the base of coniferous and deciduous trees, especially oaks.

Additional materials examined. U.S.A. MISSOURI: Barry County, Cassville, at approximately 36.5586, -93.6833, elevation: 301 m, 26 May 2019, on nymph of cicada buried in soil, collected by Aaron Peters, (OSC-M-052005) U.S.A. MISSOURI: Barry County, Cassville, at approximately 36.6501, -93.7031, elevation: 382 m, 16 May 2019, on nymph of cicada buried in soil, collected by Aaron Peters (OSC-M-052007) U.S.A. MISSOURI: Barry County, Cassville, at approximately 36.5586, -93.6833, elevation: 301 m, 4 April 2020, on nymph of cicada buried in soil, collected by Aaron Peters (OSC-M-052009, living culture: ARSEF 14610). U.S.A. KENTUCKY: Lincoln County, Crab Orchard, at approximately 36.464, -84.51, elevation: 290 m, 19 April 2021, on nymph of cicada buried in

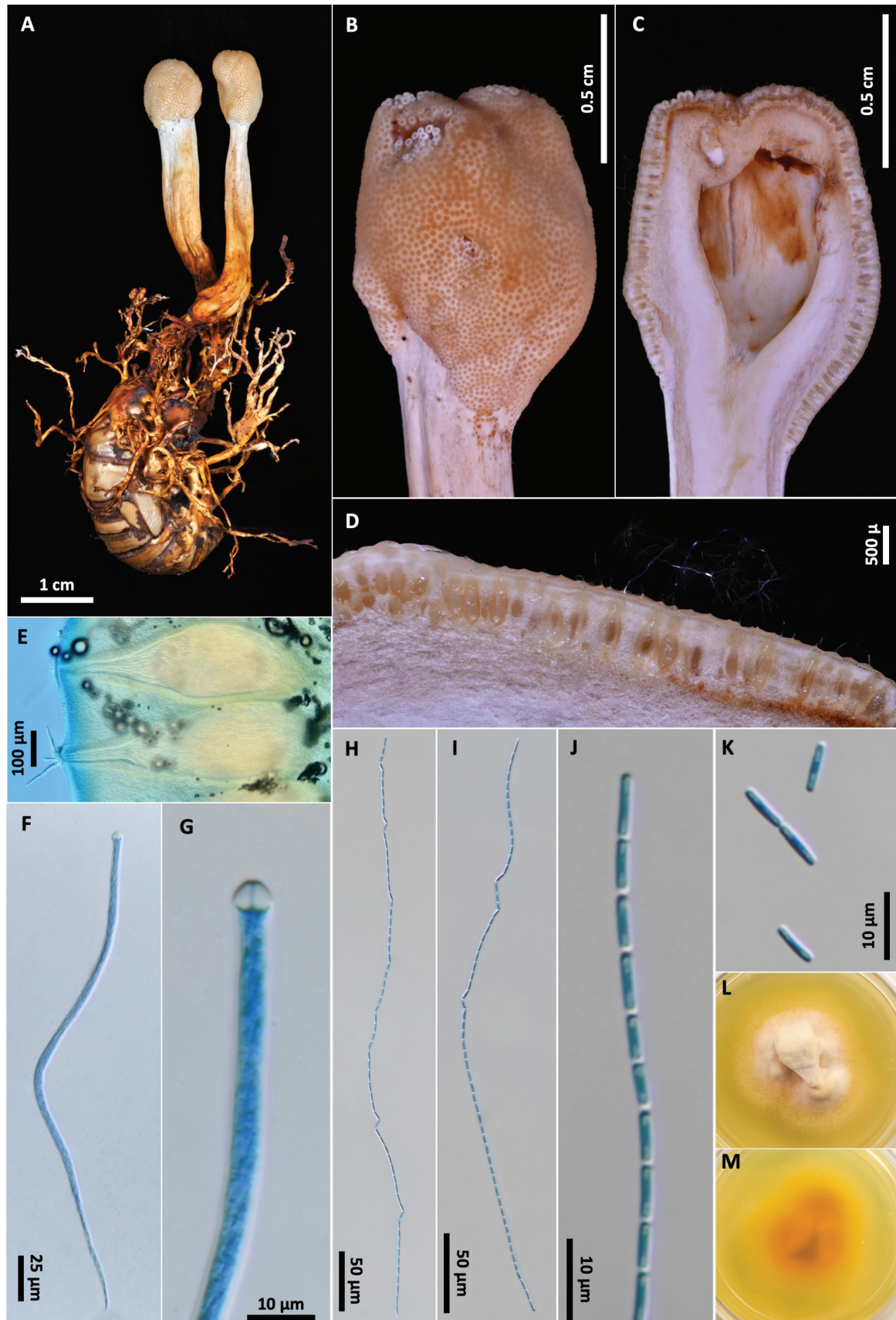


Figure 4. *Paraisaria pseudoheteropoda* **A** OSC-M-052022 **B** fertile head **C, D** cross section of fertile head showing arrangement of perithecia **E** perithecia **F** ascus **G** ascus apex **H, I** ascospores **J** ascospore tip **K** part-spores **L, K** colonies on PDA 61 d (**L** obverse, **M** reverse).

soil, collected by Michael Roberts (OSC-M-052015). U.S.A. TENNESSEE: Putnam County, Cookerville, at approximately 36.163, -85.501, elevation: 337 m, 17 April 2022, on nymph of cicada buried in soil in mixed hardwood forest comprising *Quercus* sp., *Fagus* sp., *Populus* sp. and *Arundinaria gigantea*, collected by Jamie Newman (OSC-M-052019). U.S.A. TENNESSEE: Putnam County, Silver Point, at approximately 36.1409, -85.7374, elevation: 180 m, 17 April 2022, on nymph of cicada buried in soil among *Acer negundo*, *Carpinus caroliniana*, *Carya* sp., *Quercus rubra*, *Lindera* sp., *Amphicarpaea bracteata*, *Phlox divaricata*, *Salvia lyrata*. collected by Holly Taylor (OSC-M-052020). U.S.A. ARKANSAS: Searcy County, Grinder's Ferry, at approximately 35.983, -92.719, elevation: 222 m, 14 May 2022, on nymphs of cicadae buried in soil, in near *Quercus* sp., *Carya* sp., and *Juniperus virginiana*, collected by Kerri McCabe (OSC-M-052021). U.S.A. MISSOURI: Barry County, Roaring River, at approximately 36.5593, -93.683, elevation: 296 m, 24 May 2022, on nymphs of cicadae buried in soil, collected by Aaron Peters, (OSC-M-052023). U.S.A. VIRGINIA: Albemarle County, Charlottesville, at approximately 38.0812, -78.4657, elevation: 133 m, 31 May 2022, on nymph of cf. *Neotibicen* sp. (Cicadidae, Hemiptera) buried in soil near *Acer rubrum*, collected by Amelio Little (OSC-M-052024). U.S.A. MISSOURI: Barry County, Roaring River, at approximately 36.5583, -93.6836, elevation: 305 m, 25 May 2022, on nymphs of cicadae buried in soil, collected by Aaron Peters, (OSC-M-052025). U.S.A. ALABAMA: St. Clair County, Leeds, at approximately 33.5540, -86.5382, elevation: 198 m, 12 March 2023, on nymphs of cicadae buried in soil, collected by Courtney Mynick, (OSC-M-053266). U.S.A. ALABAMA: Jefferson County, Birmingham, at approximately 33.4402, -86.8894, elevation: 195 m, 16 March 2023, on nymphs of cicadae buried in soil, collected by Bucky Raeder, (OSC-M-053267).

Notes. This species is the only *Paraisaria* species known to occur on cicadas in North America. In morphology and geographic distribution, it overlaps with *P. insignis* but that species is distinguished by its strict occurrence on Coleoptera. *P. pseudoheteropoda* sometimes has a pallid stroma which is not observed in *P. insignis*.

***Paraisaria insignis* (Cooke & Ravenel) Tehan & Spatafora, comb. nov.**

MycoBank No: 849763

Fig. 5

Cordyceps insignis Cooke & Ravenel, *Grevillea* 12(no. 61): 38 (1883). Basionym. *Ophiocordyceps insignis* (Cooke & Ravenel) G.H. Sung, J.M. Sung, Hywel-Jones & Spatafora, *Stud. Mycol.* 57: 43 (2007). Synonym.

Type. U.S.A. SOUTH CAROLINA, "seaboard", 4 January 1881, on larva coleoptera, collected by H. W. Ravenel. (Holotype: Ravenel 3251, K-M 1434269).

Epitype designated here: U.S.A. ARKANSAS: Saline County, Avilla, at approximately 34.713, -92.587, elevation: 169 m, 2 April 2021, on larva of *Prionus imbricornis* (Cerambycidae, Coleoptera) buried in soil near *Quercus* sp., collected by Jay Justice (OSC-M-052013, ex-type living culture ARSEF 14611).

Description. Stromata capitate, unbranched, growing singly to gregarious, in groups of up to four stromata on a single host. Stromata 20–52.5 mm long. Ascogenous portion brown, globose to oblong, 8–22 mm long × 7–16 mm wide,

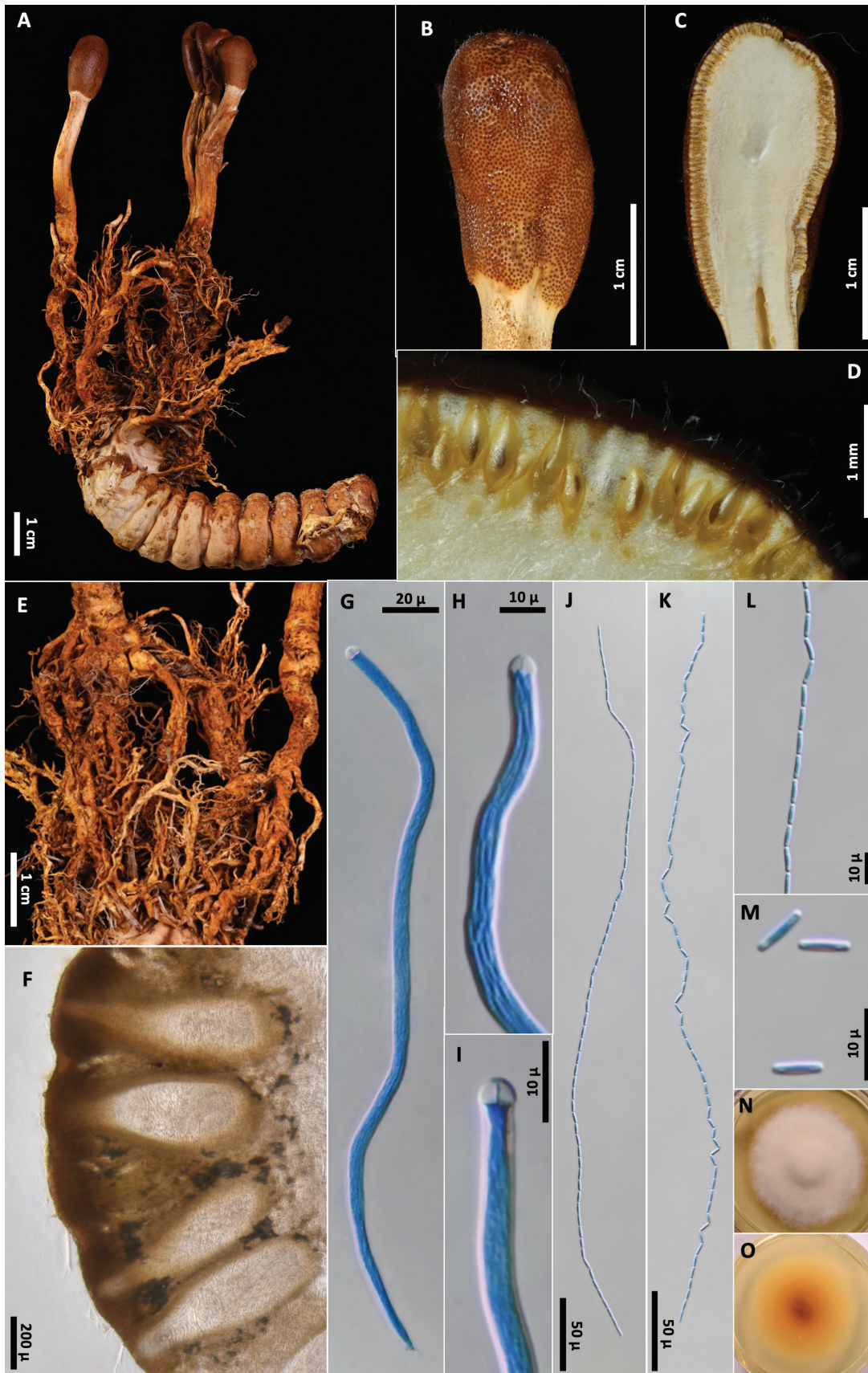


Figure 5. *Paraisaria insignis* **A** OSC-M-052013 Epitype **B** fertile head **C, D** cross section of fertile head showing arrangement of perithecia **E** rhizomorphs **F** perithecia **G** ascus **H, I** asci apices **J–L** ascospores **M** part-spores **N, O** colony on PDA 70 d (**N** obverse, **O** reverse).

papillate with ostioles of perithecia. Stipe golden yellow to reddish orange, sometimes furfureous toward upper half, 14–25 × 4–9 mm long, attached to hypogeous host by thick mats of fibrous, tangled, yellow to reddish orange rhizomorphs, extending 25–45 mm. Mycelial growth occurring between, and sometimes over, larval segments, forming a thin membrane. Perithecia embedded, obclavate, brown, (520–)640–800(840) × (160–)185–250(–270) μm. Asci hyaline, cylindrical, up to 380 μ long × (3.8–)4.0–5.9(–7.5) μm, possessing abruptly thickened apex. Ascospores hyaline, filiform, smooth, disarticulating into 64 part-spores. Part-spores, cylindrical, 6.3–9.0(–10.5) × 2.5–3.5 μm. Growing on larvae of *Prionus* cf. *imbricornis*. (Cerambycidae, Coleoptera).

Culture characteristics. Colonies on PDA 70 days at 20 °C, 37.5 mm, white, reverse reddish brown to yellow. Mycelium septate, smooth-walled hyaline. No conidial state was observed.

Host. larvae of *Prionus* cf. *imbricornis*. (Cerambycidae, Coleoptera)

Habitat. Specimens occur on hypogeous larvae of coleoptera typically at the base of oak trees.

Additional materials examined. U.S.A. ARKANSAS: Saline County, Avilla, at approximately 34.713, -92.587, elevation: 169 m, 18 March 2018, on larva of *Prionus imbricornis* (Cerambycidae, Coleoptera) buried in soil near *Quercus* sp., collected by Jay Justice (OSC.164134). U.S.A. ARKANSAS: Saline County, Avilla, at approximately 34.713, -92.587, elevation: 169 m, 2 April 2018, on larva of *Prionus imbricornis* (Cerambycidae, Coleoptera) buried in soil near *Quercus* sp., collected by Jay Justice (OSC.164135, living culture: ARSEF 14615). U.S.A. ARKANSAS: Saline County, Avilla, at approximately 34.713, -92.587, elevation: 169 m, 21 April 2018, on larva of *Prionus imbricornis* (Cerambycidae, Coleoptera) buried in soil near *Quercus* sp., collected by Jay Justice (OSC.164136). U.S.A. ARKANSAS: Pulaski County, North Little Rock, at approximately 34.7989, -92.312, elevation: 99 m, 17 April 2018, on larva of *Prionus imbricornis* (Cerambycidae, Coleoptera) buried in soil near *Quercus* sp., and *Ulmus* sp., collected by Sheila Griffin (OSC.164137). U.S.A. MISSOURI: Barry County, Cassville, at approximately 36.6116, -93.6938, elevation: 381 m, 16 April 2019, on larva of *Prionus imbricornis* (Cerambycidae, Coleoptera) buried in soil, collected by Aaron Peters (OSC-M-052004). U.S.A. TEXAS: Harris County, Friendswood, at approximately 29.5501, -95.1972, 19 m, 15 February 2020, on larva of Coleoptera, cf. *Prionus imbricornis* buried in soil, collected by Brett Jackson (OSC-M-052008). U.S.A. MISSISSIPPI: Otibbeha County, at approximately 33.4576, -88.7859, elevation: 109 m, 29 March 2021, on larva of Coleoptera buried in soil near *Quercus* sp., collected by Carol Siniscalchi (OSC-M-052014). U.S.A. ARKANSAS: Saline County, Avilla, at approximately 34.713, -92.587, elevation: 169 m, 21 April 2018, on larva of *Prionus imbricornis* (Cerambycidae, Coleoptera) buried in soil near *Quercus* sp., collected by Jay Justice (OSC-M-052018, living culture: ARSEF 14617). U.S.A. GEORGIA: Greene County, Greensboro, at approximately 33.556, -83.262, elevation 152 m, 25 March 2023, on larva of coleoptera, buried in soil, collected by Patti Chaco (OSC-M-053264). U.S.A. GEORGIA: Bibb County, Musella, at approximately 32.8491, -83.8886, elevation 145 m, 2 April 2023, on larva of coleoptera, buried in soil near *Quercus phellos*, collected by Rose Payne (OSC-M-053265).

Notes. Recent collections of this species were initially determined to not match any described species and were given the provisional name *Paraisaria tortuosa*, which was used in a doctoral dissertation (Tehan 2022), and in confer-

ence presentations. The conspecificity with *Ophiocordyceps insignis* (= *Cordyceps insignis*) was considered but it was difficult to reconcile Cooke's description of the stroma as "livid purple". However, that species was described from a dried specimen and the true colors of the fresh specimen were evidently not observed by the authority. Petch (1935) cast doubt on the accurate description of the color of *C. insignis* and though the original host is not able to be precisely identified, Petch's analysis here is helpful, suggesting based on morphology that the host is one that pupates in wood, which accords with the host of recent collections identified as *Prionus imbricornis*. Ultimately, chemical comparison of fresh collections to the holotype was definitive in the identification of the fresh collections, and strongly supports the combination into *Paraisaria*.

***Paraisaria monticola* (Mains) Tehan & Spatafora, comb. nov.**

MycoBank No: 849764

Fig. 6

Cordyceps monticola Mains, *Mycologia* 32(3): 310 (1940). Basionym.

Ophiocordyceps monticola (Mains) G.H. Sung, J.M. Sung, Hywel-Jones & Spatafora, *Stud. Mycol.* 57: 45 (2007). Synonym.

Materials examined. Type: U.S.A. TENNESSEE, Monroe County, Vonore, June 1936, on adult *Neocurtilla hexadactyla*. collected by G. L. Williams. (BPI 634610).

Notes. *P. monticola* is known to occur on adult Northern mole cricket, *Neocurtilla hexadactyla* (= *Grylotalpa hexadactyla*, Orthoptera, Grylotalpidae). Other pathogens of mole crickets, Grylotalpidae include *Beauveria grylotalpidicola*, *Beauveria sinensis*, *Cordyceps neogrylotalpae*, *Ophiocordyceps grylotalpae*, *Ophiocordyceps krachonicola*, and *Polycephalomycs albiramus*, all of which are only known from east Asia. Lloyd (1920) reported *C. grylotalpae* from a mole cricket collected in Louisiana, USA, but that specimen was immature, and bore only cylindrical immature stromata with no ascogenous tissue. Owing to the absence of microanatomical character data available for *C. grylotalpae*, and the lack of genetic data available for either species, future studies could compare *P. monticola* to *C. grylotalpae* by chemical means, focusing on paraisariamide content of the fungal endosclerotium. *P. monticola* is only known from the type collection.

Additional *Paraisaria* specimens examined

Two additional collections were examined which were phylogenetically closest to *P. cascadenis* but occurring on undetermined insect hosts, outside of the known geographic distribution of *Cyphoderris monstrosa*, the host of *P. cascadenis*. Together they form a clade which is sister to *P. cascadenis*. We do not consider these collections to be conspecific to *P. cascadenis*, but their formal description was not within the scope of the present study owing to lack of adequate sampling and host data. We anticipate that they represent two distinct new species, the description of which requires further sampling. U.S.A., CALIFORNIA: Mendocino County, Ukiah, at approximately 39.1568, -123.2328, elevation: 352 m, 5 April 2019, on undetermined insect host buried in soil, collected by Warren Cardimona (OSC-M-052011) U.S.A., IOWA: Johnson County, Solon, at

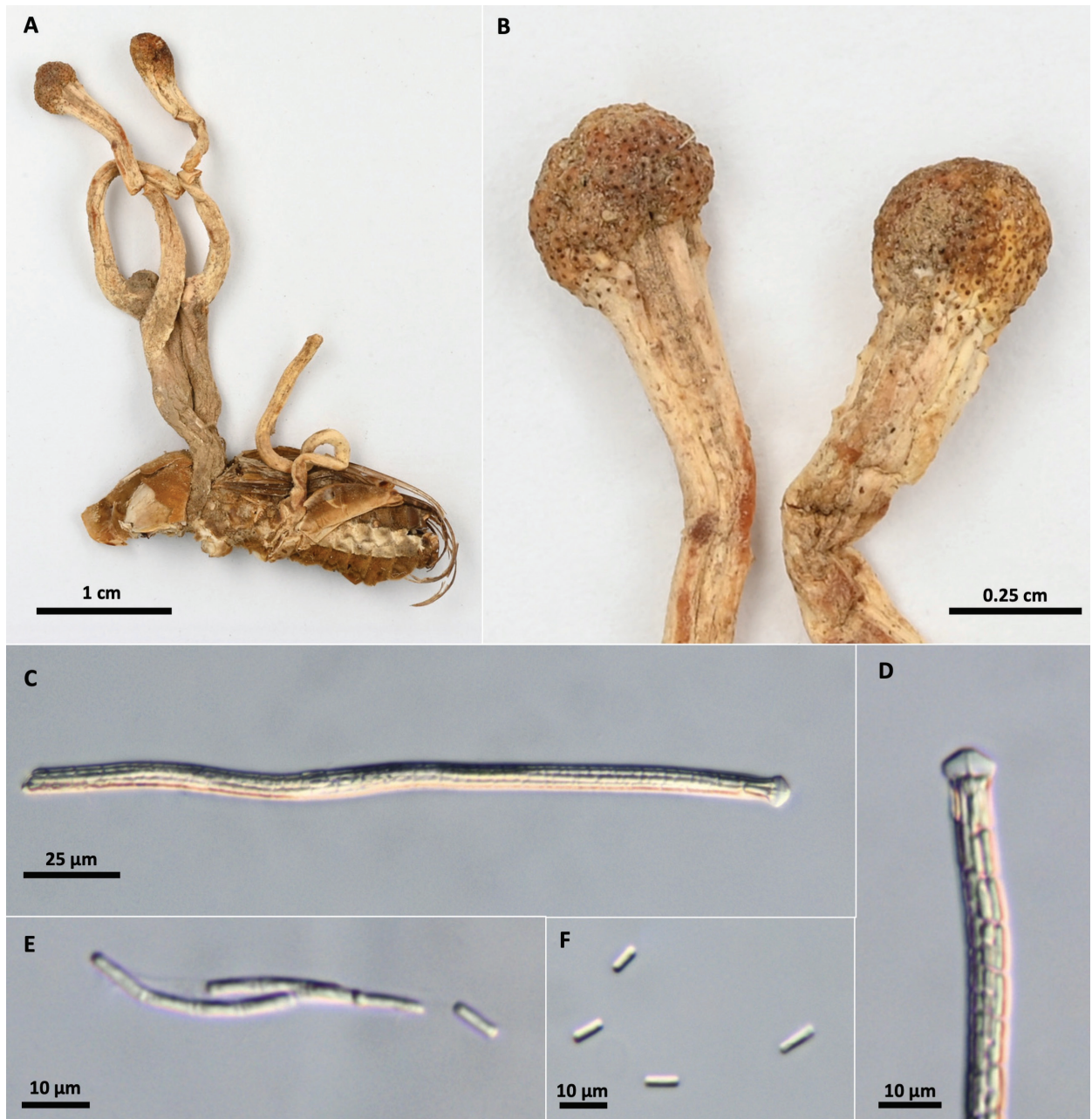


Figure 6. *Paraisaria monticola* **A** holotype BPI 634610 **B** fertile head **C** ascus **D** ascus apex **E** portion of ascospore **F** part spores.

approximately 41.7572, -91.5457, elevation: 238 m, 30 June 2022, on undetermined insect host buried in soil, collected by Ross Salinas (OSC-M-052026).

Discussion

In this study, two new *Paraisaria* species are described and two known species are combined into *Paraisaria*. The entomopathogenic fungal genus *Paraisaria* thus currently comprises 18 formally described species which occur on six continents, as deduced from a combination of herbarium records (MycoPortal 2023) and citizen science observations (iNaturalist 2023). The extent of *Paraisaria* diversity both in North America and worldwide is not comprehensively reflected in this study, which warrants future studies of this group. The results of our phylogenetic

and chemical analyses support the presence of additional cryptic diversity yet to be elucidated. For such a geographically widespread genus, there has been a relative paucity of sampling and analyses of *Paraisaria* specimens globally. Continued study of this group promises to reveal additional new *Paraisaria* species, each with the potential for new specialized metabolite discovery. In this study, *Paraisaria* populations in North America prove to be enriched in species falling within the *Paraisaria heteropoda* complex. Species in this clade are characterized by fruiting bodies with yellow, brown, and reddish hues and prodigious orange to brown rhizomorphs attaching to hypogeous insect hosts. Aboveground portions of the fruiting bodies in some respects resemble the truffle parasite, *Tolypocladium capitatum*, with which they have been compared (Cooke 1883), and with which they are frequently confused. Numerous host shifts have accompanied speciation in the *P. heteropoda* complex with species occurring on insect hosts in orders Hemiptera, Diptera, Coleoptera, and Orthoptera. Host identification is critical for field identification of North American *Paraisaria* species. *P. insignis* and *P. pseudoheteropoda* overlap extensively in fruiting body morphology and geographic distribution but are easily distinguished by their respective distinct hosts. *P. insignis* occurs strictly on coleopteran hosts and *P. pseudoheteropoda* is the only known *Paraisaria* species to occur on cicadas in North America. *P. cascadenensis* and *P. monticola* both occur on orthopteran hosts, but the geographic distribution of *P. cascadenensis* appears to be restricted to montane regions of the Pacific Northwest, which accords with the distribution of its host, *Cyphoderris monstrosa*. *P. monticola* is only known from the type specimen collected in Vonore, TN. Re-collection efforts for this species would be valuable and could focus on records of its host *Neocurtilla hexadactyla*, in the vicinity of the type locality. Notably, *N. hexadactyla* is widely distributed, and may support a wide distribution of *P. monticola*.

The life cycles of *Paraisaria* species, including mode of infection of their insect hosts, their possible occurrence in soil, as endophytes, saprophytic, and nematophagous nutritional modes, are not well characterized. Owing to the observation that *Paraisaria* species produce fruiting bodies in spring months in North America, we hypothesize that they colonize their insect hosts in the prior season and overwinter as endosclerotia which are observed to possess high concentrations of cyclopeptide specialized metabolites. The molecular structures, biological activities, and chemical ecology of *Paraisaria* specialized metabolites are the focus of ongoing studies (Tehan 2022).

The targeted LC-MS analysis of specialized metabolites from fungi that are only partially represented in phylogenetic analyses represents a robust application of chemotaxonomy to resolve species. Fungi that produce cyclopeptides may be especially good candidates for chemotaxonomic profiling as many cyclopeptides are particularly resistant to degradation by oxidation, heating, or proteolytic cleavage (Haque and Grayson 2020). Chemotaxonomic profiling of stable metabolites also provides a framework for the analysis of fungal groups lacking genetic data for type specimens, whereby type specimens that afford only chemical data can be linked to samples for which both chemical and genetic data are available, if both types of data resolve species groups. The lack of genetic data for type material is especially challenging when type specimens are very old and possess degraded, highly-fragmented DNA, and for which no suitable neotype has been designated. Micromorphological characters lack robustly distinct differences between *Paraisaria* species for use in reliable species di-

agnoses. It was thus critical to compare chemical profiles of recent collections of *P. insignis* to the holotype to rigorously establish their conspecificity. Conservation of the general paraisariamide chemotype also supports paraisariamides as chemotaxonomic markers for genus *Paraisaria*, as these compounds were detected in the endosclerotia of all *Paraisaria* specimens analyzed. These markers are substantially more durable than DNA over long periods of time as is evident from the definitive detection of these compounds in the 142-year-old holotype of *P. insignis*. Notably, the shape of chromatograms was visually identical between old and new specimens, indicating that even the relative abundance of paraisariamide congeners within a sample is preserved. LC-MS/MS profiling surveys should be conducted across *Paraisaria* species and related groups of fungi to assess the extent of the paraisariamide molecular family and confirm the utility of these metabolites as chemotaxonomic markers.

Other specialized metabolite families may offer promise as critical chemotaxonomic markers, depending on the relative stability of their biosynthetic genes over time, and whether or not they are reliably expressed. For example, genomic analyses show that the cyclosporin genotype is highly conserved within the insect pathogen, *Tolypocladium inflatum* (Ophiocordycipitaceae), whereas peptaibiotics have evolved rapidly (Olarite et al. 2019) though neither cyclosporins nor peptaibiotics are detected by LCMS in every *Tolypocladium* strain exhibiting those genotypes (Blount 2018; Tehan et al. 2022).

Ophiocordyceps blattae, the type species of the large genus *Ophiocordyceps*, presents another system for potential chemotyping to compare with the various paraphyletic clades of *Ophiocordyceps*. Grounding of genus *Ophiocordyceps* in a type species to strictly define a core *Ophiocordyceps* clade and circumscribe other clades, has remained a longstanding problem owing to the rarity of the type species, and age of its holotype specimen. Increasingly routine chemical profiling by high resolution LC-MS and metabolomics analysis applied to the characterization of fungi in taxonomic studies adds an additional layer of phenotypic assessment that could be indispensable for taxon circumscriptions. Increasing efforts to profile and characterize specialized metabolites in fungi will not only provide useful data for taxonomists but is critical for understanding fungal ecology and may also guide pharmaceutical drug discovery efforts. These pursuits are highly complementary, as demonstrated here and in ongoing research. The isolation, structure elucidation, organic synthesis, biosynthesis, biological characterization, and chemical ecology of the paraisariamides are the focus of ongoing research.

Acknowledgements

Any opinions, findings, and conclusions or recommendations expressed in this material are those of the author(s) and do not necessarily reflect the views of the National Science Foundation. We thank Dr. Jessie Uehling and Kyle Gervers at the Oregon State University herbarium for assistance with processing loans and accessioning specimens, Lee Davies at the Fungarium of Royal Botanic Gardens, Kew (K), and Shannon Dominick at the U.S. National Fungus Collections (BPI) for assistance processing herbarium loans. We thank Dr. Kathryn Bushley, Michael Wheeler, and Nin Knight at the USDA ARSEF collection for assistance with culture curation. We thank Dr. Chris Marshall at Oregon State University for assistance in the identification of insect hosts.

Additional information

Conflict of interest

The authors have declared that no competing interests exist.

Ethical statement

No ethical statement was reported.

Funding

This research was supported in part by the National Institutes of Health via NCCIH 1T32 AT010131 (support of RMT) and NIGMS 1R01GM132649 (KLM), the National Science Foundation (DEB-135944 to JWS, KLM), The Sonoma County Mycological Society, The Oregon Mycological Society, and The Cascade Mycological Society.

Author contributions

Conceptualization: RMT, JWS, KLM. Methodology: RMT, JWS, KLM. Formal analysis: RMT. Investigation: RMT, CBD. Resources: JWS, KLM. Data Curation: RMT, EGB, CBD. Writing - Original draft: RMT. Writing - Review and Editing: RMT, KLM, JWS. Visualization: RMT, EGB. Supervision: JWS, KLM. Project administration: RMT. Funding Acquisition: RMT, KLM, JWS.

Author ORCIDs

Richard M. Tehan  <https://orcid.org/0000-0001-7039-3610>

Connor B. Dooley  <https://orcid.org/0009-0007-5692-1182>

Edward G. Barge  <https://orcid.org/0000-0001-8473-7867>

Kerry L. McPhail  <https://orcid.org/0000-0003-2076-1002>

Joseph W. Spatafora  <https://orcid.org/0000-0002-7183-1384>

Data availability

All of the data that support the findings of this study are available in the main text or Supplementary Information.

References

- Araújo JPM, Evans HC, Kepler R, Hughes DP (2018) Zombie-ant fungi across continents: 15 new species and new combinations within *Ophiocordyceps*. I. Myrmecophilous hirsutelloid species. *Studies in Mycology* 90(1): 119–160. <https://doi.org/10.1016/j.simyco.2017.12.002>
- Araújo JPM, Lebert BM, Vermeulen S, Brachmann A, Ohm RA, Evans HC, de Bekker C (2022) Masters of the manipulator: Two new hypocrealean genera, *Niveomyces* (Cordycipitaceae) and *Torrubiellomyces* (Ophiocordycipitaceae), parasitic on the zombie ant fungus *Ophiocordyceps camponoti-floridani*. *Persoonia* 49(1): 171–194. <https://doi.org/10.3767/persoonia.2022.49.05>
- Ban S, Sakane T, Nakagiri A (2015) Three new species of *Ophiocordyceps* and overview of anamorph types in the genus and the family Ophiocordyceptaceae. *Mycological Progress* 14(1): 1017. <https://doi.org/10.1007/s11557-014-1017-8>
- Blount RR (2018) Secondary Metabolism in *Tolypocladium*: Characterization, Ecology, Evolution and Regulation [Doctoral Dissertation]. Department of Botany and Plant Pathology, Oregon State University. Corvallis, OR.

- Castlebury LA, Rossman AY, Sung GH, Hyten AS, Spatafora JW (2004) Multi-gene phylogeny reveals new lineage for *Stachybotrys chartarum*, the indoor air fungus. *Mycological Research* 108(8): 864–872. <https://doi.org/10.1017/S0953756204000607>
- Cedeño-Sánchez M, Charria-Girón E, Lambert C, Luangsa-ard JJ, Decock C, Franke R, Brönstrup M, Stadler M (2023) Segregation of the genus *Parahyphoxylon* (Hyphoxylaceae, Xylariales) from *Hyphoxylon* by a polyphasic taxonomic approach. *MycKeys* 95: 131–162. <https://doi.org/10.3897/mycokeys.95.98125>
- Chaverri P, Samuels GJ, Hodge KT (2005) The genus *Podocrella* and its nematode killing anamorph *Harposporium*. *Mycologia* 97(2): 433–443. <https://doi.org/10.1080/15572536.2006.11832819>
- Cooke MC (1883) Some exotic fungi. *Grevillea* 12(61): 37–39.
- Delacroix G (1893) Travaux du Laboratoire de Pathologie Végétale. *Bulletin de la Société Mycologique de France* 9: 260–268.
- Doan UV, Mendez Rojas B, Kirby R (2017) Unintentional ingestion of *Cordyceps* fungus-infected cicada nymphs causing ibotenic acid poisoning in Southern Vietnam. *Clinical Toxicology (Philadelphia, PA)* 55(8): 893–896. <https://doi.org/10.1080/15563650.2017.1319066>
- Edgar RC (2004) MUSCLE: Multiple sequence alignment with high accuracy and high throughput. *Nucleic Acids Research* 32(5): 1792–1797. <https://doi.org/10.1093/nar/gkh340>
- Gardes M, Bruns TD (1993) ITS primers with enhanced specificity for basidiomycetes - application to the identification of mycorrhizae and rusts. *Molecular Ecology* 2(2): 113–118. <https://doi.org/10.1111/j.1365-294X.1993.tb00005.x>
- Haque FM, Grayson SM (2020) The synthesis, properties and potential applications of cyclic polymers. *Nature Chemistry* 12(5): 433–444. <https://doi.org/10.1038/s41557-020-0440-5>
- Hofstetter V, Miadlikowska J, Kauff F, Lutzoni F (2007) Phylogenetic comparison of protein-coding versus ribosomal RNA-coding sequence data: A case study of the Lecanoromycetes (Ascomycota). *Molecular Phylogenetics and Evolution* 44(1): 412–426. <https://doi.org/10.1016/j.ympev.2006.10.016>
- iNaturalist (2023) iNaturalist. <https://www.inaturalist.org/> [Accessed 15 August 2023]
- Johnson D, Sung GH, Hywel-Jones NL, Luangsa-Ard JJ, Bischoff JF, Kepler RM, Spatafora JW (2009) Systematics and evolution of the genus *Torrubiella* (Hypocreales, Ascomycota). *Mycological Research* 113(3): 279–289. <https://doi.org/10.1016/j.mycres.2008.09.008>
- Kauff F, Lutzoni F (2002) Phylogeny of the Gyalectales and Ostropales (Ascomycota, Fungi): Among and within order relationships based on nuclear ribosomal RNA small and large subunits. *Molecular Phylogenetics and Evolution* 25(1): 138–156. [https://doi.org/10.1016/S1055-7903\(02\)00214-2](https://doi.org/10.1016/S1055-7903(02)00214-2)
- Kepler RM, Kaitsu Y, Tanaka E, Shimano S, Spatafora JW (2011) *Ophiocordyceps pulvinata* sp. nov., a pathogen with a reduced stroma. *Mycoscience* 52(1): 39–47. <https://doi.org/10.1007/S10267-010-0072-5>
- Kepler RM, Sung GH, Harada Y, Tanaka K, Tanaka E, Hosoya T, Bischoff JF, Spatafora JW (2012) Host jumping onto close relatives and across kingdoms by *Tyrannicordyceps* (Clavicipitaceae) gen. nov. and *Ustilaginoidea* (Clavicipitaceae). *American Journal of Botany* 99(3): 552–561. <https://doi.org/10.3732/ajb.1100124>
- Kepler R, Ban S, Nakagiri A, Bischoff J, Hywel-Jones N, Owensby CA, Spatafora JW (2013) The phylogenetic placement of hypocrealean insect pathogens in the genus

- Polycephalomyces*: An application of One Fungus One Name. *Fungal Biology* 117(9): 611–622. <https://doi.org/10.1016/j.funbio.2013.06.002>
- Kepler RM, Luangsa-Ard JJ, Hywel-Jones NL, Quandt CA, Sung GH, Rehner SA, Aime MC, Henkel TW, Sanjuan T, Zare R, Chen M, Li Z, Rossman AY, Spatafora JW, Shrestha B (2017) A phylogenetically-based nomenclature for Cordycipitaceae (Hypocreales). *IMA Fungus* 8(2): 335–353. <https://doi.org/10.5598/imafungus.2017.08.02.08>
- Kil YS, Risinger AL, Petersen CL, Mooberry SL, Cichewicz RH (2020) Leucino-statins from *Ophiocordyceps* spp. and *Purpureocillium* spp. demonstrate selective antiproliferative effects in cells representing the luminal androgen receptor subtype of triple negative breast cancer. *Journal of Natural Products* 83(6): 2010–2024. <https://doi.org/10.1021/acs.jnatprod.0c00404>
- Krasnoff SB, Reátegui RF, Wagenaar MM, Gloer JB, Gibson DM (2005) Cicadapeptins I and II: New Aib-containing peptides from the entomopathogenic fungus *Cordyceps heteropoda*. *Journal of Natural Products* 68(1): 50–55. <https://doi.org/10.1021/np0497189>
- Li CR, Ming L, Fan MZ, Li ZZ (2004) *Paraisaria gracilioides* comb. nov., the anamorph of *Cordyceps gracilioides*. *Mycosystema* 23(1): 165–166.
- Lloyd CG (1920) *Mycological Notes* 62. *Mycological Writings* 6(62): 904–944.
- Mongkolsamrit S, Noisripoom W, Arnarnart N, Lamlerthton S, Himaman W, Jangsantear P, Samson RA, Luangsa-ard JJ (2019) Resurrection of *Paraisaria* in the Ophiocordycipitaceae with three new species from Thailand. *Mycological Progress* 18(9): 1213–1230. <https://doi.org/10.1007/s11557-019-01518-x>
- MycoPortal (2023) Mycological Collections data Portal. <https://www.mycportal.org/portal/collections> [Accessed 11 August 2023]
- Olarte RA, Menke J, Zhang Y, Sullivan S, Slot JC, Huang Y, Badalamenti JP, Quandt AC, Spatafora JW, Bushley KE (2019) Chromosome rearrangements shape the diversification of secondary metabolism in the cyclosporin producing fungus *Tolypocladium inflatum*. *BMC Genomics* 20(1): 1–23. <https://doi.org/10.1186/s12864-018-5399-x>
- Petch T (1935) Notes on entomogenous fungi. *Transactions of the British Mycological Society* 19(3): 161–194. [https://doi.org/10.1016/S0007-1536\(35\)80008-9](https://doi.org/10.1016/S0007-1536(35)80008-9)
- Pluskal T, Castillo S, Villar-Briones A, Orešič M (2010) MZmine 2: Modular framework for processing, visualizing, and analyzing mass spectrometry-based molecular profile data. *BMC Bioinformatics* 11(1): 395. <https://doi.org/10.1186/1471-2105-11-395>
- Quandt CA, Kepler RM, Gams W, Araújo JPM, Ban S, Evans HC, Hughes D, Hywel-Jones N, Li Z, Luangsa-ard JJ, Rehner SA, Sanjuan T, Sato H, Shrestha B, Sung GH, Yao YJ, Zare R, Spatafora JW (2014) Phylogenetic-based nomenclatural proposals for Ophiocordycipitaceae (Hypocreales) with new combinations in *Tolypocladium*. *IMA Fungus* 5(1): 14. <https://doi.org/10.5598/imafungus.2014.05.01.12>
- Rehner SA, Samuels GJ (1994) Taxonomy and phylogeny of *Gliocladium* analyzed from nuclear large subunit ribosomal DNA sequences. *Mycological Research* 98(6): 625–634. [https://doi.org/10.1016/S0953-7562\(09\)80409-7](https://doi.org/10.1016/S0953-7562(09)80409-7)
- Samarakoon T, Wang SY, Alford MH (2013) Enhancing PCR amplification of DNA from recalcitrant plant specimens using a trehalose-based additive. *Applications in Plant Sciences* 1(1): 1200236. <https://doi.org/10.3732/apps.1200236>
- Samson RA, Brady BL (1983) *Paraisaria*, a new genus for *Isaria dubia*, the anamorph of *Cordyceps gracilis*. *Transactions of the British Mycological Society* 81(2): 285–290. [https://doi.org/10.1016/S0007-1536\(83\)80081-3](https://doi.org/10.1016/S0007-1536(83)80081-3)
- Sanjuan TI, Franco-Molano AE, Kepler RM, Spatafora JW, Tabima J, Vasco-Palacios AM, Restrepo S (2015) Five new species of entomopathogenic fungi from the Amazon

- and evolution of neotropical *Ophiocordyceps*. *Fungal Biology* 119(10): 901–916. <https://doi.org/10.1016/j.funbio.2015.06.010>
- Schoch CL, Seifert KA, Huhndorf S, Robert V, Spouge JL, Levesque CA, Chen W, Consortium FB (2012) Nuclear ribosomal internal transcribed spacer (ITS) region as a universal DNA barcode marker for Fungi. *Proceedings of the National Academy of Sciences of the United States of America* 109(16): 6241–6246. <https://doi.org/10.1073/pnas.1117018109>
- Spatafora JW, Sung GH, Sung JM, Hywel-Jones NL, White Jr JF (2007) Phylogenetic evidence for an animal pathogen origin of ergot and the grass endophytes. *Molecular Ecology* 16(8): 1701–1711. <https://doi.org/10.1111/j.1365-294X.2007.03225.x>
- Sung GH, Spatafora JW, Zare R, Hodge KT, Gams W (2001) A revision of *Verticillium* sect. *Prostrata*. II. Phylogenetic analyses of SSU and LSU nuclear rDNA sequences from anamorphs and teleomorphs of the Clavicipitaceae. *Nova Hedwigia* 72(3–4): 311–328. <https://doi.org/10.1127/nova.hedwigia/72/2001/311>
- Sung GH, Hywel-Jones NL, Sung JM, Luangsa-ard JJ, Shrestha B, Spatafora JW (2007) Phylogenetic classification of *Cordyceps* and the clavicipitaceous fungi. *Studies in Mycology* 57: 5–59. <https://doi.org/10.3114/sim.2007.57.01>
- Tehan RM (2022) Drug discovery and chemical ecology investigations of specialized metabolism in *Tolypocladium* and *Paraisaria*. Doctoral Dissertation. College of Pharmacy, Oregon State University. Corvallis, OR.
- Tehan RM, Blount RR, Goold RL, Mattos DR, Spatafora NR, Tabima JF, Gazis R, Wang C, Ishmael JE, Spatafora JW, McPhail KL (2022) Tolypocladamide H and the proposed Tolypocladamide NRPS in *Tolypocladium* species. *Journal of Natural Products* 85(5): 1363–1373. <https://doi.org/10.1021/acs.jnatprod.2c00153>
- The Orthopterists' Society (2023) The Orthopterists' Society. <https://orthsoc.org/sina/339m.htm> [Accessed 12 August 2023]
- Umeyama A, Okada M, Nakamura Y, Suenaga M, Nakano M, Imakawa H, Hashimoto T, Kumada T, Adachi K, Oku N, Kawabata T, Shizuri Y, Ishiyama Y, Otoguro K, Omura S (2011) Isolation and structure of a novel cyclic peptide derived from *Cordyceps sinensis*, *Ophiocordyceps heteropoda*, and the marine microorganism *Photobacterium* sp. [Poster]. *Proceedings of the natural organic compounds debate*. https://www.jstage.jst.go.jp/article/tennenyuki/53/0/53_385/_article/-char/ja/
- Vilgalys R, Hester M (1990) Rapid genetic identification and mapping of enzymatically amplified ribosomal DNA from several *Cryptococcus* species. *Journal of Bacteriology* 172(8): 4238–4246. <https://doi.org/10.1128/jb.172.8.4238-4246.1990>
- Vu D, Groenewald M, De Vries M, Gehrman T, Stielow B, Eberhardt U, Al-Hatmi A, Groenewald JZ, Cardinali G, Houbraeken J, Boukhout T, Crous PW, Robert V, Verkley GJM (2019) Large-scale generation and analysis of filamentous fungal DNA barcodes boosts coverage for kingdom fungi and reveals thresholds for fungal species and higher taxon delimitation. *Studies in Mycology* 92(1): 135–154. <https://doi.org/10.1016/j.simyco.2018.05.001>
- Wang M, Carver JJ, Phelan VV, Sanchez LM, Garg N, Peng Y, Nguyen DD, Watrous J, Kapon CA, Luzzatto-Knaan T, Porto C, Bouslimani A, Melnik AV, Meehan MJ, Liu W-T, Crüsemann M, Boudreau PD, Esquenazi E, Sandoval-Calderón M, Kersten RD, Pace LA, Quinn RA, Duncan KR, Hsu C-C, Floros DJ, Gavilan RG, Kleigrewe K, Northen T, Dutton RJ, Parrot D, Carlson EE, Aigle B, Michelsen CF, Jelsbak L, Sohlenkamp C, Pevzner P, Edlund A, McLean J, Piel J, Murphy BT, Gerwick L, Liaw C-C, Yang Y-L, Humpf H-U, Maansson M, Keyzers RA, Sims AC, Johnson AR, Sidebottom AM, Sedio BE, Klitgaard A, Larson CB, Boya PCA, Torres-Mendoza D, Gonzalez DJ, Silva DB,

- Marques LM, Demarque DP, Pociute E, O'Neill EC, Briand E, Helfrich EJN, Granatosky EA, Glukhov E, Ryffel F, Houson H, Mohimani H, Kharbush JJ, Zeng Y, Vorholt JA, Kurita KL, Charusanti P, McPhail KL, Nielsen KF, Vuong L, Elfeki M, Traxler MF, Engene N, Koyama N, Vining OB, Baric R, Silva RR, Mascuch SJ, Tomasi S, Jenkins S, Macherla V, Hoffman T, Agarwal V, Williams PG, Dai J, Neupane R, Gurr J, Rodríguez AMC, Lamsa A, Zhang C, Dorrestein K, Duggan BM, Almaliti J, Allard P-M, Phapale P, Nothias L-F, Alexandrov T, Litaudon M, Wolfender J-L, Kyle JE, Metz TO, Peryea T, Nguyen D-T, VanLeer D, Shinn P, Jadhav A, Müller R, Waters KM, Shi W, Liu X, Zhang L, Knight R, Jensen PR, Palsson BØ, Pogliano K, Lington RG, Gutiérrez M, Lopes NP, Gerwick WH, Moore BS, Dorrestein PC, Bandeira N (2016) Sharing and community curation of mass spectrometry data with Global Natural Products Social Molecular Networking. *Nature Biotechnology* 34(8): 828–837. <https://doi.org/10.1038/nbt.3597>
- Wang YH, Ban S, Wang WJ, Li Y, Wang K, Kirk PM, Bushley KE, Dong CH, Hawksworth DL, Yao YJ (2021) *Pleurocordyceps* gen. nov. for a clade of fungi previously included in *Polycephalomyces* based on molecular phylogeny and morphology. *Journal of Systematics and Evolution* 59(5): 1065–1080. <https://doi.org/10.1111/jse.12705>
- Wei DP, Wanasinghe DN, Xu JC, To-Anun C, Mortimer PE, Hyde KD, Elgorban AM, Madawala S, Suwannarach N, Karunarathna SC, Tibpromma S, Lumyong S (2021) Three novel entomopathogenic fungi from China and Thailand. *Frontiers in Microbiology* 11: 608991. <https://doi.org/10.3389/fmicb.2020.608991>
- White TJ, Bruns TD, Lee S, Taylor JW (1990) Amplification and direct sequencing of fungal ribosomal RNA genes for phylogenetics. In: Innis MA, Gelfand DH, Sninsky JJ, White TJ (Eds) *PCR protocols: A guide to the methods and applications*. Academic Press, 315–322. <https://doi.org/10.1016/B978-0-12-372180-8.50042-1>

Supplementary material 1

Endosclerotia LCMS feature list

Author: Richard M. Tehan

Data type: csv

Explanation note: This table comprises processed LCMS data for methanol extracts of the endosclerotia of 19 vouchered specimens.

Copyright notice: This dataset is made available under the Open Database License (<http://opendatacommons.org/licenses/odbl/1.0/>). The Open Database License (ODbL) is a license agreement intended to allow users to freely share, modify, and use this Dataset while maintaining this same freedom for others, provided that the original source and author(s) are credited.

Link: <https://doi.org/10.3897/mycokeys.100.110959.suppl1>

Taxonomy and evolution history of two new litter-decomposing *Ciliochorella* (Amphisphaeriales, Sporocadaceae)

Jia-Yu Song¹, Hai-Xia Wu^{1,2}, Jin-Chen Li¹, Wei-Feng Ding^{1,2}, Cui-Ling Gong¹, Xiang-Yu Zeng³, Nalin N. Wijayawardene⁴, Da-Xin Yang⁵

¹ International Fungal Research and Development Centre, Institute of Highland Forest Science, Chinese Academy of Forestry, Kunming 650224, China

² Key Laboratory of Breeding and Utilization of Resource Insects, National Forestry and Grassland Administration, Kunming 650224, China

³ Department of Plant Pathology, College of Agriculture, Guizhou University, Guiyang 550025, China

⁴ Centre for Yunnan Plateau Biological Resources Protection and Utilization, College of Biological Resource and Food Engineering, Qujing Normal University, Qujing, Yunnan 655011, China

⁵ Kunming Branch (KMB), Chinese Academy of Sciences (CAS), Kunming, Yunnan 650204, China

Corresponding author: Hai-Xia Wu (aileen2008haixia@gmail.com)

Abstract

The genus *Ciliochorella* is a group of pestalotioid fungi, which typically occurs in subtropical and tropical areas. Species from the *Ciliochorella* genus play important roles in the decomposition of litter. In this study, we introduce two new species (*Ciliochorella chinensis* **sp. nov.** and *C. savannica* **sp. nov.**) that were found on leaf litter collected from savanna-like vegetation in hot dry valleys of southwestern China. Phylogenetic analyses of combined LSU, ITS and *tub2* sequence datasets indicated that *C. chinensis* and *C. savannica* respectively form a distinct clade within the *Ciliochorella* genus. The comparison of the morphological characteristics indicated that the two new species are well differentiated within this genus species. Analysis of the evolutionary history suggests that *Ciliochorella* originated from the Eurasian continent during the Paleogene (38 Mya). Further, we find that both new species can produce cellulase and laccase, playing a decomposer role.

Key words: Ancestral biogeography, leaf litter degradation, morphology, new taxa, time dating



Academic editor: Xinlei Fan

Received: 1 July 2023

Accepted: 21 October 2023

Published: 13 November 2023

Citation: Song J-Y, Wu H-X, Li J-C, Ding W-F, Gong C-L, Zeng X-Y, Wijayawardene NN, Yang D-X (2023) Taxonomy and evolution history of two new litter-decomposing *Ciliochorella* (Amphisphaeriales, Sporocadaceae). MycoKeys 100: 95–121. <https://doi.org/10.3897/mycokeys.100.108863>

Copyright: © Jia-Yu Song et al.

This is an open access article distributed under terms of the Creative Commons Attribution License (Attribution 4.0 International – CC BY 4.0).

Introduction

Fungi thrive on diverse ecosystems and environments as pathogens, mutualists, and saprobes (Bucher et al. 2004; Schmit and Mueller 2007; Jobard et al. 2010; Hyde et al. 2020; Lai et al. 2021). As decomposers of nature, fungi are involved in the degradation of lignin and cellulose (Bisaria and Ghose 1981; Hatakka 1994; Adlini et al. 2014). The extracellular lignin-degrading enzymes of fungi mainly comprise two types, peroxidases and laccases (Pointing et al. 2005; Floudas et al. 2012). Some plant-specific pathogenic fungi use laccases to counter the effects of tannic acid, which also has anti-viral activities (Dong and Changsun 2021). As such, laccase activity is also considered a virulence factor in many fungal diseases.

Ciliochorella Sydow & Mitter (1935), typified by *C. mangiferae* Syd., is an important genus of pestalotioid fungi (Sutton 1980; Nag Raj 1993; Lee et al. 2006; Tanaka et al. 2011; Tangthirasun et al. 2015; Wijayawardene et al. 2016; Liu et al. 2019a). Most taxa classified as pestalotioid fungi are phytopathogens that cause a variety of diseases in plants, some of which are saprobes or endophytes that are widely distributed in tropical and temperate regions (Benjamin and Guba 1961; Barr 1975; Nag Raj 1993; Maharachchikumbura et al. 2016). Liu et al. (2019a) and Wijayawardene et al. (2022a) placed this genus in Sporocadaceae (Ascomycota, Sordariomycetes, Amphisphaerales).

Ciliochorella is an asexually typified, coelomycetous genus with nine species listed in the Index Fungorum (2023). However, only six species are accepted in the Species Fungorum (2023) due to the following two reports: 1) Subramanian and Ramakrishnan (1956) proposed *Shanoria* Subram. & Ramakr., a new genus, to accommodate *Ciliochorella bambusarum* Shanor as *Shanoria bambusarum* (Shanor) Subram. & K. Ramakr.; 2) Nag Raj (1993) synonymized *Ciliochorella eucalypti* T.S. Viswan. and *Ciliochorella indica* Kalani under *C. mangiferae*. The genus is characterized by cylindrical, straight, or slightly curved conidia with septate pale brown middle cells, and colorless end cells bearing a single, eccentric appendage (Nag Raj 1993; Allegrucci et al. 2011; Hyde et al. 2016; Wijayawardene et al. 2016).

There are few studies that focused on the divergence time estimation of *Ciliochorella*, whereas some published studies are based on a larger classification scale (such as the order and the class). Divergence time can provide insights into the history of a given group of fungi species and its taxonomic placement (Li et al. 2005; Vijaykrishna et al. 2006; Beimforde et al. 2014; Pérez-Ortega et al. 2016; Samarakoon et al. 2016; Li et al. 2023). Samarakoon et al. (2016; 2022) estimated the divergence time of the Xylariomycetidae, including one species of *Ciliochorella* (*C. mangiferae*), diverged approximately 201–252 Mya in the Early Mesozoic (Samarakoon et al. 2022). Chen et al. (2023) conducted detailed genomic studies on the divergence time of members in Sordariomycetes, which included nine species of Sporocadaceae. The results show that the divergence time of Sporocadaceae is about 90.56 Mya. In addition to estimating divergence times, ancestral state reconstruction is also a viable strategy for studying evolutionary history. Ancestral state reconstruction can reveal the origin and evolution of a species and provide a basis for species classification (Omland 1999; Ismail et al. 2016; Royer-Carenzi and Didier 2016; Gao and Wu 2022; Li et al. 2022). However, relevant research examining the ancestral reconstruction of *Ciliochorella* is lacking.

Studies on the litter decomposition of *Ciliochorella* have demonstrated oxidative enzymatic activity using *in-vitro* cultures of *Ciliochorella buxifolia* demonstrated by Troncozo et al. (2015). It is also worth noting that *C. mangiferae* is an important litter-decomposing taxon in tropical countries, especially in India (Masilamani and Muthumary 1994). This genus may be involved in the leaf decomposition process, but not all species in this genus have been verified to have this function (Saparrat et al. 2010).

The primary objectives of this study were: 1) to delineate the taxonomic status of newly collected *Ciliochorella*-like species; 2) to estimate the evolutionary history of *Ciliochorella*; and 3) to determine the litter-decomposing function of this genus species in nature based on the screening of cellulase and laccase production.

Methods

Morphological studies

Two *Ciliochorella*-like taxa were collected from leaf litter (dead leaves from an unidentified plant species) in the savanna-like vegetation of hot dry valleys in southwestern China. The samples were placed in paper bags and transported to the laboratory for further observation. Following Wu et al. (2014), the collected samples were processed and examined by microscopes: photographs of ascomata were taken by using a compound stereomicroscope (KEYENCE CORPORATION V.1.10 with camera VHZ20R). Hand sections were made under a stereomicroscope (OLYMPUS SZ61) and mounted in water and blue cotton Photomicrographs of fungal structures were taken with a compound microscope (Nikon ECLIPSE 80i).

The images used for the figures were processed using the software Adobe Photoshop CC v. 2015.5.0 software (Adobe Systems, San Jose, CA, USA).

The specimens were deposited in the herbarium of IFRD (International Fungal Research & Development Centre; Institute of Highland Forest Science, Chinese Academy of Forestry, Kunming, China) and the cultures were deposited in the International Fungal Research & Development Center Culture Collection (IFRDCC) at the Research Institute of Highland Forest Science, Chinese Academy of Forestry, Kunming, China.

Single spore isolation was performed following the procedure published by Choi et al. (1999) and Chomnunti et al. (2014). Germinated spores were individually transferred to potato dextrose agar (PDA) medium and incubated at 26 °C for 48 h. Colony characteristics were observed and measured after two weeks at 26 °C.

Newly introduced taxa were registered at Fungal Names (<https://nmdc.cn/fungalnames/>) and obtained identifiers.

DNA isolation, amplification and sequencing

Genomic DNA was extracted from mycelia growing on PDA at room temperature using the Forensic DNA Kit (OMEGA, USA) according to the manufacturer's instructions. The primers LR0R and LR5 were used to amplify the 28S large subunit (LSU) rDNA (Vilgalys and Hester 1990). The internal transcribed spacer (ITS) rDNA was amplified and sequenced with the primers ITS5 and ITS4 (White et al. 1990). The primers T12 and T22 were used to amplify the β -tubulin (*tub2*) (O'Donnell and Cigelnik 1997). The following PCR protocol was used: initial denaturation at 98 °C for 2 min, then 30 cycles, i) 98 °C denaturation for 10 s, ii) 56 °C annealing for 10 s, and iii) 72 °C extension for 10 s (ITS) or 20 s (LSU and *tub2*) followed by a final extension at 72 °C for 1 min. All PCR products were sequenced by Biomed (Beijing, China).

Sequence alignments and phylogenetic analyses

BioEdit version 7.0.5.3 was used to re-assemble sequences generated from forward and reverse primers to obtain the integrated sequences (Hall 1999). The sequences used by literature and closely related taxa from NCBI BLAST results (Table 1). Sequence alignments were performed in MAFFT (<https://mafft.cbrC.jp/alignment/server/>) (Katoh et al. 2019), and alignments were manually

Table 1. Selected taxa in this study with their corresponding GenBank accession numbers and distribution information.

Species	Location	Voucher/ Strains	GenBank accession numbers			Reference
			LSU	ITS	<i>tub2</i>	
<i>Ciliochorella castaneae</i>	East Asia (Japan); South Asia (India)	HHUF 28799	AB433277	–	–	Nag Raj 1993; Endo et al.2008
<i>C. castaneae</i>	East Asia (Japan); South Asia (India)	HHUF 28800	AB433278	–	–	Nag Raj 1993; Endo et al. 2008
<i>C. chinensis</i>	East Asia (China)	IFRD 9468	OP902256	OP902250	OQ918680	In this study
<i>C. dipteroearpi</i>	Southeast Asia (Thailand)	MFLUCC 22-0132	OP912990	OP912991	–	Nethmini et al. 2023
<i>C. mangiferae</i> *	Southeast Asia (Thailand); South Asia (India, Pakistan); America (Cuba); Africa (Nigeria, Sierra Leone);	MFLUCC 12-0310	KF827445	KF827444	KF827478	Nag Raj 1993; Masilamani and Muthumary 1994; Tangthirasunun et al. 2015
<i>C. phanericola</i>	Southeast Asia (Thailand)	MFLUCC 14-0984	KX789681	KX789680	KX789682.1	Hyde et al. 2016
<i>C. savannica</i>	East Asia (China)	IFRD 9467	OP902279	OP902251	OQ926205	In this study
	East Asia (China)	IFRD 9473	OQ867459	OQ867475	OQ926206	In this study
<i>Discosia</i> aff. <i>brasiliensis</i>	Unknown	NBRC 104199	AB593707	AB594775	AB594185	Tanaka et al. 2011
<i>D. aff. pleurochaeta</i>	Unknown	KT2188	AB593713	AB594781	AB594179	Tanaka et al. 2011
<i>D. artocreas</i> *	Unknown	NBRC 8975	AB593705	AB594773	AB594172	Tanaka et al. 2011
<i>D. brasiliensis</i>	Southeast Asia (Thailand)	NTCL095	KF827437	KF827433	KF827470	Tangthirasunun et al. 2015
<i>D. celtidis</i>	East Asia (China)	MFLU 18-2581	MW114406	NR_174839	–	Tennakoon et al. 2021
<i>D. fagi</i>	Europe (Italy)	MFLU 14-0299A	KM678048	KM678040	–	Li et al. 2015
<i>D. fici</i>	East Asia (China)	MFLU 19-2704	MW114409.1	NR_174840	–	Tennakoon et al. 2021
<i>D. italica</i>	Europe (Italy)	MFLU 14-0298C	KM678044	KM678041	–	Li et al. 2015
<i>D. macrozambiae</i>	Oceania (Australia)	CPC 32113	MH327855	MH327819	MH327894	Crous et al. 2018
<i>D. pini</i>	Unknown	MAFF 410149	AB593708	AB594776	AB594174	Tanaka et al. 2011
<i>D. pseudoartocreas</i>	Europe (Austria)	CBS 136438	MH877640	NR_132068	MH554672	Crous et al. 2013
	Unknown	DUCC5154	MH844788	MH844763	–	Tanaka et al. 2011
<i>D. querci</i>	East Asia (China)	MFLU 18-0097	MW114405	MW114326	–	Tennakoon et al. 2021
<i>D. tricellularis</i>	Unknown	NBRC 32705	AB593728	AB594796	AB594188	Tanaka et al. 2011
<i>D. yakushimensis</i>	East Asia (Japan)	MAFF 242774	AB593721	AB594789	AB594187	Tanaka et al. 2011
<i>Discostroma tosta</i>	Unknown	HKUCC 1004	AF382380	–	–	Tang et al. 2007
<i>Discost. fuscillum</i>	Europe (Italy)	MFLUCC 14-0052	KT005514	KT005515	–	Senanayake et al. 2015
<i>Discost. stoneae</i>	Unknown	NBRC 32690	AB593729	AB594797	–	Tanaka et al. 2011
<i>Immersidiscosia eucalypti</i> *	East Asia (Japan)	NBRC 104195	AB593722	AB594790	–	Tanaka et al. 2011
<i>I. eucalypti</i> *	East Asia (Japan)	NBRC 104196	AB593723	AB594791	–	Tanaka et al. 2011
	East Asia (Japan)	NBRC 104197	AB593724.1	AB594792	–	Tanaka et al. 2011
	East Asia (Japan)	MAFF 242781	AB593725	AB594793	–	Tanaka et al. 2011
	Unknown	MFLU 16-1372	MF173608	MF173609	–	Tennakoon et al. 2021
<i>Neopestalotiopsis protearum</i> *	Africa (Zimbabwe)	CBS 114178	JN712564	JN712498	KM199463	Maharachchikumbura et al. 2014
<i>N. rosae</i>	Oceania (New Zealand)	CBS 101057	KM116245	KM199359	KM199429	Maharachchikumbura et al. 2014
<i>Pestalotiopsis knightiae</i>	Oceania (New Zealand)	CBS 114138	KM116227	KM199310	KM199408	Maharachchikumbura et al. 2014
<i>P. malayana</i>	Southeast Asia (Malaysia)	CBS 102220	KM116238	KM199306	KM199411	Maharachchikumbura et al. 2014
<i>P. spathuliappendiculata</i>	Oceania (Australia)	CBS 144035	MH554366	MH554172	MH554845	Liu et al. 2019
<i>Pseudopestalotiopsis cocos</i>	Southeast Asia (Indonesia)	CBS 272.29	KM116276	KM199378	KM199467	Maharachchikumbura et al. 2014

Species	Location	Voucher/ Strains	GenBank accession numbers			Reference
			LSU	ITS	tub2	
<i>Ps. theae</i> *	East Asia (China), Southeast Asia (Thailand)	MFLUCC 12-0055	KM116282	JQ683727	JQ683711	Maharachchikumbura et al. 2014
<i>Robillarda africana</i>	Africa (South Africa)	CBS 122.75	KR873281	KR873253	MH554656	Crous et al. 2015
<i>R. roystoneae</i>	East Asia (China)	CBS 115445	KR873282	KR873254	KR873317	Crous et al. 2015
	East Asia (China)	MFLUCC 19-0060	MW114402	MW114323	–	Tennakoon et al. 2021
<i>R. sessilis</i> *	Europe (Germany)	CBS 114312	KR873284	KR873256	KR873319	Crous et al. 2015
<i>R. terrae</i>	South Asia (India)	CBS 587.71	KJ710459	KJ710484	MH554734	Crous et al. 2015
<i>Seimatosporium azaleae</i>	Unknown	MAFF 237478	AB593730	AB594798	AB594189	Tanaka et al. 2011
<i>S. bisepatum</i>	Oceania (Australia)	CPC 13584	JN871208	JN871199	MH554749	Barber et al. 2011
<i>S. botan</i>	America (Chile)	HMUC 316PD	–	JN088483	–	Díaz et al. 2012
<i>S. cornicola</i>	Europe (Italy)	MFLUCC 14-0448	–	KU974967	–	Wijayawardene et al. 2016
<i>S. cornii</i>	Europe (Italy)	MFLUCC 14-1208	KT868531	KT868532	–	Perera et al. 2016
<i>S. elegans</i>	Oceania (Australia)	NBRC 32674	AB593733	AB594801	MH554683	Tanaka et al. 2011
<i>S. eucalypti</i>	Africa (South Africa)	CPC 156	JN871209	JN871200	MH704627	Barber et al. 2011
<i>S. falcatum</i>	Oceania (Australia)	CPC 13578	JN871213	JN871204	MH554668	Barber et al. 2011
<i>S. grevilleae</i>	Africa (South Africa)	ICMP 10981	AF382372	AF405304	–	Jeewon et al. 2002
<i>S. italicum</i>	Europe (Italy)	MFULCC 14-1196	NG_064463	NR_157485	–	Hyde et al. 2017
<i>S. leptospermi</i>	Oceania (New Zealand)	ICMP 11845	AF382373	–	–	Jeewon et al. 2002
<i>S. obtusum</i>	Oceania (Australia)	CPC 12935	JN871215	JN871206	MH554669	Barber et al. 2011
<i>S. physocarpi</i>	Europe (Russia)	MFLUCC 14-0625	KT198723	KT198722	MH554676	Norphanphoun et al. 2015
<i>S. pistaciae</i>	West Asia (Iran)	CBS 138865	KP004491	KP004463	MH554674	Norphanphoun et al. 2015
<i>S. pseudorosae</i>	Europe (Italy)	MFLUCC 14-0468	KU359035	–	–	Li et al. 2015
<i>S. pseudorosarum</i>	Europe (Italy)	MFLUCC 14-0466	KT281912	KT284775	–	Ariyawansa et al. 2015
<i>S. rosae</i> *	Europe (Russia)	MFLUCC 14-0621	KT198727	KT198726	LT853253	Norphanphoun et al. 2015
<i>S. rosicola</i>	Europe (Italy)	MFLU 16-0239	MG829069	MG828958	–	Wanasinghe et al. 2018
	Europe (Italy)	MFLUCC 15-0564	MG829070	MG828959	–	Wanasinghe et al. 2018
<i>S. sorbi</i>	Europe (Italy)	MFLUCC 14-0469	KT281911	KT284774	–	Ariyawansa et al. 2015
<i>S. tostum</i>	Unknown	NBRC 32626	AB593727	AB594795	–	Rossmann et al. 2016
<i>S. vaccinii</i>	Oceania (New Zealand)	ICMP 7003	AF382374	–	–	Jeewon et al. 2002
<i>S. vitis</i>	Europe (Italy)	MFLUCC 14-0051	KR920362	NR_156595	–	Senanayake et al. 2015
<i>S. walkeri</i>	Oceania (Australia)	CPC 17644	JN871216	JN871207	MH554769	Barber et al. 2011
<i>Seiridium cancrinum</i>	Africa (Kenya)	CBS 226.55 = IMI 052256	MH554241	LT853089	LT853236	Liu et al. 2019
<i>Seir. cupressi</i>	Africa (Kenya)	CBS 224.55 = IMI 052254	MH554240	LT853083	LT853230	Liu et al. 2019
<i>Seir. eucalypti</i>	Oceania (Australia)	CBS 343.97	MH554251	MH554034	MH554710	Liu et al. 2019
<i>Seir. kartense</i>	Oceania (Australia)	CBS 142629 = CPC 20183	–	LT853100	LT853247	Liu et al. 2019
<i>Seir. kenyanium</i>	Africa (Kenya)	CBS 228.55 = IMI 052257	MH554242	LT853098	LT853245	Liu et al. 2019
<i>Seir. marginatum</i> *	Europe (Austria)	CBS 140404	–	KT949916	–	Jaklitsch et al. 2016
	Europe (France)	CBS 140403	MH554223	KT949914	LT853249	Liu et al. 2019
<i>Seir. neocupressi</i>	Europe (Italy)	CBS 142625 = CPC 23786	MH554329	LT853079	LT853226	Liu et al. 2019
<i>Seir. papillatum</i>	Oceania (Australia)	CBS 340.97	DQ414531	LT853102	LT853250	Liu et al. 2019
<i>Seir. phyllicae</i>	Tristan da Cunha (Atlantic islands)	CBS 133587 = CPC 19964	–	LT853091	LT853238	Liu et al. 2019
<i>Seir. pseudocardinale</i>	Europe (Portugal)	CBS 122613 = CMW 1648	MH554206	LT853096	LT853243	Liu et al. 2019

Species	Location	Voucher/ Strains	GenBank accession numbers			Reference
			LSU	ITS	tub2	
<i>Seir. unicorna</i>	Oceania (New Zealand)	CBS 538.82 = NBRC 32684	MH554269	LT853088	LT853235	Liu et al. 2019
<i>Strickeria kochii</i> *	Europe (Austria)	C143	KT949918	KT949918	–	Jaklitsch et al. 2016
<i>St. kochii</i> *	Europe (Austria)	C149	KT949920	KT949920	–	Jaklitsch et al. 2016
<i>Phlogicylindrium uniforme</i>	Oceania (Australia)	CBS 131312	JQ044445	JQ044426	MH704634	Crous et al. 2015

Type species are marked with an asterisk "*". New species are given in bold.

adjusted where necessary using BioEdit version 7.0.5.3. The sequence data set for subsequent analyses were obtained with the sequence fragments using R-based ape package (Paradis and Schliep 2019).

Phylogenetic analyses were performed using the CIPRES Science Gateway V.3.3 (<https://www.phylo.org/>). For maximum likelihood (ML) analyses, we used RAxML-HPC2 on XSEDE (8.2.12). *Phlogicylindrium uniforme* (CBS 131312) was selected as the outgroup taxon. One thousand non-parametric bootstrap iterations were performed using the "GTRGAMMA" algorithm. For Bayesian analysis, jModelTest2 on XSEDE (2.1.6) was used to estimate the best-fitting model for the combined LSU, ITS and *tub2* genes, and the GTR+I+G model was the best fit. In MrBayes on XSEDE (3.2.7a), four simultaneous Markov chains were run for 2,000,000 generations; trees were sampled and printed every 2,000 generations. The first 25% of all trees were submitted to the burn-in phase and discarded, while the remaining trees were used to compute posterior probabilities in the majority rule consensus tree (Cai et al. 2006, 2008; Wu et al. 2011; Zeng et al. 2019).

Divergence time estimations

In this study, two secondary calibration nodes for the divergence time estimation of *Ciliochorella* were implemented to calibrate the tree: Node 1 was composed of *Phlogicylindrium* (outgroup, Phlogicylindriaceae) and 10 genera from the Sporocadaceae, which diverged 76 Mya; for Node 2 we used *Discosia*, *Robillarda* and the other seven genera (*Ciliochorella*, *Neopestalotiopsis*, *Pestalotiopsis*, *Pseudopestalotiopsis*, *Seimatosporium*, *Seiridium* and *Strickeria*), which diverged 44 Mya (Samarakoon et al. 2016). A maximum likelihood (ML) tree was used as input data and the data were analyzed via R8S 1.81 (<https://sourceforge.net/projects/r8s/>). The divergence time of *Ciliochorella* was estimated based on the PL (Penalized likelihood) method and TN algorithm (truncated Newton algorithm) obtained via R8S (Fig. 2). The R8S program only needs the second calibration node to estimate divergence times, and some methods in this program, such as NPRS (Nonparametric rate smoothing) and PL, which were first proposed by the author, are currently challenging to implement in similar software programs (Sanderson 2003). The PL method and TN algorithm have been implemented to estimate divergence times using data from the ML tree and secondary calibration nodes (Sanderson 2003). The ancient map is based on the results of Peng et al. (2023).

Reconstruction of ancestral biogeographic

RASP (<http://mnh.scu.edu.cn/soft/blog/RASP>) was used to reconstruct the ancestral biogeography in this study. It is a tool to infer the ancestral state

using S-DIVA (Statistical Dispersal-Vicariance Analysis), Lagrange (DEC), Bayes-Lagrange (S-DEC), BayArea, BBM (Bayesian Binary MCMC), Bayestraits and BioGeoBEARS packages (Yu et al. 2015, 2020). Members of *Ciliochorella* were coded based on their collection locality according to references (Table 1). Based on the distribution data in the table, six geographic regions were defined: A = Asia, B = America, C = Europe, D = Africa, E = Oceania, F = Tristan da Cunha, G = Unknown, using species from Asia, America, Europe, Africa, Oceania and Tristan da Cunha. In MrBayes on XSEDE (3.2.7a), chains were run for 2,000,000 generations; trees were sampled and printed every 2,000 generations. RASP 4.2 was used to reconstruct the ancestral state, and the most-optimal model was BAYAREALIKE.

Screening of cellulase and laccase production

Cellulase screening was performed by the Congo red test (Liu and Fan 2012). A fungal cake with a diameter of 8 mm was isolated from the edge of the 7-day old colony and inoculated on solid PDA medium. After 7 days of inoculation, the culture was stained with 1 mg/mL Congo red solution for 10 min, and washed and fixed with 1 mol/L NaCl for 30 min.

Screening for laccase activity in the lignin peroxidase system requires the use of guaiacol-PDA solid medium (Wang et al. 2016), including PDA medium 40.20 g, agar 3.00 g, guaiacol 0.40 mL and distilled water to 1 L with 121 °C sterilization 30 min. The obtained strain was cultured at 26 °C for 7 days, and the fungal cake with a diameter of 8 mm was taken from the growing mycelium at the edge of the colony and inoculated on solid guaiacol-PDA medium. The growth of the strain was observed for 7 days of inoculation.

The supernatant was incubated on a shaker (150 rpm) for 12 hours at 26 °C, followed by centrifugation at 12,000 rpm to obtain a crude enzyme solution. The Thermo Varioskan Flash multifunctional enzyme reader has a characterized absorption peak at 540 nm, which can be used to assess cellulase activity based on changes in absorbance values. Laccase activity was characterized by the change in absorbance at 420 nm and the enzyme activity of the crude enzyme liquid was determined using the Laccase Activity Detection Kit (www.boxbio.cn). The experiment was repeated three times.

Results

Phylogenetic analyses

We analyzed a three-locus (LSU, ITS, *tub2*) data set of *Ciliochorella*. This data set consists of 203 sequences, including 75 LSU sequences, 75 ITS sequences and 53 *tub2* sequences from 80 taxa. The concatenated sequences have 2338 characters including gaps. The two topological trees obtained by maximum likelihood (ML) and Bayesian were found to be similar, and the best-scoring RAxML tree was used as the representative tree (Fig. 1). Bootstrap values of ML greater than 50% are shown on the phylogenetic tree, while values of Bayesian posterior probabilities greater than 0.5 are shown on the tree (Fig. 1).

Phylogenetic analysis showed that *Ciliochorella* species formed a clade with bootstrap values of 70% (in ML analysis) and Bayesian posterior probability of

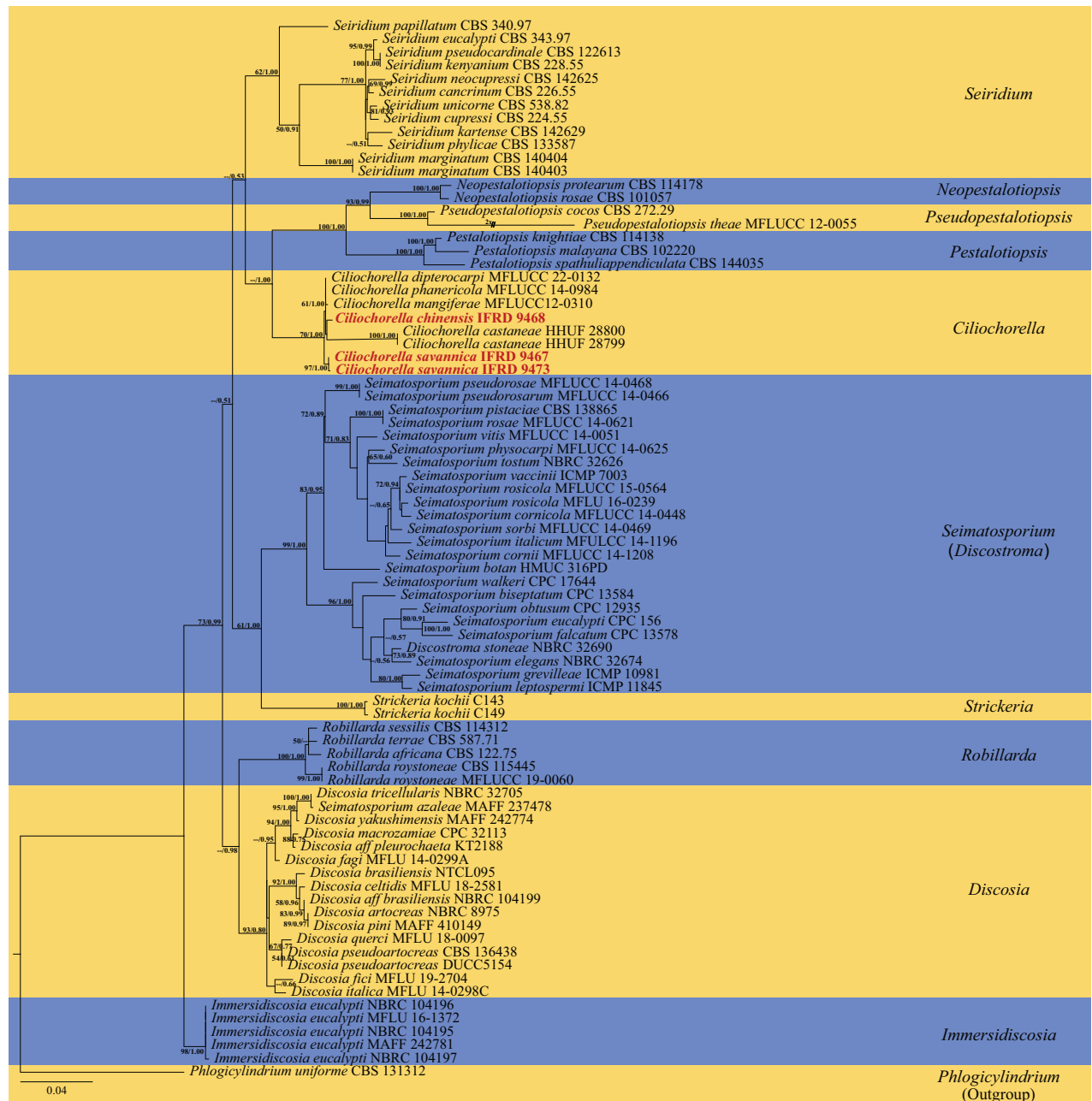


Figure 1. Phylogenetic tree of maximum likelihood analyses showing the relationships of *Ciliochorella* species based on combined LSU, ITS and *tub2* data set analysis. Bootstrap values of maximum likelihood values greater than 50% are shown on the left, while values for Bayesian posterior probabilities greater than 0.5 are shown on the right. *Discostroma* is the sexual morph of *Seimatosporium*. New species are shown in bold and red, followed by their strain number.

1.00 (as a result of new species, the genus forms a separate clade). *Pestalotiopsis*, *Pseudopestalotiopsis*, and *Neopestalotiopsis* formed a clade with bootstrap values of 100% and Bayesian posterior probabilities of 1.00. Notably, this clade was adjacent to the *Ciliochorella* clade. In addition, *Ciliochorella* was also close to *Seiridium* (Fig. 1).

Ciliochorella savannica is distinguished from other *Ciliochorella* in the phylogenetic tree and has a high support rate with 97% ML and 1.00 Bayesian posterior probabilities. *Ciliochorella chinensis* has a close relationship with *C. castaneae* (HHUF 28800).

Divergence time estimation

According to divergence time estimates (Fig. 2), the age of *Ciliochorella* is about 38 Mya in the Paleogene period and falling in the recommended divergence times of Xylariomycetidae by Samarakoon et al. (2016). The ten genera of Sporocadaceae were all originated in the Paleogene. The genus of *Immersidiscosia* initially diverged about 49 Mya. *Discosia* and *Robillarda* formed one clade, with a divergence of time about 35 Mya. The other seven genera formed one clade: *Neopestalotopsis* diverged about at 25 Mya, divergence times of *Pestalotopsis* in the analysis is about 28 Mya, *Pseudopestalotopsis* diverged about at 25 Mya, *Seimatosporium* diverged about at 35 Mya, *Seiridium* diverged about at 41 Mya and *Strickeria* diverged about at 35 Mya.

Ancestral biogeographic reconstruction analysis for *Ciliochorella*

Analysis of ancestral biogeographic reconstructions revealed that *Ciliochorella* species originated in Asia (Fig. 3, node 139). Dispersal, vicariance, extinction, and other historical events affected the biogeographic distribution of individual species. The evolutionary history of the ancestors of the genus *Ciliochorella* showed that the species of this genus underwent 45 dispersals, 27 vicariations, and 2 extinctions (Fig. 3, the blue circle represents dispersal, the green circle represents vicariance, and the yellow circle represents extinction). From approximately the Middle Paleogene, dispersal and vicariance events were frequent. In the early Paleogene, dispersal and extinction events occurred among ancestors of *Pestalotopsis*, *Pseudopestalotopsis*, *Neopestalotopsis*, and *Ciliochorella*. After these events, *Ciliochorella* began to evolve independently of other genera (Fig. 3, node 140). *Pestalotopsis*, *Pseudopestalotopsis*, and *Neopestalotopsis* are predicted to share the same ancestral biogeographic area (Fig. 3, node 132). Dispersal events occurred two times with *Ciliochorella* in the late Paleogene (about 30 Mya), which was followed by a period where *Ciliochorella* began spreading in Africa and America (Fig. 3, node 135). The result of the ancestral biogeographic reconstruction supported the notion that the Eurasian continent was the center of origin for *Ciliochorella*: the estimated ancestral distributions for nodes of the complex and its clades included both Asia and Europe (Fig. 3, node 139).

Taxonomy

***Ciliochorella* Syd., in Sydow & Mitter, *Annls mycol.* 33(1/2): 62 (1935)**

Fungal Names: FN 7657

Type species. *Ciliochorella mangiferae* Syd., *Annls Mycol.* 33(1/2): 63 (1935).
Fungal Names: FN 270484.

Notes. *Ciliochorella* is an asexually typified genus. Most species of this genus are saprophytic with the exception of *Ciliochorella castaneae* Munjal. The conidiomata of *Ciliochorella* species are generally round, semi-immersed, and longitudinally lenticular. A prominent feature observed during the early stage of germination is apical and basal cells of conidia-produced germ tubes, and a vacuolated state of the protoplasm (Masilamani and Muthumary 1994).

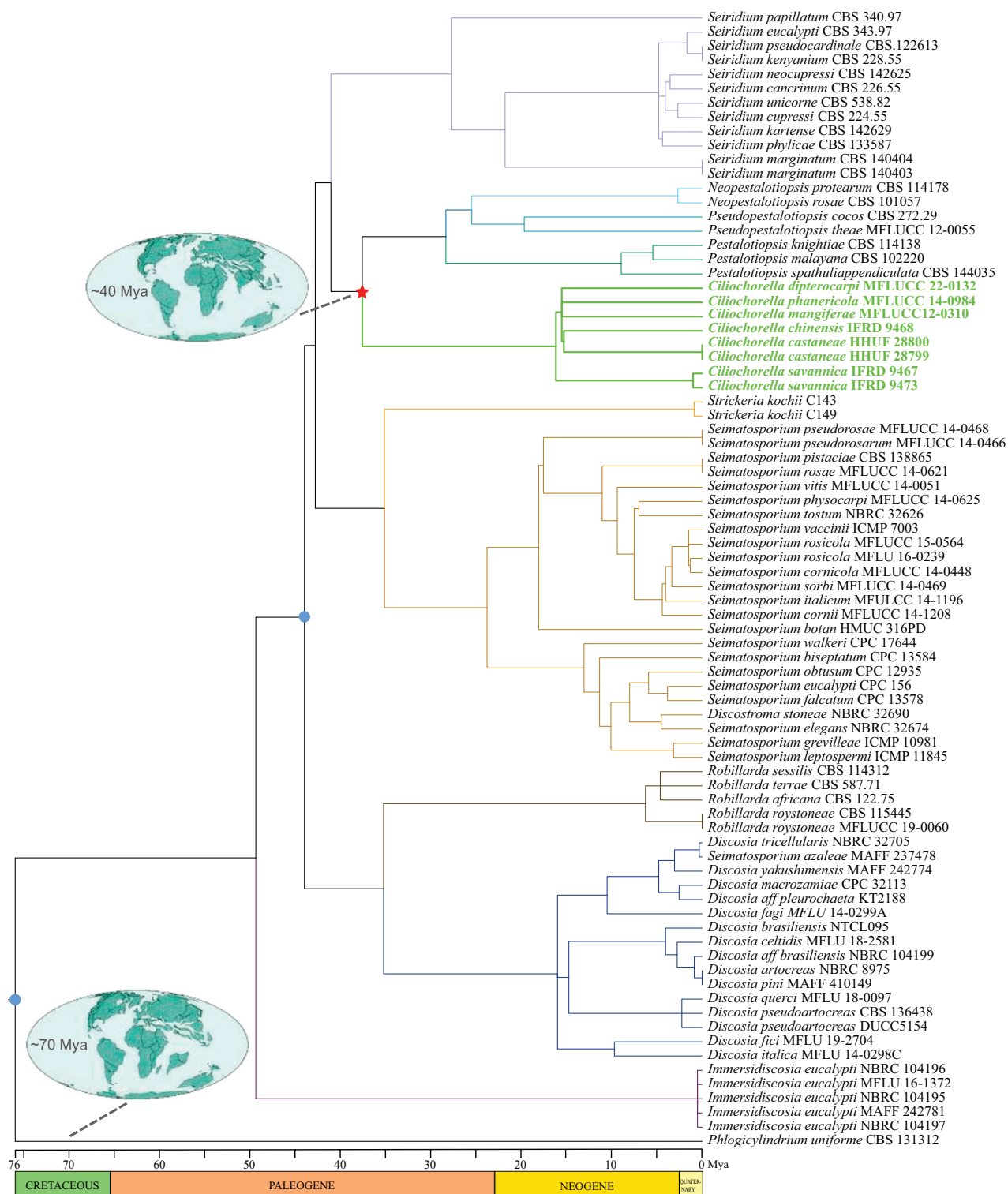


Figure 2. Divergence time tree based on ML analysis. Divergence times of all nodes were estimated by R8S software using two calibration points. The blue circles and the red star indicate secondary points and the divergence time of *Ciliochorella* respectively. *Ciliochorella* species are shown in bold and green. Maps were adopted from Peng et al (2023).

Conidiophores arise from the thin-walled, and are almost colorless cells of the basal or basal and parietal tissue, mostly reduced to conidiogenous cells. Occasionally, they are sparsely septate, branched or unbranched, colorless, smooth, invested in mucus (Sutton 1980; Nag Raj 1993). Conidiogenous cells

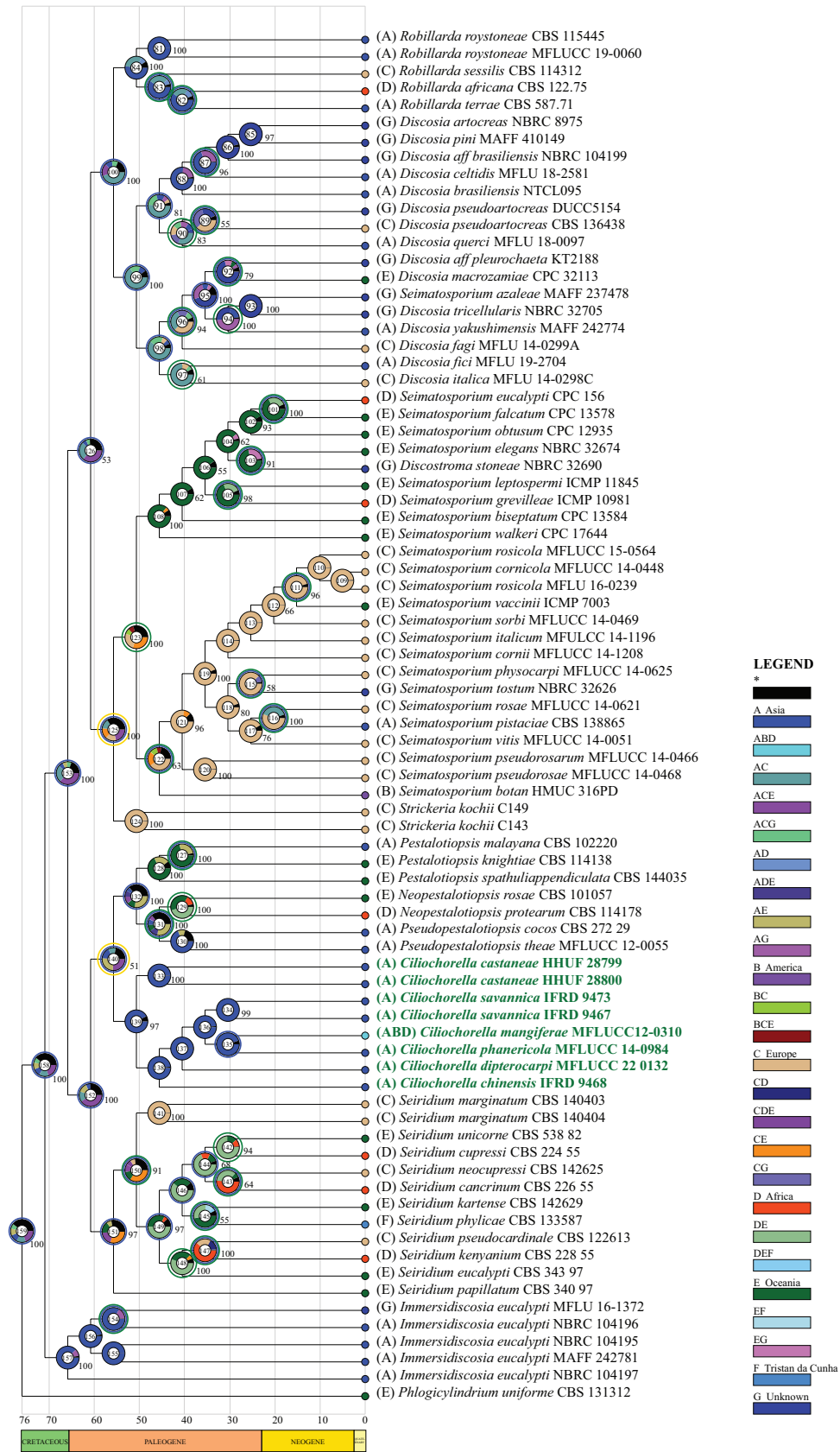


Figure 3. Ancestral biogeographic reconstructions are based on Bayesian trees. Each event is represented by a node number. Bayesian posterior probabilities are shown (≥ 50). A colored circle near the number at the nodes indicates the following: blue represents dispersal, green represents vicariance, and yellow represents extinction. *Ciliochorella* species are shown in bold and green.

are discrete, ampulliform, or conical with a long neck, colorless, and smooth. Conidia are cylindrical, straight, or slightly curved with septate pale brown middle cells and colorless end cells with appendages at one or both ends (Lee et al. 2006; Allegrucci et al. 2011; Tangthirasunun et al. 2015; Hyde et al. 2016; Wijayawardene et al. 2016; Liu et al. 2019a).

There are four *Ciliochorella* species for which molecular data is available on the NCBI repository (i.e. *C. castaneae*; *C. dipteroearpi* Samaradiwakara, Lumyong & K.D. Hyde; *C. mangiferae* and *C. phanericola* Norph., T.C. Wen & K.D. Hyde). *Ciliochorella mangiferae* is the earliest recorded species and described by Sydow and Mitter (1935) as the type species of this genus. Tangthirasunun et al. (2015) discovered a new record of *C. mangiferae* in Thailand and provided some its molecular data for this species. The first discovery of *C. castaneae* was in India (Nag Raj 1993), but Endo et al. (2008) added a new record for this species in Japan and also added molecular data. Samaradiwakara et al. (2023) discovered *C. dipteroearpi* and analyzed the species molecularly. For the other species of this genus, there is still no molecular data available, and comprise *C. splendida* Nag Raj & R.F. Castañeda and *C. buxifoliae* Allegr., Ellegr. & Aramb (Nag Raj 1993; Allegrucci et al. 2011). The morphological characteristics of all *Ciliochorella* species are provided in Table 2.

Ciliochorella chinensis H.X. Wu & J.C. Li, sp. nov.

Fungal Names: FN 571291

Etymology. The species epithet reflects China where the species of *Ciliochorella* was first collected country.

Holotype. IFRD9468.

Description. Saprobic on leaf litter. **Asexual morph:** Coelomycetous. **Conidiomata** 894–1314 µm diameter (\bar{x} = 1055 µm, n = 14), unilocular, semi-immersed, circular areas, dark brown, mostly aggregated, sometimes solitary, forming a papilla in the center (Fig. 4a–c). **Conidiomata wall** comprises a few

Table 2. The comparison of micro-morphological characteristics of *Ciliochorella*.

Species	Host-Substratum	Conidiomata diam (µm)	Conidiomata with a papillary	Conidia (µm)	Mean conidium length/width ratio	Basal appendages number	Reference
<i>Ciliochorella buxifoliae</i>	<i>Scutia buxifolia</i>	300–500	–	19–21×2.5–2.7	7:1	1	Allegrucci et al. 2011
<i>C. castaneae</i>	<i>Castanea europaea</i>	450–650	Yes	13–19×2.5–3.2 (Ave.16.0×3.0)	11.1:1	1	Nag Raj 1993; Endo et al. 2008
<i>C. chinensis</i>	Unidentified leaf litter	894–1314	Yes	13.9–17.9×3.3–4.1 (Ave.15.7×3.6)	4.4:1	1	In this study
<i>C. dipteroearpi</i>	<i>Dipteroearpaceae alatus</i>	650–800	No	9–18×1–3 (Ave.14×2)	7:1	1	Nethmini et al. 2023
<i>C. mangiferae</i>	<i>Mangifera indica</i>	400–800	–	32–43×2.5–3.5 (Ave. 37×3)	12.3:1	1	Nag Raj 1993
<i>C. phanericola</i>	<i>Phanera purpurea</i>	1000–1200	No	13–15×2.8–3.5 (Ave. 15×3.7)	4.1:1	1	Hyde et al. 2016
<i>C. savannica</i>	Unidentified leaf litter	530–952	Yes	11–16×2–3 (Ave.14×2.6)	5.4:1	0	In this study
<i>C. splendida</i>	<i>Quercus oleoides</i> subsp. <i>Sagrana</i>	–	–	24–40×2.5–3 (Ave. 32×2.7)	11.8:1	1	Nag Raj 1993

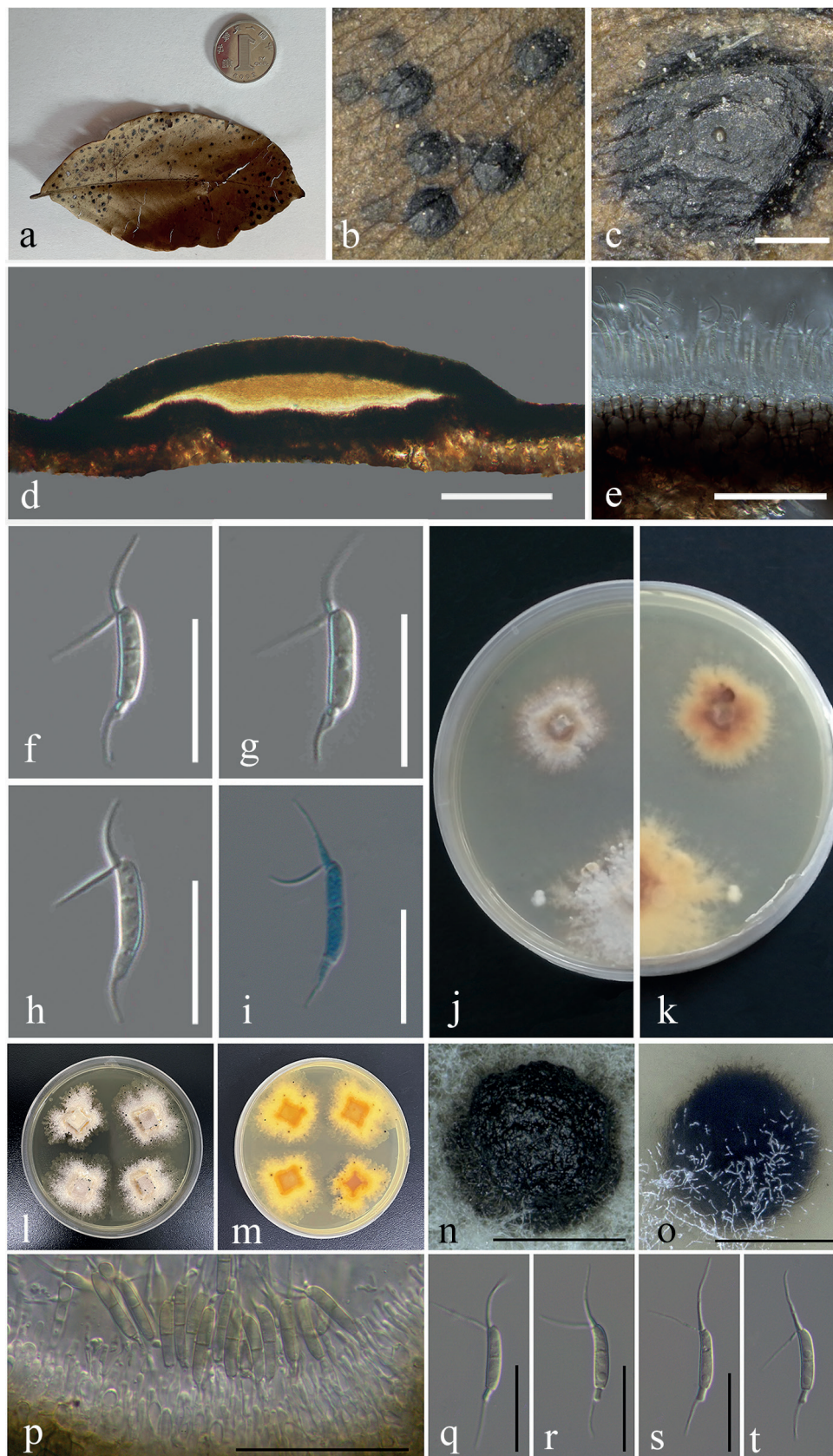


Figure 4. *Ciliochorella chinensis* (IFRD9468, holotype; IFRDCC3202, ex-type strain) **a, b** the specimen **c** surface of fruiting bodies **d** longitudinal section of the conidioma **e** peridium **f–h** mature conidia **i** mature conidia in cotton blue **j, k** colonies on PDA (**k** from below) **l, m** colonies on PDA (**m** from below) **n** fruiting bodies on PDA **o** fruiting bodies in PDA **p** peridium **q–t** mature conidia. Scale bars: 400 μm (**c, n, o**); 200 μm (**d**); 40 μm (**p**); 20 μm (**e**); 10 μm (**f–i, q–t**).

to several layers of cells of *textura angularis*, with the innermost layer thin, transparent, and precisely arranged, the outer layer dark brown to black (Fig. 4d). **Conidiophores** appear to be reduced to conidiogenous cells. **Conidiogenous cells** are enteroblastic phialidic, formed from the innermost layer of the wall, hyaline to pale brown, and smooth (Fig. 4e). **Conidia** 14–18 × 3–4 μm (\bar{x} = 15.7 × 3.6 μm, n = 12), excluding apical and basal appendages, mean conidium length/width ratio = 4.4:1, navicular to subcylindrical, slightly curved, 1-septate, wide middle two cells with apical cell transformed into two forked filiform cellular appendages, 9–16 μm (\bar{x} = 12.5 μm, n = 20), the narrow basal cell with basal appendage, 4–7 μm (\bar{x} = 5.4 μm, n = 11), colorless to light brown, with guttules on the conidia surface (Fig. 4f–i). **Sexual morph**: Unknown.

Culture characteristics. Colonies on PDA, reaching 4.4 cm (n = 3) diam after 7 days at 26 °C, producing dense mycelium, irregular circular, margin rough, white (Fig. 4j, k). Conidia germinated and grew deep into the medium. There was a clear boundary between the center and the most marginal part. The culture grew fruiting bodies after about four months on PDA medium at 26 °C (Fig. 4l, m). The morphology of conidiophores and conidia in the semi-immersed or fully embedded medium was consistent with that found under natural conditions (Fig. 4n–t).

Material examined. CHINA. Yunnan Province, Yuanjiang County, Yuanjiang National Nature Reserve (Xiaohedi), on dead leaves of an unidentified plant, 23°28'33"N, 102°21'1"E, elevation 423 m, June 2021, Hai-Xia Wu, Jin-Chen Li, and Xin-Hao Li (IFRD9468, **holotype**; IFRDCC3202, **ex-type**).

Notes. The phylogenetic tree shows that *Ciliochorella chinensis* has a close relationship with *C. castaneae* (HHUF 28800) (Fig. 1). A BLAST search conducted within GenBank, the match for LSU showed a 98.72% similarity to *C. castaneae* (HHUF 28800, this species only has LSU) across a query coverage of 95%. At present, the phylogenetic relationship in this genus is not comprehensive enough, so the classification depends greatly on their morphology. Morphologically, the conidiomata of *C. chinensis* have a papillary, which the conidiomata of *C. phanericola* lack. The conidiomata of both species display different sizes (Table 2).

***Ciliochorella savannica* H.X. Wu & J.Y. Song, sp. nov.**

Fungal Names: FN 571290

Etymology. Epithet derived from the type locality (Yuanjiang Savanna Ecosystem Research Station).

Holotype. IFRD9467.

Description. **Saprobic** on leaf litter. **Asexual morph**: Coelomycetous. **Conidiomata** 530–950 μm diameter (\bar{x} = 758 μm, n = 23), unilocular, semi-immersed, circular areas, black, mostly aggregated, sometimes solitary, with a papilla central circular ostiole (Fig. 5a–c). **Conidiomata wall** comprises a few to several layers of cells of *textura angularis*, with the inner layer being mostly thin, brown, whereas the outer layer appears dark brown to black. The longitudinal section is lenticular, the base is well developed (Fig. 5d). **Conidiophores** are reduced to conidiogenous cells. **Conidiogenous cells** enteroblastic phialidic, formed from the innermost layer of the wall, hyaline to pale brown, smooth (Fig. 5e). **Conidia** 11–16 × 2–3 μm (\bar{x} = 14 × 2.6 μm, n = 22) excluding apical appendages,

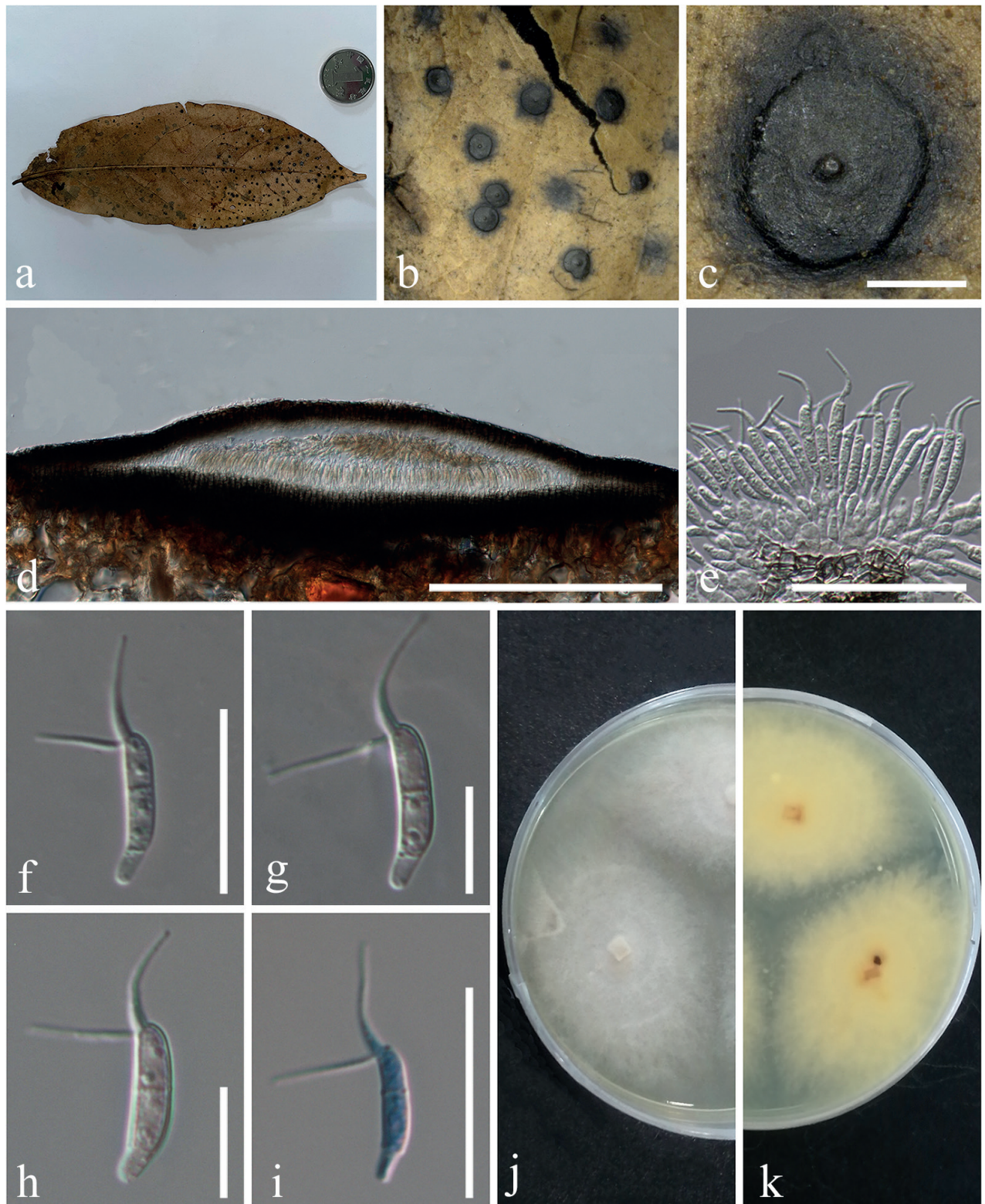


Figure 5. *Ciliochorella savannica* (IFRD:9467, holotype; IFRDCC:3201, ex-type) **a, b** the specimen **c** surface of fruiting bodies **d** longitudinal section of the conidioma **e** peridium **f–h** mature conidia **i** mature conidia in cotton blue **j, k** colonies on PDA (**k** from below). Scale bars: 400 μm (**c**); 200 μm (**d**); 20 μm (**e**); 10 μm (**f–i**).

mean conidium length/width ratio = 5.4:1, navicular to subcylindrical, slightly curved, 1-septate, narrow basal cell, wide middle two cells with apical cell transformed into two forked filiform cellular appendages 7–13 μm (\bar{x} = 10 μm ,

n = 22), 2–4-guttulates on the surface of the conidia, without basal appendages (Fig. 5f–i). **Sexual morph:** Unknown.

Culture characteristics. Conidia germinated and hyphae grew in emission form from the center to the outside (Fig. 5j, k). Colonies growing on PDA, reaching a diameter of 4.4 cm (n = 3) after 7 days at 26 °C, producing dense mycelium, circular, margin rough. Surface white from the surrounding of the mycelium on PDA and pale yellow in reverse.

Material examined. CHINA. Yunnan Province, Yuanjiang County, Yuanjiang Savanna Ecosystem Research Station (Xishuangbanna Tropical Botanical Garden, Chinese Academy of Sciences), 23°28'31"N, 102°10'38"E, 579 m, on dead leaves of an unidentified plant, June 2021, Hai-Xia Wu, Jin-Chen Li, and Xin-Hao Li (IFRD9467, **holotype**; IFRD9473, **paratype**; IFRDCC3201, **ex-type**).

Notes. Two strains of *Ciliochorella savannica* (holotype and paratype) correspond to *Ciliochorella* described by Sydow and Mitter (1935). The phylogenetic analysis showed that this species is only distantly related to other species in *Ciliochorella*. The number of different bases in ITS and LSU sequences of holotype and paratype was 7 (1033/1040) and 4 (1406/1410), respectively. These two strains of *C. savannica* formed a subclade within *Ciliochorella*, with 97% ML and 1.00 Bayesian posterior probabilities (Fig. 1). They differ morphologically from other species in conidiomata size (530–952 µm) and mean conidium length/width ratio (5.4:1) (Table 2). The significant characteristic is that *C. savannica* has conidia that lack basal appendages, whereas *Ciliochorella* species have this characteristic.

Enzyme activity screening

The temperature was maintained at 26 °C. After 7 days of inoculation, Congo red staining was used to determine whether the strain had cellulase production ability (Fig. 6a, d). The results showed that both *C. chinensis* and *C. savannica* produced discoloring circles on the solid medium, with the discoloration of *C. savannica* being more pronounced. This indicates that cellulase plays a role in the cellulose degradation of both species.

Guaiacol-PDA solid medium was used to screen for laccase, and the temperature was set at 26 °C. The results were as follows: *C. chinensis* had a lighter color reaction on the solid medium until after 12 days (Fig. 6b, c) while *C. savannica* showed a color reaction obvious on the solid medium after 10 days (Fig. 6e, f).

The enzyme activity of the supernatant was determined by the Thermo Varioskan Flash enzyme marker. The average content of cellulose and laccase for *C. savannica* was 4.97 U/ml (n = 3) and 1.16 U/ml (n = 3); and for *C. chinensis*, the average cellulose content was 5.05 U/ml (n = 3) and laccase content was 1.71 U/ml (n = 3) (Fig. 6g). This suggests that laccase participates in lignin degradation of both species. There is no strong positive correlation between color reaction and numerical value, and the specific reasons need to be further explored.

Discussion

Ciliochorella species play important roles in the decomposition of litter (Saparit et al. 2010), and as such are a part of the carbon cycle throughout the world.

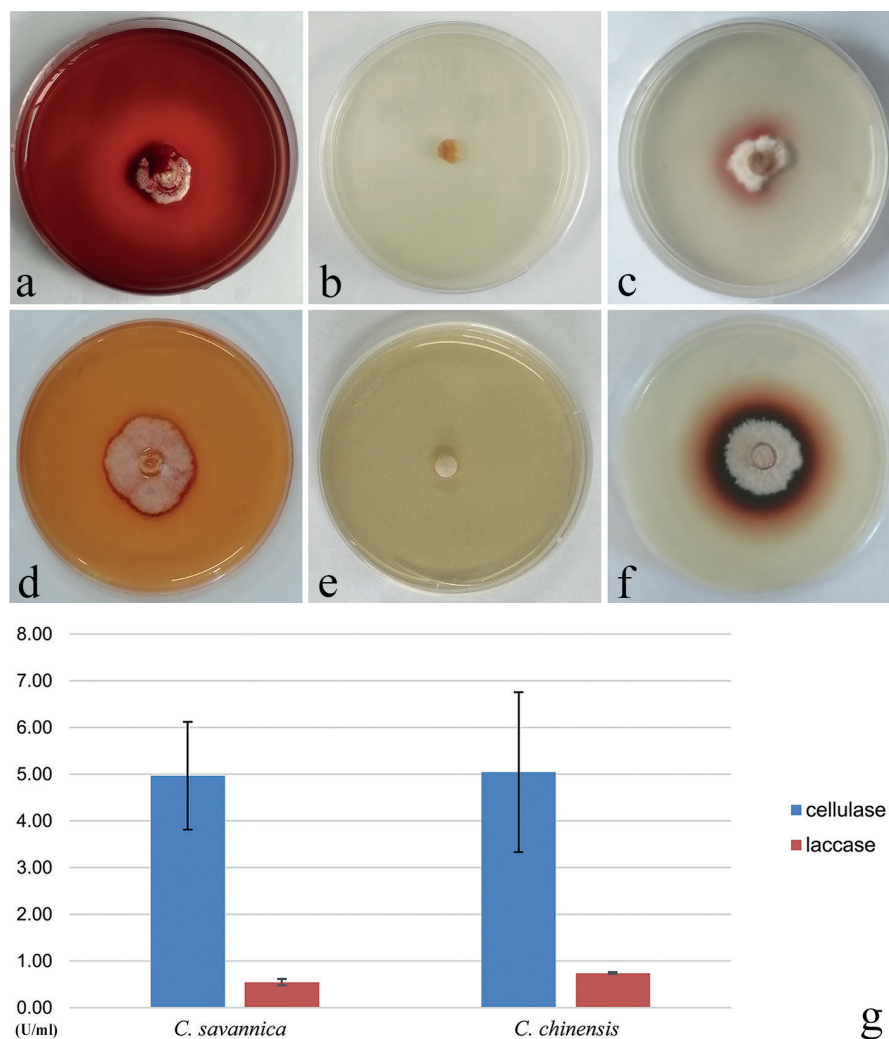


Figure 6. Screening of enzyme activity in culture **a** *C. chinensis* was cultured on solid PDA medium for 7 days and stained with Congo red stain **b** *C. chinensis* on solid guaiacol-PDA medium after 1 day **c** *C. chinensis* on solid guaiacol-PDA medium after 12 days **d** *C. savannica* was cultured on PDA solid medium for 7 days and stained with Congo red stain **e** *C. savannica* on guaiacol-PDA solid medium 1 day **f** *C. savannica* on solid guaiacol-PDA medium for 10 days **g** determination of enzyme activity.

The main body of *Ciliochorella* research has focused on the phylogeny and morphology of these fungi (Kalani 1963; Seshadri et al. 1969; Nag Raj 1993; Endo et al. 2008; Allegrucci et al. 2011; Hyde et al. 2016; Samaradiwakara et al. 2023). By contrast, the evolutionary history of *Ciliochorella*, whether based on DNA sequence analysis or the ecosystem studies, has received less attention and has remained unclear.

Wijayawardene et al. (2022b) stated that the subtropical to tropical regions in Asia will be an important region for discovering new fungal taxa, specifically asexually typified taxa. In China, the savanna-like vegetation has a unique geography and complex topography, which has contributed to the formation of various habitats with high biodiversity (Zhu and Tan 2022). Investigations have been carried out in the savanna-like vegetation in hot dry valleys of southwestern China, and this site is referred to as the “Chinese savanna”. However, only a few reports have focused on fungi in this habitat, most of which have concentrated on endophytic and soil fungi (He et al. 2011; Ruan 2011; Yi et al.

2011). In addition, most *Ciliochorella* species were recorded from Asia except for *C. buxifoliae* and *C. splendida*, both of which occur in America (Nag Raj 1993; Endo et al. 2008; Allegrucci et al. 2011; Tangthirasunun et al. 2015; Hyde et al. 2016). According to the best of our knowledge, *Ciliochorella* species have not been recorded from China before. Our studies resulted in the discovery of two new *Ciliochorella* species: *C. chinensis* and *C. savannica*. This finding not only contributed two new species to the growing catalog of microfungal species found in the *Chinese savanna*, but also represents the first *Ciliochorella* specimens reported for China. The two new species in this paper have been characterized based on phylogenetic analysis (Fig. 1) and morphological characteristics (Table 2). They belong to the genus *Ciliochorella*, which is part of the Sporocadaceae family, and the result is consistent with previous studies (Samarakoon et al. 2016; Liu et al. 2019a; Tennakoon et al. 2021).

The study of fossil fungi has become an essential tool for understanding fungal evolution and diversification, as well as elucidating the relationships of fungi to other organisms in the historical context of a given ecosystem (Taylor et al. 2015; Liu et al. 2019b; Samarakoon et al. 2019; Li et al. 2023). Despite wide distribution and large population, the majority of fungi (mycelia) are readily decomposed after death, resulting in a scarcity of fungal fossils that can be utilized for research concerning evolution (Tao and Chen 2020). In this report, we used the r8s program based on molecular clocks and two secondary calibration nodes to assess divergence times, which allowed us to estimate the emergence of the *Ciliochorella* at around 38 Mya during the Paleogene (Fig. 2). The Cretaceous-Paleogene mass extinction caused the disappearance of numerous groups, and its aftermath saw the rapid diversification of surviving species (Klein et al. 2021). According to the results of this study, *Ciliochorella* appeared in the middle and late periods of the Paleogene explosion of species. In addition, recent phylogeny and genomic studies used for the divergence time of Sordariomycetes indicate that relying solely on genus-level estimations may lack sufficient evidence and could potentially introduce errors (Chen et al. 2023). However, the divergence time estimated in this study does not conflict with the results based on genomic data.

The ancestral biogeography of *Ciliochorella* was investigated for the first time in this study. The result showed that the ancestor of *Ciliochorella* species originated from the Eurasian continent during the late Cretaceous. From approximately the late Cretaceous to the early Paleogene, there were some dispersal, vicariance and extinction events, which may be related to extreme climate incidents (Hu and Liu 2003). At about 30 Mya, there are two dispersal events that occurred within *Ciliochorella*. Up to this point, *Ciliochorella* species have been only found in Asia, Africa and America (Nag Raj 1993; Masilamani and Muthumary 1994; Endo et al. 2008; Tangthirasunun et al. 2015; Hyde et al. 2016). The results of our study clarify the evolutionary history of *Ciliochorella* ancestors and also provide a reference for the estimation of the divergence times of similar genera.

Some pathogenic plant fungi eliminate the effects of plant antiviral and tannic acid via laccase activity (Dong and Changsun 2021). By screening *Ciliochorella chinensis* and *C. savannica* strains on the medium, we found that both new species produce laccase and cellulase. They are involved in the decomposition of

lignin and cellulose of leaf litter in their natural habitat, but their decomposition efficiency needs further study. Hyde et al. (2016) identify *C. phanericola* as a pathogen. The present study also supports the idea that *Ciliochorella* may have a potential role as a pathogenic plant fungus.

Acknowledgements

The authors are deeply grateful to Prof. Kirst King-Jones (University of Alberta) for language improvement.

Additional information

Conflict of interest

The authors have declared that no competing interests exist.

Ethical statement

No ethical statement was reported.

Funding

This study was supported by the National Natural Science Foundation of China (grant No. 32170024) the Grant for Essential Scientific Research of National Nonprofit Institute (No. CAFYBB2019QB005), and the Yunnan Province Ten Thousand Plan of Youth Top Talent Project (No. YNWR-QNBJ-2018-267).

Author contributions

Methodology, H.-X. W., W.-F. D. and J.-Y. S.; formal analysis, H.-X. W. and J.-Y. S.; resources, H.-X. W., J.-C. L. and J.-Y. S.; sampling guidance, D.-X. Y.; data curation, J.-Y. S., J.-C. L., C.-L. G. and H.-X. W.; writing—original draft preparation, J.-Y. S. and H.-X. W.; writing—review and editing, J.-Y. S., H.-X. W., N. W. and X.-Y. Z.; project administration, H.-X. W.; funding acquisition, H.-X. W. All authors have read and agreed to the published version of the manuscript.

Author ORCIDs

Jia-Yu Song  <https://orcid.org/0000-0002-0884-7594>

Hai-Xia Wu  <https://orcid.org/0000-0002-7169-6717>

Jin-Chen Li  <https://orcid.org/0000-0001-8977-1829>

Wei-Feng Ding  <https://orcid.org/0000-0002-2471-8071>

Cui-Ling Gong  <https://orcid.org/0009-0005-9282-0974>

Xiang-Yu Zeng  <https://orcid.org/0000-0003-1341-1004>

Nalin N. Wijayawardene  <https://orcid.org/0000-0003-0522-5498>

Da-Xin Yang  <https://orcid.org/0009-0008-9985-4669>

Data availability

All of the data that support the findings of this study are available in the main text.

References

Adlini NI, Fibriarti BL, Roza RM (2014) Seleksi mikroba selulolitik dalam mendegradasi lignin asal tanah gambut desa rimbo panjang kabupaten kampar riau.

- Allegrucci N, Eládes L, Cabello M, Arambarri A (2011) New species *Koorchaloma* and *Ciliochorella* from xeric forests in Argentina. *Mycotaxon* 115(1): 175–181. <https://doi.org/10.5248/115.175>
- Ariyawansa HA, Hyde KD, Jayasiri SC, Buyck B, Chethana KWT, Dai DQ, Dai YC, Daranagama DA, Jayawardena RS, Lücking R, Ghobad-Nejhad M, Niskanen T, Thambugala KM, Voigt K, Zhao RL, Li G-J, Doilom M, Boonmee S, Yang ZL, Cai Q, Cui Y-Y, Bahkali AH, Chen J, Cui BK, Chen JJ, Dayarathne MC, Dissanayake AJ, Ekanayaka AH, Hashimoto A, Hongsanan S, Jones EBG, Larsson E, Li WJ, Li Q-R, Liu JK, Luo ZL, Maharachchikumbura SSN, Mapook A, McKenzie EHC, Norphanphoun C, Konta S, Pang KL, Perera RH, Phookamsak R, Phukhamsakda C, Pinruan U, Randrianjohany E, Singtripop C, Tanaka K, Tian CM, Tibpromma S, Abdel-Wahab MA, Wanasinghe DN, Wijayawardene NN, Zhang J-F, Zhang H, Abdel-Aziz FA, Wedin M, Westberg M, Ammirati JF, Bulgakov TS, Lima DX, Callaghan TM, Callac P, Chang C-H, Coca LF, Dal-Forno M, Dollhofer V, Fliegerová K, Greiner K, Griffith GW, Ho H-M, Hofstetter V, Jeewon R, Kang JC, Wen T-C, Kirk PM, Kytövuori I, Lawrey JD, Xing J, Li H, Liu ZY, Liu XZ, Liimatainen K, Lumbsch HT, Matsumura M, Moncada B, Nuankaew S, Parnmen S, de Azevedo Santiago ALCM, Sommai S, Song Y, de Souza CAF, de Souza-Motta CM, Su HY, Suetrong S, Wang Y, Wei S-F, Wen TC, Yuan HS, Zhou LW, Réblová M, Fournier J, Camporesi E, Luangsa-ard JJ, Tasanathai K, Khonsanit A, Thanakitpipattana D, Somrithipol S, Diederich P, Millanes AM, Common RS, Stadler M, Yan JY, Li XH, Lee HW, Nguyen TTT, Lee HB, Battistin E, Marsico O, Vizzini A, Vila J, Ercole E, Eberhardt U, Simonini G, Wen H-A, Chen X-H, Miettinen O, Spirin V, Hernawati (2015) Erratum to: Fungal diversity notes 111–252—taxonomic and phylogenetic contributions to fungal taxa. *Fungal Diversity* 75(1): 27–274. <https://doi.org/10.1007/s13225-015-0346-5>
- Barber PA, Crous PW, Groenewald JZ, Pascoe IG, Keane P (2011) Reassessing *Vermisporium* (Amphisphaeriaceae), a genus of foliar pathogens of eucalypts. *Persoonia – Molecular Phylogeny and Evolution of Fungi* 27(1): 90–118. <https://doi.org/10.3767/003158511X617381>
- Barr ME (1975) *Pestalospaeria*, a new genus in the Amphisphaeriaceae. *Mycologia* 67(1): 187–194. <https://doi.org/10.1080/00275514.1975.12019740>
- Beimforde C, Feldberg K, Nylinder S, Rikkinen J, Tuovila H, Dörfelt H, Gube M, Jackson DJ, Reitner J, Seyfullah LJ, Schmidt AR (2014) Estimating the Phanerozoic history of the Ascomycota lineages: Combining fossil and molecular data. *Molecular Phylogenetics and Evolution* 78: 386–398. <https://doi.org/10.1016/j.ympev.2014.04.024>
- Benjamin CR, Guba EF (1961) Monograph of *Monochaetia* and *Pestalotia*. *Mycologia* 52(6): e966. <https://doi.org/10.2307/3755860>
- Bisaria VS, Ghose TK (1981) Biodegradation of cellulosic materials: Substrates, microorganisms, enzymes and products. *Enzyme and Microbial Technology* 3(2): 90–104. [https://doi.org/10.1016/0141-0229\(81\)90066-1](https://doi.org/10.1016/0141-0229(81)90066-1)
- Bucher VVC, Pointing SB, Hyde KD, Reddy CA (2004) Production of wood decay enzymes, loss of mass, and lignin solubilization in wood by diverse tropical freshwater fungi. *Microbial Ecology* 48(3): 331–337. <https://doi.org/10.1007/s00248-003-0132-x>
- Cai L, Jeewon R, Hyde KD (2006) Phylogenetic investigations of Sordariaceae based on multiple gene sequences and morphology. *Mycological Research* 110(2): 137–150. <https://doi.org/10.1016/j.mycres.2005.09.014>
- Cai L, Guo XY, Hyde KD (2008) Morphological and molecular characterization of a new anamorphic genus *Cheirosporium*, from freshwater in China. *Persoonia* 20(1): 53–58. <https://doi.org/10.3767/003158508X314732>

- Chen YP, Su PW, Hyde KD, Maharachchikumbura SSN (2023) Phylogenomics and diversification of Sordariomycetes. *Mycosphere: Journal of Fungal Biology* 14(1): 414–451. <https://doi.org/10.5943/mycosphere/14/1/5>
- Choi Y, Hyde KD, Ho W (1999) Single spore isolation of fungi. *Fungal Diversity* 3: 29–38.
- Chomnunti P, Hongsanan S, Aguirre-Hudson B, Tian Q, Peršoh D, Dhamsi MK, Alias AS, Xu JC, Liu XZ, Stadler M, Hyde KD (2014) The sooty moulds. *Fungal Diversity* 66(1): 1–36. <https://doi.org/10.1007/s13225-014-0278-5>
- Crous PW, Wingfield MJ, Guarro J, Cheewangkoon R, van der Bank M, Swart WJ, Stchigel AM, Cano-Lira JF, Roux J, Madrid H, Damm U, Wood AR, Shuttleworth LA, Hodges CS, Munster M, de Jesús Yáñez-Morales M, Zúñiga-Estrada L, Cruywagen EM, De Hoog GS, Silvera C, Najafzadeh J, Davison EM, Davison PJN, Barrett MD, Barrett RL, Manamgoda DS, Minnis AM, Kleczewski NM, Flory SL, Castlebury LA, Clay K, Hyde KD, Maússe-Sitoe SND, Chen S, Lechat C, Hairaud M, Lesage-Meessen L, Pawłowska J, Wilk M, Śliwińska-Wyrzychowska A, Mętrak M, Wrzosek M, Pavlic-Zupanc D, Maleme HM, Slippers B, Mac Cormack WP, Archuby DI, Grünwald NJ, Tellería MT, Dueñas M, Martín MP, Marinowitz S, de Beer ZW, Perez CA, Gené J, Marin-Felix Y, Groenewald JZ (2013) Fungal Planet description sheets: 154–213. *Persoonia* 31(4): 188–296. <https://doi.org/10.3767/003158513X675925>
- Crous PW, Carris LM, Giraldo A, Groenewald JZ, Hawksworth DL, Hernández-Restrepo M, Jaklitsch WM, Lebrun MH, Schumacher RK, Stielow JB, der Linde EJ, Vilcãne J, Voglmayr H, Wood AR (2015) The Genera of Fungi – fixing the application of the type species of generic names – G 2: *Allantophomopsis*, *Latorua*, *Macrodiplodiopsis*, *Macrohilum*, *Milospium*, *Protostegia*, *Pyricularia*, *Robillarda*, *Rotula*, *Septoriella*, *Torula*, and *Wojnowicia*. *IMA Fungus* 6(1): 163–198. <https://doi.org/10.5598/imafungus.2015.06.01.11>
- Crous PW, Wingfield MJ, Burgess TI, Hardy GESJ, Gené J, Guarro J, Baseia IG, García D, Gusmão LFP, Souza-Motta CM, Thangavel R, Adamčík S, Barili A, Barnes CW, Bezerra JDP, Bordallo JJ, Cano-Lira JF, de Oliveira RJV, Ercole E, Hubka V, Iturrieta-González I, Kubátová A, Martín MP, Moreau PA, Morte A, Ordoñez ME, Rodríguez A, Stchigel AM, Vizzini A, Abdollahzadeh J, Abreu VP, Adamčíková K, Albuquerque GMR, Alexandrova AV, Álvarez Duarte E, Armstrong-Cho C, Banniza S, Barbosa RN, Bellanger JM, Bezerra JL, Cabral TS, Caboň M, Caicedo E, Cantillo T, Carnegie AJ, Carmo LT, Castañeda-Ruiz RF, Clement CR, Čmoková A, Conceição LB, Cruz RHSF, Damm U, da Silva BDB, da Silva GA, da Silva RMF, Santiago ALCMA, de Oliveira LF, de Souza CAF, Déniel F, Dima B, Dong G, Edwards J, Félix CR, Fournier J, Gibertoni TB, Hosaka K, Iturriaga T, Jadan M, Jany J-L, Jurjević Ž, Kolařík M, Kušan I, Landell MF, Leite Cordeiro TR, Lima DX, Loizides M, Luo S, Machado AR, Madrid H, Magalhães OMC, Marinho P, Matočec N, Mešić A, Miller AN, Morozova OV, Neves RP, Nonaka K, Nováková A, Oberlies NH, Oliveira-Filho JRC, Oliveira TGL, Papp V, Pereira OL, Perrone G, Peterson SW, Pham THG, Raja HA (2018) Fungal Planet description sheets: 716–784. *Persoonia* 40(4): 240–393. <https://doi.org/10.3767/persoonia.2018.40.10>
- Díaz GA, Elfar K, Latorre BA (2012) First report of *Seimatosporium* botan associated with trunk disease of grapevine (*Vitis vinifera*) in Chile. *Plant Disease* 96(11): e1696. <https://doi.org/10.1094/PDIS-05-12-0478-PDN>
- Dong JS, Changsun C (2021) Antiviral bioactive compounds of mushrooms and their antiviral mechanisms: A review. *Viruses* 13(2): e350. <https://doi.org/10.3390/v13020350>
- Endo M, Hatakeyama S, Harada Y, Tanaka K (2008) Description of a coelomycete *Ciliochorella castaneae* newly found in Japan, and notes on the distribution and phylogeny. *Nippon Kingakkai Kaiho* 49: 115–120.

- Floudas D, Binder M, Riley R, Barry K, Blanchette RA, Henrissat B, Martinez AT, Otilar R, Spatafora JW, Yadav JS, Aerts A, Benoit I, Boyd A, Carlson A, Copeland A, Coutinho PM, deVries RP, Ferreira P, Findley K, Foster B, Gaskell J, Glotzer D, Górecki P, Heitman J, Hesse C, Hori C, Igarashi K, Jurgens JA, Kallen N, Kersten P, Kohler A, Kües U, Kumar TKA, Kuo A, LaButti K, Larrondo LF, Lindquist E, Ling A, Lombard V, Lucas S, Lundell T, Martin R, McLaughlin DJ, Morgenstern I, Morin E, Murat C, Nagy LG, Nolan M, Ohm RA, Patyshakuliyeva A, Rokas A, Ruiz-Dueñas FJ, Sabat G, Salamov A, Samejima M, Schmutz J, Slot JC, John FS, Stenlid J, Sun H, Sun S, Syed K, Tsang A, Wiebenga A, Young D, Pisabarro A, Eastwood DC, Martin F, Cullen D, Grigoriev IV, Hibbett DS (2012) The Paleozoic Origin of Enzymatic Lignin Decomposition Reconstructed from 31 Fungal Genomes. *Science* 336: 1715–1719. <https://doi.org/10.1126/science.1221748>
- Gao Y, Wu M (2022) Modeling pulsed evolution and time-independent variation improves the confidence level of ancestral and hidden state predictions in continuous traits. *Systematic Biology* 71(5): 1225–1232. <https://doi.org/10.1093/sysbio/syac016>
- Hall TA (1999) BioEdit: A user-friendly biological sequence alignment program for Windows 95/98/NT. *Nucleic Acids Symposium Series* 41: 95–98.
- Hatakka A (1994) Lignin-modifying enzymes from selected white-rot fungi: Production and role from in lignin degradation. *FEMS Microbiology Reviews* 13(2–3): 125–135. <https://doi.org/10.1111/j.1574-6976.1994.tb00039.x>
- He CM, Wei DQ, Li HY, Xie HW, He XL (2011) Endophytic fungal diversity of five dominant plant species in the dry-hot valley of Yuanjiang, Yunnan Province, China. *Acta Ecologica Sinica* 31(12): 3315–3321.
- Hu XM, Liu ZF (2003) Extreme climate events from the Cretaceous to Early Tertiary. *Diqiu Kexue Jinzhan* 18(5): 681–690. <https://doi.org/10.3321/j.issn:1001-8166.2003.05.007>
- Hyde KD, Hongsanan S, Jeewon R, Jeewon R, Bhat DJ, McKenzie EHC, Jones EBG, Phookamsak R, Ariyawansa HA, Boonmee S, Zhao Q, Abdel-Aziz FA, Abdel-Wahab MA, Banmai S, Chomnunti P, Cui BK, Daranagama DA, Das K, Dayarathne MC, de Silva NI, Dissanayake AJ, Doilom M, Ekanayaka AH, Gibertoni TB, Góes-Neto A, Huang SK, Jayasiri SC, Jayawardena RS, Konta S, Lee HB, Li WJ, Lin CG, Liu LK, Lu YZ, Luo ZL, Manawasinghe IS, Manimohan P, Mapook A, Niskanen T, Norphanphoun C, Papizadeh M, Perera RH, Phukhamsakda C, Richter C, de Santiago ALCM, Drechsler-Santos ER, Senanayake IC, Tanaka K, Tennakoon TMDS, Thambugala KM, Tian Q, Tibpromma S, Thongbai B, Vizzini A, Wanasinghe DN, Wijayawardene NN, Wu HX, Yang J, Zeng XY, Zhang H, Zhang JF, Bulgakov TS, Camporesi E, Bahkali AH, Amoozegar MA, Araujo-Neta LS, Ammirati JF, Baghela A, Bhatt RP, Bojantchev D, Buyck B, da Silva GA, de Lima CLF, de Oliveira RJV, de Souza CAF, Dai YC, Dima B, Duong TT, Ercole E, Mafalda-Freire F, Ghosh A, Hashimoto A, Kamolhan S, Kang JC, Karunarathna SC, Kirk PM, Kytövuori I, Lantieri A, Liimatainen K, Liu ZY, Liu XZ, Lücking R, Medardi G, Mortimer PE, Nguyen TTT, Promputtha I, Anil Raj KN, Reck MA, Lumyong S, Shahzadeh-Fazeli SA, Stadler M, Soudi MR, Su HY, Takahashi T, Tangthirasunun N, Uniyal P, Wang Y, Wen YC, Xu JC, Zhang ZK, Zhao YC, Zhou JL, Zhu L (2016) Fungal diversity notes 367–490: Taxonomic and phylogenetic contributions to fungal taxa. *Fungal Diversity* 80: 1–270. <https://doi.org/10.1007/s13225-016-0373-x>
- Hyde KD, Norphanphoun C, Abreu VP, Bazzicalupo A, Thilini CKW, Clericuzio M, Dayarathne MC, Dissanayake AJ, Ekanayaka AH, He MQ, Hongsanan S, Huang SK, Jayasiri SC, Jayawardena RS, Karunarathna A, Konta S, Kušan I, Lee H, Li JF, Lin CG, Liu NG, Lu YZ, Luo ZL, Manawasinghe IS, Mapook A, Perera RH, Phookamsak R, Phukhamsakda C, Siedlecki I, Soares AM, Tennakoon DS, Tian Q, Tibpromma S, Wanasinghe DN, Xiao

- YP, Yang J, Zeng XY, Abdel-Aziz FA, Li WJ, Senanayake IC, Shang QJ, Daranagama DA, de Silva NI, Thambugala KM, Abdel-Wahab MA, Bahkali AH, Berbee ML, Boonmee S, Bhat DJ, Bulgakov TS, Buyck B, Camporesi E, Castañeda-Ruiz RF (2017) Fungal diversity notes 603–708: Taxonomic and phylogenetic notes on genera and species. *Fungal Diversity* 87(1): 1–235. <https://doi.org/10.1007/s13225-017-0391-3>
- Hyde KD, Jeewon R, Chen YJ, Bhunjun CS, Calabon MS, Jiang HB, Lin CG, Norphanphoun C, Sysouphanthong P, Pem D, Tibpromma S, Zhang Q, Doilom M, Jayawardena RS, Liu JK, Maharachchikumbura SSN, Phukhamsakda C, Phookamsak R, Al-Sadi AM, Thongklang N, Wang Y, Gafforov Y, Gareth JEB, Lumyong S (2020) The numbers of fungi: Is the descriptive curve flattening? *Fungal Diversity* 103(4): 219–271. <https://doi.org/10.1007/s13225-020-00458-2>
- Index Fungorum (2023) Index Fungorum. <http://indexfungorum.org/> [Accessed on 15 June 2023]
- Ismail SI, Batzer JC, Harrington TC, Crous PW, Lavrov DV, Li H, Gleason ML (2016) Ancestral state reconstruction infers phytopathogenic origins of sooty blotch and flyspeck fungi on apple. *Mycologia* 108(2): 15–36. <https://doi.org/10.3852/15-036>
- Jaklitsch WM, Gardiennet A, Voglmayr H (2016) Resolution of morphology-based taxonomic delusions: *Acrocordiella*, *Basiseptospora*, *Blogiascospora*, *Clypeosphaeria*, *Hymenoplella*, *Lepteutypa*, *Pseudapiolella*, *Requienella*, *Seiridium* and *Strickeria*. *Persoonia* 37(1): 82–105. <https://doi.org/10.3767/003158516X690475>
- Jeewon R, Liew ECY, Hyde KD (2002) Phylogenetic relationships of *Pestalotiopsis* and allied genera inferred from ribosomal DNA sequences and morphological characters. *Molecular Phylogenetics and Evolution* 25(3): 378–392. [https://doi.org/10.1016/S1055-7903\(02\)00422-0](https://doi.org/10.1016/S1055-7903(02)00422-0)
- Jobard M, Rasconi S, Sime-Ngando T (2010) Diversity and functions of microscopic fungi: A missing component in pelagic food webs. *Aquatic Sciences* 72(3): 255–268. <https://doi.org/10.1007/s00027-010-0133-z>
- Kalani IK (1963) Some new records of *Ciliochorella* spp. from India. *Mycopathologia* 19(3): 238–240. <https://doi.org/10.1007/BF02051252>
- Katoh K, Rozewicki J, Yamada KD (2019) MAFFT online service: Multiple sequence alignment, interactive sequence choice and visualization. *Briefings in Bioinformatics* 20(4): 1160–1166. <https://doi.org/10.1093/bib/bbx108>
- Klein CG, Pisani D, Field DJ, Lakin R, Wills MA, Longrich NR (2021) Evolution and dispersal of snakes across the Cretaceous–Paleogene mass extinction. *Nature Communications* 12(1): e5335. <https://doi.org/10.1038/s41467-021-25136-y>
- Lai GD, Qin CS, Zhao DY, Qiu HL, Yang H, Tian LY, Lian T, Xu JZ (2021) Isolation and Screening of Cellulose Degrading Strains. *Forest Environmental Science* 037: 24–32. [In Chinese]
- Lee S, Crous PW, Wingfield MJ (2006) Pestalotioid fungi from Restionaceae in the Cape Floral Kingdom. *Studies in Mycology* 55: 175–187. <https://doi.org/10.3114/sim.55.1.175>
- Li Y, Hyde KD, Jeewon R, Cai L, Vijaykrishna D, Zhang K (2005) Phylogenetics and evolution of nematode-trapping fungi (Orbiliiales) estimated from nuclear and protein coding genes. *Mycologia* 97(5): 1034–1046. <https://doi.org/10.1080/15572536.2006.11832753>
- Li WJ, Liu JK, Bhat DJ, Camporesi E, Chomnunti P (2015) Molecular phylogenetic analysis reveals two new species of *Discosia* from Italy. *Phytotaxa* 203(1): 37–46. <https://doi.org/10.11646/phytotaxa.203.1.3>
- Li JC, Wu HX, Li YY, Li XH, Song JY, Suwannarach N, Wijayawardene NN (2022) Taxonomy, phylogenetic and ancestral area reconstruction in *Phyllachora*, with four

- novel species from Northwestern China. *Journal of Fungi* 8(5): e520. <https://doi.org/10.3390/jof8050520>
- Li JF, Jiang HB, Jeewon R, Hongsanan S, Bhat DJ, Tang SM, Lumyong S, Mortimer PE, Xu JC, Camporesi E, Bulgakov TS, Zhao GJ, Suwannarach N, Phookamsak R (2023) *Alternaria*: Update on species limits, evolution, multi-locus phylogeny, and classification. *Studies in Fungi* 8(1): 1–61. <https://doi.org/10.48130/SIF-2023-0001>
- Liu S, Fan BQ (2012) Screening of a straw cellulose-degrading fungi QSH3-3 and study on its characteristics of cellulase production. *Plant Nutrition and Fertilizer Science* 18(1): 218–226.
- Liu F, Bonthond G, Groenewald JZ, Cai L, Crous PW (2019a) Sporocadaceae, a family of coelom-ycetous fungi with appendage-bearing conidia. *Studies in Mycology* 92(1): 287–415. <https://doi.org/10.1016/j.simyco.2018.11.001>
- Liu NG, Hyde KD, Bhat DJ, Jumpathong J, Liu JK (2019b) Morphological and phylogenetic studies of *Pleopunctum* gen. nov. (Phaeoseptaceae, Pleosporales) from China. *Mycosphere: Journal of Fungal Biology* 10(1): 757–775. <https://doi.org/10.5943/mycosphere/10/1/17>
- Maharachchikumbura SSN, Hyde KD, Groenewald JZ, Xu J, Crous PW (2014) *Pestalotiopsis* revisited. *Studies in Mycology* 79(1): 121–186. <https://doi.org/10.1016/j.simyco.2014.09.005>
- Maharachchikumbura SSN, Hyde KD, Jones EBG, McKenzie EHC, Bhat DJ, Dayarathne MC, Huang SK, Norphanphoun C, Senanayake IC, Perera RH, Shang QJ, Xiao YP, D'souza MJ, Hongsanan S, Jayawardena RS, Daranagama DA, Konta S, Goonasekara ID, Zhuang WY, Jeewon R, Phillips AJL, AbdelWahab MA, Al-Sadi AM, Bahkali AH, Boonmee S, Boonyuen N, Cheewangkoon R, Dissanayake AJ, Kang JC, Li QR, Liu JK, Liu XZ, Liu ZY, Luangsa-ard JJ, Pang KL, Phookamsak R, Promputtha I, Suetrong S, Stadler M, Wen TC, Wijayawardene NN (2016) Families of Sordariomycetes. *Fungal Diversity* 79(1): 1–317. <https://doi.org/10.1007/s13225-016-0369-6>
- Masilamani S, Muthumary J (1994) Development of conidiomata in *Ciliochorella mangiferae*. *Mycological Research* 98(8): 857–861. [https://doi.org/10.1016/S0953-7562\(09\)80254-2](https://doi.org/10.1016/S0953-7562(09)80254-2)
- Nag Raj TR (1993) *Coelomycetous Anamorphs with Appendage-Bearing Conidia*. Mycologue Publications, Canada.
- Norphanphoun C, Maharachchikumbura SSN, Daranagama DA, Bulgakov TS, Bhat DJ, Bahkali AH, Hyde KD (2015) Towards a backbone tree for *Seimatosporium*, with *S. physocarpis* sp. nov. *Mycosphere: Journal of Fungal Biology* 6(3): 385–400. <https://doi.org/10.5943/mycosphere/6/3/12>
- O'Donnell K, Cigelnik E (1997) Two divergent intragenomic rADN ITS2 types within a monophyletic lineage of the fungus fusarium are nonorthologous. *Molecular Phylogenetics and Evolution* 7: 103–116. <https://doi.org/10.1006/mpev.1996.0376>
- Omland KE (1999) The assumptions and challenges of ancestral state reconstructions. *Systematic Biology* 3(3): 604–611. <https://doi.org/10.1080/106351599260175>
- Paradis E, Schliep K (2019) APE 5.0: An environment for modern phylogenetics and evolutionary analyses in R. *Bioinformatics* 35(3): 526–528. <https://doi.org/10.1093/bioinformatics/bty633>
- Peng CG, Wu DD, Ren JL, Peng ZL, Ma ZF, Wu W, Lv YY, Wang Z, Deng C, Jiang K, Parkinson CL, Qi Y, Zhang ZY, Li JT (2023) Large-scale snake genome analyses provide insights into vertebrate development. *Cell* 186(14): 2959–2976. <https://doi.org/10.1016/j.cell.2023.05.030>

- Perera RH, Maharachchikumbura SSN, Bahkali AH, Camporesi E, Jones EBG, Phillips AJL, Hyde KD (2016) Sexual morph of *Seimatosporium cornii* found on *Cornus sanguinea* in Italy. *Phytotaxa* 257(1): 51–60. <https://doi.org/10.11646/phytotaxa.257.1.3>
- Pérez-Ortega S, Garrido-Benavent I, Grube M, Olmo R, de los Ríos A (2016) Hidden diversity of marine borderline lichens and a new order of fungi: Collemopsidiales (Dothideomyceta). *Fungal Diversity* 80(1): 285–300. <https://doi.org/10.1007/s13225-016-0361-1>
- Pointing SB, Pelling AL, Smith GJD, Hyde KD, Reddy CA (2005) Screening of basidiomycetes and xylariaceous fungi for lignin peroxidase and laccase gene-specific sequences. *Mycological Research* 109(1): 115–124. <https://doi.org/10.1017/S0953756204001376>
- Rossmann AY, Allen WC, Castlebury LA (2016) New combinations of plant-associated fungi resulting from the change to one name for fungi. *IMA Fungus* 7(1): 1–7. <https://doi.org/10.5598/imafungus.2016.07.01.01>
- Royer-Carenzi M, Didier G (2016) A comparison of ancestral state reconstruction methods for quantitative characters. *Cold Spring Harbor Laboratory* 404: 126–142. <https://doi.org/10.1016/j.jtbi.2016.05.029>
- Ruan LF (2011) Studies on dark septate endophytes (DSE) in the dry-hot valley of Yuan River, Yunnan Province. Master dissertation of Yunnan University, Yunnan, China. [In Chinese]
- Samaradiwakara NP, de Farias ARG, Tennakoon DS, Aluthmuhandiram JVS, Bhunjun CS, Chethana KWT, Kumla J, Lumyong S (2023) Appendage-bearing Sordariomycetes from *Dipterocarpus alatus* Leaf Litter in Thailand. *Journal of Fungi* 9(6): e625. <https://doi.org/10.3390/jof9060625>
- Samarakoon MC, Hyde KD, Promputtha I, Hongsanan S, Mapook A (2016) Evolution of Xylariomycetidae (Ascomycota: Sordariomycetes). *Mycosphere: Journal of Fungal Biology* 7(11): 1746–1761. <https://doi.org/10.5943/mycosphere/7/11/9>
- Samarakoon MC, Hyde KD, Hongsanan S, McKenzie EHC, Ariyawansa HA, Promputtha I, Zeng ZY, Tian Q, Liu JK (2019) Divergence time calibrations for ancient lineages of Ascomycota classification based on a modern review of estimations. *Fungal Diversity* 96(1): 285–346. <https://doi.org/10.1007/s13225-019-00423-8>
- Samarakoon MC, Hyde KD, Maharachchikumbura SSN, Stadler M, Jones EBG, Promputtha I, Suwannarach N, Camporesi E, Bulgakov TS, Liu JK (2022) Taxonomy, phylogeny, molecular dating and ancestral state reconstruction of Xylariomycetidae (Sordariomycetes). *Fungal Diversity* 112(1): 1–88. <https://doi.org/10.1007/s13225-021-00495-5>
- Sanderson MJ (2003) r8s: Inferring absolute rates of molecular evolution and divergence times in the absence of a molecular clock. *Bioinformatics* 19(2): 301–302. <https://doi.org/10.1093/bioinformatics/19.2.301>
- Saparrat MCN, Estevez JM, Troncozo MI, Arambarri AM, Balatti PA (2010) In-vitro depolymerization of *Scutia buxifolia* leaf-litter by a dominant Ascomycota *Ciliochorella* sp. *International Biodeterioration & Biodegradation* 64(3): 262–266. <https://doi.org/10.1016/j.ibiod.2010.02.001>
- Schmit JP, Mueller GM (2007) An estimate of the lower limit of global fungal diversity. *Biodiversity and Conservation* 16(1): 99–111. <https://doi.org/10.1007/s10531-006-9129-3>
- Senanayake IC, Maharachchikumbura SSN, Hyde KD, Bhat JD, Jones EBG, McKenzie EHC, Dai DQ, Daranagama DA, Dayaratne MC, Goonasekara ID, Konta S, Li WJ, Shang QJ, Stadler M, Wijayawardene NN, Xiao YP, Norphanphoun C, Li QR, Liu XZ, Bahkali AH, Kang JC, Wang Y, Wen TC, Wendt L, Xu JC, Camporesi E (2015) Towards un-

- raveling relationships in Xylariomycetidae (Sordariomycetes). *Fungal Diversity* 73(1): 73–144. <https://doi.org/10.1007/s13225-015-0340-y>
- Seshadri VS (1969) Critical observations on the fungus genus *Ciliochorella*. *Mycopathologia* 38(1–2): 129–131. <https://doi.org/10.1007/BF02051682>
- Species Fungorum (2023) Species Fungorum. <https://speciesfungorum.org/> [Accessed on 15 June 2023]
- Subramanian CV, Ramakrishnan K (1956) *Ciliochorella* Sydow, *Plagionema* Subram & Ramakr, and *Shanoria* gen. nov. *Transactions of the British Mycological Society* 39(3): 314–318. [https://doi.org/10.1016/S0007-1536\(56\)80016-8](https://doi.org/10.1016/S0007-1536(56)80016-8)
- Sutton BC (1980) *The Coelomycetes. Fungi Imperfecti with Pycnidia, Acervuli and Stromata*. Commonwealth Mycological Institute, UK.
- Sydow H, Mitter JH (1935) *Fungi Indici II*. *Annales mycologici* 33: 46–71.
- Tanaka K, Endo M, Hirayama K, Okane I, Hosoya T, Sato T (2011) Phylogeny of *Discosia* and *Seimatosporium*, and introduction of *Adisciso* and *Immersidiscosia* genera nova. *Persoonia – Molecular Phylogeny and Evolution of Fungi* 26(1): 85–98. <https://doi.org/10.3767/003158511X576666>
- Tang AMC, Jeewon R, Hyde KD (2007) Phylogenetic utility of protein (RPB2, β -tubulin) and ribosomal (LSU, SSU) gene sequences in the systematics of Sordariomycetes (Ascomycota, Fungi). *Antonie van Leeuwenhoek* 91(4): 327–349. <https://doi.org/10.1007/s10482-006-9120-8>
- Tangthirasunun N, Silar P, Bhat DJ, Maharachchikumbura SSN, Wijayawardene NN, Bahkali AH, Hyde KD (2015) Morphology and phylogeny of two appendaged genera of coelomycetes: *Ciliochorella* and *Discosia*. *Sydowia* 67: 217–226. <https://doi.org/10.12905/0380.sydowia67-2015-0217>
- Tao X, Chen SL (2020) Research progress on fungal fossils. *Junwu Xuebao* 39(2): 211–222. [In Chinese]
- Taylor TN, Krings M, Taylor EL (2015) 10 Fungal Diversity in the Fossil Record. *Systematics and Evolution*: 259–78. https://doi.org/10.1007/978-3-662-46011-5_10
- Tennakoon DS, Kuo CH, Maharachchikumbura SSN, Thambugala KM, Gentekaki E, Phillips AJL, Bhat DJ, Wanasinghe DN, de Silva NI, Promputtha I, Hyde KD (2021) Taxonomic and phylogenetic contributions to *Celtis formosana*, *Ficus ampelas*, *F. septica*, *Macaranga tanarius* and *Morus australis* leaf litter inhabiting microfungi. *Fungal Diversity* 108(1): 1–215. <https://doi.org/10.1007/s13225-021-00474-w>
- Troncozo MI, Go'mez RP, Arambarri AM, Balatti PA, Bucsinzky AMM, Saparrat MCN (2015) Growth and oxidative enzymatic activity of in-vitro cultures of *Ciliochorella buxifolia*. *Mycoscience* 56(1): 58–65. <https://doi.org/10.1016/j.myc.2014.03.003>
- Vijaykrishna D, Jeewon R, Hyde KD (2006) Molecular taxonomy, origins and evolution of freshwater ascomycetes. *Fungal Diversity* 23: 351–390.
- Vilgalys R, Hester M (1990) Rapid genetic identification and mapping of enzymatically amplified ribosomal DNA from several *Cryptococcus* species. *Journal of Bacteriology* 172(8): 4238–4246. <https://doi.org/10.1128/jb.172.8.4238-4246.1990>
- Wanasinghe DN, Phukhamsakda C, Hyde KD, Jeewon R, Lee HB, Jones EBG, Tibpromma S, Tennakoon DS, Dissanayake AJ, Jayasiri SC, Gafforov Y, Camporesi E, Bulgakov TS, Ekanayake AH, Perera RH, Samarakoon MC, Goonasekara ID, Mapook A, Li WJ, Senanayake IC, Li JF, Norphanphoun C, Doilom M, Bahkali AH, Xu JC, Mortimer PE, Tibell L, Tibell S, Karunarathna SC (2018) Fungal diversity notes 709–839: Taxonomic and phylogenetic contributions to fungal taxa with an emphasis on fungi on Rosaceae. *Fungal Diversity* 89(1): 1–236. <https://doi.org/10.1007/s13225-018-0395-7>

- Wang K, Han YF, Liang ZQ (2016) Screening of superior lignin-degrading thermotolerant fungal strains from Wuyi Mountains and assessment of their degradation effects on straw lignin. *Junwu Xuebao* 35(10): 1169–1177. [In Chinese]
- White TJ, Bruns TD, Lee SB, Taylor JW, Innis MA, Gelfand DH, Sninsky J (1990) Amplification and Direct Sequencing of Fungal Ribosomal RNA Genes for Phylogenetics. *PCR Protocols*. Academic Press, 315–322. <https://doi.org/10.1016/B978-0-12-372180-8.50042-1>
- Wijayawardene N, Goonasekara ID, Erio C, Wang Y, An YL (2016) Two new seimatosporium species from Italy. *Mycosphere: Journal of Fungal Biology* 7(2): 204–213. <https://doi.org/10.5943/mycosphere/7/2/9>
- Wijayawardene NN, Hyde KD, Dai DQ, Sánchez-García M, Goto BT, Saxena RK, Erdoğdu M, Selçuk F, Rajeshkumar KC, Aptroot A, Błaszczowski J, Boonyuen N, da Silva GA, de Souza FA, Dong W, Ertz D, Haelewaters D, Jones EBG, Karunarathna SC, Kirk PM, Kukwa M, Kumla J, Leontyev DV, Lumbsch HT, Maharachchikumbura SSN, Marguno F, Martínez-Rodríguez P, Mešić A, Monteiro JS, Oehl F, Pawłowska J, Pem D, Pfliegler WP, Phillips AJL, Pošta A, He MQ, Li JX, Raza M, Sruthi OP, Suetrong S, Suwannarach N, Tedersoo L, Thiyagaraja V, Tibpromma S, Tkalčec Z, Tokarev YS, Wanasinghe DN, Wijesundara DSA, Wimalaseana SDMK, Madrid H, Zhang GQ, Gao Y, Sánchez-Castro I, Tang LZ, Stadler M, Yurkov A, Thines M (2022a) Outline of Fungi and fungus-like taxa – 2021. *Mycosphere: Journal of Fungal Biology* 13(1): 53–453. <https://doi.org/10.5943/mycosphere/13/1/2>
- Wijayawardene NN, Phillips AJL, Pereira DS, Dai DQ, Aptroot A, Monteiro JS, Druzhinina IS, Cai F, Fan X, Selbmann L, Coleine C, Castañeda-Ruiz RF, Kukwa M, Flakus A, Fiuza PO, Kirk PM, Kumar KCR, Arachchi ISL, Suwannarach N, Tang LZ, Boekhout T, Tan CS, Jayasinghe RPPK, Thines M (2022b) Forecasting the number of species of asexually reproducing fungi (Ascomycota and Basidiomycota). *Fungal Diversity* 114(1): 463–490. <https://doi.org/10.1007/s13225-022-00500-5>
- Wu HX, Schoch CL, Boonmee S, Bahkali AH, Chomnunti P, Hyde KD (2011) A reappraisal of Microthyriaceae. *Fungal Diversity* 51(1): 189–248. <https://doi.org/10.1007/s13225-011-0143-8>
- Wu HX, Li YM, Ariyawansa HA, Li WJ, Yang H, Hyde KD (2014) A new species of *Microthyrium* from Yunnan, China. *Phytotaxa* 176(1): 213–218. <https://doi.org/10.11646/phytotaxa.176.1.21>
- Yi ZY, Shi LL, Chen AQ, Zou XM, Cao KF (2011) Soil fungal communities along the vegetation gradient in hot-dry valley of Yuanjiang, Yunnan ProvinC. *Chinese Agricultural Science Bulletin* 27(22): 89–93.
- Yu Y, Harris AJ, Blair C, He XJ (2015) RASP (Reconstruct Ancestral State in Phylogenies): A t-tool for historical biogeography. *Molecular Phylogenetics and Evolution* 87: 46–49. <https://doi.org/10.1016/j.ympev.2015.03.008>
- Yu Y, Blair C, He XJ (2020) RASP 4: Ancestral State Reconstruction Tool for multiple genes and characters. *Molecular Biology and Evolution* 37(2): 604–606. <https://doi.org/10.1093/molbev/msz257>
- Zeng XY, Wu HX, Hongsanan S, Jeewon R, Wen TC, Maharachchikumbura SSN, Chomnunti P, Hyde KD (2019) Taxonomy and the evolutionary history of Micropeltidaceae. *Fungal Diversity* 97(1): 393–436. <https://doi.org/10.1007/s13225-019-00431-8>
- Zhu H, Tan YH (2022) Flora and Vegetation of Yunnan, Southwestern China: Diversity, Origin and Evolution. *Diversity* 14(5): e340. <https://doi.org/10.3390/d14050340>

Taxonomic and phylogenetic characterisations of six species of Pleosporales (in Didymosphaeriaceae, Roussoellaceae and Nigrogranaceae) from China

Hongmin Hu^{1,2*}, Minghui He^{1,2*}, Youpeng Wu¹, Sihan Long¹, Xu Zhang¹, Lili Liu³, Xiangchun Shen^{1,2}, Nalin N. Wijayawardene^{4,5}, Zebin Meng⁶, Qingde Long¹, Jichuan Kang⁷, Qirui Li^{1,2}

1 State Key Laboratory of Functions and Applications of Medicinal Plants, Guizhou Medical University, Guiyang, Guizhou province, China

2 The High Efficacy Application of Natural Medicinal Resources Engineering Center of Guizhou Province (The Key Laboratory of Optimal Utilization of Natural Medicine Resources), School of Pharmaceutical Sciences, Guizhou Medical University, University Town, Gui'an New District, Guiyang, Guizhou province, China

3 Key Laboratory of Infectious Immune and Antibody Engineering of Guizhou Province, Cellular Immunotherapy Engineering Research Center of Guizhou Province, Immune Cells and Antibody Engineering Research Center of Guizhou Province, School of Biology and Engineering, Guizhou Medical University, Guiyang, Guizhou province, China

4 Center for Yunnan Plateau Biological Resources Protection and Utilization, College of Biological Resource and Food Engineering, Qujing Normal University, Qujing, Yunnan province, China

5 Tropical Microbiology Research Foundation, 96/N/10, Meemanagoda Road, 10230 Pannipitiya, Sri Lanka

6 Guizhou Tea Seed Resource Utilization Engineering Research Center, Guizhou Education University, Guiyang, Guizhou province, China

7 The Engineering and Research Center for Southwest Bio-Pharmaceutical Resources of National Education Ministry of China, Guizhou University, Guiyang, Guizhou province, China

Corresponding authors: Qirui Li (lqrnd2008@163.com); Qingde Long (longqingde@gmc.edu.cn)



Academic editor: J. Luangsa-ard

Received: 12 July 2023

Accepted: 27 October 2023

Published: 29 November 2023

Citation: Hu H, He M, Wu Y, Long S, Zhang X, Liu L, Shen X, Wijayawardene NN, Meng Z, Long Q, Kang J, Li Q (2023) Taxonomic and phylogenetic characterisations of six species of Pleosporales (in Didymosphaeriaceae, Roussoellaceae and Nigrogranaceae) from China. MycoKeys 100: 123–151. <https://doi.org/10.3897/mycokeys.100.109423>

Copyright: © Hongmin Hu et al.

This is an open access article distributed under terms of the Creative Commons Attribution License (Attribution 4.0 International – CC BY 4.0).

Abstract

Pleosporales comprise a diverse group of fungi with a global distribution and significant ecological importance. A survey on Pleosporales (in Didymosphaeriaceae, Roussoellaceae and Nigrogranaceae) in Guizhou Province, China, was conducted. Specimens were identified, based on morphological characteristics and phylogenetic analyses using a dataset composed of ITS, LSU, SSU, *tef1* and *rpb2* loci. Maximum Likelihood (ML) and Bayesian analyses were performed. As a result, three new species (*Neokalmusia karka*, *Nigrograna schinifolium* and *N. trachycarpus*) have been discovered, along with two new records for China (*Roussoella neopustulans* and *R. doimaesalongensis*) and a known species (*Roussoella pseudohysterioides*). Morphologically similar species and phylogenetically close taxa are compared and discussed. This study provides detailed information and descriptions of all newly-identified taxa.

Key words: phylogeny, saprophytic fungi, taxonomy, three new taxa

Introduction

The order Pleosporales was formally established by Luttrell and Barr (1987) and is characterised by perithecioid ascomata with a papillate apex, ostioles with or without periphyses, cellular pseudoparaphyses, bitunicate asci and ascospores of varying shapes, pigmentation and septation (Zhang et al. 2012).

* These authors contributed equally as co-first authors.

As one of the largest orders in the Dothideomycetes, it comprises a quarter of all dothideomycetous species (Ahmed et al. 2014b). Species in this order are found in various habitats and can be epiphytes, endophytes or parasites of living leaves or stems, hyperparasites on fungi or insects, lichenised or saprobes of dead plant stems, leaves or bark (Ramesh 2003; Kruijs et al. 2006). In this study, we identified six species belonging to the order Pleosporales from the families Didymosphaeriaceae Munk, Nigrogranaceae Jaklitsch & Voglmayr and Roussoellaceae Jian et al. in Guizhou, China (Wijayawardene et al. 2022).

The family Didymosphaeriaceae, introduced by Munk (1953) and typified by *Didymosphaeria fuckeliana*, can be placed in the order Pleosporales. *Neokalmusia* was introduced to Didymosphaeriaceae by Ariyawansa et al. (2014a). Currently, only eight *Neokalmusia* species are listed in Index Fungorum (accession date: 25 July 2023). Members of Didymosphaeriaceae are known to form numerous different types of life modes, including saprobes, pathogens or endophytes and can be found both on land and in water (Gonçalves et al. 2019; Hongsanan et al. 2020). In the study of this paper, *Neokalmusia karka* is taken from the dead culms of the *Phragmites karka* (Retz.) Trin. ex Steud. Shilihe Beach Park, Huaxi, Guizhou Province, China.

Roussoellaceae was established to accommodate three genera, *Neoroussoella* Jian K. Liu et al., *Roussoella* Sacc. and *Roussoellopsis* I. Hino & Katum., based on molecular phylogenetic studies (Liu et al. 2014). The genus *Roussoella* has cylindrical asci with *Cytoplea* asexual morphs, which distinguishes it from other genera (Liu et al. 2014). Another feature reported for the genus *Roussoella* is the high stability of the ascus exotunica, particularly in 3% potassium hydroxide (KOH). This is quite common for nearly all fungi treated here, while only in *Nigrograna* can fissitunicate ascus dehiscence be seen rather frequently (Jaklitsch and Voglmayr 2016). Nigrogranaceae was established to accommodate *Nigrograna*, with *N. mackinnonii* (Borelli) Gruyter et al. as the type species (Jaklitsch and Voglmayr 2016). As the only genus in the family Nigrogranaceae, *Nigrograna* was established despite lacking strong bootstrap values support in ITS/*tef1*-based phylogenetic trees (Kolařík et al. 2017; Mapook et al. 2020; Zhang et al. 2020a; Wijayawardene et al. 2020). Species of *Nigrograna* may be interpreted as a result of cryptic speciation, as, morphologically, they show only subtle differences (Jaklitsch and Voglmayr 2016). Twenty-three *Nigrograna* species are listed in Index Fungorum (accession date: 25 July 2023).

In this study, we collected dead branches in Guizhou Province, China. Examination of the wood revealed three novel fungal species, two species that are newly recorded in China and one known species of Pleosporales. To elucidate their taxonomic placement and relationships with related species, we conducted morphological observations and phylogenetic analyses, based on combined ITS, LSU, SSU, *tef1*, and *rpb2* sequences. Detailed descriptions of the morphological features of these species along with their molecular characterisation are provided.

Materials and methods

Fungal sampling, isolating and morphology

Fresh fungal specimens were collected in Duyun, Zunyi, Qiannan Prefecture and Guiyang, Guizhou Province and were brought back to the laboratory in self-seal-

ing bags. The specimens were then examined for their macroscopic characteristics using a Nikon SMZ 745 series stereomicroscope and photographed, using a Canon 700D digital camera. Micro-morphological structures were photographed using a Nikon digital camera (Canon 700D) that was attached to a light microscope (Nikon Ni). Melzer's iodine reagent was used to test the apical apparatus structures for amyloid reaction. Measurements of the specimens were registered using Tarosoft (R) Image FrameWork 80 software. The photo plates were arranged and improved using Adobe Photoshop CS6 software. Pure cultures were obtained with the single spore isolation method (Long et al. 2019) and the cultures were grown on potato dextrose agar (PDA) for preservation and observation of the anamorph (Rogers and Ju 1996). The specimens were deposited in the Herbaria of Guizhou Medical University (**GMB**) and Kunming Institute of Botany, Chinese Academy of Sciences (**KUN-HKAS**). Living cultures were deposited at the Guizhou Medical University Culture Collection (**GMBC**).

DNA extraction, polymerase chain reaction (PCR) amplification

The pure cultures were cultivated on potato dextrose agar (PDA) medium (Weigh 40.1g of potato dextrose agar (Shanghai Bawei Microbial Technology Co., Ltd.), add 1L of sterile water, and dissolve by heating until boiling. After dissolution, distribute the solution into conical flasks and place them in a high-pressure sterilizer for sterilization. Sterilization conditions are set at 121 degrees Celsius for 30 minutes. After sterilization, add a small amount of injectable potassium penicillin (Huamu) and injectable streptomycin sulfate (Huamu) into the culture medium and mix well. Pour the mixture into disposable culture dishes for later use. This step should be performed in aseptic conditions inside a laminar flow hood.) at 25 °C in the dark for 15–20 days. Fresh mycelium was collected by scraping it with a surgical knife and then transferred to a 1.5 ml centrifuge tube. DNA extraction was performed according to the instructions provided in the Biospin Fungus Genomic DNA Extraction Kit (BIOMIGA®).

The amplification of internal transcribed spacers (ITS), small subunit rDNA (SSU), large subunit rDNA (LSU), translation elongation factor 1-gene region (*tef1*) and RNA polymerase II second largest subunit (*rpb2*) was achieved using ITS5/ITS4, NS1/NS4, LR0R/LR5, EF1-938F/EF1-2218R and fRPB2-5f/fRPB2-7cr primers (Tibpromma et al. 2018; Vu et al. 2019; Wijesinghe et al. 2020; Dissanayake et al. 2021). The polymerase chain reaction (PCR) for the amplification of ITS, SSU, LSU, *tef1* and *rpb2* loci were performed using the Eppendorf Mastercycler nexus (SimpliAmp Thermal Cycler, A24811, SimpliAmp, China) gradient under the conditions specified in Table 1. Subsequently, the PCR fragments were sent to Sangon Biotech (Shanghai) Co., China, for sequencing. Amplification conditions using the Polymerase Chain Reaction is shown in Table 2. The obtained sequences were deposited in GenBank and are listed in Table 3.

Phylogenetic analysis

BioEdit v.7.0 was used to verify the quality of sequences (Hall TA 1999) and MAFFT v.7.215 (<http://mafft.cbrc.jp/alignment/server/index.html>) was employed to generate single gene alignments (Kato and Standley 2013). The file format was converted using ALTER (Alignment Transformation Environment)

Table 1. PCR conditions used for ITS, SSU, LSU, *tef1* and *rpb2* loci.

Genes	Initial period	Cycles, denaturation, annealing and elongation	Final extension
ITS, LSU, SSU, <i>tef1</i>	95°C for 5 min	35 cycles of denaturation at 94 °C for 1 min, annealing at 52°C for 1 min, elongation at 72°C for 1.5 min	72°C for 10 minutes
<i>rpb2</i>	95°C for 5 min	35 cycles of denaturation at 95°C for 1 minute, annealing at 54°C for 2 minutes, elongation at 72°C for 1.5 minutes	72°C for 10 minutes

Table 2. Composition of PCR reaction system.

Components	Volumetry	Concentration
2× Tap PCR Mix	12.5 µl	1×
Primer 1	1 µl	10µM µl ⁻¹
Primer	1 µl	10µM µl ⁻¹
DNA template	1 µl	0.1-0.2 µg µl ⁻¹
ddH ₂ O	Up to 25 µl	

Table 3. Taxa and corresponding GenBank accession numbers of sequences used in the phylogenetic analysis of Didymosphaeriaceae, Roussoellaceae and Nigrogranaceae.

Species	Strain	GenBank Accession Numbers					References
		ITS	SSU	LSU	<i>tef1</i>	<i>rpb2</i>	
<i>Alloconiothyrium camelliae</i>	NTUCC 17-032-1 ^T	MT112294	MT071221	MT071270	MT232967	–	(Kolařík et al. 2017)
<i>Arthopyrenia</i> sp.	UTHSC DI16–362	LT796905	LN907505	–	LT797145	LT797065	(Crous et al. 2015)
<i>Austropleospora ochracea</i>	KUMCC 20-0020 ^T	MT799859	MT808321	MT799860	MT872714	–	(Dissanayake et al. 2021)
<i>A. keteleeriae</i>	MFLUCC 18-1551 ^T	NR_163349	MK347910	NG_070075	MK360045	–	(Mapook et al. 2020)
<i>Biatrispora antibiotica</i>	CCF 1998	LT221894	–	–	–	–	(Kolařík et al. 2017)
<i>B. carollii</i>	CCF 4484 ^T	LN626657	–	–	LN626668	–	(Kolařík et al. 2017)
<i>B. mackinnonii</i>	E9303e	–	–	–	LN626673	–	(Kolařík et al. 2017)
<i>B. peruviansis</i>	CCF 4485 ^T	LN626658	–	–	LN626671	–	(Kolařík et al. 2017)
<i>Bimuria omanensis</i>	SQUCC 15280 ^T	NR_173301	–	NG_071257	MT279046	–	(Wijesinghe et al. 2020)
<i>B. novae-zelandiae</i>	CBS 107.79 ^T	MH861181	AY016338	AY016356	DQ471087	–	(Vu et al. 2019)
<i>Chromolaenicola nanensis</i>	MFLUCC 17-1477	MN325014	MN325008	MN325002	MN335647	–	(Liu et al. 2014)
<i>C. siamensis</i>	MFLUCC 17-2527 ^T	NR_163337	MK347866	NG_066311	MK360048	–	(Mapook et al. 2020)
<i>C. thailandensis</i>	MFLUCC 17-1475	MN325019	MN325013	MN325007	MN335652	–	(Liu et al. 2014)
<i>C. lampangensis</i>	MFLUCC 17-1462 ^T	MN325016	MN325010	MN325004	MN335649	–	(Liu et al. 2014)
<i>Cylindroaseptospora leucaena</i>	MFLUCC 17-2424	NR_163333	MK347856	NG_066310	MK360047	–	(Mapook et al. 2020)
<i>Deniquelata hypolithi</i>	CBS 146988 ^T	MZ064429	–	NG_076735	MZ078250	–	(Ariyawansa et al. 2020b)
<i>D. barringtoniae</i>	MFLUCC 16-0271	MH275059	–	MH260291	MH412766	–	(Tibpromma et al. 2018)
<i>Didymocrea sadasivani</i>	CBS 438.65	MH858658	DQ384066	DQ384103	–	–	(Vu et al. 2019)
<i>Didymosphaeria rubi-ulmifolii</i>	MFLUCC 14-0023 ^T	–	NG_063557	KJ436586	–	–	(Jayasiri et al. 2019)
<i>Kalmusia erioi</i>	MFLU 18-0832 ^T	MN473058	MN473046	MN473052	MN481599	–	(Vu et al. 2019)
<i>K. italica</i>	MFLUCC 13-0066 ^T	KP325440	KP325442	KP325441	–	–	(Vu et al. 2019)
<i>K. variisporum</i>	CBS 121517 ^T	NR_145165	–	JX496143	–	–	(Wijesinghe et al. 2020)
<i>K. ebuli</i>	CBS 123120 ^T	KF796674	JN851818	JN644073	–	–	(Dissanayake et al. 2021)
<i>Kalmusibambusa triseptata</i>	MFLUCC 13-0232	KY682697	KY682696	KY682695	–	–	(Tibpromma et al. 2018)
<i>Karstenula rhodostoma</i>	CBS 690.94	–	GU296154	GU301821	GU349067	–	(Crous et al. 2021)
<i>Laburnicola hawksworthii</i>	MFLUCC 13-0602 ^T	KU743194	KU743196	KU743195	–	–	(Ariyawansa et al. 2014)
<i>Letendreaa helminthicola</i>	CBS 884.85	MK404145	AY016345	AY016362	MK404174	–	(Tibpromma et al. 2018)
<i>L. muriformis</i>	MFLUCC 16-0290 ^T	KU743197	KU743199	KU743198	KU743213	–	(Ariyawansa et al. 2014)
<i>L. padouk</i>	CBS 485.70	–	GU296162	AY849951	–	–	(Zhang et al. 2013)
<i>L. cordylinicola</i>	MFLUCC 11 0148 ^T	NR_154118	KM214001	NG_059530	–	–	(Wijayawardene et al. 2020)
<i>Montagnula chromolaenicola</i>	MFLUCC 17-1469 ^T	NR_168866	NG_070157	NG_070948	MT235773	–	(Liu et al. 2014)
<i>M. cirsii</i>	MFLUCC 13 0680	KX274242	KX274255	KX274249	KX284707	–	(Hyde et al. 2020)
<i>M. krabiensis</i>	MFLUCC 16-0250 ^T	MH275070	MH260343	MH260303	MH412776	–	(Tibpromma et al. 2018)

Species	Strain	GenBank Accession Numbers					References
		ITS	SSU	LSU	tef1	rpb2	
<i>M. thailandica</i>	MFLUCC 17-1508 ^T	MT214352	NG_070158	NG_070949	MT235774	–	(Liu et al. 2014)
<i>M. bellevaliae</i>	MFLUCC 14-0924 ^T	NR_155377	KT443904	KT443902	KX949743	–	(Ariyawansa et al. 2014)
<i>Neorousoella alishanense</i>	FU31016	MK503816	MK503822	–	MK336181	MN037756	(Verkley et al. 2014)
<i>N. bambusae</i>	MFLUCC 11–0124	KJ474827	KJ474839	–	KJ474848	KJ474856	(Dissanayake et al. 2021)
<i>N. brevispora</i>	KT2313 ^T	LC014574	AB524460	AB524601	AB539113	–	(Tanaka et al. 2015)
<i>N. brevispora</i>	KT1466	LC014573	AB524459	AB524600	AB539112	–	(Tanaka et al. 2015)
<i>N. heveae</i>	MFLUCC 17–1983	MH590693	MH590689	–	–	–	(Wanasinghe et al. 2018)
<i>N. jonahhulmei</i>	KUMCC 21-0819	ON007044	ON007040	ON007049	ON009134	–	(Wanasinghe et al. 2016)
<i>N. karka</i>	GMB0494^T	OR120445	OR120442	OR120432	OR150020	–	This study
<i>N. karka</i>	GMB0500	OR120438	OR120433	OR120443	OR150021	–	This study
<i>N. kunmingensis</i>	KUMCC 18-0120 ^T	MK079886	MK079887	MK079889	MK070172	–	(Vu et al. 2019)
<i>N. lenispora</i>	GZCC 16-0020 ^T	–	KX791431	–	–	–	(Hyde et al. 2020)
<i>N. scabrispora</i>	KT1023	LC014575	AB524452	AB524593	AB539106	–	(Tanaka et al. 2015)
<i>N. solani</i>	CPC 26331 ^T	KX228261	KX228312	–	–	–	(Wijayawardene et al. 2014)
<i>N. thailandica</i>	MFLUCC 16-0405 ^T	NR_154255	KY706137	NG_059792	KY706145	–	(Thambugala et al. 2015)
<i>Neokalmusia arundinis</i>	MFLUCC 15-0463 ^T	NR_165852	NG_068372	NG_068237	KY244024	–	(Thambugala et al. 2015)
<i>Nigrograna antibiotica</i>	CCF 4378 ^T	JX570932	–	–	JX570934	–	(Kolařík et al. 2018)
<i>Nigrograna cangshanensis</i>	MFLUCC15-0253 ^T	KY511063	–	–	KY511066	–	(Crous et al. 2015)
<i>N. chromolaenae</i>	MFLUCC 17-1437 ^T	MT214379	–	–	MT235801	–	(Liu et al. 2014)
<i>N. didymospora</i>	MFLUCC 11-0613	–	KP091435	KP091434	–	–	(Haridas et al. 2020)
<i>N. fuscidula</i>	CBS 141556 ^T	KX650550	–	–	KX650525	–	(Feng et al. 2019)
<i>N. fuscidula</i>	CBS 141476	KX650547	–	–	KX650522	–	(Feng et al. 2019)
<i>N. hydei</i>	GZCC 19-0050 ^T	NR_172415	–	–	MN389249	–	(Zhang et al. 2020)
<i>N. impatientis</i>	GZCC 19-0042 ^T	NR_172416	–	–	MN389250	–	(Zhang et al. 2020)
<i>N. leucaenae</i>	MFLUCC 18–1544	MK347767	MK347984	–	MK360067	MK434876	(Mapook et al. 2020)
<i>N. locuta-pollinis</i>	CGMCC 3.18784	MF939601	–	–	MF939613	–	(Ahmed et al. 2014)
<i>N. locuta-pollinis</i>	LC11690	MF939603	–	–	MF939614	–	(Ahmed et al. 2014)
<i>N. mackinnonii</i>	CBS 674.75 ^T	NR_132037	–	–	KF407986	–	(Ariyawansa et al. 2015)
<i>N. mackinnonii</i>	E5202H	JX264157	–	–	JX264154	–	(Phukhamsakda et al. 2018)
<i>N. magnoliae</i>	GZCC 17-0057	MF399066	–	–	MF498583	–	(Zhang et al. 2020)
<i>N. magnoliae</i>	MFLUCC 20-0020 ^T	MT159628	–	–	MT159605	–	(Liu et al. 2014)
<i>N. mycophila</i>	CBS 141478 ^T	KX650553	–	–	KX650526	–	(Feng et al. 2019)
<i>N. mycophila</i>	CBS 141483	KX650555	–	–	KX650528	–	(Feng et al. 2019)
<i>N. norvegica</i>	CBS 141485 ^T	KX650556	–	–	–	–	(Feng et al. 2019)
<i>N. obliqua</i>	CBS 141477 ^T	KX650560	–	–	KX650531	–	(Feng et al. 2019)
<i>N. obliqua</i>	CBS 141475	KX650558	–	–	KX650530	–	(Feng et al. 2019)
<i>N. rhizophorae</i>	MFLUCC 18-0397 ^T	MN047085	–	–	MN077064	–	(Poli et al. 2020)
<i>N. samueliana</i>	NFCCI-4383 ^T	MK358817	–	–	MK330937	–	(Poli et al. 2020)
<i>N. schinifolium</i>	GMB0498^T	OR120434	–	–	OR150022	–	This study
<i>N. schinifolium</i>	GMB0504	OR120441	–	–	OR150023	–	This study
<i>N. thymi</i>	MFLUCC 14-1096 ^T	KY775576	–	–	KY775578	–	(Crous et al. 2015)
<i>N. trachycarpus</i>	GMB0499^T	OR120437	–	–	OR150024	–	This study
<i>N. trachycarpus</i>	GMB0505	OR120440	–	–	OR150025	–	This study
<i>N. yasuniana</i>	YU.101026 ^T	HQ108005	–	–	LN626670	–	(Kolařík et al. 2018)
<i>Occultibambusa pustula</i>	MFLUCC 11-0502 ^T	KU940126	–	–	–	–	(Crous et al. 2014)
<i>O. bambusae</i>	MFLUCC 13-0855 ^T	KU940123	–	–	KU940193	–	(Crous et al. 2014)
<i>Paracamarosporium fagi</i>	CPC 24890 ^T	NR_154318	–	NG_070630	–	–	(Ariyawansa et al. 2014)
<i>P. cyclothrioides</i>	CBS 972.95	JX496119	AY642524	JX496232	–	–	(Schoch et al. 2009)
<i>P. estuarinum</i>	CBS 109850 ^T	JX496016	AY642522	JX496129	–	–	(Verkley et al. 2014)
<i>P. hawaiiense</i>	CBS 120025 ^T	JX496027	EU295655	JX496140	–	–	(Verkley et al. 2014)
<i>P. robiniae</i>	MFLUCC 14–1119 ^T	KY511142	KY511141	–	KY549682	–	(Crous et al. 2015)
<i>P. rosarum</i>	MFLUCC 17–6054 ^T	NR_157529	NG_059872	–	MG829224	–	(Hyde et al. 2016)
<i>P. rosicola</i>	MFLUCC 15-0042	NR_157528	MG829153	MG829047	–	–	(Hyde et al. 2016)

Species	Strain	GenBank Accession Numbers					References
		ITS	SSU	LSU	tef1	rpb2	
<i>Paramassariosphaeria anthostomoides</i>	CBS 615.86	MH862005	GU205246	GU205223	–	–	(Vu et al. 2019)
<i>Paraphaeosphaeria rosae</i>	MFLUCC 17-2547 ^T	MG828935	MG829150	MG829044	MG829222	–	(Hyde et al. 2016)
<i>Pararousoella mukdahanensis</i>	KUMCC 18-0121	MH453489	MH453485	–	MH453478	MH453482	(Flakus et al. 2019)
<i>Parathyridaria ramulicola</i>	CBS 141479 ^T	KX650565	KX650565	–	KX650536	KX650584	(Feng et al. 2019)
<i>Phaeodothis winteri</i>	CBS 182.58	–	GU296183	GU301857	–	–	(Zhang et al. 2013)
<i>Pseudocamarosporium propinquum</i>	MFLUCC 13-0544 ^T	KJ747049	KJ819949	KJ813280	–	–	(Thambugala et al. 2017)
<i>Pseudodidymocytis lobariellae</i>	KRAM Flakus 25130 ^T	NR_169714	NG_070349	NG_068933	–	–	(Tanaka et al. 2015)
<i>Pseudoneoconiothyrium euonymi</i>	CBS 143426 ^T	MH107915	MH107961	–	–	MH108007	(Valenzuela-Lopez et al. 2017)
<i>Pseudopithomyces entadae</i>	MFLUCC 17-0917 ^T	–	MK347835	NG_066305	MK360083	–	(Mapook et al. 2020)
<i>Pseudorousoella chromolaenae</i>	MFLUCC 17–1492 ^T	MT214345	MT214439	–	MT235769	–	(Liu et al. 2014)
<i>P. elaeicola</i>	MFLUCC 15–0276a	MH742329	MH742326	–	–	–	(Liu et al. 2014)
<i>P. kunmingensis</i>	MFLUCC 17-0314	MF173607	MF173606	MF173605	–	–	(Mapook et al. 2020)
<i>P. pteleae</i>	MFLUCC 17-0724 ^T	NR_157536	MG829166	MG829061	MG829233	–	(Hyde et al. 2016)
<i>P. rosae</i>	MFLUCC 15-0035 ^T	MG828953	MG829168	MG829064	–	–	(Hyde et al. 2016)
<i>P. ulmi-minoris</i>	MFLUCC 17-0671 ^T	NR_157537	MG829167	MG829062	–	–	(Hyde et al. 2016)
<i>Rousoella acaciae</i>	CBS:138873 ^T	KP004469	KP004497	–	–	–	(Karunaratna et al. 2019)
<i>R. aquatic</i>	MFLUCC 18-1040 ^T	NR171975	NG073797	–	–	–	(Liu et al. 2014)
<i>R. chiangraina</i>	MFLUCC 10-0556 ^T	NR155712	NG059510	–	–	–	(Dissanayake et al. 2021)
<i>R. doimaesalongensis</i>	MFLUCC 14-0584 ^T	NR165856	NG068241	–	KY651249	KY678394	(Thambugala et al. 2015)
<i>R. doimaesalongensis</i>	GMB0497	OR116188	OR117732	–	OR150026	–	This study
<i>R. doimaesalongensis</i>	GMB0503	OR120435	OR120444	–	OR150027	–	This study
<i>R. elaeicola</i>	MFLUCC 15-15-0276a	MH742329	MH742326	–	–	–	(Crous et al. 2015)
<i>R. euonymi</i>	CBS:143426 ^T	MH107915	MH107961	–	–	MH108007	(Valenzuela-Lopez et al. 2017)
<i>R. guttulata</i>	MFLUCC 20-0102 ^T	NR172428	NG075383	–	–	–	(Senwana et al. 2018)
<i>R. hysteroioides</i>	CBS 546.94	MH862484	MH874129	–	KF443399	KF443392	(Vilgalys et al. 1990)
<i>R. intermedia</i>	CBS 170.96	KF443407	KF443382	–	KF443398	KF443394	(Crous et al. 2013)
<i>R. japonensis</i>	MAFF 239636 ^T	NR155713	–	–	–	–	(Dissanayake et al. 2021)
<i>R. kunmingensis</i>	HKAS 101773 ^T	MH453491	MH453487	–	MH453480	MH453484	(Flakus et al. 2019)
<i>R. magnatum</i>	MFLUCC 15-0185 ^T	–	KT281980	–	–	–	(Jiang et al. 2019)
<i>R. mangrovei</i>	MFLU 17-1542 ^T	MH025951	MH023318	–	MH028246	MH028250	(Jaklitsch and Voglmayr 2016)
<i>R. margidorensis</i>	MUT 5329 ^T	NR169906	MN556322	–	MN605897	MN605917	(Tibpromma et al. 2017)
<i>R. mediterranea</i>	MUT5369 ^T	KU314947	MN556324	–	MN605899	MN605919	(Tibpromma et al. 2017)
<i>R. mexicana</i>	CPC 25355 ^T	KT950848	KT950862	–	–	–	(Crous et al. 2015a)
<i>R. mukdahanensis</i>	MFLU 11-0237 ^T	NR155722	–	–	–	–	(Crous et al. 2014)
<i>R. multiplex</i>	GMB0316 ^T	ON479891	–	ON479892	–	–	(Dong et al. 2020)
<i>R. neopustulans</i>	MFLUCC 11-0609 ^T	KJ474833	KJ474841	–	KJ474850	–	(Dissanayake et al. 2021)
<i>R. neopustulans</i>	GMB0496	OR120436	OR120446	–	–	–	This study
<i>R. neopustulans</i>	GMB0502	OR116176	OR117714	–	–	–	This study
<i>R. nitidula</i>	MFLUCC 11-0634	KJ474834	KJ474842	–	KJ474851	KJ474858	(Dissanayake et al. 2021)
<i>R. padinae</i>	MUT 5503 ^T	–	MN556327	–	MN605902	MN605922	(Tibpromma et al. 2017)
<i>R. percutanea</i>	CBS 868.95	KF322118	KF366449	–	KF407987	KF366452	(Ahmed et al. 2014a)
<i>R. pseudohysteroioides</i>	GMBC0009 ^T	MW881445	MW881451	–	–	MW883345	(Zhang et al. 2020)
<i>R. pseudohysteroioides</i>	GMB0495	OR116175	OR117737	–	OR150028	–	This study
<i>R. pseudohysteroioides</i>	GMB0501	OR120447	OR120439	–	OR150029	–	This study
<i>R. pustulans</i>	KT 1709	–	AB524623	–	AB539116	AB539103	(Zhang et al. 2020)
<i>R. scabrispora</i>	MFLUCC 14-0582	KY026583	KY000660	–	–	–	(Zhang et al. 2020)
<i>R. siamensis</i>	MFLUCC 11-0149 ^T	KJ474837	KJ474845	–	KJ474854	KJ474861	(Dissanayake et al. 2021)
<i>R. thailandica</i>	MFLUCC 11-0621 ^T	KJ474838	KJ474846	–	–	–	(Dissanayake et al. 2021)
<i>R. tuberculata</i>	MFLUCC 13-0854 ^T	KU940132	KU863121	–	KU940199	–	(Crous et al. 2014)
<i>R. verrucispora</i>	CBS 125434 ^T	KJ474832	–	–	–	–	(Dissanayake et al. 2021)

Species	Strain	GenBank Accession Numbers					References
		ITS	SSU	LSU	<i>tef1</i>	<i>rpb2</i>	
<i>R. yunnanensis</i>	HKAS 101762	MH453492	MH453488	–	MH453481	–	(Flakus et al. 2019)
<i>Roussoellopsis macrospora</i>	MFLUCC 12-0005	–	KJ474847	–	KJ474855	KJ474862	(Dissanayake et al. 2021)
<i>R. tosaensis</i>	KT 1659	–	AB524625	–	AB539117	AB539104	(Zhang et al. 2020)
<i>Setoarthopyrenia chromolaenae</i>	MFLUCC 17-1444	MT214344	MT214438	–	MT235768	MT235805	(Liu et al. 2014)
<i>Spegazzinia deightonii</i>	yone 212	–	AB797292	AB807582	AB808558	–	(Tanaka et al. 2015)
<i>S. radermacherae</i>	MFLUCC 17-2285 ^T	MK347740	MK347848	MK347957	MK360088	–	(Mapook et al. 2020)
<i>S. tessartha</i>	NRRL 54913	JQ673429	AB797294	AB807584	AB808560	–	(Tanaka et al. 2015)
<i>Thyridaria acaciae</i>	CBS 138873	KP004469	KP004497	–	–	–	(Liu et al. 2014)
<i>T. broussonetiae</i>	CBS 141481	NR_147658	KX650568	–	KX650539	KX650586	(Karunaratna et al. 2019)
<i>Torula herbarum</i>	CBS 111855	KF443409	KF443386	–	KF443403	KF443396	(Crous et al. 2013)
<i>T. hollandica</i>	CBS 220.69	KF443406	KF443384	–	–	KF443393	(Crous et al. 2013)
<i>Tremateia arundicola</i>	MFLU 16-1275	KX274241	KX274254	KX274248	KX284706	–	(Hyde et al. 2020)
<i>T. chromolaenae</i>	MFLUCC 17-1425 ^T	NR_168868	NG_070160	NG_068710	MT235778	–	(Tanaka et al. 2015)
<i>T. guiyangensis</i>	GZAAS01	KX274240	KX274253	KX274247	KX284705	–	(Hyde et al. 2020)
<i>T. murispora</i>	GZCC 18-2787	NR_165916	MK972750	MK972751	MK986482	–	(Feng et al. 2019)
<i>T. thailandensis</i>	MFLUCC 17-1430 ^T	NR_168869	NG_070161	NG_068711	MT235781	–	(Liu et al. 2014)
<i>Verrucoconiothyrium nitidae</i>	CBS:119209	EU552112	–	EU552112	–	–	(Wanasinghe et al. 2018)
<i>Xenocamarosporium acaciae</i>	CPC 24755 ^T	NR_137982	–	NG_058163	–	–	(Crous et al. 2015b)
<i>Xenorossoella triseptata</i>	MFLUCC 17-1438	MT214343	MT214437	–	MT235767	MT235804	(Liu et al. 2014)

Notes: Type specimens or Ex-type specimens are marked with T; “–”: indicates no sequence available in GenBank; newly-generated sequences are indicated in bold.

Abbreviations: **CBS:** Centraalbureau voor Schimmelcultures, Utrecht, The Netherlands; **CPC:** Culture collection of Pedro Crous, housed at the Westerdijk Fungal Biodiversity Institute; **GMB:** Culture collection of Guizhou Medical University; **HKAS:** Herbarium of Cryptogams Kunming Institute of Botany Academia Sinica, Chinese Academy of Sciences, Kunming, China; **HKUC:** Hong Kong University Culture Collection; **KT:** K. Tanaka; **KUMCC:** Kunming Institute of Botany Culture Collection, Chinese Science Academy, Kunming, China; **MAFF:** Ministry of Agriculture, Forestry and Fisheries, Japan; **MFLUCC:** Mae Fah Luang University Culture Collection, Chiang Rai, Thailand; **NFCCI:** National Fungal Culture Collection of India; **Others:** information not available.

(<http://www.sing-group.org/ALTER/>). Maximum Likelihood (ML) analyses and Bayesian posterior probabilities (BYPP), based on a combination of ITS, LSU, *tef1* and *rpb2* sequence data, were performed using RAxML-HPC BlackBox and MrBayes v. 3.2.7a tools in the CIPRES Science Gateway platform (Liang et al. 2020). GTR+I+G was estimated as the best-fit substitution model by ModelTest2 on XSEDE v.2.1.6. (Posada and Crandall 1998).

Bayesian Inference (BI) analysis was conducted using MrBayes v.3.2.7a (Ronquist et al. 2012) and posterior probabilities (PP) were determined through Markov Chain Monte Carlo sampling (MCMC). Six simultaneous Markov chains for 3,000,000 generations were run and trees were sampled every 1,000th generation.

The trees were visualised using FigTree v.1.4.4, and formatted using Adobe Illustrator CS v.6. Branches with Maximum-Likelihood bootstrap values (MLBP) equal to or greater than 75% and Bayesian posterior probabilities (BYPP) greater than 0.95 are indicated. The combined loci alignment and resulting phylogenetic trees were submitted to TreeBASE (<https://www.treebase.org>, submission number: ID 30482; ID 30483; ID 30484).

Results

Phylogenetic analyses

Phylogenetic analyses of Didymosphaeriaceae (Fig. 1), Roussoellaceae (Fig. 2), and Nigrogranaceae (Fig. 3) were performed separately, with corresponding parameters presented in Table 4.

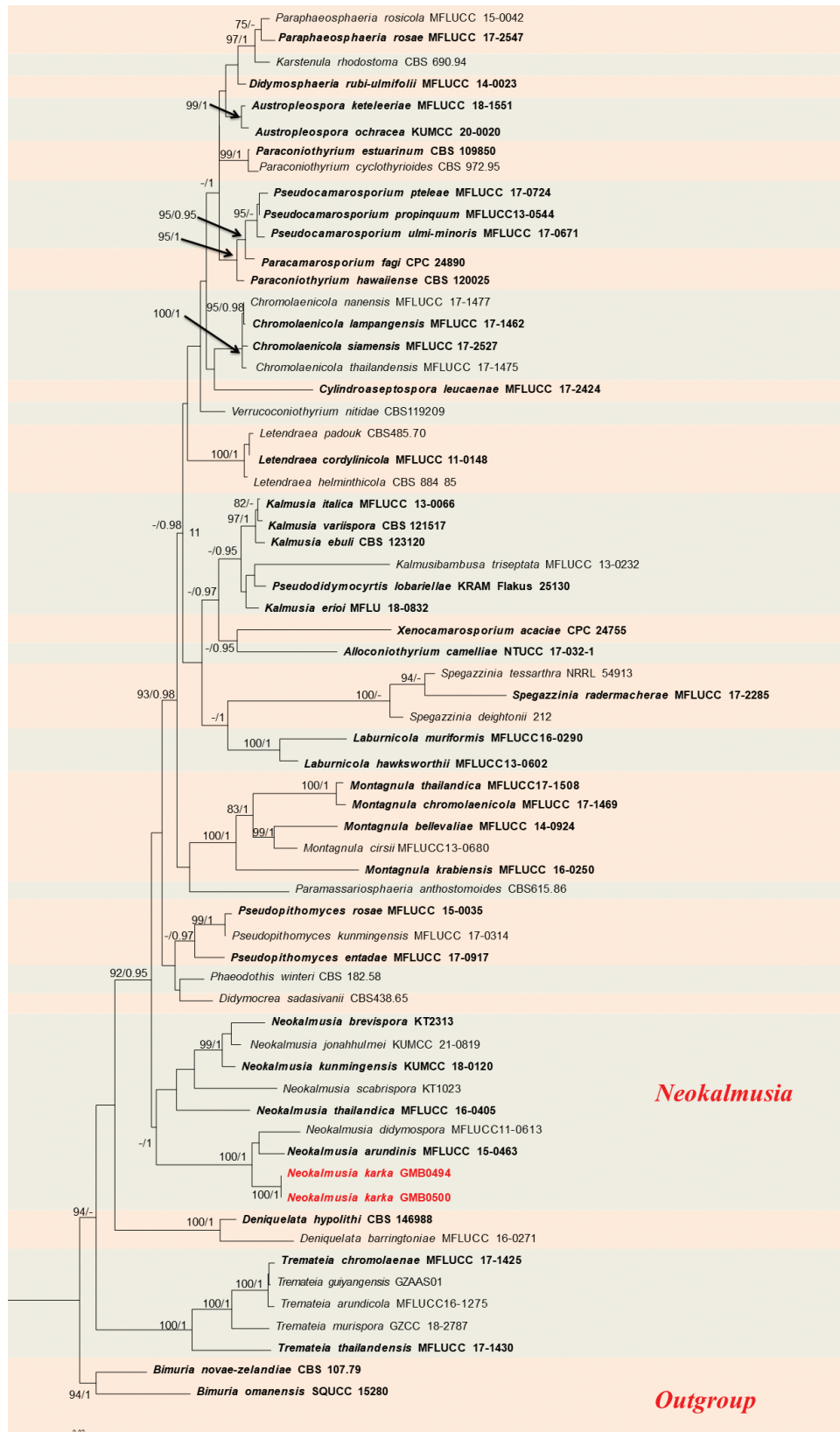


Figure 1. RAxML phylogram of Didymosphaeriaceae, based on a combined dataset of partial ITS, LSU, SSU and *tef1* DNA sequences. The tree is rooted by *Bimuria novae-zelandiae* (CBS 107.79) and *Bimuria omanensis* (SQUCC 15280). Bootstrap supports (MLB) and Bayesian posterior probabilities (BYPP) are given as MLB/BYPP above the branches. Sequences from newly-generated isolates are in red, bold letters, while those of ex-type isolates are shown in black, bold letters.

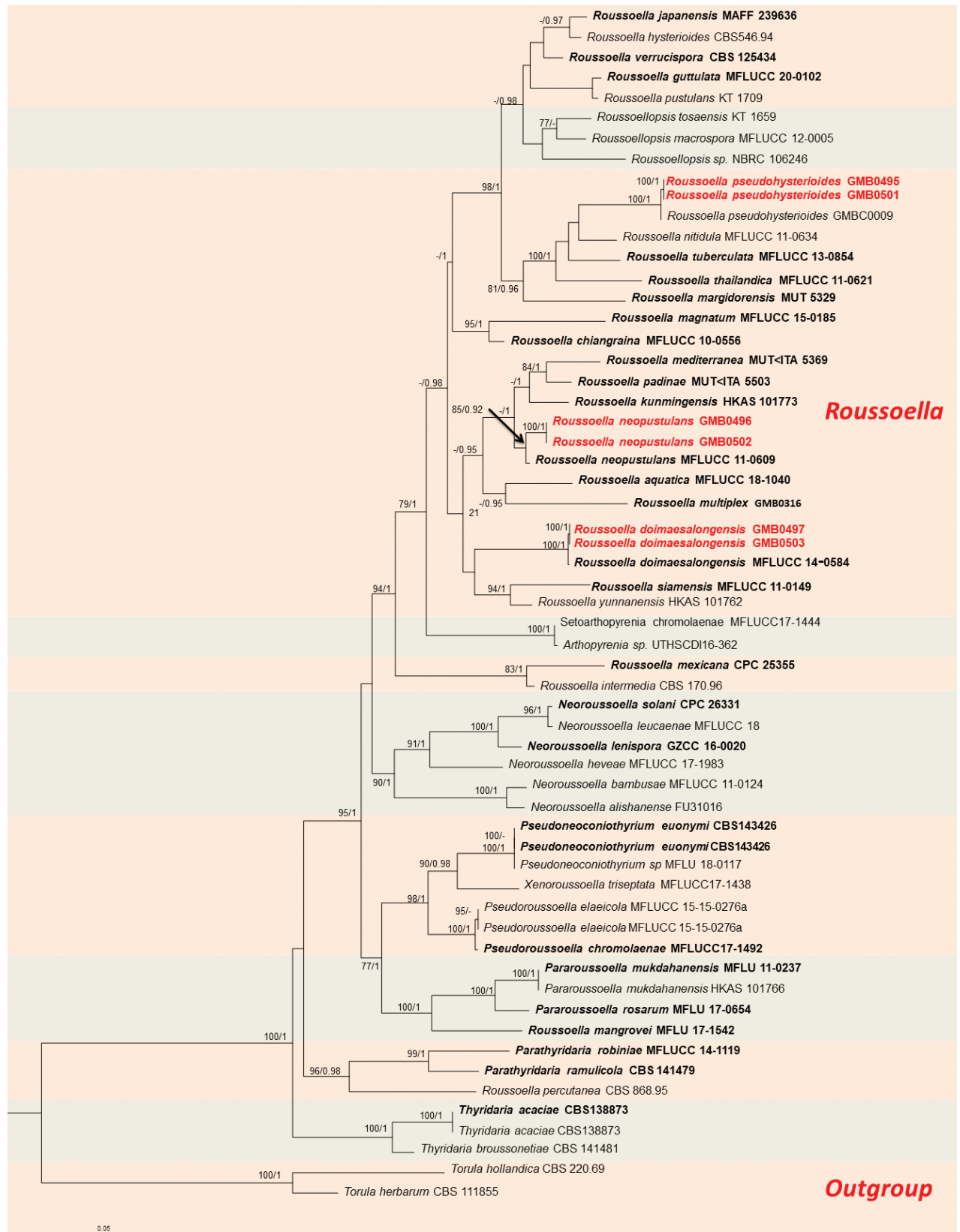


Figure 2. RAxML phylogram of Roussoellaceae, based on a combined dataset of partial ITS, LSU, *tef1* and *rpb2* DNA sequences. The tree is rooted by *Torula hollandica* (CBS 220.69) and *T. herbarum* (CBS 111855). Bootstrap supports ML (MLB ≥ 75%) and Bayesian posterior probabilities (BYPP ≥ 0.95) are given as MLB/BYPP above the branches. Sequences from newly-generated isolates are in red, bold letters, while those of ex-type isolates are shown in black, bold letters.

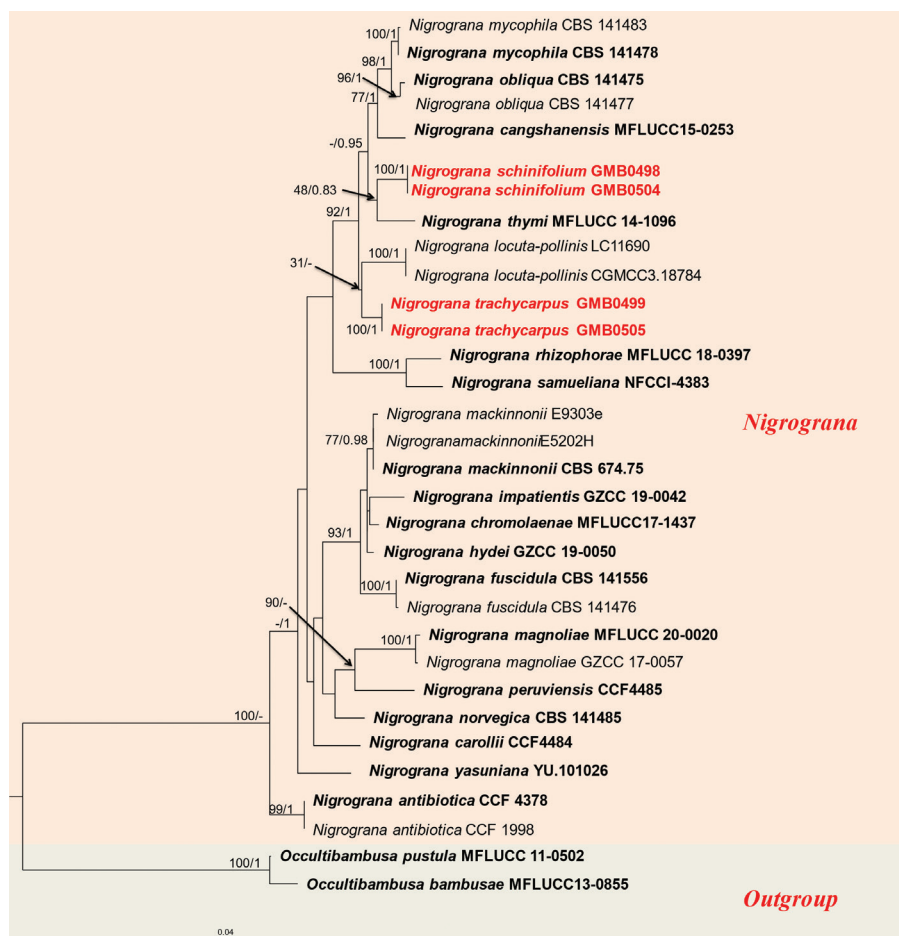


Figure 3. RAxML phylogram of Nigrogranaceae, based on a combined dataset of ITS and *tef1* DNA sequences. The tree is rooted by *Occultibambusa pustula* (MFLUCC 11-0502) and *O. bambusae* (MFLUCC 13-0855). Bootstrap supports ML (MLB $\geq 75\%$) and Bayesian posterior probabilities (BYPP ≥ 0.95) are given as MLB/BYPP above the branches. Sequences from newly-generated isolates are in red, bold letters, while those of ex-type isolates are shown in black, bold letters.

Table 4. Results of Maximum-Likelihood (ML) and Bayesian (BI) analyses for each sequenced dataset.

Analyses	Didymosphaeriaceae	Roussoellaceae	Nigrogranaceae
Number of taxa	64	59	32
Gene regions	ITS, LSU, SSU and <i>tef1</i>	ITS, LSU, <i>tef1</i> and <i>rpb2</i>	ITS and <i>tef1</i>
Number of character positions (including gaps)	2423	2267	868
ML optimisation likelihood value	-13324.603084	-16237.062124	-3695.409391
Distinct alignment patterns in the matrix	584	773	240
Number of undetermined characters or gaps (%)	14.26%	27.45%	7.87%
Estimated base frequencies	A	0.237970	0.229686
	C	0.246811	0.293625
	G	0.277468	0.242370
	T	0.237752	0.234319
Substitution rates	AC	1.764988	1.598706
	AG	2.187844	2.533043
	AT	1.416956	1.640025
	CG	1.132266	0.752494
	CT	7.848138	8.062830
	GT	1.000000	1.000000
Proportion of invariable sites (I)	0.595845	0.544120	0.487317
Gamma distribution shape parameter (a)	0.516792	0.502253	0.634309
Number of generated trees in BI	14806	10678	9932
Average standard deviation of split frequencies	0.006852	0.004431	0.004939

Taxonomy

Didymosphaeriaceae Munk, 1953

Neokalmusia Ariyawansa & K.D. Hyde, *Fungal Diversity* 68: 92 (2014b)

MycoBank No: 550700

Notes. *Neokalmusia* was established by Ariyawansa et al. (2014b) to accommodate two bambusicolous taxa, *N. brevispora* and *N. scabrispora*, previously referred to *Kalmusia*. Members of *Neokalmusia* are characterised by solitary sphaeroid ascomata, a peridium of small pseudoparenchymatous cells, clavate basal asci with very long pedicels, very thin pseudoparaphyses and distoseptate, smooth-walled ascospores (Ariyawansa et al. 2014b; Zhang et al. 2020a). In this study, we introduce a new species of *Neokalmusia*, based on a combination of morphological and molecular analyses (Fig. 1).

Neokalmusia karka H. M. Hu & Q. R. Li, *sp. nov.*

MycoBank No: 851046

Fig. 4

Type material. Holotype: GMB0494.

Etymology. In reference to the host, *Phragmites karka* (Retz.) Trin. ex Steud.

Description. Saprobic on dead culms of *P. karka*.

Sexual morph: Clypeus visible as black dots on the host surface, breaking through slightly raised cracks at the centre. **Ascomata** 241–386 × 161–231 μm (average = 375 × 197 μm, n = 5), smooth, semi-immersed, scattered, solitary or in small groups, black, oval, with ostiole. **Peridium** 12–20 μm wide, composed of a few layers of thin-walled, brown to dark brown, cells of textura angularis. **Hamathecium** comprising 1.5–2.8 μm wide, numerous, cellular, pseudoparaphyses, embedded in a mucilaginous matrix. **Asci** 80–109 × 10–14 μm (average = 95 × 11.4 μm, n = 15), 8-spored, bitunicate, fissitunicate, cylindrical-clavate, with bulbous pedicel, apically rounded with an indistinct ocular chamber, with a J-subapical ring. **Ascospores** 14–17 × 4–6 μm (average = 15.8 × 5.3 μm, n = 30), overlapping 1–2-seriate, fusiform, pale brown to brown, 1-septate, constricted at the septum, often enlarged near septum in the upper cell, distinctly verrucose on the surface, without a mucilaginous sheath. **Asexual morph:** undetermined.

Culture characters. After 4 weeks of cultivation at 25 °C, the colonies on PDA measure around 2–2.5 cm in diameter. The surface appears smooth to velvety with an entire or slightly irregular margin, ranging from white to grey olivaceous. The colour is white near the margin with dense circular to filamentous growth. The reverse side of the colonies black to greenish-olivaceous.

Specimens examined. CHINA, Guizhou Province, Zunyi City, Suiyang County, Kuanqwashui Nature Reserve (28°31'51.04"N, 107°9'33.65"E), 1544 m elev., on decaying culms, 12 October 2022, Y.P. Wu and H.M. Hu, 2022KKS49 (GMB0494, holotype; GMBC0494, ex-type; KUN-HKAS 129179, isotype).

Other examined material. CHINA, Guizhou Province, Huaxi District, Shilihetan Wetland Park (26°41'34.3"N, 106°67'68.8"E), 1500 m elev., on decaying culms, 8 October 2022, Y.P. Wu and H.M. Hu, 2022SLZH11 (GMB0500; GMBC0500, living culture).



Figure 4. *Neokalmusia karka* (GMB0494, holotype) **A** type specimen **B, C** appearance of ascomata on substrate **D, E** longitudinal section of an ascoma **F** peridium **G** pseudoparaphyses **H–K** asci **L–N** ascospores **O, J** ascus subapical ring in Melzer's Reagent. Scale bars: 0.5 mm (**B–D**); 10 μ m (**E–O**).

Notes. This fungus shares morphological characters similar to *Neokalmusia* in having immersed ascomata, a clypeus-like structure composed of thin-walled cells and verrucose ascospores (Tanaka et al. 2009; Ariyawansa et al. 2014b). Other than *Neokalmusia karka*, only two species, *N. arundinis* Thambug. & K.D. Hyde and *N. didymospora* D.Q. Dai & K.D. Hyde have been reported with 1-septate ascospores. However, *N. karka* can be distinguished, based on differences in asci size (*N. karka*, 80–109 × 10–14 µm; *N. arundinis* 60–85 × (7.5–) 8.5–10.5 µm; *N. didymospora* 125–160 × 9.5–14 µm) and the obvious oval shape of its ascomata (Wanasinghe et al. 2018; Flakus et al. 2019). In our phylogram, *Neokalmusia karka* formed a well-supported separate clade (100% ML, 1 BYPP; Fig. 1) in a sister relationship with *N. arundinis* and *N. didymospora*. The macro and micro-morphological differences and phylogenetic analyses support the recognition of *N. karka* as a new species (Fig. 1).

Roussoellaceae Jian K. Liu, Phook., D.Q. Dai & K.D. Hyde 2014

***Roussoella* Sacc., Atti Inst. Veneto Sci. lett., ed Arti, Sér. 6 6: 410 (1888)**

MycoBank No: 541317

Notes. the genus *Roussoella* was introduced by Saccardo et al. (1888), with *R. nitidula* Sacc. & Paol. as the type species, which was collected from bamboo in Malaysia. This family is characterised as having semi-immersed to immersed, solitary or gregarious, clypeate ascostromata containing trabeculate pseudoparaphyses embedded in a gel matrix, long cylindrical to clavate bitunicate asci with or without obvious fissitunicate dehiscence and brown, 2-celled ornamented ascospores (Liu et al. 2014). In this study, we introduce three new records of *Roussoella* species, based on morpho-anatomical and molecular analyses (Fig. 2).

***Roussoella pseudohysterioides* D.Q. Dai & K.D. Hyde, in Dai et al., Fungal Diversity 82(1): 37 (2017)**

MycoBank No: 552026

Fig. 5

Descriptions. See Dai et al. (2017).

Specimen examined. CHINA, Guizhou Province, Huaxi District, Shiliheta Wetland Park (26°43'34.3"N, 106°67'68.8"E), 1542 m elev., on decaying bamboo, 8 October 2022, Y.P Wu and H.M Hu, 2022SLZH6 (GMB0495; GMBC0495, living culture).

Notes. Phylogenetic analyses of the combined ITS, LSU, *tef1* and *rpb2* gene sequences showed that the sequence from our 2022SLZH6 collection clusters together with *Roussoella pseudohysterioides* (MFLU 15-1209), with strong support (100% ML, 1 BYPP; Fig. 2). The morphological characteristics of our specimen are also consistent with those of *R. pseudohysterioides*, which was originally described from decaying bamboo culms in Thailand (Dai et al. 2017). In China, it had previously been reported from Yunnan Province (Jiang et al. 2019). This is the second report of this species in China, representing a new record for Guizhou Province.



Figure 5. *Roussoella pseudohysterioides* (GMB0495) **A** specimen **B, C** appearance of ascomata on substrate **D** cross-section of ascostromata **E** longitudinal section of an ascoma **F** peridium **G** pseudoparaphyses **H–I** asci **J–M** ascospores. Scale bars: 0.5 mm (**B–D**); 10 μ m (**E–M**).

Roussoella neopustulans D.Q. Dai, J.K. Liu & K.D. Hyde, in Liu et al. *Phytotaxa* 181(1): 15 (2014)

MycoBank No: 550664

Fig. 6

Descriptions. See Liu et al. (2014).

Specimens examined. CHINA, Guizhou Province, Huaxi District, Guiyang Huaxi National Urban Wetland Park (26°2'2.34"N, 106°34'16.22"E), on dead branch

of bamboo, 12 October 2022, 1130 m elev., Y.P Wu and H.M Hu, 2022HX25 (GMB0496; GMBC0496, living culture).

Notes. The sequence of our *Rousoella neopustulans* (2022HX25) forms a well-supported clade (85% ML, 0.92 BYPP; Fig. 2) with *R. neopustulan* (MFLUCC 11-0609). *Rousoella neopustulans* was originally introduced by Liu et al. (2014), with a description of the sexual morph only. Dai et al. (2017) provided a comprehensive description and illustrations for both the sexual and asexual morphs of this species. Our collection exhibits identical morphological characteristics to those detailed by Dai et al. (2017). This is the first report of this species in China.

***Rousoella doimaesalongensis* Thambugala & K.D. Hyde, *Mycosphere* 8 (4): 782 (2017)**

MycoBank No: 553169

Fig. 7

Descriptions. See Thambugala et al. (2017).

Specimen examined. CHINA, Guizhou Province, Huaxi District, Shiliheta Wetland Park (26°23'23.4"N, 106°67'56.4"E), 1511 m elev., on dead bamboo branches, 8 October 2022, Y.P Wu and H.M Hu, 2022SLHT14 (GMB0497; GMBC0497, living culture).

Notes. In our phylogram (Fig. 2), the sequence of our collection clustered with *Rousoella doimaesalongensis* with robust support (100% ML, 1 BYPP). *Rousoella doimaesalongensis* was originally found on decaying bamboo culms in Thailand (Thambugala et al. 2017). Morphologically, our specimens match the description provided by Thambugala et al. (2017) and this species was first reported in China by Seong et al. (2022).

Nigrogranaceae Jaklitsch & Voglmayr, 2016

***Nigrograna* Gruyter, Verkley & Crous, *Stud. Mycol.* 75: 31 (2012) [2013]**

MycoBank No: 564794

Notes. *Nigrograna* was described by De Gruyter et al. (2012) as a monotypic genus. *Nigrograna* is characterised by black ascomata, clavate, short pedicellate asci and pale to chocolate brown, asymmetric, fusoid to narrowly ellipsoid, septate ascospores (Zhang et al. 2020a).

***Nigrograna schinifolium* H. M. Hu & Q. R. Li, sp. nov.**

MycoBank No: 849204

Fig. 8

Type material. Holotype. GMB0498.

Etymology. With reference to the host, *Zanthoxylum schinifolium* Sieb. & Zucc.

Description. Saprobitic on dead stem of *Z. schinifolium*.

Sexual morph: Ascomata 198–320 µm wide, 105–160 µm high, solitary or aggregated in small groups, black, semi-immersed, appearing as slightly raised regions. **Ostioles** are black, lined with paraphyses. **Peridium** 26–39 µm wide,

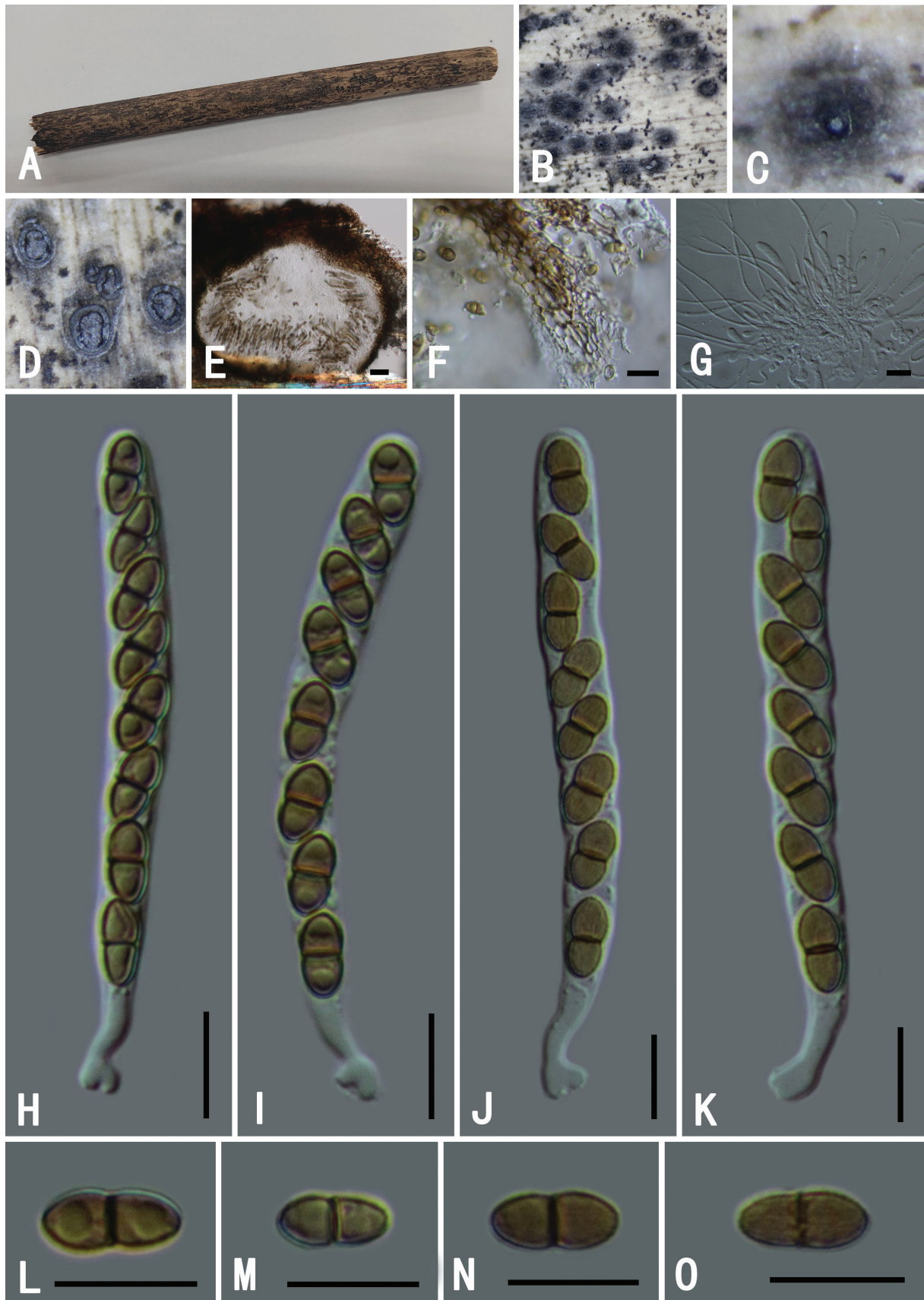


Figure 6. *Roussouella neopustulans* (GMB0496) **A** specimen **B, C** appearance of ascomata on substrate **D** cross-section of ascostromata **E** longitudinal section of an ascoma **F** peridium **G** pseudoparaphyses **H–K** asci **L–O** ascospores. Scale bars: 0.5 mm (**B–D**); 10 μ m (**E–O**).

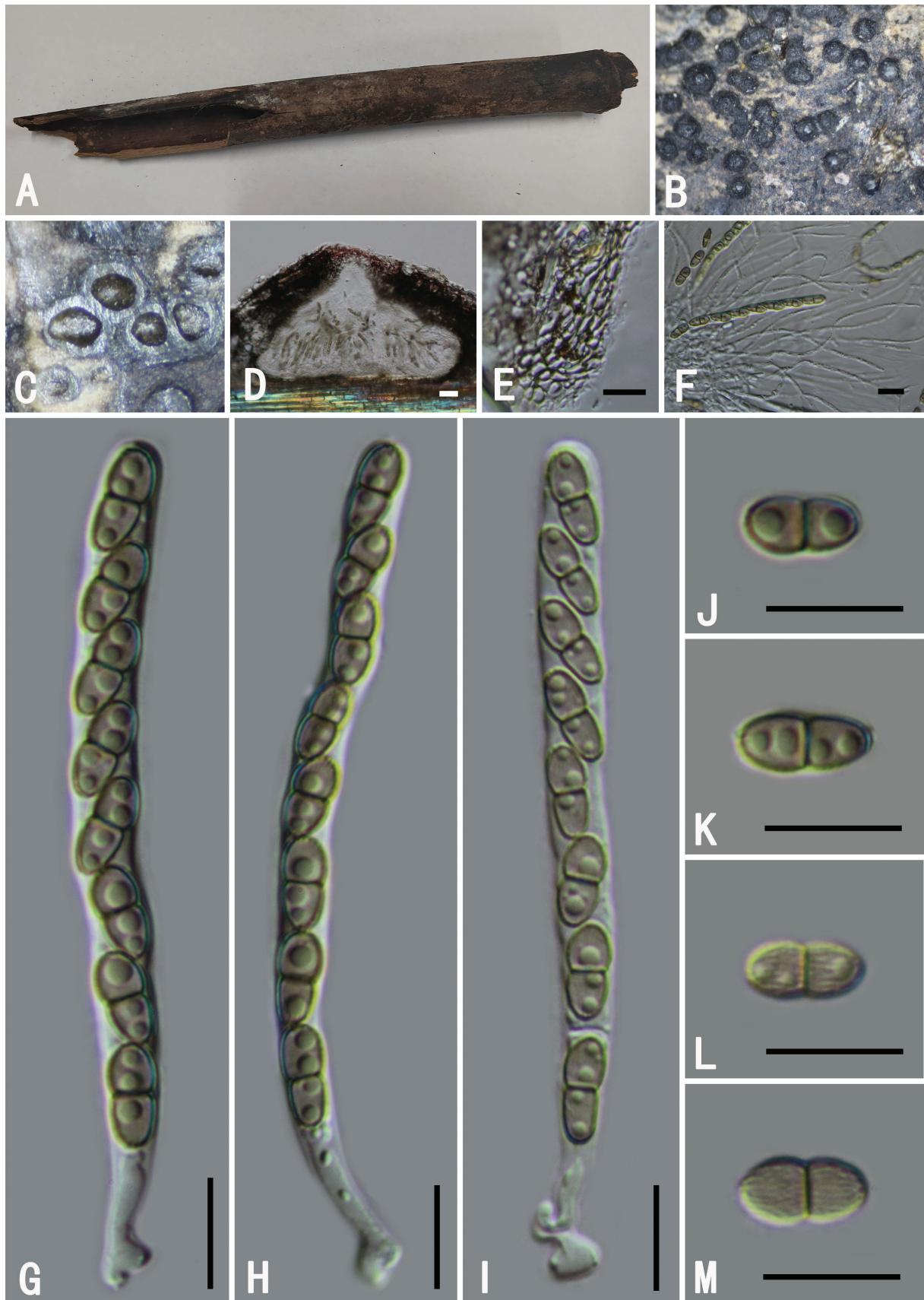


Figure 7. *Rousoella doimaesalongensis* (GMB0497) **A** specimen **B** appearance of ascomata on substrate **C** cross-section of ascostromata **D** longitudinal section of an ascoma **E** peridium **F** pseudoparaphyses **G–I** asci **J–M** ascospores. Scale bars: 0.5 mm (**B–C**); 10 μ m (**D–M**).

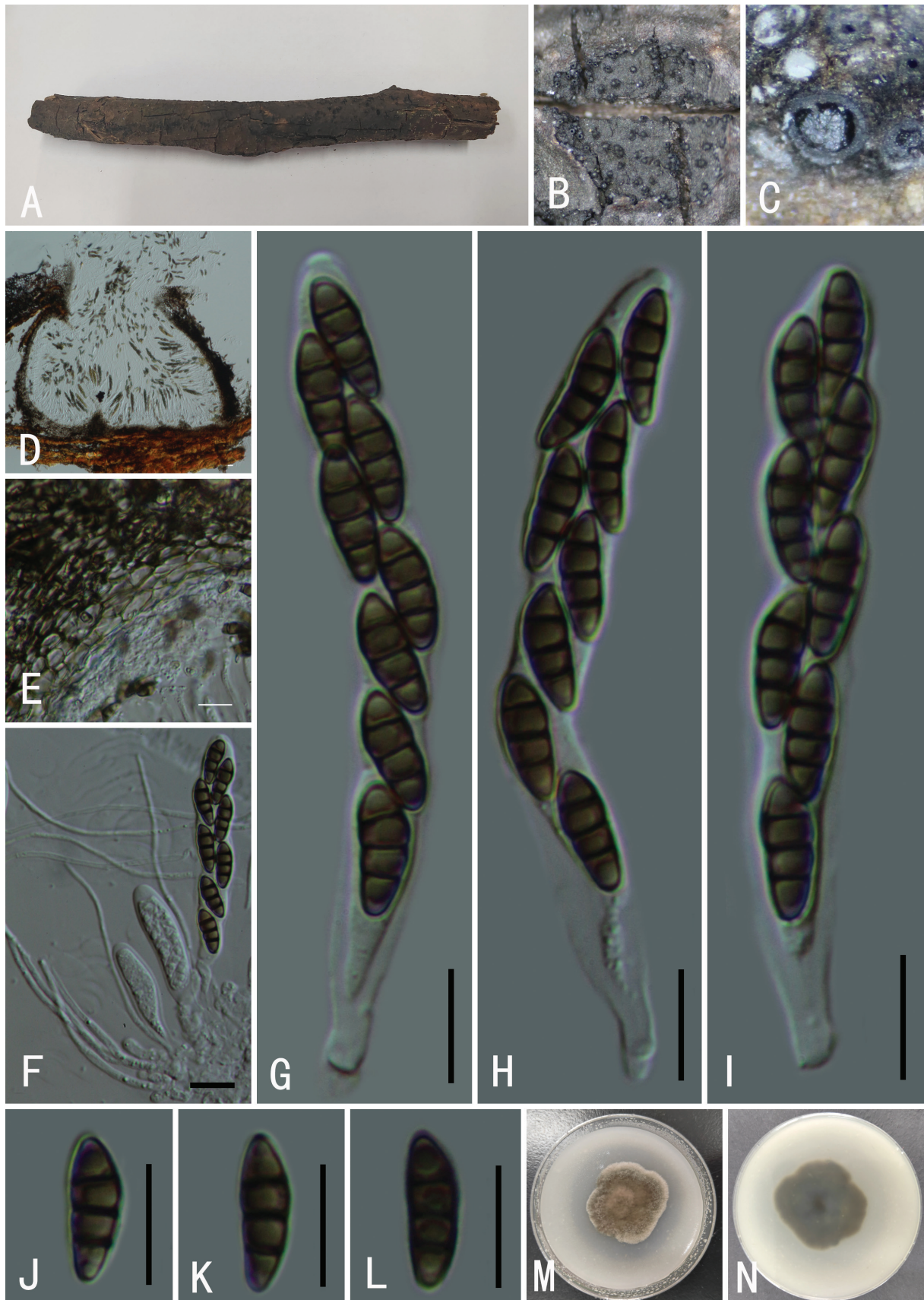


Figure 8. *Nigrograna schinifolium* (GMB0498) **A** specimen **B** appearance of ascomata on substrate **C** cross-section of ascomata **D** longitudinal section of an ascoma **E** peridium **F** pseudoparaphyses **G–I** asci **J–L** ascospores **M, N** culture on PDA. Scale bars: 0.5 mm (**B–C**); 10 μ m (**D–L**).

comprising several fused layers of "textura angularis", thin-walled and pale brown at the interior, becoming darker and thicker-walled to the outside. **Hamathecium** comprising 1–2 µm wide, cylindrical to filiform, septate, branched, pseudoparaphyses, embedded in a gelatinous matrix. **Asci** 44–59 × 8–10 µm (average = 51.5 × 9.3 µm, n = 25), 8-spored, bitunicate, fissitunicate, cylindrical to broadly filiform, with a short stipe and knob-like base, apically rounded with a minute ocular chamber. **Ascospores** 10–14 × 2.8–4 µm (average = 11.6 × 3.3 µm, n = 40), broadly fusiform to inequilaterally ellipsoid, with the second cell slightly enlarged, straight or slightly curved, with obtuse to rounded ends, hyaline when immature, becoming brown to dark brown at maturity, 3-euseptate, slightly constricted at the median septum. **Asexual morph**: undetermined.

Culture characters. After 4 weeks at 25 °C, colonies on PDA have a diameter of 2–2.5 cm and are circular, slightly raised to umbonate and dull with an entire edge. They appear floccose and smooth and droplets can be observed due to cellular respiration, water formation or antibiotic production. Colonies from the upper region have brown to cream-coloured margins and blackish-brown centres, while their reverse is white to yellowish-brown at the margin and blackish-brown in the centre.

Specimen examined. CHINA, Guizhou Province, Qiannan Prefecture, Sandu Shui Autonomous County, Yao Man Mountain National Forest Park (25°94'18.76"N, 107°95'70.09"E), 563 m elev., on branches of *Zanthoxylum schinifolium*, 28 September 2022, Y.P. Wu, 2022YRS36 (GMB0498, holotype, GMBC0498, ex-type; KUN-HKAS 12983, isotype).

Other examined material. CHINA, Guizhou Province, Huaxi District, Shilihetan Wetland Park (26°23'13.4"N, 106°66'56.4"E), 1501 m elev., on branches of *Zanthoxylum schinifolium*, 8 October 2022, Y.P. Wu and H.M. Hu, 2022SLHT44 (GMB0504; GMBC0504, living culture).

Notes. *Nigrograna schinifolium* and *N. thymi* Mapook et al. form a monophyletic clade with moderate support (MPBP 48%, BYPP 0.83, Fig. 3). However, *N. schinifolium* is distinguished by having 3-septate ascospores (Hyde et al. 2017). Morphologically, *N. schinifolium* can be distinguished from other species of *Nigrograna* by its shorter asci and ascospores (Hyde et al. 2017; Zhao et al. 2018; Zhang et al. 2020a). Our research confirms *N. schinifolium* is a new species.

***Nigrograna trachycarpus* H. M. Hu & Q. R. Li, sp. nov.**

MycoBank No: 849205

Fig. 9

Type material. Holotype: GMB0499.

Etymology. Named after the host genus *Trachycarpus* from which the fungus was isolated.

Description. Saprobic or parasitic on dead culms of *Trachycarpus* sp.

Sexual morph: Ascomata 160–380 µm wide, 100–210 µm high, pyriform to globose, scattered or clustered in small groups, black, immersed, the base remaining immersed in the substrate, smooth, with ostiole. **Ostiole** single, central, flattened, with a short neck, without paraphyses. **Peridium** 22–34 µm wide, multi-layered, composed of 4–6 rows of heavily pigmented, light brown

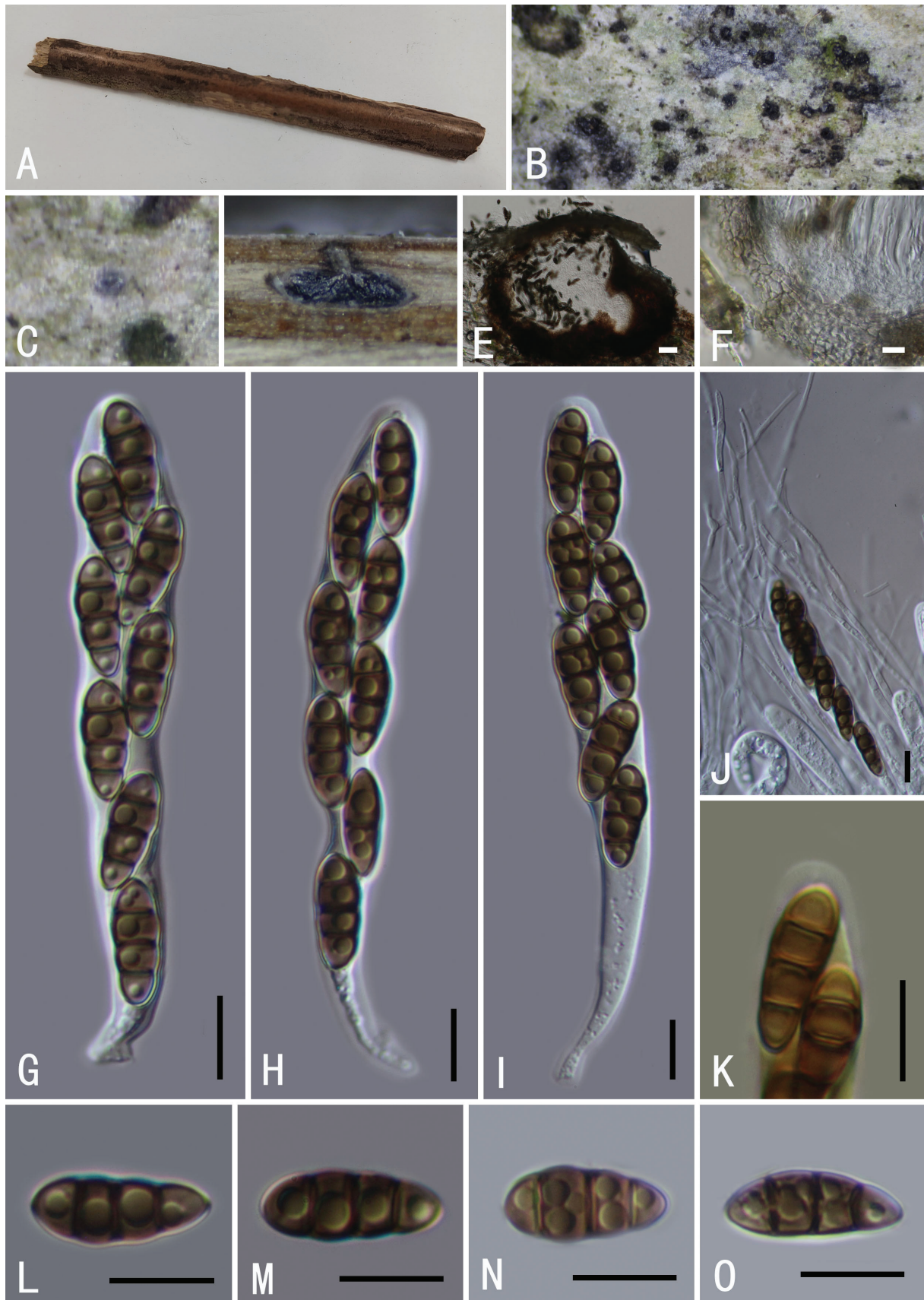


Figure 9. *Nigrograna trachycarpus* (GMB0499) **A** specimen **B, C** appearance of ascomata on substrate **D, E** longitudinal section of an ascoma **F** peridium **G–I** asci **J** pseudoparaphyses **K** J-ascus subapical ring in Melzer's **L–O** ascospores. Scale bars: 0.5 mm (**B–D**); 10 μ m (**E–O**).

to dark brown cells of textura angularis. **Hamathecium** comprising numerous 1.4–2.2 µm diameter, filamentous, unbranched, anastomosing, septate pseudoparaphyses. **Asci** 86–126 × 11–13 µm (average = 99 × 12 µm, n = 25), 8-spored, bitunicate, with fissitunicate dehiscence occurring rarely, elliptical, shortly pedicellate, apically rounded, with an ocular chamber, with a J-subapical ring. **Ascospores** 15–17 × 5–7 µm (average = 16.3 × 6.1 µm, n = 40), hyaline to yellow brown, 2–3-septate, deeply constricted at second septum, tapering to each end, the widest point at second cell from apex, smooth-walled, distinctly guttulate, without a sheath or appendages. **Asexual morph**: undetermined.

Culture characteristics. After 4 weeks at 25 °C on PDA, colonies typically reach 2–2.5 cm in diameter. They present a circular shape with a dense and elevated centre, while appearing sparse and radiating at the margin. The colonies exhibit colours ranging from dark grey to pale olivaceous when viewed from above and from dark olivaceous to black on reverse.

Specimen examined. CHINA, Guizhou Province, Guiyang Huaxi National Urban Wetland Park (26°2'2.34"N, 106°34'16.22"E), 1130 m elev., on decaying culms of *Trachycarpus* sp., 12 October 2022, Y.P. Wu and H.M. Hu, 2022 HXGY11 (GMB0499, holotype, GMBC0499, ex-type; KUN-HKAS 12984, isotype).

Other examined material. CHINA, Guizhou Province, Qiannan Prefecture, Sandu Shui Autonomous County, Yao Man Mountain National Forest Park (25°93'18.76"N, 107°95'15.66"E), 540 m elev., on decaying bamboo culms of *Trachycarpus* sp.; 28 September 2022; Y.P. Wu, 2022YRS50 (GMB050; GMBC0505, living culture).

Notes. In the phylogenetic analysis, *Nigrograna trachycarpus* and *N. locuta-pollinis* F. Liu & L. Cai formed a monophyletic branch within the *Nigrograna* genus, with a bootstrap support value of 31% (Fig. 3). However, this relationship remained consistent in repeated phylogenetic analyses. Sequences generated from the cultures of *N. trachycarpus* are similar to sharing an ITS similarity of 70.7% (with 57/488 gaps) and a *tef1* similarity of 89.8% (with 0/481 gaps). Morphologically, *N. trachycarpus* can be distinguished by its larger ascospores, measuring 16.3 × 6.1 µm, in contrast to *N. schinifolium*'s ascospores, 11.6 × 3.3 µm. Morphologically, it is close to *N. impatientis* J.F. Zhang, J.K. Liu & Z.Y. Liu, but the latter typically has ascocarps in groups of 2–6 with ostiole necks penetrating the host surface together. Moreover, the *N. trachycarpus* possesses longer asci (measuring 99 × 12 µm) and larger ascospores (measuring 16.3 × 6.1 µm) compared to *N. impatientis* (asci measuring 48 × 8, ascospores measuring 12 × 4.3 µm) (Zhang et al. 2020a).

Discussion

In this study, based on phylogenetic trees of combined ITS, LSU, SSU, *tef1* and *rpb2* sequences and morphology, we described and illustrated three new species of micro-fungi on dead woody litter, viz., *Neokalmusia karka* (Didymosphaeriaceae), *Nigrograna schinifolium* and *N. trachycarpus* (Nigrogranaceae) and records of three species of *Roussoella* (Roussoellaceae). Didymosphaeriaceae was introduced by Munk (1953) and is one of the most diverse families within the *Pleosporales*, with a total of 33 genera (Thambugala et al. 2015; Haridas et al. 2020). We included all of these *Didymosphaeriaceae* genera in our phylogenetic analysis. We used a dataset that combines ITS, LSU, SSU, *tef1*

and *rpb2* genes for this purpose. *Neokalmusia* formed a well-supported monophyletic clade within *Didymosphaeriaceae*, while the newly-discovered species, *N. karka*, exhibited a distinct separation from other known *Neokalmusia* species, supported by strong phylogenetic values.

Nigrograna, which is the only genus within *Nigrogranaeae*, is globally distributed and ecologically diverse. Amongst its species, *N. mackinnonii* is the most widely distributed species, mainly found in deciduous forests in Canada and northern USA. *Nigrograna bergmaniae* is mainly distributed in Europe, while *N. novae-zelandiae* was discovered in New Zealand. Approximately one-quarter of existing species live as saprotrophs on the bark or corticated twigs of various hardwoods (Phukhamsakda et al. 2018; Jayasiri et al. 2019). *Nigrograna schinifolium* was collected from rotten wood, while *N. trachycarpus* was obtained from decaying culms. Notably, several *Nigrograna* species have been established in recent studies without strong bootstrap value support. This finding suggests that these two species, *N. schinifolium* and *N. trachycarpus*, belong to the genus *Nigrograna* with strong evidence supporting this classification.

This study unveils valuable insights about saprophytic fungi, shedding light on their distribution and diversity within the Guizhou Region. It also identified three new species, which are important for the study of fungal taxonomy and further enriches our understanding of these microscopic organisms. Moreover, the study highlights the ongoing instability within the existing taxonomic system, emphasising the necessity for addressing these taxonomic challenges through processes such as re-collection, confirmation and sequencing of samples.

Additional information

Conflict of interest

The authors have declared that no competing interests exist.

Ethical statement

No ethical statement was reported.

Funding

This research was supported by National Natural Science Foundation of China (31960005, 32000009 and 32170019); Science and Technology Department Foundation of Guizhou Province ([2018]2322); Qianhe Talents, Science and Technology Department of Guizhou Province ([2015]4029); Guizhou Provincial Education Department Scientific Research Project for Higher Education Institutions ([2022]064); National Natural Science Foundation of China Karst Centre Project U1812403-4-4.

Author contributions

Conceptualization, Jichuan Kang, Qirui Li, Xiangchun Shen; investigation, Hongmin Hu, Youpeng Wu, Qingde Long; morpho-logical examinations, molecular sequencing, and phylogenetic analyses, Xu Zhang, Sihan Long and Youpeng Wu; specimen identification, Hongmin Hu and Qirui Li; writing—original draft preparation, Hongmin Hu, Minghui He; writing—review and editing, Nalin N. Wijayawardene, Zebin Meng; supervision, Qirui Li. All authors have read and agreed to the published version of the manuscript.

Author ORCIDs

Hongmin Hu  <https://orcid.org/0000-0003-3894-3269>

Sihan Long  <https://orcid.org/0000-0002-8346-3646>

Nalin N. Wijayawardene  <https://orcid.org/0000-0003-0522-5498>

Data availability

All of the data that support the findings of this study are available in the main text.

References

- Ahmed SA, Stevens DA, van de Sande WW, Meis JF, De Hoog GJ (2014a) *Rousoella percutanea*, a novel opportunistic pathogen causing subcutaneous mycoses. *Medical Mycology* 52(7): 689–698. <https://doi.org/10.1093/mmy/myu035>
- Ahmed SA, Van De Sande W, Stevens DA, Fahal A, Van Diepeningen A, Menken S, De Hoog GS (2014b) Revision of agents of black-grain eumycetoma in the order Pleosporales. *Persoonia* 33(1): 141–154. <https://doi.org/10.3767/003158514X684744>
- Ariyawansa HA, Camporesi E, Thambugala KM, Mapook A, Kang JC, Alias SA, Chukeatirote E, Thines M, McKenzie EH, Hyde KD (2014a) Confusion surrounding Didymosphaeria–phylogenetic and morphological evidence suggest Didymosphaeriaceae is not a distinct family. *Phytotaxa* 176. <https://doi.org/10.11646/phytotaxa.176.1.12>
- Ariyawansa HA, Tanaka K, Thambugala KM, Phookamsak R, Tian Q, Camporesi E, Hyde KD (2014b) A molecular phylogenetic reappraisal of the Didymosphaeriaceae (= Montagnulaceae). *Fungal Diversity* 68(1): 69–104. <https://doi.org/10.1007/s13225-014-0305-6>
- Ariyawansa HA, Hyde KD, Jayasiri SC, Buyck B, Chethana KT, Dai DQ, Dai YC, Daranagama DA, Jayawardena RS, Lücking R, Ghobad-Nejhad M, Niskanen T, Thambugala KM, Voigt K, Zhao RL, Li G-J, Doilom M, Boonmee S, Yang ZL, Cai Q, Cui Y-Y, Bahkali AH, Chen J, Cui BK, Chen JJ, Dayarathne MC, Dissanayake AJ, Ekanayaka AH, Hashimoto A, Hongsanan S, Jones EBG, Larsson E, Li WJ, Li Q-R, Liu JK, Luo ZL, Maharachchikumbura SSN, Mapook A, McKenzie EHC, Norphanphoun C, Konta S, Pang KL, Perera RH, Phookamsak R, Phukhamsakda C, Pinruan U, Randrianjohany E, Singtripop C, Tanaka K, Tian CM, Tibpromma S, Abdel-Wahab MA, Wanasinghe DN, Wijayawardene NN, Zhang J-F, Zhang H, Abdel-Aziz FA, Wedin M, Westberg M, Ammirati JF, Bulgakov TS, Lima DX, Callaghan TM, Callac P, Chang C-H, Coca LF, Dal-Forno M, Dollhofer V, Fliegerová K, Greiner K, Griffith GW, Ho H-M, Hofstetter V, Jeewon R, Kang JC, Wen T-C, Kirk PM, Kytövuori I, Lawrey JD, Xing J, Li H, Liu ZY, Liu XZ, Liimatainen K, Lumbsch HT, Matsumura M, Moncada B, Nuankaew S, Parmen S, de Azevedo Santiago ALCM, Sommai S, Song Y, de Souza CAF, de Souza-Motta CM, Su HY, Suetrong S, Wang Y, Wei S-F, Wen TC, Yuan HS, Zhou LW, Réblová M, Fournier J, Camporesi E, Luangsa-ard JJ, Tasanathai K, Khonsanit A, Thanakitpipattana D, Somrithipol S, Diederich P, Millanes AM, Common RS, Stadler M, Yan JY, Li XH, Lee HW, Nguyen TTT, Lee HB, Battistin E, Marsico O, Vizzini A, Vila J, Ercole E, Eberhardt U, Simonini G, Wen H-A, Chen X-H, Miettinen O, Spirin V, Hernawati (2015) Fungal diversity notes 111–252–Taxonomic and phylogenetic contributions to fungal taxa. *Fungal Diversity* 75(1): 27–274. <https://doi.org/10.1007/s13225-015-0346-5>
- Ariyawansa HA, Tsai I, Thambugala KM, Chuang WY, Lin SR, Hozzein WN, Cheewangkoon R (2020) Species diversity of Pleosporalean taxa associated with *Camellia sinensis* (L.) Kuntze in Taiwan. *Scientific Reports* 10(1): 1–20. <https://doi.org/10.1038/s41598-020-69718-0>

- Barr, Margaret E (1987) *Prodromus to Class Loculoascomycetes*. Amherst. University of Massachusetts, Massachusetts.
- Crous P, Cowan D, Maggs-Kölling G, Yilmaz N, Thangavel R, Wingfield M, Noordeloos ME, Dima B, Brandrud TE, Groenewald JZ (2021) Fungal planet description sheets: 1182–1283. *Persoonia. Molecular Phylogeny and Evolution of Fungi* 46: 313. <https://doi.org/10.3767/persoonia.2021.46.11>
- Crous PW, Wingfield M, Guarro J, Hernández-Restrepo M, Sutton D, Acharya K, Barber P, Boekhout T, Dimitrov R, Groenewald JZ (2015b) Fungal planet description sheets: 320–370. *Persoonia* 34(1): 167–266. <https://doi.org/10.3767/003158515X688433>
- Crous PW, Wingfield MJ, Guarro J, Cheewangkoon R, van der Bank M, Swart WJ, Stchigel AM, Cano-Lira JF, Roux J, Madrid H, Damm U, Wood AR, Shuttleworth LA, Hodges CS, Munster M, de Jesús Yáñez-Morales M, Zúñiga-Estrada L, Cruywagen EM, De Hoog GS, Silvera C, Najafzadeh J, Davison EM, Davison PJN, Barrett MD, Barrett RL, Manamgoda DS, Minnis AM, Kleczewski NM, Flory SL, Castlebury LA, Clay K, Hyde KD, Maússe-Sitoe SND, Chen S, Lechat C, Hairaud M, Lesage-Meessen L, Pawłowska J, Wilk M, Śliwińska-Wyrzychowska A, Mętrak M, Wrzosek M, Pavlic-Zupanc D, Maleme HM, Slippers B, Mac Cormack WP, Archuby DI, Grünwald NJ, Tellería MT, Dueñas M, Martín MP, Marincowitz S, de Beer ZW, Perez CA, Gené J, Marin-Felix Y, Groenewald JZ (2013) Fungal planet description sheets: 154–213. *Persoonia* 31(1): 188–296. <https://doi.org/10.3767/003158513X675925>
- Crous PW, Wingfield MJ, Roux J, Richardson DM, Strasberg D, Shivas RG, Alvarado P, Edwards J, Moreno G, Sharma R, Sonawane MS, Tan YP, Altés A, Barasubiyé T, Barnes CW, Blanchette RA, Boertmann D, Bogó A, Carlavilla JR, Cheewangkoon R, Daniel R, de Beer ZW, Yáñez-Morales M de Jesús, Duong TA, Fernández-Vicente J, Geering ADW, Guest DI, Held BW, Heykoop M, Hubka V, Ismail AM, Kajale SC, Khem-muk W, Kolařík M, Kurli R, Lebeuf R, Lévesque CA, Lombard L, Magista D, Manjón JL, Marincowitz S, Mohedano JM, Nováková A, Oberlies NH, Otto EC, Paguigan ND, Pascoe IG, Pérez-Butrón JL, Perrone G, Rahi P, Raja HA, Rintoul T, Sanhueza RMV, Scarlett K, Shouche YS, Shuttleworth LA, Taylor PWJ, Thorn RG, Vawdrey LL, Solano-Vidal R, Voitek A, Wong PTW, Wood AR, Zamora JC, Groenewald JZ (2015a) Fungal planet description sheets: 371–399. *Persoonia* 35: 264–327. <https://doi.org/10.3767/003158515X690269>
- Crous PW, Wingfield MJ, Schumacher R, Summerell BA, Giraldo A, Gené J, Guarro J, Wanasinghe D, Hyde KD, Groenewald JZ (2014) Fungal planet description sheets: 281–319. *Persoonia* 33(1): 212–289. <https://doi.org/10.3767/003158514X685680>
- Dai DQ, Phookamsak R, Wijayawardene NN, Li WJ, Bhat DJ, Xu JC, Taylor JE, Hyde KD, Chukeatirote EJ (2017) Bambusicolous fungi. *Fungal Diversity* 82(1): 1–105. <https://doi.org/10.1007/s13225-016-0367-8>
- De Gruyter J, Woudenberg JHC, Aveskamp MM, Verkley GJM, Groenewald JZ, Crous PW (2012) Rediposition of phoma-like anamorphs in Pleosporales. *Studies in Mycology* 75: 1–36. <https://doi.org/10.3114/sim0004>
- Dissanayake LS, Wijayawardene NN, Samarakoon MC, Hyde KD, Kang JC (2021) The taxonomy and phylogeny of *Austropleospora ochracea* sp. nov. (Didymosphaeriaceae) from Guizhou, China. *Phytotaxa* 491(3): 217–229. <https://doi.org/10.11646/phyto-taxa.491.3.2>
- Dong W, Wang B, Hyde KD, McKenzie EH, Raja HA, Tanaka K, Abdel-Wahab MA, Abdel-Aziz FA, Doilom M, Zhang H (2020) Freshwater Dothideomycetes. *Fungal Diversity* 105(1): 319–575. <https://doi.org/10.1007/s13225-020-00463-5>

- Feng Y, Zhang SN, Liu ZY (2019) *Tremateia murispora* sp. nov. (Didymosphaeriaceae, Pleosporales) from Guizhou, China. *Phytotaxa* 416: 79–87. <https://doi.org/10.11646/phytotaxa.416.1.10>
- Flakus A, Etayo J, Miadlikowska J, Lutzoni F, Kukwa M, Matura N, Rodriguez-Flakus P (2019) Biodiversity assessment of ascomycetes inhabiting Lobariella lichens in Andean cloud forests led to one new family, three new genera and 13 new species of lichenicolous fungi. *Plant and Fungal Systematics*. 64(2): 283–344. <https://doi.org/10.2478/pfs-2019-0022>
- Gonçalves MFM, Vicente TFL, Esteves AC, Alves A (2019) *Neptunomyces aureus* gen. et sp. nov. (Didymosphaeriaceae, Pleosporales) isolated from algae in Ria de Aveiro, Portugal. *MycKeys* 60: 31–44. <https://doi.org/10.3897/mycokeys.60.37931>
- Hall TA (1999) BioEdit: a user-friendly biological sequence alignment editor and analysis program for Windows 95/98/NT. In *Proceedings of the Nucleic acids symposium series*. Nucleic acids symposium series, 95–98. <https://doi.org/10.1021/bk-1999-0734.ch008>
- Haridas S, Albert R, Binder M, Bloem J, LaButti K, Salamov A, Andreopoulos B, Baker S, Barry K, Grigoriev IV (2020) 101 Dothideomycetes genomes: A test case for predicting lifestyles and emergence of pathogens. *Studies in Mycology* 96: 141–153. <https://doi.org/10.1016/j.simyco.2020.01.003>
- Hongsanan S, Hyde KD, Phookamsak R, Wanasinghe DN, McKenzie EHC, Sarma VV, Boonmee S, Lücking R, Bhat DJ, Liu NG, Tennakoon DS, Pem D, Karunarathna A, Jiang SH, Jones EBG, Phillips AJL, Manawasinghe IS, Tibpromma S, Jayasiri SC, Sandamali DS, Jayawardena RS, Wijayawardene NN, Ekanayaka AH, Jeewon R, Lu YZ, Dissanayake AJ, Zeng XY, Luo ZL, Tian Q, Phukhamsakda C, Thambugala KM, Dai DQ, Chethana KWT, Samarakoon MC, Ertz D, Bao DF, Doilom M, Liu JK, PérezOrtega S, Suija A, Senwanna C, Wijesinghe SN, Konta S, Niranjana M, Zhang SN, Ariyawansa HA, Jiang HB, Zhang JF, Norphanphoun C, de Silva NI, Thiyagaraja V, Zhang H, Bezerra JDP, Miranda-González R, Aptroot A, Kashiwadani H, Harishchandra D, Sérusiaux E, Aluthmuhandiram JVS, Abeywickrama PD, Devadatha B, Wu HX, Moon KH, Gueidan C, Schumm F, Bundhun D, Mapook A, Monkai J, Chomnunti P, Suetrong S, Chaiwan N, Dayarathne MC, Yang J, Rathnayaka AR, Bhunjun CS, Xu JC, Zheng JS, Liu G, Feng Y, Xie N (2020) Refined families of Dothideomycetes: Dothideomycetidae and Pleosporomycetidae. *Mycosphere* 11(1): 1553–2107. <https://doi.org/10.5943/mycosphere/11/1/13>
- Hyde KD, Dong Y, Phookamsak R, Jeewon R, Bhat DJ, Jones EG, Liu NG, Abeywickrama PD, Mapook A, Sheng J (2020) Fungal diversity notes 1151–1276: Taxonomic and phylogenetic contributions on genera and species of fungal taxa. *Fungal Diversity* 100(1): 5–277. <https://doi.org/10.1007/s13225-020-00439-5>
- Hyde KD, Hongsanan S, Jeewon R, Bhat DJ, McKenzie EH, Jones EG, Phookamsak R, Ariyawansa HA, Boonmee S, Zhu L (2016) Fungal diversity notes 367–490: Taxonomic and phylogenetic contributions to fungal taxa. *Fungal Diversity* 80: 1–270. <https://doi.org/10.1007/s13225-016-0373-x>
- Hyde KD, Norphanphoun C, Abreu VP, Bazzicalupo A, Thilini Chethana K, Clericuzio M, Dayarathne MC, Dissanayake AJ, Ekanayaka AH, He MQ, Hongsanan S, Huang S-K, Jayasiri SC, Jayawardena RS, Karunarathna A, Konta S, Kušan I, Lee H, Li J, Lin C-G, Liu N-G, Lu Y-Z, Luo Z-L, Manawasinghe IS, Mapook A, Perera RH, Phookamsak R, Phukhamsakda C, Siedlecki I, Soares AM, Tennakoon DS, Tian Q, Tibpromma S, Wanasinghe DN, Xiao Y-P, Yang J, Zeng X-Y, Abdel-Aziz FA, Li W-J, Senanayake IC,

- Shang Q-J, Daranagama DA, de Silva NI, Thambugala KM, Abdel-Wahab MA, Bahkali AH, Berbee ML, Boonmee S, Bhat DJ, Bulgakov TS, Buyck B, Camporesi E, Castañeda-Ruiz RF, Chomnunti P, Doilom M, Dovana F, Gibertoni TB, Jadan M, Jeewon R, Jones EBG, Kang J-C, Karunarathna SC, Lim YW, Liu J-K, Liu Z-Y, Plautz Jr HL, Lumyong S, Maharachchikumbura SSN, Matočec N, McKenzie EHC, Mešić A, Miller D, Pawłowska J, Pereira OL, Promputtha I, Romero AI, Ryvarden L, Su H-Y, Suetrong S, Tkalčec Z, Vizzini A, Wen T-C, Wisitrassameewong K, Wrzosek M, Xu J-C, Zhao Q, Zhao R-L, Mortimer PE (2017) Fungal diversity notes 603–708: Taxonomic and phylogenetic notes on genera and species. *Fungal Diversity* 87(1): 1–235. <https://doi.org/10.1007/s13225-017-0391-3>
- Jaklitsch W, Voglmayr H (2016) Hidden diversity in Thyridaria and a new circumscription of the Thyridariaceae. *Studies in Mycology* 85(1): 35–64. <https://doi.org/10.1016/j.simyco.2016.09.002>
- Jayasiri S, Hyde K, Jones E, McKenzie E, Jeewon R, Phillips A, Bhat D, Wanasinghe D, Liu J, Karunarathna SC (2019) Diversity, morphology and molecular phylogeny of Dothideomycetes on decaying wild seed pods and fruits. *Mycosphere* 10(1): 1–186. <https://doi.org/10.5943/mycosphere/10/1/1>
- Jiang HB, Hyde KD, Jayawardena RS, Doilom M, Xu J, Phookamsak R (2019) Taxonomic and phylogenetic characterizations reveal two new species and two new records of *Roussoella* (Roussoellaceae, Pleosporales) from Yunnan, China. *Mycological Progress* 18(4): 577–591. <https://doi.org/10.1007/s11557-019-01471-9>
- Karunarathna A, Phookamsak R, Jayawardena RS, Cheewangkoon R, Hyde KD, Kuo CH (2019) The holomorph of *Neoroussoella alishanense* sp. nov. (Roussoellaceae, Pleosporales) on *Pennisetum purpureum* (Poaceae). *Phytotaxa* 406(4): 218–236. <https://doi.org/10.11646/phytotaxa.406.4.1>
- Katoh K, Standley DM (2013) MAFFT multiple sequence alignment software version 7: Improvements in performance and usability. *Molecular Biology and Evolution* 30(4): 772–780. <https://doi.org/10.1093/molbev/mst010>
- Kolařík M (2018) New taxonomic combinations in endophytic representatives of the genus *Nigrograna*. *Czech Mycology* 70(2): 123–126. <https://doi.org/10.33585/cmy.70202>
- Kolařík M, Spakowicz DJ, Gazis R, Shaw J, Kubátová A, Nováková A, Chudíčková M, Forcina GC, Kang KW, Narváez-Trujillo A (2017) *Biatriospora* (Ascomycota: Pleosporales) is an ecologically diverse genus including facultative marine fungi and endophytes with biotechnological potential. *Plant Systematics and Evolution* 303(1): 35–50. <https://doi.org/10.1007/s00606-016-1350-2>
- Kruys S, Eriksson OE, Wedin M (2006) Phylogenetic relationships of coprophilous Pleosporales (Dothideomycetes, Ascomycota), and the classification of some bitunicate taxa of unknown position. *Mycological Research* 110(5): 527–536. <https://doi.org/10.1016/j.mycres.2006.03.002>
- Liang H, Gagné JD, Faye A, Rodrigue D, Brisson J (2020) Ground tire rubber (GTR) surface modification using thiol-ene click reaction: Polystyrene grafting to modify a GTR/polystyrene (PS) blend. *Progress in Rubber, Plastics and Recycling Technology* 36(2): 81–101. <https://doi.org/10.1177/1477760619895016>
- Liu JK, Phookamsak R, Dai DQ, Tanaka K, Jones BG, Xu J-C, Chukeatirote E, Hyde KD (2014) Roussoellaceae, a new pleosporalean family to accommodate the genera *Neoroussoella* gen. nov., *Roussoella* and *Roussoellopsis*. *Phytotaxa* 181(1): 1–33. <https://doi.org/10.11646/phytotaxa.181.1.1>

- Long QD, Liu LL, Zhang X, Wen TC, Kang JC, Hyde KD, Shen XC, Li QR (2019) Contributions to species of Xylariales in China-1. *Durotheca* species. *Mycological Progress* 18(3): 495–510. <https://doi.org/10.1007/s11557-018-1458-6>
- Mapook A, Hyde KD, McKenzie EH, Jones EG, Bhat DJ, Jeewon R, Stadler M, Samarakoon MC, Malaithong M, Purahong W (2020) Taxonomic and phylogenetic contributions to fungi associated with the invasive weed *Chromolaena odorata* (Siam weed). *Fungal Diversity* 101(1): 1–175. <https://doi.org/10.1007/s13225-020-00444-8>
- Munk A (1953) The system of the pyrenomycetes. A contribution to a natural classification of the group Sphaeriales *sensu* Lindau. *Dansk Bot Ark* 15: 1–163.
- Phukhamsakda C, Bhat DJ, Hongsanan S, Xu JC, Stadler M, Hyde KD (2018) Two novel species of *Neoaquastroma* (Parabambusicolaceae, Pleosporales) with their phoma-like asexual morphs. *MycKeys* 34: 47–62. <https://doi.org/10.3897/mycokeys.34.25124>
- Poli A, Bovio E, Ranieri L, Varese GC, Prigione V (2020) News from the sea: A new genus and seven new species in the Pleosporalean families Roussoellaceae and Thyridariaceae. *Diversity* 12(4): 144. <https://doi.org/10.3390/d12040144>
- Posada D, Crandall KA (1998) MODELTEST: Testing the model of DNA substitution. *Bioinformatics* 14(9): 817–818. <https://doi.org/10.1093/bioinformatics/14.9.817>
- Ramesh C, (2003) Loculoascomycetes from India. *Frontiers of Fungal Diversity in India: Prof. Kamal Festschrift*, 457–479.
- Rogers JD, Ju YM (1996) *Entoleuca mammata* comb. nov. for *Hypoxylon mammatum* and the genus *Entoleuca*. *Mycotaxon* 59: 441–448. <https://doi.org/10.1007/s11557-017-1311-3>
- Ronquist F, Teslenko M, Van Der Mark P, Ayres DL, Darling A, Höhna S, Larget B, Liu L, Suchard MA, Huelsenbeck JP (2012) MrBayes 3.2: Efficient Bayesian phylogenetic inference and model choice across a large model space. *Systematic Biology* 61(3): 539–542. <https://doi.org/10.1093/sysbio/sys029>
- Saccardo PA (1888) *Sylloge Hymenomyceteae*, Vol. VI. Polyporeae, Hydneae, Thelephoreae, Clavarieae, Tremellineae. *Sylloge Fungorum* 6: 1–928.
- Schoch CL, Crous PW, Groenewald JZ, Boehm EW, Burgess TI, de Gruyter J, de Hoog GS, Dixon LJ, Grube M, Gueidan C, Harada Y, Hatakeyama S, Hirayama K, Hosoya T, Huhndorf SM, Hyde KD, Jones EB, Kohlmeyer J, Kruys A, Li YM, Lücking R, Lumbsch HT, Marvanová L, Mbatchou JS, McVay AH, Miller AN, Mugambi GK, Muggia L, Nelsen MP, Nelson P, Owensby CA, Phillips AJ, Phongpaichit S, Pointing SB, Pujade-Renaud V, Raja HA, Plata ER, Robbertse B, Ruibal C, Sakayaroj J, Sano T, Selbmann L, Shearer CA, Shirouzu T, Slippers B, Suetrong S, Tanaka K, Volkmann-Kohlmeyer B, Wingfield MJ, Wood AR, Woudenberg JH, Yonezawa H, Zhang Y, Spatafora JW (2009) A class-wide phylogenetic assessment of Dothideomycetes. *Stud Mycol* 64: 1-15S10. <https://doi.org/10.3114/sim.2009.64.01>.
- Senwanna C, Hyde KD, Phookamsak R, Jones EG, Cheewangkoon R (2018) *Coryneum heveanum* sp. nov. (Coryneaceae, Diaporthales) on twigs of Para rubber in Thailand. *MycKeys* 75: 75–90. <https://doi.org/10.3897/mycokeys.43.29365>
- Seong KL, Kallol D, Soo MH, Sang JS, Seung YL, Hee YJ (2023) Morphological and Phylogenetic Analyses Reveal a New Species of Genus *Monochaetia* Belonging to the Family Sporocadaceae in Korea. *Mycobiology* 51(2): 87–93. <https://doi.org/10.1080/12298093.2022.2038843>
- Tanaka K, Hirayama K, Yonezawa H, Hatakeyama S, Harada Y, Sano T, Shirouzu T, Hosoya TJ (2009) Molecular taxonomy of bambusicolous fungi: Tetraplosphaeriaceae, a new pleosporalean family with Tetraploa-like anamorphs. *Studies in Mycology* 64: 175–209. <https://doi.org/10.3114/sim.2009.64.10>

- Tanaka K, Hirayama K, Yonezawa H, Sato G, Toriyabe A, Kudo H, Hashimoto A, Matsumura M, Harada Y, Hosoya T (2015) Revision of the Massarineae (Pleosporales, Dothideomycetes). *Studies in Mycology* 82(1): 75–136. <https://doi.org/10.1016/j.simyco.2015.10.002>
- Thambugala K, Wanasinghe D, Phillips A, Camporesi E, Bulgakov T, Phukhamsakda C, Ariyawansa H, Goonasekara I, Phookamsak R, Hyde KD (2017) Mycosphere notes 1–50: Grass (Poaceae) inhabiting Dothideomycetes. *Mycosphere* 8(4): 697–796. <https://doi.org/10.5943/mycosphere/8/4/13>
- Thambugala KM, Hyde KD, Tanaka K, Tian Q, Wanasinghe DN, Ariyawansa HA, Jayasiri SC, Boonmee S, Camporesi E, Liu ZY (2015) Towards a natural classification and backbone tree for Lophiostomataceae, Floricolaceae, and Amorosiaceae fam. nov. *Fungal Diversity* 74(1): 199–266. <https://doi.org/10.1007/s13225-015-0348-3>
- Tibpromma S, Hyde KD, Jeewon R, Maharachchikumbura SS, Liu JK, Bhat DJ, Jones EG, McKenzie EH, Camporesi E, Bulgakov TS, Doilom M, de Azevedo Santiago ALCM, Das K, Manimohan P, Gibertoni TB, Lim YW, Ekanayaka AH, Thongbai B, Lee HB, Yang J-B, Kirk PM, Sysouphanthong P, Singh SK, Boonmee S, Dong W, Raj KNA, Latha KPD, Phookamsak R, Phukhamsakda C, Konta S, Jayasiri SC, Norphanphoun C, Tennakoon DS, Li J, Dayarathne MC, Perera RH, Xiao Y, Wanasinghe DN, Senanayake IC, Goonasekara ID, de Silva NI, Mapook A, Jayawardena RS, Dissanayake AJ, Manawasinghe IS, Chethana KWT, Luo Z-L, Hapuarachchi KK, Baghela A, Soares AM, Vizzini A, Meiras-Ottoni A, Mešić A, Dutta AK, de Souza CAF, Richter C, Lin C-G, Chakrabarty D, Daranagama DA, Lima DX, Chakraborty D, Ercole E, Wu F, Simonini G, Vasquez G, da Silva GA, Plautz Jr HL, Ariyawansa HA, Lee H, Kušan I, Song J, Sun J, Karmakar J, Hu K, Semwal KC, Thambugala KM, Voigt K, Acharya K, Rajeshkumar KC, Ryvarden L, Jadan M, Hosen MI, Mikšić M, Samarakoon MC, Wijayawardene NN, Kim NK, Matočec N, Singh PN, Tian Q, Bhatt RP, de Oliveira RJV, Tulloss RE, Aamir S, Kaewchai S, Marathe SD, Khan S, Hongsanan S, Adhikari S, Mehmood T, Bandyopadhyay TK, Svetasheva TY, Nguyen TTT, Antonín V, Li W-J, Wang Y, Indoliya Y, Tkalčec Z, Elgorban AM, Bahkali AH, Tang AMC, Su H-Y, Zhang H, Promputtha I, Luangsa-ard J, Xu J, Yan J, Ji-Chuan K, Stadler M, Mortimer PE, Chomnunti P, Zhao Q, Phillips AJL, Nontachaiyapoom S, Wen T-C, Karunarathna SC (2017) Fungal diversity notes 491–602: Taxonomic and phylogenetic contributions to fungal taxa. *Fungal Diversity* 83(1): 1–261. <https://doi.org/10.1007/s13225-017-0378-0>
- Tibpromma S, Hyde KD, McKenzie EH, Bhat DJ, Phillips AJ, Wanasinghe DN, Samarakoon MC, Jayawardena RS, Dissanayake AJ, Karunarathna SC (2018) Fungal diversity notes 840–928: Micro-fungi associated with Pandanaceae. *Fungal Diversity* 93(1): 1–160. <https://doi.org/10.1007/s13225-018-0408-6>
- Valenzuela-Lopez N, Sutton DA, Cano-Lira JF, Paredes K, Wiederhold N, Guarro J, Stchigel AM (2017) Coelomycetous fungi in the clinical setting: Morphological convergence and cryptic diversity. *Journal of Clinical Microbiology* 55(2): 552–567. <https://doi.org/10.1128/JCM.02221-16>
- Verkley G, Dukik K, Renfurm R, Göker M, Stielow JB (2014) Novel genera and species of coniothyrium-like fungi in Montagnulaceae (Ascomycota). *Persoonia* 32(1): 25–51. <https://doi.org/10.3767/003158514X679191>
- Vu D, Groenewald M, De Vries M, Gehrman T, Stielow B, Eberhardt U, Al-Hatmi A, Groenewald JZ, Cardinali G, Verkley GJ (2019) Large-scale generation and analysis of filamentous fungal DNA barcodes boosts coverage for kingdom fungi and reveals thresholds for fungal species and higher taxon delimitation. *Studies in Mycology* 92(1): 135–154. <https://doi.org/10.1016/j.simyco.2018.05.001>

- Wanasinghe DN, Jones EB, Camporesi E, Dissanayake AJ, Kamolhan S, Mortimer PE, Xu J, Abd-Elsalam KA, Hyde KD (2016) Taxonomy and phylogeny of *Laburnicola* gen. nov. and *Paramassariosphaeria* gen. nov. (Didymosphaeriaceae, Massariaceae, Pleosporales). *Fungal Biology* 120(11): 1354–1373. <https://doi.org/10.1016/j.funbio.2016.06.006>
- Wanasinghe DN, Phukhamsakda C, Hyde KD, Jeewon R, Lee HB, Gareth Jones E, Tibpromma S, Tennakoon DS, Dissanayake AJ, Karunarathna SC (2018) Fungal diversity notes 709–839: Taxonomic and phylogenetic contributions to fungal taxa with an emphasis on fungi on Rosaceae. *Fungal Diversity* 89(1): 1–236. <https://doi.org/10.1007/s13225-018-0395-7>
- Wijayawardene N, Hyde KD, Al-Ani L, Tedersoo L, Aps SF (2020) Outline of Fungi and fungi-like taxa. *Mycosphere* 11(1): 1160–1456. <https://doi.org/10.5943/mycosphere/11/1/8>
- Wijayawardene NN, Hyde KD, Bhat DJ, Camporesi E, Schumacher RK, Chethana KT, Wikee S, Bahkali AH, Wang Y (2014) Camarosporium-like species are polyphyletic in Pleosporales; introducing *Paracamarosporium* and *Pseudocamarosporium* gen. nov. in Montagnulaceae. *Cryptogamie. Mycologie* 35(2): 177–198. <https://doi.org/10.7872/crym.v35.iss2.2014.177>
- Wijayawardene NN, Hyde KD, Dai DQ, Sánchez-García M, Goto BT, Magurno F (2022) Outline of Fungi and fungus-like taxa–2021. *Mycosphere* 13(1): 53–453. <https://doi.org/10.5943/mycosphere/13/1/2>
- Wijesinghe SN, Wanasinghe DN, Maharachchikumbura SS, Wang Y, Al-Sadi AM, Hyde KD (2020) *Bimuria omanensis* sp. nov. (Didymosphaeriaceae, Pleosporales) from Oman. *Phytotaxa* 449(2): 97–108. <https://doi.org/10.11646/phytotaxa.449.2.1>
- Zhang JF, Liu JK, Thambugala KM, Yang J, Meng ZH, Liu ZY (2020a) Two new species and a new record of *Nigrograna* (Nigrogranaceae, Pleosporales) from China and Thailand. *Mycological Progress* 19(11): 1365–1375. <https://doi.org/10.1007/s11557-020-01633-0>
- Zhang JY, Phookamsak R, Boonmee S, Hyde KD, Dai DQ, Lu YZ (2020b) *Roussoella guttulata* (Roussoellaceae, Pleosporales), a novel bambusicolous ascomycete from Thailand. *Phytotaxa* 471: 221–233. <https://doi.org/10.11646/phytotaxa.471.3.4>
- Zhang Y, Crous PW, Hyde SK (2012) Pleosporales. *Fungal Diversity* 53(1): 1–221. <https://doi.org/10.1007/s13225-011-0117-x>
- Zhang Y, Fournier J, Phookamsak R, Bahkali AH, Hyde KD (2013) Halotthiaceae fam. nov. (Pleosporales) accommodates the new genus *Phaeoseptum* and several other aquatic genera. *Mycologia* 105(3): 603–609. <https://doi.org/10.3852/11-286>
- Zhao Y, Zhang Z, Cai L, Peng W, Liu FJ (2018) Four new filamentous fungal species from newly-collected and hive-stored bee pollen. *Mycosphere* 9(6): 1089–1116. <https://doi.org/10.5943/mycosphere/9/6/3>

Exploring diversity within the genus *Tulostoma* (Basidiomycota, Agaricales) in the Pannonian sandy steppe: four fascinating novel species from Hungary

Péter Finy^{1,2}, Mikael Jeppson³, Dániel G. Knapp^{1,4}, Viktor Papp⁵, László Albert², István Ölvedi², Károly Bóka¹, Dóra Varga¹, Gábor M. Kovács¹, Bálint Dima¹

1 Department of Plant Anatomy, Institute of Biology, Eötvös Loránd University, Pázmány Péter sétány 1/C, Budapest 1117, Hungary

2 Hungarian Mycological Society, Könyves Kálmán krt. 40. Budapest 1087, Hungary

3 University of Gothenburg, Biological and Environmental Sciences, P.O. Box 461, SE-40530 Göteborg, Sweden

4 Department of Forestry and Wood Technology, Linnaeus University, Växjö, Sweden

5 Department of Botany, Hungarian University of Agriculture and Life Sciences, Villányi út 29–43, H-1118 Budapest, Hungary

Corresponding author: Bálint Dima (cortinarius1@gmail.com)

Abstract

Steppe vegetation on sandy soil in Hungary has recently been revealed as one of the hot spots in Europe for the stalked puffballs (genus *Tulostoma*). In the framework of the taxonomic revision of gasteroid fungi in Hungary, four *Tulostoma* species are described here as new to science: *T. dunense*, *T. hungaricum*, *T. sacchariolens* and *T. shaihuludii*. The study is based on detailed macro- and micromorphological investigations (including light and scanning electron microscopy), as well as a three-locus phylogeny of nrDNA ITS, nrDNA LSU and *tef1-α* sequences. The ITS and LSU sequences generated from the type specimen of *T. cretaceum* are provided and this resolved partly the taxonomy of the difficult species complex of *T. aff. cretaceum*.

Key words: Gasteroid, hot spot, molecular systematics, Pannonian inland sand dune thicket, phylogeny, taxonomy, Tulostomataceae



Academic editor: María P. Martín

Received: 9 September 2023

Accepted: 27 October 2023

Published: 29 November 2023

Citation: Finy P, Jeppson M, Knapp DG, Papp V, Albert L, Ölvedi I, Bóka K, Varga D, Kovács GM, Dima B (2023) Exploring diversity within the genus *Tulostoma* (Basidiomycota, Agaricales) in the Pannonian sandy steppe: four fascinating novel species from Hungary. MycoKeys 100: 153–170. <https://doi.org/10.3897/mycokeys.100.112458>

Copyright: © Péter Finy et al.

This is an open access article distributed under terms of the Creative Commons Attribution License (Attribution 4.0 International – CC BY 4.0).

Introduction

The genus *Tulostoma* was erected by Persoon (1794, 1801) encompassing two species, *T. brumale* and *T. squamosum*. Several new species have since been added from all continents, except Antarctica. In a monograph of the genus based on type studies, Wright (1987) accepted 139 species worldwide. Later studies generally confirmed those species concepts, nevertheless reduced some of the species to synonymy (e.g. Moreno et al. (1992, 1997); Altés et al. (1999); Jeppson et al. (2017)). With the introduction of molecular methods in taxonomy, unexpected species diversity has been detected and new, formerly unknown species have been described. In Europe, Jeppson et al. (2017) suggested Mediterranean grassland regions of the Iberian Peninsula, as well as steppe habitats in East Central Europe, as hot-spot areas for species diversity in *Tulostoma*. Jeppson et al. (2017)

described two novel species with type localities in Central Hungary (*T. grandisporum*, *T. pannonicum*), but their phylogenetic and morphological results indicated the presence of at least 19 previously-undescribed European species of *Tulostoma*, nine of which had been collected in Hungary. The species diversity in Eastern Europe was further emphasised by Rusevska et al. (2019) who reported four species from North Macedonia distinct from all known and described species.

In Europe, Hungary has an exceptionally large diversity of gasteroid taxa mainly due to the suitable habitats of the Pannonian sandy steppe areas of the country (Fig. 1). The *Festucetum vaginatae* plant communities are characteristic on open, continental sandy soils, dominated by the grass species *Festuca vaginata* which also occur on open steppe mosaics between the poplar–juniper sand dune thickets (Bölöni et al. 2011; Rimóczi et al. 2011). Gasteroid fungi occur especially in those areas where *Stipa borysthenica*, *Fumana procumbens* or *Juniperus communis* are present (Fig. 1).

In this paper, we propose four species of *Tulostoma* new to science, two of which were retrieved previously by Jeppson et al. (2017) as *Tulostoma* sp. 1 and *T. aff. cretaceum*. Additionally, we present two further species identified through subsequent collections and field investigations. One of the new species was previously reported from Hungary under the name *T. volvulatum* (Hollós 1904; Siller and Vasas 1995; Siller et al. 2005) and *T. obesum* (Siller et al. 2006; Rimóczi et al. 2011) which is listed as a protected species by Hungarian law.



Figure 1. Habitats of *Tulostoma* species in Hungary: **a** *T. hungaricum* in Orgovány **b** *T. sacchariolens* in Orgovány **c** *T. dunense* in Izsák (Soltszentimre) **d** *T. shaihuludii* in Izsák (Soltszentimre). Photos: P. Finy.

Materials and methods

Samples of *Tulostoma* were collected in Hungary over a period of more than 25 years. Collecting has mostly been performed in the sandy habitats of the Great Hungarian Plain on both sides of the Danube (Kiskunság, Mezőföld). Studied collections were deposited in the herbaria BP (only holotypes), GB and in the Department of Plant Anatomy, Eötvös Loránd University (abbreviated further as ELTE).

Macromorphological study

Mature basidiomata of *Tulostoma* were collected and studied under a stereomicroscope, regarding their macromorphological characteristics (size, colour, shape of the spore-sac (capitulum), type of mouth (ostiole), type of exoperidium as well as features of the stem), in accordance with Wright (1987). In situ or ex situ photo-documentation of each sample was carried out.

Microscopy

Microscopic features were studied under an Olympus BH-2 light microscope. Samples were mounted in lactophenol-cotton blue and heated to boiling temperature. Measurements were performed under 1000× magnification and calculated digitally using Piximètre software (www.piximetre.fr). Spore dimensions are given without the ornamentation of the spore walls. Small pieces of peridium and gleba from dried basidiomata were prepared, fixed to stubs, coated with gold and examined under a Hitachi S2460N (Hitachi Ltd., Tokyo, Japan) scanning electron microscope (SEM) at 22 kV accelerating voltage.

Molecular study

Total DNA extraction was carried out with the E.Z.N.A. SP Fungal DNA Mini Kit (Omega Bio-Tek, Norcross, GA, USA) and NucleoSpin Plant II Mini Kit (Macherey-Nagel, Düren, Germany) following the instructions of the manufacturers. The ITS (internal transcribed spacer) region of the nrDNA which is the universal fungal DNA barcode region (Schoch et al. 2012) was amplified using the primer pairs ITS1F/ITS4 (White et al. 1990; Gardes and Bruns 1993) as described in Papp and Dima (2018). The primers LR0R (Rehner and Samuels 1994) and LR5 (Vilgalys and Hester 1990) were used to amplify the partial 28S nrRNA gene (LSU) of the nrDNA operon region. The primers EF1-983F and EF1-2218R (Rehner and Buckley 2005) were used to amplify part of the translation elongation factor 1 α (*tef1- α*). Sequencing of the amplicons with the primers used for amplification was carried out by LGC Genomics (Berlin, Germany). The sequences were compiled from electrophoregrams using the Staden software package (Staden et al. 2000) and CodonCode Aligner package (CodonCode Corp., Centerville, Massachusetts, USA). Sequences of each locus (ITS, LSU and *tef1- α*), together with sequences of respective species downloaded from GenBank mainly based on Jeppson et al. (2017), were aligned separately with the online MAFFT version 7 using the E-INS-i strategy (Katoh and Standley 2013) (Table 1). The alignments were checked and edited in MEGA7 (Kumar et al. 2016) and concatenated to one dataset in SeaView 5 (Gouy et al. 2021). Bayesian Inference (BI) analyses were performed with MrBayes 3.1.2 (Ron-

quist and Huelsenbeck 2003) using a GTR + G substitution model. Four Markov chains were run for 10,000,000 generations, sampling every 1,000 generations with a burn-in value set at 4,000 sampled trees. Maximum Likelihood (ML) phylogenetic analysis was carried out with the raxmlGUI 1.3 implementation (Silvestro and Michalak 2012; Stamatakis 2014). The GTR + G nucleotide substitution model and ML estimation of base frequencies were applied for the partitions. ML bootstrap (BS) analysis with 1,000 replicates was used to test the support of the branches. *Tulostoma pulchellum* (MJ7833) and *T. striatum* (Fritz 2010-2) served as outgroups. Intra- and interspecific genetic differences were calculated by dividing the number of differences (substitutions and/or indels) found in the whole ITS region by the length of the region. Phylogenetic trees were visualised and edited in MEGA 7 (Kumar et al. 2016) and deposited together with the alignments at Figshare repository (10.6084/m9.figshare.24112749). Newly-generated sequences were submitted to GenBank. Studied voucher collections are presented in Table 1.

Table 1. Sequences used in this study. Newly-generated sequences are marked in boldface.

Name	Strain/Voucher	Country	ITS	LSU	TEF	References
<i>Tulostoma ahmadii</i>	HUP SH-33b, holotype	Pakistan	KP738712	–	–	Hussain et al. (2016)
<i>Tulostoma albicans</i>	B2092, P.S. Catcheside 1266	Australia	–	MK278628	–	Varga et al. (2019)
<i>Tulostoma albicans</i>	Cope, NY, Holotype	United States	KX576548	–	–	Jeppson et al. (2017)
<i>Tulostoma beccarianum</i>	Finy2	Hungary	KU519076	KU519076	KU843959	Jeppson et al. (2017)
<i>Tulostoma beccarianum</i>	Herb. Bresadola (S), holotype	Italy	KX640979	–	–	Jeppson et al. (2017)
<i>Tulostoma berkeleyi</i>	JLH MyCoPortal 6604754	United States	MK578704	MK578704	–	Unpublished
<i>Tulostoma brumale</i>	Finy9	Hungary	KU519059	KU519059	KU843944	Jeppson et al. (2017)
<i>Tulostoma calcareum</i>	Finy4	Hungary	KU519088	KU519088	KU843895	Jeppson et al. (2017)
<i>Tulostoma calcareum</i>	MJ6965, holotype	Sweden	KU519086	KU519086	KU843881	Jeppson et al. (2017)
<i>Tulostoma calongei</i>	MJ8773, holotype	Spain	KU518973	KU518973	KU844000	Jeppson et al. (2017)
<i>Tulostoma caespitosum</i> cf.	SNMH9	Slovakia	MK907419	MK907419	–	Unpublished
<i>Tulostoma caespitosum</i> cf.	MJ881114	Spain	KU519031	KU519031	KU843978	Jeppson et al. (2017)
<i>Tulostoma caespitosum</i> cf.	AH15040	Spain	KU519032	KU519032	KU843979	Jeppson et al. (2017)
<i>Tulostoma cretaceum</i>	NY737977, holotype	United States	OR722641	OR722660	–	This study
<i>Tulostoma cretaceum</i> cf. 1	Knudsen0107	Russia	KU518993	KU518993	KU843988	Jeppson et al. (2017)
<i>Tulostoma cretaceum</i> cf. 2	AH13672	Spain	KU518998	KU518998	KU843991	Jeppson et al. (2017)
<i>Tulostoma cretaceum</i> cf. 2	AH3995	Spain	KU518999	KU518999	KU843992	Jeppson et al. (2017)
<i>Tulostoma cretaceum</i> cf. 2	MJ6194	Spain	KU518997	KU518997	KU843989	Jeppson et al. (2017)
<i>Tulostoma cretaceum</i> cf. 2	MJ9304	Spain	KU519000	KU519000	KU843990	Jeppson et al. (2017)
<i>Tulostoma cretaceum</i> cf. 3	FP-2023-05-11-1	Kazakhstan	OR722639	OR722658	–	This study
<i>Tulostoma cretaceum</i> cf. 3	FP-2023-05-11-4	Kazakhstan	OR722640	OR722659	–	This study
<i>Tulostoma cretaceum</i> cf. 3	SNMH10	Kazakhstan	MK907420	MK907420	–	Unpublished
<i>Tulostoma cretaceum</i> cf.	MJ3821	Hungary	KU518994	KU518994	KU843993	Jeppson et al. (2017)
<i>Tulostoma cyclophorum</i>	MJ8862	Hungary	KU518985	KU518985	KU843963	Jeppson et al. (2017)
<i>Tulostoma domingueziae</i>	MLHC24 (CORD), holotype	Argentina	HQ667594	HQ667597	–	Caffot et al. (2011)
<i>Tulostoma dunense</i>	BP112640, holotype	Hungary	OR722622	OR722648	OR707014	This study
<i>Tulostoma dunense</i>	DB-2021-11-21-2	Hungary	OR722626	–	–	This study
<i>Tulostoma dunense</i>	FP-2019-12-07	Hungary	OR722617	OR722643	OR707009	This study
<i>Tulostoma dunense</i>	FP-2020-12-06	Hungary	OR722618	OR722644	OR707010	This study
<i>Tulostoma dunense</i>	FP-2022-01-02-1	Hungary	OR722619	OR722645	OR707011	This study
<i>Tulostoma dunense</i>	FP-2021-01-02	Hungary	OR722620	OR722646	OR707012	This study
<i>Tulostoma dunense</i>	FP-2016-06-05	Hungary	OR722621	OR722647	OR707013	This study
<i>Tulostoma dunense</i>	FP-2021-02-18	Hungary	OR722623	OR722649	OR707015	This study
<i>Tulostoma dunense</i>	FP-2015-12-06	Hungary	OR722624	OR722650	OR707016	This study
<i>Tulostoma dunense</i>	FP-2016-12-11	Hungary	OR722625	OR722651	OR707017	This study
<i>Tulostoma dunense</i>	MJ6103 (as cf. <i>cretaceum</i>)	Hungary	KU518995	KU518995	KU843994	Jeppson et al. (2017)
<i>Tulostoma dunense</i>	MJ7759 (as cf. <i>cretaceum</i>)	Hungary	KU518996	KU518996	KU843995	Jeppson et al. (2017)

Name	Strain/Voucher	Country	ITS	LSU	TEF	References
<i>Tulostoma eckbladii</i>	Sivertsen930717, TRH9565, holotype	Norway	KU519069	KU519069	KU843952	Jeppson et al. (2017)
<i>Tulostoma excentricum</i>	BPI 729284, holotype	United States	KU519055	KU519055	–	Jeppson et al. (2017)
<i>Tulostoma fimbriatum</i>	Finy8	Hungary	KU518968	KU518968	KU843912	Jeppson et al. (2017)
<i>Tulostoma fimbriatum</i>	Månsson 991010, epitype	Sweden	KU518963	KU518963	KU843904	Jeppson et al. (2017)
<i>Tulostoma fulvellum</i>	Kabát 970428	Slovakia	KU518991	KU518991	KU844001	Jeppson et al. (2017)
<i>Tulostoma giovanellae</i>	MJ8706	Spain	KU519071	KU519071	KU843954	Jeppson et al. (2017)
<i>Tulostoma grandisporum</i>	Finy10	Hungary	KU519005	KU519005	KU843922	Jeppson et al. (2017)
<i>Tulostoma grandisporum</i>	MJ8907, holotype	Hungary	KU519003	KU519003	KU843924	Jeppson et al. (2017)
<i>Tulostoma hungaricum</i>	BP112641, holotype	Hungary	OR722630	OR722653	–	This study
<i>Tulostoma hungaricum</i>	FP-2019-01-23	Hungary	OR722627	–	–	This study
<i>Tulostoma hungaricum</i>	FP-2021-02-19	Hungary	OR722628	–	–	This study
<i>Tulostoma hungaricum</i>	FP-2022-01-02-2	Hungary	OR722629	OR722652	OR707021	This study
<i>Tulostoma kotlabae</i>	Brůžek 140918	Czech Republic	KU519028	KU519028	KU843977	Jeppson et al. (2017)
<i>Tulostoma kotlabae</i>	Kotlaba (PRM 704203), holotype	Slovakia	KX576544	KX576544	–	Jeppson et al. (2017)
<i>Tulostoma</i> cf. <i>kotlabae</i>	MJ5996	Hungary	KU519016	KU519016	KU843966	Jeppson et al. (2017)
<i>Tulostoma</i> cf. <i>kotlabae</i>	Finy1	Hungary	KU519017	KU519017	KU843967	Jeppson et al. (2017)
<i>Tulostoma</i> cf. <i>kotlabae</i>	MJ7795	Hungary	KU519020	KU519020	KU843970	Jeppson et al. (2017)
<i>Tulostoma laceratum</i>	NY834492	United States	OR722642	OR722661	–	This study
<i>Tulostoma lloydii</i>	Lahti 201210	Italy	KU518990	KU518990	KU843965	Jeppson et al. (2017)
<i>Tulostoma lusitanicum</i>	LISU-MGA-8	Portugal	KX576542	KX576542	–	Jeppson et al. (2017)
<i>Tulostoma lysocephalum</i>	Long 9639, holotype	United States	KU519034	KU519034	–	Jeppson et al. (2017)
<i>Tulostoma melanocyclus</i>	MJ090418	Hungary	KU519106	KU519106	KU843890	Jeppson et al. (2017)
<i>Tulostoma</i> cf. <i>nanum</i>	MJ4976	Hungary	KU519036	KU519036	KU843968	Jeppson et al. (2017)
<i>Tulostoma niveum</i>	MJ7692	Sweden	KU519078	KU519078	KU843932	Jeppson et al. (2017)
<i>Tulostoma obesum</i>	Cooke 2715, isotype	United States	KX576541	KX576541	–	Jeppson et al. (2017)
<i>Tulostoma obesum</i>	MJ8695	Spain	KU518986	KU518986	KU843985	Jeppson et al. (2017)
<i>Tulostoma pannonicum</i>	MJ7764, holotype	Hungary	KU519010	KU519010	–	Jeppson et al. (2017)
<i>Tulostoma pannonicum</i>	MJ7803	Hungary	KU519011	KU519011	KU843996	Jeppson et al. (2017)
<i>Tulostoma pseudopulchellum</i>	AH 11603, paratype	Spain	KU519012	KU519012	KU843997	Jeppson et al. (2017)
<i>Tulostoma pseudopulchellum</i>	AH 11605, holotype	Spain	KX513827	KX513827	–	Jeppson et al. (2017)
<i>Tulostoma pulchellum</i>	MJ7833	Hungary	KU518957	KU518957	KU843928	Jeppson et al. (2017)
<i>Tulostoma punctatum</i>	BPI 729033, lectotype	United States	KC333071	KC333071	–	Jeppson et al. (2017)
<i>Tulostoma punctatum</i>	MJ7472	Slovakia	KU518952	KU518952	KU843875	Jeppson et al. (2017)
<i>Tulostoma pygmaeum</i> cf.	Brůžek 131207	Slovakia	KU519041	KU519041	KU843931	Jeppson et al. (2017)
<i>Tulostoma rufum</i>	BPI 704578, holotype	United States	KU519107	KU519107	–	Jeppson et al. (2017)
<i>Tulostoma sacchariolens</i>	BP112642, holotype	Hungary	OR722632	OR722654	OR707020	This study
<i>Tulostoma sacchariolens</i>	FP-2019-12-06	Hungary	OR722631	–	–	This study
<i>Tulostoma sacchariolens</i>	FP-2021-01-24b	Hungary	OR722633	–	–	This study
<i>Tulostoma sacchariolens</i>	FP-2021-02-18	Hungary	OR722634	OR722655	–	This study
<i>Tulostoma shaihuludii</i>	BP112643, holotype	Hungary	OR722637	OR722657	OR707019	This study
<i>Tulostoma shaihuludii</i>	FP-2020-12-01	Hungary	OR722635	–	–	This study
<i>Tulostoma shaihuludii</i>	FP-2020-12-27	Hungary	OR722636	OR722656	OR707018	This study
<i>Tulostoma shaihuludii</i>	FP-2017-12-09	Hungary	OR722638	–	–	This study
<i>Tulostoma shaihuludii</i>	MJ7762	Hungary	KU518979	KU518979	KU843981	Jeppson et al. (2017)
<i>Tulostoma simulans</i>	MJ3844	Hungary	KU519052	KU519052	KU843941	Jeppson et al. (2017)
<i>Tulostoma</i> sp. 10	MJ3813	Hungary	KU519029	KU519029	–	Jeppson et al. (2017)
<i>Tulostoma</i> sp. 14	MJ5004	Spain	KU519039	KU519039	KU843999	Jeppson et al. (2017)
<i>Tulostoma</i> sp. 20	MJ5015	Spain	KU519067	KU519067	KU843950	Jeppson et al. (2017)
<i>Tulostoma</i> sp. 21	AH11698	Spain	KX640986	KX640986	–	Jeppson et al. (2017)
<i>Tulostoma squamosum</i>	Larsson 260-06	France	KU519097	KU519097	KU843892	Jeppson et al. (2017)
<i>Tulostoma striatum</i>	Fritz 2010-2	Mongolia	KU518958	KU518958	KU843929	Jeppson et al. (2017)
<i>Tulostoma submembranaceum</i>	AH15132, holotype	Mexico	KX513826	KX513826	–	Jeppson et al. (2017)
<i>Tulostoma submembranaceum</i> cf.	MJ9296	Spain	KU519014	KU519014	KU843984	Jeppson et al. (2017)
<i>Tulostoma subsquamosum</i>	MJ4945	Hungary	KU519091	KU519091	KU843899	Jeppson et al. (2017)
<i>Tulostoma verrucosum</i>	CCB142	United States	MG663293	MG663293	–	Unpublished
<i>Tulostoma winterhoffii</i>	MJ7761	Hungary	KU518976	KU518976	KU843916	Jeppson et al. (2017)
<i>Tulostoma xerophilum</i>	Long 9688, BPI 802484, holotype	United States	KX576549	–	–	Jeppson et al. (2017)

Results

Phylogenetic analysis

The three-locus molecular phylogenetic analyses of the newly-generated and representative *Tulostoma* sequences were based on 94 ITS, 76 LSU and 60 *tef1-a* (Table 1) and 3321 characters. In this study, 26 ITS, 26 LSU and 13 *tef1-a* sequences were newly gained, including the ITS and LSU sequences of the holotype of *Tulostoma cretaceum* (Table 1). Phylogenetic trees from ML and BI analyses showed congruent topologies and the sequences representing the four new species proposed here formed strongly-supported clades (MLBS/BIPP = 100%/1.00). The best scoring ML tree is shown in Fig. 2.

Taxonomy

***Tulostoma dunense* Finy, Jeppson, L. Albert, Ölvedi, Dima & V. Papp, sp. nov.**

MycoBank No: MB 849931

Fig. 3

Holotype. HUNGARY, Tolna, Németskér, open sandy grassland, 18 Oct 2020, P. Finy, I. Ölvedi, FP-2020-10-18 (BP112640, isotype GB). GenBank: ITS OR722622, LSU OR722648, *tef1* OR707014.

Etymology. The epithet refers to the continental, open, bare sandy habitat of this species, similar to coastal dunes.

Description. Spore-sac subglobose, depressed-globose, 10–20 mm. Exoperidium hyphal, encrusting sand only at the base of the spore-sac. Endoperidium tough, chalky white or dirty-dingy white, with age becoming greyish, young basidiomata with velvety surface. Mouth prominent, fibrillose-lacerate, irregular sometimes remains unopened for a long time and splits later due to mechanical pressure (wind or trampling). Socket distantly separated from the stem. Stem 35–80 × 1.5–5 mm, initially white, then ochraceous, with age greyish–blackish, longitudinally furrowed, at the base with a volva and a prominent, easily broken pseudorhiza. Gleba ferruginous to brick-red brown, usually scattered on the surface of the spore-sac. Capillitium brown, 2.5–10 µm in diameter with walls 0.7–2.5 µm in diameter, fragile, breaking up at septal levels in 40–350 µm long segments with rounded, not widened ends, rarely branching. Spores subglobose to oval, 4.6–5.2 × 4.0–4.8 µm (av. 4.4 × 4.9 µm), smooth under LM and SEM.

Habitat and distribution. The psammophilous species *Tulostoma dunense* known so far only from sandy areas of the Great Hungarian Plain of Hungary. It occurs on both sides of the Danube (Kiskunság, Dél-Mezőföld), where open dunes appear. It mainly grows solitary, deep in the sand in large, open sandy areas to bare spots.

Notes. *Tulostoma dunense* was previously recorded in Hungary by Hollós (1904), Siller and Vasas (1995), Babos (1999), Siller et al. (2005), Siller et al. (2006) and Rimóczi et al. (2011) under the names of *T. volvulatum*, *T. obesum* and *T. aff. cretaceum*. Hollós (1904) included both *T. giovanellae* and *T. dunense* under the name *T. volvulatum* (nom. rej., Altés et al. (1999)) and recorded it in urban places in the City of Kecskemét (now *T. giovanellae*) as well as in sand dunes (now the new species, *T. dunense*). The brownish colour of the capillitium characteristic of specimens from sand dunes and largely absent in those from

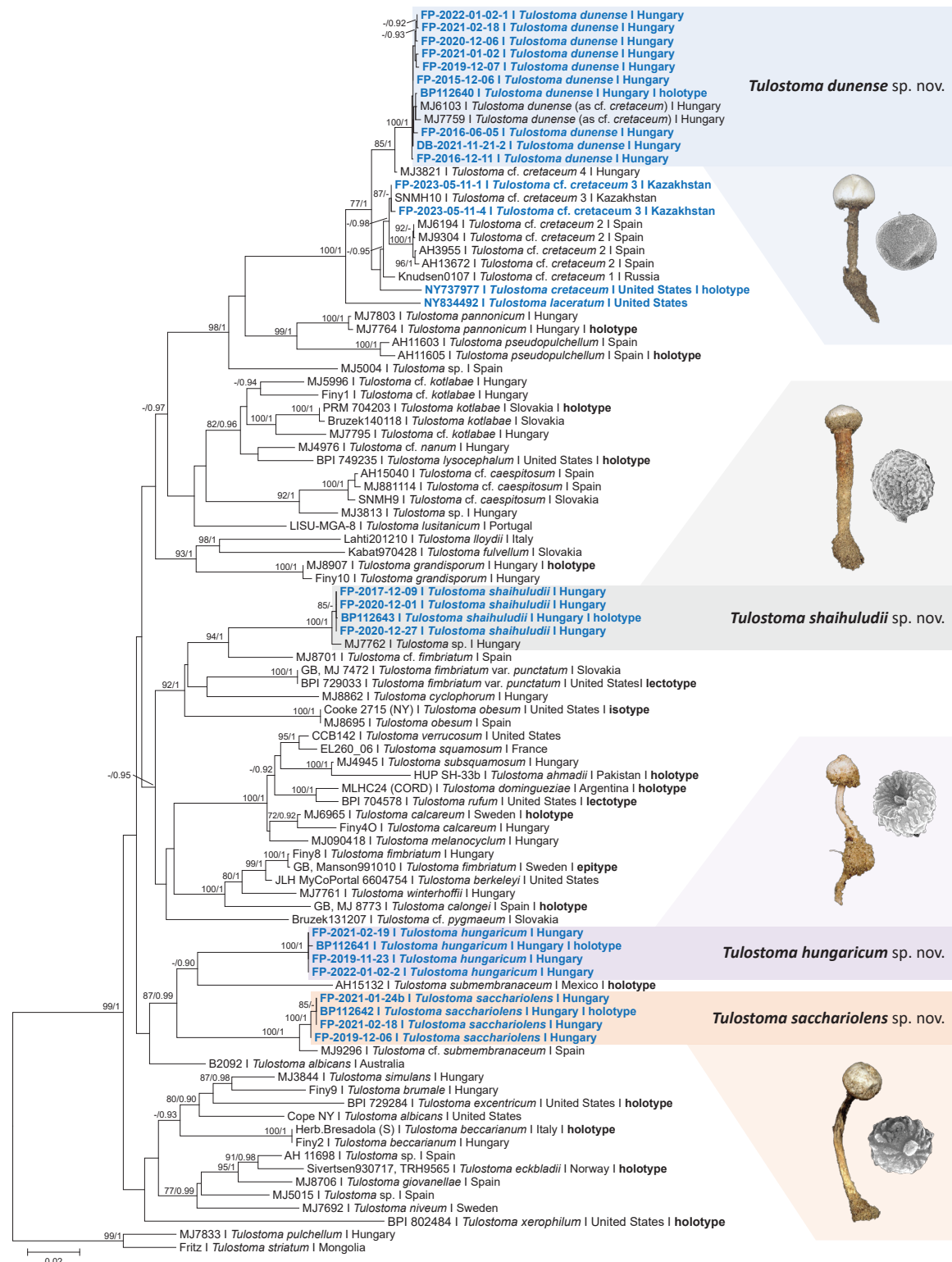


Figure 2. Maximum Likelihood (RAxML) tree of concatenated nrDNA ITS, nrDNA LSU and *tf1-α* sequences of representative species of the genus *Tulostoma* and the four newly-introduced species in the present study. Sequences obtained in this study are shown in bold blue. After the voucher number, the species and the country of origin are shown. Then, the type specimens are indicated. ML bootstrap support values (≥ 70) are shown before slashes and Bayesian posterior probabilities (≥ 0.90) are shown after slashes. Highlighted sections indicate affiliations to the four novel *Tulostoma* species: *T. dunense*, *T. hungaricum*, *T. sacchariolens* and *T. shaihuludii*. The illustrations exhibit basidiomata and basidiospore characteristics of the novel species. *Tulostoma pulchellum* (MJ7833) and *T. striatum* (Fritz) served as multiple outgroups. The scale bar indicates expected changes per site per branch.

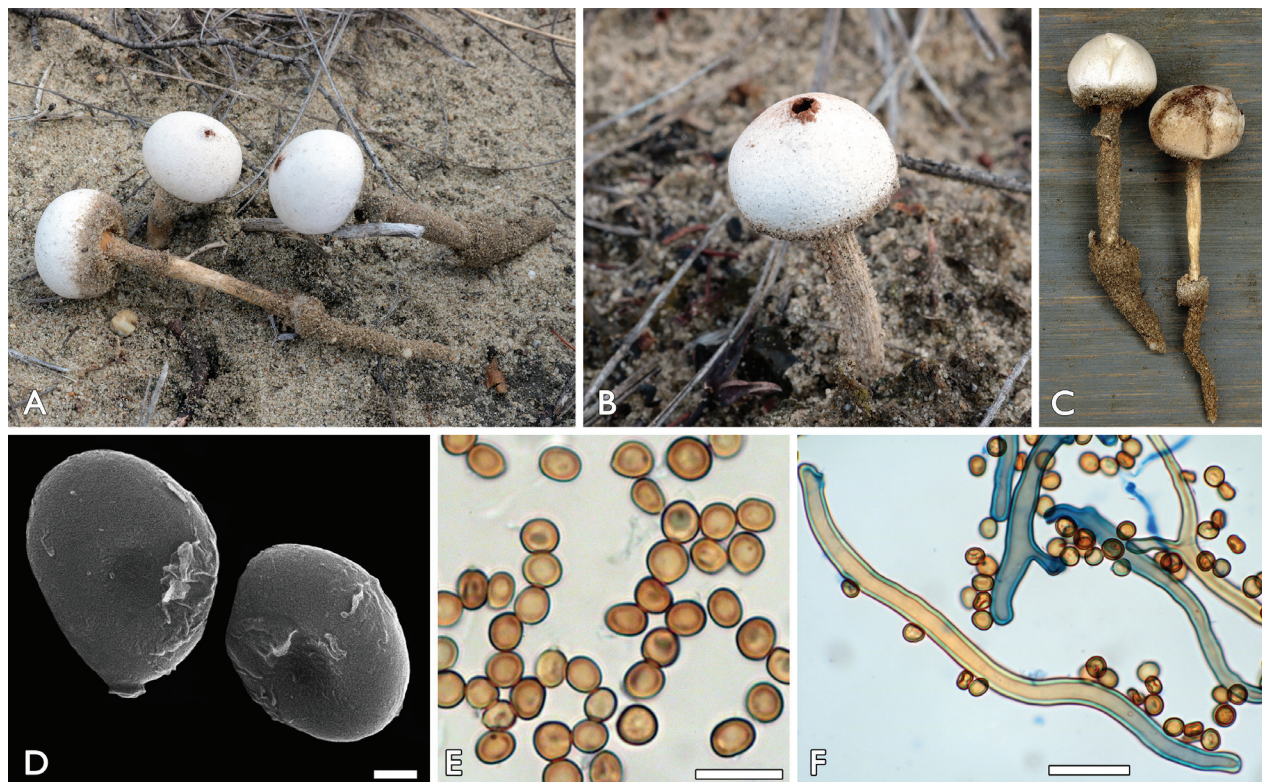


Figure 3. *Tulostoma dunense*: **a, c–f** FP-2020-10-18 (BP112640, holotype), Németskér **b** FP-2021-01-02, Tázlár **a–c** basidiocarps **d, e** basidiospores **f** capillitium with basidiospores. Scale bars: 1 μm (**d**); 10 μm (**e**); 10 μm (**f**). Photos: **a, b, e, f** P. Finy **c** L. Albert **d** K. Bóka.

urban habitats, was considered a result of the maturation process. Later (Hollós 1913) corrected his earlier concept and concluded that some of the synonyms he had listed under *T. vulvatum* in his publication (Hollós 1904), in fact belonged to a complex of several species. He added illustrations of their different types of capillitia (Hollós 1913: tables 3 and 4) and concluded that his concept of *T. vulvatum* from the sand dunes was a synonym of *T. kansense*, a smooth-spored species with brownish capillitium described from North America. The capillitium in the samples from urban habitats clearly showed the undulating inner walls of the capillitium typical of *T. giovanellae* (Hollós 1913: table 3, fig. 6), although Hollós did not identify them under this name. Some 50 years later, Nagy and Babos (1969) recorded *T. giovanellae* growing on a pavement at the base of a house wall in Budapest. It matched partly the material cited by Hollós (1904) as *T. vulvatum*, but was decidedly different from the species growing in the sand dunes. Babos (1999) later came to the same conclusion. Altés et al. (1999) studied the holotype material of *T. vulvatum* and concluded that it was a synonym of *T. giovanellae* characterised by ornamented spores. They also studied the holotype material of *T. obesum* with which they identified European collections with completely smooth spores from steppe habitats and the name *T. vulvatum* was rejected. Rimóczy et al. (2011) accordingly identified the Hungarian species of the sand dunes as *T. obesum*. Molecular data (Jeppson et al. 2017) later showed that the Hungarian "*T. obesum*" was not identical with the American holotype of *T. obesum*, but was closely related to another American species described as *T. cretaceum*. It was recovered as *T. aff. cretaceum* by Jeppson et al. (2017). The *T. aff. cretaceum* from Hungary belongs to a complex

of cryptic species with a strong geographical isolation. The type of *T. cretaceum* was studied and successfully sequenced by Gube (2009), but the ITS and LSU sequences have remained unpublished. We have kindly received these sequences from Matthias Gube allowing us to include them in the phylogenetic analyses. The phylogenetic analyses showed that the type of *T. cretaceum* formed a distinct lineage within this complex (Fig. 1), proving that this North American species is different from the European and Asian lookalikes. Therefore, the Hungarian collections are proposed here as a novel species, *T. dunense*, which is closely related to samples of *T. aff. cretaceum* collected in Hungary, Kazakhstan and in the Russian Federation as well as in Spain (Fig. 1). The main features to distinguish *T. dunense* from the other species in the complex are mainly phylogenetic and geographical-based data. *Tulostoma dunense* has been a protected species under Hungarian law since 2005, but to date, it has erroneously been treated under various misinterpreted and dubious names, i.e. *T. volvulatum*, *T. obesum* and *T. aff. cretaceum*. The ITS region of *T. dunense* differs from its closest clade represented by a single sequence (*T. cf. cretaceum* MJ3821, see Fig. 2) by at least 13 substitution and indel positions, which is a similarity of 98%. This sequence might represent a different species, but further collections need to be studied to clarify its taxonomic status. In contrast, low intraspecific genetic variation was detected in *T. dunense* (0–4 substitution and indel positions). The ITS and LSU sequences of an old collection identified by Long (www.mycportal.org) under the name *Schizostoma laceratum* (NY834492) collected in 1941 in New Mexico, were provided for us by Matthias Gube. Our phylogenetic analyses indicate that this specimen belongs to the *T. cretaceum* complex as a distinct lineage. On the other hand, the nomenclature of the genus *Schizostoma*, as well as the species *S. laceratum* (Fries 1829; Lévillé 1846), seems to be problematic and needs further clarification.

Specimens examined. HUNGARY, Bács-Kiskun, Ágasegyháza, in open sand, 18 Feb 2021, P. Finy, FP-2021-02-18 (ELTE); Bócsa, in open sand, 7 Dec 2019, P. Finy, FP-2019-12-07 (ELTE); Fülöpháza, 11 Apr 2006, T. Knutsson, T. Gunnarsson, J. Jeppson, M. Jeppson, MJ7759 (GB), *Ibidem*, in open sand, 5 Jun 2016, P. Finy, FP-2016-06-05 (ELTE); Izsák (Soltszentimre), in open sand, 21 Nov 2019, A. Nagy, B. Dima, DB-2021-11-21-2 (ELTE); Kéleshalom, in open sand, 6 Dec 2015, P. Finy, FP-2015-12-06 (ELTE); *Ibidem*, in open sand, 2 Jan 2022, P. Finy, I. Ölvedi, FP-2022-01-02-1 (ELTE); Tázlár, in open sand, 11 Dec 2016, P. Finy, FP-2016-12-11 (ELTE); *Ibidem*, in open sand, 2 Jan 2021, P. Finy, FP-2021-01-02 (ELTE). Pest, Örkény, former military training field, sand steppe vegetation, in open sand, 5 Nov 2001, J. Jeppson, M. Jeppson, MJ6103 (GB), *Ibidem*, in open sand, 6 Dec 2020, P. Finy, L. Albert, FP-2020-12-06 (ELTE).

***Tulostoma hungaricum* Finy, Jeppson, L. Albert, Ölvedi & Dima, sp. nov.**

MycoBank No: MB 849932

Fig. 4

Holotype. HUNGARY, Bács-Kiskun, Bócsa, open sandy grassland, on sandy sites with scattered vegetation, near *Juniperus communis* shrubs 24 Jan 2021, P. Finy, FP-2021-01-24a (BP112641, isotype GB). GenBank: ITS OR722630, LSU OR722653.

Etymology. With reference to Hungary where it was discovered.

Description. Spore-sac subglobose, 3–6 mm. Exoperidium hyphal, heavily encrusting sand grains. Endoperidium white, pitted from adhering sand grains. Mouth small, fibrillose-fimbriate with a small and inconspicuous mouth. Socket inconspicuous. Stem slender, 9–15 × 1–1.5 mm, whitish, not bulbous. Gleba ochraceous brown. Capillitium elastic, 2–6 µm in diameter with walls 0.5–2 µm in diameter and moderate branching. Septa in general not widened. Basidiospores subglobose, 4.9–5.7 × 4.5–5.1 µm (av. 5.2 × 4.8 µm), varied in size, with fine, but visible ornamentation. SEM-photos show low verrucae coalescing in short lines.

Habitat and distribution. *Tulostoma hungaricum* occurs in the calcareous, sandy steppe areas, in dry and exposed habitats on bare sand. It has, to date, been found on the sheltered and sun-exposed, extremely warm sandy spots on the south-facing sides of *Juniperus communis*. So far, it has only been found in few localities of the Kiskunság National Park, Central Hungary.

Notes. *Tulostoma hungaricum* is the smallest *Tulostoma* species in Europe. It sometimes shares its habitat with *T. pannonicum*, another species forming small basidiomata. The latter is, however, easily distinguished on its ochraceous stem, membranous exoperidium and smaller spores. *Tulostoma hungaricum* is an isolated species belonging to the well-supported Clade 7 according to Jeppson et al. (2017), together with *T. submembranaceum* from Mexico, *T. cf. submembranaceum* from Spain and the below-described new species *T. sacchariolens*. In the ITS region, *T. hungaricum* differs from its closest species (*T. submembranaceum*, see Fig. 1) by almost 90 substitution and indel positions, which is a similarity of 87%. Low intraspecific genetic variability was observed in *T. hungaricum* by a difference of 0–3 substitution and indel positions.



Figure 4. *Tulostoma hungaricum*: **a, c–g** FP-2021-01-24a (BP112641, holotype), Bócsa **b** FP-2019-11-23, Orgovány **a–c** basidiocarps **d, e** basidiospores **f, g** capillitium with basidiospores. Scale bars: 1 µm (**d**); 10 µm (**e**); 20 µm (**f, g**). Photos: **a, b, e–g** P. Finy **c** L. Albert **d** K. Bóka.

Specimens examined. HUNGARY, Bács-Kiskun, Kéleshalom, open sandy grassland, near *Juniperus communis*, 2 Jan 2022, P. Finy, I. Ölvedi, L. Albert, FP-2022-01-02-2 (ELTE); Orgovány, open sandy grassland, near *Juniperus communis*, 23 Nov 2019, P. Finy, I. Ölvedi, L. Albert, FP-2019-11-23 (ELTE); Ibidem, open sandy grassland, near *Juniperus communis*, 19 Feb 2021, P. Finy, I. Ölvedi, L. Albert, FP-2021-02-19 (ELTE).

Morphologically examined specimens. HUNGARY, Bács-Kiskun, Bócsa, open sandy grassland, near *Juniperus communis*, 3 Dec 2022, P. Finy, I. Ölvedi, L. Albert, FP-2022-12-03 (herb. Finy); Fülöpháza, open sandy grassland, near *Juniperus communis*, 14 Jan 2023, P. Finy, I. Ölvedi, L. Albert, FP-2023-01-14 (herb. Finy); Pest, Tatárszentgyörgy, open sandy grassland, near *Juniperus communis*, 17 Dec 2022, I. Ölvedi, OP-2022-12-17 (herb. Ölvedi).

***Tulostoma sacchariolens* Finy, Jeppson, L. Albert, Ölvedi & Dima, sp. nov.**

MycoBank No: MB 849933

Fig. 5

Holotype. HUNGARY, Bács-Kiskun, Bócsa, open disturbed sandy grassland, in a sand pit, on bare ground, 24 Jan 2021, I. Ölvedi, P. Finy, L. Albert, OP20210124 (BP112642, isotype GB). GenBank: ITS OR722632, LSU OR722654, tef1 OR707020.

Etymology. The epithet refers to its unique sweetish floral smell reminiscent of that of, for example, *Hebeloma sacchariolens*.

Description. Spore-sac subglobose, often flattened to depressed or hemispherical, 5–9 µm. Exoperidium hyphal, heavily encrusting sand, more persistent at the base of the spore-sac. Endoperidium white or dirty white, pitted from detached sand grains. Mouth delicately fimbriate. Socket conspicuous, forming a thickening on the upper part of the stem. Stem 25–50 × 1.5–2.5 mm, whitish, ornamented with orange to reddish fibrils, with age remarkably blackening, thickening towards the base, bulbous. The mature basidiomata have a pronounced sweet floral smell, reminiscent of *Hebeloma sacchariolens* Quél. or *Freesia* flowers. Gleba ferruginous brown. Capillitium 2.5–7 µm in diameter with walls 0.8–2.2 µm in diameter, lumen in general scarce, mostly straight, little branching. Most septa slightly widened. Spores subglobose, 4.6–5.3 × 4.1–5 µm (av. 4.6–4.9 µm), with coarse elongated ornamentation. SEM-photos show developed crests arranged in lines.

Habitat and distribution. Recorded in calcareous, sandy steppe areas, mostly in sunny open habitats with sparse vegetation, often in trampled or otherwise disturbed places. It is currently known only from a few localities in the sandy areas of the Danube–Tisza interfluves in Central Hungary.

Notes. With its fragrant smell and blackening stem, *Tulostoma sacchariolens* has a unique combination of characters within the genus, easily separating it from any known *Tulostoma* species. *Tulostoma sacchariolens* belongs to Clade 7 according to Jeppson et al. (2017) together with *T. cf. submembranaceum* (MJ9296, see Fig. 2) from Spain, *T. submembranaceum* from Mexico and the above-described *T. hungaricum*. It differs from its sister species (*T. cf. submembranaceum*) in the ITS region by more than 20 substitution and indel positions, which is a similarity of 96%. The intraspecific genetic variability in the ITS region amongst three sequences of *T. sacchariolens* was zero (Fig. 1), while the ITS sequence of FP-2019-12-06 had six polymorphic sites.

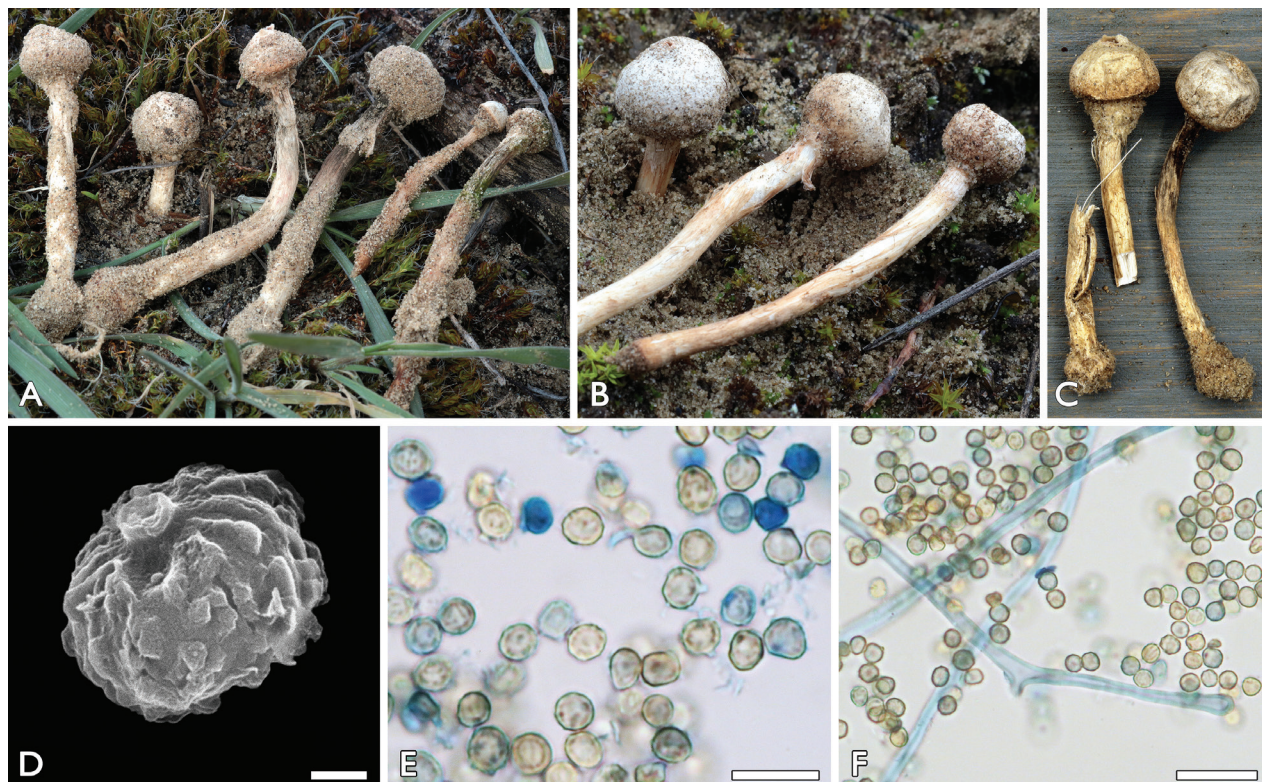


Figure 5. *Tulostoma sacchariolens*: **a, e** FP-2021-02-18, Orgovány **b** FP-2019-12-06, Bócsa **c, d, f** OP-2021-01-24 (BP112642, holotype), Bócsa **a–c** basidiocarps **d, e** basidiospores **f** capillitium with basidiospores. Scale bars: 1 μm (**d**); 10 μm (**e**); 20 μm (**f**). Photos: **a, b, e, f** P. Finy **c** L. Albert **d** K. Bóka.

Specimens examined. HUNGARY, Bács-Kiskun: Bócsa, open sandy grassland, 6 Dec 2019, P. Finy, FP-2019-12-06 (ELTE); Ibidem, open sandy grassland, 24 Jan 2021, P. Finy, I. Ölvedi, L. Albert, FP-2021-01-24b (ELTE); Orgovány, open sandy grassland, 18 Feb 2021, P. Finy, I. Ölvedi FP-2021-02-18 (ELTE).

Morphologically examined specimens. HUNGARY, Bács-Kiskun: Bócsa, open sandy grassland, 3 Dec 2022, P. Finy, FP-2022-12-03 (herb. Finy); Fülöpháza, open sandy grassland, 14 Jan 2023, P. Finy, FP-2023-01-14 (herb. Finy); Orgovány, open sandy grassland, 4 Dec 2021, P. Finy, I. Ölvedi, L. Albert, FP-2021-12-04 (herb. Finy); Pest, Örkény, open sandy grassland, 12 Jan 2022, I. Ölvedi, OP-2022-01-12 (herb. Ölvedi); Ibidem, open sandy grassland, 10 Dec 2022, P. Finy, I. Ölvedi, L. Albert, FP-2022-12-10 (herb. Finy).

***Tulostoma shaihuludii* Finy, Jeppson, L. Albert, Ölvedi, D.G. Knapp & Dima, sp. nov.**

MycoBank No: MB 849934

Fig. 6

Holotype. HUNGARY, Bács-Kiskun, Tázlár, open sandy grassland, 11 Dec 2016, P. Finy, FP-2016-12-11 (BP112643, isotype GB). GenBank: ITS OR722637, LSU OR722657, tef1 OR707019.

Etymology. The epithet refers to its being reminiscent of the sandworm Shai-Hulud of the fictional planet Arrakis from the science fiction novel series *Dune* by Frank Herbert.

Description. Spore-sac subglobose, often flattened to depressed, 7–18 mm, relatively small compared to the size of the stem. Exoperidium hyphal, encrusting sand at the base of the spore-sac. Endoperidium white or greyish-white, pitted from detached sand grains. Mouth fimbriate, somewhat prominent. Socket developed, slightly separated from the stem. The spore-sac rarely detaches from the stem. Stem 30–70 × 3–6 mm, yellowish-brown to orange brown or reddish-brown, with age darkening, longitudinally furrowed, scaly, often curved, at the base slightly bulbous, with a conspicuous, but fragile pseudorhiza. Gleba ferruginous-cinnamon-brown. Capillitium 3.5–7 µm in diameter with walls 0.3–3.2 µm in diameter, mostly straight, sparsely branched, inner wall often undulating. Septa not or slightly widened. Abundant, thin-walled, septate capillitium hyphae present amongst normal capillitium threads. Basidiospores globose, sometimes flattened, 4.1–5.2 × 3.5–4.7 µm (av. 4.1 × 4.6 µm), finely asperulate, ornamentation not always visible under LM. SEM photos show fine warts arranged in lines forming a dense network.

Habitat and distribution. Occurs in dry and loose calcareous, open sandy habitats of the *Festucetum vaginatae* natural grasslands. It mainly grows solitary, deeply rooted in the sand in spots with bare sand. It is currently known only from the sandy areas of Central Hungary.

Notes. *Tulostoma shaihuludii* is similar in stature to *T. fimbriatum* and *T. winterhoffii*, but can be easily distinguished by its habitat (open sand) and its microcharacters, particularly the spore wall ornamentation. It belongs to Clade 2 according to Jeppson et al. (2017) and it forms a sister clade of *Tulostoma* cf. *fimbriatum*

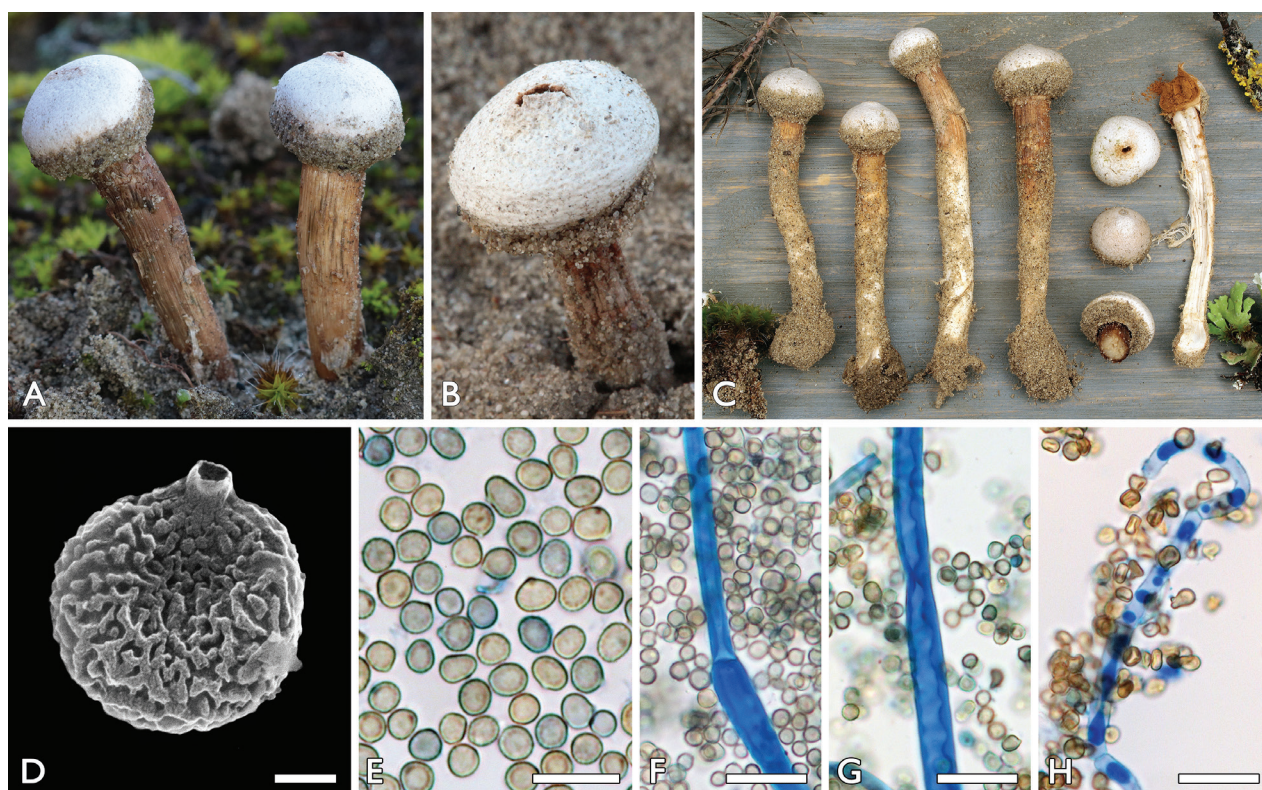


Figure 6. *Tulostoma shaihuludii*: **a** FP-2020-12-01-3, Fülöpháza **b, d–g** FP-2016-12-11 (BP112643, holotype), Tázlár **c** AL-2021-01-24, Bócsa **h** FP-2017-12-09, Orgovány **a–c** basidiocarps **d, e** basidiospores **f, g** capillitium with basidiospores **h** thin-walled, septate capillitium hyphae. Scale bars: 1 µm (**d**); 10 µm (**e**); 20 µm (**f–h**). Photos: **a, b, e–h** P. Finy **c** L. Albert **d** K. Bóka.

(MJ8701 as “*T. sp2*” in Jeppson et al. (2017)) from which it differs in the ITS region by 45 substitution and indel positions, which is a similarity of 93%. The intraspecific genetic variability of *T. shaihuludii* is low (0–3 substitution and indels positions).

Specimens examined. HUNGARY, Bács-Kiskun, Fülöpháza, Fülöpházi homokbuckák, sand steppe vegetation, 11 Apr 2006, J. Jeppson, M. Jeppson, MJ7762 (GB); Ibidem, open sandy grassland, 1 Dec 2020, P. Finy, I. Ölvedi, FP-2020-12-01-3 (ELTE); Orgovány, open sandy grassland, 9 Dec 2017, P. Finy, FP-2017-12-09 (ELTE); Pirtó, open sandy grassland, 27 Dec 2020, P. Finy, L. Albert, FP-2020-12-27 (ELTE).

Morphologically examined specimens. HUNGARY, Bács-Kiskun, Bócsa, open sandy grassland, 7 Dec 2019, P. Finy, FP-2019-12-07 (herb. Finy); Ibidem, open sandy grassland, 24 Jan 2021, P. Finy, L. Albert, I. Ölvedi, FP-2021-01-24 (herb. Finy), AL-2021-01-24 (herb. Albert); Ibidem, open sandy grassland, 4 Dec 2021, P. Finy, I. Ölvedi, FP-2021-12-04 (herb. Finy); Ibidem, open sandy grassland, 3 Dec 2022, P. Finy, FP-2022-12-03 (herb. Finy); Fülöpháza, open sandy grassland, 2 Dec 2018, P. Finy, FP-2018-12-02 (herb. Finy); Ibidem, open sandy grassland, 16 Jan 2022, P. Finy, I. Ölvedi, FP-2022-01-16 (herb. Finy); Izsák (Soltszentimre), open sandy grassland, 4 Feb 2016, P. Finy, FP-2016-02-04 (herb. Finy); Ibidem, open sandy grassland, 14 Dec 2016, P. Finy, FP-2016-12-14 (herb. Finy); Ibidem, open sandy grassland, 17 Jan 2019, P. Finy, FP-2019-01-17 (herb. Finy); Ibidem, open sandy grassland, 16 Dec 2020, P. Finy, FP-2020-12-16-1 (herb. Finy); Kéleshalom, open sandy grassland, 6 Dec 2015, P. Finy, FP20151206 (herb. Finy); Ibidem, open sandy grassland, 2 Jan 2022, P. Finy, I. Ölvedi, FP-2022-01-02-3 (herb. Finy); Kiskunhalas, open sandy grassland, 22 Dec 2019, P. Finy, FP-2019-12-22 (herb. Finy); Ibidem, open sandy grassland, 5 Jan 2023, P. Finy, I. Ölvedi, FP-2023-01-05 (herb. Finy); Kunbaracs, open sandy grassland, 5 Feb 2022, P. Finy, I. Ölvedi, FP-2022-02-05 (herb. Finy); Orgovány, open sandy grassland, 13 Aug 2017, P. Finy, FP-2017-08-13 (herb. Finy); Ibidem, open sandy grassland, 18 Feb 2021, P. Finy, I. Ölvedi, FP-2021-02-18 (herb. Finy); Pirtó, open sandy grassland, 16 Jan 2016, P. Finy, FP-2016-01-16 (herb. Finy); Tázlár, open sandy grassland, 11 Dec 2016, P. Finy, FP-2016-12-11 (herb. Finy); Pest, Örkény, open sandy grassland, 12 Jan 2022, I. Ölvedi, OP-2022-01-12 (herb. Ölvedi); Tatárszentgyörgy, open sandy grassland, 1 Jan 2022, I. Ölvedi, OP-2022-01-01 (herb. Ölvedi); Ibidem, open sandy grassland, 10 Dec 2022, P. Finy, FP-2022-12-10 (herb. Finy); Ibidem, open sandy grassland, 17 Dec 2022, I. Ölvedi, OP-2022-12-17 (herb. Ölvedi); Tolna, Paks, open sandy grassland, 4 Feb 2018, P. Finy, FP-2018-02-04 (herb. Finy); Ibidem, open sandy grassland, 22 Jan 2021, P. Finy, FP-2021-01-22 (herb. Finy); Ibidem, open sandy grassland, 9 Jan 2022, I. Ölvedi, P. Finy, OP-2022-01-09 (herb. Ölvedi); Ibidem, open sandy grassland, 27 Feb 2022, P. Finy, FP-2022-02-27 (herb. Finy).

Discussion

The results of our study further emphasise the high species diversity amongst the stalked puffballs (*Tulostoma*) in East Central Europe, as previously indicated by Jeppson et al. (2017). In Hungary, so far 19 species have been recorded, including the four new species proposed in this study. The Pannonian, dry and sandy grasslands between the rivers Danube and Tisza, as well as adjacent areas in Central Hungary, harbour to date 66% of all described species of *Tulostoma* known to occur in Europe (29 spp.). The dry, sandy grasslands in Central Hungary have a long continuity as natural grasslands or as sheep pastures and

are characterised by steppe flora and fauna. Both natural and grazed habitats are rich in gasteroid fungi, but usually their species composition is different. The summer and autumn temperatures in the sand are extremely high and the yearly precipitation is low. The dry and drought-resisting basidiomata of *Tulostoma* species could be considered as adaptations to xeric conditions. The development of the basidiomata occurs mainly in late autumn and early winter.

Tulostoma species are generally rare (although locally abundant) and the current knowledge of their population structures in Europe is limited. However, their occurrences are highly dependent on the habitat status where they grow and changes in land management are likely to be detrimental to their populations. A vast majority of the European *Tulostoma* species are Red-Listed in the countries where they occur (<http://www.eccf.eu/redlists-en.ehtml>).

In addition to the four novel species proposed herein, the results from previous works (e.g. Jeppson et al. (2017)) and our ongoing studies indicate the presence of many more undescribed species of *Tulostoma* in Central Europe.

Acknowledgements

The work was supported by the ÚNKP-22-5 New National Excellence Program of the Ministry for Culture and Innovation from the source of the National Research, Development and Innovation Fund, the National Research, Development and Innovation Office of Hungary (FK-143061, the ELTE Institutional Excellence Program 2020 (TKP2020-IKA-05), Diagnostics and Therapy 2). Bálint Dima is grateful to the János Bolyai Research Scholarship of the Hungarian Academy of Sciences. We thank to Csilla Gergely for her assistance in laboratory work. We are grateful to Matthias Gube (Germany) for allowing us to publish the type sequences of *Tulostoma cretaceum* and the sequences of *Schizostoma laceratum*.

Additional information

Conflict of interest

The authors have declared that no competing interests exist.

Ethical statement

No ethical statement was reported.

Funding

New National Excellence Program of the Ministry for Culture and Innovation from the source of the National Research, Development and Innovation Fund (Hungary); National Research, Development and Innovation Office (Hungary); János Bolyai Research Scholarship of the Hungarian Academy of Sciences.

Author contributions

Conceptualisation: PF, BD. Methodology: PF, MJ, DGK, VP, KB, DV, BD. Validation: PF, MJ, LA, IÖ. Formal analysis: PF, MJ, DGK, DV, BD. Investigation: PF, MJ, LA, IÖ, KB, BD. Resources: PF, MJ, LA, IÖ, BD. Data Curation: PF, MJ, DGK, LA, IÖ, DV, BD. Writing - Original draft: PF, MJ, VP, BD. Writing - Review and Editing: PF, MJ, DGK, VP, LA, IÖ, KB, DV, GMK, BD. Visualisation: PF, DGK, VP, LA, IÖ, KB. Supervision: MJ, GMK, BD. Funding Acquisition: GMK, BD.

Author ORCIDs

Dániel G. Knapp  <https://orcid.org/0000-0002-7568-238X>

Viktor Papp  <https://orcid.org/0000-0001-6994-8156>

Károly Bóka  <https://orcid.org/0000-0002-1324-3592>

Gábor M. Kovács  <https://orcid.org/0000-0001-9509-4270>

Bálint Dima  <https://orcid.org/0000-0003-2099-3903>

Data availability

All the data that support the findings of this study are available in the main text or in publicly accessible data repositories, as indicated in the text.

References

- Altés A, Moreno G, Wright JE (1999) Notes on *Tulostoma volvulatum* and *T. giovanellae*. *Mycological Research* 103(1): 91–98. <https://doi.org/10.1017/S0953756298006704>
- Babos M (1999) Higher fungi (Basidiomycotina) of the Kiskunság National Park and its environs. In: Lőkös L, Rajczy M (Eds) *The flora of the Kiskunság National Park 2. Cryptogams*, Hungarian Natural History Museum, Budapest, 199–298.
- Bölöni J, Molnár Zs, Kun A [Eds] (2011) *Magyarország élőhelyei. A hazai vegetációtípusok leírása és határozója. ÁNÉR 2011*. MTA ÖBKI, Vácrátót.
- Caffot MLH, Domínguez LS, Hosaka K, Crespo EM (2011) *Tulostoma domingueziae* sp. nov. from *Polylepis australis* woodlands in Córdoba Mountains, central Argentina. *Mycologia* 103(5): 1047–1054. <https://doi.org/10.3852/10-266>
- Fries EM (1829) *Systema mycologicum*. Vol. 3. Gryphiswaldiae, 524 pp. + 202 pp.
- Gardes M, Bruns TD (1993) ITS primers with enhanced specificity for basidiomycetes – application to the identification of mycorrhizae and rusts. *Molecular Ecology* 2(2): 113–118. <https://doi.org/10.1111/j.1365-294X.1993.tb00005.x>
- Gouy M, Tannier E, Comte N, Parsons DP (2021) Seaview version 5: A multiplatform software for multiple sequence alignment, molecular phylogenetic analyses, and tree reconciliation. In: Katoh K. (Ed.) *Multiple Sequence Alignment. Methods in Molecular Biology*, vol 2231. Humana, New York, NY, 241–260. https://doi.org/10.1007/978-1-0716-1036-7_15
- Gube M (2009) *Ontogeny and phylogeny of gasteroid members of Agaricaceae (Basidiomycetes)*. PhD Dissertation, University of Jena, Jena, Germany, 145 pp. <https://d-nb.info/999990691/34>
- Hussain S, Yousaf N, Afshan NS, Niazi AR, Ahmad H, Khalid AN (2016) *Tulostoma ahmadii* sp. nov. and *T. squamosum* from Pakistan. *Turkish Journal of Botany* 40: 218–225. <https://doi.org/10.3906/bot-1501-9>
- Hollós L (1904) *Die Gasteromyceten Ungarns*. Oswald Weigel, Leipzig.
- Hollós L (1913) *Zu den Gasteromyceten Ungarns – Magyarország Gasteromycetái-hoz*. *Magyar Botanikai Lapok* 12(6–7): 194–200.
- Jeppson M, Altés A, Moreno G, Nilsson RH, Loarce Y, de Bustos A, Larsson E (2017) Unexpected high species diversity among European stalked puffballs – a contribution to the phylogeny and taxonomy of the genus *Tulostoma* (Agaricales). *MycKeys* 21: 33–88. <https://doi.org/10.3897/mycokeys.21.12176>
- Katoh K, Standley DM (2013) MAFFT multiple sequence alignment software version 7: Improvements in performance and usability. *Molecular Biology and Evolution* 30(4): 772–780. <https://doi.org/10.1093/molbev/mst010>

- Kumar S, Stecher G, Tamura K (2016) MEGA7: Molecular Evolutionary Genetics Analysis Version 7.0 for Bigger Datasets. *Molecular Biology and Evolution* 33(7): 1870–1874. <https://doi.org/10.1093/molbev/msw054>
- Léveillé J-H (1846) Description des champignons de l'herbier du muséum de Paris. *Annales des Sciences Naturelles sér. 3. Botanique* 5: 111–166.
- Moreno G, Altés A, Wright JE (1992) *Tulostoma squamosum*, *T. verrucosum* and *T. musooriense* are the same species. *Mycotaxon* 43: 61–68.
- Moreno G, Altés A, Ochoa C, Wright JE (1997) Notes on type materials of *Tulostoma*. Some species with mixed holotypes. *Mycological Research* 101(8): 957–965. <https://doi.org/10.1017/S0953756297003572>
- Nagy L, Babos M (1969) Vorkommen einer seltenen Stielbovist-Art (*Tulostoma giovanellae* Bres. in Ungarn). *Mikológiai Közlemények* 1969(2): 115–121.
- Papp V, Dima B (2018) New systematic position of *Aurantiporus alborubescens* (Meruliaceae, Basidiomycota), a threatened old-growth forest polypore. *Mycological Progress* 17(3): 319–332. <https://doi.org/10.1007/s11557-017-1356-3>
- Persoon CH (1794) Neuer Versuch einer systematischen Eintheilung der Schwämme. *Neues Magazin für die Botanik* 1: 63–128.
- Persoon CH (1801) *Synopsis Methodica Fungorum*. Gottingae.
- Rehner SA, Buckley E (2005) A *Beauveria* phylogeny inferred from nuclear ITS and EF1-a sequences: Evidence for cryptic diversification and links to *Cordyceps* teleomorphs. *Mycologia* 97(1): 84–98. <https://doi.org/10.3852/mycologia.97.1.84>
- Rehner SA, Samuels GJ (1994) Taxonomy and phylogeny of *Gliocladium* analysed from nuclear large subunit ribosomal DNA sequences. *Mycological Research* 98(6): 625–634. [https://doi.org/10.1016/S0953-7562\(09\)80409-7](https://doi.org/10.1016/S0953-7562(09)80409-7)
- Rimóczi I, Jeppson M, Benedek L (2011) Characteristic and rare species of Gasteromycetes in Eupannonicum. *Fungi Non Delineati : Raro Vel Haud Perspecte et Explorate Descripti aut Definite Picti*: 56–57. [Edizioni Candusso, Alassio]
- Ronquist F, Huelsenbeck JP (2003) MRBAYES 3: Bayesian phylogenetic inference under mixed models. *Bioinformatics (Oxford, England)* 19(12): 1572–1574. <https://doi.org/10.1093/bioinformatics/btg180>
- Rusevska K, Calonge FD, Karadelev M, Martín MP (2019) Fungal DNA barcode (ITS nrDNA) reveals more diversity than expected in *Tulostoma* from Macedonia. *Turkish Journal of Botany* 43(1): 102–115. <https://doi.org/10.3906/bot-1804-38>
- Schoch CL, Seifert KA, Huhndorf S, Robert V, Spouge JL, Levesque CA, Chen W, Bolchacova E, Voigt K, Crous PW, Miller AN, Wingfield MJ, Aime MC, An K-D, Bai F-Y, Barreto RW, Begerow D, Bergeron M-J, Blackwell M, Boekhout T, Bogale M, Boonyuen N, Burgaz AR, Buyck B, Cai L, Cai Q, Cardinali G, Chaverri P, Coppins BJ, Crespo A, Cubas P, Cummings C, Damm U, de Beer ZW, de Hoog GS, Del-Prado R, Dentinger B, Diéguez-Uribeondo J, Divakar PK, Douglas B, Dueñas M, Duong TA, Eberhardt U, Edwards JE, Elshahed MS, Fliegerova K, Furtado M, García MA, Ge Z-W, Griffiths GW, Griffiths K, Groenewald JZ, Groenewald M, Grube M, Gryzenhout M, Guo L-D, Hagen F, Hambleton S, Hamelin RC, Hansen K, Harrold P, Heller G, Herrera C, Hirayama K, Hirooka Y, Ho H-M, Hoffmann K, Hofstetter V, Högnabba F, Hollingsworth PM, Hong S-B, Hosaka K, Houbraken J, Hughes K, Huhtinen S, Hyde KD, James T, Johnson EM, Johnson JE, Johnston PR, Jones EBG, Kelly LJ, Kirk PM, Knapp DG, Kõljalg U, Kovács GM, Kurtzman CP, Landvik S, Leavitt SD, Ligtenstoffer AS, Liimatainen K, Lombard L, Luangsa-ard JJ, Lumbsch HT, Maganti H, Maharachchikumbura SSN, Martín MP, May TW, McTaggart AR, Methven AS, Meyer W, Moncalvo J-M, Mongkolsamrit S, Nagy LG, Nilsson RH, Niskanen T, Nyilasi I, Okada G, Okane I, Olariaga I, Otte J, Papp T, Park

- D, Petkovits T, Pino-Bodas R, Quaedvlieg W, Raja HA, Redecker D, Rintoul TL, Ruibal C, Sarmiento-Ramírez JM, Schmitt I, Schüßler A, Shearer C, Sotome K, Stefani FOP, Stenroos S, Stielow B, Stockinger H, Suetrong S, Suh S-O, Sung G-H, Suzuki M, Tanaka K, Tedersoo L, Telleria MT, Tretter E, Untereiner WA, Urbina H, Vágvölgyi C, Vialle A, Vu TD, Walther G, Wang Q-M, Wang Y, Weir BS, Weiß M, White MM, Xu J, Yahr R, Yang ZL, Yurkov A, Zamora J-C, Zhang N, Zhuang W-Y, Schindel D (2012) Nuclear ribosomal internal transcribed spacer (ITS) region as a universal DNA barcode marker for Fungi. *Proceedings of the National Academy of Sciences of the United States of America* 109(16): 6241–6246. <https://doi.org/10.1073/pnas.1117018109>
- Siller I, Vasas G (1995) Red list of macrofungi of Hungary (revised edition). *Studia Botanica Hungarica* 26: 7–14.
- Siller I, Vasas G, Pál-Fám F, Bratek Z, Zagyva I, Fodor L (2005) Hungarian distribution of the legally protected macrofungi species. *Studia Botanica Hungarica* 36: 131–163.
- Siller I, Dima B, Albert L, Vasas G, Fodor L, Pál-Fám F, Bratek Z, Zagyva I (2006) Protected macrofungi in Hungary. *Mikol. Közlemények. Clusiana* 45(1–3): 3–158.
- Silvestro D, Michalak I (2012) RaxmlGUI: A graphical front-end for RAxML. *Organisms, Diversity & Evolution* 12(4): 335–337. <https://doi.org/10.1007/s13127-011-0056-0>
- Staden R, Beal KF, Bonfield JK (2000) The Staden package, 1998. In: Misener S, Krawetz SA (Eds) *Bioinformatics methods and protocols*. Humana Press, 115–130. <https://doi.org/10.1385/1-59259-192-2:115>
- Stamatakis A (2014) RAxML Version 8: a tool for phylogenetic analysis and post-analysis of large phylogenies. *Bioinformatics* 30: 1312–1313. <https://doi.org/10.1093/bioinformatics/btu033>
- Varga T, Krizsán K, Földi Cs, Dima B, Sánchez-García M, Sánchez-Ramírez S, Szöllősi G, Szarkándi GJ, Papp V, Albert L, Angelini C, Antonín V, Bougher N, Buchanan P, Buyck B, Bense V, Catcheside P, Cooper J, Dämon W, Desjardin D, Finy P, Geml J, Hughes K, Justo AF, Karasiński D, Kautmanova I, Kerr S, Kiss B, Kocsubé S, Kotiranta H, Lechner BE, Liimatainen K, Lukács Z, Morgado L, Niskanen T, Noordeloos ME, Ortiz-Santana B, Ovrebo C, Rácz N, Savchenko A, Shiryayev A, Soop K, Spirin V, Szébenyi Cs, Tomsovsky M, Tulloss RE, Uehling J, Vágvölgyi Cs, Papp T, Martin FM, Miettinen O, Hibbett DS, Nagy LG (2019) Megaphylogeny resolves global patterns of mushroom diversification. *Nature Ecology & Evolution* 3(4): 668–678. <https://doi.org/10.1038/s41559-019-0834-1>
- Vilgalys R, Hester M (1990) Rapid genetic identification and mapping of enzymatically amplified ribosomal DNA from several *Cryptococcus* species. *Journal of Bacteriology* 172(8): 4238–4246. <https://doi.org/10.1128/jb.172.8.4238-4246.1990>
- White TJ, Bruns T, Lee S, Taylor JW (1990) Amplification and direct sequencing of fungal ribosomal RNA genes for phylogenetics. In: Innis MA, Gelfand DH, Sninsky JJ, White TJ (Eds) *PCR protocols: A guide to the methods and applications*. Academic Press, New York, 315–322. <https://doi.org/10.1016/B978-0-12-372180-8.50042-1>
- Wright JE (1987) The genus *Tulostoma* (Gasteromycetes) – A world monograph. *Bibliotheca Mycologica* 113. Berlin, Stuttgart, 338 pp.

Morphophylogenetic evidence reveals four new fungal species within Tetraplosphaeriaceae (Pleosporales, Ascomycota) from tropical and subtropical forest in China

Xia Tang^{1,2,3}, Rajesh Jeewon^{4,5}, Yong-Zhong Lu^{1,6}, Abdulwahed Fahad Alrefaei⁵,
Ruvishika S. Jayawardena^{2,3}, Rong-Ju Xu^{2,3}, Jian Ma^{2,3}, Xue-Mei Chen⁷, Ji-Chuan Kang¹

1 Engineering and Research Center for Southwest Biopharmaceutical Resource of National Education Ministry of China, Guizhou University, Guiyang, 550025, Guizhou Province, China

2 Center of Excellence in Fungal Research, Mae Fah Luang University, Chiang Rai, 57100, Thailand

3 School of Science, Mae Fah Luang University, Chiang Rai, 57100, Thailand

4 Department of Health Sciences, Faculty of Medicine and Health Sciences, University of Mauritius, Reduit, Mauritius

5 Department of Zoology, College of Science, King Saud University, P.O. Box 2455, Riyadh 11451, Saudi Arabia

6 School of Food and Pharmaceutical Engineering, Guizhou Institute of Technology, Guiyang, Guizhou Province 550003, China

7 Center for Yunnan Plateau Biological Resources Protection and Utilization, College of Biological Resource and Food Engineering, Qujing Normal University, Qujing 655011, China

Corresponding authors: Rajesh Jeewon (r.jeewon@uom.ac.mu); Ji-Chuan Kang (jckang@gzu.edu.cn)



Academic editor: C. S. Bhunjun
Received: 22 September 2023
Accepted: 9 November 2023
Published: 6 December 2023

Citation: Tang X, Jeewon R, Lu Y-Z, Alrefaei AF, Jayawardena RS, Xu R-J, Ma J, Chen X-M, Kang J-C (2023) Morphophylogenetic evidence reveals four new fungal species within Tetraplosphaeriaceae (Pleosporales, Ascomycota) from tropical and subtropical forest in China. MycoKeys 100: 171–204. <https://doi.org/10.3897/mycokeys.100.113141>

Copyright: © Xia Tang et al.
This is an open access article distributed under terms of the Creative Commons Attribution License (Attribution 4.0 International – CC BY 4.0).

Abstract

Tetraplosphaeriaceae (Pleosporales, Ascomycota) is a family with many saprobes recorded from various hosts, especially bamboo and grasses. During a taxonomic investigation of microfungi in tropical and subtropical forest regions of Guizhou, Hainan and Yunnan provinces, China, several plant samples were collected and examined for fungi. Four newly discovered species are described based on morphology and evolutionary relationships with their allies inferred from phylogenetic analyses derived from a combined dataset of LSU, ITS, SSU, and *tub2* DNA sequence data. Detailed illustrations, descriptions and taxonomic notes are provided for each species. The four new species of Tetraplosphaeriaceae reported herein are *Polyplosphaeria guizhouensis*, *Polyplosphaeria hainanensis*, *Pseudotetraploa yunnanensis*, and *Tetraploa hainanensis*. A checklist of Tetraplosphaeriaceae species with available details on their ecology is also provided.

Key words: Anamorphic fungi, checklist, Dothideomycetes, ribosomal genes, species diversity, taxonomy

Introduction

The Southwestern part of China is characterised by a tropical to subtropical climate and several provinces are well known for their high diversity of plants as well as fungi (Feng and Yang 2018; Hyde et al. 2020b; Bao et al. 2021; Yang et al. 2023). Yunnan province, for example, is considered a hotspot for species diversity. Over the last few decades, there has been a number of studies that have reported novel fungal species from this region (Jeewon et al. 2003; Luo et al. 2017, 2018; Huang et al. 2018; Su et al. 2018; Yang et al. 2019; Hyde et al. 2020b;

Bao et al. 2021; Mortimer et al. 2021). So far more than 6000 fungal species described alone from Yunnan province (Feng and Yang 2018). Guizhou, as a prominent example of China's karst landform (also referred to as a 'karst province'), is also characterised by a geomorphological diversity that can be directly related to species diversity. It boasts a distinctive geographical environment and a special climate that fosters the growth of numerous rare, endangered, and indigenous plant, animal, and fungal species. Over the past few decades, extensive research has focused on fungi, encompassing both macro and microfungi, leading to the identification and documentation of roughly over 2,500 fungal species in Guizhou province (Zhou et al. 2018, 2020a, 2020b, 2022; Dissanayake et al. 2020; Chen et al. 2021; Yang et al. 2023). Hainan Province, the largest island in the Indo-Burma biodiversity hotspot, contains extensive and well-preserved tropical forests (Huang et al. 2023). Recent studies have indicated the presence of diverse fungal species in Hainan, with roughly over 1000 fungal species. Most of these fungi are macrofungi (Zhang et al. 1994; Li et al. 2010; Hapuarachchi et al. 2018; Huang et al. 2023). With our current fungal biodiversity estimates and given that mycologists anticipate many more species remain to be discovered especially in explored habitats, this research study has been undertaken to investigate microfungi in this region, and potentially discover new fungal species.

Tetraplosphaeriaceae was introduced by Tanaka et al. (2009) to accommodate the massarina-like species that produced tetraploa-like anamorphs in culture with *Tetraplosphaeria* as its type genus. Tetraplosphaeriaceae is known to be widely distributed on various hosts, with most species reported from bamboo or grasses (Poaceae) (Tanaka et al. 2009; Ariyawansa et al. 2015; Li et al. 2016), while *Tetraploa* species occur on diverse hosts (Hyde et al. 2013). Tetraplosphaeriaceae was first described to accommodate five genera: *Polyplosphaeria* Kaz. Tanaka & K. Hiray, *Pseudotetraploa* Kaz. Tanaka & K. Hiray, *Quadricrura* Kaz. Tanaka & K. Hiray, *Tetraplosphaeria* Kaz. Tanaka & K. Hiray, and *Triplosphaeria* Kaz. Tanaka & K. Hiray (Tanaka et al. 2009). Hyde et al. (2013) treated the type genus, *Tetraplosphaeria* as a synonym of *Tetraploa* according to nomenclatural priority. Ariyawansa et al. (2015) accepted *Shrungabeeja* in Tetraplosphaeriaceae based on morphological and molecular evidence from *S. longiappendiculata*. Later, *Ernakulamia* was accommodated in Tetraplosphaeriaceae based on morphology and phylogenetic analyses of combined ITS, LSU and *tub2* sequence data (Delgado et al. 2017; Hyde et al. 2020a). Pem et al. (2019) transferred *Byssolophis* from the genera incertae sedis to Tetraplosphaeriaceae based on its massarina-like morphology and phylogenetic analyses based on combined LSU, SSU, *tef1-a*, and *rpb2* sequence data. Hongsanan et al. (2020) provided a taxonomic update on families of Dothideomycetes and eight genera were accepted in Tetraplosphaeriaceae. Recently, Li et al. (2021) discovered a freshwater fungus that had a close phylogenetic affinity with *Ernakulamia* and *Shrungabeeja* in Tetraplosphaeriaceae and accommodated it in a new genus *Aquatisphaeria* based on morphology and phylogeny. To date, Tetraplosphaeriaceae consists of nine genera (Hongsanan et al. 2020; Li et al. 2021; Wijayawardene et al. 2022).

Most members of Tetraplosphaeriaceae contain anamorphic species (Wijayawardene et al. 2022). However, *Pseudotetraploa*, *Tetraploa*, and *Triplosphaeria* exhibit both teleomorphs and anamorphs (Wijayawardene et al. 2022), while *Byssolophis* is only known in its teleomorphic morph (Tanaka et al. 2009; Ariyawansa et al. 2015; Pem et al. 2019; Hongsanan et al. 2020; Li et al. 2021;

Jayawardena et al. 2023). Tetraplosphaeriaceae is characterized by massarina-like teleomorph morphs but can be distinguished from other families by its immersed to superficial, glabrous or brown hyphae at sides of ascomata with flattened bases and cylindrical to clavate, short pedicellate 8-spored asci which are narrowly fusiform to broadly cylindrical, septate, hyaline to pale brown ascospores, usually with a complete sheath or appendage-like sheath (Tanaka et al. 2009; Hyde et al. 2013). The anamorphs are tetraploa-like hyphomycetes having micronematous to macronematous, erect, unbranched, septate, with presence or absence of conidiophores, monoblastic, terminal conidiogenous cells sometimes indistinguishable from creeping hyphae, solitary, cylindrical to obpyriform, comprising 3–8 columns or internal hyphal structure conidia, mostly verrucose at the conidial base and with 2–8-setose appendages (Tanaka et al. 2009; Hyde et al. 2013; Hongsanan et al. 2020).

In this study, the aim is to characterize anamorphic fungal species collected from the southern part of China. The objectives are to 1) to describe novel species collected from Guizhou, Hainan, and Yunnan provinces in China, based on morphological examination of fresh specimens; 2) to document morphological differences and similarities with extant species; 3) to establish four new species within the family Tetraplosphaeriaceae with support from results generated from phylogenetic analyses of LSU, ITS, SSU, and *tub2* DNA sequence data; 4) to provide a worldwide checklist of Tetraplosphaeriaceae species with available details on their ecology.

This study will undoubtedly increase our understanding of fungal diversity in China.

Materials and methods

Sample collection, isolation and morphological studies

Fresh samples of unidentified decaying wood and decaying bamboo were collected in Guizhou (Xingyi city, Xianheping National Forest Park), Hainan (Wuzhishan city, Wuzhishan National Nature Reserve), and Yunnan (Puer city, Ailao mountains) provinces respectively. During the collection period, the environmental conditions at the different regions were as follows: Guizhou-average temperature of 26 °C, subtropical climate, humid environment during autumn; Hainan-average temperature of 29 °C, tropical climate, humid environment during autumn; Yunnan-average temperature of 22 °C, subtropical climate, humid environment during spring. The samples were placed in Ziplock bags, labelled with a marker pen, and observed using the stereomicroscope (Motic SMZ-171). The procedure for specimen collection, observation and isolation follows that of Senanayake et al. (2020) and Tang et al. (2022). The morphological measurements were performed by the Tarosoft (R) Image Frame Work tool (IFW 0.97 version), and photoplates were created using the Adobe Photoshop 2019 program (Adobe Systems, USA).

After morphological examination, the specimens were deposited at the herbaria of Kunming Institute of Botany, Chinese Academy of Sciences (**HKAS**), Kunming, China, and the Guizhou Academy of Agriculture Sciences (**GZAAS**), Guiyang, China, respectively. The ex-type cultures were deposited at the Guizhou Culture Collection (**GZCC**) in China and the Kunming Institute of Botany Culture Collection (**KUNCC**). Faces of Fungi and Index Fungorum numbers are provided as in Jayasiri

et al. (2015) and Index Fungorum (2023). Species recognition and justifications for new species establishment were done based on the guide-lines provided by Jeewon and Hyde (2016), Chethana et al. (2021) and Pem et al. (2021).

DNA extraction, PCR amplification and sequencing

Fresh mycelium was scraped from the living culture and transferred to 1.5 mL microcentrifuge tubes and kept in a refrigerator at -20 °C. Total genomic DNA was extracted using the DNA extraction kits (Sangon Biotech (Shanghai) Co. Ltd., China). DNA template amplifications were performed by Polymerase Chain Reaction (PCR) using primer pairs, ITS5/ITS4 for ITS (White et al. 1990), NS1/NS4 for SSU (White et al. 1990), LR0R/LR5 for LSU (Vilgalys and Hester 1990, Cubeta et al. 1991), and BT1/BT2b for *tub2* (Glass and Donaldson 1995). For other details pertaining to DNA extraction, PCR amplifications, sequencing, and phylogenetic analyses, see Tang et al. (2022). The polymerase chain reaction was carried out in a volume of 50 µL, and the reagents that were used were as follows: DNA template (2 µL), forward primers (2 µL), reverse primers (2 µL), 2 × Taq PCR Master Mix (25 µL) and 19 µL of ddH₂O (double-distilled water). PCR profiles are as follows: 35 cycles, and the annealing temperatures for each gene are 52 °C for 1 minute and extension at 72 °C for 90 seconds in LSU, ITS and SSU; and 55 °C for 50 s and elongation at 72 °C for 1 minute for *tub2*. Verification of PCR products was done on 1% agarose gels before being sent to China's Sangon Biotech (Shanghai) Co., Ltd. for sequencing.

Phylogenetic analyses

The forward and reverse primers of the newly generated sequence were assembled by the Contig Ex-press v3.0.0 application, and the most similar taxa were found by BLASTn (<https://blast.ncbi.nlm.nih.gov/Blast.cgi>) in NCBI. A combination of different DNA sequence data (LSU, ITS, SSU, and *tub2*), which are close hits and similar to other Tetraplospora species in GenBank (Table 1), were downloaded to be further analysed along with our new taxa. Each sequence data was aligned by the online version of MAFFT v. 7 (<https://mafft.cbrc.jp/alignment/server/index.html>) through the "auto" option (Katoh et al. 2017). Multiple genes were assembled by SequenceMatrix (Vaidya et al. 2011). The aligned sequence was trimmed by trimAl v 1.2 with the 'gappyout' option (Capella-Gutiérrez et al. 2009). The phylogenetic analyses in this study were based on the maximum likelihood (ML), and Bayesian inference (BI) by using a combined sequence dataset of LSU, ITS, SSU, and *tub2*.

Analyses under different criteria such as maximum likelihood (ML) and Bayesian inference (BI) were processed in the CIPRES web portal (Miller et al. 2010) by using the "RAxML-HPC v.8 on XSEDE" tool, and the tool "MrBayes on XSEDE", respectively (Huelsenbeck and Ronquist 2001; Swofford 2002; Stamatakis et al. 2008; Ronquist et al. 2012).

For BI, MrModeltest v2 was used for the selection of the best-fit model for each gene region. The Markov Chain Monte Carlo (MCMC) algorithm was launched with four chains running concurrently from a random tree topology. The burn-in factor was set at 25%, and the sampling interval for trees was set to every 1000th generation. The Posterior Probabilities (PP) for the remaining

Table 1. Taxa used in this study and their GenBank accession numbers for LSU, ITS, SSU and *tub2* sequence data.

Taxa name	Strain Numbers	GenBank Accession Numbers			
		LSU	SSU	ITS	<i>tub2</i>
<i>Amniculicola immersa</i>	CBS 123083T	NG_056964	NG_062796	–	–
<i>A. parva</i>	CBS 123092T	NG_056970	NG_016504	–	–
<i>Aquatisphaeria thailandica</i>	MFLUCC 21–0025T	MW890763	MW890967	MW890969	–
<i>Aq. Thailandica</i>	DLUCC B151	MW890764	MW890968	–	–
<i>Byssolophis sphaerioides</i>	IFRDCC 2053	GU301805	GU296140	–	–
<i>Ernakulamia cochinchinensis</i>	MFLUCC 18–1237	MN913716	MT864326	MT627670	–
<i>E. krabiensis</i>	MFLUCC 18–0237T	MK347990	MK347880	MK347773	–
<i>E. tanakae</i>	NFCCI 4615T	MN937211	–	MN937229	MN938312
<i>E. xishuangbannaensis</i>	KUMCC 17–0187T	MH260314	MH260354	MH275080	–
<i>Polyposphaeria fusca</i>	KT 2124	AB524607	AB524466	AB524791	AB524853
<i>Po. Fusca</i>	KT 1616T	AB524604	AB524463	AB524789	AB524851
<i>Po. guizhouensis</i>	GZCC 23–0598T	OR438888	–	OR427327	OR449118
<i>Po. Hainanensis</i>	GZCC 23–0599T	OR438889	OR438285	OR427323	OR449115
<i>Po. Hainanensis</i>	GZCC 23–0600	OR438890	–	OR427324	–
<i>Po. Thailandica</i>	MFLUCC 15–0840T	KU248767	–	KU248766	–
<i>Po. nabanheensis</i>	KUMCC 16–0151T	MH260312	MH260352	MH275078	MH412745
<i>Po. pandanicola</i>	MFLUCC 17–2266T	MH260313	MH260353	MH275079	–
<i>Pseudotetraploa bambusicola</i>	CGMCC 3.20939T	ON332933	ON332923	ON332915	–
<i>Ps. bambusicola</i>	UESTCC 22.0005	ON332934	ON332924	ON332916	–
<i>Ps. curviappendiculata</i>	JCM 12852T	AB524608	AB524467	AB524792	AB524854
<i>Ps. Javanica</i>	JCM 12854	AB524611	AB524470	AB524795	AB524857
<i>Ps. Longissima</i>	JCM 12853T	AB524612	AB524471	AB524796	AB524858
<i>Ps. rajmachiensis</i>	NFCCI 4618T	MN937204	–	MN937222	–
<i>Ps. Yunnanensis</i>	KUNCC 10464T	OR438891	–	OR449073	–
<i>Quadricrura bicornis</i>	CBS 125427T	AB524613	AB524472	AB524797	AB524859
<i>Q. meridionalis</i>	CBS 125684T	AB524614	AB524473	AB524798	AB524860
<i>Q. septentrionalis</i>	CBS 125429	AB524615	AB524474	AB524799	AB524861
<i>Shrungabeeja aquatica</i>	MFLUCC 18–0664T	MT627663	–	MT627722	–
<i>S. longiappendiculata</i>	BCC 76463T	KT376472	KT376471	KT376474	–
<i>S. longiappendiculata</i>	BCC 76464	KT376473	–	KT376475	–
<i>S. fluviatilis</i>	GZCC 20–0505T	–	–	–	–
<i>S. fluviatilis</i>	GZCC 19–0511	MW133853	MW134631	–	–
<i>S. vadirajensis</i>	MFLUCC 17–2362	MN913685	–	MT627681	–
<i>Tetraploa aquatica</i>	MFLU 19–0996	MT530453	MT530454	MT530449	–
<i>T. aquatica</i>	MFLUCC 19–0995T	MT530452	–	MT530448	–
<i>T. aristata</i>	CBS 996.70	AB524627	AB524486	AB524805	AB524867
<i>T. bambusae</i>	KUMCC 21–0844T	ON077067	ON077073	ON077078	ON075065
<i>T. dwibahubeeja</i>	NFCCI 4621T	MN937207	–	MN937225	MN938308
<i>T. dwibahubeeja</i>	NFCCI 4623	MN937208	–	MN937226	MN938309
<i>T. endophytica</i>	CBS 147114T	MW659165	–	KT270279	–
<i>T. hainanensis</i>	GZCC 23–0601T	OR438892	OR438286	OR427325	OR449116
<i>T. hainanensis</i>	GZCC 23–0602	OR438893	–	OR427326	OR449117
<i>T. juncicola</i>	CBS 149046	ON603800	–	ON603780	–
<i>T. nagasakiensis</i>	KUMCC 18–0109	MK079891	MK079888	MK079890	–
<i>T. nagasakiensis</i>	KT 1682T	AB524630	AB524489	AB524806	AB524868

Taxa name	Strain Numbers	GenBank Accession Numbers			
		LSU	SSU	ITS	<i>tub2</i>
<i>T. pseudoaristata</i>	NFCCI 4624T	MN937214	–	MN937232	MN938315
<i>T. pseudoaristata</i>	NFCCI 4625	MN937212	–	MN937230	MN938313
<i>T. puzheheiensis</i>	MFLUCC 20–0151T	MT627655	–	MT627744	–
<i>T. sasicola</i>	KT 563T	AB524631	AB524490	AB524807	AB524869
<i>T. thailandica</i>	MFLUCC 21–0030T	MZ412530	MZ413274	MZ412518	–
<i>T. thrayabahubeeja</i>	NFCCI 4627T	MN937217	–	MN937235	MN938318
<i>T. thrayabahubeeja</i>	NFCCI 4628	MN937215	–	MN937233	MN938316
<i>T. yunnanensis</i>	MFLUCC 19–0319T	MN913735	MT864341	MT627743	–
<i>T. yakushimensis</i>	KT 1906T	AB524632	AB524491	AB524808	AB524870
<i>T. cylindrica</i>	KUMCC 20–0205T	MT893204	MT893203	MT893205	MT899417
<i>T. cylindrica</i>	ZHKUCC 22–0087	ON555688	ON555690	ON555689	ON564477
<i>T. dashaoensis</i>	KUMCC 21–0010T	OL473555	OL473556	OL473549	OL505601
<i>T. obpyriformis</i>	KUMCC 21–0011T	OL473554	OL473557	OL473558	OL505600
<i>Tetraploa</i> sp.1	KT 1684	AB524628	AB524487	–	–
<i>Tetraploa</i> sp.2	KT 2578	AB524629	AB524488	–	–
<i>T. tetraploa</i>	CY112	–	–	HQ607964	–
<i>Triplosphaeria acuta</i>	KT 1170T	AB524633	AB524492	AB524809	AB524871
<i>Tr. Cylindrica</i>	NBRC 106247	AB524636	AB524495	AB524811	AB524873
<i>Tr. cylindrica</i>	KT 1800	AB524635	AB524494	AB524810	AB524872
<i>Tr. maxima</i>	KT 870T	AB524637	AB524496	AB524812	AB524874
<i>Tr. yezoensis</i>	KT 1715T	AB524638	AB524497	AB524813	AB524875
<i>Tr. yezoensis</i>	KT 1732	AB524639	AB524498	AB524814	AB524876
<i>Triplosphaeria</i> sp.	HHUF 27481	AB524640	AB524499	AB524815	AB524877
<i>Triplosphaeria</i> sp.	KT 2546	AB524641	AB524500	AB524816	AB524878

Notes: Ex-type strains are indicated by “T” at the end of the strain number, and newly generated sequences are in bold. Abbreviations: **BCC**: Biotec Culture Collection, Bangkok, Thailand; **CBS**: Westerdijk Fungal Biodiversity Institute, Utrecht, the Netherlands; **CGMCC**: China General Microbiological Culture Collection Centre, Beijing, China; **DLUCC**: Dali University Culture Collection, Yunnan, China; **GZCC**: Guizhou Culture Collection, Guizhou, China; **HHUF**: Herbaria of Hiroasaki University; **IFRDCC**: Culture Collection, International Fungal Research and Development Centre, Chinese Academy of Forestry, Kunming, China; **JCM**: the Japan Collection of Microorganisms, Japan; **KUNCC**: Kunming Institute of Botany Culture Collection; **KT**: Kazuaki Tanaka; **MFLUCC**: Mae Fah Luang University Culture Collection, Chiang Rai, Thailand; **MFLU**: Mae Fah Luang University Herbarium Collection; **NBRC**: Nite Biological Resource Center, Department of Biotechnology, National Institute of Technology and Evaluation, Japan; **NFCCI**: National Fungal Culture Collection of India NFCCI-A National Facility; **UESTCC**: University of Electronic Science and Technology Culture Collection, Chengdu, China; **ZHKUCC**: Zhongkai University of Agriculture and Engineering Culture Collection, Guangzhou, China. **A.** = *Amniculicola*. **Aq.** = *Aquatishphaeria*. **E.** = *Ernakulamia*. **Po.** = *Polyposphaeria*. **Ps.** = *Pseudotetraploa*. **Q.** = *Quadricrura*. **S.** = *Shrungabeeja*. **T.** = *Tetraploa*. **Tr.** = *Triplosphaeria*.

trees were computed. Adobe Illustrator and FigTree were used to view trees. Bootstrap support and Bayesian posterior probabilities above 70 and 0.9 were considered as high support respectively.

Results

Phylogenetic analyses

For the phylogenetic analyses, a combined DNA sequence data of 68 taxa on LSU, ITS, SSU, and *tub2* was used and analysed under the ML and PP criteria. The data matrix comprised 2995 total characters, including gaps (LSU: 1–848 bp, ITS: 849–1372 bp, SSU: 1373–2363 bp, *tub2*: 2364–2995 bp). Phylogenetic reconstructions with broadly comparable topologies were recovered from the combined dataset of ML and PP analyses. The top-scoring

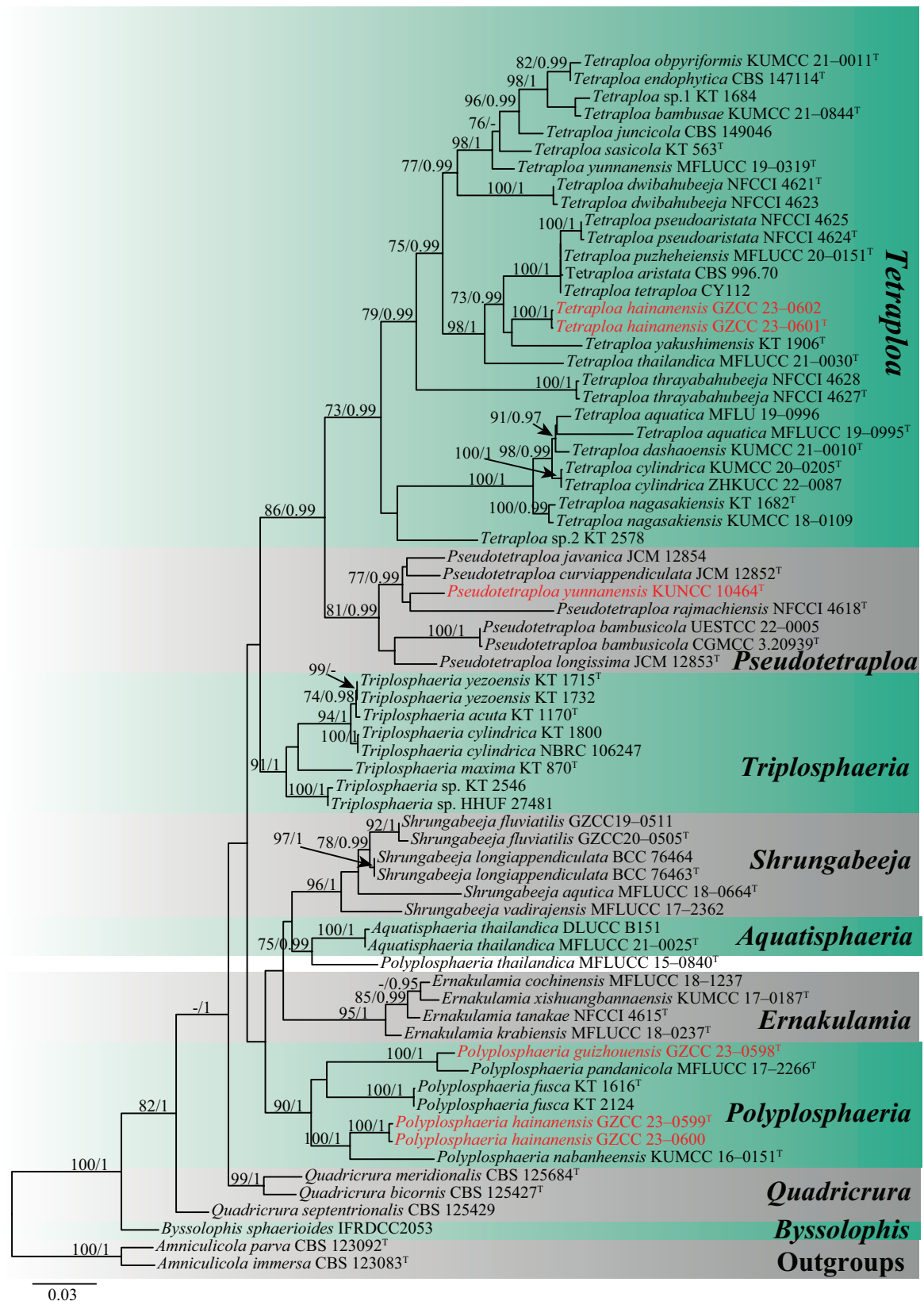


Figure 1. Phylogenetic construction of Tetraplospora using RAxML-based maximum likelihood analysis of a combined LSU, ITS, SSU, and *tub2* DNA sequence dataset. Bootstrap support values for maximum likelihood (ML) equal to or greater than 70% and Bayesian posterior probabilities (PP) equal to or greater than 0.95 PP are shown above the nodes. The tree is rooted with *Amniculicola immersa* (CBS 123083) and *A. parva* (CBS 123092). Newly generated strains are in red, and the type strains are indicated using "T" in superscript.

RAXML tree is shown in Fig. 1, with a final ML optimization likelihood value of -17569.286960 (ln). In the RAXML analysis, the GTRGAMMA+I-Invar model was used and the results showed 969 unique alignment patterns and 25.50% of indeterminate characters. Base frequency estimates were as follows: A = 0.243260, C = 0.247998, G = 0.277213, T = 0.231530; substitution rates were as follows: AC = 3.027135, AG = 4.828263, AT = 2.159193, CG = 1.385950, CT = 10.517436, GT = 1.000000; gamma distribution shape parameter alpha = 0.166037; and tree-length has been as follows: 1.837225. The best-fit models for the BPP analysis were GTR+I+G for LSU, ITS, and *tub2* gene regions; HKY+I+G for the SSU gene region. With a final average standard deviation of split frequencies of 0.009909, Bayesian posterior probabilities from MCMC were analysed. The new taxa analysed herein all belong to the Tetraplosphaeriaceae clade based on the results of the combined LSU, ITS, SSU, and *tub2* sequence data analysis.

Taxonomy

Tetraplosphaeriaceae Kaz. Tanaka & K. Hiray, Studies in Mycology 64: 177 (2009)

MycoBank No: 515253

Facesoffungi Number: FoF06665

Type genus. *Tetraploa* Berk. & Broome, Ann. Mag. Nat. Hist. 5: 459, t. 11:6 (1850).

Description. *Teleomorph* see Tanaka et al. (2009). *Anamorph* Conidiophores absent. Conidiogenous cells monoblastic. Conidia composed of 3–8 columns or internal hyphal structure, brown, mostly verrucose at the base, with more than 3–8 setose appendages (Tanaka et al. 2009).

Notes. Tetraplosphaeriaceae was described by Tanaka et al. (2009) to accommodate the species which has massarina-like teleomorphic morph and tetraploa-like anamorphs based on a combined SSU and LSU DNA sequence data and established five genera. To date, the members of Tetraplosphaeriaceae are mainly distributed on Poaceae and unidentified decayed wood as saprobes and pathogens from aquatic and terrestrial habitats (Tanaka et al. 2009; Hyde et al. 2013; Hongsanan et al. 2020; Yu et al. 2022; Li et al. 2021). It now contains nine genera and 69 species (Tanaka et al. 2009; Pem et al. 2019; Hongsanan et al. 2020; Li et al. 2021; Liao et al. 2022).

Polyposphaeria Kaz. Tanaka & K. Hirayama, Studies in Mycology 64: 192 (2009)

MycoBank No: 515256

Facesoffungi Number: FoF06668

Type species. *Polyposphaeria fusca* Kaz. Tanaka & K. Hirayama, Studies in Mycology 64: 193 (2009).

Description. *Teleomorph* see Tanaka et al. (2009). *Anamorph* Conidiophores absent. Conidiogenous cells monoblastic. Conidia globose to subglobose, with thin peel-like outer wall of conidia, composed of numerous internal hyphae at the inside, brown, almost smooth, verrucose at the base. Appendages with 3 to 8 setose appendages, brown, straight (Tanaka et al. 2009).

Notes. Tanaka et al. (2009) established *Polyposphaeria* and typified with *Po. fusca* based on a combined SSU and LSU DNA sequence data. All the members of *Polyposphaeria* were reported as saprobes from various plant hosts, such as *Pleioblastus chino*, *Phyllostachys bambusoides* and Pandanaceae (Tanaka et al. 2009; Li et al. 2016; Tibpromma et al. 2018). *Polyposphaeria* is distributed in Japan, China and Thailand in terrestrial habitats (Tanaka et al. 2009; Li et al. 2016; Tibpromma et al. 2018). Dong et al. (2020) transferred *Po. xishuangbannaensis* into *Ernakulamia* based on phylogenetic analyses and differences in morphology. In this study, two new *Polyposphaeria* species are introduced from unidentified decaying wood from China. The genus contains six species viz. *Polyposphaeria guizhouensis*, *Po. hainanensis*, *Po. fusca*, *Po. nabanheensis*, *Po. pandanicola* and *Po. thailandica* (Tanaka et al. 2009; Li et al. 2016; Tibpromma et al. 2018; This study; Table 2).

***Polyposphaeria guizhouensis* X. Tang, Jayaward., R. Jeewon & J.C. Kang, sp. nov.**

Mycobank No: 900950

Facesoffungi Number: FoF14571

Fig. 2

Etymology. The specific epithet '*guizhouensis*' refers to the place where the fungus was collected, Guizhou Province, China.

Holotype. GZAAS 23–0600.

Description. *Saprobic* on unidentified decaying wood in the forest. **Teleomorph** not observed. **Anamorph** Hyphomycetous. **Colonies** effuse, gregarious on host substrate, brown to dark brown. **Mycelium** semi-immersed or immersed, pale brown, branched, septate. **Conidiophores** absent. **Conidiogenous cells** forming directly on creeping hyphae, integrated, monoblastic, determinate. **Conidia** 34–61 × 41–63 µm (\bar{x} = 51 × 51 µm, n = 20), globose to subglobose to turbinate, solitary, olivaceous-green to brown, verrucose and darker at base, with setose appendages on surface. **Appendages** with two forms, solitary, cylindrical, unbranched, septate, smooth, brown at base and paler towards to apex, long appendages 51–152 × 3–5 µm (\bar{x} = 89 × 4.0 µm, n = 20), wide at the base, 2–6-septate, arising from apical part of conidia; short appendages 13–38 × 2.5–6 µm (\bar{x} = 25 × 4 µm, n = 20), wide at the base, 0–3-septate, arising randomly from conidial apex.

Culture characteristics. Conidia germinated on PDA and incubate at room temperature (25 °C). Colonies circular, cottony, flat, slightly grey with an undulate margin, forming three concentric zonation, margin regular, brownish grey. The reverse side is greenish grey in the centre, with a dark brown margin and pigment.

Material examined. CHINA, Guizhou Province, Xingyi City, Xianheping National Forest Park, on unidentified decaying wood, 25 September 2021, Xia Tang, xhp08 (GZAAS 23–0600, holotype), ex-type culture GZCC 23–0598.

Notes. The phylogenetic results (Fig. 1) showed that *Polyposphaeria guizhouensis* is sister to *Po. pandanicola* within *Polyposphaeria* with high support (ML = 100, BPP = 1). The comparison of pairwise nucleotides showed that *Polyposphaeria guizhouensis* is different from *Po. pandanicola* in 2/801 bp (0.2%) in LSU and 11/460 (2.5%) in ITS. Thus, we describe *Polyposphaeria guizhouensis* herein as a novel species in *Polyposphaeria* following recommendations proposed by Jeewon and Hyde (2016) and Chethana et al. (2021).



Figure 2. *Polyposphaeria guizhouensis* (GZAAS 23-0600, holotype) **a** colonies on decaying wood **b, c** colonies on natural substrates **d–n** conidia bearing appendages **o** germinating conidium **p** colony on PDA (front at right, reverse at left). Scale bars: 50 μm (**d–o**).

Table 2. Tetraplosphaeriaceae species and their country, life cycle, habitat, host and reference.

Species name	Country	Life cycle	Habitat	Host	Reference
<i>Aquatrisphaeria thailandica</i>	Thailand	saprobic	freshwater	decaying wood	Li et al. (2021)
<i>Byssolophis byssiseda</i>	France	saprobic	terrestrial	branch of <i>Carpinus</i> , decaying wood	Zhang et al. (2012)
<i>B. sphaerioides</i>	Finland, UK	saprobic	terrestrial	decaying stemp of <i>Rubus</i> , decaying wood birch	Berkeley and Broome (1854); Karsten (1870)
<i>Ernakulamia cochinchensis</i>	Argentina, Cuba, India, Japan, Malaysia, Mexico, Panama, Thailand	saprobic	freshwater, terrestrial	<i>Astrocaryum standleyanum</i> , <i>Benthamidia japonica</i> , dead leaves, dead spathes of <i>Cocos nucifera</i> , decomposing leaves of <i>Satakentia liukivensis</i> , <i>Freycinetia multi</i> , palm tree, <i>Ilex</i> sp., <i>Ocotea leucoxylon</i> , <i>Pandanus tectorius</i> , <i>P. monticola</i> , submerged wood, <i>Syagrus romanzoffiana</i> , <i>Stewartia monadelpha</i> , <i>Vitex</i> sp.	Ellis (1976); Holubová-Jechová and Mercado (1986); Holubová-Jechová (1989); Mercado et al. (1997, 2005); Taylor and Hyde (2003); Delgado and Mena (2004); Capdet and Romero (2010); Whitton et al. (2012); Delgado et al. (2017); Dong et al. (2020); Farr and Rossm (2023)
<i>E. krabiensis</i>	Thailand	saprobic	terrestrial	<i>Acacia</i> sp.	Jayasiri et al. (2019)
<i>E. tanakae</i>	India	saprobic	terrestrial	dead spathes of <i>Cocos nucifera</i>	Hyde et al. (2020a)
<i>E. xishuangbannaensis</i>	China	saprobic	terrestrial	dead leaves of <i>Pandanus</i> sp.	Tibpromma et al. (2018); Dong et al. (2020)
<i>Polyposphaeria guizhouensis</i>	China	saprobic	terrestrial	unidentified decaying wood	This study
<i>Po. Hainanensis</i>	China	saprobic	terrestrial	unidentified decaying wood	This study
<i>Po. Fusca</i>	Japan	saprobic	terrestrial	culms of <i>Chimonobambusa marmorea</i> , culms of <i>Phyllostachys bambusoides</i> , culms of <i>Pleioblastus chino</i> , culms of <i>Sasa kurilensis</i>	Tanaka et al. (2009)
<i>Po. thailandica</i>	Thailand	saprobic	terrestrial	decaying bamboo	Li et al. (2016)
<i>Po. nabanheensis</i>	China	saprobic	terrestrial	decaying leaves of <i>Pandanus</i> sp.	Tibpromma et al. (2018)
<i>Po. pandanicola</i>	China	saprobic	terrestrial	decaying leaves of <i>Pandanus</i> sp.	Tibpromma et al. (2018)
<i>Pseudotetraploa bambusicola</i>	China	saprobic	terrestrial	dead branches of Bamboo	Yu et al. (2022)
<i>Ps. curviappendiculata</i>	Japan	saprobic	terrestrial	culms of <i>Sasa kurilensis</i>	Tanaka et al. (2009)
<i>Ps. yunnanensis</i>	China	saprobic	freshwater	bamboo	This study
<i>Ps. Javanica</i>	Indonesia, Japan	saprobic	terrestrial	culms of decaying <i>Bambusa glaucescens</i> , culms of <i>Phyllostachys bambusoides</i> , culms of <i>Pleioblastus chino</i> , culms of <i>Sasa</i> sp., dead bark of broad-leaved tree, dead stems of an unidentified herbaceous plant	Hatakeyama et al. (2005); Tanaka et al. (2009); Rifai et al. (2014)
<i>Ps. longissima</i>	Japan	saprobic	terrestrial	culms of <i>Pleioblastus chino</i>	Tanaka et al. (2009)
<i>Ps. rajmachiensis</i>	India	saprobic	terrestrial	decaying bamboo culms, <i>Dendrocalamus stocksii</i> (Poaceae)	Hyde et al. (2020a)
<i>Quadricrura bicornis</i>	Japan	saprobic	terrestrial	culms of <i>Sasa kurilensis</i> , leaf litter of a conifer	Tanaka et al. (2009)
<i>Q. meridionalis</i>	Japan	saprobic	terrestrial	bamboo	Tanaka et al. (2009)
<i>Q. septentrionalis</i>	Japan	saprobic	terrestrial	culms of <i>Sasa kurilensis</i>	Tanaka et al. (2009)
<i>Shrungabeeja aquatica</i>	Thailand	saprobic	freshwater	submerged wood	Dong et al. (2020)

Species name	Country	Life cycle	Habitat	Host	Reference
<i>S. longiappendiculata</i>	Thailand	saprobic	terrestrial	dead culm of <i>Bambusa</i> sp. (Poaceae)	Ariyawansa et al. (2015)
<i>S. vadirajensis</i>	Brazil, China, India	saprobic	terrestrial	dead branches of unidentified plant	Rao and Reddy (1981); Zhang et al. (2009)
<i>S. begoniae</i>	China	saprobic	terrestrial	dead branches of <i>Begonia semperflorens</i>	Zhang et al. (2009)
<i>S. melicopes</i>	China	saprobic	terrestrial	dead branches of <i>Melicope triphylla</i>	Zhang et al. (2009)
<i>S. piepenbringiana</i>	Panama	saprobic	terrestrial	dead Poaceae	Kirschner et al. (2017)
<i>S. fluviatilis</i>	China	saprobic	freshwater	submerged decaying twig	Yang et al. (2023)
<i>Tetraploa abortiva</i>	Argentina	saprobic	freshwater	N/A	Arambarri et al. (1987)
<i>T. aquatica</i>	China	saprobic	freshwater	submerged decaying wood	Li et al. (2020)
<i>T. aristata</i>	Africa, Barbados, Bolivia, China, Cuba, Denmark, Eire, Europe, Fiji, Germany, Ghana, Hong Kong (China), India, Italy, Japan, Jamaica, Malaysia, Nepal, New Caledonia, Pakistan, Papua New Guinea (New Britain), Philippines, Puerto Rico, Sierra Leone, Thailand, The Dominican Republic, The Netherlands, Uganda, Venezuela, USA(Alabama)	pathogenic (human), saprobic	terrestrial	<i>Alpinia formosa</i> , <i>Ammophila arenaria</i> , <i>Anadelphia leptocoma</i> , <i>Andropogon</i> , <i>Angelica sylvestris</i> , <i>Avena pralensis</i> , <i>Axonopus</i> , <i>Bambusa</i> , <i>Carex paniculata</i> , <i>Cladium mariscus</i> , <i>Cladium selloana</i> , <i>Cocos</i> , <i>Cortaderia</i> , <i>Cymbopogon afronardus</i> , <i>Cyperus longus</i> , <i>Dactylis</i> , <i>Deschampsia</i> , <i>Erianthus</i> , <i>Euchlaena</i> , <i>Festuca</i> , <i>Gynerium argenteum</i> , <i>Gynerium</i> , <i>Heracleum sphondylium</i> , <i>Heteropogon</i> , <i>Hevea brasiliensis</i> , <i>Juncus</i> , <i>Musa</i> , <i>Phalaris arundinacea</i> , <i>Phaseolus</i> , <i>Phoenix</i> , <i>Phormium</i> , <i>Phragmites communis</i> , <i>Poa pratensis</i> , <i>Pteridium aquilinum</i> , <i>Saccharum officinarum</i> , <i>Sorghum</i> , straw, <i>Triticum</i> , unnamed host, wheat stubble, <i>Zea</i>	Ellis (1949, 1971); Markham et al. (1990); Tanaka et al. (2009); Senwana et al. (2021)
<i>T. bambusae</i>	China	saprobic	terrestrial	dead twigs of bamboo	Phookamsak et al. (2022)
<i>T. biformis</i>	Japan	saprobic	terrestrial	dead bark of broad-leaved tree	Matsushima and Matsushima (1996)
<i>T. circinata</i>	India	saprobic	terrestrial	decaying bamboo twig	Pratibha and Bhat (2008)
<i>T. conata</i> F	India	N/A	N/A	N/A	Saxena and Sarkar (1986); Gupta (2002)
<i>T. cylindrica</i>	China	saprobic	terrestrial	decaying stems of <i>Saccharum arundinaceum</i> (Poaceae)	Liao et al. (2022)
<i>T. dashaoensis</i>	China	saprobic	terrestrial	dead stem of <i>Saccharum arundinaceum</i>	Jayawardena et al. (2023)
<i>T. divergens</i>	USA (Mississippi)	saprobic	terrestrial	leaves of <i>Panicum agrostidiforme</i>	Tracy and Earle (1895)
<i>T. dwibahubeeja</i>	India	saprobic	terrestrial	decaying spathes of <i>Cocos nucifera</i>	Hyde et al. (2020a)
<i>T. ellisii</i>	Argentina, USA (New Jersey), Zimbabwe	saprobic	terrestrial	<i>Chloris</i> , <i>Dactylis</i> , <i>Hevea brasiliensis</i> , stalks of <i>Zea mays</i>	Cooke and Ellis (1879); Ellis (1971); Senwana et al. (2021)
<i>T. endophytica</i>	Germany	endophytic	terrestrial	roots of <i>Microthlaspi perfoliatum</i>	Crous et al. (2021)
<i>T. hainanensis</i>	China	Saprobic	terrestrial	unidentified decaying wood	This study
<i>T. indica</i> ^F	India	N/A	N/A	N/A	Saxena and Khare (1991)
<i>T. josettae</i> ^F	France	N/A	N/A	N/A	Nuñez Otaño et al. (2022)
<i>T. juncicola</i>	The Netherlands	saprobic	terrestrial	dead culm of <i>Juncus inflexus</i> (Juncaceae)	Crous et al. (2022)

Species name	Country	Life cycle	Habitat	Host	Reference
<i>T. muscicola</i>	Spain	N/A	N/A	fronds of <i>Aneura multifida</i> , <i>Lophozia quinqueidentata</i>	González Fragoso (1916)
<i>T. nagasakiensis</i>	Japan, China	saprobic	terrestrial	culms of bamboo	Hyde et al. (2013, 2019)
<i>T. obpyriformis</i>	China	saprobic	terrestrial	dead grass under <i>Saccharum arundinaceum</i> (Gramineae)	Unpublished
<i>T. opaca</i>	China	saprobic	terrestrial	dead culms of bamboo, decaying branches of unidentified tree	Zhao et al. (2009)
<i>T. pseudoaristata</i>	India	saprobic	terrestrial	decaying spathes of <i>Cocos nucifera</i> (Arecaceae)	Hyde et al. (2020a)
<i>T. puzheheensis</i>	China	saprobic	freshwater	submerged wood	Dong et al. (2020)
<i>T. sasicola</i>	China, Japan	saprobic	terrestrial	culms of <i>Sasa senanensis</i> , dead leaves of <i>Pennisetum purpureum</i> (Poaceae)	Tanaka et al. (2009); Hyde et al. (2020a)
<i>T. scabra</i>	USA	N/A	terrestrial	<i>Scirpus</i> sp.	Harkness (1885)
<i>T. scheueri</i>	UK	saprobic	freshwater, terrestrial	leaves of <i>Carex acutiformis</i> , rotten leaves	Scheuer (1991); Hyde et al. (2013)
<i>T. setifera</i>	Hungary	saprobic	terrestrial	rotten wood	Révay (1993)
<i>T. siwalika</i> ^f	N/A	N/A	N/A	N/A	Saxena et al. (1987)
<i>T. taugourdeaui</i> ^f	India	N/A	N/A	N/A	Saxena and Sarkar (1986)
<i>T. thailandica</i>	Thailand	saprobic	freshwater	Submerged decaying wood	Bao et al. (2021)
<i>T. thrayabahubeeja</i>	India	saprobic	terrestrial	decaying spathes of <i>Cocos nucifera</i> (Arecaceae)	Hyde et al. (2020a)
<i>T. yakushimensis</i>	Japan	saprobic	terrestrial	culms of <i>Arundo donax</i>	Tanaka et al. (2009); Hyde et al. (2013)
<i>T. yunnanensis</i>	China, Thailand	saprobic	freshwater	submerged wood	Dong et al. (2020)
<i>Tetraploa</i> sp. 1	Japan	saprobic	terrestrial	culms of bamboo	Tanaka et al. (2009)
<i>Tetraploa</i> sp. 2	Japan	saprobic	terrestrial	culms of Gramineae	Tanaka et al. (2009)
<i>Triplosphaeria cylindrica</i>	Japan	saprobic	terrestrial	culms of <i>Sasa kurilensis</i>	Tanaka et al. (2009)
<i>Tr. maxima</i>	Japan	saprobic	terrestrial	culms of <i>Sasa kurilensis</i>	Tanaka et al. (2009)
<i>Tr. yezoensis</i>	Japan	saprobic	terrestrial	culms of <i>Sasa palmata</i>	Tanaka et al. (2009)
<i>Tr. acuta</i>	Japan	saprobic	freshwater	submerged culms of bamboo	Tanaka et al. (2009)
<i>Triplosphaeria</i> sp.	Japan	saprobic	terrestrial	culms of <i>Sasa kurilensis</i>	Tanaka et al. (2009)

Fossil fungi were indicated "F"; N/A: Not available or cannot find; Newly species indicate in bold.

***Polyposphaeria hainanensis* X. Tang, Jayaward., R. Jeewon & J.C. Kang, sp. nov.**

MycoBank No: 900951

Facesoffungi Number: FoF14665

Figs 3, 4

Etymology. The specific epithet '*hainanensis*' refers to the place where the fungus was collected, Hainan Province, China.

Holotype. GZAAS 23–0601

Description. **Saprobic** on unidentified decaying wood in the forest. **Teleomorph** not observed. **Anamorph** Hyphomycetous. **Colonies** effuse, gregarious on host substrate, brown to blackish brown. **Mycelium** semi-immersed or immersed, dark brown, branched, septate. **Conidiophores** absent. **Conidiogenous**

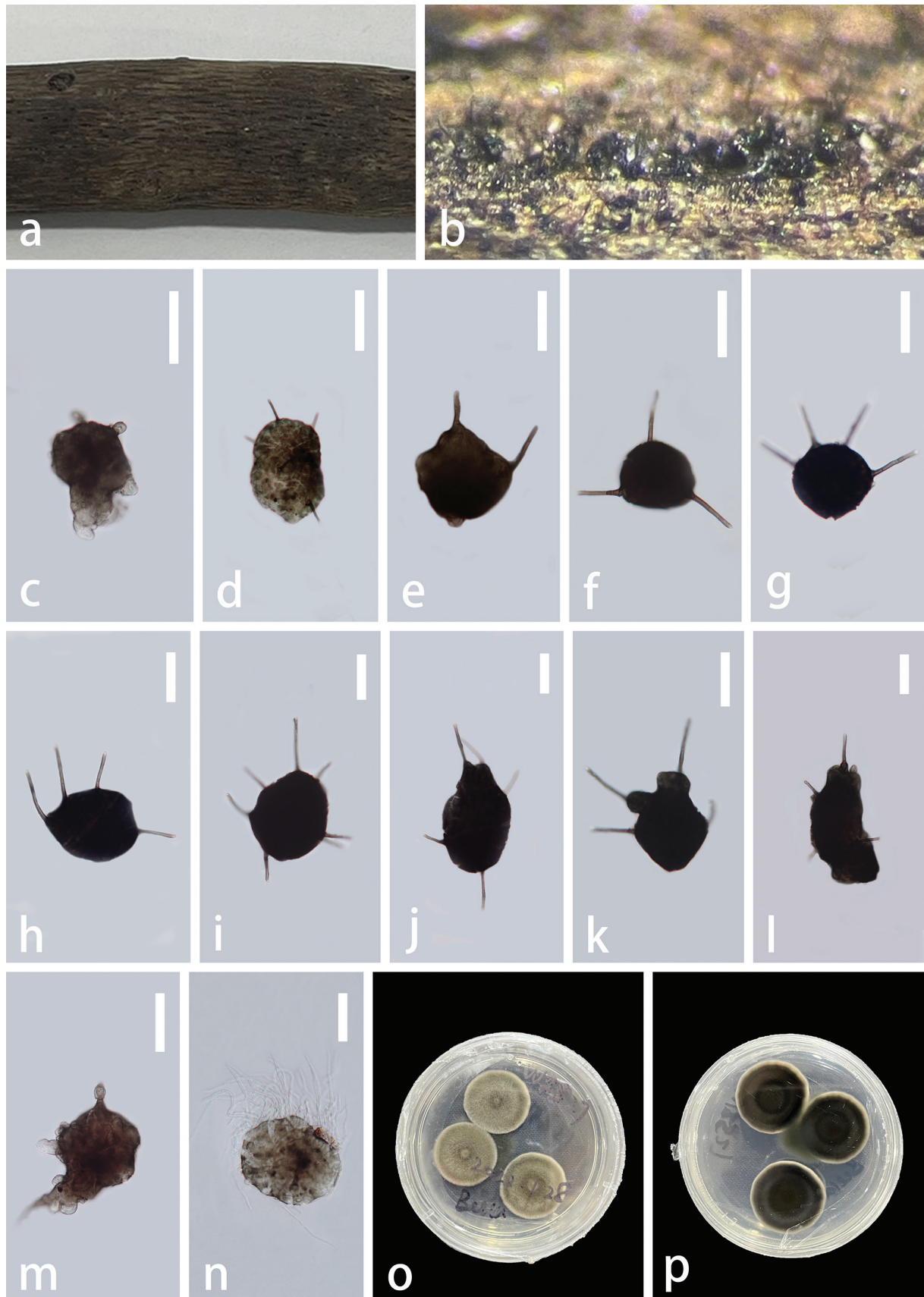


Figure 3. *Polyposphaeria hainanensis* (GZAAS 23-0601, holotype) **a** colonies on decay wood **b** colonies on natural substrates **c–m** conidia bearing appendages **n** germinating conidium **o** colony on PDA (from front) **p** colony on PDA (from reverse). Scale bars: 50 µm (**c–n**).



Figure 4. *Polyposphaeria hainanensis* (GZAAS 23-0602, paratype) **a** colonies on decay wood **b, c** colonies on natural substrates **d–o** conidia bearing appendages **p** colony on PDA (from front) **q** colony on PDA (from reverse). Scale bars: 100 μm (**d–i, k–m**); 50 μm (**j, n, o**).

cells indistinguishable from creeping hyphae, integrated, monoblastic, determinate. **Conidia** 49–134.5 × 52–90.5 μm (\bar{x} = 86 × 71 μm, n = 20), globose, subglobose, obconical, broadly ellipsoidal to broadly pyriform, variable in shape, sometimes with thin peel on the outer wall of conidia, internally filled with a mass of hyaline, solitary, brown to dark brown, smooth. **Appendages** 36–58 × 3–5.5 μm (\bar{x} = 44.5 × 4 μm, n = 20), cylindrical, solitary, straight or flexuous, unbranched and almost hyaline at the apex, 0–4-septate, smooth, round at apex, pervasive.

Culture characteristics. Conidia germinated from both ends on PDA and incubated at room temperature (25 °C). Colonies circular, cottony, flat, olivaceous with a slightly grey entire margin. The reverse side is an olive drab, which gradually extends outwards to form a deep colour ring in the centre with a pale grey margin and no pigment.

Material examined. CHINA, Hainan Province, Wuzhishan City, Wuzhishan National Nature Reserve, on unidentified decaying wood, 25 September 2021, Zili Li, WZS27 (GZAAS 23–0601, holotype), ex-type culture GZCC 23–0599; WZS31 (GZAAS 23–0602, paratype), culture GZCC 23–0600.

Notes. Based on the phylogenetic analysis (Fig. 1), two of our *Polyposphaeria* collections share similar morphology and clustered together with high support (ML = 100, and BPP = 1). The base pair differences between the two strains (GZCC 23–0599 and GZCC 23–0600) were: LSU = 0.2% (2/834), ITS = 0.1% (1/840), respectively, therefore, we considered them as the same species according to the guidelines for species delineation proposed by Jeewon and Hyde (2016). The phylogenetic result (Fig.1) showed that *Polyposphaeria hainanensis* is sister to *Po. nabanheensis* within *Polyposphaeria*. Based on the comparison of the morphological characters with other species in *Polyposphaeria*, our collection can be distinct in having obconical, broadly ellipsoidal to broadly pyriform, variable conidial shape (without verrucose at the base) and pervasive appendages. The comparison of pairwise nucleotides showed that *Polyposphaeria hainanensis* is different from *Po. nabanheensis* in 24/826 bp (3%) in LSU, 20/758 (2.6%) in SSU, 17/472 (3.6%) in ITS and 16/344 (5%) in *tub2*. Thus, we describe *Polyposphaeria hainanensis* herein as a novel species in *Polyposphaeria* according to the guidelines of Jeewon and Hyde (2016) and Chethana et al. (2021).

***Pseudotetraploa* Kaz. Tanaka & K. Hirayama, Studies in Mycology 64: 193 (2009)**

MycoBank No: 515257

Facesoffungi Number: FoF06669

Type species. *Pseudotetraploa curviappendiculata* (Sat. Hatak., Kaz. Tanaka & Y. Harada) Kaz. Tanaka & K. Hirayama, Studies in Mycology 64: 195 (2009).

Description. **Teleomorph morph** not observed. **Anamorph Mycelium** superficial. **Conidiophores** absent. **Conidiogenous cells** monoblastic, indistinguishable from creeping hyphae. **Conidia** composed of 4 to 8 columns, obpyriform to long obpyriform, brown to dark brown, almost smooth, verrucose at the base, pseudoseptate, with setose appendages at the apical part. **Appendages** mostly 4, rarely 6 to 8, curved or straight (Tanaka et al. 2009).

Notes. Tanaka et al. (2009) established *Pseudotetraploa* (Ps.) with three species, which were previously described in *Tetraploa* and typified by *Ps. curviappendiculata* based on a combined SSU and LSU DNA sequence data. *Pseudotetraploa* species

are reported as saprobes on bamboo, dead bark of the broad-leaved tree, and unidentified herbaceous plants in Japan, China, and India (Hatakeyama et al. 2005; Tanaka et al. 2009; Hyde et al. 2020a; Yu et al. 2022). *Pseudotetraploa* is only known in its anamorphic state and dwells in terrestrial habitats and contains six species viz. *Ps. bambusicola*, *Ps. curviappendiculata*, *Ps. javanica*, *Ps. longissima*, *Ps. Rajmachiensis*, and *Ps. yunnanensis* (Hatakeyama et al. 2005; Tanaka et al. 2009; Hyde et al. 2020a; Yu et al. 2022; This study; Table 2). In this study, a new *Pseudotetraploa* species isolated from bamboo is introduced.

***Pseudotetraploa yunnanensis* X. Tang, Jayaward., R. Jeewon & J.C. Kang, sp. nov.**

MycoBank No: 900963

Facesoffungi Number: FoF14666

Fig. 5

Etymology. The specific epithet '*yunnanensis*' refers to the place where the fungus was collected, Yunnan Province, China.

Holotype. HKAS 129442.

Description. *Saprobic* on bamboo. *Teleomorph* not observed. *Anamorph* Hyphomycetous. **Colonies** effuse, gregarious on host substrate, brown to dark brown. **Mycelium** superficial, hyaline to pale brown. **Conidiophores** absent. **Conidiogenous cells** micronematous, mononematous, monoblastic, integrated, usually undistinguishable from superficial hyphae. **Conidia** 67–120 × 16.5–35 µm (\bar{x} = 95 × 24 µm, n = 20), solitary, septate, brown to dark brown, ovoid to obclavate or narrowly obpyriform, consisting of 3–6 columns of cells, rounded at the base 19–36 µm wide (\bar{x} = 26 µm, n = 20), slightly constricted at septa, rarely branched and make V-shaped conidia; setose appendages at the apical part 15–87 × 3.5–7 µm (\bar{x} = 37 × 5 µm, n = 20), appendages 3–6 in number, 1–8-septate, brown at the base and almost hyaline at the apex, smooth, unbranched, shorter appendage is straight and longer appendage is curved.

Culture characteristics. Conidia germinated from both ends on PDA and incubated at room temperature (25 °C). Colonies circular, cottony, flat, slightly grey with an entire margin, containing a circular white mycelium in the centre. The reverse side is a pale brown in the centre that gradually extends outwards while the colour changes to pale grey, with a brown margin and no pigment.

Material examined. CHINA, Yunnan Province, Puer City, Ailao mountains, on bamboo, May 23, 2022, Rong-Ju Xu, ALS 29 (HKAS 129442, holotype), ex-type culture KUNCC 10464.

Notes. *Pseudotetraploa yunnanensis* is similar to *Ps. curviappendiculata* and *Ps. longissima*. However, *Pseudotetraploa yunnanensis* differs from *Ps. curviappendiculata* in having branched and V-shaped conidia, consisting of 3–6 columns of cells with 3–6 apical appendages, larger conidia [67–120 µm vs. 52–67(–75) µm] in length and [16–35 µm vs. 15–22 µm] in width, while *Ps. curviappendiculata* consists of 4–5 columns of cells with 4 apical appendages; *Pseudotetraploa yunnanensis* differs from *Ps. longissima* in having smaller conidia [67–120 µm vs. (98–)110–148(–155) µm] in length and [16–35 µm vs. 18–25 µm] in width, without verrucose at the base. The phylogenetic analysis showed that *Pseudotetraploa yunnanensis* is sister to *Ps. rajmachiensis* and *Ps. javanica*. The comparison of



Figure 5. *Pseudotetraploa yunnanensis* (HKAS 129442, holotype) **a, b** colonies on natural substrates **c–n** conidia. Scale bars: 20 μm (**c**); 50 μm (**d–n**).

pairwise nucleotides showed that *Pseudotetraploa yunnanensis* is different from *Ps. rajmachiensis* in 27/1021 bp (2.6%) in LSU and 30/560 (6%) in ITS; *Pseudotetraploa yunnanensis* is different from *Ps. javanica* in 11/1020 bp (1.1%) in LSU and 17/538 (3.2%) in ITS. Thus, we describe *Pseudotetraploa yunnanensis* herein as a novel species in *Pseudotetraploa* according to the guidelines Jeewon and Hyde (2016) and Chethana et al. (2021).

***Tetraploa* Berk. & Broome, Ann. Mag. Nat. Hist. 5: 459, t. 11:6 (1850)**

MycoBank No: 10199

Facesoffungi Number: FoF06666

= *Tetraplosphaeria* Kaz. Tanaka & K. Hiray., in Tanaka et al., Stud. Mycol. 64: 177 (2009).

Type species. *Tetraploa aristata* Berk. & Broome, Ann. Mag. Nat. Hist. 5: 459 (1850).

Description. **Teleomorph** see Tanaka et al. (2009). **Anamorph *Tetraploa*** sensu stricto **Conidiophores** absent. **Conidiogenous cells** monoblastic. **Conidia** composed of 4 columns, short-cylindrical, brown, verrucose at the base, euseptate, with 4 setose appendages at the apex (Tanaka et al. 2009).

Notes. Tanaka et al. (2009) established *Tetraplosphaeria* to accommodate pleosporalean species that have massarina/lophiostoma-like teleomorph and anamorphs belonging to *Tetraploa* sensu stricto based on a combined SSU and LSU DNA sequence data. Later, Hyde et al. (2013) treated *Tetraploa* as a synonym of *Tetraplosphaeria*, which has been applied previously to anamorphic species and used *Tetraploa* instead of *Tetraplosphaeria*. Species of *Tetraploa* are mainly reported as saprobes, distributed in freshwater and terrestrial habitats, and only *T. aristata* has been reported as a pathogen on various plants and human pathogen that cause cysts (Markham et al. 1990; Tanaka et al. 2009; Hyde et al. 2013; Liao et al. 2022). *Tetraploa* has been recovered from more than 80 plants, such as bamboo culms, submerged wood, palms, and *Poaceae*, on the leaves of *Acer* and liverworts (Ellis 1949; Ando 1992; Hyde et al. 2013; Liao et al. 2022). Saxena et al. (2021) mentioned that *Frasnacritetrus* is probably a fossil of *Tetraploa*. Nuñez Otaño et al. (2022) considered *Frasnacritetrus* as a synonym of *Tetraploa* and transferred five *Frasnacritetrus* fossil species into *Tetraploa* viz. *Tetraploa conata*, *T. indica*, *T. josettae*, *T. siwalika* and *T. taugourdeau* based on the observation that the spores of both fossil and contemporary species exhibit identical morphological characteristics. To date, there are 35 species accepted in *Tetraploa* (Wijayawardene et al. 2022; Jayawardena et al. 2023; this study; Table 2). In this study, a new *Tetraploa* species is introduced.

***Tetraploa hainanensis* X. Tang, Jayaward., R. Jeewon & J.C. Kang, sp. nov.**

MycoBank No: 900952

Facesoffungi Number: FoF14667

Figs 6, 7

Etymology. The specific epithet '*hainanensis*' refers to the place where the fungus was collected, Hainan Province, China.

Holotype. GZAAS 23–0603.

Description. **Saprobic** on unidentified decaying wood in forest. **Teleomorph** Not observed. **Anamorph** Hyphomycetous. **Colonies** effuse, gregarious on host substrate, brown to dark brown. **Mycelium** semi-immersed or immersed, pale brown, branched, septate. **Conidiophores** absent. **Conidiogenous cells** integrated, monoblastic, determinate. **Conidia** 30–46 × 18–36 µm (\bar{x} = 38 × 27 µm, n = 20), cylindrical with obtuse ends, pale brown to brown, verrucose, composed of four columns of cells, sometimes five columns of cells, 4–5-septate in each

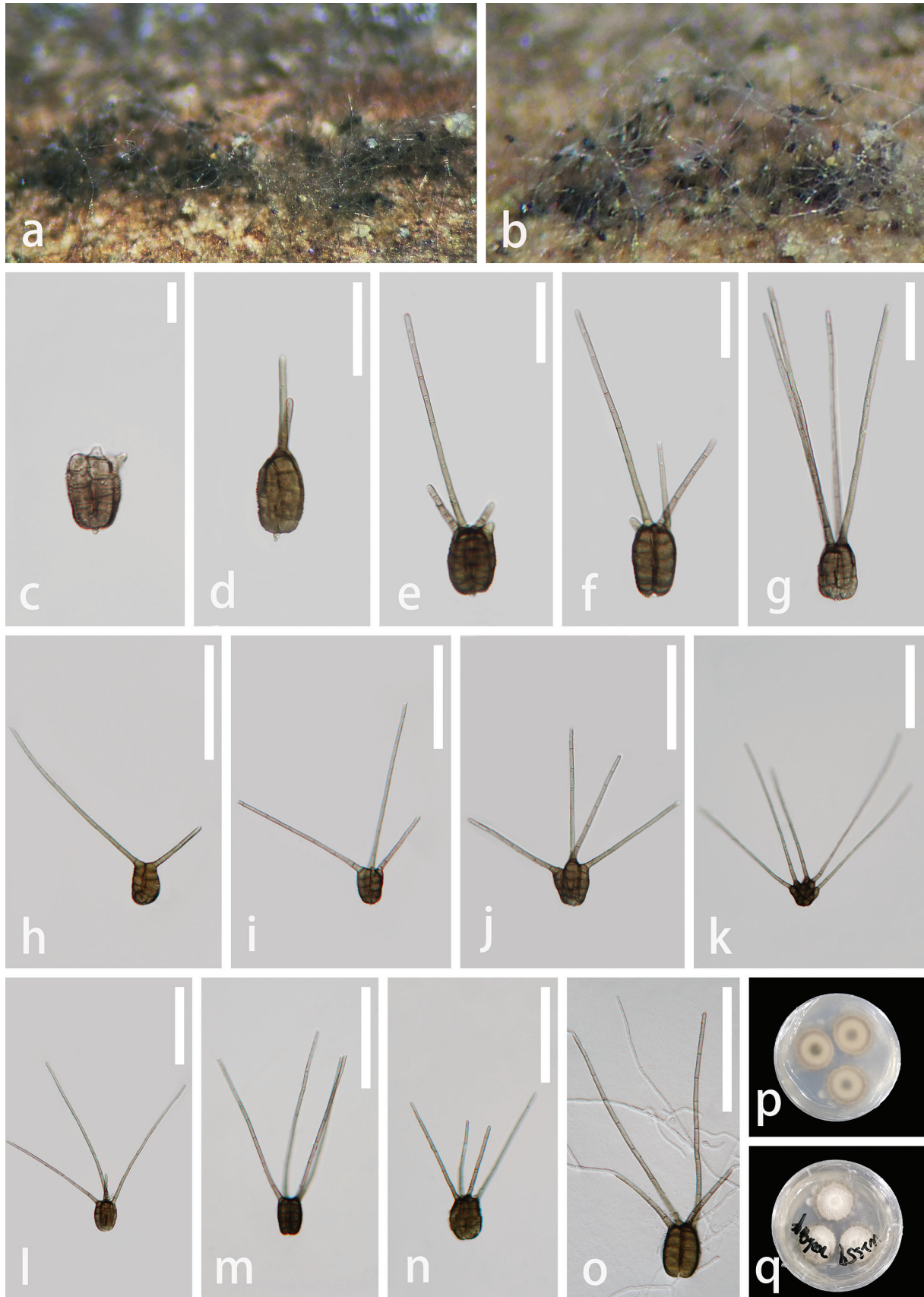


Figure 6. *Tetraploa hainanensis* (GZAAS 23-0603, holotype) **a, b** colonies on natural substrates **c-n** conidia bearing 1–5 appendages **o** germinating conidium **p** colony on PDA (from reverse) **q** colony on PDA (from front). Scale bars 20 μm (**c**); 50 μm (**d-g**); 100 μm (**h-o**).

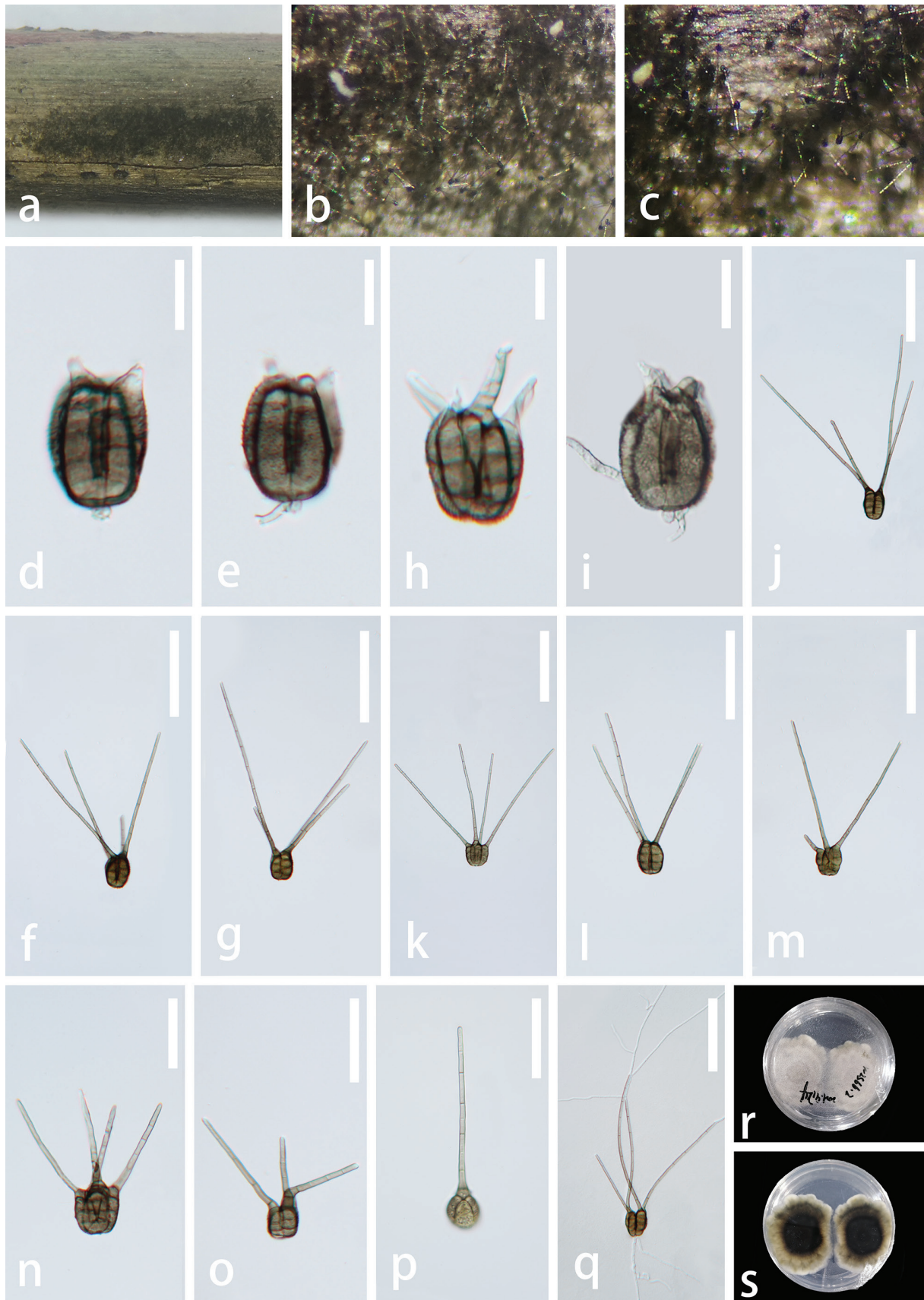


Figure 7. *Tetraploa hainanensis* (GZAAS 23-0604, paratype) **a** colonies on decay wood **b, c** colonies on natural substrates **d–p** conidia bearing 1–4 appendages **q** germinating conidium **r** colony on PDA (from front) **s** colony on PDA (from reverse). Scale bars: 20 μm (**d–g**); 100 μm (**h–l, o, q**); 50 μm (**m, n, p**).

column, smooth, mostly with four apical appendages, some with one or two or five appendages. **Appendages** 52–209 × 3–6 μm (\bar{x} = 140 × 4 μm, n = 20) cylindrical, solitary, unbranched, guttulate, septate, wide at the base, divergent, pale brown to brown, 5–16-septate, straight or slightly flexuous, smooth-walled.

Culture characteristics. Conidia germinated from both ends on PDA and incubated at room temperature (25 °C). Colonies circular, cottony, flat, slightly grey with an entire margin, contain a circular white mycelium in the centre. The reverse side is a pale brown in the centre that gradually extends outwards while the colour changes to pale grey, with a brown margin and no pigment.

Material examined. CHINA, Hainan Province, Wuzhishan City, Wuzhishan National Nature Reserve, on unidentified decaying wood, 25 September 2021, Zili Li, WZS59 (GZAAS 23–0603, holotype), ex-type culture GZCC 23–0601; WZS66.2 (GZAAS 23–0604, paratype), culture GZCC 23–0602.

Notes. *Tetraploa hainanensis* is morphologically similar to *T. pseudoaristata*. However, *Tetraploa hainanensis* can be distinguished from *T. pseudoaristata* in having larger conidia (30.5–46 × 18–36 μm vs. 22–31 × 15–20 μm) with four columns of cells, sometimes five columns of cells, and longer appendages (52–209 × 3–6 μm vs. 23–107 × 2–5 μm), commonly four in number, sometimes five. Based on the phylogenetic analysis, two of our *Tetraploa* collections which share similar morphology clustered together with high support (ML = 100, and BPP = 1 (Fig. 1)). The base pair differences between the two strains were: LSU = 0.1% (1/806), ITS = 0% (0/516), and *tub2* = 0% (1/633), respectively. Therefore, we considered them as the same species according to the guidelines for species delineation proposed by Jeewon and Hyde (2016). *Tetraploa hainanensis* forms a distinct lineage but close to *T. yakushimensis* and *T. tetraploa*. However, *Tetraploa hainanensis* differs from *T. yakushimensis* by having four or five columns and appendages, while *T. yakushimensis* has only four columns and appendages; *Tetraploa hainanensis* differs from *T. tetraploa* in having four or five columns and shorter appendages (52–209 × 3–6 μm vs. 263–350 × 2–3 μm), while *T. tetraploa* has only four columns and slender appendages. The comparison of pairwise nucleotide showed that *Tetraploa hainanensis* is different from *T. yakushimensis* in 31/620 bp (3%) in LSU, 7/814 (0.98%) in ITS, and 87/450 (19%) in *tub2* and *Tetraploa hainanensis* is different from *T. tetraploa* in 31/620 bp (3%) in LSU, 7/814 (0.98%) in ITS, and 87/450 (19%) in *tub2*. Based on the combination of morphological characters and multigene phylogeny, we describe *Tetraploa hainanensis* herein as a distinct species according to the guidelines of Jeewon and Hyde (2016) and Chethana et al. (2021).

Discussion

Hyde et al. (2018) reported that more than 95% of fungi collected in northern Thailand could be new to science and there is a dire need to collect more samples from a wide variety of hosts to better understand fungal diversity estimates. In the same way, fungal diversity in Yunnan, Guizhou and Hainan is expected to be rather high. In this study, collections of decayed wood samples and bamboo were done to assess which fungal species are potentially colonising them. Our study reveals four anamorphic fungal species that belong to the family Tetraplosphaeriaceae. In this study, we characterise two new anamorphic species collected from unidentified decayed wood samples that belong to *Polypliosphaeria*. In *Polypliosphaeria* this study brings the number of species to

six. The first new species is described as *Po. guizhouensis* and our multigene phylogeny depict a close relationship to *Po. pandanicola*. The latter was collected from fallen dead and decaying leaves of *Pandanus* sp. in China (Tibpromma et al. 2018) and characterized by micronematous conidiophores; monoblastic, incomplete globose connected to base of conidia conidiogenous cell with guttules, hyaline; globose to subglobose, solitary, verrucose at base conidia with almost hyaline at apex, unbranched setose appendages on surface. However, *Po. guizhouensis* differs in having turbinate conidia which are verrucose and darker at the base. Furthermore, it possesses a longer conidium base and two types of appendages originating from the apical part of the conidia. With regard to DNA sequence data comparison, *Po. guizhouensis* differs from *Po. pandanicola* (MFLUCC 17–2266) in having 11 out of 460 (2.5%) and 2 out of 801 (0.2%) different base pairs (bp) in the ITS alignments and LSU gene respectively. Our second new species, named *Polyposphaeria hainanensis*, forms a strongly supported subclade with *Po. nabanheensis*. The latter was collected from fallen dead and decaying leaves of *Pandanus* sp. in China (Tibpromma et al. 2018). It is characterised by monoblastic, hyaline conidiogenous cells with guttules; oval to ellipsoid conidia, made up of 2–3 cells, and verrucose at base, rough-walled, with apical setose appendages. However, *Po. hainanensis* differs with regards to having an obconical, broadly ellipsoidal to broadly pyriform, variable shaped conidia (no verrucose at the base) and pervasive appendages. Comparison of available LSU, ITS, SSU and *tub2* sequences also reveal differences in base pairs that support species distinctiveness. For instance, *Po. hainanensis* differs from *Po. nabanheensis* in having 24/826 bp (3% difference) in LSU, 20/758 (2.6% difference) in SSU, 17/472 (3.6% difference) in ITS and 16/344 (5% difference) in *tub2*. Another peculiar finding when we analysed the relationships of *Polyposphaeria* species, we found that two strains of *Polyposphaeria thailandica* (MFLU 15–3273) and *Aquatisphaeria thailandica* (MFLUCC 21–0025 and DLUCC B151) clustered together with 75% ML/0.99 BPP support and sister to species of *Shrungabeeja*. However, it's important to note that this relationship lacked significant statistical support, a pattern observed in various previous studies as well (Li et al. 2021; Liao et al. 2022). *Aquatisphaeria thailandica* has been reported as a saprobe on submerged decaying wood in China. It is characterised by macronematous, mononematous, solitary, unbranched conidiophores with 3–4 septa; monoblastic, integrated, terminal, subcylindrical conidiogenous cells; and acrogenous, solitary, subglobose or turbinate, muriform, dictyoseptate conidia with 3–4 (mostly 4) cylindrical, upward appendages with 1–2-septa. At the same time, *Po. thailandica* is recognised as a saprobe found in decaying bamboo in Thailand. It is characterised by monoblastic conidiogenous cells; acrogenous, solitary, globose, obovoid, pyriform, ellipsoidal, obconical, muriform, verrucose conidia with 2–5-septate appendages, occasionally, two conidia are associated together at the basal cell (Li et al. 2016; Li et al. 2020). Based on the phylogenetic analyses, it seems that *Po. thailandica* is a member of *Aquatisphaeria*. There is not much taxonomic data available for *Aquatisphaeria*, hence we recommend that further collections of this genus are required to elucidate its relationships to *Po. thailandica*. Alternatively, there might be a need to relook into the taxonomy of *Po. thailandica* and verify whether the DNA sequences submitted are reliable.

The third anamorphic species was collected from bamboo in Yunnan, China and subsequently assigned to *Pseudotetraploa*. To date, five species have been

reported, and this study extends the known species count to six. The new species is described as *Ps. yunnanensis* and our multigene phylogeny depicts a close relationship to *Ps. rajmachiensis*. The latter was collected from decaying bamboo culms in India (Hyde et al. 2020a) and characterised by the absence of conidiophores; micronematous, mononematous, monoblastic conidiogenous cells; ovoid to obclavate or obpyriform conidia, minutely verrucose at the base; unbranched, septate, setose appendages at the apical part, consisting of two appendages with one straight and one curved. However, *Ps. yunnanensis* differs in having larger conidia that rarely separate, consisting of 3–6 columns of cells, forming a V-shape conidia, 3–6 apical appendages. In terms of DNA sequence data comparison, *Ps. yunnanensis* differs from *Ps. rajmachiensis* (NFCCI 4618) in LSU by 27/1021 bp (2.6% difference) and in ITS by 30/560 bp (6% difference).

The last anamorphic species was collected from unidentified decaying wood in Hainan, China, and was assigned to *Tetraploa*. With the addition of this species, the genus now comprises a total of 35 species. The new species is described as *T. hainanensis*, and the multigene phylogeny depicts a close relationship to *T. yakushimensis*. The latter was collected on culms of *Arundo donax* in Japan (Tanaka et al. 2009) and characterised by the absence of conidiophores; monoblastic conidiogenous cells; solitary, short cylindrical, brown, verruculose conidia, composed of 4 columns with 4 apical setose appendages. However, *T. hainanensis* differs in having four or five culms and appendages. In terms of DNA sequence data comparison, *T. hainanensis* differs from *T. yakushimensis* (KT 1906) in 31/620 bp (3% difference) in LSU, 7/814 (0.98% difference) in ITS, and 87/450 (19% difference) in *tub2*.

Tetraplosphaeriaceae is a well-known family in terrestrial habitats with mostly saprobes being reported so far, and previous and recent studies have shown that Tetraplosphaeriaceae is widely associated with many plants in different countries. In this work, we describe four new Tetraplosphaeriaceae species based on phylogenetic and morphological comparisons with allied taxa, update the phylogeny of the Tetraplosphaeriaceae family and also provide a checklist of species with other details (Table 2). To date, there are 69 species in Tetraplosphaeriaceae, of which 23 species (including this study) are from China. This study enriches the diversity of fungi in China of Tetraplosphaeriaceae species.

Acknowledgements

The authors are grateful to Shaun Pennycook for his suggestions on naming the new fungus. In addition, the authors also would like to thank Mae Fah Luang University for its support in the tuition fee scholarship. This work was supported by the Distinguished Scientist Fellowship Program (DSFP) at King Saud University, Riyadh, Saudi Arabia.

Additional information

Conflict of interest

The authors have declared that no competing interests exist.

Ethical statement

No ethical statement was reported.

Funding

This work was funded by grants from the National Natural Science Foundation of China (NSFC Grants Nos. 32170019 & 31460011) and the Open Fund Program of Engineering Research Centre of Southwest Bio-Pharmaceutical Resources, Ministry of Education, Guizhou University No. GZUKEY20160702. The authors are grateful to the Thailand Research Fund grant “Impact of climate change on fungal diversity and biogeography in the Greater Mekong Sub-region” (RDG6130001).

Author contributions

Xia Tang conducted the experiments, analysed the data, and wrote the first draft of the manuscript. Rajesh Jeewon, Yong-Zhong Lu, Ruvishika S. Jayawardena and Ji-Chuan Kang planned the experiments. Xia Tang, Jian Ma and Rong-Ju Xu analysed the data. Xia Tang and Xue-Mei Chen conducted the experiments. Rajesh Jeewon, Yong-Zhong Lu, Ruvishika S. Jayawardena, Abdulwahed Fahad Alrefaei and Ji-Chuan Kang corrected and revised the manuscript. Yong-Zhong Lu and Ji-Chuan Kang funded the experiments. All authors revised and agreed to the published version of the manuscript.

Author ORCIDs

Xia Tang  <https://orcid.org/0000-0003-2705-604X>

Rajesh Jeewon  <https://orcid.org/0000-0002-8563-957X>

Yong-Zhong Lu  <https://orcid.org/0000-0002-1033-5782>

Abdulwahed Fahad Alrefaei  <https://orcid.org/0000-0002-3761-6656>

Ruvishika S. Jayawardena  <https://orcid.org/0000-0001-7702-4885>

Rong-Ju Xu  <https://orcid.org/0000-0002-3968-8442>

Jian Ma  <https://orcid.org/0009-0008-1291-640X>

Xue-Mei Chen  <https://orcid.org/0009-0004-8631-0735>

Ji-Chuan Kang  <https://orcid.org/0000-0002-6294-5793>

Data availability

All of the data that support the findings of this study are available in the main text. DNA sequences generated have been submitted to Genbank.

References

- Ando K (1992) A study of terrestrial aquatic hyphomycetes. *Nippon Kingakkai Kaiho* 33: 415–425. [In Japanese]
- Arambarri A, Cabello M, Mengascini A (1987) New hyphomycetes from Santiago River. II. (Buenos Aires Province, Argentina). *Mycotaxon* 30: 263–267.
- Ariyawansa HA, Hyde KD, Jayasiri SC, Buyck B, Chethana KWT, Dai DQ, Dai YC, Daranagama DA, Jayawardena RS, Lücking R, Ghobad-Nejhad M, Niskanen T, Thambugala KM, Voigt K, Zhao RL, Li GJ, Doilom M, Boonmee S, Yang ZL, Cai Q, Cui YY, Bahkali AH, Chen J, Cui BK, Chen JJ, Dayarathne MC, Dissanayake AJ, Ekanayaka AH, Hashimoto A, Hongsanan S, Jones EBG, Larsson E, Li WJ, Li QR, Liu JK, Luo ZL, Maharachchikumbura SSN, Mapook A, McKenzie EHC, Norphanphoun C, Konta S, Pang KL, Perera RH, Phookamsak R, Phukhamsakda C, Pinruan U, Randrianjohany E, Singtripop C, Tanaka K, Tian CM, Tibpromma S, Abdel-Wahab MA, Wanasinghe DN, Wijayawardene NN, Zhang JF, Zhang H, Abdel-Aziz FA, Wedin M, Westberg M, Ammirati JF, Bulgakov TS, Lima DX, Callaghan TM, Callac P, Chang CH, Coca LF, Dal-Forno M, Dollhofer V, Fliiegerová K, Greiner K, Griffith GW, Ho HM, Hofstetter V, Jeewon R, Kang JC, Wen TC, Kirk PM, Kytövuori I, Lawrey JD,

- Xing J, Li H, Liu ZY, Liu XZ, Liimatainen K, Lumbsch HT, Matsumura M, Moncada B, Nuankaew S, Parnmen S, de Azevedo Santiago ALCM, Sommai S, Song Y, de Souza CAF, de Souza-Motta CM, Su HY, Suetrong S, Wang Y, Wei SF, Wen TC, Yuan HS, Zhou LW, Réblová M, Fournier J, Camporesi E, Luangsa-ard JJ, Tasanathai K, Khonsanit A, Thanakitpipattana D, Somrithipol S, Diederich P, Millanes AM, Common RS, Stadler M, Yan JY, Li X, Lee HW, Nguyen TTT, Lee HB, Battistin E, Marsico O, Vizzini A, Vila J, Ercole E, Eberhardt U, Simonini G, Wen HA, Chen XH, Miettinen O, Spirin V, Hernawati (2015) Fungal diversity notes 111–252 – Taxonomic and phylogenetic contributions to fungal taxa. *Fungal Diversity* 75(1): 27–274. <https://doi.org/10.1007/s13225-015-0346-5>
- Bao DF, Hyde KD, McKenzie EHC, Jeewon R, Su HY, Nalumpang S, Luo ZL (2021) Biodiversity of lignicolous freshwater hyphomycetes from China and Thailand and description of sixteen species. *Journal of Fungi (Basel, Switzerland)* 7(8): 669. <https://doi.org/10.3390/jof7080669>
- Berkeley MJ, Broome CE (1854) XLIII. – Notices of British Fungi. *Annals & Magazine of Natural History* 13(78): 458–469. <https://doi.org/10.1080/03745485709495104>
- Capdet M, Romero AI (2010) Fungi from palms in Argentina. 1. *Mycotaxon* 112(1): 339–355. <https://doi.org/10.5248/112.339>
- Capella-Gutiérrez S, Silla-Martínez JM, Gabaldón T (2009) trimAl: A tool for automated alignment trimming in large-scale phylogenetic analyses. *Bioinformatics (Oxford, England)* 25(15): 1972–1973. <https://doi.org/10.1093/bioinformatics/btp348>
- Chen WH, Han YF, Liang JD, Liang ZQ (2021) Taxonomic and phylogenetic characterizations reveal four new species of *Simplicillium* (Cordycipitaceae, Hypocreales) from Guizhou, China. *Scientific Reports* 11(1): 15300. <https://doi.org/10.1038/s41598-021-94893-z>
- Chethana KWT, Manawasinghe IS, Hurdeal VG, Bhunjun CS, Appadoo MA, Gentekaki E, Raspé O, Promputtha I, Hyde KD (2021) What are fungal species and how to delineate them? *Fungal Diversity* 109(1): 1–25. <https://doi.org/10.1007/s13225-021-00483-9>
- Cooke MC, Ellis JB (1879) New Jersey fungi. *Grevillea* 8(45): 11–16. <https://doi.org/10.1086/326617>
- Crous PW, Cowan DA, Maggs-Kölling G, Yilmaz N, Thangavel R, Wingfield MJ, Noordeloos ME, Dima B, Brandrud TE, Jansen GM, Morozova OV, Vila J, Shivas RG, Tan YP, Bishop-Hurley S, Lacey E, Marney TS, Larsson E, Le Floch G, Lombard L, Nodet P, Hubka V, Alvarado P, Berraf-Tebbal A, Reyes JD, Delgado G, Eichmeier A, Jordal JB, Kachalkin AV, Kubátová A, Maciá-Vicente JG, Malysheva EF, Papp V, Rajeshkumar KC, Sharma A, Spetik M, Szabóová D, Tomashevskaya MA, Abad JA, Abad ZG, Alexandrova AV, Anand G, Arenas F, Ashtekar N, Balashov S, Bañares Á, Baroncelli R, Bera I, Biketova AY, Blomquist CL, Boekhout T, Boertmann D, Bulyonkova TM, Burgess TI, Carnegie AJ, Cobo-Diaz JF, Corriol G, Cunnington JH, da Cruz MO, Damm U, Davoodian N, de A Santiago ALCM, Dearnaley J, de Freitas LWS, Dhileepan K, Dimitrov R, Di Piazza S, Fatima S, Fuljer F, Galera H, Ghosh A, Giraldo A, Glushakova AM, Gorczak M, Gouliamova DE, Gramaje D, Groenewald M, Gansch CK, Gutiérrez A, Holdom D, Houbraken J, Ismailov AB, Istel Ł, Iturriaga T, Jeppson M, Jurjević Ž, Kalinina LB, Kapitonov VI, Kautmanová I, Khalid AN, Kiran M, Kiss L, Kovács Á, Kurose D, Kušan I, Lad S, Læssøe T, Lee HB, Luangsa-ard JJ, Lynch M, Mahamedi AE, Malysheva VF, Mateos A, Matočec N, Mešić A, Miller AN, Mongkolsamrit S, Moreno G, Morte A, Mostowfizadeh-Ghahamfarsa R, Naseer A, Navarro-Ródenas A, Nguyen TTT, Noisripoom W, Ntandu JE, Nuytinck J, Ostrý V, Pankratov TA, Pawłowska J, Pecenka J, Pham THG, Polhorský A, Pošta A, Raudabaugh DB, Reschke K, Rodríguez A, Romero M, Rooney-Latham S, Roux J, Sandoval-Denis M, Smith MTh, Steinrücken TV, Svetasheva TY, Tkalčec Z, van der Linde EJ, Vegte Mvd, Vauras J, Verbeken A, Visagie CM, Vitelli JS, Volobuev SV, Weill A, Wrzosek M,

- Zmitrovich IV, Zvyagina EA, Groenewald JZ (2021) Fungal Planet description sheets: 1182–1283. *Persoonia* 46: 313. <https://doi.org/10.3767/persoonia.2021.46.11>
- Crous PW, Boers J, Holdom D, Osieck ER, Steinrucken TV, Tan YP, Vitelli JS, Shivas RG, Barrett M, Boxshall A-G, Broadbridge J, Larsson E, Lebel T, Pinruan U, Sommai S, Alvarado P, Bonito G, Decock CA, De la Peña-Lastra S, Delgado G, Houbaken J, Maciá-Vicente JG, Raja HA, Rigueiro-Rodríguez A, Rodríguez A, Wingfield MJ, Adams SJ, Akulov A, AL-Hidmi T, Antonín V, Arauzo S, Arenas F, Armada F, Aylward J, Bellanger J-M, Berraf-Tebbal A, Bidaud A, Boccardo F, Cabero J, Calleda F, Corriol G, Crane JL, Dearnaley JDW, Dima B, Dovana F, Eichmeier A, Esteve-Raventós F, Fine M, Ganzert L, García D, Torres-García D, Gené J, Gutiérrez A, Iglesias P, Istel Ł, Jangsantear P, Jansen GM, Jeppson M, Karun NC, Karich A, Khamsuntorn P, Kokkonen K, Kolarik M, Kubátová A, Labuda R, Lagashetti AC, Lifshitz N, Linde C, Loizides M, Luangsa-ard JJ, Lueangjaroenkit P, Mahadevakumar S, Mahamedi AE, Malloch DW, Marinowicz S, Mateos A, Moreau P-A, Miller AN, Molia A, Morte A, Navarro-Ródenas A, Nebesářová J, Nigrone E, Nuthan BR, Oberlies NH, Pepori AL, Rämä T, Rapley D, Reschke K, Robicheau BM, Roets F, Roux J, Saavedra M, Sakolrak B, Santini A, Ševčíková H, Singh PN, Singh SK, Somrithipol S, Spletik M, Sridhar KR, Starink-Willemse M, Taylor VA, van Iperen AL, Vauras J, Walker AK, Wingfield BD, Yarden O, Cooke AW, Manners AG, Pegg KG, Groenewald JZ (2022) Fungal Planet description sheets: 1383–1435. *Persoonia* 48(1): 261–371. <https://doi.org/10.3767/persoonia.2022.48.08>
- Cubeta MA, Echandi E, Abernethy T, Vilgalys R (1991) Characterization of anastomosis groups of binucleate *Rhizoctonia* species using restriction analysis of an amplified ribosomal RNA gene. *Phytopathology* 81(11): 1395–1400. <https://doi.org/10.1094/Phyto-81-1395>
- Delgado G, Koukol O, Cáceres O, Piepenbring M (2017) The phylogenetic placement of *Ernakulamia cochinchinensis* within Pleosporales (Dothideomycetes, Ascomycota). *Cryptogamie. Mycologie* 38(4): 435–452. <https://doi.org/10.7872/crym/v38.iss4.2017.435>
- Delgado-Rodríguez G, Mena-Portales J (2004) Hifomicetos (hongos anamórficos) de la reserva ecológica “Alturas de Banao” (Cuba). *Boletín de la Sociedad Micológica de Madrid* 28: 115–124.
- Dissanayake AJ, Chen YY, Liu JK (2020) Unravelling *Diaporthe* species associated with woody hosts from karst formations (Guizhou) in China. *Journal of Fungi (Basel, Switzerland)* 6(4): 251. <https://doi.org/10.3390/jof6040251>
- Dong W, Wang B, Hyde KD, McKenzie EHC, Raja HA, Tanaka K, Abdel-Wahab MA, Abdel-Aziz FA, Doilom M, Phookamsak R, Hongsanan S, Wanasinghe DN, Yu XD, Wang GN, Yang H, Yang J, Thambugala KM, Tian Q, Luo ZL, Yang JB, Miller AN, Fournier J, Boonmee S, Hu DM, Nalumpang S, Zhang H (2020) Freshwater Dothideomycetes. *Fungal Diversity* 105(1): 319–575. <https://doi.org/10.1007/s13225-020-00463-5>
- Ellis MB (1949) *Tetraploa*. *Transactions of the British Mycological Society* 32(3–4): 246–251. [https://doi.org/10.1016/S0007-1536\(49\)80013-1](https://doi.org/10.1016/S0007-1536(49)80013-1)
- Ellis MB (1971) Dematiaceous hyphomycetes. *Dematiaceous hyphomycetes*.
- Ellis RP (1976) A procedure for standardizing comparative leaf anatomy in the Poaceae. I. The leaf-blade as viewed in transverse section. *Bothalia* 12(1): 65–109. <https://doi.org/10.4102/abc.v12i1.1382>
- Farr DF, Rossman AY (2023) Fungal Databases, US National Fungus Collections, ARS, USDA. 2020. <https://nt.ars-grin.gov/fungaldatabases/> [Accession date: 9 August, 2023]
- Feng B, Yang Z (2018) Studies on diversity of higher fungi in Yunnan, southwestern China: A review. *Plant Diversity* 40(4): 165–171. <https://doi.org/10.1016/j.pld.2018.07.001>
- Glass NL, Donaldson GC (1995) Development of primer sets designed for use with the PCR to amplify conserved genes from filamentous ascomycetes. *Applied*

- and Environmental Microbiology 61(4): 1323–1330. <https://doi.org/10.1128/aem.61.4.1323-1330.1995>
- González Frago R (1916) Hongos sobre muscineas. Boletín de la Real Sociedad Española de Historia Natural 16: 367–370.
- Gupta A (2002) Algal/fungal spores from Early Tertiary sediments of Sirmour District, Himachal Pradesh, India. Tertiary Research 21(1/4): 128–154.
- Hapuarachchi KK, Karunarathna SC, Raspé O, De Silva KH, Thawthong A, Wu XL, Kakumyan P, Hyde KD, Wen TC (2018) High diversity of *Ganoderma* and *Amauroderma* (Ganodermataceae, Polyporales) in Hainan Island, China. Mycosphere: Journal of Fungal Biology 9(5): 931–982. <https://doi.org/10.5943/mycosphere/9/5/1>
- Harkness HW (1885) Fungi of the Pacific Coast. Bulletin of the California Academy of Sciences 1(3): 159–176.
- Hatakeyama S, Tanaka K, Harada Y (2005) Bambusicolous fungi in Japan (5): Three species of *Tetraploa*. Mycoscience 46(3): 196–200. <https://doi.org/10.1007/S10267-005-0233-0>
- Holubová-Jechová V, Mercado-Sierra A (1986) Studies on Hyphomycetes from Cuba IV. Dematiaceous Hyphomycetes from the Province PinardelRio. Česká Mykologie 40: 142–164.
- Holubová-Jechová V (1989) Hyphomycetes from Loma de la Coca and some localities of La Habana and Matanzas provinces, Cuba. Acta Botánica Cubana 76: 1–15.
- Hongsanan S, Hyde KD, Phookamsak R, Wanasinghe DN, McKenzie EHC, Sarma VV, Boonmee S, Lücking R, Bhat DJ, Liu NG, Tennakoon DS, Pem D, Karunarathna A, Jiang SH, Jones EBG, Phillips AJL, Manawasinghe IS, Tibpromma S, Jayasiri SC, Sandamali DS, Jayawardena RS, Wijayawardene NN, Ekanayaka AH, Jeewon R, Lu YZ, Dissanayake AJ, Zeng XY, Luo ZL, Tian Q, Phukhamsakda C, Thambugala KM, Dai DQ, Chethana KWT, Samarakoon MC, Ertz D, Bao DF, Doilom M, Liu JK (2020) Refined families of Dothideomycetes: Dothideomycetidae and Pleosporomycetidae. Mycosphere: Journal of Fungal Biology 11(1): 1553–2107. <https://doi.org/10.5943/mycosphere/11/1/13>
- Huang SK, Maharachchikumbura SSN, Jeewon R, Bhat JD, Phookamsak R, Hyde KD, Al-Sadi AM, Kang JC (2018) *Lecanicillium subprimulinum* (Cordycipitaceae, Hypocreales), a novel species from Baoshan, Yunnan. Phytotaxa 348(2): 99–108. <https://doi.org/10.11646/phytotaxa.348.2.4>
- Huang T, Su LJ, Zeng NK, Lee SM, Lee SS, Thi BK, Zhang WH, Ma J, Huang HY, Jiang S, Tang LP (2023) Notes on *Amanita* section Validae in Hainan Island, China. Frontiers in Microbiology 13: 1087756. <https://doi.org/10.3389/fmicb.2022.1087756>
- Huelsenbeck JP, Ronquist F (2001) MRBAYES: Bayesian inference of phylogenetic trees. Bioinformatics (Oxford, England) 17(8): 754–589. <https://doi.org/10.1093/bioinformatics/17.8.754>
- Hyde KD, Jones G, Liu JK, Ariyawansa H, Boehm E, Boonmee S, Braun U, Chomnunti P, Crous PW, Dai DQ, Diederich P, Dissanayake A, Doilom M, Doveri F, Hongsanan S, Jayawardena R, Lawrey JD, Li YM, Liu YX, Lücking R, Monkai J, Muggia L, Nelsen MP, Pang KL, Phookamsak R, Senanayake IC, Shearer CA, Suetrong S, Tanaka K, Thambugala KM, Wijayawardene NN, Wikee S, Wu HX, Zhang Y, Aguirre-Hudson B, Alias SA, Aptroot A, Bahkali AH, Bezerra JL, Bhat DJ, Camporesi E, Chukeatirote E, Gueidan C, Hawksworth DL, Hirayama K, Hoog SD, Kang JC, Knudsen K, Li WJ, Li XH, Liu ZY, Mapook A, McKenzie EHC, Miller AN, Mortimer PE, Phillips AJL, Raja HA, Scheuer C, Schumm F, Taylor JE, Tian Q, Tibpromma S, Wanasinghe DN, Wang Y, Xu JC, Yacharoen S, Yan JY, Zhang M (2013) Families of Dothideomycetes. Fungal Diversity 63(1): 1–313. <https://doi.org/10.1007/s13225-013-0263-4>

- Hyde KD, Norphanphoun C, Chen J, Dissanayake AJ, Doilom M, Hongsanan S, Jayawardena RS, Jeewon R, Perera RH, Thongbai B, Wanasinghe DN, Wisitrassameewong K, Tibpromma S, Stadler M (2018) Thailand's amazing diversity: Up to 96% of fungi in northern Thailand may be novel. *Fungal Diversity* 93(1): 215–239. <https://doi.org/10.1007/s13225-018-0415-7>
- Hyde KD, Tennakoon DS, Jeewon R, Bhat DJ, Maharachchikumbura SS, Rossi W, Leonardi M, Lee HB, Mun HY, Houbraken J, Nguyen TTT, Jeon SJ, Frisvad JC, Wanasinghe DN, Lücking R, Aptroot A, Cáceres MES, Karunarathna SC, Hongsanan S, Phookamsak R, de Silva NI, Thambugala KM, Jayawardena RS, Senanayake IC, Boonmee S, Chen J, Luo ZL, Phukhamsakda C, Pereira OL, Abreu VP, Rosado AWC, Bart B, Randrianjohany E, Hofstetter V, Gibertoni TB, da Silva Soares AM, Plautz Jr HL, Sotão HMP, Xavier WKS, Bezerra JDP, de Oliveira TGL, de Souza-Motta CM, Magalhães OMC, Bundhun D, Harishchandra D, Manawasinghe IS, Dong W, Zhang SN, Bao DF, Samarakoon MC, Pem D, Karunarathna A, Lin CG, Yang J, Perera RH, Kumar V, Huang SK, Dayarathne MC, Ekanayaka AH, Jayasiri SC, Xiao YP, Konta S, Niskanen T, Liimatainen K, Dai YC, Ji XH, Tian XM, Mešić A, Singh SK, Phutthacharoen K, Cai L, Sorvongxay T, Thiyagaraja V, Norphanphoun C, Chaiwan N, Lu YZ, Jiang HB, Zhang JF, Abeywickrama PD, Aluthmuhandiram JVS, Brahmanage RS, Zeng M, Chethana T, Wei DP, Réblová M, Fournier J, Nekvindová J, Barbosa RDN, dos Santos JEF, de Oliveira NT, Li GJ, Ertz D, Shang QJ, Phillips AJL, Kuo CH, Camporesi E, Bulgakov TS, Lumyong S, Jones EBG, Chomnunti P, Gentekaki E, Bungartz F, Zeng XY, Fryar S, Tkalčec Z, Liang J, Li GS, Wen TC, Singh PN, Gafforov Y, Promptuttha I, Yasanthika E, Goonasekara ID, Zhao RL, Zhao Q, Kirk PM, Liu JK, Yan JY, Mortimer PE, Xu JC, Doilom M (2019) Fungal diversity notes 1036–1150: Taxonomic and phylogenetic contributions on genera and species of fungal taxa. *Fungal Diversity* 96(1): 1–242. <https://doi.org/10.1007/s13225-019-00429-2>
- Hyde KD, Dong Y, Phookamsak R, Jeewon R, Bhat DJ, Jones EBG, Liu NG, Abeywickrama PD, Mapook A, Wei D, Perera RH, Manawasinghe IS, Pem D, Bundhun D, Karunarathna A, Ekanayaka AH, Bao DF, Li J, Samarakoon MC, Chaiwan N, Lin CG, Phutthacharoen K, Zhang SN, Senanayake IC, Goonasekara ID, Thambugala KM, Phukhamsakda C, Tennakoon DS, Jiang HB, Yang J, Zeng M, Huanraluek N, Liu JK, Wijesinghe SN, Tian Q, Tibpromma S, Brahmanage RS, Boonmee S, Huang SK, Thiyagaraja V, Lu YZ, Jayawardena RS, Dong W, Yang EF, Singh SK, Singh SM, Rana S, Lad SS, Anand G, Devadatha B, Niranjana M, Sarma VV, Liimatainen K, Aguirre-Hudson B, Niskanen T, Overall A, Alvarenga RLM, Gibertoni TB, Pfliegler WP, Horváth E, Imre A, Alves AL, da Silva Santos AC, Tiago PV, Bulgakov TS, Wanasinghe DN, Bahkali AH, Doilom M, Elgorban AM, Maharachchikumbura SSN, Rajeshkumar KC, Haelewaters D, Mortimer PE, Zhao Q, Lumyong S, Xu JC, Sheng J (2020a) Fungal diversity notes 1151–1276: Taxonomic and phylogenetic contributions on genera and species of fungal taxa. *Fungal Diversity* 100(1): 5–277. <https://doi.org/10.1007/s13225-020-00439-5>
- Hyde KD, Norphanphoun C, Maharachchikumbura SSN, Bhat DJ, Jones EBG, Bundhun D, Chen YJ, Bao DF, Boonmee S, Calabon MS, Chaiwan N, Chethana KWT, Dai DQ, Dayarathne MC, Devadatha B, Dissanayake AJ, Dissanayake LS, Doilom M, Dong W, Fan XL, Goonasekara ID, Hongsanan S, Huang SK, Jayawardena RS, Jeewon R, Karunarathna A, Konta S, Kumar V, Lin CG, Liu JK, Liu NG, Luangsa-ard J, Lumyong S, Luo ZL, Marasinghe DS, McKenzie EHC, Niego AGT, Niranjana M, Perera RH, Phukhamsakda C, Rathnayaka AR, Samarakoon MC, Sama-rakoon SMBC, Sarma VV, Senanayake IC, Shang QJ, Stadler M, Tibpromma S, Wanasinghe DN, Wei DP, Wijaya-wardene NN, Xiao YP, Yang J, Zeng XY, Zhang SN, Xiang MM (2020b) Refined families of Sordariomycetes. *Mycosphere: Journal of Fungal Biology* 11(1): 306–1060. <https://doi.org/10.5943/mycosphere/11/1/7>

- Index Fungorum (2023) The Index Fungorum database. <http://www.indexfungorum.org> [Accessed June 24, 2023]
- Jayasiri SC, Hyde KD, Ariyawansa HA, Bhat J, Buyck B, Cai L, Dai YC, Abd-Elsalam KA, Ertz D, Hidayat I, Jeewon R, Jones EBG, Bahkali AH, Karunarathna SC, Liu JK, Luangsa-ard JJ, Lumbsch HT, Maharachchikumbura SSN, McKenzie EHC, Moncalvo JM, Ghobad-Nejhad M, Nilsson H, Pang KL, Pereira OL, Phillips AJL, Raspé O, Rollins AW, Romero AI, Etayo J, Selçuk F, Stephenson SL, Suetrong S, Taylor JE, Tsui CKM, Vizzini A, Abdel-Wahab MA, Wen TC, Boonmee S, Dai DQ, Daranagama DA, Dissanayake AJ, Ekanayaka AH, Fryar SC, Hongsanan S, Jayawardena RS, Li WJ, Perera RH, Phookamsak R, de Silva NI, Thambugala KM, Tian Q, Wijayawardene NN, Zhao RL, Zhao Q, Kang JC, Promputtha I (2015) The Faces of Fungi database: Fungal names linked with morphology, phylogeny and human impacts. *Fungal Diversity* 74(1): 3–18. <https://doi.org/10.1007/s13225-015-0351-8>
- Jayasiri SC, Hyde KD, Jones EBG, McKenzie EHC, Jeewon R, Phillips AJL, Bhat DJ, Wannasinghe DN, Liu JK, Lu YZ, Kang JC, Xu JC, Karunarathna SC (2019) Diversity, morphology and molecular phylogeny of Dothideomycetes on decaying wild seed pods and fruits. *Mycosphere* 10(1): 1–186. <https://doi.org/10.5943/mycosphere/10/1/1>
- Jayawardena RS, Hyde KD, Wang S, Sun YR, Suwannarach N, Sysouphanthong P, Abdel-Wahab MA, Abdel-Aziz FA, Abeywickrama PD, Abreu VP, Armand A, Aptroot A, Bao DF, Begerow D, Bellanger JM, Bezerra JDP, Bundhun D, Calabon MS, Cao T, Cantillo T, Carvalho JLVR, Chaiwan N, Chen CC, Courtecuisse R, Cui BK, Damm U, Denchev CM, Denchev TT, Deng CY, Devadatha B, de Silva NI, Santos LA, Dubey NK, Dumez S, Fernandez HS, Firmino AL, Gafforov Y, Gajanayake AJ, Gomdola D, Gunaseelan S, He SC, Htet ZH, Kaliyaperumal M, Kemler M, Kezo K, Kularathnage ND, Leonardi M, Li JP, Liao CF, Liu S, Loizides M, Luangharn T, Ma J, Madrid H, Mahadevakumar S, Maharachchikumbura SSN, Manamgoda DS, Martín MP, Mekala N, Moreau P-A, Mu YH, Pahoua P, Pem D, Pereira OL, Phonrob W, Phukhamsakda C, Raza M, Ren GC, Rinaldi AC, Rossi W, Samarakoon BC, Samarakoon MC, Sarma VV, Senanayake IC, Singh A, Souza MF, Souza-Motta CM, Spielmann AA, Su WX, Tang X, Tian XG, Thambugala KM, Thongklang N, Tennakoon DS, Wannathes N, Wei DP, Welti S, Wijesinghe SN, Yang HD, Yang YH, Yuan HS, Zhang H, Zhang JY, Balasuriya A, Bhunjun CS, Bulgakov TS, Cai L, Camporesi E, Chomnunti P, Deepika YS, Doilom M, Duan WJ, Han SL, Huanraluek N, Gareth Jones EB, Lakshmidevi N, Li Y, Lumyong S, Luo ZL, Khuna S, Kumla J, Manawasinghe IS, Mapook A, Punyaboon W, Tibpromma S, Lu YZ, Yan JY, Wang Y (2023) Fungal diversity notes 1512–1610: Taxonomic and phylogenetic contributions on genera and species of fungal taxa. *Fungal Diversity* 117(1): 1–272. <https://doi.org/10.1007/s13225-022-00513-0>
- Jeewon R, Hyde KD (2016) Establishing species boundaries and new taxa among fungi: Recommendations to resolve taxonomic ambiguities. *Mycosphere* 7(11): 1669–1677. <https://doi.org/10.5943/mycosphere/7/11/4>
- Jeewon R, Cai L, Zhang K, Hyde KD (2003) *Dyrithiopsis lakefuxianensis* gen et sp. nov. from Fuxian Lake, Yunnan, China and notes on the taxonomic confusion surrounding *Dyrithium*. *Mycologia* 95(5): 911–920. <https://doi.org/10.1080/15572536.2004.11833050>
- Karsten PA (1870) *Symbolae ad mycologiam Fennicam*. I. Notiser ur Sällskapetets pro Fauna et Flora Fennica Förhandlingar. 11: 211–268.
- Katoh K, Rozewicki J, Yamada KD (2017) MAFFT online service: Multiple sequence alignment, interactive sequence choice and visualization. *Briefings in Bioinformatics* 20(4): 1160–1166. <https://doi.org/10.1093/bib/bbx108>
- Kirschner R, Villarreal RV, Hofmann TA (2017) A new species of *Shrungabeeja* (Tetraplosphaeriaceae) and new records of saprobic dematiaceous hyphomycetes on Poaceae from the high mountains of Panama. *Sydowia* 69: 153–160.

- Li WL, Bao DF, Bhat DJ, Su HY (2020) *Tetraploa aquatica* (Tetraplosphaeriaceae), a new freshwater fungal species from Yunnan Province, China. *Phytotaxa* 459(2): 181–189. <https://doi.org/10.11646/phytotaxa.459.2.8>
- Li HJ, He SH, Cui BK (2010) *Polypores* from Bawangling Nature Reserve, Hainan Province. *Junwu Xuebao* 29(6): 828–833.
- Li GJ, Hyde KD, Zhao RL, Hongsanan S, Abdel-Aziz FA, Abdel-Wahab MA, Alvarado P, Alves-Silva G, Ammirati JF, Ariyawansa HA, Baghela A, Bahkali AH, Beug M, Bhat DJ, Bojantchev D, Boonpratuang T, Bulgakov TS, Camporesi E, Boro MC, Ceska O, Chakraborty D, Chen JJ, Chethana KWT, Chomnunti P, Consiglio G, Cui BK, Dai DQ, Dai YC, Daranagama DA, Das K, Dayarathne MC, De Crop E, De Oliveira RJV, de Souza CAF, de Souza JI, Dentinger BTM, Dissanayake AJ, Doilom M, Drechsler-Santos ER, Ghobad-Nejhad M, Gilmore SP, Góes-Neto A, Gorczak M, Haitjema CH, Hapuarachchi KK, Hashimoto A, He MQ, Henske JK, Hirayama K, Iribarren MJ, Jayasiri SC, Jayawardena RS, Jeon SJ, Jerônimo GH, Jesus AL, Jones EBG, Kang JC, Karunarathna SC, Kirk PM, Konta S, Kuhnert E, Langer E, Lee HS, Lee HB, Li WJ, Li XH, Liimatainen K, Lima DX, Lin CG, Liu JK, Liu XZ, Liu ZY, Luangsa-ard JJ, Lücking R, Lumbsch HT, Lumyong S, Leaño EM, Marano AV, Matsumura M, McKenzie EHC, Mongkolsamrit S, Mortimer PE, Nguyen TTT, Niskanen T, Norphanphoun C, O'Malley MA, Parmen S, Pawłowska J, Perera RH, Phookamsak R, Phukhamsakda C, Pires-Zottarelli CLA, Raspé O, Reck MA, Rocha SCO, de Santiago ALCMA, Senanayake IC, Setti L, Shang QJ, Singh SK, Sir EB, Solomon KV, Song J, Srikitikulchai P, Stadler M, Suetrong S, Takahashi H, Takahashi T, Tanaka K, Tang LP, Thambugala KM, Thanakitpipattana D, Theodorou MK, Thongbai B, Thummarukcharoen T, Tian Q, Tibpromma S, Verbeken A, Vizzini A, Vlasák J, Voigt K, Wanasinghe DN, Wang Y, Weerakoon G, Wen HA, Wen TC, Wijayawardene NN, Wongkanoun S, Wrzosek M, Xiao YP, Xu JC, Yan JY, Yang J, Da Yang S, Hu Y, Zhang JF, Zhao J, Zhou LW, Peršoh D, Phillips AJL, Maharachchikumbura SSN (2016) Fungal diversity notes 253–366: Taxonomic and phylogenetic contributions to fungal taxa. *Fungal Diversity* 78(1): 1–237. <https://doi.org/10.1007/s13225-016-0366-9>
- Li WL, Bao DF, Liu NG, Hyde KD, Liu JK (2021) *Aquatisphaeria thailandica* gen. et sp. nov. (Tetraplosphaeriaceae, Pleosporales) from freshwater habitat in Thailand. *Phytotaxa* 513(2): 118–128. <https://doi.org/10.11646/phytotaxa.513.2.3>
- Liao CF, Dong W, Chethana KT, Pem D, Phookamsak R, Suwannarach N, Doilom M (2022) Morphological and phylogenetic evidence reveal *Tetraploa cylindrica* sp. nov. (Tetraplosphaeriaceae, Pleosporales) from *Saccharum arundinaceum* (Poaceae) in Yunnan Province, China. *Phytotaxa* 554(2): 189–200. <https://doi.org/10.11646/phytotaxa.554.2.7>
- Luo ZL, Bhat DJ, Jeewon R, Boonmee S, Bao DF, Zhao YC, Hong-Mei Chai HM, Su HY, Su XJ, Hyde KD (2017) Molecular phylogeny and morphological characterization of asexual fungi (Tubeufiaceae) from freshwater habitats in Yunnan, China. *Cryptogamie. Mycologie* 38(1): 27–53. <https://doi.org/10.7872/crym/v38.iss1.2017.27>
- Luo ZL, Hyde KD, Bhat DJ, Jeewon R, Maharachchikumbura SS, Bao DF, Li WL, Su XJ, Yang XY, Su HY (2018) Morphological and molecular taxonomy of novel species Pleurotheciaceae from freshwater habitats in Yunnan, China. *Mycological Progress* 17(5): 511–530. <https://doi.org/10.1007/s11557-018-1377-6>
- Markham WD, Key RD, Padhye AA, Ajello L (1990) Phaeohyphomycotic cyst caused by *Tetraploa aristata*. *Medical Mycology* 28(2): 147–150. <https://doi.org/10.1080/02681219080000191>
- Matsushima K, Matsushima T (1996) *Fragmenta Mycologica II*. *Matsushima Mycological Memoirs* 9: 31–40.

- Mercado-Sierra A, González-Fraginals G, Mena-Portales J, Rodríguez-Morejón K (1997) Las Palmas y su relación como sustratos de Hongos Microscópicos (Hifomicetes) en Cuba. *Boletín de la Sociedad Micológica de Madrid* 22: 33–44.
- Miller MA, Pfeiffer W, Schwartz T (2010) Creating the CIPRES Science Gateway for inference of large phylogenetic trees. 2010 Gateway Computing Environments Workshop (GCE). Institute of Electrical and Electronics Engineers, New Orleans, LA, 1–8. <https://doi.org/10.1109/GCE.2010.5676129>
- Mortimer PE, Jeewon R, Xu JC, Lumyong S, Wanasinghe DN (2021) Morpho-phylo taxonomy of novel dothideomycetous fungi associated with dead woody twigs in Yunnan Province, China. *Frontiers in Microbiology* 12: 654683. <https://doi.org/10.3389/fmicb.2021.654683>
- Nuñez Otaño NB, Bianchinotti MV, Romero IC, Perez Pincheira E, Saxena RK, Saparrat MCN (2022) Fossil *Tetraploa* redefinition and potential contribution of dark pigments for the preservation of its spores in the fossil record. *Mycosphere* 13(1): 188–206. <https://doi.org/10.5943/mycosphere/si/1f/6>
- Pem D, Jeewon R, Bhat DJ, Doilom M, Boonmee S, Hongsanan S, Promputtha I, Xu JC, Hyde KD (2019) *Mycosphere Notes* 275–324: A morphotaxonomic revision and typification of obscure Dothideomycetes genera (incertae sedis). *Mycosphere* 10(1): 1115–1246. <https://doi.org/10.5943/mycosphere/10/1/22>
- Pem D, Jeewon R, Chethana KWT, Hongsanan S, Doilom M, Suwannarach N, Hyde KD (2021) Species concepts of Dothideomycetes: Classification, phylogenetic inconsistencies and taxonomic standardization. *Fungal Diversity* 109(1): 283–319. <https://doi.org/10.1007/s13225-021-00485-7>
- Phookamsak R, Jiang HB, Suwannarach N, Lumyong S, Xu JC, Xu S, Liao CF, Chomnunti P (2022) Bambusicolous fungi in pleosporales: Introducing four novel taxa and a new habitat record for *Anastomitrabeculia didymospora*. *Journal of Fungi* (Basel, Switzerland) 8(6, no. 630): 1–35. <https://doi.org/10.3390/jof8060630>
- Pratibha J, Bhat DJ (2008) New and unusual fungi from Mahabaleshwar, India. *Mycotaxon* 105: 423–431.
- Rao VG, Reddy KA (1981) Two new Hyphomycetes. *Iranian Journal of Botany* 4(1): 108–114.
- Révay A (1993) Some new or interesting hyphomycetes from Hungary. *Nova Hedwigia* 56: 473–482.
- Rifai MA, Zainuddin H, Cholil A (2014) The Javanese species of *Tetraploa*. *Reinwardtia* 10(4): 419–423.
- Ronquist F, Teslenko M, Van Der Mark P, Ayres DL, Darling A, Höhna S, Larget B, Liu L, Suchard MA, Huelsenbeck JP (2012) MrBayes 3.2: Efficient Bayesian Phylogenetic Inference and model choice across a large model space. *Systematic Biology* 61(3): 539–542. <https://doi.org/10.1093/sysbio/sys029>
- Saxena RK, Khare S (1991) Fungal remains from the Neyveli formation of Tiruchirapalli District, Tamil Nadu, India. *Geophytology* 21(1): 37–43.
- Saxena RK, Sarkar S (1986) Morphological study of *Frasnacritetrus taugourdeau* emend. From tertiary sediments of himachal pradesh, India. *Review of Palaeobotany and Palynology* 46(3–4): 209–225. [https://doi.org/10.1016/0034-6667\(86\)90015-1](https://doi.org/10.1016/0034-6667(86)90015-1)
- Saxena RK, Singh HP, Rao MR (1987) Palynology of the Tatrot – Pinjor sequence exposed between Masol and Kiratpur in Ambala District, Haryana. *Geophytology* 17: 270–284.
- Saxena RK, Wijayawardene NN, Dai DQ, Hyde KD, Kirk PM (2021) Diversity in fossil fungal spores. *Mycosphere* 12(1): 670–874. <https://doi.org/10.5943/mycosphere/12/1/8>
- Scheuer C (1991) *Massarina tetraploa* sp. nov., the teleomorph of *Tetraploa aristata*. *Mycological Research* 95(1): 126–128. [https://doi.org/10.1016/S0953-7562\(09\)81370-1](https://doi.org/10.1016/S0953-7562(09)81370-1)

- Senanayake IC, Rathnayaka AR, Marasinghe DS, Calabon MS, Gentekaki E, Lee HB, Hurdeal VG, Pem D, Dissanayake LS, Wijesinghe SN, Bundhun D, Nguyen TT, Goonasekara ID, Abeywickrama PD, Bhunjun CS, Jayawardena RS, Wanasinghe DN, Jeewon R, Bhat DJ, Xiang MM (2020) Morphological approaches in studying fungi: Collection, examination, isolation, sporulation and preservation. *Mycosphere* 11(1): 2678–2754. <https://doi.org/10.5943/mycosphere/11/1/20>
- Senwanna C, Mapook A, Samarakoon MC, Karunarathna A, Wang Y, Tang AMC, Haituk S, Suwannarach N, Hyde KD, Cheewangkoon R (2021) Ascomycetes on Para rubber (*Hevea brasiliensis*). *Mycosphere* 12(1): 1334–1512. <https://doi.org/10.5943/mycosphere/12/1/18>
- Sierra AM, Guarro J, Heredia G (2005) The hyphomycete genus *Piricauda*, with the description of a new species. *Mycological Research* 109(6): 723–728. <https://doi.org/10.1017/S0953756205002522>
- Stamatakis A, Hoover P, Rougemont J (2008) A rapid bootstrap algorithm for the RAxML Web servers. *Systematic Biology* 57(5): 758–771. <https://doi.org/10.1080/10635150802429642>
- Su XJ, Luo ZL, Jeewon R, Bhat DJ, Bao DF, Li WL, Hao YE, Su HY, Hyde KD (2018) Morphology and multigene phylogeny reveal new genus and species of Torulaceae from freshwater habitats in northwestern Yunnan, China. *Mycological Progress* 17(5): 531–545. <https://doi.org/10.1007/s11557-018-1388-3>
- Swofford DL (2002) PAUP*: Phylogenetic analysis using parsimony (and other methods), version 4.0 b10. MA: Sinauer Associates, Sunderland, UK.
- Tanaka K, Hirayama K, Yonezawa H, Hatakeyama S, Harada Y, Sano T, Shirouzu T, Hosoia T (2009) Molecular taxonomy of bambusicolous fungi: Tetraplosporaaceae, a new pleosporalean family with tetraploa-like anamorphs. *Studies in Mycology* 64: 175–209. <https://doi.org/10.3114/sim.2009.64.10>
- Tang X, Jayawardena RS, Stephenson SL, Kang JC (2022) A new species *Pseudoplagiostoma diptercarpicola* (Pseudoplagiostomataceae, Diaporthales) found in northern Thailand on members of the Diptercarpaceae. *Phytotaxa* 543(4): 233–243. <https://doi.org/10.11646/phytotaxa.543.4.3>
- Taylor JE, Hyde KD (2003) Microfungi of tropical and temperate palms. *Fungal Diversity Research Series* 12:1–459.
- Tibpromma S, Hyde KD, McKenzie EHC, Bhat DJ, Phillips AJL, Wanasinghe DN, Samarakoon MC, Jayawardena RS, Dissanayake AJ, Tennakoon DS, Doilom M, Phookamsak R, Tang AMC, Xu J, Mortimer PE, Promputtha I, Maharachchikumbura SSN, Khan S, Karunarathna SC (2018) Fungal diversity notes 840–928: Microfungi associated with Pandanaceae. *Fungal Diversity* 93(1): 1–160. <https://doi.org/10.1007/s13225-018-0408-6>
- Tracy SM, Earle FS (1895) New species of parasitic fungi. *Bulletin of the Torrey Botanical Club* 22(4): 174–208. <https://doi.org/10.2307/2477854>
- Vaidya G, Lohman DJ, Meier R (2011) SequenceMatrix: Concatenation software for the fast assembly of multi-gene datasets with character set and codon information. *Cladistics* 27(2): 171–180. <https://doi.org/10.1111/j.1096-0031.2010.00329.x>
- Vilgalys R, Hester M (1990) Rapid genetic identification and mapping of enzymatically amplified ribosomal DNA from several *Cryptococcus* species. *Journal of Bacteriology* 172(8): 4238–4246. <https://doi.org/10.1128/jb.172.8.4238-4246.1990>
- White TJ, Bruns T, Lee SJWT, Taylor J (1990) Amplification and direct sequencing of fungal ribosomal RNA genes for phylogenetics. *PCR protocols: a guide to methods and applications* 18: 315–322. <https://doi.org/10.1016/B978-0-12-372180-8.50042-1>

- Whitton SR, McKenzie EH, Hyde KD (2012) Anamorphic fungi associated with Pandanaceae. *Fungal Diversity Research Series* 21: 125–353. https://doi.org/10.1007/978-94-007-4447-9_4
- Wijayawardene NN, Hyde KD, Dai DQ, Sánchez-García M, Goto BT, Saxena RK, Erdoğdu M, Selçuk F, Rajeshkumar KC, Aptroot A, Błaszczowski J, Boonyuen N, da Silva GA, de Souza FA, Dong W, Ertz D, Haelewaters D, Jones EBG, Karunarathna SC, Kirk PM, Kukwa M, Kumla J, Leontyev DV, Lumbsch HT, Maharachchikumbura SSN, Marguno F, Martínez-Rodríguez P, Mešić A, Monteiro JS, Oehl F, Pawłowska J, Pem D, Pfliegler WP, Phillips AJL, Pošta A, He MQ, Li JX, Raza M, Sruthi OP, Suetrong S, Suwannarach N, Tedersoo L, Thiyagaraja V, Tibpromma S, Tkáčec Z, Tokarev YS, Wanasinghe DN, Wijesundara DSA, Wimalaseana SDMK, Madrid H, Zhang GQ, Gao Y, Sánchez-Castro I, Tang LZ, Stadler M, Yurkov A, Thines M (2022) Outline of Fungi and fungus-like taxa – 2021. *Mycosphere* 13(1): 53–453. <https://doi.org/10.5943/mycosphere/13/1/2>
- Yang CL, Xu XL, Jeewon R, Boonmee S, Liu YG, Hyde KD (2019) *Acremonium arthrinii* sp. nov., a mycopathogenic fungus on *Arthrinium yunnanum*. *Phytotaxa* 420(4): 283–299. <https://doi.org/10.11646/phytotaxa.420.4.4>
- Yang J, Liu LL, Jones EG, Hyde KD, Liu ZY, Bao DF, Liu NG, Li WL, Sheng HW, Yu XD, Liu JK (2023) Freshwater fungi from karst landscapes in China and Thailand. *Fungal Diversity* 119(1): 1–212. <https://doi.org/10.1007/s13225-023-00514-7>
- Yu XD, Zhang SN, Liu JK (2022) Morpho-phylogenetic evidence reveals novel pleosporalean taxa from Sichuan Province, China. *Journal of Fungi (Basel, Switzerland)* 8(7): 720. <https://doi.org/10.3390/jof8070720>
- Zhang WM, Bi ZS, Li TH, Zheng GY (1994) Taxonomic studies on the genus *Entoloma* from Hainan Province of China (II). *Acta Mycologica Sinica* 13(4): 260–263.
- Zhang K, Ma LG, Zhang XG (2009) New species and records of *Shrungabeeja* from southern China. *Mycologia* 101(4): 573–578. <https://doi.org/10.3852/09-006>
- Zhang Y, Crous PW, Schoch CL, Hyde KD (2012) Pleosporales. *Fungal Diversity* 53(1): 1–221. <https://doi.org/10.1007/s13225-011-0117-x>
- Zhao GZ, Liu XZ, Xie XM, Cao AX (2009) Saprobitic dematiaceous hyphomycetes from Shennongjia region, China. *Nova Hedwigia* 88(1–2): 217–227. <https://doi.org/10.1127/0029-5035/2009/0088-0217>
- Zhou YM, Zhi JR, Ye M, Zhang ZY, Yue WB, Zou X (2018) *Lecanicillium cauligalbarum* sp. nov. (Cordycipitaceae, Hypocreales), a novel fungus isolated from a stemborer in the Yao Ren National Forest Mountain Park, Guizhou. *MycKeys* 59(43): 59–74. <https://doi.org/10.3897/mycokeys.43.30203>
- Zhou YM, Zou X, Zhi JR, Xie JQ, Jiang T (2020a) Fast recognition of *Lecanicillium* spp., and its virulence against *Frankliniella occidentalis*. *Frontiers in Microbiology* 11: 561381. <https://doi.org/10.3389/fmicb.2020.561381>
- Zhou YM, Xie W, Ye JQ, Zhang T, Li DY, Zhi JR, Zou X (2020b) New potential strains for controlling *Spodoptera frugiperda* in China: *Cordyceps cateniannulata* and *Metarhizium rileyi*. *BioControl* 65(6): 663–672. <https://doi.org/10.1007/s10526-020-10035-w>
- Zhou YM, Zhi JR, Qu JJ, Zou X (2022) Estimated divergence times of *Lecanicillium* in the Family Cordycipitaceae provide insights into the attribution of *Lecanicillium*. *Frontiers in Microbiology* 13: 859886. <https://doi.org/10.3389/fmicb.2022.859886>

Identification and fungicide sensitivity of *Microdochium chrysopogonis* (Ascomycota, Amphisphaeriaceae), a new species causing tar spot of *Chrysopogon zizanioides* in southern China

Xiang Lu¹, Mengxian Mai¹, Wenhui Tan¹, Muyan Zhang¹, Jie Xie¹, Yi Lu¹, Xue Li Niu¹, Wu Zhang²

¹ School of Life Sciences and Technology, Lingnan Normal University, Zhanjiang 524048, China

² School of Geographical Science, Lingnan Normal University, Zhanjiang 524048, China

Corresponding author: Wu Zhang (ldzw1987@163.com)

Abstract

Vetiver grass (*Chrysopogon zizanioides*) has received extensive attention in recent years due to its diverse applications in soil and water conservation, heavy metal remediation, as well as essential oil and phenolic acids extraction. In 2019, the emergence of tar spot disease on *C. zizanioides* was documented in Zhanjiang, Guangdong Province, China. Initially, the disease manifested as black ascomata embedded within leaf tissue, either scattered or clustered on leaf surfaces. Subsequently, these ascomata became surrounded by fisheye lesions, characterised by brown, elliptical, necrotic haloes, which eventually coalesced, resulting in leaf withering. Koch's postulates demonstrated that the fungus isolated from these lesions was the causal agent. Microscopic examination showed that the pathogen morphologically belonged to *Microdochium*. The phylogenetic tree inferred from the combined ITS, LSU, *tub2* and *rpb2* sequences revealed the three isolates including GDMCC 3.683, LNU-196 and LNU-197 to be a novel species of *Microdochium*. Combining the results of phylogenetic, pathogenicity and morphological analyses, we propose a new species named *M. chrysopogonis* as the causal agent of *C. zizanioides* in southern China. The optimum growth temperature for *M. chrysopogonis* was determined to be 30 °C. The in vitro fungicide sensitivity of *M. chrysopogonis* was determined using a mycelial growth assay. Four demethylation-inhibiting (DMI) fungicides, including difenoconazole, flusilazole, propiconazole and tebuconazole and one methyl benzimidazole carbamate (MBC) fungicide, carbendazim, were effective against *M. chrysopogonis*, with mean 50% effective concentration (EC₅₀) values of 0.077, 0.011, 0.004, 0.024 and 0.007 µg/ml, respectively. These findings provide essential references for the precise diagnosis and effective management of *M. chrysopogonis*.

Key words: fungicide sensitivity, multilocus phylogeny, new taxon, pathogenicity, tar spot



Academic editor: C. Phukhamsakda
Received: 7 September 2023
Accepted: 19 November 2023
Published: 6 December 2023

Citation: Lu X, Mai M, Tan W, Zhang M, Xie J, Lu Y, Niu XL, Zhang W (2023) Identification and fungicide sensitivity of *Microdochium chrysopogonis* (Ascomycota, Amphisphaeriaceae), a new species causing tar spot of *Chrysopogon zizanioides* in southern China. MycoKeys 100: 205–232. <https://doi.org/10.3897/mycokeys.100.112128>

Copyright: © Xiang Lu et al.
This is an open access article distributed under terms of the Creative Commons Attribution License (Attribution 4.0 International – CC BY 4.0).

Introduction

Vetiver (*Chrysopogon zizanioides*) is one of the main grasses in tropical and subtropical areas (Maurya et al. 2023). With a large root system that penetrates deep into the soil, *C. zizanioides* is strongly tolerant to adverse environments, such as drought, salinity and heavy metals. Recently, vetiver has been widely

utilised in various applications, such as land restoration, soil and water conservation and phytoremediation of heavy metal-contaminated soils (Chen et al. 2021). Moreover, the essential oil and phenolic acids extracted from vetiver root possess significant aromatic and biological properties, giving it an important role in perfumery, the food industry and medicine (David et al. 2019; Moon et al. 2020).

To our knowledge, four diseases on *C. zizanioides* have been reported, namely, leaf blight caused by *Curvularia trifolii* in India (Babu et al. 2021), root and basal stem rot caused by *Gaeumannomyces graminicola* (Lin et al. 2019), leaf spot caused by *Phoma herbarum* (Zhang et al. 2017) and leaf streak caused by *Stenocarpella chrysopogonis* (Jia et al. 2023).

Microdochium species were originally introduced with the type species, *M. phragmitis*, identified on the leaves of *Phragmites australis* in Germany (Sydow 1924). Presently, there are 49 species included in this genus. However, only a subset of these species can induce diseases, primarily affecting grasses and cereals. For example, *M. albescens* (also referred to as *Monographella albescens*) typically induces leaf scald and grain discoloration in rice, leading to a global reduction in rice yield (Araujo et al. 2016; Dirchwolf et al. 2023). *M. bolleyi* is recognised for inducing root necrosis and basal rot in creeping bent grass in Korea, as well as causing root rot on triticale in Kazakhstan (Hong et al. 2008; Alkan et al. 2021). *M. nivale* and *M. majus* frequently result in the occurrence of pink snow mould or Fusarium Patch on wheat, barley and turf grass in cold to temperate regions (Ren et al. 2015; Abdelhalim et al. 2020). *M. opuntiae* leads to brown spotting on *Opuntia* (Braun 1995). *M. poae* triggers leaf blight disease in turf-grasses, such as *Poa pratensis* and *Agrostis stolonifera* (Liang et al. 2019). *M. paspali* is recognised for its ability to cause leaf blight in seashore paspalum (*Paspalum vaginatum*) (Zhang et al. 2015). *M. panattonianum* has the potential to induce anthracnose in lettuce (Galea et al. 1986). *M. sorghi* is accountable for the formation of zonate leaf spots and decay on sorghum species (Stewart et al. 2019).

The application of fungicides has always been an effective approach for disease control. In recent decades, demethylation-inhibiting (DMI) fungicides have emerged as a significant and extensive group of fungicides, exhibiting notable efficacy in the control of diseases caused by the *Microdochium* genus. Notably, compounds such as prochloraz, difenoconazole, propiconazole, metconazole, myclobutanil, tebuconazole and triticonazole have shown substantial antifungal efficacy against *M. panattonianum*, *M. majus* and *M. nivale* (Wicks et al. 1994; Debieu et al. 2000; Glynn et al. 2008; Mao et al. 2023). Additionally, fungicide subgroups, including phenylpyrrole (PP) fungicides, such as fludioxonil, dicarboximides, such as iprodione and quinone outside inhibitors (QoIs), such as trifloxystrobin, have demonstrated noteworthy efficacy in the management of diseases induced by *M. nivale* (Glynn et al. 2008; Koch et al. 2015; Aamlid et al. 2017). Therefore, to promote effective control against tar spot of *C. zizanioides*, it is necessary to determine the sensitivity of the pathogen to fungicides.

The main objectives of this study were to identify the pathogenic fungi causing tar spot of *C. zizanioides* in southern China on the basis of morphological characteristics and multigene sequence analysis; to determine the pathogenicity to *C. zizanioides*; and to determine the inhibitory effect of fungicides against mycelial growth of the pathogen.

Materials and methods

Sample collection and fungal isolation

Leaves exhibiting symptoms of tar spot on *C. zizanioides* were collected in fields of the Grass Research Station of Lingnan Normal University (LNU), Zhanjiang, Guangdong, China. Leaf segments (0.5 × 0.5 cm) from the transition zone from diseased to healthy tissue were cut and surface-sterilised for 30 s with 75% ethanol and 2% sodium hypochlorite (NaClO) for 1 min, rinsed with distilled water 3 times, dried on sterile filter paper and placed on 2% potato dextrose agar (PDA) (Crous et al. 2021b). Additionally, ascomata developing on the surface of diseased tissue were gently scraped using a sterile scalpel. Subsequently, a small number of ascospores were transferred and evenly spread on to the surface of a water agar (WA) plate. Hyphal tips originating from leaf tissue fragments and single germinating conidia were transferred on to PDA medium. They were then incubated at 30 °C in darkness (Polizzi et al. 2009). After a period of 7 days, the isolates were transferred on to PDA slants and preserved at 4 °C in the culture collection of Lingnan Normal University. Additionally, they were deposited in the Guangdong Microbial Culture Collection Center (GDMCC) in Guangzhou, China. The holotype specimen was preserved in the Herbarium of the Chinese Academy of Forestry (CAF) in Beijing, China.

Morphological characterisation

Colonies were subcultured on 2% malt extract agar (MEA) and oatmeal agar (OA) at 30 °C for 10 days in the dark (Crous et al. 2009). Colony colour was characterised using Rayner's Mycological Color Chart (Rayner 1970) and colony diameters were measured after incubation for 10 days at 30 °C in the dark. Morphological characters of ascomata, asci, ascospores, sporodochia, hyphae, conidiomata, conidiophores, conidiogenous cells and conidia were determined in sterile water using an Olympus BX53 compound microscope (Tokyo, Japan), equipped with cellSens Dimension software (version 1.17).

DNA extraction, PCR amplification and sequencing

Fungal genomic DNA was extracted from mycelia grown on PDA medium after 10 days using the ENZA Fungal DNA Miniprep Kit (Omega Bio-tek, Doraville, Norcross, GA, U.S.A.), according to the protocol of manufacturer. Four loci, including internal transcribed spacer (ITS) rDNA region, large subunit ribosomal acid (LSU) rDNA region, RNA polymerase II second largest subunit gene (*rpb2*) and part of the beta-tubulin gene (*tub2*), were amplified by the following primer pairs: ITS1 and ITS4 for ITS (White et al. 1990), LR0R and LR5 for LSU (Vilgalys and Hester 1990), RPB150F (Jewell and Hsiang 2013) and fRPB2-7Cr (Liu et al. 1999) and Btub526F and Btub1332R (Jewell and Hsiang 2013). The polymerase chain reaction (PCR) conditions were as follows: 94 °C for 5 min; 94 °C for 30 s, annealing temperature for 45 s and 72 °C for 1 min, 35 cycles; and a final extension step at 72 °C for 10 min. The annealing temperature for ITS and LSU was 54 °C, for *tub2* was 55 °C and for *rpb2* was 57 °C. PCR products were sequenced by Sangon Biotech Co., Ltd. (Shanghai, China). Sequences were edited and assembled using DNAMAN version 5.2.2 and deposited in the NCBI GenBank nucleotide database (Table 1).

Table 1. Strains included in the phylogenetic analyses with collection details and GenBank accession numbers.

Species	Voucher	Country	GenBank Accession Number			
			LSU	ITS	<i>tub2</i>	<i>rpb2</i>
<i>Microdochium albescens</i>	CBS 290.79	Ivory Coast	KP858950	KP859014	KP859078	KP859123
	CBS 291.79	Ivory Coast	KP858932	KP858996	KP859059	KP859105
	CBS 243.83	Unknown country	KP858930	KP858994	KP859057	KP859103
<i>M. bolleyi</i>	CBS 172.63	Germany	MH869857	MH858255	–	–
	CBS 540.92	Syria	KP858946	KP859010	KP859073	KP859119
	Kaz_Mb01	Kazakhstan	–	MW301448	–	–
	Kaz_Mb02	Kazakhstan	–	MW301449	–	–
	CBS 137.64	Netherlands	MH870023	MH858394	–	–
	CPC 25994	Canada	KP858954	KP859018	KP859074	KP859127
	CBS 102891	Germany	MH874405	–	–	–
	CBS 618.72	Germany	MH872294	MH860598	–	–
<i>M. chrysanthemoides</i>	CGMCC 3.17929 ^T	China	KU746736	KU746690	KU746781	–
	CGMCC 3.17930	China	KU746735	KU746689	KU746782	–
<i>M. chuxiongense</i>	YFCC 8794 ^T	China	OK586160	OK586161	OK556901	OK584019
<i>M. citrinidiscum</i>	CBS 109067 ^T	Peru	KP858939	KP859003	KP859066	KP859112
<i>M. colombiense</i>	CBS 624.94 ^T	Colombia	KP858935	KP858999	KP859062	KP859108
<i>M. dawsoniorum</i>	BRIP 65649 ^T	Australia	ON394569	MK966337	–	–
	BRIP 67439	Australia	OM333563	MN492650	–	ON624208
<i>M. fisheri</i>	CBS 242.90 ^T	UK	KP858951	KP859015	KP859079	KP859124
	NFCCI 4083	India	KY777594	KY777595	–	–
	C30 ITI	Sri Lanka	–	MT875317	–	–
<i>M. graminearum</i>	CGMCC 3.23525 ^T	China	OP104016	OP103966	OP236029	OP236026
	CGMCC 3.23524	China	OP104015	OP103965	OP242835	OP236026
<i>M. hainanense</i>	SAUCC210781 ^T	China	OM959323	OM956295	OM981146	OM981153
	SAUCC210782	China	OM959324	OM956296	OM981147	OM981154
<i>M. indocalami</i>	SAUCC1016 ^T	China	MT199878	MT199884	MT435653	MT510550
<i>M. insulare</i>	BRIP 75114a	Australia	OQ892168	OQ917075	–	OQ889560
<i>M. lycopodium</i>	CBS 146.68	The Netherlands	KP858929	KP858993	KP859056	KP859102
	CBS 109397	Germany	KP858940	KP859004	KP859067	KP859113
	CBS 109398	Germany	KP858941	KP859005	KP859068	KP859114
	CBS 109399	Germany	KP858942	KP859006	KP859069	KP859115
	CBS 125585 ^T	Austria	KP858952	KP859016	KP859080	KP859125
<i>M. maculosum</i>	COAD 3358 ^T	Brazil	OK966953	OK966954	–	OL310501
<i>M. majus</i>	CBS 741.79	Germany	KP858937	KP859001	KP859064	KP859110
	10099	France	–	JX280597	JX280563	JX280560
	10098	France	–	–	JX280564	JX280561
	99027	Canada	–	JX280583	JX280566	–
	200107	Norway	–	KT736191	KT736253	KT736287
<i>M. miscanthi</i>	SAUCC211092 ^T	China	OM957532	OM956214	OM981141	OM981148
	SAUCC211093	China	OM957533	OM956215	OM981142	OM981149
	SAUCC211094	China	OM957534	OM956216	OM981143	OM981150
<i>M. musae</i>	CBS 143500 ^T	Malaysia	MH107942	MH107895	MH108041	MH108003
	CBS 143499	Malaysia	MH107941	MH107894	MH108040	–

Species	Voucher	Country	GenBank Accession Number			
			LSU	ITS	tub2	rpb2
<i>M. musae</i>	CBS 111018	Costa Rica	–	AY293061	–	–
	CPC 11240	Mauritius	MH107944	MH107897	MH108043	–
	CPC 16258	Mexico	MH107945	MH107898	MH108044	–
	CPC 11234	Mauritius	MH107943	MH107896	MH108042	–
	CPC 32681	Malaysia	MH107946	MH107899	–	–
<i>M. neoqueenslandicum</i>	CBS445.95	The Netherlands	KP858933	KP858997	KP859060	KP859106
	CBS108926 ^T	New Zealand	KP858938	KP859002	KP859065	KP859111
<i>M. nivale</i>	CBS 116205 ^T	UK	KP858944	KP859008	KP859071	KP859117
	200114	Norway	–	KT736185	–	KT736279
	200119	Norway	–	KT736199	KT736240	KT736263
	200120	Norway	–	KT736210	KT736221	KT736273
	200566	Norway	–	KT736220	KT736224	–
	201050	Norway	–	KT736217	KT736236	KT736257
<i>M. novae-zelandiae</i>	CBS 143847	New Zealand	–	LT990655	LT990608	LT990641
	CPC 29693	New Zealand	–	LT990656	LT990609	LT990642
<i>M. paspali</i>	CBS 138620 ^T	China	–	KJ569509	KJ569514	–
	CBS 138621	China	–	KJ569510	KJ569515	–
	CBS 138622	China	–	KJ569511	KJ569516	–
<i>M. phragmitis</i>	CBS 285.71 ^T	Poland	KP858949	KP859013	KP859077	KP859122
	CBS 423.78	Germany	KP858948	KP859012	KP859076	KP859121
<i>M. poae</i>	CGMCC3.19170 ^T	China	–	MH740898	MH740914	MH740906
	LC12115	China	–	MH740901	MH740917	MH740909
	LC12116	China	–	MH740902	MH740918	MH740910
	LC12117	China	–	MH740903	MH740919	MH740911
	LC12118	China	–	MH740897	MH740913	MH740905
	LC12119	China	–	MH740899	MH740915	MH740907
	LC12120	China	–	MH740904	MH740920	MH740912
	LC12121	China	–	MH740900	MH740916	MH740908
<i>M. ratticaudae</i>	BRIP 68298 ^T	Australia	MW481666	MW481661	–	MW626890
<i>M. rhopalostylidis</i>	CBS 145125 ^T	New Zealand	MK442532	MK442592	MK442735	MK442667
<i>M. salmonicolor</i>	NC14-294	South Korea	MK836108	MK836110	–	–
<i>M. seminicola</i>	CBS 122706	Switzerland	KP858943	KP859007	KP859070	KP859116
	CBS 122707	Switzerland	KP858947	KP859011	KP859081	KP859120
	CBS 139951 ^T	Switzerland	KP858974	KP859038	KP859101	KP859147
	KAS1516	Canada	KP858961	KP859025	KP859088	KP859134
	KAS3574	Switzerland	KP858973	KP859037	KP859100	KP859146
	KAS3158	Canada	KP858970	KP859034	KP859097	KP859143
	KAS1527	Canada	KP858966	KP859030	KP859093	KP859139
	KAS1473	Canada	KP858955	KP859019	KP859082	KP859128
<i>M. shilinense</i>	CGMCC 3.23531 ^T	China	OP104022	OP103972	OP242834	–
<i>M. sinense</i>	SAUCC211097 ^T	China	OM959225	OM956289	OM981144	OM981151
	SAUCC211098	China	OM959226	OM956290	OM981145	OM981152
<i>M. sorghi</i>	CBS 691.96	Cuba	KP858936	KP859000	KP859063	KP859109
<i>Microdochium</i> sp.	SAUCC1017	China	MT199879	MT199885	MT435654	–
<i>M. tainanense</i>	CBS 269.76 ^T	Taiwan	KP858945	KP859009	KP859072	KP859118
	CBS 270.76	Taiwan	KP858931	KP858995	KP859058	KP859104

Species	Voucher	Country	GenBank Accession Number			
			LSU	ITS	<i>tub2</i>	<i>rpb2</i>
<i>M. trichocliadiopsis</i>	CBS 623.77 ^T	Unknown country	KP858934	KP858998	KP859061	KP859107
<i>M. triticicola</i>	RR 241	UK	–	AJ748691	–	–
<i>M. chrysopogonis</i>	GDMCC 3.683	China	MT988024	MT988022	MW002441	MW002444
	LNU-196	China	MT988023	MT988020	MW002442	MW002445
	LNU-197	China	MT988025	MT988021	MW002443	MW002446
<i>M. yunnanense</i>	SAUCC1018	China	MT199880	MT199886	MT435655	–
	SAUCC1015	China	MT199877	MT199883	MT435652	MT510549
	SAUCC1012	China	MT199876	MT199882	–	MT510548
	SAUCC1011 ^T	China	MT199875	MT199881	MT435650	MT510547
<i>Thamnomycetes dendroidea</i>	CBS 123578	France	KY610467	FN428831	KY624313	KY624232

Note: "T" denotes ex-type strain. Newly-generated sequences are indicated in bold. "–" means no data available in GenBank.

Phylogenetic analyses

The sequences of the strains from *C. zizanioides* and those of *Microdochium* species, as well as the outgroup *Idriella lunata* obtained from NCBI GenBank, were aligned with MAFFT version 7 using the default settings. Manual adjustments were made to optimise the alignment in MEGA version 7.0 (Kato and Standley 2013; Kumar et al. 2016). To elucidate the taxonomic phylogenetic relationships, single and concatenated ITS, LSU, *rpb2* and *tub2* sequence alignments were subjected to analysis by applying Bayesian Inference (BI) using MrBayes version 3.2.5 and Maximum Likelihood (ML) using RAxML on the CIPRES portal (www.phylo.org) (Swoford 2002; Crous et al. 2006; Ronquist et al. 2012). For BI analysis, the best evolutionary model was determined through the utilisation of MrModelTest version 2.2 (Nylander 2004). Subsequently, in MrBayes v. 3.2.5, the Markov Chain Monte Carlo 180 (MCMC) algorithm was used to generate phylogenetic trees. The first 25% of saved trees were discarded as the burn-in phase. Posterior probabilities (PPs) were determined from the remaining trees prior to calculation of the 50% majority rule consensus trees; PP values exceeding 0.90 were considered significant. The ML analyses were performed by using RAxML-HPC BlackBox version 8.2.6, based on 1000 bootstrap replicates. A general time reversible (GTR) model was applied with gamma-distributed rate variation. Bootstrap values (BSs) equal to or higher than 70% were regarded as significant. The phylogenetic tree was viewed in Fig-Tree version 1.4.4 (Rambaut 2018) and edited by Adobe Illustrator CC2018.

Pathogenicity test

Three isolates of *M. chrysopogonis* (GDMCC 3.683, LNU-196 and LNU-197) were used to conduct the pathogenicity test. *C. zizanioides* plants were cultivated within a greenhouse, utilising plastic pots containing field-collected soil from the location where the plants had been established. The isolates were cultured on PDA for 2 weeks at 30 °C in the dark to collect conidia.

For the detached leaf assay, 1-cm wide leaves were harvested from 2-month-old plants cultivated in a greenhouse, washed under running tap water, surface disinfected with 70% ethanol for 1 min, rinsed with sterile water for 30 seconds and finally air-dried on sterilised filter paper. The conidial suspension was adjusted to a concentration of 1×10^6 conidia/ml in sterile distilled water. An equivalent volume

of sterile distilled water was used as a control. Leaf blades were then wounded with a sterilised pin and each leaf was sprayed with 2 ml of conidial suspension. All inoculated and control leaves were placed in a moist chamber at 25 °C with 100% relative humidity (RH) under cool fluorescent light with a 12-h photoperiod. After seven days, the disease incidence was assessed and calculated as the percentage of leaves with leaf tar spot symptoms. Each treatment consisted of five replicates and the experiment was conducted three times.

For the attached leaf assay, the leaf blades of healthy leaves were also pin-pricked and the conidial suspension was adjusted to a concentration of 2×10^6 conidia/ml in sterile distilled water. An equivalent volume of sterile distilled water was used as a control. In each treatment, five plants were included, with each plant being sprayed with approximately 20 ml of inoculum. All sprayed and control plants were incubated in a plastic container in a greenhouse at 25 ± 2 °C under cool fluorescent light with a 12-h photoperiod. For the first 3 days, the plastic container was covered with transparent polyethylene bags to maintain a high humidity. The disease incidence was assessed 10 days post inoculation and calculated as the percentage of plants displaying tar spot symptoms. Each treatment had three replicates and the pathogenicity test was repeated twice.

To fulfil Koch's postulates, symptomatic leaf tissues were subjected to surface sterilisation as described above. Subsequently, these tissues were plated on to PDA medium to enable the re-isolation of the fungi. These isolates were identified, based on comparison of the cultures with those of the original strains. Furthermore, the identifications were confirmed by sequencing of the isolates.

Effect of temperature on mycelial growth rate

Mycelial growth rates of *M. chrysopogonis* isolates were assessed across various temperatures. Mycelial plugs with a diameter of 5 mm were excised using a sterile hole puncher from the periphery of 10-day-old PDA cultures. Subsequently, they were translocated to the central area of 90 mm PDA Petri dishes. The cultures were subjected to incubation across a temperature range of 5, 10, 15, 20, 25, 30, 35, 40 and 45 °C. Four replicate plates per isolate were prepared for each temperature. The plates were enveloped using Parafilm (Bemis Company, Neenah, WI, U.S.A.) and then positioned within plastic containers prior to their placement in incubators. The colony diameter was measured along two mutually perpendicular axes and the mean of these two measurements was documented as the radial colony diameter. Following a 10-day duration, mycelial growth rates were determined, based on colony diameter and subsequently quantified in millimetres per day. Each treatment was replicated four times.

Fungicide sensitivity

To determine possible control measures for this pathogen in the field, six groups including nine fungicides were tested for their ability to inhibit the growth of *M. chrysopogonis* in vitro. Fungicide sensitivity assays were conducted, based on methods developed by Yin et al. (2019). The commercial formulations of fungicides were serially diluted using sterilised distilled water. These diluted solutions were added to autoclaved PDA medium that had been cooled to 55 °C to obtain the desired concentrations in micrograms per millilitre (Table 2). Isolates were cul-

tured on PDA plates at 30 °C for 10 days in darkness to supply inoculum. Mycelial discs (5 mm in diameter) from the periphery of colonies actively growing on PDA were positioned at the centre of the fungicide-amended plates and unamended (control) plates. The plates were then incubated at a temperature of 30 °C in darkness for a duration of 2 weeks. Subsequently, the diameter of each colony was measured along two perpendicular axes and the mean diameter was recalibrated by deducting the diameter of the original plug utilised for inoculation. The effective concentration for 50% mycelial growth inhibition (EC_{50}) was estimated by performing a regression analysis of the percentage of mycelial growth inhibition against the \log_{10} of fungicide concentrations. Each treatment was replicated four times.

Statistical analysis

The dataset was tested for variance homogeneity using the Levene test. If the variances were equal, an analysis of variance (ANOVA) followed by a least significant difference (LSD) test was conducted. In cases where the variances were unequal, the Dunnett T3 test was applied. All statistical analyses were carried out using IBM SPSS version 20.0 (SPSS Inc., Chicago, IL, U.S.A.). The significance threshold for detecting treatment disparities was set at $P < 0.05$.

Results

Disease symptoms and isolation of the pathogen

From 2019 to 2022, a previously unknown disease of vetiver grass occurred during late spring and early autumn at the Grass Research Station of Lingnan Normal University (LNU) in Guangdong Province, China. Symptoms consistently appeared on 85% of *C. zizanioides* grown under field conditions. The initial symptoms appeared as small and scattered punctate spots (< 1 cm) embedded within the leaf tissue. Gradually, these spots clustered on leaf surfaces. Subsequently, brown, elliptical, fish-eye necrotic haloes emerged, encircling the lesion spots and aligning parallel to the leaf veins (Fig. 1A–C). As these necrotic haloes coalesced, the leaf underwent chlorosis and wilting, eventually leading to blighting of the entire plant. Ascospores were visible on the diseased leaf surfaces.

Table 2. List of the fungicides used in this study.

Active ingredient	Chemical family	Trade name	FRAC code	Concentration ($\mu\text{g/ml}$)
Pyrimethanil	anilino-pyrimidines	Syngenta	9	0, 0.01, 0.1, 1, 10, 100
Difenoconazole	triazoles	Syngenta	3	0, 0.01, 0.1, 1, 10, 100
Fludioxonil	phenylpyrroles	Syngenta	12	0, 1, 10, 30, 100, 300
Iprodione	dicarboximides	Syngenta	2	0, 1, 10, 30, 100, 300
Flusilazole	triazoles	Syngenta	3	0, 0.001, 0.01, 0.1, 1, 10
Propiconazole	triazoles	BASF	3	0, 0.0016, 0.008, 0.04, 0.2, 1
Carbendazim	benzimidazoles	Syngenta	1	0, 0.0016, 0.008, 0.04, 0.2, 1
Metalaxyl	acylalanines	BASF	4	0, 10, 30, 100, 300, 1000
Tebuconazole	triazoles	Bayer	3	0, 0.0016, 0.008, 0.04, 0.2, 1

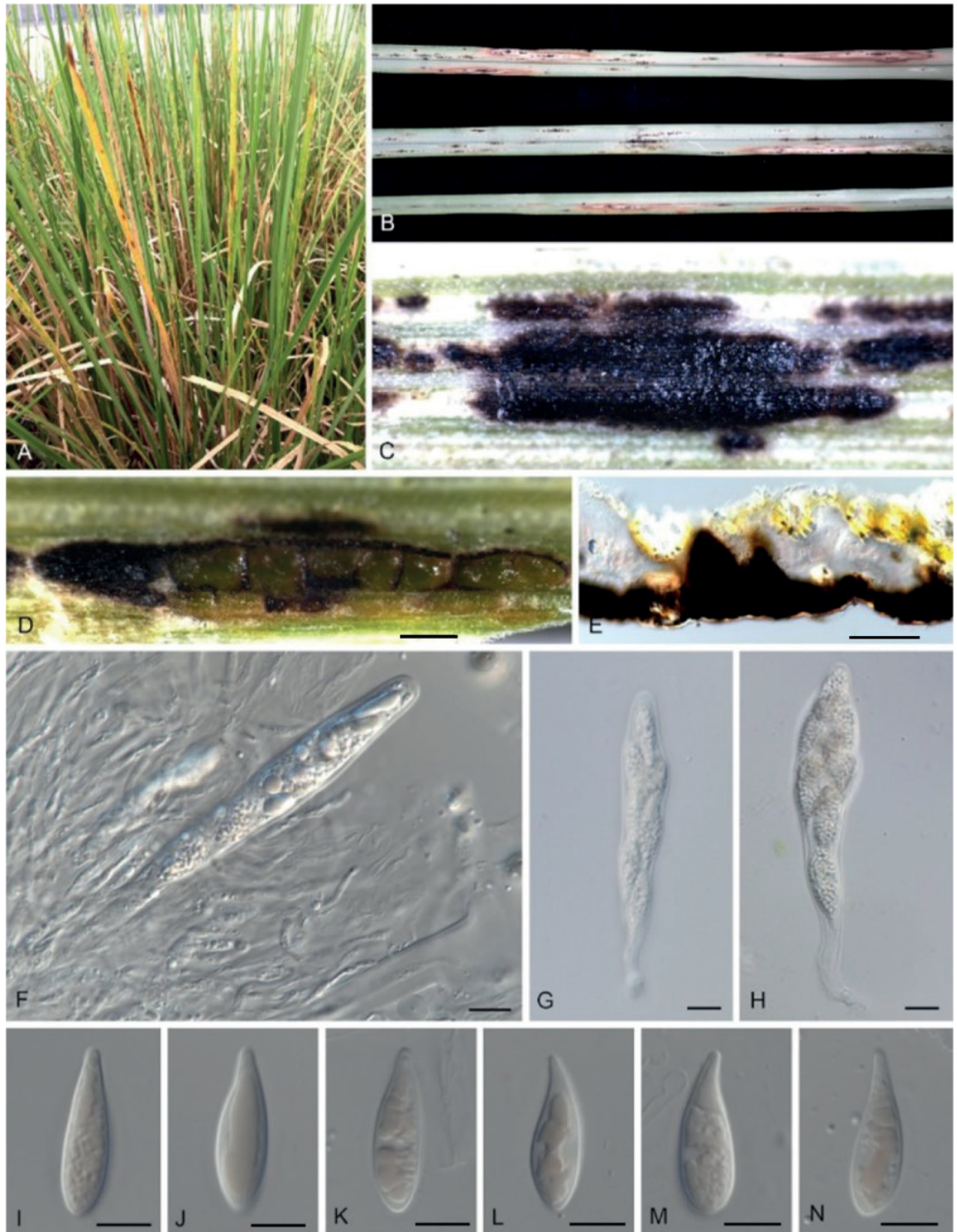


Figure 1. Disease symptoms and morphological characters of *Microdochium chrysopogonis* on infected leaf tissue (CAF 800053) **A–C** tar spot symptoms of *Chrysopogon zizanioides* from natural infection in the field **D** appearance of immersed ascomata on infected leaves **E** ascomata in longitudinal section **F–H** asci **I–N** ascospores. Scale bars: 100 μ m (**D, E**); 10 μ m (**F–H**).

A total of 67 isolates were obtained on PDA. As the colony morphology of the isolates was consistent, three representative isolates (GDMCC 3.683, LNU-196 and LNU-197), one from each field, were selected for further studies.

Phylogeny

Based on a Megablast search on NCBI's GenBank nucleotide database, the closest hits for the ITS sequence of strain GDMCC 3.683 were *M. dawsoniorum* sequences with 98% identity (538/551, MK966337; 532/543, MN492650) and a *Microdochium* sp. sequence with 97% identity (545/562, FJ536210). The closest hits for LSU sequence of this strain were *M. dawsoniorum* sequences with 99% identity (868/871, OM333563; 864/867, ON394569) and a *M. yunnanense* sequence with 99% identity (875/882, MT199880). The closest hits for its *rpb2* sequence were *M. tainanense* sequences with 85% identity (711/841, KP859118 and KP859104) and a *M. neoqueenslandicum* sequence with 83% identity (698/842, KP859106). The closest hits for *tub2* sequence were a *M. tainanense* sequence with 95% identity (661/697, KP859058), a *M. neoqueenslandicum* sequence with 95% identity (665/703, KP859060) and a *M. colombiense* sequence with 95% identity (658/695, KP859062). Therefore, molecular analyses with all available *Microdochium* species were performed. The alignment of each single locus and concatenated sequence dataset of ITS, LSU, *rpb2* and *tub2* were used to confirm species resolution in *Microdochium*.

There were in total 99 aligned sequences, including the outgroup, *Thamnomycetes dendroidea*. A total of 3,033 characters (547 bp from the ITS, 843 bp from LSU, 848 bp from *tub2* and 795 bp from *rpb2*) were included in the phylogenetic analyses. RAxML analysis of the combined dataset yielded a best scoring tree with a final ML optimisation likelihood value of -21,329.537402 (ln). The matrix had 1,096 distinct alignment patterns with 27.41% undetermined characters or gaps. The tree length was 3.410120. Estimated base frequencies were: A = 0.234382, C = 0.267827, G = 0.258835, T = 0.238956; substitution rates were AC = 1.101009, AG = 4.781387, AT = 1.240884, CG = 0.955029, CT = 6.933148 and GT = 1.000000; gamma distribution shape parameter $\alpha = 0.152657$. Based on the results of MrModelTest, the SYM + I + gamma for ITS, GTR + I + gamma for LSU and *rpb2* and HKY + I + gamma model for *tub2* were selected as the best fit models for Bayesian analyses. A total of 47,402 trees were generated by BI, amongst which 11,851 trees were discarded as the burn-in phase and the remaining 35,551 trees were used to calculate the posterior probabilities (PPs). The BI consensus tree confirmed the tree topology obtained with ML. The well-supported clade (1/100) formed by the three strains from *C. zizanioides* clustered with high support (1/100) with *M. dawsoniorum* (0.92/97), which was sister to one single-strain clade representing *M. ratticaude*. This clade clustered with high support (0.92/93) with the clade formed by *M. albescens*, *M. seminicola*, *M. graminearum*, *M. shilinense*, *M. insulare*, *M. paspali*, *M. citrinidiscum*, *M. sorghi*, *M. tainanense* and *M. trichocladiopsis* strains. The *M. neoqueenslandicum* clade (1/100) was basal to this clade (Fig. 2). Single gene-based phylogenies are presented in the Suppl. material 1. Nonetheless, these individual gene trees did not yield a conclusive taxonomic classification for the new species, in contrast to the comprehensive resolution achieved through the concatenated sequence analysis.

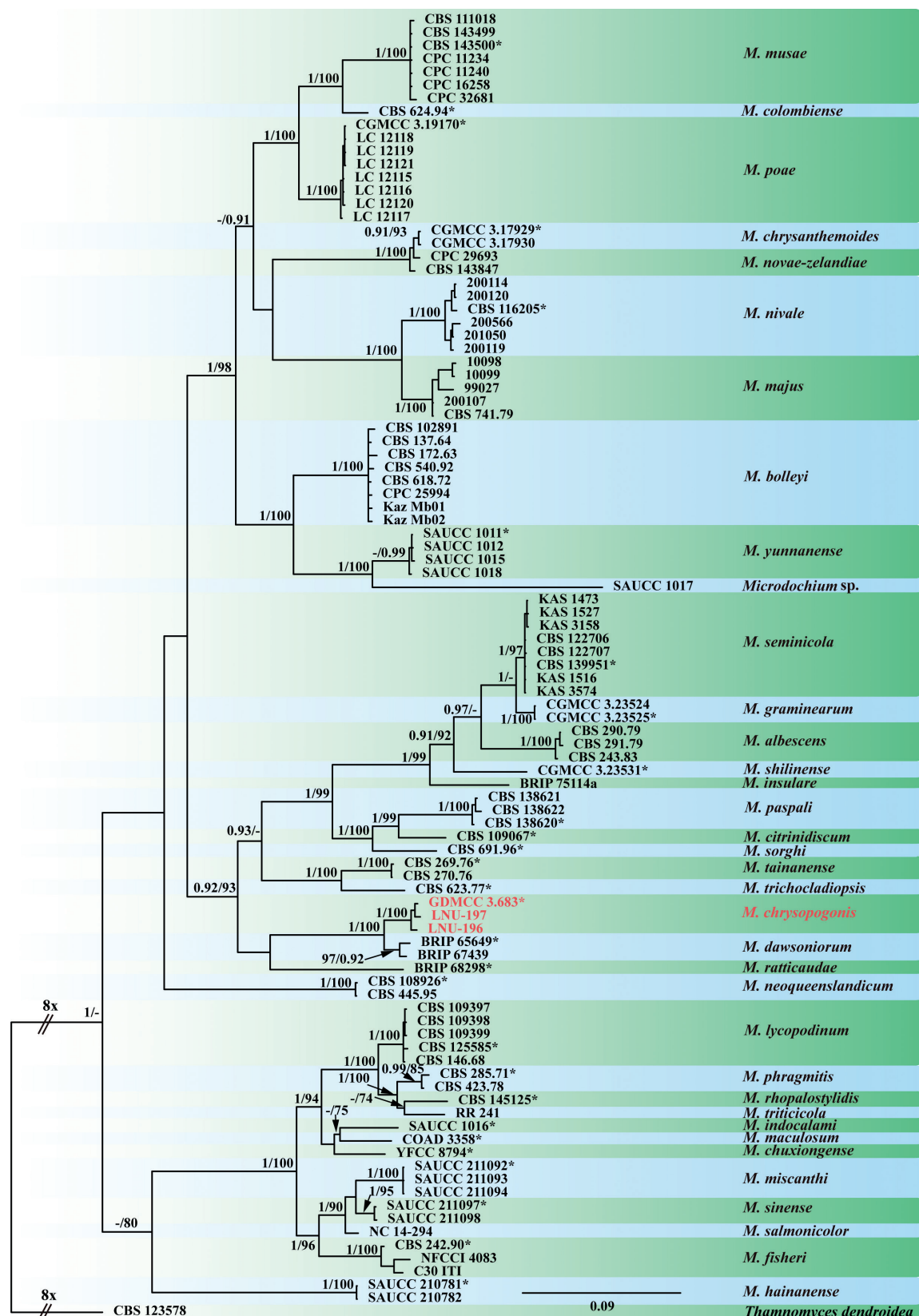


Figure 2. Phylogenetic tree inferred from a Maximum Likelihood analysis, based on a combined alignment of ITS, LSU, *tub2* and *rpb2* sequences from 99 isolates of *Microdochium* sp. Bootstrap support values obtained with ML above 70% and Bayesian (BI) posterior probability values above 0.90 are shown at the nodes (BI/ML). The tree was rooted to *Thamnomycetes dendroidea* CBS 123578. Numbers of ex-type strains are emphasised with an asterisk and species are delimited with shaded blocks. Isolates of *M. chrysopogonis* are indicated with lighter text.

Taxonomy

Based on multilocus phylogenetic analyses, the three strains isolated from *C. zizanioides* represent a previously unknown species within the genus *Microdochium* that is closely related to *M. dawsoniorum* and *M. ratticaudae*. Morphological data placed the new species in the genus *Microdochium*. This species is characterised below.

***Microdochium chrysopogonis* W. Zhang & X. Lu, sp. nov.**

MycoBank No: 845624

Figs 1, 3

Etymology. Name refers to *Chrysopogon*, the host genus from which this fungus was collected.

Description. **Sexual morph** on infected leaf tissue of the host plant (CAF 800054). **Ascomata** perithecial, 300–350 µm diam., solitary or in groups, immersed, pale brown to black, subglobose to oval, uniloculate, non-ostiolate. **Paraphyses** filiform, hyaline, straight or curved, apically free. **Asci** 50–60 × 10–18, \bar{x} = 55 × 13 µm (n = 50), hyaline, fasciculate, unitunicate, oblong to narrowly clavate, fusiform, 8 biseriate spores with a short stipe. **Ascospores** clavate, hyaline, guttulate, 20–22 × 8–11.5, \bar{x} = 21 × 9 µm (n = 50), aseptate, smooth. **Sporodochia** salmon-pink, slimy. **Conidiophores** reduced to conidiogenous cells. **Conidiogenous cells** with percurrent proliferation, hyaline, smooth, aseptate, ampulliform or obpyriform, 10–23 × 8–11.5, \bar{x} = 17 × 9.5 µm (n = 50). **Conidia** fusiform, lunate, curved, solitary, guttulate, variable in length, 0–1-septate, 18–72 × 2–3.5, \bar{x} = 38.5 × 3 µm (n = 50), apex rounded, base usually flattened. **Chlamydospores** not observed. Vegetative hyphae on PDA (GDMCC 3.683) superficial and immersed, septate, branched, hyaline, smooth, 1–5.5 µm wide.

Culture characteristics. Colonies on PDA reaching 4.0–4.5 cm within seven days in the dark at 30 °C, flat, white cottony aerial mycelium, dense, saffron rounded sporodochia produced after 3 weeks; reverse saffron. On MEA, sparse white cottony aerial mycelium, orange rounded sporodochia produced; reverse salmon-pink. On OA, periphery with white scarce cottony aerial mycelium, concentric rings of orange rounded sporodochia produced; reverse orange.

Type. China, Guangdong Province, Zhanjiang City, field of the Grass Research Station of Lingnan Normal University (LNU), from a leaf of vetiver grass (*Chrysopogon zizanioides*) with leaf tar spot disease, September 2019, W. Zhang & X. Lu, holotype CAF 800054, ex-type living strain GDMCC 3.683.

Additional materials examined. China, Guangdong Province, Zhanjiang City, field of the Grass Research Station of Lingnan Normal University (LNU), from a leaf of vetiver grass (*C. zizanioides*) with leaf tar spot disease, September 2019, W. Zhang & X. Lu, strain LNU-196; China, Guangdong Province, Zhanjiang City, field of the Grass Research Station of Lingnan Normal University (LNU), from a leaf of vetiver grass (*C. zizanioides*) with leaf tar spot disease, September 2019, W. Zhang & X. Lu, strain LNU-197.

Notes. A multilocus phylogenetic analysis of the ITS, LSU, *tub2* and *rpb2* loci placed three strains of *M. chrysopogonis* in a distinct and monophyletic clade (1/100) sister to *M. dawsoniorum* and *M. ratticaudae*. Notably, *M. chrysopogonis*

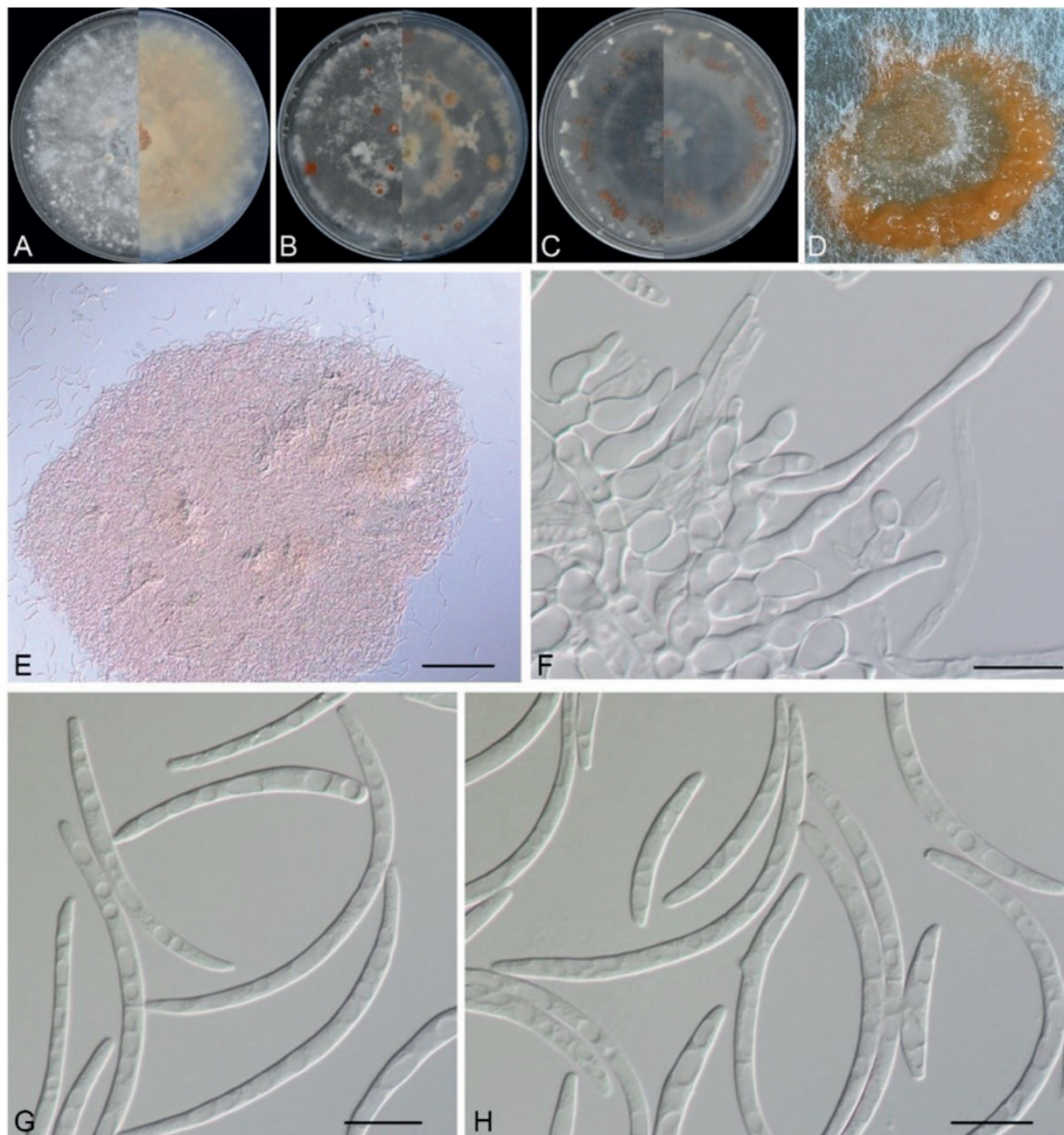


Figure 3. *Microdochium chrysopogonis* (from ex-type: GDMCC 3.683) **A** colonies after 7 days on PDA **B** colonies after 7 days on MEA **C** colonies after 7 days on OA **D** colony overview of the sporodochia on PDA in culture after incubation for three weeks **E** aggregated conidiophores **F** conidiophores with conidiogenous cells **G, H** conidia. Scale bars: 20 μm (**B**).

has longer conidia ($18\text{--}72 \times 2\text{--}3.5 \mu\text{m}$) than *M. ratticaudae* ($7\text{--}11 \times 1.5\text{--}2.5 \mu\text{m}$) and wider conidia than *M. dawsoniorum* ($25\text{--}75 \times 1\text{--}2 \mu\text{m}$). Furthermore, the conidia of *M. chrysopogonis* are guttulate and 0–1-septate, while those of *M. dawsoniorum* are 0–3-septate and those of *M. ratticaudae* are aseptate. The conidiogenous cells of *M. chrysopogonis* appear as percurrent, ampulliform or obpyriform, whereas those of *M. ratticaudae* are indistinct from the hyphae and those of *M. dawsoniorum* are cylindrical to irregular and flexuous. Additionally, the conidiogenous cells of *M. chrysopogonis* ($10\text{--}23 \times 8\text{--}11.5 \mu\text{m}$) are wider than those of *M. ratticaudae* ($20\text{--}30 \times 1\text{--}2 \mu\text{m}$) (Table 3). Differences are also evident in the sexual morph of these three species. In particular, the sexual

morph is not observed in *M. dawsoniorum*. Ascomata size varies, with that of *M. ratticaudae* (100–160 μm) being smaller than that of *M. chrysopogonis* (300–350 μm). Ascospores of *M. ratticaudae* (14–24 \times 4–7 μm) are fusoid to navicular, while those of *M. chrysopogonis* are clavate, guttulate and wider (20–22 \times 8–11.5 μm). In addition, *M. ratticaudae* features abundant, pale to olivaceous brown, subglobose or cylindrical chlamydospores, while these are not observed in *M. chrysopogonis* (Crous et al. 2020, 2021a; Table 3). Consequently, based on both morphological characteristics and phylogenetic analyses, all three isolates of *M. chrysopogonis* were proposed as a new species.

Pathogenicity test

The symptoms observed on leaves of *C. zizanioides* after inoculation with the representative isolate GDMCC 3.683 were similar to those observed in the field. No symptoms were observed on the leaves of the negative controls (Fig. 4). The average disease incidence of detached leaves that were wounded and sprayed with the isolates GDMCC 3.683, LNU-196 and LNU-197 was 93.3%, 80.0% and 93.3%, respectively. The average disease incidence of whole plants after spraying with the same isolates was 76.7%, 73.3% and 73.3%, respectively (Fig. 5). Koch's postulates were fulfilled by successful re-isolation of the fungal strains from all leaf spot tissues inoculated with the three isolates. The morphology and DNA sequences of the isolates re-isolated from the inoculated tissues were consistent with those of the strains used for inoculations.

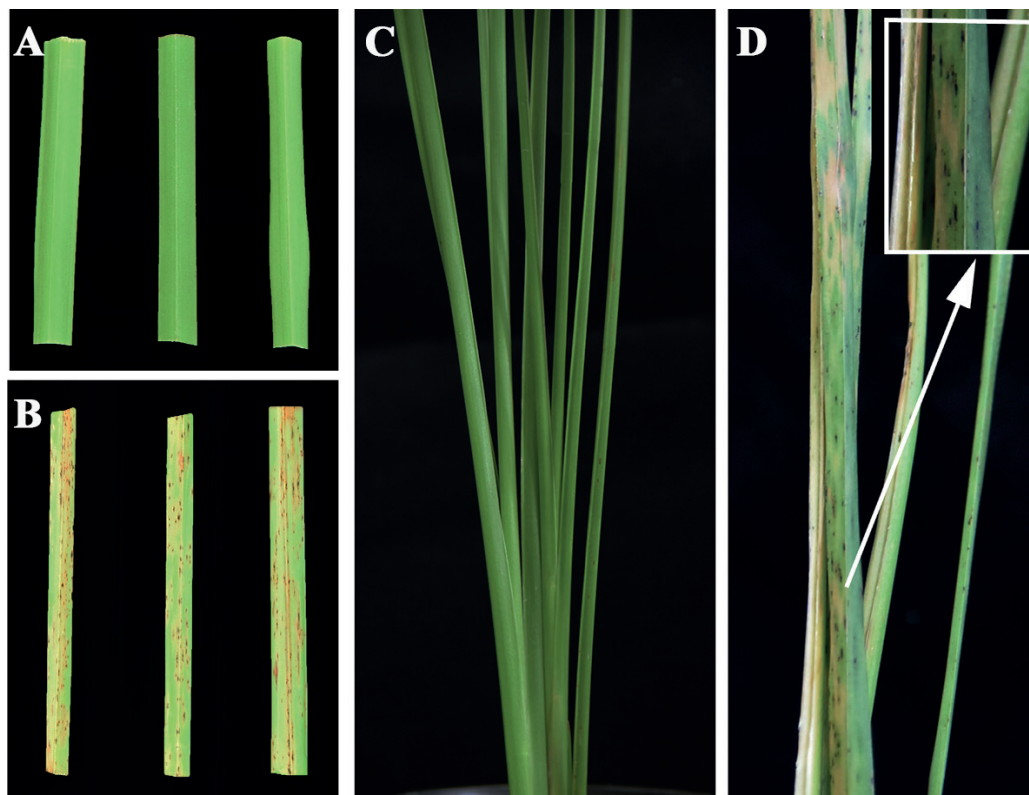


Figure 4. Tar spot symptoms of *Chrysopogon zizanioides* 7 days after spraying on detached leaves (**A**, **B**) and 10 days after spraying on leaves attached to whole plants (**C**, **D**) with *Microdochium chrysopogonis* isolate GDMCC 3.683 (**B**, **D**) and sterilised water (**A**, **C**).

Table 3. Morphological characters of *Microdochium chrysopogonis* and its related species.

Taxa		<i>M. albescens</i>	<i>M. citrinidiscum</i>	<i>M. neoqueenslandicum</i>	<i>M. paspali</i>	<i>M. semini-cola</i>	<i>M. trichocladitopsis</i>	<i>M. tainanense</i>	<i>M. sorghi</i>	<i>M. dawsoniorum</i>	<i>M. ratticaudae</i>	<i>M. graminearum</i>	<i>M. shilinese</i>	<i>M. chrysopogonis</i>
Asexual morph	Conidia	falcate, slightly to strongly curved, apex pointed	cylindrical, clavate, obovoid	lunate, allantoid, curved	falcate, apex pointed	cylindrical to fusiform, straight or curved	oblong, fusiform to obovoid, straight or curved	lunate	filiform, narrowly acicular fusiform, obclavate	flexuous to falcate, sometimes with a geniculation, acute at the tip, narrow at the base	fusoid, falcate, acute at the apex and narrowed at the base	n/a	n/a	fusiform, lunate, curved, guttulate
		Size (µm) 11–16 × 3.5–4.5	7–31 × 2–3	4–9 × 1.5–3	7–20.5 × 2.5–4.5	19–54 × 3–4.5	6–18 × 2–3.5	10–15 × 2–3	20–90 × 1.5–4.5	25–75 × 1–2	7–11 × 1.5–2.5	n/a	n/a	18–72 × 2–3.5
Conidiogenous cells	Septa	0–1(–3)	0–3	0(–1)	0–3	0(–3)(–5)	0(–1)	0–1	1–7(–10)	0–3	aseptate	n/a	n/a	0–1
	Shape	subcylindrical, doliform to obpyriform	denticulate, cylindrical	ampulliform, lageniform to subcylindrical	ampulliform, lageniform to cylindrical	ampulliform to lageniform	cylindrical to clavate, straight but often curved at the tip	sympodial, apical, cylindrical or ampulliform with conspicuous rhachides	sympodial, ovoid, ampulliform to obclavate	cylindrical to irregular, flexuous, narrowed towards the tip	indistinct from hyphae, terminal, solitary.	n/a	n/a	n/a
Sexual morph	Chlamydospores	n/a	n/a	n/a	n/a	n/a	present	n/a	n/a	n/a	subglobose or cylindrical	n/a	n/a	n/a
	Perithecia	150–180 × 90–120	n/a	n/a	n/a	110–149	n/a	n/a	n/a	n/a	100–160	n/a	n/a	300–350
	Asci	40–85 × 8–12	n/a	n/a	n/a	41–66 × 7.6–11	n/a	n/a	n/a	n/a	50–75 × 10–14	55–77.5 × 9.5–15.	50–76 × 7–10	50–60 × 10–18
	Ascospores	14–23 × 3.5–4.5	n/a	n/a	n/a	12–22 × 3–4.5	n/a	n/a	n/a	n/a	14–24 × 4–7	16.5–24 × 4–5.5	14–18 × 3–5.5	20–22 × 8–11.5
References	Septa	1–3(–5)	n/a	n/a	n/a	0–3	n/a	n/a	n/a	n/a	aseptate	0–3	0–3	aseptate
		Hernández-Restrepo et al. (2016)	Hernández-Restrepo et al. (2016)	Hernández-Restrepo et al. (2016)	Zhang et al. (2015) (Continued on next page)	Hernández-Restrepo et al. (2016)	Hernández-Restrepo et al. (2016)	De Hoog & Hermandides-Nijhof (1977)	Braun (1995)	Crous et al. (2020) (Continued on next page)	Crous et al. (2021a)	Gao et al. (2022)	Gao et al. (2022)	Gao et al. (2022)

Note: "n/a" means not provided in the literature.

Effect of temperature on mycelial growth

The mycelial growth of *M. chrysopogonis* was significantly affected by temperature ($P < 0.01$). All three isolates of *M. chrysopogonis* grew between 10 and 40 °C, with maximum growth observed at 30 °C (Fig. 6). No isolates grew at 5 or 45 °C after 3 days. The highest average mycelial growth rate was observed at 30 °C (26.5 ± 2.0 mm/day), followed by 25 °C (20.1 ± 4.7 mm/day).

Fungicide sensitivity

The EC_{50} values of various fungicides were analysed for their effectiveness against *M. chrysopogonis* isolates. A total of 17 isolates of *M. chrysopogonis* were collected from diseased leaves spanning the period from 2019 to 2022.

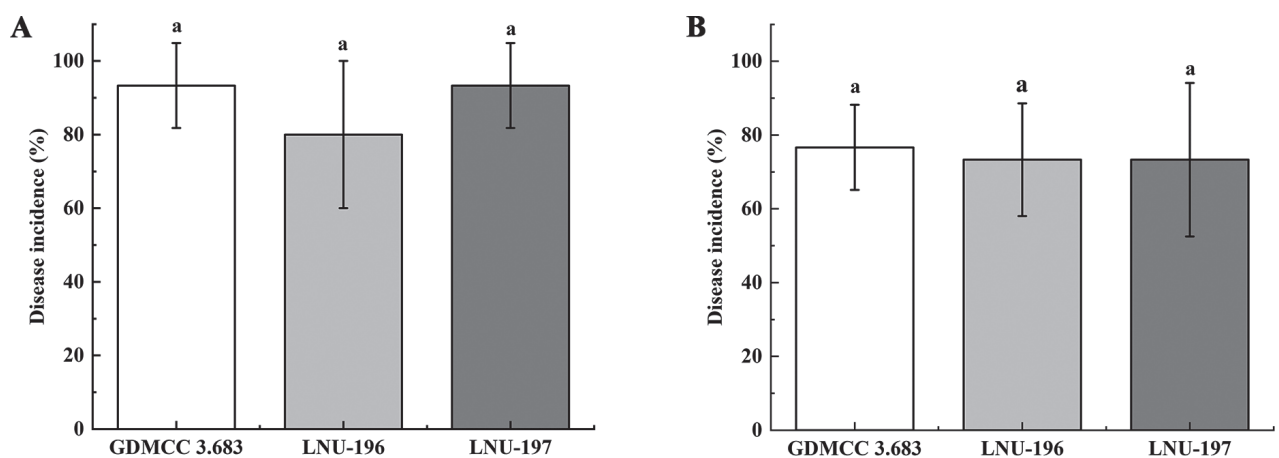


Figure 5. Disease incidence of tar spot symptoms on *Chrysopogon zizanioides* for leaves 7 days after spraying detached leaves (A) and for whole plants 10 days after spraying leaves attached to potted plants (B), respectively, with *Microdochium chrysopogonis* isolates GDMCC 3.683, LNU-196 and LNU-197. Values are shown as the means, with the error bars representing the standard error. For each pathogen, columns with the same letter indicate means that are not significantly different according to a least significant difference (LSD) test ($P < 0.05$).

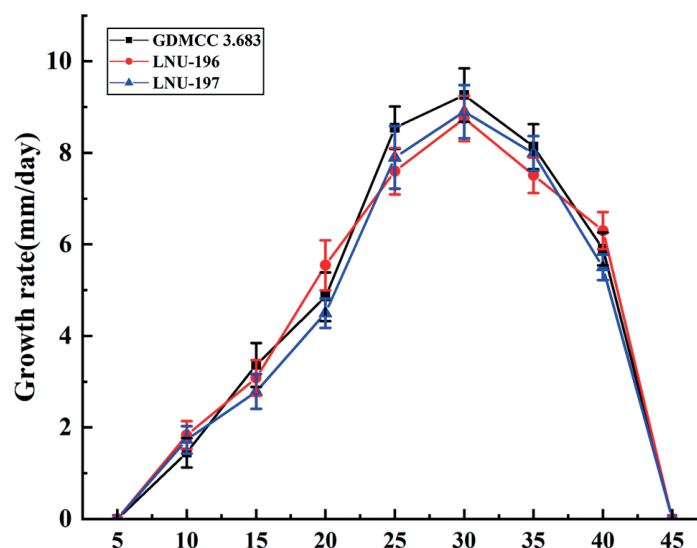


Figure 6. Colony growth rate of three isolates, GDMCC 3.683, LNU-196 and LNU-197, of *Microdochium chrysopogonis* from *Chrysopogon zizanioides* under different temperatures. Error bars represent the standard error.

The frequency distribution showed that difenoconazole, fludioxonil, flusilazole, carbendazim and iprodione exhibited distributions resembling normal curves, while pyrimethanil, propiconazole, metalaxyl and tebuconazole displayed unimodal curves (Fig. 7). EC_{50} values for the inhibition of 17 *M. chrysopogonis* isolates, based on mycelial radial growth, varied across fungicide treatments ($P < 0.05$) (Table 4). Amongst the tested fungicides, flusilazole had the lowest EC_{50} values, with a notably concentrated response range of 0.001 to 0.007 $\mu\text{g}/\text{ml}$ and an average of 0.004 $\mu\text{g}/\text{ml}$. Tebuconazole closely followed with a slightly narrower range, exhibiting values ranging from 0.002 to 0.009 $\mu\text{g}/\text{ml}$ and an average of 0.007 $\mu\text{g}/\text{ml}$. Furthermore, there was no significant difference between flusilazole and tebuconazole. Propiconazole displayed EC_{50} values spanning from 0.006 to 0.016 $\mu\text{g}/\text{ml}$, with an average of 0.011 $\mu\text{g}/\text{ml}$, while those of carbendazim ranged from 0.008 to 0.031 $\mu\text{g}/\text{ml}$, with an average of 0.024 $\mu\text{g}/\text{ml}$. In contrast, those of difenoconazole exhibited a broader range, varying from 0.013 to 0.127 $\mu\text{g}/\text{ml}$, with a mean value of 0.077 $\mu\text{g}/\text{ml}$, while those of pyrimethanil ranged from 0.054 to 0.605 $\mu\text{g}/\text{ml}$, with an average of 0.411 $\mu\text{g}/\text{ml}$. Those of ip-

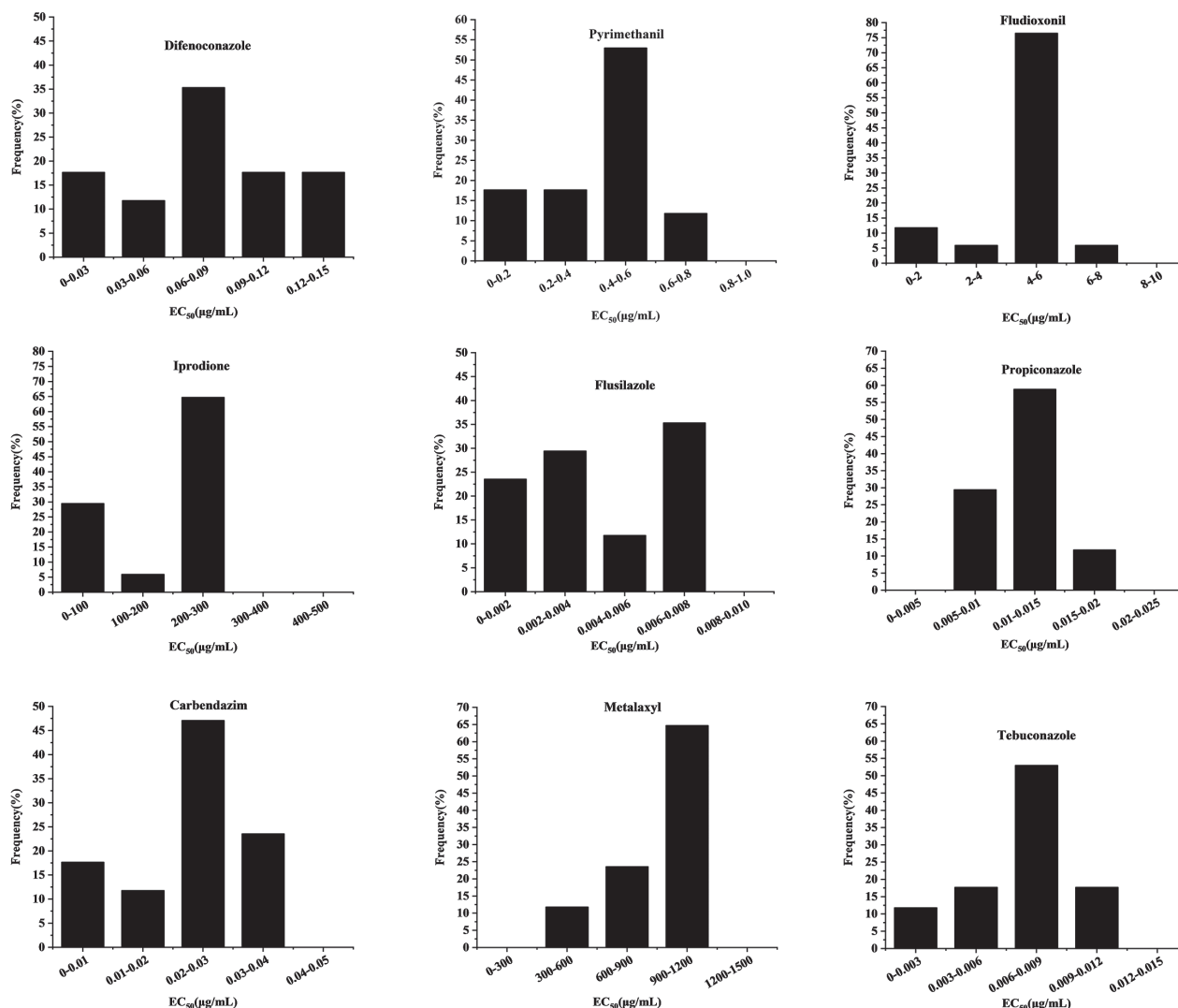


Figure 7. Frequency distribution of the 50% effective concentration (EC_{50}) values of six groups including nine fungicides for *Microdochium chrysopogonis* isolates, based on mycelial growth from 2019 to 2022.

Table 4. In vitro sensitivity ranges and mean 50% effective concentration (EC_{50}) values for the inhibition of *Microdochium chrysopogonis*.

Fungicide	EC_{50} ($\mu\text{g/ml}$)		
	Lowest	Highest	Mean \pm SE
Difenoconazole	0.013	0.127	0.077 \pm 0.039e
Pyrimethanil	0.054	0.605	0.411 \pm 0.180d
Fludioxonil	0.014	6.128	4.525 \pm 1.626c
Iprodione	15.018	260.335	193.031 \pm 99.462b
Flusilazole	0.001	0.007	0.004 \pm 0.003h
Propiconazole	0.006	0.016	0.011 \pm 0.003g
Carbendazim	0.008	0.031	0.024 \pm 0.009f
Metalaxyl	302.785	1056.896	892.677 \pm 236.145a
Tebuconazole	0.002	0.009	0.007 \pm 0.002h

Note: The letters indicate the comparison amongst the different fungicide treatments. Means followed by the same letter do not differ according to a post hoc Dunnett T3 test ($p < 0.05$).

rodione, on the other hand, spanned from 15.018 to 260.335 $\mu\text{g/ml}$, with an average of 193.031 $\mu\text{g/ml}$. Metalaxyl exhibited the highest EC_{50} value, displaying the widest range amongst all fungicides, extending from 302.785 to 1056.896 $\mu\text{g/ml}$ with an average of 892.677 $\mu\text{g/ml}$. Overall, these findings indicate varying degrees of sensitivity to different fungicides amongst *M. chrysopogonis* isolates. These variations in sensitivity could be essential considerations for designing effective fungicide application strategies against vetiver leaf tar spot disease.

The inhibition of mycelial growth revealed that all nine fungicides exhibited a reduction in fungal growth in vitro when compared to plates without amendments. The effectiveness of these fungicides in diminishing the mycelial growth of the isolates was contingent upon both the specific chemical compound and its concentration. Four DMI fungicides, namely, difenoconazole, propiconazole, flusilazole and tebuconazole and one MBC fungicide, carbendazim, displayed strong activity against *M. chrysopogonis* growth at concentrations below 1 $\mu\text{g/ml}$, specifically at concentrations of 1, 0.2, 0.1, 0.2 and 0.2 $\mu\text{g/ml}$, respectively (Fig. 8). However, *M. chrysopogonis* showed a tendency to exhibit better growth in the presence of pyrimethanil, fludioxonil, iprodione and metalaxyl, with mycelial growth being completely inhibited at concentrations exceeding 100 $\mu\text{g/ml}$ (Fig. 8).

Discussion

In a survey of disease on *C. zizanioides* in Guangdong Province, China, from 2019 to 2022, tar spot was the predominant leaf spot disease. Isolation, morphological features, multilocus phylogenetic analysis and pathogenicity tests confirmed that a new *Microdochium* species, *M. chrysopogonis* was the causal agent. To effectively control the disease, the sensitivity of *M. chrysopogonis* to six groups of fungicides, including nine fungicides was determined. Results indicated that four DMI fungicides, namely difenoconazole, propiconazole, flusilazole and tebuconazole and one MBC fungicide, carbendazim, were highly effective against the new species.

The morphology of the new species is introduced along with its sexual and asexual morphological features, which are consistent with the following of *Microdochium*: pale brown to black, subglobose to oval, uniloculate, perithecial

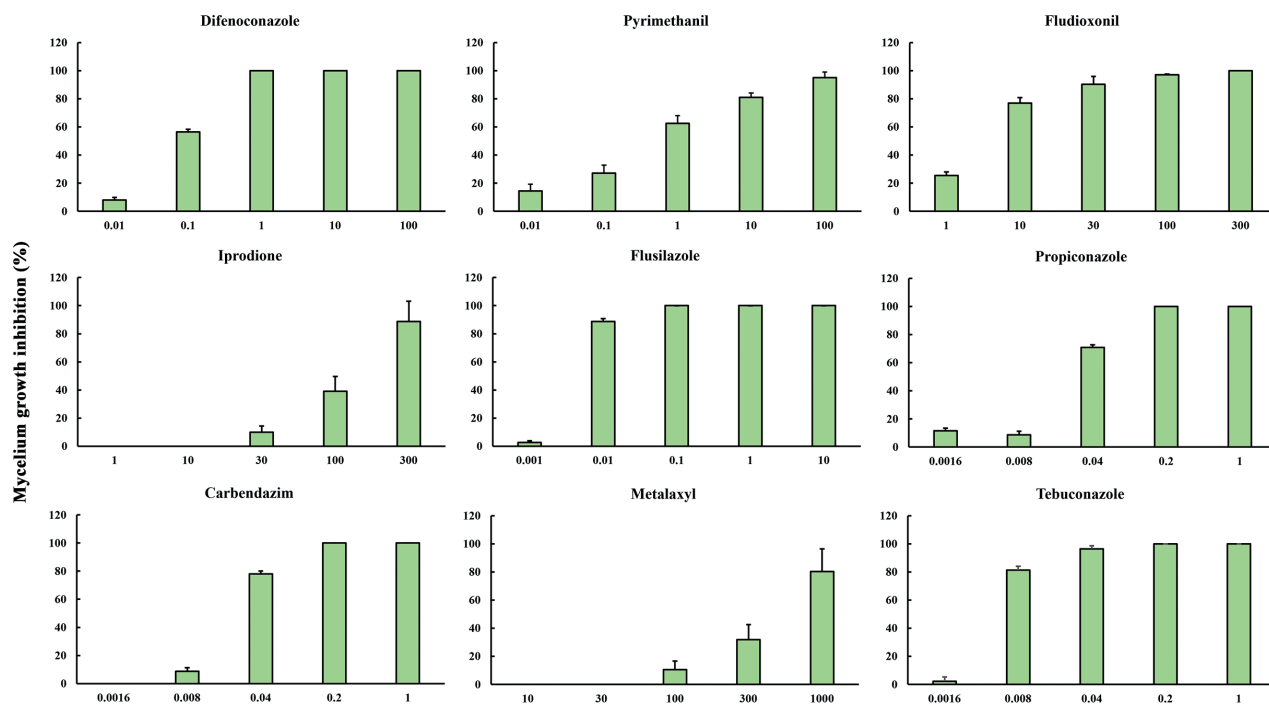


Figure 8. Effect of fungicides on the mycelial growth of *Microdochium chrysopogonis*. Values are shown as the means, with the error bars representing the standard error.

ascomata; hyaline, fasciculate, unitunicate, oblong to narrowly clavate, eight biserial spores with short stipe asci, from which hyaline, clavate, smooth ascospores arise. Conidiophores reduced to hyaline, smooth, aseptate, percurrent, ampulliform or obpyriform, conidiogenous cells, from which hyaline, 0–1-septate, fusiform, lunate conidia with the apex rounded and base flattened usually arise (Figs 1, 3) (Hernández-Restrepo et al. 2016). The concatenated ITS, LSU, *tub2* and *rpb2* sequences were able to identify species in *Microdochium* and proved to be suitable barcoding markers in the process of species resolution (Hernández-Restrepo et al. 2016). Phylogenetic analysis indicated that *M. chrysopogonis* formed a distinct well-supported clade (1/100) and was closely related to *M. dawsoniorum* and *M. ratticaudae* (Fig. 2). Nevertheless, the classification of the new species in the genus *Microdochium* is well supported by morphology, based on sexual and asexual morphs, which are different from those of *M. dawsoniorum* and *M. ratticaudae*.

Temperature is a major factor affecting plant disease epidemics. In recent years, tar spot disease of *C. zizanioides* has become increasingly prevalent in Guangdong Province, China, especially in hot and rainy summers. Thus, the effect of temperature on the growth rate of *M. chrysopogonis* in vitro was evaluated in this study. There were no significant differences in the minimum and optimum growth temperatures amongst the three isolates and the optimum growth temperature was 30 °C (Fig. 6). Research revealed that the highest growth rate of *M. paspali* occurred at 25–28 °C and *M. majus*, *M. seminicola* and *M. nivale* strains in Russia and Europe grew optimally at 20–25 °C (Doohan et al. 2003; Gagkaeva et al. 2020), while *M. nivale* from Slovakia grew better at temperatures below 20 °C (Hudec and Muchová 2010). Thus, the optimum growth temperature varies amongst *Microdochium* species.

A previous study showed that *P. herbarum* could initially induce leaf spots and blight on vetiver grass, causing round or irregular dark brown spots, which

are similar to the symptoms on *M. chrysopogonis* (Zhang et al. 2017). However, the symptoms on *M. chrysopogonis* were different from those on *P. herbarum* in the later period. Specifically, *P. herbarum* caused fusiform or irregular with red-dish-brown margins on the host plant, whereas *M. chrysopogonis* caused fish-eye necrotic haloes surrounding the spot lesions on leaves. Additionally, the disease incidences were different. *P. herbarum* affected 26% to 42% of plants, while *M. chrysopogonis* showed a 100% disease incidence. Given the high disease incidence associated with *M. chrysopogonis* and its induction of leaf spots on vetiver grass, as well as the identification of this new species, it is imperative to conduct future studies addressing the host spectrum, epidemic conditions, biological characteristics and distribution patterns of *M. chrysopogonis*.

The effectiveness of biofungicides, such as bacterial seed treatments using *Pseudomonas* and *Pantoea* in controlling diseases caused by *Microdochium*, has been established (Johansson et al. 2003). However, there remains substantial reliance on registered chemical fungicides. Currently, research on fungicide sensitivity within *Microdochium* mainly focuses on three species: *M. panattonianum*, *M. majus* and *M. nivale*. Six groups of fungicides, namely, MBCs, DMIs, Qols, SDHIs, PPs, and dicarboximides, have been shown to have significant inhibitory activity (Kaneko and Ishii 2009; Aamlid et al. 2017, 2018; Matušinsky et al. 2017; Gagkaeva et al. 2022). In this study, consistent with previous findings, four DMI fungicides (difenoconazole, propiconazole, flusilazole and tebuconazole) and one MBC fungicide (carbendazim) exhibited significant inhibitory effects on the growth of *M. chrysopogonis*, with mean EC_{50} values of 0.077, 0.011, 0.004, 0.024 and 0.007 $\mu\text{g/ml}$, respectively (Table 4). However, dicarboximides (iprodione), which were effective against snow mould and *Microdochium* patch caused by *M. nivale* on turf-grass in previous studies (Gourlie and Hsiang 2017), showed ineffectiveness in this study, with a mean EC_{50} value of 193.031 $\mu\text{g/ml}$. Additionally, while the PP fungicide fludioxonil demonstrated good antifungal activity against *M. majus* in other research (Mao et al. 2023), the isolates in this study displayed only moderate sensitivity to fludioxonil, with an EC_{50} value of 4.525 $\mu\text{g/ml}$ and complete inhibition of mycelial growth required concentrations exceeding 100 $\mu\text{g/ml}$ (Table 4, Fig. 8). These variations in fungicide sensitivity could be attributed to genetic structural changes, introducing bias in chemical control efficacy (Matušinsky et al. 2019). Furthermore, the response of the same pathogen to fungicides can vary amongst regions. For example, the DMI fungicides, tebuconazole and metconazole, were reported to be ineffective against *M. nivale* in the Czech Republic and France (Ioos et al. 2005; Matušinsky et al. 2019). Similarly, *M. nivale* exhibited sensitivity to SDHI fungicides, including pydiflumetofen, fluxapyroxad and penthiopyrad, in vitro, but these fungicides were ineffective in providing acceptable control under field conditions in the USA (Hockemeyer and Koch 2022). These differences may be attributed to variations in environmental factors, such as temperature and humidity, as well as diverse biological characteristics, including epidemiology, fungicide sensitivity and aggressive nature of the pathogen (Abdelhalim et al. 2020). Overall, this study offers valuable insights into fungicide application strategies for effectively managing the disease. Further research is needed to analyse the influences of environmental variables and conduct field trials to validate the effects of DMI fungicides, ultimately enhancing the ability to successfully manage vetiver leaf tar spot disease.

Acknowledgements

We thank the Herbarium of the Chinese Academy of Forestry for helping with the preservation of plant specimens.

Additional information

Conflict of interest

The authors have declared that no competing interests exist.

Ethical statement

No ethical statement was reported.

Funding

This research was financially supported by the Guangdong Basic and Applied Basic Research Foundation (2020A1515110167), School-level Talents Project of Lingnan Normal University (ZL 2034), Natural Science Foundation of Guangdong Province, China (2023A1515011676) and Key Scientific Research Platform and Project of Guangdong Education Department (2021KCXTD054)

Author contributions

Xiang Lu, Xue-Li Niu and Wu Zhang carried out the investigation and sampling. Xiang Lu and Wu Zhang conducted the morphological and phylogenetic analysis. Xiang Lu and Wu Zhang carried out the pathogenicity test. Xiang Lu, Meng-Xian Mai, Wen-Hui Tan, Mu-Yan Zhang, Jie Xie and Yi Lu undertook the fungicide sensitivity experiment. Xiang Lu wrote, edited and reviewed the manuscript. Xiang Lu and Wu Zhang reviewed the manuscript and provided funding. All authors have read and agreed to the published version of the manuscript.

Author ORCIDs

Xiang Lu  <https://orcid.org/0000-0001-9582-1319>

Mengxian Mai  <https://orcid.org/0009-0001-3824-2895>

Wenhui Tan  <https://orcid.org/0009-0008-6054-2174>

Muyan Zhang  <https://orcid.org/0009-0005-8880-9780>

Jie Xie  <https://orcid.org/0009-0002-4200-0140>

Yi Lu  <https://orcid.org/0009-0003-0848-2390>

Data availability

All of the data that support the findings of this study are available in the main text or Supplementary Information.

References

- Aamlid TS, Espevig T, Tronsmo A (2017) Microbiological products for control of *Microdochium nivale* on golf greens. *Crop Science* 57(2): 559–566. <https://doi.org/10.2135/cropsci2016.05.0301>
- Aamlid TS, Niemeläinen O, Paaske K, Widmark D, Ruuttunen P, Kedonperä A (2018) Evaluation of a petroleum-derived spray oil for control of *Microdochium* patch and turf-grass spring performance on Nordic golf greens. *Agronomy Journal* 110(6): 2189–2197. <https://doi.org/10.2134/agronj2018.07.0475>

- Abdelhalim M, Brurberg MB, Hofgaard IS, Rognli OA, Tronsmo AM (2020) Pathogenicity, host specificity and genetic diversity in Norwegian isolates of *Microdochium nivale* and *Microdochium majus*. *European Journal of Plant Pathology* 156(3): 885–895. <https://doi.org/10.1007/s10658-020-01939-5>
- Alkan M, Özer G, İmren M, Özdemir F, Morgounov A, Dababat AA (2021) First report of *Fusarium culmorum* and *Microdochium bolleyi* causing root rot on *Triticale* in Kazakhstan. *Plant Disease* 105(7): e2015. <https://doi.org/10.1094/PDIS-12-20-2659-PDN>
- Araujo L, Paschoalino RS, Rodrigues FÁ (2016) Microscopic aspects of silicon-mediated rice resistance to leaf scald. *Phytopathology* 106(2): 132–141. <https://doi.org/10.1094/PHTO-04-15-0109-R>
- Babu S, Rameshkumar S, Prakash M (2021) Vetiver-a Blessing to Coastal Ecosystem for an Integral Prosperity and Ecological Stability. *Coastal Agriculture and Climate Change*. CRC Press, Florida, 13 pp. <https://doi.org/10.1201/9781003245285-11>
- Braun U (1995) A Monograph of *Cercospora*, *Ramularia* and Allied Genera (Phytopathogenic Hyphomycetes). IHW Verlag, Eching, 2 pp.
- Chen XW, Wong JTF, Wang JJ, Wong MH (2021) Vetiver grass-microbe interactions for soil remediation. *Critical Reviews in Environmental Science and Technology* 51(9): 897–938. <https://doi.org/10.1080/10643389.2020.1738193>
- Crous PW, Slippers B, Wingfield MJ, Rheeder J, Marasas WFO, Philips AJL, Alves A, Burgess T, Barber P, Groenewald JZ (2006) Phylogenetic lineages in the Botryosphaeriaceae. *Studies in Mycology* 55: 235–253. <https://doi.org/10.3114/sim.55.1.235>
- Crous PW, Verkley GJM, Groenewald JZ, Samson RA (2009) *Fungal Biodiversity*. American Phytopathological Society, St. Paul, 269 pp.
- Crous PW, Wingfield MJ, Chooi Y-H, Gilchrist CLM, Lacey E, Pitt JI, Roets F, Swart WJ, Cano-Lira JF, Valenzuela-Lopez N, Hubka V, Shivas RG, Stchigel AM, Holdom DG, Jurjević Ž, Kachalkin AV, Lebel T, Lock C, Martín MP, Tan YP, Tomashevskaya MA, Vitelli JS, Baseia IG, Bhatt VK, Brandrud TE, De Souza JT, Dima B, Lacey HJ, Lombard L, Johnston PR, Morte A, Papp V, Rodríguez A, Rodríguez-Andrade E, Semwal KC, Tegart L, Abad ZG, Akulov A, Alvarado P, Alves A, Andrade JP, Arenas F, Asenjo C, Ballarà J, Barrett MD, Berná LM, Berraf-Tebbal A, Bianchinotti MV, Bransgrove K, Burgess TI, Carmo FS, Chávez R, Čmoková A, Dearnaley JDW, Santiago ALCMA, Freitas-Neto JF, Denman S, Douglas B, Dovana F, Eichmeier A, Esteve-Raventós F, Farid A, Fedosova AG, Ferisin G, Ferreira RJ, Ferrer A, Figueiredo CN, Figueiredo YF, Reinoso-Fuentealba CG, Garrido-Benavent I, Cañete-Gibas CF, Gil-Durán C, Glushakova AM, Gonçalves MFM, González M, Górczak M, Gorton C, Guard FE, Guarizo AL, Guarro J, Gutiérrez M, Hamal P, Hien LT, Hocking AD, Houbaken J, Hunter GC, Inácio CA, Jourdan M, Kapitonov VI, Kelly L, Khanh TN, Kislo K, Kiss L, Kiyashko A, Kolařík M, Kruse J, Kubátová A, Kučera V, Kučerová I, Kušan I, Lee HB, Levicán G, Lewis A, Liem NV, Liimatainen K, Lim HJ, Lyons MN, Maciá-Vicente JG, Magaña-Dueñas V, Mahiques R, Malysheva EF, Marbach PAS, Marinho P, Matočec N, McTaggart AR, Mešić A, Morin L, Muñoz-Mohedano JM, Navarro-Ródenas A, Nicolli CP, Oliveira RL, Otsing E, Ovrebø CL, Pankratov TA, Paños A, Paz-Conde A, Pérez-Sierra A, Phosri C, Pintos Á, Pošta A, Prencipe S, Rubio E, Saitta A, Sales LS, Sanhueza L, Shuttleworth LA, Smith J, Smith ME, Spadaro D, Spetik M, Sochor M, Sochorová Z, Sousa JO, Suwannasai N, Tedersoo L, Thanh HM, Thao LD, Tkáčec Z, Vaghefi N, Venzhik AS, Verbeken A, Vizzini A, Voyron S, Wainhouse M, Whalley AJS, Wrzosek M, Zapata M, Zeil-Rolfe I, Groenewald JZ (2020) *Fungal Planet description sheets: 1042–1111*. *Persoonia* 44(1): 301–459. <https://doi.org/10.3767/persoonia.2020.44.11>
- Crous PW, Cowan DA, Maggs-Kölling G, Yilmaz N, Thangavel R, Wingfield MJ, Noorde-loos ME, Dima B, Brandrud TE, Jansen GM, Morozova OV, Vila J, Shivas RG, Tan YP,

- Bishop-Hurley S, Lacey E, Marney TS, Larsson E, Le Floch G, Lombard L, Nodet P, Hubka V, Alvarado P, Berraf-Tebbal A, Reyes JD, Delgado G, Eichmeier A, Jordal JB, Kachalkin AV, Kubátová A, Maciá-Vicente JG, Malysheva EF, Papp V, Rajeshkumar KC, Sharma A, Spetik M, Szabóová D, Tomashevskaya MA, Abad JA, Abad ZG, Alexandrova AV, Anand G, Arenas F, Ashtekar N, Balashov S, Bañares Á, Baroncelli R, Bera I, Biketova AYU, Blomquist CL, Boekhout T, Boertmann D, Bulyonkova TM, Burgess TI, Carnegie AJ, Cobo-Diaz JF, Corriol G, Cunnington JH, da Cruz MO, Damm U, Davoodian N, de A Santiago ALCM, Dearnaley J, de Freitas LWS, Dhileepan K, Dimitrov R, Di Piazza S, Fatima S, Fuljer F, Galera H, Ghosh A, Giraldo A, Glushakova AM, Gorczak M, Gouliamova DE, Gramaje D, Groenewald M, Gunsch CK, Gutiérrez A, Holdom D, Houbraken J, Ismailov AB, Istel Ł, Iturriaga T, Jeppson M, Jurjević Ž, Kalinina LB, Kapitonov VI, Kautmanová I, Khalid AN, Kiran M, Kiss L, Kovács Á, Kurose D, Kušan I, Lad S, Læssøe T, Lee HB, Luangsa-ard JJ, Lynch M, Mahamedi AE, Malysheva VF, Mateos A, Matočec N, Mešić A, Miller AN, Mongkolsamrit S, Moreno G, Morte A, Mostowfizadeh-Ghalamfarsa R, Naseer A, Navarro-Ródenas A, Nguyen TTT, Noisripoom W, Ntandu JE, Nuytinck J, Ostrý V, Pankratov TA, Pawłowska J, Pecenka J, Pham THG, Polhorský A, Pošta A, Raudabaugh DB, Reschke K, Rodríguez A, Romero M, Rooney-Latham S, Roux J, Sandoval-Denis M, Smith MTh, Steinrucken TV, Svetasheva TY, Tkalčec Z, van der Linde EJ, Vegte M, Vauras J, Verbeken A, Visagie CM, Vitelli JS, Volobuev SV, Weill A, Wrzosek M, Zmitrovich IV, Zvyagina EA, Groenewald JZ (2021a) Fungal Planet description sheets: 1182–1283. *Persoonia* 46: 313–528. <https://doi.org/10.3767/persoonia.2021.46.11>
- Crous PW, Osieck ER, Jurjević Ž, Boers J, Van Iperen AL, Starink-Willemse M, Dima B, Balashov S, Bulgakov TS, Johnston PR, Morozova OV, Pinruan U, Sommai S, Alvarado P, Decock CA, Lebel T, McMullan-Fisher S, Moreno G, Shivas RG, Zhao L, Abdollahzadeh J, Abrinbana M, Ageev DV, Akhmetova G, Alexandrova AV, Altés A, Amaral AGG, Angelini C, Antonín V, Arenas F, Asselman P, Badali F, Baghela A, Bañares A, Barreto RW, Baseia IG, Bellanger J-M, Berraf-Tebbal A, Biketova AYU, Bukharova NV, Burgess TI, Cabero J, Câmara MPS, Cano-Lira JF, Ceryngier P, Chávez R, Cowan DA, de Lima AF, Oliveira RL, Denman S, Dang QN, Dovana F, Duarte IG, Eichmeier A, Erhard A, Esteve-Raventós F, Fellin A, Ferisin G, Ferreira RJ, Ferrer A, Finy P, Gaya E, Geering ADW, Gil-Durán C, Glässnerová K, Glushakova AM, Gramaje D, Guard FE, Guarnizo AL, Haelewaters D, Halling RE, Hill R, Hirooka Y, Hubka V, Iliushin VA, Ivanova DD, Ivanushkina NE, Jangsantear P, Justo A, Kachalkin AV, Kato S, Khamsuntorn P, Kirtsideli IY, Knapp DG, Kochkina GA, Koukol O, Kovács GM, Kruse J, Kumar TKA, Kušan I, Læssøe T, Larsson E, Lebeuf R, Levicán G, Loizides M, Marinho P, Luangsa-ard JJ, Lukina EG, Magaña-Dueñas V, Maggs-Kölling G, Malysheva EF, Malysheva VF, Martín B, Martín MP, Matočec N, McTaggart AR, Mehrabi-Koushki M, Mešić A, Miller AN, Mironova P, Moreau P-A, Morte A, Müller K, Nagy LG, Nanu S, Navarro-Ródenas A, Nel WJ, Nguyen TH, Nóbrega TF, Noordeloos ME, Olariaga I, Overton BE, Ozerskaya SM, Palani P, Pancorbo F, Papp V, Pawłowska J, Pham TQ, Phosri C, Popov ES, Portugal A, Pošta A, Reschke K, Reul M, Ricci GM, Rodríguez A, Romanowski J, Ruchikachorn N, Saar I, Safi A, Sakolrak B, Salzmann F, Sandoval-Denis M, Sangwichein E, Sanhueza L, Sato T, Sastoque A, Senn-Irlet B, Shibata A, Siepe K, Somrithipol S, Spetik M, Sridhar P, Stchigel AM, Stuskova K, Suwannasai N, Tan YP, Thangavel R, Tiago I, Tiwari S, Tkalčec Z, Tomashevskaya MA, Tonegawa C, Tran HX, Tran NT, Trovão J, Trubitsyn VE, Van Wyk J, Vieira WAS, Vila J, Visagie CM, Vizzini A, Volobuev SV, Vu DT, Wangsawat N, Yaguchi T, Ercole E, Ferreira BW, de Souza AP, Vieira BS, Groenewald JZ (2021b) Fungal Planet description sheets: 1284–1382. *Persoonia* 47: 178–374. <https://doi.org/10.3767/persoonia.2021.47.06>

- David A, Wang F, Sun X, Li H, Lin J, Li P, Deng G (2019) Chemical composition, antioxidant, and antimicrobial activities of *Vetiveria zizanioides* (L.) nash essential oil extracted by carbon dioxide expanded ethanol. *Molecules* (Basel, Switzerland) 24(10): 1897. <https://doi.org/10.3390/molecules24101897>
- Debieu D, Bach J, Arnold A, Brousset S, Gredt M, Taton M, Rahier A, Malosse C, Leroux P (2000) Inhibition of ergosterol biosynthesis by morpholine, piperidine, and spiroketalamine fungicides in *Microdochium nivale*: Effect on sterol composition and sterol $\Delta 8 \rightarrow \Delta 7$ -isomerase activity. *Pesticide Biochemistry and Physiology* 67(2): 85–94. <https://doi.org/10.1006/pest.2000.2485>
- Dirchwolf PM, Moschini RC, Gutiérrez SA, Carmona MA (2023) Modelling of the effects of environmental factors on rice grain discoloration incidence in Corrientes province, Argentina. *Journal of Phytopathology* 171(1): 12–22. <https://doi.org/10.1111/jph.13150>
- Doohan FM, Brennan J, Cooke BM (2003) *Epidemiology of Mycotoxin Producing Fungi*. Springer, Dordrecht, 129 pp.
- Gagkaeva TY, Orina AS, Gavrilova OP, Gogina NN (2020) Evidence of *Microdochium* Fungi associated with cereal grains in Russia. *Microorganisms* 8(3): e340. <https://doi.org/10.3390/microorganisms8030340>
- Gagkaeva T, Orina A, Gavrilova O, Usoltseva M, Crouch JA, Normann K, Entwistle K, Torp T, Espevig T (2022) In vitro fungicide sensitivity of *Clariireedia*, *Fusarium*, and *Microdochium* isolates from grasses. *International Turfgrass Society Research Journal* 14(1): 972–980. <https://doi.org/10.1002/its2.139>
- Galea VJ, Price TV, Sutton BC (1986) Taxonomy and biology of the lettuce anthracnose fungus. *Transactions of the British Mycological Society* 86(4): 619–628. [https://doi.org/10.1016/S0007-1536\(86\)80065-1](https://doi.org/10.1016/S0007-1536(86)80065-1)
- Glynn NC, Hare MC, Edwards SG (2008) Fungicide seed treatment efficacy against *Microdochium nivale* and *M. majus* in vitro and in vivo. *Pest Management Science* 64(8): 793–799. <https://doi.org/10.1002/ps.1558>
- Gourlie R, Hsiang T (2017) Resistance to dicarboximide fungicides in a Canadian population of *Microdochium nivale*. *International Turfgrass Society Research Journal* 13(1): 133–138. <https://doi.org/10.2134/itsrj2016.06.0497>
- Hernández-Restrepo M, Groenewald JZ, Crous PW (2016) Taxonomic and phylogenetic re-evaluation of *Microdochium*, *Monographella* and *Idriella*. *Persoonia* 36(1): 57–82. <https://doi.org/10.3767/003158516X688676>
- Hockemeyer K, Koch PL (2022) Field evaluations and in vitro sensitivity of *Microdochium nivale* to succinate dehydrogenase (SDHI) fungicides. *International Turfgrass Society Research Journal* 14(1): 951–957. <https://doi.org/10.1002/its2.48>
- Hong SK, Kim WG, Choi HW, Lee SY (2008) Identification of *Microdochium bolleyi* associated with basal rot of creeping bent grass in Korea. *Mycobiology* 36(2): 77–80. <https://doi.org/10.4489/MYCO.2008.36.2.077>
- Hudec K, Muchová D (2010) Influence of temperature and species origin on *Fusarium* spp. and *Microdochium nivale* pathogenicity to wheat seedlings. *Plant Protection Science* 46(2): 59–65. <https://doi.org/10.17221/12/2009-PPS>
- Ioos R, Belhadj A, Menez M, Faure A (2005) The effects of fungicides on *Fusarium* spp. and *Microdochium nivale* and their associated trichothecene mycotoxins in French naturally-infected cereal grains. *Crop Protection* 24(10): 894–902. <https://doi.org/10.1016/j.cropro.2005.01.014>
- Jewell LE, Hsiang T (2013) Multigene differences between *Microdochium nivale* and *Microdochium majus*. *Botany* 91(2): 99–106. <https://doi.org/10.1139/cjb-2012-0178>

- Jia X, Zheng X, Damm U, Lu X, Niu XL, Feng Y, Zhang W (2023 [June 04]) *Stenocarpella chrysopogonis*, a new species causing leaf streak disease of *Chrysopogon zizanioides* in southern China. *Plant Disease* PDIS-02-23-0383-SR. <https://doi.org/10.1094/PDIS-02-23-0383-SR>
- Johansson PM, Johnsson L, Gerhardson B (2003) Suppression of wheat-seedling diseases caused by *Fusarium culmorum* and *Microdochium nivale* using bacterial seed treatment. *Plant Pathology* 52(2): 219–227. <https://doi.org/10.1046/j.1365-3059.2003.00815.x>
- Kaneko I, Ishii H (2009) Effect of azoxystrobin on activities of antioxidant enzymes and alternative oxidase in wheat head blight pathogens *Fusarium graminearum* and *Microdochium nivale*. *Journal of General Plant Pathology* 75(5): 388–398. <https://doi.org/10.1007/s10327-009-0178-9>
- Katoh K, Standley DM (2013) MAFFT multiple sequence alignment software version 7: Improvements in performance and usability. *Molecular Biology and Evolution* 30(4): 772–780. <https://doi.org/10.1093/molbev/mst010>
- Koch PL, Stier JC, Kerns JP (2015) Snow cover has variable effects on persistence of fungicides and their suppression of microdochium patch on amenity turfgrass. *Plant Pathology* 64(6): 1417–1428. <https://doi.org/10.1111/ppa.12379>
- Kumar S, Stecher G, Tamura K (2016) MEGA7: Molecular evolutionary genetics analysis version 7.0 for bigger datasets. *Molecular Biology and Evolution* 33(7): 1870–1874. <https://doi.org/10.1093/molbev/msw054>
- Liang J, Li G, Zhao M, Cai L (2019) A new leaf blight disease of turfgrasses caused by *Microdochium poae*, sp. nov. *Mycologia* 111(2): 265–273. <https://doi.org/10.1080/00275514.2019.1569417>
- Lin JM, Liu JX, Niu XL, Zhang W (2019) Root and basal stem rot caused by *Gaeumannomyces graminicola* on *Vetiveria zizanioides* in southern China. *Plant Disease* 103(8): e2128. <https://doi.org/10.1094/PDIS-12-18-2161-PDN>
- Liu YJ, Whelen S, Hall BD (1999) Phylogenetic relationships among ascomycetes: Evidence from an RNA polymerase II subunit. *Molecular Biology and Evolution* 16(12): 1799–1808. <https://doi.org/10.1093/oxfordjournals.molbev.a026092>
- Mao Y, Wu J, Song W, Zhao B, Zhao H, Cai Y, Wang J-X, Zhou M, Duan Y (2023) Occurrence and chemical control strategy of wheat brown foot rot caused by *Microdochium majus*. *Plant Disease* 107(11): 3523–3530. <https://doi.org/10.1094/PDIS-02-23-0392-RE>
- Matušinsky P, Svačinová I, Jonavičienė A, Tvarůžek L (2017) Long-term dynamics of causative agents of stem base diseases in winter wheat and reaction of Czech *Oculimacula* spp. and *Microdochium* spp. populations to prochloraz. *European Journal of Plant Pathology* 148(1): 199–206. <https://doi.org/10.1007/s10658-016-1082-8>
- Matušinsky P, Svobodová LL, Svačinová I, Havis N, Hess M, Tvarůžek L (2019) Population genetic structure of *Microdochium majus* and *Microdochium nivale* associated with foot rot of cereals in the Czech Republic and adaptation to penthiopyrad. *European Journal of Plant Pathology* 155(1): 1–12. <https://doi.org/10.1007/s10658-019-01737-8>
- Maurya R, Yadav P, Krishna R, Kulkarni P, Rastogi S, Mohapatra S, Srivastava S, Akhtar MQ, Shukla AK, Chauhan HS, Verma RK, Chanotiya CS, Shasany AK (2023) Transcriptome and metabolome analysis of sesquiterpene diversity in Indian vetiver (*Chrysopogon zizanioides* L. Roberty). *Industrial Crops and Products* 200: e116798. <https://doi.org/10.1016/j.indcrop.2023.116798>
- Moon UR, Durge AA, Kumar M (2020) Value addition of khus (*Vetiveria zizanioides* L. Nash) root extracts by elicitor and heat treatment. *Industrial Crops and Products* 144: e112037. <https://doi.org/10.1016/j.indcrop.2019.112037>

- Nylander JAA (2004) MrModeltest 2.0. MrModeltest Version 2. Uppsala University, Uppsala.
- Polizzi G, Aiello D, Vitale A, Giuffrida F, Groenewald JZ, Crous PW (2009) First report of shoot blight, canker, and gummosis caused by *Neoscytalidium dimidiatum* on citrus in Italy. *Plant Disease* 93(11): 1215–1215. <https://doi.org/10.1094/PDIS-93-11-1215A>
- Rambaut A (2018) FigTree v.1.4.4. University of Edinburgh, Edinburgh.
- Rayner RW (1970) A Mycological Colour Chart. Commonwealth Mycological Institute & British Mycological Society, Kew, 34 pp.
- Ren R, Yang X, Ray RV (2015) Comparative aggressiveness of *Microdochium nivale* and *M. majus* and evaluation of screening methods for *Fusarium* seedling blight resistance in wheat cultivars. *European Journal of Plant Pathology* 141(2): 281–294. <https://doi.org/10.1007/s10658-014-0541-3>
- Ronquist F, Teslenko M, van der Mark P, Ayres DL, Darling A, Höhna S, Larget B, Liu L, Suchard MA, Huelsenbeck JP (2012) MrBayes 3.2: Efficient bayesian phylogenetic inference and model choice across a large model space. *Systematic Biology* 61(3): 539–542. <https://doi.org/10.1093/sysbio/sys029>
- Stewart S, Rodríguez M, Mattos N, Abreo E, Stewart S, Rodríguez M, Mattos N, Abreo E (2019) First report of zonate leaf spot in sorghum caused by *Microdochium sorghi* in Uruguay. *Agrociencia* 23(2): 94–98. <https://doi.org/10.31285/AGRO.23.74>
- Swofford D (2002) PAUP*. phylogenetic analysis using parsimony (*and other methods). version 4.0b10. Sinauer Associates, Sunderland.
- Sydow H (1924) Mycotheca germanica. Fasc. XLII–XLV (No. 20512250). *Annales Mycologici* 22: 257–268.
- Vilgalys R, Hester M (1990) Rapid genetic identification and mapping of enzymatically amplified ribosomal DNA from several *Cryptococcus* species. *Journal of Bacteriology* 172(8): 4238–4246. <https://doi.org/10.1128/jb.172.8.4238-4246.1990>
- White TJ, Bruns T, Lee S, Taylor J (1990) Amplification and Direct Sequencing of Fungal Ribosomal RNA Genes for Phylogenetics. *PCR Protocols: a Guide to Methods and Applications*. Academic Press, San Diego, 482 pp. <https://doi.org/10.1016/B978-0-12-372180-8.50042-1>
- Wicks TJ, Hall B, Pezzaniti P (1994) Fungicidal control of anthracnose (*Microdochium panattonianum*) on lettuce. *Australian Journal of Experimental Agriculture* 34(2): 277–283. <https://doi.org/10.1071/EA9940277>
- Yin LF, Du SF, Chaisiri C, Cheewangkoon R, Luo CX (2019) Phylogenetic analysis and fungicide baseline sensitivities of *Monilia mumeicola* in China. *Plant Disease* 103(9): 2231–2236. <https://doi.org/10.1094/PDIS-11-18-1953-RE>
- Zhang W, Nan Z, Tian P, Hu M, Gao Z, Li M, Liu G (2015) *Microdochium paspali*, a new species causing seashore paspalum disease in southern China. *Mycologia* 107(1): 80–89. <https://doi.org/10.3852/14-119>
- Zhang W, Liu JX, Huo PH (2017) *Phoma herbarum* causes leaf spots and blight on Vetiver grass (*Vetiveria zizanioides* L.) in southern China. *Plant Disease* 101(10): e1823. <https://doi.org/10.1094/PDIS-04-17-0519-PDN>

Supplementary material 1

Phylogenetic tree inferred from a maximum likelihood analysis based on a combined alignment of ITS sequences of 97 isolates of the *Microdochium* sp.

Authors: Xiang Lu, Mengxian Mai, Wenhui Tan, Muyan Zhang, Jie Xie, Yi Lu, Xue Li Niu, Wu Zhang

Data type: tif

Explanation note: Bootstrap support values obtained with ML above 70% and Bayesian (BI) posterior probability values above 0.90 are shown at the nodes (BI/ML). The designated outgroup taxa are *Thamnomycetes dendroidea* CBS 123578. Numbers of ex-type strains are emphasized with an asterisk and species are delimited with shaded blocks. Isolates of *M. chrysopogonis* are indicated with lighter text.

Copyright notice: This dataset is made available under the Open Database License (<http://opendatacommons.org/licenses/odbl/1.0/>). The Open Database License (ODbL) is a license agreement intended to allow users to freely share, modify, and use this Dataset while maintaining this same freedom for others, provided that the original source and author(s) are credited.

Link: <https://doi.org/10.3897/mycokeys.100.112128.suppl1>

Supplementary material 2

Phylogenetic tree inferred from a maximum likelihood analysis based on a combined alignment of LSU sequences of 72 isolates of the *Microdochium* sp.

Authors: Xiang Lu, Mengxian Mai, Wenhui Tan, Muyan Zhang, Jie Xie, Yi Lu, Xue Li Niu, Wu Zhang

Data type: tif

Explanation note: Bootstrap support values obtained with ML above 70% and Bayesian (BI) posterior probability values above 0.90 are shown at the nodes (BI/ML). The designated outgroup taxa are *Thamnomycetes dendroidea* CBS 123578. Numbers of ex-type strains are emphasized with an asterisk and species are delimited with shaded blocks. Isolates of *M. chrysopogonis* are indicated with lighter text.

Copyright notice: This dataset is made available under the Open Database License (<http://opendatacommons.org/licenses/odbl/1.0/>). The Open Database License (ODbL) is a license agreement intended to allow users to freely share, modify, and use this Dataset while maintaining this same freedom for others, provided that the original source and author(s) are credited.

Link: <https://doi.org/10.3897/mycokeys.100.112128.suppl2>

Supplementary material 3

Phylogenetic tree inferred from a maximum likelihood analysis based on a combined alignment of *rpb2* sequences of 71 isolates of the *Microdochium* sp.

Authors: Xiang Lu, Mengxian Mai, Wenhui Tan, Muyan Zhang, Jie Xie, Yi Lu, Xue Li Niu, Wu Zhang

Data type: tif

Explanation note: Bootstrap support values obtained with ML above 70% and Bayesian (BI) posterior probability values above 0.90 are shown at the nodes (BI/ML). The designated outgroup taxa are *Thamnomycetes dendroidea* CBS 123578. Numbers of ex-type strains are emphasized with an asterisk and species are delimited with shaded blocks. Isolates of *M. chrysopogonis* are indicated with lighter text.

Copyright notice: This dataset is made available under the Open Database License (<http://opendatacommons.org/licenses/odbl/1.0/>). The Open Database License (ODbL) is a license agreement intended to allow users to freely share, modify, and use this Dataset while maintaining this same freedom for others, provided that the original source and author(s) are credited.

Link: <https://doi.org/10.3897/mycokeys.100.112128.suppl3>

Supplementary material 4

Phylogenetic tree inferred from a maximum likelihood analysis based on a combined alignment of *tub2* sequences of 80 isolates of the *Microdochium* sp.

Authors: Xiang Lu, Mengxian Mai, Wenhui Tan, Muyan Zhang, Jie Xie, Yi Lu, Xue Li Niu, Wu Zhang

Data type: tif

Explanation note: Bootstrap support values obtained with ML above 70% and Bayesian (BI) posterior probability values above 0.90 are shown at the nodes (BI/ML). The designated outgroup taxa are *Thamnomycetes dendroidea* CBS 123578. Numbers of ex-type strains are emphasized with an asterisk and species are delimited with shaded blocks. Isolates of *M. chrysopogonis* are indicated with lighter text.

Copyright notice: This dataset is made available under the Open Database License (<http://opendatacommons.org/licenses/odbl/1.0/>). The Open Database License (ODbL) is a license agreement intended to allow users to freely share, modify, and use this Dataset while maintaining this same freedom for others, provided that the original source and author(s) are credited.

Link: <https://doi.org/10.3897/mycokeys.100.112128.suppl4>

The phylogeny and taxonomy of *Upretia* (Caloplacoideae, Teloschistaceae), reveal three new species from Southwestern China

Lijuan Li^{1,2}^{*}, Yanyun Zhang³^{*}, Christian Printzen², Lisong Wang^{1,4}, Xinyu Wang^{1,4}

¹ Key Laboratory for Plant Diversity and Biogeography of East Asia, Kunming Institute of Botany, Chinese Academy of Sciences, Kunming 650201, China

² Senckenberg Research Institute and Natural History Museum, 60325, Frankfurt am Main, Germany

³ College of Life Science, Anhui Normal University, Wuhu 241000, China

⁴ Yunnan Key Laboratory for Fungal Diversity and Green Development, Kunming Institute of Botany, Chinese Academy of Sciences, Kunming 650201, China

Corresponding authors: Lisong Wang (wanglisong@mail.kib.ac.cn); Xinyu Wang (wangxinyu@mail.kib.ac.cn)

Abstract

Several specimens of *Upretia* from Southwest China are morphologically and phylogenetically distinct from currently recognized species in the genus. These specimens are here accommodated within a new species, *Upretia zeorina* Li J. Li & Printzen. It is characterized by an areolate to squamulose thallus with brown to blackish brown upper surface, pruinose, zeorine type apothecia, black discs, narrowly bacilliform conidia, and the production of gyrophoric acid. Two other specimens of *Upretia* from China are distinct from currently accepted species and tentatively referred to as *Upretia* sp. 1 and *Upretia* sp. 2. A key to all known species of *Upretia* is also provided.

Key words: Chemistry, Hengduan Mountains, lichen, phylogenetic analyses, zeorine type apothecia



Academic editor: Cecile Gueidan

Received: 21 August 2023

Accepted: 12 November 2023

Published: 7 December 2023

Citation: Li L, Zhang Y, Printzen C, Wang L, Wang X (2023) The phylogeny and taxonomy of *Upretia* (Caloplacoideae, Teloschistaceae), reveal three new species from Southwestern China. MycoKeys 100: 233–243. <https://doi.org/10.3897/mycokeys.100.111446>

Copyright: © Lijuan Li et al.

This is an open access article distributed under terms of the Creative Commons Attribution License (Attribution 4.0 International – CC BY 4.0).

Introduction

The family Teloschistaceae is one of the largest families of lichenized fungi, including more than 1000 known species, and divided into four subfamilies, Brownlielloideae, Caloplacoideae, Teloschistoideae and Xanthorioideae (Gaya et al. 2012; Arup et al. 2013; Kondratyuk et al. 2015). The originally monotypic genus *Upretia* S. Y. Kondr., A. Thell & J. S. Hur was described in the subfamily Caloplacoideae. Its type species, i.e., *U. amarkantakana* (Y. Joshi & Upreti) S.Y. Kondr. & A. Thell from India is characterized by a partly pruinose, lobate to subsquamulose, olivaceous grey to brown thallus, lecanorine apothecia, small ascospores and narrowly bacilliform conidia (Kondratyuk et al. 2018). Subsequently, two more species were reported, *U. hueana* (B. de Lesd.) S. Y. Kondr. et Upreti from India and *U. squamulosa* Y. Y. Zhang & Li S. Wang from China (Zhang et al. 2019; Mishra et al. 2020).

* These authors contributed equally to this work.

Our field work along the collection routes of Handel-Mazzetti (1914–1915) (Zahlbruckner 1930) in Hengduan Mountains, Southwest China, yielded specimens of the family Teloschistaceae, which had polarilocular ascospores and that were phylogenetically close to the genus *Upretia*. Analyses of morphological traits and phylogenetic evidence suggest that these specimens are distinct from currently recognized species. Our Chinese specimens represented three morphospecies, of which only one was shared by multiple accessions. The latter are accommodated within a new species, i.e., *Upretia zeorina* Li J. Li & Printzen, whereas the other two specimens are tentatively referred to *Upretia* sp. 1 and *Upretia* sp. 2. A key to all the known species of *Upretia* is also provided.

Materials and methods

Phenotypic studies

The specimens examined are deposited in Lichen Herbarium, Kunming Institute of Botany, Chinese Academy of Sciences (**KUN**), and the Herbarium Senckenbergianum Frankfurt/M. (**FR**).

External morphological characters were studied on air-dried material under a stereomicroscope (Zeiss Stemi SV11). Anatomical features were studied using a light microscope (Zeiss Axioskop 2 plus) on transverse sections of apothecia and thalli, cut with a freezing microtome (Zeiss HYRAX KS 34) to 16–20 µm thickness and mounted in water, Lugol's iodine solution (I) and lactophenol cotton blue (LCB).

Spot tests were conducted using the following reagents: a 10% aqueous solution of potassium hydroxide (KOH) (K), saturated aqueous solution of sodium hypochlorite NaClO (C). High performance thin layer chromatography (HPTLC) was performed in solvents A, B' and C to detect lichen secondary metabolites (Culberson and Kristinsson 1970; Arup et al. 1993). Substances were identified according to Orange et al. (2001).

DNA extraction, PCR and sequencing

Total DNA was extracted from specimens using the GeneOn Plant DNA Extraction Kit (GeneOn BioTech, Changchun, China) by the magnetic bead method or the DNA secure Plant Kit (Tiangen Biotech, Beijing, China). The fungal internal transcribed spacer (ITS) region of the rDNA repeat was amplified via polymerase chain reaction (PCR) using the primers ITS1F (Gardes and Bruns 1993) and ITS4A (Larena et al. 1999). PCRs were performed in 25 µL volumes using Illustra PuReTaq Ready-To-Go PCR Beads (GE Healthcare Life Sciences, Little Chalfont, Buckinghamshire, UK) containing 5 µL of DNA extract and 1 µL (10mM) of each primer; or in 25 µL reactions containing 12.5 µL 2× Taq PCR Mix (Tiangen Biotech, Beijing, China), 0.5 µL of each primer, 10.5 µL ddH₂O and 1 µL of DNA. Cycling conditions included initial denaturation at 94 °C for 5 min, followed by 4 cycles at 94 °C for 30 s, 54 °C for 45 s, and 72 °C for 60 s, 30 cycles at 94 °C for 30 s, 48 °C for 30 s, and 72 °C for 60 s, and a final extension at 72 °C for 10 min. The PCR products were sequenced by MacroGen Europe (Amsterdam, The Netherlands) or TsingKe Biological Technology (Kunming, China).

Phylogenetic analyses

We used nrITS sequences to construct a phylogenetic tree with more species of the subfamily Caloplacoideae (Table 1). Sequences were assembled and edited in Geneious Prime 2021.0.3 (<https://www.geneious.com/>). Dataset was aligned using the MAFFT v.7 online service (<https://mafft.cbrc.jp/alignment/server/index.html>, Katoh and Standley (2013)). The final alignment included 25 taxa with 562 bp.

Phylogenetic reconstructions were carried out using maximum likelihood and Bayesian inference. Maximum likelihood phylogeny was inferred using the online version of IQ-TREE (<http://iqtree.cibiv.univie.ac.at/>, Trifinopoulos et al. 2016) with automated substitution model selection with three partitions (ITS1, 5.8S rDNA, ITS2). The best-fit model was selected according to the Bayesian information criterion (BIC) for individual per partition as: TNe+G4 for ITS1, K2P+I for 5.8S, TNe+I for ITS2. The Branch support was assessed using both ultra-fast bootstrap approximation (UFBoot) (Minh et al. 2013) with 1000 replicates

Table 1. Specimens used for the phylogenetic analyses including collection information and GenBank accession numbers for nrITS sequences. Newly obtained sequences in this study are in bold.

Species name	Voucher details	Country	GenBank No.
<i>Caloplaca cerina</i>	Elvebakk 03-084 (TROM)	Norway	KC179425
<i>Caloplaca monacensis</i>	Malíček 8255 (JM)	Ukraine	MG773668
<i>Caloplaca stillicidiorum</i>	Gueidan s.n. (BCN)	France	EU639607
<i>Fauriea chujaensis</i>	Kondratyuk SK D07 (KoLRI)	South Korea	KX793095
<i>Fauriea orientochinensis</i>	Wang & Hur SK710 (KoLRI)	China	KX793097
<i>Ioplaca pindarensis</i>	Aptroot 56827 (ABL)	China	JQ301672
<i>Upretia amarkantakana</i> 1	Kondratyuk SK E23 (LWG)	India	MG652763
<i>Upretia amarkantakana</i> 2	Kondratyuk SK J21 (LWG)	India	MG652765
<i>Upretia amarkantakana</i> 3	Kondratyuk SK J59 (LWG)	India	MG652766
<i>Upretia squamulosa</i> 1	Wang et al. 17-56088 (KUN)	China	MH497054
<i>Upretia squamulosa</i> 2	Wang et al. 15-47423 (KUN)	China	MH497055
<i>Upretia squamulosa</i> 3	Wang et al. 16-50148 (KUN)	China	MH497056
<i>Upretia squamulosa</i> 4	Wang et al. 13-41007 (KUN)	China	MH497059
<i>Upretia zeorina</i> 1	Wang et al. 19-63056 (KUN & FR)	China	MW798796
<i>Upretia zeorina</i> 2	Wang et al. 19-63058 (KUN & FR)	China	MW798795
<i>Upretia zeorina</i> 3	Wang et al. 17-56125 (KUN)	China	OP806864
<i>Upretia zeorina</i> 4	Wang et al. 17-56127 (KUN)	China	OP806866
<i>Upretia zeorina</i> 5	Wang et al. 14-43393 (KUN)	China	OP806863
<i>Upretia zeorina</i> 6	Wang et al. 16-50177 (KUN)	China	OP806865
<i>Upretia zeorina</i> 7	Wang et al. 19-63045 (KUN)	China	OP806871
<i>Upretia zeorina</i> 8	Wang et al. 19-63040 (KUN)	China	OP806870
<i>Upretia zeorina</i> 9	Wang et al. 19-62891 (KUN)	China	OP806868
<i>Upretia zeorina</i> 10	Wang et al. 19-62896 (KUN)	China	OP806869
<i>Upretia</i> sp.1	Wang et al. 19-62841 (KUN)	China	OP806862
<i>Upretia</i> sp.2	Wang et al. 14-43454 (KUN)	China	OP806867

and the Shimodaira-Hasegawa-like approximate likelihood ratio test (SH-aLRT) (Guindon et al. 2010) with 1000 replicates. Nodes with support values of both UFBoot \geq 95% and SH-aLRT \geq 80% were considered as well-supported (Minh et al. 2013). Bayesian reconstruction of phylogeny was performed with MrBayes 3.2.6 (Ronquist et al. 2012) to infer phylogenetic trees applying the models inferred by ModelFinder (Kalyaanamoorthy et al. 2017) as: GTR+G for ITS1 and ITS2, K2P+I for 5.8S. Two parallel runs of four Markov chains each were run for 2 million generations, sampling every 1000th generation, and the first 25% discarded as burn-in. The average standard deviation of split frequencies had fallen below 0.01 at the end of the analysis. SH-aLRT \geq 80%, UFBoot \geq 95% and Bayesian posterior probabilities \geq 0.95 were visualized on the ML tree.

Results and discussion

The nrITS dataset comprised 25 terminals, and 12 of them represented newly generated sequences in this study that were deposited in GenBank. All the reported species of *Upretia* with available sequences in GenBank were used in our study.

Phylogenetic inferences resolved the specimens of *Upretia* as a highly supported (SH-aLRT = 96.6%, UFBoot = 98%, PP = 1.00) monophyletic group (Fig. 1), sister grouped to *Ioplaca pindarensis*. Ten of the newly collected Chinese specimens compose a robust clade (SH-aLRT = 98.4%, UFBoot = 99%, PP = 1.00) that is strongly supported as sister (97.7%, UFBoot = 99%, PP = 1.00) to the Chinese species *U. squamulosa*. Two other Chinese specimens (*Upretia* sp.1 and *Upretia* sp. 2) compose a grade subtending the Indian species *U. amarkantakana*, from which they differ in several phenotypic characters (see discussion below). In our preliminary phylogenetic analysis, we included all the available sequences of *Upretia* from GenBank. The type species *U. amarkantakana*, with four samples, appears paraphyletic at the base of *Upretia*, with *U. amarkantakana* SK J20 (ITS-MG652764, mtSSU-MG652767) (Kondratyuk et al. 2018) as basal to three further samples of *U. amarkantakana* and the remainder of the genus. The result is in agreement with Zhang et al. (2019) that the true phylogenetic position and delimitation of the species *U. amarkantakana* is not clear. Therefore, we exclude this sample from our final analysis here and do not show it in the phylogenetic tree (Fig. 1).

Taxonomy

Upretia zeorina Li J. Li & Printzen, sp. nov.

MycoBank No: 849819

Fig. 2A–F

Diagnosis. Thallus epilithic, brown to blackish brown, areolate to squamulose, partly pruinose; apothecia zeorine type, disc black; ascospores polarilocular, 11.5–18.0 \times 6.5–11.0 μ m; conidia narrowly bacilliform, 4.0–6.0 \times 0.5 μ m. Containing gyrophoric acid.

Type. CHINA. Sichuan Prov.: Huili Co., on the way from Huili to Jiaopingdu, elev. 1880 m, 26°21'N, 102°23'E, on rock, 11 Apr 2019, Wang Lisong et al. 19-63056 (KUN-L-66526–**Holotype**, FR-0183125–**Isotype**); GenBank No.: ITS-MW798796, mtSSU-MW798794.

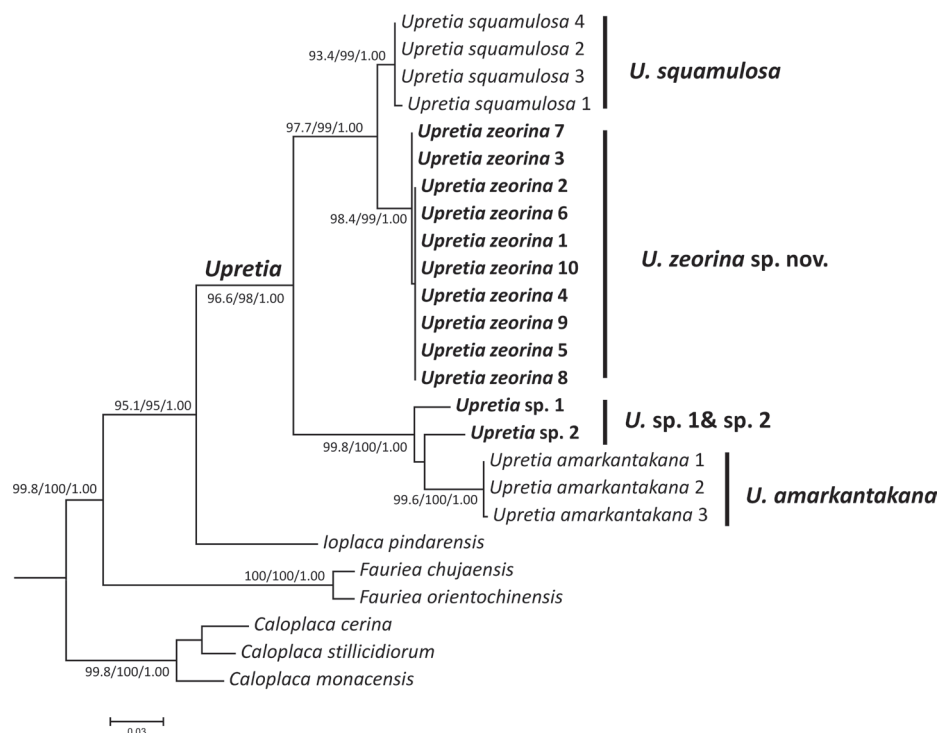


Figure 1. Phylogenetic tree generated from Maximum Likelihood based on nrITS sequences data. SH-aLRT support (%) ≥ 80 / ultrafastbootstrap support (%) ≥ 95 / Bayesian posterior probabilities (PPs) ≥ 0.95 are given above the nodes.

Description. Thallus areolate to squamulose, irregular in outline, squamules plane, adnate, rarely raised and free from substrate at edges, entire or rarely incised, 0.5–2.5 mm in diam. Upper surface brown to blackish brown, smooth or sparingly fissured, partly weakly shiny, \pm white pruinose, mostly at the edges. Lower surface dark on the rising edge, without rhizines. Upper cortex brown, ca. 20 μm high; algal layer continuous, ca. 50–60 μm high, photobiont trebouxoid; medulla grey, ca. 120–160 μm high; lower cortex lacking.

Apothecia zeorine type, sessile, numerous, scattered to aggregated, rounded or irregular when aggregated, up to 1.2 mm in diam.; disc slightly concave to plane, black; proper margin persistent, slightly raised above or level with disc, brownish black, weakly shiny, consisting of interwoven hyphae, uppermost lateral part ca. 30–80 μm thick; thalline margin concolorous with the thallus, 30–130 μm thick, with olive cortical layer, 10–20 μm thick. Hymenium colorless, I+ blue, ca. 70–90 μm ; epihymenium with brown pigment, 10–20 μm ; paraphyses septate, rarely branched, ca. 2.0 μm wide, dark brown and swollen up to 4.0 μm at the tips; subhymenium and hypothecium colorless, 80–160 μm . Asci *Teloschistes*-type, 8-spored, 55–65 \times 14–16 μm . Ascospores hyaline, polarilocular, ellipsoid to broadly ellipsoid, 11.5–18.0 \times 6.5–11.0 μm , septum 6.0–9.0 μm . Pycnidia immersed, wall dark olive, conidia narrowly bacilliform, 4.0–6.0 \times ca. 0.5 μm .

Chemistry. Thallus and apothecia thalline margin K-, C+ red; HPTLC: only gyrophoric acid was detected.

Ecology and distribution. On exposed rock in arid valley, at elevations between 1520 and 1880 m along the Jinsha-jiang River. Only known from Sichuan and Yunnan Provinces, China (Fig. 3).

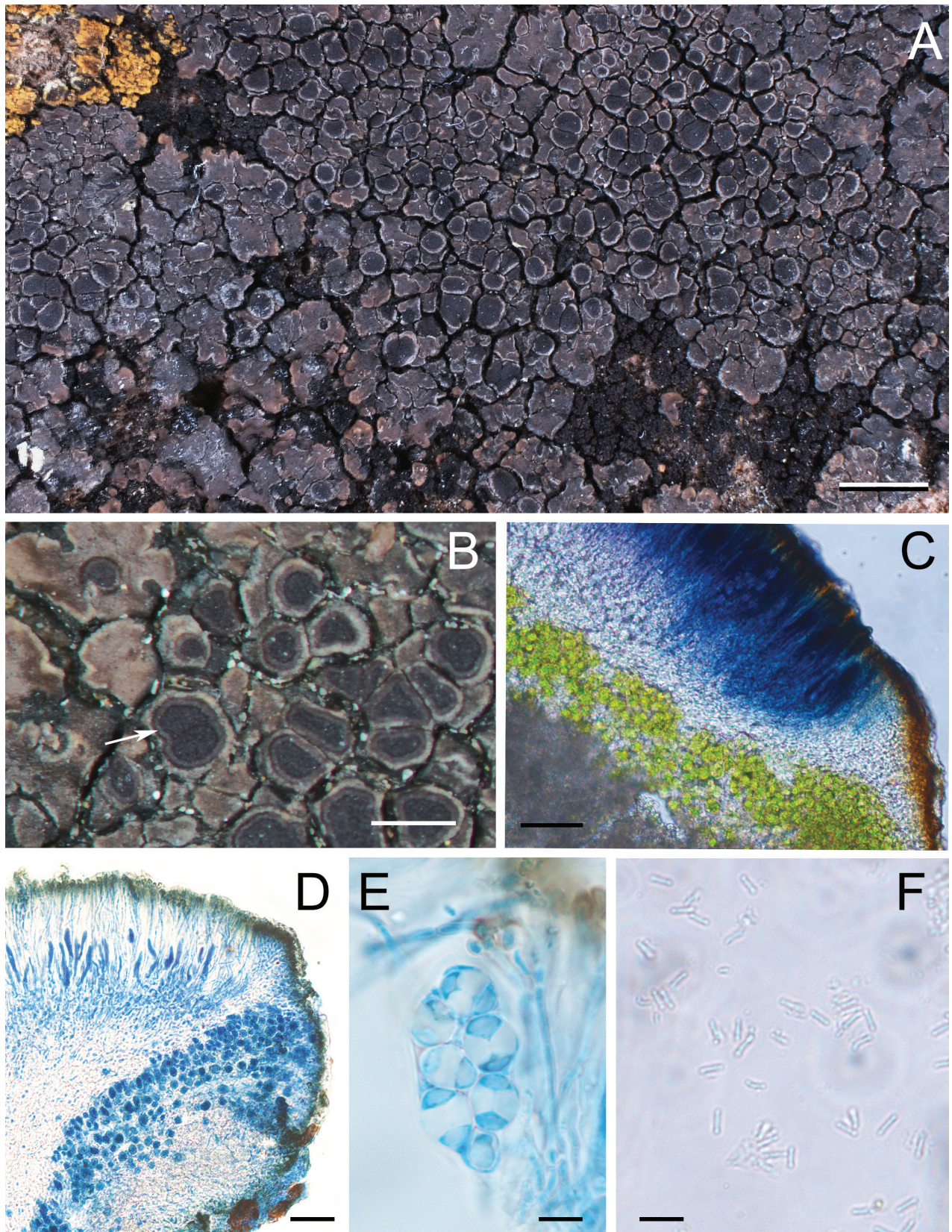


Figure 2. The new species *Upretia zeorina* **A** habitus and lichen thallus **B** zeorine type apothecia, proper margin raised above disc (arrow) **C** section of apothecia in Lugol's iodine (I), hymenium I+ blue, proper margin I- **D** section of apothecia in lactophenol cotton blue (LCB) **E** asci in lactophenol cotton blue, with polarilocular ascospores **F** shortly bacilliform conidia of the new species. Scale bars: 2 mm (**A**); 1 mm (**B**); 50 µm (**C**); 20 µm (**D**); 10 µm (**E**, **F**).

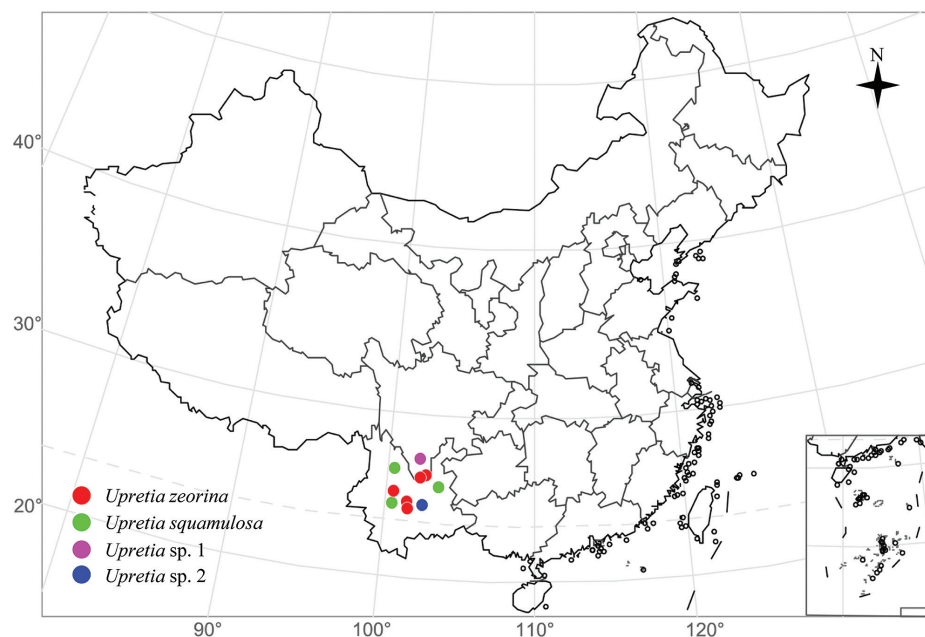


Figure 3. Locations of species of the genus *Upretia* in China. The map was obtained from National Platform for Common Geospatial Information Services (<https://www.tianditu.gov.cn/>).

Etymology. Named due to its zeorine type of apothecia with a thalline outer and a proper inner margin.

Notes. *Upretia amarkantakana*, the type species of the genus *Upretia* known from India, differs from the new species by the olive-grey to brownish grey thallus with lobate margin, the lecanorine apothecia and orange to brown apothecial disc, the smaller ascospores ($8.5\text{--}9.0\text{--}10.0 \times 4.0\text{--}5.0 \mu\text{m}$) and shorter conidia ($1.0\text{--}2.0\text{--}3.0 \times 0.5\text{--}1.0 \mu\text{m}$), and the absence of gyrophoric acid (Joshi and Upreti 2006; Kondratyuk et al. 2018).

Upretia squamulosa is similar to the new species with similar ascospores size ($11.5\text{--}17.5 \times 7.5\text{--}10.0 \mu\text{m}$), squamulose thallus without lobate margin, the presence of gyrophoric acid, and similar distribution in Southwestern China (along the Jinshajiang River), but differs by having imbricate squamules with a non-pruinose, greyish green to brown upper surface, larger apothecia (up to 2 mm diam.) with a pale brown to brown disc, hyaline and slightly swollen paraphyses tips, and the presence of lecanoric acid (Zhang et al. 2019). Apothecia of *U. squamulosa* are usually lecanorine with the thalline margin at the early stage, and soon becoming zeorine, inner proper margin could be distinguished in sections, ca. $25\text{--}50 \mu\text{m}$ thick, thalline margin concolorous with the thallus, ca. $20\text{--}30 \mu\text{m}$ thick.

Molecular data are not available for *U. hueana*, and hence its phylogenetic relationships *U. zeorina* cannot be assessed, but the species distinctly differs by its squamulose to lobed thallus with brown surface, lecanorine apothecia with brown disc, smaller ascospores ($8.5\text{--}11.0\text{--}12.5 \times 5.0\text{--}8.5 \mu\text{m}$ vs. $11.5\text{--}18.0 \times 6.5\text{--}11.0 \mu\text{m}$), the presence of parietin and the absence of gyrophoric acid (Wetmore 1996; Joshi and Upreti 2007; Mishra et al. 2020). As far as the currently known species in the genus *Upretia* are concerned, the Indian species differ from the Chinese species by their smaller ascospores, the secondary metabolites, and a preference for growing at lower altitudes (500–1050m) (Joshi and Upreti 2006; Kondratyuk et al. 2018; Mishra et al. 2020).

Mishra et al. (2020) mentioned that *Caloplaca cupreorufa* Zahlbr., may belong to *Upretia* due to its brownish thallus and brownish pigment in walls of outer cortical cells. The species was collected by Handel-Mazzetti 1914 in Setschwan (Sichuan province, China) in a dry subtropical valley (Zahlbruckner 1930), close to the localities where the specimens of the new species were collected, but it differs by its smaller areoles (0.3–0.7 mm vs. 0.5–2.5 mm), its brown apothecial disc, lacking an inner proper margin, its apically unswollen and frequently branched paraphyses and its smaller ascospores (12.5–14.0 × 7.5–8.5 µm vs. 11.5–18.0 × 6.5–11.0 µm) (Zahlbruckner 1930; Wetmore 1994).

Two specimens of *Upretia* from Sichuan and Yunnan, i.e., *Upretia* sp. 1 and *Upretia* sp. 2 in figure 1, compose a clade with *U. amarkantakana*. They resemble the latter by their crustose thallus with lobate margins, but differ by the smaller areoles (0.2–0.5 mm) and shorter lobes (≤ 1.2 mm). *Upretia* sp.1 is characterized by the green thallus with partly pruinose on the margins, yellow medulla, and the presence of gyrophoric acid, whereas *Upretia* sp. 2 is characterized by a continuously pruinose upper surface, white medulla and the absence of gyrophoric acid. Unfortunately, only one sample has been collected each for these two putative species, respectively, and only the specimen of *Upretia* sp. 2 contains apothecia which are of the zeorine to lecanorine type. Therefore, we temporarily refrain from describing these two samples as new species until more populations and data are available. However, their morphological distinction within the genus *Upretia* highlights the further diversity of the genus in China, especially in the Hengduan Mountains.

Additional specimens examined. *Upretia zeorina*: China. Sichuan Prov.: Huili Co., on the way from Huili to Jiaopingdu, elev. 1736–1880 m, 26°21'N, 102°19'E, on rock, 11 Apr 2019, Wang Lisong et al. 19-63058 (KUN-L-66528, FR-0183126, mtSSU- MW798793), 19-63045 (KUN-L-66515), 19-63039 (KUN-L-66509), 19-63040 (KUN-L-66510), 19-63046 (KUN-L-66516), 19-62891 (KUN-L-66432), 19-62896 (KUN-L-66437); Yunnan Prov., Heqing Co., Zhongjiang Village, elev. 1540 m, 26°30'N, 100°23'E, on rock, 8 July 2016, Wang Lisong et al. 16-50177 (KUN-L-53525); Yuanmou Co., Langbapu Soil Forest, elev. 1526 m, 25°42'N, 101°41'E, on rock, 21 Apr 2014, Wang Lisong et al. 14-43393 (KUN-L-45200), on the way from Yuanmou to Yongren, elev. 1520 m, 25°58'N, 101°43'E, on rock, 1 July 2017, Wang Lisong et al. 17-56127 (KUN-L-59563), 17-56125 (KUN-L-59561), 18-58007 (KUN-L-61584).

Upretia squamulosa: China. Yunnan Prov.: Huize Co., Zhehai Town, elev. 1720m, 26°21'N, 102°19'E, on rock, 18 June 2015, Wang Xinyu et al. 15-47423 (KUN-L-50312-holotype, FR-0264988-isotype), 15-47427 (KUN-L-50316); Yulong Co., on the way from Lijiang to Ninglang, elev. 1871 m, 27°03'N, 100°30'E, on rock, 9 Apr 2019, Wang Lisong et al. 19-62704 (KUN-L-66245), Jiangbianxin Village, elev. 1720 m, 26°31'N, 103°42'E, on rock, 9 Dec 2013, Wang Lisong et al. 18-58077 (KUN-L-61568).

Upretia sp. 1: China. Sichuan Prov.: Dechang Co., on the way from Dechang to Huili, elev. 1320 m, 27°18'N, 102°19'E, on rock, 11 Apr 2019, Wang Lisong et al. 19-62841 (KUN-L-66382).

Upretia sp. 2: China. Yunnan Prov.: Yunlong Vil., Yunlong water reservoir, elev. 2100 m, 25°51'N, 102°22'E, on rock, 18 Apr 2014, Wang Lisong et al. 14-43454 (KUN-L-45260).

World key to species of *Upretia*

- 1 Thallus distinctly lobate at the margin..... **2**
 - Thallus without a lobate margin..... **4**
- 2 Lobes long, (0.5–)1.5–2.5(–3.5) mm in length, upper surface olive-grey to brownish grey, partly pruinose..... ***U. amarkantakana***
 - Lobes shorter than 1.2 mm in length, known from Southwestern China **3**
- 3 Thallus partly pruinose on the margins, medulla yellow, producing gyrophoric acid ***U. sp. 1***
 - Thallus totally pruinose on the upper surface, medulla white, with zeorine to lecanorine type apothecia, lacking gyrophoric acid..... ***U. sp. 2***
- 4 Thallus blackish brown, partially with pruina, apothecial disc zeorine-type, blackish..... ***U. zeorina***
 - Thallus brownish, without pruina, apothecial disc lecanorine-type, brown **5**
- 5 Apothecia 0.5–2.5 mm diam., ascospores 11.5–17.5 × 7.5–10.0 µm, producing lecanoric acid in addition to gyrophoric acid, only known from Southwestern China ***U. squamulosa***
 - Apothecia 0.3–1.0 mm diam., ascospores 8.5–11.0(–12.5) × 5.0–8.5 µm, only producing parietin instead of gyrophoric acid, known from Mexico and India ***U. hueana***

Acknowledgements

We would like to thank the Herbarium KUN for specimen support, Heike Kappes from the Grunelius-Möllgaard-Lab of the Senckenberg Research Institute for technical support.

Additional information

Conflict of interest

The authors have declared that no competing interests exist.

Ethical statement

No ethical statement was reported.

Funding

This study was supported by DFG grant Pr 567/19-1 to CP; the Second Tibetan Plateau Scientific Expedition and Research Program (STEP), grant number 2019QZKK0503; Youth Innovation Promotion Association CAS, grant number 2020388 and National Natural Science Foundation of China, grant number 31970022.

Author contributions

LL & YZ conducted the lab work, analyzed the data, and wrote the manuscript. CP, LW & XW supervised the research, revised the manuscript, and provided funding.

Author ORCIDs

Lijuan Li  <https://orcid.org/0000-0003-1048-1971>

Yanyun Zhang  <https://orcid.org/0000-0002-0902-5066>

Christian Printzen  <https://orcid.org/0000-0002-0871-0803>

Lisong Wang  <https://orcid.org/0000-0003-3721-5956>

Xinyu Wang  <https://orcid.org/0000-0003-2166-6111>

Data availability

All of the data that support the findings of this study are available in the main text.

References

- Arup U, Ekman S, Lindblom L, Mattsson JE (1993) High performance thin layer chromatography (HPTLC), an improved technique for screening lichen substances. *Lichenologist* 25(1): 61–71. <https://doi.org/10.1006/lich.1993.1018>
- Arup U, Søchting U, Frödén P (2013) A new taxonomy of the family Teloschistaceae. *Nordic Journal of Botany* 31(1): 1683. <https://doi.org/10.1111/j.1756-1051.2013.00062.x>
- Culberson CF, Kristinsson H (1970) A standardized method for the identification of lichen products. *Journal of Chromatography A* 46: 85–93. [https://doi.org/10.1016/S0021-9673\(00\)83967-9](https://doi.org/10.1016/S0021-9673(00)83967-9)
- Gardes M, Bruns TD (1993) ITS primers with enhanced specificity for basidiomycetes - application to the identification of mycorrhizae and rusts. *Molecular Ecology* 2(2): 113–118. <https://doi.org/10.1111/j.1365-294X.1993.tb00005.x>
- Gaya E, Högnabba F, Holguin Á, Molnar K, Fernández-Brime S, Stenroos S, Arup U, Søchting U, Boom PVD, Lücking R, Sipman HJM and Lutzoni F (2012) Implementing a cumulative supermatrix approach for a comprehensive phylogenetic study of the Teloschistales (Pezizomycotina, Ascomycota). *Molecular Phylogenetics and Evolution* 63(2): 374–387. <https://doi.org/10.1016/j.ympev.2012.01.012>
- Guindon S, Dufayard JF, Lefort V, Anisimova M, Hordijk W, Gascuel O (2010) New algorithms and methods to estimate maximum-likelihood phylogenies: assessing the performance of PhyML 3.0. *Systematic Biology* 59(3): 307–321. <https://doi.org/10.1093/sysbio/syq010>
- Joshi Y, Upreti DK (2006) *Caloplaca amarkantakana*, a new species in the *Caloplaca sideritis* group from India. *The Lichenologist* 38(6): 537–540. <https://doi.org/10.1017/S0024282906006360>
- Joshi Y, Upreti DK (2007) New species and new records of the lichen genus *Caloplaca* from India. *The Lichenologist* 39(6): 505–508. <https://doi.org/10.1017/S0024282907006834>
- Kalyaanamoorthy S, Minh BQ, Wong TKF, Von Haeseler A, Jermini LS (2017) ModelFinder: fast model selection for accurate phylogenetic estimates. *Nature Methods* 14(6): 587–589. <https://doi.org/10.1038/nmeth.4285>
- Katoh K, Standley DM (2013) MAFFT Multiple Sequence Alignment Software Version 7: Improvements in Performance and Usability. *Molecular Biology and Evolution* 30(4): 772–780. <https://doi.org/10.1093/molbev/mst010>
- Kondratyuk SY, Kärnefelt I, Thell A, Elix JA, Kim J, Kondratyuk AS, Hur JS (2015) Brownlieoideae, a new subfamily in the Teloschistaceae (Lecanoromycetes, Ascomycota). *Acta Botanica Hungarica* 57(3–4): 321–341. <https://doi.org/10.1556/034.57.2015.3-4.6>
- Kondratyuk SY, Persson P, Hansson M, Mishra GK, Nayaka S, Liu D, Hur JS, Thell A (2018) *Upretia*, a new caloplacoid lichen genus (Teloschistaceae, Lichen-Forming Ascomycota) from India. *Cryptogam Biodiversity and Assessment, Special Volume*, e-ISSN: 2456–0251, 22–31. <https://doi.org/10.21756/cab.esp5>
- Larena I, Salazar O, González V, Julián MC, Rubio V (1999) Design of a primer for ribosomal DNA internal transcribed spacer with enhanced specificity for ascomycetes.

- Journal of Biotechnology 75(2–3): 187–194. [https://doi.org/10.1016/S0168-1656\(99\)00154-6](https://doi.org/10.1016/S0168-1656(99)00154-6)
- Minh BQ, Nguyen MAT, Von Haeseler A (2013) Ultrafast approximation for phylogenetic bootstrap. *Molecular Biology and Evolution* 30(5): 1188–1195. <https://doi.org/10.1093/molbev/mst024>
- Mishra GK, Upreti DK, Nayaka S, Thell A, Kärnefelt I, Lőkös L, Hur JS, Sinha GP, Kondratyuk SY (2020) Current taxonomy of the lichen family Teloschistaceae from India with descriptions of new species. *Acta Botanica Hungarica* 62(3–4): 309–391. <https://doi.org/10.1556/034.62.2020.3-4.5>
- Orange A, James PW, White FJ (2001) *Microchemical methods for the identification of lichens*. British Lichen Society, 107 pp.
- Ronquist F, Teslenko M, van der Mark P, Ayres DL, Darling A, Höhna S, Larget B, Liu L, Suchard MA, Huelsenbeck JP (2012) MrBayes 3.2: efficient Bayesian phylogenetic inference and model selection across a large model space. *Systematic Biology* 61(3): 539–542. <https://doi.org/10.1093/sysbio/sys029>
- Trifinopoulos J, Nguyen LT, Von Haeseler A, Minh BQ (2016) W-IQ-TREE: a fast online phylogenetic tool for maximum likelihood analysis. *Nucleic Acids Research* 44: W232–W235. <https://doi.org/10.1093/nar/gkw256>
- Wetmore CM (1994) The lichen genus *Caloplaca* in North and Central America with brown or black apothecia. *Mycologia* 86(6): 813–838. <https://doi.org/10.1080/00275514.1994.12026488>
- Wetmore CM (1996) The *Caloplaca sideritis* group in North and Central America. *The Bryologist* 99(3): 292–314. <https://doi.org/10.2307/3244301>
- Zahlbruckner A (1930) Lichenes. In: Handel-Mazzetti H (Ed.) *Symbolae sinicae. Botanische Ergebnisse der Expedition der Akademie der Wissenschaften in Wien nach Südwest-China 1914-1918. III*. J. Springer, Wien, 254 pp.
- Zhang YY, Wang XY, Li LJ, Søchting U, Yin AC, Wang SQ, Wang LS (2019) *Upretia squamulosa*, a new lichen species from the arid valley of Jinsha-Jiang River, China. *Phytotaxa* 402(6): 288–294. <https://doi.org/10.11646/phytotaxa.402.6.3>

New nephridiophagid genera (Fungi, Chytridiomycota) in a mallow beetle and an earwig

Renate Radek¹, Christian Wurzbacher², Jürgen F. H. Strassert³

¹ Evolutionary Biology, Institute of Biology, Free University of Berlin, 14195 Berlin, Germany

² Chair of Urban Water Systems, Engineering, Technical University of Munich, 85748 Garching, Germany

³ Evolutionary and Integrative Ecology, Leibniz Institute of Freshwater Ecology and Inland Fisheries, 12587 Berlin, Germany

Corresponding authors: Jürgen F. H. Strassert (juergen.strassert@igb-berlin.de); Renate Radek (renate.radek@fu-berlin.de)

Abstract

Nephridiophagids are unicellular fungi (Chytridiomycota) that infect the Malpighian tubules of insects. Most species have been found in cockroach hosts and belong to the genus *Nephridiophaga*. Three additional genera have been described from beetles and an earwig. Here, we characterise morphologically and molecular phylogenetically the nephridiophagids of the European earwig *Forficula auricularia* and the mallow beetle *Podagrica malvae*. Their morphology and life cycle stages resemble those of other nephridiophagids, but their rRNA gene sequences support the existence of two additional genera. Whereas the earwig nephridiophagid (*Nephridiochytrium forficulae* **gen. nov. et sp. nov.**) forms a sister lineage of the *Nephridiophaga* cluster, the mallow beetle nephridiophagid (*Malpighivincina podagrica* **gen. nov. et sp. nov.**) represents the earliest divergent lineage within the nephridiophagids, being sister to all other species. Our results corroborate the hypothesis that different insect groups harbour distinct nephridiophagid lineages.

Key words: Chytrids, *Forficula auricularia*, Malpighian tubules, *Malpighivincina podagrica*, *Nephridiochytrium forficulae*, *Nephridiophaga*, *Podagrica malvae*, phylogeny



Academic editor: Kerstin Voigt

Received: 17 August 2023

Accepted: 27 October 2023

Published: 22 December 2023

Citation: Radek R, Wurzbacher C, Strassert JFH (2023) New nephridiophagid genera (Fungi, Chytridiomycota) in a mallow beetle and an earwig. MycoKeys 100: 245–260. <https://doi.org/10.3897/mycokeys.100.111298>

Copyright: © Renate Radek et al.

This is an open access article distributed under terms of the Creative Commons Attribution License (Attribution 4.0 International – CC BY 4.0).

Introduction

The members of Nephridiophagaceae (‘nephridiophagids’) are unicellular entomopathogens, which reproduce in the Malpighian tubules of insects (Woolever 1966; Lange 1993; Radek and Herth 1999; Voigt et al. 2021). During their life cycle, multinucleate vegetative plasmodia divide into oligo- and uninucleate stages or transform to sporogenic plasmodia. Spores develop within the sporogenic plasmodium by delimitation of a portion of cytoplasm including a generative nucleus. Degenerated vegetative (“somatic”) nuclei remain in the cytoplasm of the mother plasmodium. The occasional occurrence of bi- and tetranuclear sporoblasts implies the existence of meiosis or sexual stages (Ivanić 1937; Purrini and Rhode 1988; Radek and Herth 1999). Mature spores are mostly flattened oval, have a spore opening at one side and include a single nucleus (Fabel et al. 2000). An infection with nephridiophagids does not kill its host but reduces its fitness, leading to, for example, lessened mobility, reduced fat reserves and fewer progeny (Strassert et al. 2022).

Only recently, the controversial discussion about the systematic position of nephridiophagids has been resolved by molecular phylogenetic analyses, which recognise them as fungi in the phylum Chytridiomycota (Radek et al. 2017; Strassert et al. 2021). Presently, the four genera *Coleospora*, *Nephridiophaga*, *Oryctospora* and *Peltomyces* are included in the family Nephridiophagaceae (Wijayawardene et al. 2018, 2020). While the monospecific genera *Coleospora* and *Oryctospora* are known from beetles only (Gibbs 1959; Purrini and Weiser 1990), the two *Peltomyces* species have been found to infect a different host each (a beetle and an earwig; Léger (1909)). The majority of the hitherto described nephridiophagids (ca. 14 species) are assigned to the genus *Nephridiophaga* (Radek and Herth 1999; Wijayawardene et al. 2018; Strassert et al. 2021; Voigt et al. 2021), which was erected by Ivanić (1937) who described spores in the Malpighian tubules of the honey bee *Apis mellifera*. Due to obscurities regarding this assignment, however, a new conserved type was recently defined for *Nephridiophaga* (*Nephridiophaga blattellae* from the German cockroach *Blattella germanica*; Radek et al. (2022)). *Nephridiophaga* species are mostly known from cockroaches and nephridiophagid species isolated from cockroaches have, so far, been found to be phylogenetically closely related to each other (Strassert et al. 2021). Interestingly, the only nephridiophagid that inhabits a non-cockroach host (an earwig) and for which SSU and LSU rRNA gene sequences are publicly available, has recently been shown to branch as sister to nephridiophagids isolated from cockroaches (Strassert et al. 2021).

In this study, we morphologically and molecular phylogenetically characterise the nephridiophagids from the European earwig *Forficula auricularia* and the mallow beetle *Podagrica malvae*. We show that, despite morphological similarities to *Nephridiophaga* (the genus they had formerly been assigned to), the here formally described taxa branch not only apart from this genus in phylogenetic trees but also from each other, strengthening the hypothesis that different insect groups host own lineages of nephridiophagids.

Methods

Insects

The insects used for this study were mallow beetles, *Podagrica malvae* (Coleoptera, Chrysomelidae, Galerucinae), collected in Italy (Syracuse) and individuals of the European earwig, *Forficula auricularia* (Dermaptera, Forficulidae), collected in France (Tours). Detailed information on the collected insects and their infection status is given in Suppl. material 1. Identifications were based on morphological characteristics as well as mitochondrial COII gene sequence similarities.

Light microscopy

Beetles and earwigs were dissected in 0.9% sodium chloride (NaCl) solution. Malpighian tubules were extracted and screened under a light microscope for entomopathogens, especially for nephridiophagids. For the production of stained permanent samples, the infected tubules were then smeared on a microscopic slide, air dried, fixed in 100% methanol for 5 min, stained in Giemsa

solution (Accustain, Sigma, diluted 1:10) for 30–60 min, washed with tap water, air dried and embedded in Entellan under a cover glass. All light microscopic samples were observed under a Zeiss AxioPhot microscope equipped with a 40× objective.

Electron microscopy

Cover glasses removed from positive squash preparations were used for scanning electron microscopy (SEM). They were air dried in order to prevent parasite loss during further preparation steps. The dried cover glasses were mounted on aluminium stubs with double-sided adhesive tape, sputter-coated with gold in a Balzers SCD 40 and observed using a FEI Quanta 200 ESEM.

For transmission electron microscopy (TEM), infected tubules were fixed in 2.5% glutaraldehyde in 0.1 M cacodylate buffer (pH 7.2) and stored in a fridge for several days. The fixed tissue was then washed three times in buffer, post-fixed in 1% osmium tetroxide (OsO_4) plus 1.5% potassium ferrocyanide ($\text{K}_3[\text{Fe}(\text{CN})_6]$) for 1.5 h at room temperature, washed three times, dehydrated in a gradient of ethanol and embedded in Spurr's resin (Spurr 1969). Ultrathin sections were contrasted with saturated aqueous uranyl acetate ($[\text{UO}_2(\text{CH}_3\text{COO})_2 \cdot 2 \text{H}_2\text{O}]$) for 30 min followed by lead citrate ($\text{C}_{12}\text{H}_{10}\text{O}_{14}\text{Pb}_3$) (Reynolds 1963) for 5 min. The sections were examined with a Philips CM 120 BioTwin electron microscope.

Sample processing for molecular phylogeny

DNA from infected Malpighian tubules was extracted with the DNeasy Plant Mini Kit (Qiagen) following the manufacturer's instructions. The ribosomal operon sequence spanning the SSU, ITS, 5.8S and partial LSU region was amplified and sequenced as described in Wurzbacher et al. (2019). Briefly, the ribosomal operon was amplified with the primers NS1short and RCA95m, subsequently purified with magnetic beads (AMPure, Beckmann), barcoded and re-purified and subjected to amplicon sequencing on the PacBio RSII sequencer (Pacific Biosciences) in reads of insert mode (ROS) and an error rate filtering of 0.02. The resulting sequences were aligned, clustered and used for consensus sequence generation as described in Wurzbacher et al. (2019). The sequence of the nephridiophagid from *F. auricularia* was obtained in a similar way by Strassert et al. (2021) with the exception that the MinION (Oxford Nanopore Technologies) was used for amplicon sequencing, but the species has not been formally described.

Phylogenetic analysis

Analyses were carried out using the high-performance computing infrastructure Zedat at Freie Universität Berlin (Bennett et al. 2020). Sequences of the SSU and LSU rRNA genes from the earwig nephridiophagid and from the mallow beetle nephridiophagid were aligned together with representatives of diverse fungal lineages using MAFFT L-INS-I v. 7.055b (Katoh and Standley 2013) (Suppl. materials 2, 3) and filtered with TRIMAL v. 1.2 (Capella-Gutierrez et al. 2009) using a gap threshold of 0.3 and a similarity threshold of 0.001. The two alignments were then concatenated using SEQKIT v. 0.11.0 (Shen et al. 2016)

and a Maximum-Likelihood tree was inferred with IQ-TREE v. 1.6.12 (Nguyen et al. 2015) under the GTR+F+R5 model, which was determined with ModelFinder (Kalyaanamoorthy et al. 2017) employing the TESTNEW option. Branch support was assessed using ultrafast bootstrap approximation (Hoang et al. 2018) (UF-BOOT2; 1,000 replicates) and SH-like approximate likelihood ratio test (Guindon et al. 2010) (SH-aLRT; 1,000 replicates). PhyloBayes-MPI v. 1.8 (Lartillot et al. 2013) was used for Bayesian analysis with the GTR model and four categories for the discrete gamma distribution (31,000 generations; burn-in 3,100). Convergence of two independent Markov Chain Monte Carlo (MCMC) chains was tested with BPCOMP and confirmed with MaxDiff reaching 0.03.

Results

Nephridiophagid in *Forficula auricularia*

The lumens of the Malpighian tubules of infected earwigs were filled with different developmental stages (Fig. 1). Sporogenic plasmodia contained 13–37 (mean 19) spores ($n = 13$; Fig. 1A–C). Giemsa staining revealed the presence of residual vegetative nuclei between the mature spores (Fig. 1D) and a varying number of nuclei in vegetative plasmodia (Fig. 1F). Oval, flattened mature spores measured 5.8–6.9 (mean 6.3) μm in length and 2.9–3.5 (mean 3.2) μm in width ($n = 10$; Fig. 1E). In scanning electron micrographs, the flattened mature spores revealed a thickened rim and two different sides. One side featured a small, central, rounded spore opening (Fig. 1G), while the other one showed a homogeneous granular surface (Fig. 1H). Different stages of spore formation could be found in ultrathin sections. Regions of future spores were demarcated around single nuclei in the sporogenic plasmodia (Fig. 1I, J). Other nuclei remained in the plasmodial cytoplasm (Fig. 1J, K). Young developing spores revealed an oval, not yet flattened shape, a thin spore wall and nuclei positioned near to a pole or centrally (Fig. 1J). Their cytoplasm had about the same density as that of the mother cytoplasm. Mature spores had a typical oval flattened form and an electron-dense interior with a centrally located nucleus (Fig. 1K–M). Their spore walls were the thickest at the border and thin at the flattened sides and especially thin at the region of the spore opening (Fig. 1L, M). The spore wall was composed of five layers. The outer layer 1 and the inner layer 5 appeared as thin electron-dense lines in the sections (Fig. 1L, M). The other three layers were thicker and became less electron-dense from outside to inside. A layer of small vesicles surrounded the single spores (Fig. 1L).

Nephridiophagid in *Podagrica malvae*

The most obvious sign of an infection with nephridiophagids were the sporogenic plasmodia in the lumens of the Malpighian tubules and the plasmodia and spores released in the squash preparations (Fig. 2A–C). The sporogenic plasmodia contained 7–36 (mean 21.5) spores ($n = 21$; Fig. 1A, B). Vegetative plasmodia had varying sizes and accordingly few or many nuclei (Fig. 2B, D–F). Giemsa staining revealed single nuclei in young spores (Fig. 2G) and the typical vegetative nuclei in the mother cytoplasm of sporogenic plasmodia (Fig. 2H). The Giemsa stain was not able to penetrate the spore wall of mature spores

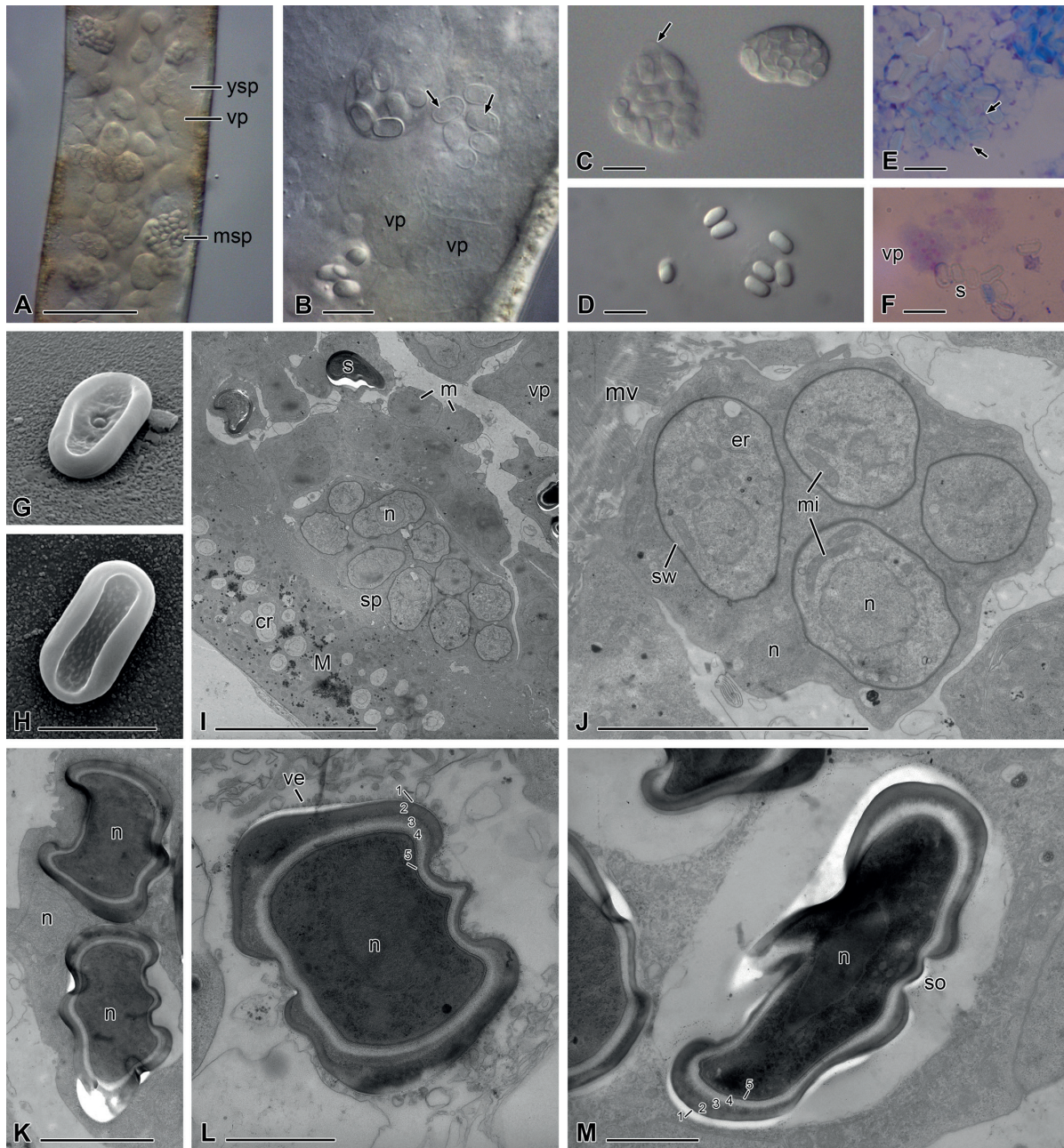


Figure 1. Nephridiophagid (*Nephridiochytrium forficulae*) from *Forficula auricularia* **A–D** differential interference microscopy (DIC) **E, F** Giemsa staining **G, H** scanning electron microscopy (SEM) **I–M** transmission electron microscopy (TEM) **A** Malpighian tubule filled with vegetative plasmodia (vp), young sporogenic plasmodia (ysp) and mature sporogenic plasmodia (msp) **B** young spores have a thin, yet transparent spore wall and a nucleus positioned near a cell pole or centrally **C** left plasmodium with large mature spores, right plasmodium with smaller, younger spores. Arrow points to plasma membrane **D** single mature spores **E** Giemsa staining reveals residual nuclei (arrows) of the plasmodium between mature spores **F** vegetative plasmodium with stained nuclei. s = spores **G, H** flattened oval spores with rim and a central spore opening on one side (**G**) **I** ultrathin section through a Malpighian tubule infected with different stages: small, uninucleate merozoites (m), vegetative plasmodia with several nuclei, sporogenic plasmodia (sp) and mature spores. n = nucleus. The epithelium of the Malpighian tubule (M) contains concretions (cr) **J** young sporogenic plasmodium containing young spores with a thin spore-wall (sw), one nucleus, endoplasmic reticulum (er) and mitochondria (mi) **K** part of a mature sporogenic plasmodium with a residual nucleus and two mature spores with a centrally located nucleus and a thick spore-wall **L** cross-section of a mature spore in the degenerating plasmodial cytoplasm. The spore wall consists of five layers (1–5). ve = vesicles **M** mature spore in longitudinal section showing the thin-walled cap of the spore opening (so). Scale bars: 50 μm (**A**); 10 μm (**B–F, I**); 5 μm (**G, H, J**); 2 μm (**K**); 1 μm (**L, M**).

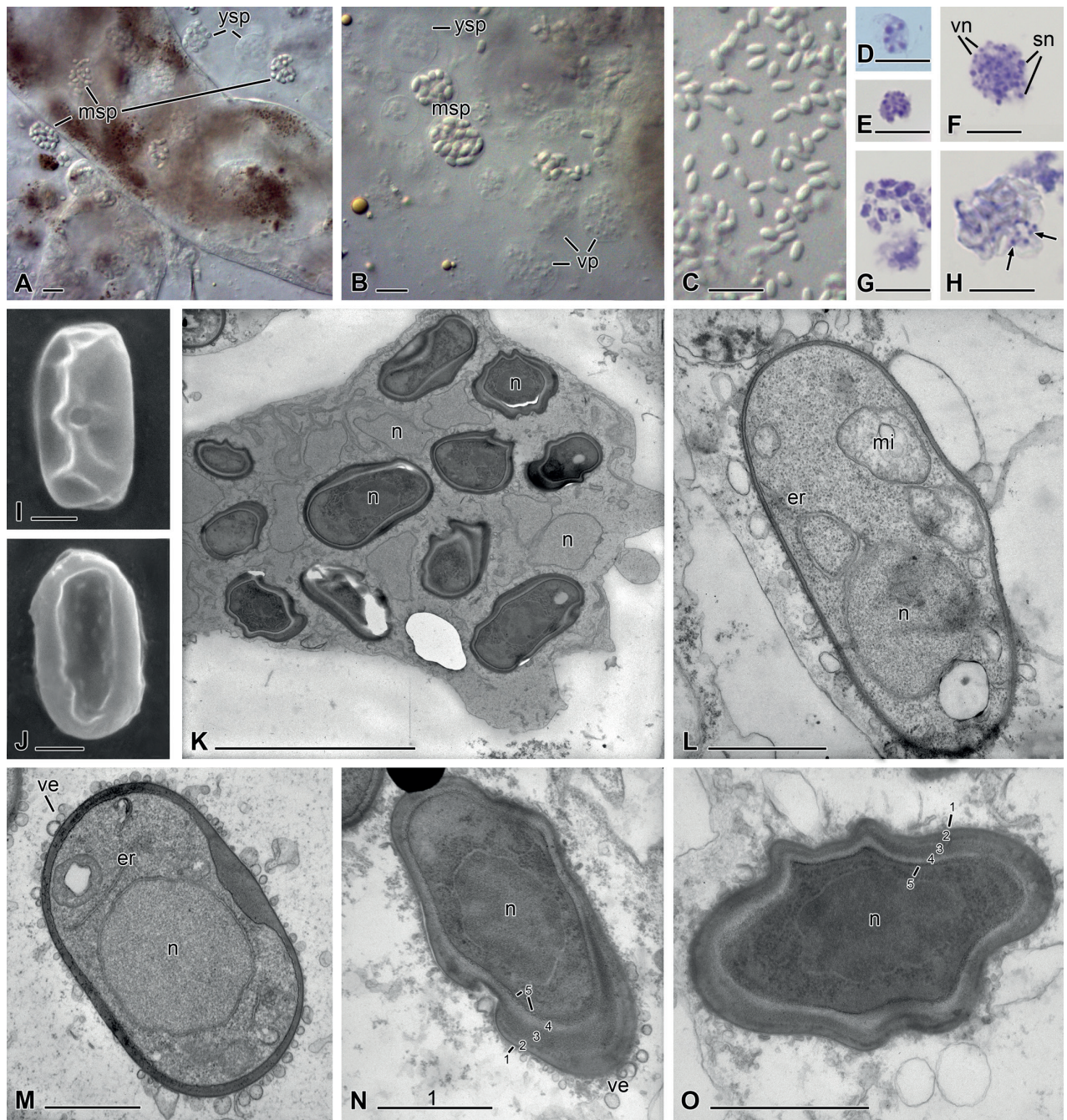


Figure 2. Nephridiophagid (*Malpighivinco podagrica*) from *Podagrica malvae* **A–C** differential interference microscopy (DIC) **D–H** Giemsa staining **I, J** scanning electron microscopy (SEM) **K–O** transmission electron microscopy (TEM) **A** fresh squash preparation of infected Malpighian tubules with young sporogenic plasmodia (ysp) and mature sporogenic plasmodia (msp) inside and outside the tubules **B** nuclei of vegetative plasmodia (vp) and young spores in sporogenic plasmodia have less contrast than mature spores **C** mature spores **D, E** vegetative plasmodia with few (**D**) or many (**E**) nuclei **F** young sporogenic plasmodium with small vegetative nuclei (vn) and larger sporogenic nuclei (sn) **G** the nuclei of thin-walled young spores are stained **H** in mature sporogenic plasmodia, only the vegetative nuclei between the spores are stained (arrows) **I, J** flattened mature spores with central spore opening on one side (**I**) **K** ultra-thin section of a sporogenic plasmodium with uninucleated mature spores and vegetative nuclei in the mother cytoplasm. n = nuclei **L** thin-walled young spore with a nucleus in polar position, mitochondria (mi) and endoplasmic reticulum (er) **M** maturing spore with attached vesicles (ve) delivering spore wall material and centrally located nucleus **N, O** mature spores with five-layered, thick spore wall, dense cytoplasm and central nucleus. Scale bars: 10 µm (**A–H**); 5 µm (**K**); 1 µm (**I, J, L–O**).

so that their nuclei remained uncontrasted (Fig. 2H). Mature spores were flattened oval (Fig. 2C, I, J) and featured a small central spore opening on one side (Fig. 2I). They measured 3.6–4.7 (mean 4.2) μm in length and 2.1–2.5 (mean 2.3) μm in width ($n = 20$). Ultrathin sections revealed more details of the sporulation process. In the sporogenic plasmodia, future spore nuclei and their surrounding cytoplasm were delimited from the mother cytoplasm by the developing spore walls (Fig. 2K–O). Thus, spores were formed inside the plasmodium, while residual vegetative nuclei remained in the mother cytoplasm (Fig. 2K). In the moderately electron-dense cytoplasm of young spores, mitochondria and endoplasmic reticulum could be seen (Fig. 2L). Their single nucleus was either located at the cell pole (Fig. 2L) or in the centre (Fig. 2M). The initially thin, electron-dense spore wall increasingly thickened, especially at its borders (Fig. 2M–O). In mature spores, the spore wall contained five layers (Fig. 2N, O). Layers 1 and 5 were thin and darkly contrasted, while the other three layers were thicker and became brighter inwards.

Phylogenetic position of nephridiophagids

Phylogenetic analyses of a concatenated SSU and LSU rRNA gene sequence alignment of the newly-described nephridiophagids along with other nephridiophagids and major fungal groups confirmed their affiliation to the Nephridiophagaceae (Fig. 3). Both the sister-relationship of the nephridiophagid from *Forficula auricularia* to *Nephridiophaga* (from cockroach hosts) as well as the sister-relationship of the nephridiophagid from *Podagrira malvae* to all other nephridiophagids was inferred with maximum support (UFBOOT2 and Bayesian posterior probability). However, whereas the branching of Nephridiophagaceae within the Chytridiomycota (as discovered before; Strassert et al. (2021)) was inferred with confidence, the exact position of the family remained ambiguous. Members of this family were nested within the Cladochytriales, but statistical support for this branching was rather low (Fig. 3). Whether or not the family Nephridiophagaceae is affiliated to the Cladochytriales or represents a distinct order (Nephridiophagales; as proposed by Doweld (2014)) could, therefore, not be resolved here.

Infection status of examined insects

All five examined earwigs collected in France were infected, i.e. they all had a high number of parasite stages in the Malpighian tubules. In contrast, only three of 16 earwigs from Germany were positive and their infection intensity was low. In addition to nephridiophagids, some of the German earwigs contained gregarines in the gut and microsporidia in the haemolymph (not shown). With nephridiophagids infected mallow beetles of the genus *Podagrira* could only be found on Sicily, Italy (3 of 14 beetles from two collection sites). Since some of the beetles were already dead at the time point of dissection, the origin and identity of similar-sized spores in the bodies of two further beetles remained unclear. We identified spores in the gut of two more beetles as microsporidia by transmission electron microscopy (not shown). None of the 30 beetles

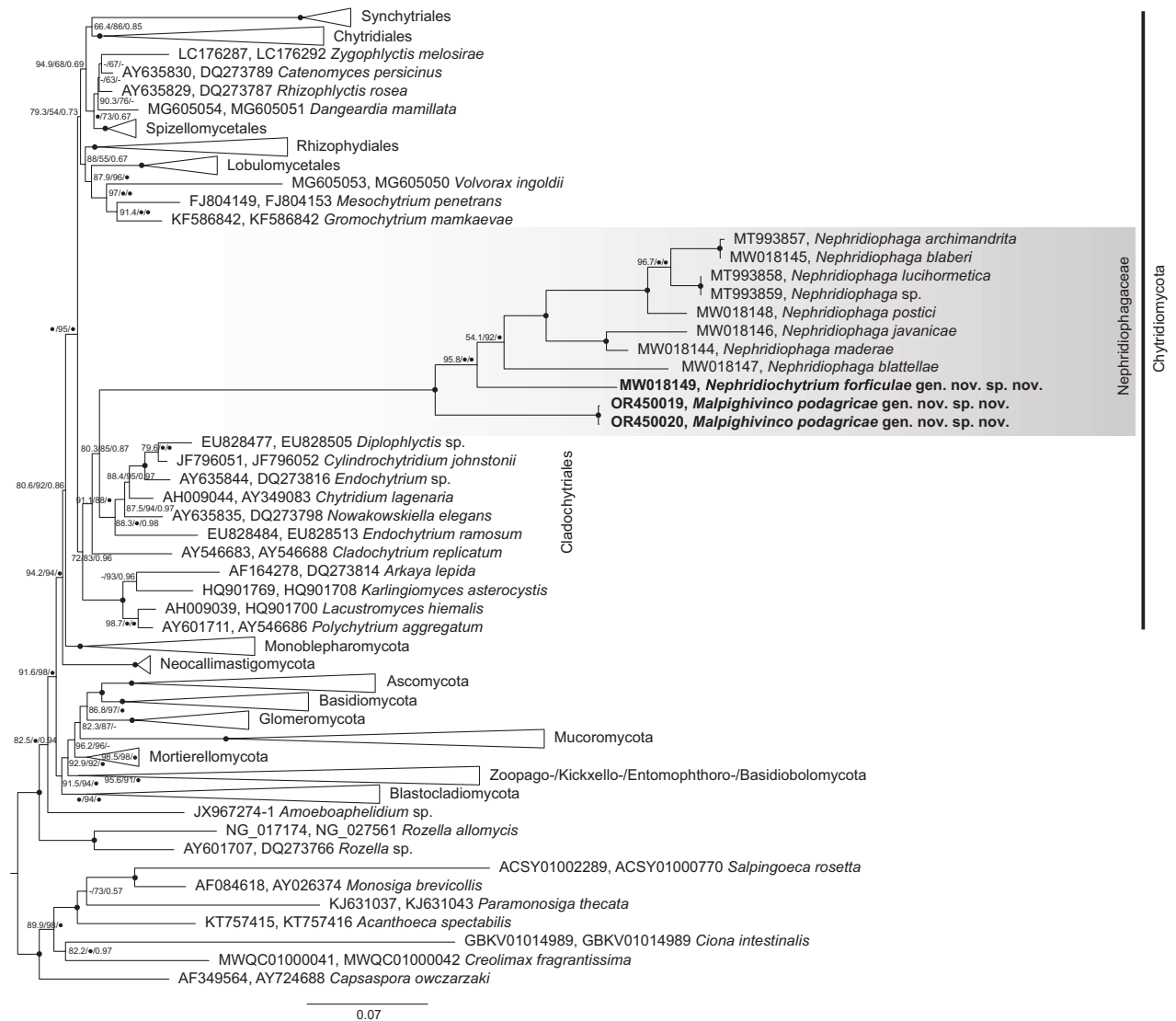


Figure 3. Phylogenetic tree inferred from a concatenated alignment of SSU and LSU rRNA genes under the GTR+F+R5 model. Branch support is given by SH-aLRT/UFBOOT2/Bayesian posterior probabilities. Black circles indicate support values $\geq 99\%$ or ≥ 0.9 and dashes indicate values $< 50\%$ or < 0.5 . Black circles at branches show $\geq 99\%$ and ≥ 0.9 support in all analyses. Sequences of the here newly-described species are marked in bold. For the nephridiophagids obtained from the two *Lucihormetica* species and from *Archimandrita tessellata*, only the SSU rRNA gene sequence was available for tree inference.

collected in Germany contained nephridiophagids. Occasionally, gregarines were found in the guts of the Italian beetles (not shown). Generally, the insects from Germany were less or not at all infected, while those collected in the Mediterranean area (France, Italy) showed a higher rate of nephridiophagids.

Discussion

In this study, we characterised two non-cockroach nephridiophagids by their morphology and SSU and LSU rRNA gene sequences. The nephridiophagid from *Forficula auricularia* was initially named by Léger (1909) as *Peltoomyces forficulae*, but, except from the information that it is very similar to

Peltomyces hyalinus from the beetle *Oloocrates abbreviatus*, hardly any further data were given. Later, the pathogen was investigated closer by light microscopy and assigned to the genus *Nephridiophaga* (*Nephridiophaga forficulae*; Ormières and Manier (1973)). According to Léger (1909), the spores measured $6.4 \times 3.3 \mu\text{m}$ and, according to Ormières and Manier (1973), their sizes were $5 \times 2.5 \mu\text{m}$ (stained) or $7 \times 4 \mu\text{m}$ (fresh). Since these size ranges match well with our measurements of fresh spores ($6.3 \times 3.2 \mu\text{m}$), we assume that we found the same pathogen species in *F. auricularia* as those authors described before. The here-presented light and electron microscopic results showed that the morphology and life cycle stages of the pathogen closely resemble *N. forficulae* and other described nephridiophagids. There were no major differences to the genera *Peltomyces* or *Nephridiophaga*. An assignment to the genera *Oryctospora* and *Coleospora* could be excluded since mature spores possessed neither “alae” (wing-like extensions), such as in *Oryctospora* nor two nuclei, such as in *Coleospora*. Spore size and number of produced spores within the sporogenic plasmodium differ within members of individual genera and, thus, do not allow us to differentiate them (Radek and Herth 1999). The layers of the spore walls of different nephridiophagid species seem to vary slightly in structure and number (Toguebaye et al. 1986; Purrini and Weiser 1990; Lange 1993; Radek and Herth 1999; Fabel et al. 2000; Radek et al. 2002). However, these differences do not allow distinction and may be influenced by, for example, fixation and contrasting conditions. The only but decisive feature justifying the erection of a new genus for the nephridiophagid from *F. auricularia* is molecular data. Our phylogenetic analyses clearly show that the earwig parasite is sister to a cluster of *Nephridiophaga* species from cockroaches. We do not retain the genus name *Peltomyces* since the type species *P. hyalinus* is from a beetle host and it does not seem to be likely that these two pathogens belong to the same genus. We, therefore, propose the new genus name *Nephridiochytrium* for the earwig pathogen and describe the new species as *Nephridiochytrium forficulae*.

Nephridiophagids have already been found in some beetles, including a mallow beetle of the genus *Podagrica* (Léger 1909; Gibbs 1959; Toguebaye et al. 1986; Purrini and Rhode 1988; Purrini and Weiser 1990). Purrini and Rhode (1988) described an infection in *Podagrica fuscicornis* and classified it as *Coelosporidium schalleri*, presuming that the spore-former belongs to the Haplosporidia. However, the ultrastructure of the type species of the genus *Coelosporidium*, *Coelosporidium chydoricola* Mesnil & Marchoux, 1897, clearly differs from that of nephridiophagids (Manier et al. 1976). An affiliation to the Haplorigidia was therefore excluded and the pathogen was transferred to the genus *Nephridiophaga* as *Nephridiophaga schalleri* (Lange 1993). The nephridiophagid from the mallow beetle *Podagrica malvae* has similar life cycle stages as the one from *P. fuscicornis*. The spore form of *N. schalleri*, however, is described as cylindrical with round poles (Purrini and Rhode 1988), while our electron microscopic studies of the nephridiophagid from *P. malvae* and from many cockroach *Nephridiophaga* species (e.g. Radek and Herth (1999); Fabel et al. (2000); Radek et al. (2017)) showed a flattened oval form. Presumably, the flattening of the spores has not been recognised in the light microscopic investigations by Purrini and Rhode (1988). However, there are other differences between our newly-described nephridiophagid and *N. schalleri*.

The sporogenic plasmodia of the new nephridiophagid from *P. malvae* contained considerably fewer (7–36 instead of 24–64) and shorter spores ($3.6\text{--}4.7 \times 2.1\text{--}2.5 \mu\text{m}$ instead of $4.5\text{--}5 \times 2.0\text{--}2.5 \mu\text{m}$). Due to these differences and the general host specificity of nephridiophagids (Woolever 1966), we presume the presence of distinct nephridiophagid species in different *Podagrica* species. The nephridiophagids from the two *Podagrica* species show no relevant morphological or life cycle differences to other nephridiophagid genera, except *Coleospora* and *Oryctospora* (see above). In our phylogenetic tree, however, the sequence from *P. malvae* was the most divergent nephridiophagid, branching apart from all other nephridiophagids from cockroaches and the earwig. Considering the need for a distinguishing genus name for this parasite, we propose the new genus name *Malpighivinco* and name the new species *Malpighivinco podagrica*.

An unusual common feature of all nephridiophagids is the presence of two types of nuclei in the sporogenic plasmodia. The larger nuclei are the future spore nuclei, while the smaller ones remain in the mother cytoplasm. The presence of two nucleus types in the context of spore formation is reminiscent of stages found in Aphelidiomycota (Tcvetkova et al. 2023) – a sister group to true fungi (Torruella et al. 2018; Strassert and Monaghan 2022) with life cycles resembling those of Chytridiomycota. The stage with two nucleus types is represented by a multinucleate plasmodium of unclear origin. While division releases zoospores inheriting one nucleus type, the remnant of the plasmodium (“monster”) retains the other nucleus type and seems to degenerate after a short motile phase (Tcvetkova et al. 2023). The presence of two nucleus types in the life cycle may be an ancient trait of (early-diverging) fungi and their fungus-like aphelid relatives.

Our study shows that all known nephridiophagid species cluster together as a well-supported monophyletic lineage within the Chytridiomycota. Moreover, the distinct clustering of the two new genera together with *Nephridiophaga* support the presumption that the nephridiophagids, similar to other parasites, evolved in parallel with their hosts. A broader host screening may help to shed light on the origin and host range of nephridiophagids. Currently, their closer affiliation remains enigmatic and whether or not nephridiophagids form a distinct order (Nephridiophagales) as supposed by Doweld (2014) or belong to the Cladochytriales will have to be scrutinised once more sequence data become available.

Taxonomy

Opisthokonta, Fungi, Chytridiomycota, Nephridiophagales, Nephridiophagaceae

***Nephridiochytrium* Radek & Strassert, gen. nov.**

MycoBank No: 850000

Etymology. “Nephridio” refers to the site of infection, the nephridia, i.e. the insect kidneys (Malpighian tubules) and “chytrium” refers to the fungal assignment within the chytrids: *Nephridiochytrium*.

Diagnosis. Typical life cycle stages and morphology of Nephridiophagaceae.

***Nephridiochytrium forficulae* Radek & Strasser, sp. nov.**

MycoBank No: 850001

Etymology. “forficulae” refers to the host, an earwig of the genus *Forficula*.

Diagnosis. Oval, flattened spores measuring 5.8–6.9 (mean 6.3) × 2.9–3.5 (mean 3.2) µm; 13–37 (mean 19) spores per sporogenic plasmodium; central capped spore-opening at one side of mature spores. Oligo- and multinucleated vegetative plasmodia.

Type host. *Forficula auricularia* Linnaeus 1758 (Dermaptera, Forficulidae). COII gene accession number MN528021.

Type host locality. Tours, France.

Syntype. Cells in Fig. 1.

Gene sequence. rDNA operon acc. no. MW018149.

***Malpighivinco* Radek & Strasser gen. nov.**

MycoBank No: 850002

Etymology. “Malpighi” refers to the Malpighian tubules as habitat and the Latin word “vinco” (verb “vincere”) means “I conquer”, i.e. the pathogens infect the Malpighian tubules: *Malpighivinco*.

Diagnosis. Typical life cycle stages and morphology of Nephridiophagaceae.

***Malpighivinco podagrica* Radek & Strasser, sp. nov.**

MycoBank No: 850003

Etymology. “podagrica” refers to the host, a mallow beetle of the genus *Podagrica*.

Diagnosis. Oval, flattened spores measuring 3.6–4.7 (mean 4.2) × 2.1–2.5 (mean 2.3) µm; 7–36 (mean 21.5) spores per sporogenic plasmodium; central capped spore-opening at one side of mature spores. Oligo- and multinucleated vegetative plasmodia.

Type host. The mallow beetle *Podagrica malvae* (Illiger 1807).

Type host locality. Sicily, Italy.

Syntype. Cells in Fig. 2.

Gene sequence. rDNA operon acc. no. OR450019 and OR450020.

Conclusions

The here-described two new genera of Nephridiophagaceae show only few morphological and life cycle differences to other members of the family. A lack of distinctive morphological features certainly is a result of adaptations to the parasitic life style. All yet detected members of nephridiophagids live in the same habitat, namely the Malpighian tubules of insects. Thus, development of special structures or new multiplication strategies were seemingly not necessary to survive in different host taxa. Nevertheless, distinct phylogenetic lineages evolved in different insect taxa. The genus *Nephridiophaga*, for example, seems to be restricted to cockroach hosts, while beetles and earwigs are infected by other nephridiophagid genera.

Acknowledgements

We thank Saskia Franke, Sebastian Helwig and Antonia Voigtländer, Berlin, for contributions during their Bachelor theses and Joël Meunier, Tours, for providing earwigs. Further, we would like to thank the German beetle specialists, Martin Lillig from Berlin and Manfred Niehuis from Landau, for determining the mallow beetles.

Additional information

Conflict of interest

The authors have declared that no competing interests exist.

Ethical statement

No ethical statement was reported.

Funding

JFHS acknowledges support from the German Research Foundation (DFG; grant STR1349/2-1, project no. 432453260). Research was partially funded by the German Federal Ministry of Education and Research (BMBF, Förderkennzeichen 033W034A). We acknowledge support by the Open Access Publication Fund of the Freie Universität Berlin.

Author contributions

Conceptualisation: RR. Methodology: RR, JFHS, CW. Investigation: RR, JFHS, CW. Visualisation: RR, JFHS. Software: CW, JFHS. Formal analysis: JFHS, CW. Data Curation: JFHS. Writing – Original draft: RR. Writing – Review and Editing: JFHS, CW.

Author ORCIDs

Renate Radek  <https://orcid.org/0000-0001-7605-7546>

Christian Wurzbacher  <https://orcid.org/0000-0001-7418-0831>

Jürgen F. H. Strassert  <https://orcid.org/0000-0001-6786-7563>

Data availability

All generated sequences were submitted to GenBank.

References

- Bennett L, Melchers B, Proppe B (2020) Curta: A general-purpose high-performance computer at ZEDAT, Freie Universität Berlin. <https://doi.org/10.17169/refubium-26754>
- Capella-Gutierrez S, Silla-Martinez JM, Gabaldon T (2009) trimAl: A tool for automated alignment trimming in large-scale phylogenetic analyses. *Bioinformatics* 25(15): 1972–1973. <https://doi.org/10.1093/bioinformatics/btp348>
- Doweld AB (2014) Nephridiophagales ord. nov. *Index Fungorum*: Published Numbers 74: 1–1.
- Fabel P, Radek R, Storch V (2000) A new spore-forming protist, *Nephridiophaga blaberi* sp. nov., in the death's head cockroach *Blaberus craniifer*. *European Journal of Protistology* 36(4): 387–395. [https://doi.org/10.1016/S0932-4739\(00\)80044-9](https://doi.org/10.1016/S0932-4739(00)80044-9)
- Gibbs AJ (1959) *Coleospora binucleata* gen. nov. spec. nov., a haplosporidian parasite found in *Gonocephalum arenarium* (Coleoptera). *Parasitology* 49(3–4): 552–558. <https://doi.org/10.1017/S0031182000027098>

- Guindon S, Dufayard JF, Lefort V, Anisimova M, Hordijk W, Gascuel O (2010) New algorithms and methods to estimate maximum-likelihood phylogenies: Assessing the performance of PhyML 3.0. *Systematic Biology* 59(3): 307–321. <https://doi.org/10.1093/sysbio/syq010>
- Hoang DT, Chernomor O, Von Haeseler A, Minh BQ, Vinh LS (2018) UFBoot2: Improving the ultrafast bootstrap approximation. *Molecular Biology and Evolution* 35(2): 518–522. <https://doi.org/10.1093/molbev/msx281>
- Ivanić M (1937) Die Entwicklungsgeschichte und die parasitäre Zerstörungsarbeit einer in den Zellen der Malpighischen Gefäße der Honigbiene (*Apis mellifera*) schmarotzenden Haplosporidie *Nephridiophaga apis* n. g. n. sp. *La Cellule* 45: 291–324.
- Kalyaanamoorthy S, Minh BQ, Wong TKF, von Haeseler A, Jermin LS (2017) ModelFinder: Fast model selection for accurate phylogenetic estimates. *Nature Methods* 14(6): 587–589. <https://doi.org/10.1038/nmeth.4285>
- Katoh K, Standley DM (2013) MAFFT multiple sequence alignment software version 7: Improvements in performance and usability. *Molecular Biology and Evolution* 30(4): 772–780. <https://doi.org/10.1093/molbev/mst010>
- Lange CE (1993) Unclassified protists of arthropods: The ultrastructure of *Nephridiophaga periplanetae* (Lutz & Splendore, 1903) n. comb., and the affinities of the Nephridiophagidae to other protists. *The Journal of Eukaryotic Microbiology* 40(6): 689–700. <https://doi.org/10.1111/j.1550-7408.1993.tb04461.x>
- Lartillot N, Rodrigue N, Stubbs D, Richer J (2013) Phylobayes mpi: Phylogenetic reconstruction with infinite mixtures of profiles in a parallel environment. *Systematic Biology* 62(4): 611–615. <https://doi.org/10.1093/sysbio/syt022>
- Léger ML (1909) Sur un mycetozoaire nouveau endoparasite des insectes. *Comptes Rendus Hebdomadaires des Séances de l'Académie des Sciences* 149(III): 239–241. <https://doi.org/10.5962/bhl.part.22028>
- Manier JF, Akbarieh M, Bouix G (1976) *Coelosporidium chydoricola* Mesnil et Marchoux, 1897: Observations ultrastructurales, données nouvelles sur le cycle et la position systématique. *Protistologica* 12: 599–612.
- Nguyen LT, Schmidt HA, Von Haeseler A, Minh BQ (2015) IQ-TREE: A fast and effective stochastic algorithm for estimating maximum-likelihood phylogenies. *Molecular Biology and Evolution* 32(1): 268–274. <https://doi.org/10.1093/molbev/msu300>
- Ormières R, Manier JF (1973) Observations sur *Nephridiophaga forficulae* (Léger, 1909) parasite des tubes de Malpighi de *Forficula auricularia*. *Annales de Parasitologie Humaine et Comparée* 48(1): 1–10. <https://doi.org/10.1051/parasite/1973481001>
- Purrini K, Rohde M (1988) Light and electron microscope studies on two new protists, *Coelosporidium schalleri* n. sp. and *Coelosporidium meloidorum* n. sp. (Protista), infecting natural populations of the flea beetle, *Podagrica fuscicornis*, and flower beetle, *Mylabris maculiventris*. *Zoologischer Anzeiger* 220: 323–333.
- Purrini K, Weiser J (1990) Light and electron microscope studies on a protozoan, *Oryctospora alata* n. gen., n. sp. (Protista: Coelosporidiidae), parasitizing a natural population of the rhinoceros beetle, *Oryctes monoceros* Oliv. (Coleoptera, Scarabaeidae). *Zoologische Beiträge* 33: 209–220.
- Radek R, Herth W (1999) Ultrastructural investigation of the spore-forming protist *Nephridiophaga blattellae* in the Malpighian tubules of the German cockroach *Blattella germanica*. *Parasitology Research* 85(3): 216–231. <https://doi.org/10.1007/s004360050538>
- Radek R, Klein G, Storch V (2002) The spore of the unicellular organism *Nephridiophaga blattellae*: Ultrastructure and substances of the spore wall. *Acta Protozoologica* 41: 169–181.

- Radek R, Wurzbacher C, Gisder S, Nilsson RH, Owerfeldt A, Genersch E, Kirk PM, Voigt K (2017) Morphologic and molecular data help adopting the insect-pathogenic nephridiophagids (Nephridiophagidae) among the early diverging fungal lineages, close to the Chytridiomycota. *MycoKeys* 25: 31–50. <https://doi.org/10.3897/mycokeys.25.12446>
- Radek R, Voigt K, Kirk PM, Strassert JFH, Lee HM (2022) (2878) Proposal to conserve the name *Nephridiophaga* (Chytridiomycota) with a conserved type. *Taxon* 71(2): 471–472. <https://doi.org/10.1002/tax.12698>
- Purrini K, Rhode M (1988) Light and electron microscope studies on two new protists, *Coelosporidium schalleri* n. sp. and *Coelosporidium meloidorum* n. sp. (Protista) infecting natural populations of the flea beetle, *Podagrica fusciocornis*, and flower beetle, *Mylabris maculiventris*. *Zoologischer Anzeiger* 5/6: 323–333.
- Reynolds ES (1963) The use of lead citrate at high pH as an electron-opaque stain in electron microscopy. *The Journal of Cell Biology* 17(1): 208–212. <https://doi.org/10.1083/jcb.17.1.208>
- Shen W, Le S, Li Y, Hu F (2016) SeqKit: A cross-platform and ultrafast toolkit for FASTA/Q file manipulation. *PLoS ONE* 11(10): e0163962. <https://doi.org/10.1371/journal.pone.0163962>
- Spurr AR (1969) A low-viscosity epoxy resin embedding medium for electron microscopy. *Journal of Ultrastructure Research* 26(1–2): 31–43. [https://doi.org/10.1016/S0022-5320\(69\)90033-1](https://doi.org/10.1016/S0022-5320(69)90033-1)
- Strassert JFH, Monaghan MT (2022) Phylogenomic insights into the early diversification of fungi. *Current Biology* 32(16): 3628–3635.e3. <https://doi.org/10.1016/j.cub.2022.06.057>
- Strassert JFH, Wurzbacher C, Hervé V, Antany T, Brune A, Radek R (2021) Long rDNA amplicon sequencing of insect-infecting nephridiophagids reveals their affiliation to the Chytridiomycota and a potential to switch between hosts. *Scientific Reports* 11(1): e396. <https://doi.org/10.1038/s41598-020-79842-6>
- Strassert JFH, Rodríguez-Rojas A, Kuropka B, Krahl J, Kaya C, Pulat H-C, Nurel M, Saroukh F, Radek R (2022) Nephridiophagids (Chytridiomycota) reduce the fitness of their host insects. *Journal of Invertebrate Pathology* 192: e107769. <https://doi.org/10.1016/j.jip.2022.107769>
- Tcvetkova VS, Pozdnyakov IR, Seliuk AO, Zorina NA, Karpov SA (2023) Vegetative cell fusion and a new stage in the life cycle of the Aphelida (Opisthosporidia). *The Journal of Eukaryotic Microbiology* 70(5): e12977. <https://doi.org/10.1111/jeu.12977>
- Togebaye BS, Manier JF, Bouix G, Marchand B (1986) *Nephridiophaga ormiersi* n. sp., protiste parasite d'*Aspidiomorpha cincta* Fabricius, 1781 (Insecte Coléoptère: Chrysomelidae). Étude ultrastructurale. *Protistologica* 22: 317–325.
- Torruella G, Grau-Bové X, Moreira D, Karpov SA, Burns JA, Sebé-Pedrós A, Völcker E, López-García P (2018) Global transcriptome analysis of the aphelid *Paraphelidium tribonemae* supports the phagotrophic origin of fungi. *Communications Biology* 1(1): e231. <https://doi.org/10.1038/s42003-018-0235-z>
- Voigt K, James TY, Kirk PM, Santiago ALCMA, Waldman B, Griffith GW, Fu M, Radek R, Strassert JFH, Wurzbacher C, Jerônimo GH, Simmons DR, Seto K, Gentekaki E, Hurdeal VG, Hyde KD, Nguyen TTT, Lee HB (2021) Early-diverging fungal phyla: Taxonomy, species concept, ecology, distribution, anthropogenic impact, and novel phylogenetic proposals. *Fungal Diversity* 109(1): 59–98. <https://doi.org/10.1007/s13225-021-00480-y>
- Wijayawardene NN, Pawłowska J, Letcher PM, Kirk PM, Humber RA, Schüßler A, Wrzosek M, Muszewska A, Okrasińska A, Istel Ł, Gęsiorska A, Mungai P, Lateef AA, Rajeshkumar KC, Sing RV, Radek R, Walther G, Wagner L, Walker C, Wijesundara DSA,

- Papizadeh M, Dolatabadi S, Shenoy BD, Tokarev YS, Lumyong S, Hyde KD (2018) Notes for genera: Basal clades of Fungi (including Aphelidiomycota, Basidiobolomycota, Blastocladiomycota, Calcarisporiellomycota, Caulochytriomycota, Chytridiomycota, Entomophthoromycota, Glomeromycota, Kickxellomycota, Monoblepharomycota, Mortierellomycota, Mucoromycota, Neocallimastigomycota, Olpidiomycota, Rozellomycota and Zoopagomycota). *Fungal Diversity* 92(1): 43–129. <https://doi.org/10.1007/s13225-018-0409-5>
- Wijayawardene NN, Hyde KD, Al-Ani LKT, Tedersoo L, Haelewaters D, Rajeshkumar KC, Zhao RL, Aptroot A, Leontyev DV, Saxena RK, Tokarev YS, Dai DQ, Letcher PM, Stephenson SL, Ertz D (2020) Outline of Fungi and fungus-like taxa. *Mycosphere: Journal of Fungal Biology* 11(1): 1060–1456. <https://doi.org/10.5943/mycosphere/11/1/8>
- Woolever P (1966) Life history and electron microscopy of a haplosporidian, *Nephridiophaga blattellae* (Crawley) n. comb., in the Malpighian tubules of the German cockroach, *Blattella germanica* (L.). *The Journal of Protozoology* 13(4): 622–642. <https://doi.org/10.1111/j.1550-7408.1966.tb01973.x>
- Wurzbacher C, Larsson E, Bengtsson-Palme J, Van den Wyngaert S, Svantesson S, Kristiansson E, Kagami M, Nilsson RH (2019) Introducing ribosomal tandem repeat barcoding for fungi. *Molecular Ecology Resources* 19(1): 118–127. <https://doi.org/10.1111/1755-0998.12944>

Supplementary material 1

Infections of *Podagrica* spp. and *Forficula auricularia* with nephridiophagids (in Malpighian tubules) and other pathogens

Authors: Renate Radek

Data type: xlsx

Explanation note: The table gives an overview on the infection status of earwigs and mallow beetle collected at different locations.

Copyright notice: This dataset is made available under the Open Database License (<http://opendatacommons.org/licenses/odbl/1.0/>). The Open Database License (ODbL) is a license agreement intended to allow users to freely share, modify, and use this Dataset while maintaining this same freedom for others, provided that the original source and author(s) are credited.

Link: <https://doi.org/10.3897/mycokeys.100.111298.suppl1>

Supplementary material 2

SSU rRNA gene sequence alignments used for phylogenetic tree reconstruction (Figure 3)

Authors: Jürgen F. H. Strassert

Data type: fa

Copyright notice: This dataset is made available under the Open Database License (<http://opendatacommons.org/licenses/odbl/1.0/>). The Open Database License (ODbL) is a license agreement intended to allow users to freely share, modify, and use this Dataset while maintaining this same freedom for others, provided that the original source and author(s) are credited.

Link: <https://doi.org/10.3897/mycokeys.100.111298.suppl2>

Supplementary material 3

LSU rRNA gene sequence alignments used for phylogenetic tree reconstruction (Figure 3)

Authors: Jürgen F. H. Strasser

Data type: fa

Copyright notice: This dataset is made available under the Open Database License (<http://opendatacommons.org/licenses/odbl/1.0/>). The Open Database License (ODbL) is a license agreement intended to allow users to freely share, modify, and use this Dataset while maintaining this same freedom for others, provided that the original source and author(s) are credited.

Link: <https://doi.org/10.3897/mycokeys.100.111298.suppl3>